

Jürgen Valldorf · Wolfgang Gessner (Eds.)

Advanced Microsystems Automotive Applications 2006

Jürgen Valldorf · Wolfgang Gessner (Eds.)

Advanced Microsystems for Automotive Applications 2006

With 287 figures

 Springer

Dr. Jürgen Valldorf
VDI/VDE Innovation + Technik GmbH
Steinplatz 1
10623 Berlin
valldorf@vdivde-it.de

Dr. Wolfgang Gessner
VDI/VDE Innovation + Technik GmbH
Steinplatz 1
10623 Berlin
gessner@vdivde-it.de

ISBN-10 3-540-33409-2 Berlin Heidelberg New York
ISBN-13 978-3-540-33409-5 Berlin Heidelberg New York

This work is subject to copyright. All rights are reserved, whether the whole or part of the material is concerned, specifically the rights of translation, reprinting, reuse of illustrations, recitation, broadcasting, reproduction on microfilms or in any other way, and storage in data banks. Duplication of this publication or parts thereof is permitted only under the provisions of the German Copyright Law of September 9, 1965, in its current version, and permission for use must always be obtained from Springer. Violations are liable to Prosecution under the German Copyright Law.

Springer is a part of Springer Science+Business Media
springer.com

© Springer-Verlag Berlin Heidelberg 2006
Printed in Germany

The use of general descriptive names, registered names, etc. in this publication does not imply, even in the absence of a specific statement, that such names are exempt from the relevant protective laws and regulations and free for general use.

Typesetting: Michael Strietzel
Cover design: deblik, Berlin

Printed on acid-free paper 62/3141/Rw-5 4 3 2 1 0

Preface

The automotive industry with more than 2 million employees is not only one of the main pillars of European economy, it is also of all economic sectors the largest R&D investor in Europe, realising 20% of the R&D expenditures of the entire manufacturing industry. Through this it constitutes a major driver for the development and diffusion of new technologies and innovations throughout the economy.

Looking back 10 years when the International Forum on Advanced Microsystems for Automotive Application (AMAA) started, enormous progress has been made in reducing casualties, emissions and in increasing comfort and performance. Microsystems in many cases provided the key functions for this progress. Although the issues the event concentrated on didn't change significantly (safety, powertrain, comfort, etc.), considerable shifts of technological paradigms and approaches can be stated.

This year the AMAA will celebrate its 10th anniversary, recapitulating objectives achieved and looking forward to new challenges for the automotive industry deriving from increasingly complex miniaturised systems driven by socio-economic requirements.

The future of microsystems will consist of integrated smart systems which are able to diagnose a situation, to describe and to qualify it. They will be able to identify and mutually address each other. They will be predictive and therefore they will be able to decide and help to decide. Smart systems will enable the automobile to interact with the environment, they will perform multiple tasks and assist a variety of activities. Smart systems will be highly reliable, often networked and energy autonomous.

There is a coincidence of the AMAA objectives and those of EPoSS, the European Technology Platform on Smart Systems Integration, contributing intensively to the development of automotive-specific smart systems. You will find a series of the EPoSS items in the programme of the 10th AMAA, which continues to be a unique exchange forum for companies in the automotive value chain.

The publication in hand also reflects these issues. It is a cut-out of new technological priorities in the area of microsystems-based smart devices and opens up a mid-term perspective of future smart systems applications in automobiles.

I would like to express my sincere thanks to the authors for their valuable contributions to this publication. I would like to thank the members of the AMAA Honorary Committee who accompanied the initiative over the last 10 years and the Steering Committee – the real backbone of the AMAA since its first beginning. Particular thanks are addressed to the European Commission for their financial support through the Innovation Relay Centre Northern Germany and to the supporting organisations CLEPA and EUCAR.

Last but not least, my thanks are addressed to the Innovation Relay Centre team at VDI/VDE-IT for their assistance with the conference, to Mr. Michael Strietzel for preparing the book for publication, and especially to Dr. Jürgen Valldorf, project manager and chairman of the AMAA.

Berlin, April 2006

Wolfgang Gessner

Public Financers

Berlin Senate for Economics and Technology

European Commision

Ministry for Economics Brandenburg

Supporting Organisations

Investitionsbank Berlin (IBB)

mstnews

ZVEI - Zentralverband Elektrotechnik- und Elektronikindustrie e.V.

Hanser automotive electronic systems

Micronews - The Yole Developpement Newsletter

enablingMNT

Co-Organisators

European Council for Automotive R&D (EUCAR)

European Association of Automotive Suppliers (CLEPA)

Advanced driver assistance systems in Europe (ADASE)

Honorary Committee

Domenico Bordone

President and CEO
Magneti Marelli S.P.A., Italy

Günter Hertel

Vice President Research and Technology
DaimlerChrysler AG, Germany

Rémi Kaiser

Director Technology and Quality
Delphi Automotive Systems Europe, France

Nevio di Giusto

President and CEO
FIAT, Italy

Karl-Thomas Neumann

CEO, Member of the Executive Board
Continental Automotive Systems, Germany

Steering Committee

Dr. Giancarlo Alessandretti	Centro Ricerche FIAT, Orbassano, Italy
Alexander Bodensohn	DaimlerChrysler AG, Frankfurt am Main, Germany
Serge Boverie	Siemens VDO Automotive, Toulouse, France
Geoff Callow	Technical & Engineering Consulting, London, UK
Bernhard Fuchsbauer	Audi AG, Ingolstadt, Germany
Kay Fürstenberg	IBEO GmbH, Hamburg, Germany
Wolfgang Gessner	VDI/VDE-IT, Berlin, Germany
Roger Grace	Roger Grace Associates, San Francisco, USA
Henrik Jakobsen	SensoNor A.S., Horten, Norway
Horst Kornemann	Continental Automotive Systems, Frankfurt am Main, Germany
Hannu Laatikainen	VTI Technologies Oy, Vantaa, Finland
Dr. Torsten Mehlhorn	Investitionsbank Berlin, Berlin, Germany
Dr. Roland Müller-Fiedler	Robert Bosch GmbH, Stuttgart, Germany
Paul Mulvanny	QinetiQ Ltd., Farnborough, UK
Dr. Andy Noble	Ricardo Consulting Engineers Ltd., Shoreham-by-Sea, UK
Ulf Palmquist	EUCAR, Brussels, Belgium
Gloria Pellischek	Clepa, Brussels, Belgium
David B. Rich	Delphi Delco Electronics Systems, Kokomo, USA
Dr. Detlef E. Ricken	Delphi Delco Electronics Europe GmbH, Rüsselsheim, Germany
Jean-Paul Rouet	Johnson Controls, Pontoise, France
Christian Rousseau	Renault S.A., Guyancourt, France
Patric Salomon	4M2C, Berlin, Germany
Ernst Schmidt	BMW AG, Munich, Germany
John P. Schuster	Motorola Inc., Northbrook Illinois, USA
Solzbacher, Florian	University of Utah, Salt Lake City, USA
Bob Sulouff	Analog Devices Inc., Cambridge, USA
Berthold Ulmer	DaimlerChrysler AG, Brussels, Belgium
Egon Vetter	Ceramet Technologies, Melbourne, Australia
Hans-Christian von der Wense	Freescale GmbH, München, Germany

Conference chair:

Dr. Jürgen Valldorf	VDI/VDE-IT, Berlin, Germany
---------------------	-----------------------------

Table of Contents

Market

Prospects for MST Sensors in Automotive Applications	3
R. Dixon, J. Bouchaud, WTC - Wicht Technologie Consulting	

Future Architecture for Inertial Sensors in Cars	13
J.C. Eloy, M. Potin, Dr. E. Mounier, Dr. P. Roussel, Yole Développement	

Safety

Three-Dimensional CMOS Image Sensor for Pedestrian Protection and Collision Mitigation	23
P. Mengel, L. Listl, B. König, C. Toepfer, M. Pellkofer, Siemens AG W. Brockherde, B. Hosticka, O. Elkhaili, O. Schrey, W. Ulfing, Fraunhofer IMS	

EVENT-ONLINE – A Service Concept for large scale Events based on FCD Technology	41
R. Willenbrock, F. Steinert, gedas deutschland GmbH W. Schönewolf, Fraunhofer IPK K. Graze, Signalbau Huber GmbH	

Advanced Pressure Sensors with high Flexibility for Side Crash Detection	45
M. Brauer, Dr. K. Krupka, Infineon Technologies AG	

Detection of Road Users in Fused Sensor Data Streams for Collision Mitigation	53
L. Walchshäusl, R. Lindl, K. Vogel, BMW Group Research and Technology T. Tatschke, FORWISS Institute for Software Systems, University of Passau	

Dynamic Pass Prediction – A New Driver Assistance System for Superior and Safe Overtaking	67
J. Loewenau, K. Gresser, D. Wisselmann, BMW Group Research and Technology W. Richter, BMW Group Development D. Rabel, S. Durekovic, NAVTEQ	

Requirement Engineering for Active Safety Pedestrian Protection Systems based on Accident Research	79
R. Fröming, V. Schindler, TU Berlin M. Kühn, VTIV	
Biologically Inspired Multi-Sensor Fusion for Adaptive Camera Stabilization in Driver-Assistance Systems	107
W. Günthner, S. Glasauer, Ph. Wagner, H. Ulbrich, TU Munich	
Low Speed Collision Avoidance System	123
J. Kibbel, H. Salow, M. Dittmer, IBEO Automobile Sensor GmbH	
Laserscanner for Multiple Applications in Passenger Cars and Trucks	129
R. Schulz, K. Fürstenberg, IBEO Automobile Sensor GmbH	
A new Approach for Obstacle Detection Based on Dynamic Vehicle Behaviour	143
M. Straßberger, BMW Group Forschung und Technik R. Lasowski, Softlab GmbH	
Far Infrared Detection Algorithms for Vulnerable Road Users Protection	155
Y. Le Guilloux, R. Moreira, S. Khaskelman, J. Lonnoy, SAGEM	
iBolt Technology – A Weight Sensing System for Advanced Passenger Safety	171
K. Kasten, A. Stratmann, M. Munz, K. Dirscherl, S. Lamers, Robert Bosch GmbH	
Object Classification exploiting High Level Maps of Intersections	187
S. Wender, T. Weiss, K. C. J. Dietmayer, University of Ulm K. Ch. Fürstenberg, IBEO Automobile Sensor GmbH	
Performance of a Time-of-Flight Range Camera for Intelligent Vehicle Safety Applications	205
S. Hsu, S. Acharya, A. Rafii, R. New, Canesta Inc.	

Powertrain

Coordinated Cylinder Pressure Based Control for Reducing Diesel Emissions Dispersion 223

M. G. Beasley, R. C. E. Cornwell, M. A. Egginton, P. M. Fussey, R. King,
A. D. Noble, T. Salamon, A. J. Truscott, Ricardo UK Ltd.
G. Landsmann, General Motors Powertrain Europe

A High Temperature Floating Gate MOSFET Driver for on the Engine Injector Control 239

P. Delatte, V. Dessard, G. Picún, O. Stevens, L. Demeûs, CISSOID S.A.

Comfort and HMI

Distributed Pressure Sensor Based on Electroactive Materials for Automotive Application 249

E. Ochoteco, J.A. Pomposo, H. Grande, Cidetec
F. Martinez, G. Obieta, Ikerlan
J. Lezama , P4Q Electronics
J. M. Iriondo, Maser Microelectronica

Intelligent Infrared Comfort Sensors for the Automotive Environment 261

L. Buydens, V. Kassovsky, R. Diels, Melexis NV

Gesture Recognition Using Novel Efficient and Robust 3D Image Processing 281

B. Liu, T. Sünkel, O. Jesorsky, R. Kompe, 3SOFT GmbH
J. Hornegger, Friedrich-Alexander University, Erlangen-Nuremberg

Network of Excellence HUMANIST - Human Centred Design for Information Society Technologies INRETS & ERT 295

A. Pauzié, French National Institute for Research in Transport and Safety

Networked Vehicle

High Speed 1Gbit/s Video Transmission with Fiber Optic Technology

307

T. Wipiejewski, F. Ho, W. Hung, S. Cheng, E. Wong, St. Ng, W. Ma, Th.
Choi, G. Egnisaban, K. Yau, T. Mangente, ASTRI

Components and Generic Sensor Technologies

Integrated Giant Magneto Resistors – a new Sensor Technology for Automotive Applications

323

W. Rössler, J. Zimmer, Th. Bever, K. Prügl, Infineon Technologies AG
W. Granig, D. Hammerschmidt, E. Katzmaier, Infineon Technologies Austria
AG

Simulating Microsystems in the Context of an Automotive Drive Application

343

G. Pelz, Ch. Decker, D. Metzner, Infineon Technologies AG
L. Voßkaemper, D. Dammers, Dolphin Integration

Miniaturized Wireless Sensors for Automotive Applications

353

R. Thomasius, D. Polityko, H. Reich, TU Berlin
M. Niedermayer, S. Grundmann, S. Guttowski, Fraunhofer IZM
R. Achterholt, Global Dynamix AG

3D-MID – Multifunctional Packages for Sensors in Automotive Applications

369

D. Moser, J. Krause, HARTING Mitronics AG

PreVENT

Towards the Automotive HMI of the Future: Mid-Term Results of the AIDE Project

379

J. Engström, J. Arwidsson, Volvo Technology Corporation
A. Amditis, ICCS I-Sense Group
L. Andreone, Centro Ricerche Fiat
K. Bengler, BMW Group Forschung und Technik GmbH
P. C. Cacciabue, European Commission – Joint Research Centre
W. Janssen, TNO Human Factors
H. Kussman Robert Bosch GmbH
F. Nathan, PSA Peugeot Citroën Automobiles

Accidentology as a Basis for Requirements and System Architecture of Preventive Safety Applications

407

M. Schulze, DaimlerChrysler AG
J. Irion, Irion Management Consulting
T. Mäkinen, Technical Research Centre of Finland (VTT)
M. Flament, ERTICO - ITS Europe

ADAS Horizon – How Digital Maps can contribute to Road Safety

427

V. Blervaque, ERTICO
K. Mezger, Daimler Chrysler Research
L. Beuk, Siemens VDO, Eindhoven
J. Loewenau, BMW Group Research and Technology

Intersection Safety – the EC Project INTERSAFE

437

B. Rössler, Volkswagen AG
K. Ch. Fürstenberg, U. Lages, IBEO Automobile Sensor GmbH

ProFusion2 – towards a Modular, Robust and Reliable Fusion Architecture for Automotive Environment Perception

451

T. Tatschke, FORWISS, University of Passau
S.-B. Park, Delphi Electronics Safety
A. Amditis, A. Polychronopoulos, ICCS, NTUA
U. Scheunert, Technical University of Chemnitz
O. Aycard, GRAVIR-IMAG INRIA

Integrating Lateral and Longitudinal Active and Preventive Safety Functions

471

A. Amditis, A. Polychronopoulos, Institute of Comm. and Computer Systems
A. Sjögren, A. Beutner, Volvo Technology Corporation
M. Miglietta, A. Saroldi, Centro Ricerche Fiat

Lane Detection for a Situation Adaptive Lane Keeping Support System, the SAFELANE System	485
N. Möhler, D. John, M. Voigtländer, Fraunhofer IVI	

Appendices

Appendix A: List of Contributors	503
Appendix B: List of Keywords	511

Prospects for MST Sensors in Automotive Applications

R. Dixon, J. Bouchaud, WTC - Wicht Technologie Consulting

Abstract

The number of passenger vehicles on the world's roads will reach an estimated 68 million light vehicles in 2008. Many vehicles will feature increasingly sophisticated safety and engine management systems as a result of the migration of sophisticated MST-based sensors from luxury into mid-range cars. The success of such sensors owes much to batch micromachining processes, which reduce component sizes and provide low power consumption devices that can be integrated with signal conditioning electronics into small packages that handle the harsh environments and deliver reliability extending over 10-15 years.

This paper examines existing and emerging markets for MST sensors deployed in airbags and vehicle dynamics, GPS navigation, and engine management. According to our estimates, the overall market for MST based automotive measurements will grow from around \$1.3 billion in 2004 to nearly \$2 billion in 2009. A particular emphasis of this article is the opportunity for inertial and pressure sensors.

1 Introduction

Automotive applications demand high-quality products that operate without failure, often under extreme conditions. Sensors in this environment must combine low cost with high reliability, sustained over production runs amounting to millions/year. These specifications have continued to be met by Microsystem solutions, which have displaced many conventional sensors due to a combination of size, low weight and compatibility with the power requirements of existing automotive electronics systems.

This success explains the increasing migration into less expensive cars. Mid-sized vehicles now contain more than 50 sensors, and luxury class cars over 100 [1]. About one third of these sensors are now MST-based. Meanwhile, the automotive sector can now be considered instrumental in the emergence of new markets for MST sensors in consumer applications and personal electronics.

The automotive market grows at about 4% annually and various estimates put the number of light passenger vehicles as around 68 million by 2008 (e.g. Strategy Analytics). Frontal impact airbags and engine monitors that improve fuel efficiency and lower emissions have historically driven sensor implementation. This is augmented by the migration of advanced safety features such as vehicle dynamics systems and anti-roll detectors, in addition to the convenience of GPS navigation. This continued implementation is expected to continue as legislators and consumers propel manufacturers to continually improve the safety, functionality, ride quality and comfort of today’s vehicles.

2 MST Sensor Applications

An overview of the applications and status for MST sensors are shown in Tab. 1. Established applications are inertial sensors for vehicle dynamics and airbags and pressure sensors for engine management, in addition to flow sensors for air intake and infrared sensors for a range of functions in traffic/road monitoring, cabin temperature control, gas sensor and air quality, anti-fog systems, tire and brake monitoring, etc.

Microsystem	Application	Status
Acceleration sensors	Front airbag, side airbag, upfront sensors, vehicle dynamic control, roll detection, GPS navigation, active suspension	Established
Yaw rate sensors (gyroscopes)	Vehicle dynamics control, roll detection, GPS navigation	Established
Pressure sensors	Air intake (MAP), atmospheric pressure (BAP), fuel vapour, turbocharger pressure, tire pressure, HVAC compressor, fuel injection, side airbag, passenger occupation, oil, diesel particle, coolant	Established
Flow sensors	Air intake, HVAC control	Established, 2008/2009
IR Sensors	Traffic/road monitoring, cabin temperature control, gas sensor and air quality, anti-fog systems, tire and brake monitoring, seat occupancy	Established
	Driver vision enhancement	2008
Inclinometers	Headlight levelling, zero setting (gyro), theft alarm, electronic parking brake	Established
Microphones	Hands free microphone, directional audio microphone arrays	2008/2009
RF MEMS switches	Automotive radar	2008

Tab. 1. Applications and status of various sensors in the automotive sector.

n engine management, manifold air pressure (MAP) and barometric air pressure (BAP) sensors represent an entrenched use for silicon micromachined pressure sensors. These devices are deformable diaphragms that employ piezoresistive or capacitive sensing principles. MAP regulates air intake pres-

sure to feedback the correct air-fuel mixture for pollution control and fuel efficiency and BAP compensates the air-fuel mix according to altitude.

Fuel vapour monitors and tire-pressure monitoring systems (TPMS) are interesting applications for pressure sensors. TPMS deployment is driven by the legislation in the US, where blowouts and flats reputedly cause 23,000 accidents and over 500 fatal accidents per year. A typical configuration is represented by a pressure sensor (and in many cases an accelerometer to save on battery power) placed on each tire that communicates with a central unit via RF and displays pressure on the dashboard.



Fig. 1. Tire pressure-monitor from Infineon and SensoNor (Courtesy of Infineon). Most TPMS modules currently contain an MST pressure sensor and an accelerometer to save battery power by signalling the transmitter to function only when the automobile is in motion.

MEMS yaw rate sensors and accelerometers are deployed in Electronic Stability Program (ESP) modules used for vehicle dynamics and determine the correct braking in corners to prevent slip or roll over. Gyroscopes also measure the roll of the vehicle and are linked to curtain airbags and seatbelt pre-tensioning systems if a critical angle is exceeded, and provide dead reckoning assistance for GPS navigation systems. Inclometers are used in headlight levelling and sensitive alarms. Inclometers correct tilt in navigation gyroscopes, provide sensitive burglar alarms and change headlight level.

Accelerometers are primarily used as sensors that send signals to fire airbags, and today's vehicles regularly feature both side and rear airbags in addition to front airbags. Intelligent front airbags have now been designed to respond differently depending on crash severity, while passenger occupancy detection

systems (PODS) determine whether it is appropriate to fire an airbag or not. Several approaches such as infrared, Hall and pressure sensors compete for this application, and are incorporated as a result of low speed incidents that triggered early airbag systems and caused fatalities, typically with young passengers. These systems are expected to be in all US vehicles by 2009, for example.

In future, the number of different MST sensors used in cars is expected to increase, e.g. for infrared devices in vision enhancement, RF MEMS switches for automotive radar, and microphones for hands free microphone and directional audio microphone arrays. These will be niche applications and not expected to represent a significant opportunity for MEMS over the next five years.

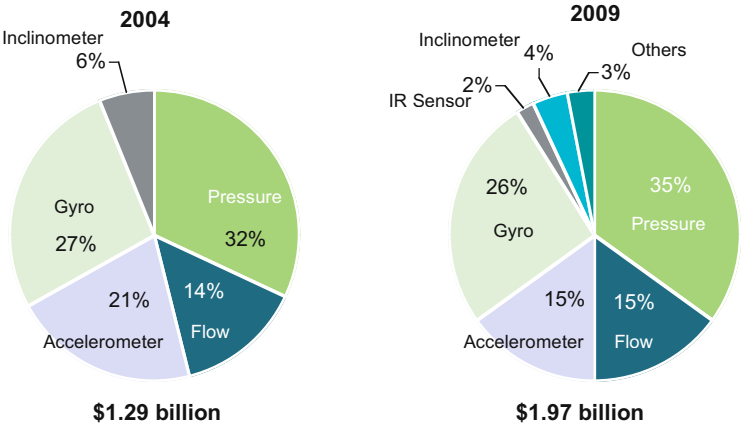


Fig. 2. Major markets for automotive sensors over the period 2004 - 2009.

3 MST Sensor Markets

The major markets are broken out by sensor type in Fig. 2. Overall, we forecast the market to grow from \$1.29 billion to \$1.97 billion over the period 2004 to 2009, a CAGR of nearly 9%. Pressure sensors make up the largest opportunity in the next five years, followed by gyroscopes for safety applications and navigation, airbag accelerometers and flow sensors, mostly for mass air flow measurement (and beginning only slowly for accurate HVAC cabin control). Inclinometers used in headlight levelling and alarms will not grow significantly over the five years and IR sensors will also remain a niche mar-

ket opportunity. The remainder of this paper concentrates on the major markets for pressure and inertial sensors.

Pressure Sensors

Pressure sensors represent the biggest market by revenue – a total of over \$677 million in 2009 – and will maintain their lead as the largest market opportunity by sensor type (see Figure 2). With the exception of TPMS this is a mature market featuring sensors for engine management using sensors priced from \$2.5 to \$6 (in 1st level packages).

The market for pressure sensors used in **TPMS** will explode to reach \$207 million from 90 million units in 2009 (see Tab. 2). This explains the highly competitive situation and large number of companies producing and developing such systems. A TPMS module typically includes pressure sensor, accelerometer, temperature sensor, signal conditioning electronics, and wireless transmitter and will cost well under \$10 per wheel by 2009.

After TPMS the biggest market is for **manifold and barometric air pressure measurement** sensors with \$175 million, followed by a vast array of under-the-bonnet sensor measurements like variable transmission oil and power steering applications, or high-pressure fuel injection systems, in coolants, braking, and so forth, together worth \$157 million. **Oil pressure sensors** can be either ceramic capacitive, silicon strain gauges bonded and fused to membranes, or piezoresistive silicon chips in silicone oil-filled reservoirs capped by stainless steel diaphragms. Oil pressure sensors increasingly use MEMS to determine condition as well as level.

	2004			2009		
	ASP [\$]	Units [millions]	Turnover [\$ millions]	ASP [\$]	Units [millions]	Turnover [\$ millions]
<i>MAP, BAP (air intake)</i>	4.20	36.00	151.20	3.50	50.00	175.00
<i>Fuel tank vapour pressure</i>	5.00	15.00	75.00	4.00	16.00	64.00
<i>Tire pressure monitoring sensor (in package, + ASIC)</i>	2.45	12.00	29.40	2.30	90.00	207.00
<i>Side airbag and passenger occupation detection</i>	3.50	13.00	45.50	2.50	30.00	75.00
<i>Other, e.g. oil, transmission, diesel particle, EGR, brake, coolant, HVAC compressor</i>	6.60	16.20	106.92	4.90	32.00	156.80
Total		92.20	408.02		218.00	677.80

Tab. 2. Market breakout for MST pressure sensors 2004-2009

In the area of **side airbags**, the much smaller crumple zone in car doors requires side impact sensors that operate up to 250 g with fast reaction time

(few milliseconds). It is worth noting that MST-based pressure sensors are considered as alternatives to accelerometers for use in side impact detection systems, e.g. from companies like Infineon. Fuel tank vapour detectors are mandatory for US markets but represent a saturated market opportunity.

The major manufacturers of pressure sensors include Bosch, Freescale (with foundry partner Dalsa), Denso, Melexis, Silicon Microstructures, Inc., Measurement Specialties, Inc. (e.g. crash test accelerometers), GE Nova Sensor, and XFAB. VTI planned to introduce pressure sensors in 2005.

TPMS system suppliers include Schröder with GE Novasensor's piezo-resistive pressure sensor, Siemens VDO, Infineon / SensoNor, Freescale, Philips (module only) and Bosch, which expects to be on the market in 1-2 years with its solution. Many others are in development.

A recent development is the gradual displacement of bulk micromachining by surface micromachining. For example, Bosch recently supplanted its previous approach – a silicon chip bonded to a glass socket using anodic wafer bonding – by a surface micromachining approach using porous silicon and processing steps designed to form a stable cavity. The method lower costs and is designed for applications of 10s of bar (metal is used above 100 bar).

Future developments will include additional demand for high-pressure sensors, such as required for common rail injection systems and cylinder pressure sensors (one per cylinder). The latter will be required for direct pressure determination inside the combustion chamber, starting with diesel engines. Lower emissions and improved fuel economy are expected to justify the high cost. Although the extreme pressure rules out silicon, future in-cylinder sensors may alleviate the need for MAP and air intake mass flow devices altogether.

Inertial Sensors

Inertial sensors comprise gyroscopes for yaw rate sensing, acceleration detectors and inclination sensors. Key requirements for the main applications comprise:

- ▶ **Vehicle dynamics (ESP)** – a yaw rate sensor, typically with a resolution of 0.1°/s, incorporated to mitigate under- and over-steering, and including 1 or sometimes 2 (up to 2 g) single-axis accelerometer(s) with high offset stability (100 mg) measure the lateral slip.
- ▶ **Roll detection** – devices with a resolution of 1°/s to trigger curtain air bags and to pre-tension seat belts in the event of rollover, with an accelerometer.

- **Navigation** – dead reckon assistance with a rate grade resolution of $0.5^\circ/\text{s}$ to assist and improve the accuracy of Global Positioning System, sometimes with an accelerometer, but mostly a gyroscope.
- **Tilt sensors (inclinometers)** - automatic handbrake, sensitive alarm systems, etc.

The total automotive inertial sensor market will grow from \$676 million in 2004 to \$854 million in 2009 (see Table 3). MEMS gyroscopes for ESP and accelerometers designed to trigger the inflation of airbags represent the largest market opportunities. However, while the number of airbags per vehicle is increasing, this is not necessarily reflected in the number of sensors, and this market will progress modestly in the next few years. ESP systems containing a 1-axis gyro and acceleration sensor will show healthy growth from \$280 million to \$382 million in five years (CAGR of over 6%).

<i>Accelerometers</i>	\$	Units (M)	Turnover (\$M)	\$	Units (M)	Turnover (\$M)
<i>Airbag (mostly 1 axis sensor)</i>	1.75	120.00	210.00	1.50	155.00	232.50
<i>Vehicle Dynamics (mostly 1 axis)</i>	5.00	11.20	56.00	3.50	19.10	66.85
<i>Tire pressure monitoring sensor*</i>	2.50	9.60	24.00	0.00	0.00	0.00
<i>Roll detection (1 axis sensor), GPS navigation assist (2/3 axis sensor)</i>	5.00	6.50	32.50	3.50	10.50	36.75
<i>Active suspension (1 axis)**</i>	15.00	0.10	1.50	15.00	0.15	2.25
<i>Gyroscopes</i>						
<i>Vehicle Dynamics (mostly 1 axis)</i>	20.00	11.20	224.00	16.50	19.10	315.15
<i>Roll detection (1 axis sensor)</i>	13.00	5.00	65.00	9.00	9.00	81.00
<i>GPS navigation assist (1 axis sensor)</i>	11.50	5.50	63.25	8.00	15.00	120.00
<i>Total</i>		169.10	676.25		227.85	854.50

Tab. 3. Market breakout MEMS inertial sensors in automotive applications 2004-2009. *Accelerometers need power and are expected to be replaced in more advanced TPMS solutions. ** Highest end vehicles only.

Gyroscopes

The biggest market for gyros is **vehicle dynamics** (so-called ESP systems) with \$315 million expected in 2009. Bosch introduced the ESP system in 1995 and has since produced 15 million systems [2]. It leads the market and shipped 4 million units in 2004, followed by BEI and Silicon Sensing Systems. ESP systems are produced in multi-million unit volumes for integrators like Robert Bosch, TRW Automotive and Continental Teves (using BEI's gyro).

A gyroscope module in an ESP system is estimated to comprise around 10-20% of the total system cost of \$500-\$600, which typically includes an MST yaw

rate sensor, accelerometer, wheel position sensors, steering wheel sensor, pressure sensors, control unit, and hydraulic modulator. Depending on how the gyro is supplied and the technology, prices range from \$15-75. The average selling price for an automotive gyro (sensing element, ASIC in a wafer level 1 package) is estimated to be \$20. The price will erode to around \$17 or less in 2009.

The gyro in a **roll detection system** does not require the same resolution as yaw sensors for vehicle dynamics because roll rates are around five times larger, although a key requirement is excellent resistance to external shock and vibration. Prices average \$13 for the gyroscope.

Navigation systems rely on the use of a compass, databases and a GPS system. When the system is started and the initial direction is established, inertial data supplied by a gyroscope is used to determine when and how much the car has turned, until the direction can be verified and updated via map matching and GPS signals. There is strong interest in GPS navigation systems in Japan, where 2.9 million units – roughly 2/3 of all new vehicles - will be fitted with these systems in 2006 [3]. Prices are generally lower, on average \$11-12 for a gyroscope in a navigation unit, because such sensors are non-safety critical.

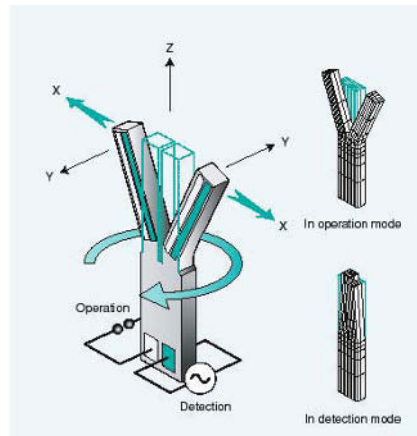


Fig. 3. Composite lithium niobate / ceramic "H" tuning fork gyro element for use in navigation and other applications (Courtesy of Fujitsu).

In terms of operation, gyros determine yaw rate (angular rotation) from the Coriolis force, and different manufacturers use different sensing principles. The established manufacturers of gyros are Bosch using either bulk or surface silicon micromachining to make capacitive measurements of a tethered proof

mass, BEI Systron Donner (now Schneider Electric) using piezoelectric actuation and sensing in a quartz tuning fork design, Silicon Sensing Systems (Sumitomo/BAE joint venture) with a magnetic solution and Analog Devices with a silicon capacitive MEMS design.

Fujitsu (see Fig. 3), Seiko Epson, Murata, Matsushita, Sony, NEC Tokin and Micro Components (owned by Swatch) are examples of other companies producing gyros, particularly for navigation. Piezoelectric materials like quartz, lithium niobate or silicon micromachined approaches are popular. OKI expects to introduce its gyro by the end of 2006. Gyros are also under development at companies looking to break the \$10 barrier, such as InvenSense, Samsung, and Fraunhofer-IST (marketed by Sensor Dynamics).

One of the expected trends over the next few years is a consolidation of increasing numbers of sensors into multifunctional modules, i.e. clustering of inertial sensors to collect information on yaw rate, roll, and for navigation dead-reckon assistance. For example, BEI Technologies (part of Schneider Electric) has developed a four-degree of freedom module with two gyros and two accelerometers.

Accelerometers

Accelerometers are used for high g (airbag) and low g (vehicle dynamics, roll detect) applications and typically employ silicon micromachining and capacitive sensing. Airbags will remain the main market for accelerometers (\$232 million in 2009), where devices will cost about \$1.50 (wafer level packaged). Major manufacturers for high g airbag sensors include Analog Devices, Freescale and Denso. VTI and Bosch supply low g sensors, which cost more than sensors for airbags (currently \$5, dropping to \$3.50 in 2009). Inclinoimeters used in tilt measurements are mostly accelerometers operating under conditions of static acceleration (Analog Devices, VTI).

Accelerometers are also used in GPS navigation systems such as Hertz's "Never Lost" system, although gyros will prevail for navigation. Tire pressure monitoring systems (TPMS) currently feature accelerometers (to inform the RF transmitter to signal the tire's pressure only when in motion to save battery power) but these will vanish from most systems by 2009 as more intelligent low-power solutions are sought.

Other potential replacement scenarios include body sound ultrasonic sensors to replace high-g accelerometers to determine and react appropriately to different kinds of crash. Siemens VDO is developing "Crash Impact Sound

Sensing”, intended for introduction in 2007, where supplementary information may be fed to safety systems using camera or radar configurations.

4 Conclusion

The market for automotive MST sensors looks bright over the next five years with growing sales for sensors that increase efficiency, reduce pollution, improve ride safety and provide additional protection in a crash situation. New types of sensor will gradually enter the market and enable automotive manufacturers to continually differentiate their product aided by sophisticated low-cost MST solutions.

5 Acknowledgements

WTC would like to acknowledge the support of NEXUS in the preparation of the data used in this article.

References

- [1] Sensoren im Automobile, Sensor Magazin 2, 2005, page 7.
- [2] Bosch reaches 10-year production milestone for electronic stability control, The Auto Channel, February 10, 2005.
- [3] Asian Telematics and navigation markets, SRD Japan, Inc, May 2004.

Dr Richard Dixon, Mr. Jérémie Bouchaud

WTC- Wicht Technologie Consulting
 Frauenplatz 5, 80331 Munich
 Germany
richard.dixon@wtc-consult.de
jeremie.bouchaud@wtc-consult.de

Keywords: inertial sensors, automotive markets, gyroscope, accelerometer, pressure sensor, MST sensors, flow sensor, inclinometer

Future Architecture for Inertial Sensors in Cars

J.C. Eloy, M. Potin, Dr. E. Mounier, Dr. P. Roussel, Yole Développement

Abstract

In the analysis of the automotive MEMS inertial market, Yole found that on the 2005-2010 period the accelerometer automotive market would have a 2% CAGR starting from 286 M\$ to 321M\$. Gyroscopes are making good promise on these same period, with a 11% CAGR expectation to reach 598M\$ in 2010. This year already the gyroscope market overcomes the accelerometer one on a market valued at 355M\$.

Two major trends that will modify the future architecture for inertia sensors are discussed in this article: the crash impact sound sensor technology is subject to change the airbag sensor market whereas the trends for integration will lead the path to future automotive IMUs.

1 Automotive Gyros are likely to generate 600M\$ Value in 2010

Gyroscope applications are today mainly divided in between consumer and automotive applications. Automotive represent today 80% of total production of gyroscopes with a 22M units market this year. Gyroscopes based automotive applications shows a high potential and dynamism

Tab. 1 describes the gyroscope automotive market on the 2005 – 2010 period.

Yole's market forecast shows that in 2010 automotive gyroscope will still account for 84% of the value generated by total MEMS angular rate production components. It is estimated that the automotive gyroscope market CAGR will range from 8% to 30%.

Three automotive applications are included in our analysis:

- ▶ Anti rollover applications
- ▶ Electronic Stability Control
- ▶ GPS Navigation

The main characteristic of the automotive field is that it requires low cost chips. The gyros' ASP is in the range \$10 to \$22, which is still considered as a high price for automotive components, thus putting a strong pressure on components manufacturers. We estimate that 54 million of gyros will be necessary in 2010 for automotive uses.

	2005			2010		
	Million units	ASP (\$)	Market (M\$)	Million units	ASP (\$)	Market (M\$)
<i>Roll over (per axis)</i>	2,5	10,0	25,0	13	7,2	93,7
<i>ESP gyroscope (per axis)</i>	12	22,0	264,0	25	15,9	396,6
<i>GPS localisation (per axis)</i>	7,5	9,0	67,5	16	6,8	107,2
<i>Other consumer applications</i>	5		41,0	27		117,0
<i>Total gyroscope market</i>	27		398	80		714

Tab. 1. Markets for MEMS-based gyroscope 2005-2010. "Others" applications include image stabilization for camcorders, cameras, and mobile phones.

Stability control and other chassis technologies are a very interesting application. This market is truly not the one with the strongest growth expected (8% CAGR from 2005 to 2010) but for sure the largest: Stability control will still counts for more than 50% of the total gyroscope market in 2010.

ESC is not a new application and in Europe it stands at a relative mature stage. Its growth dynamisms mainly comes from North America. Europe is still ahead with an average 40% market penetration against 26% in USA in 2005. But we figure out that in one year an average 4% were won on the electronics stability control equipment rate in USA. These good results are bounds to the promotion it benefited from:

- Surveys showed that SUV are more subject to loose steering control in difficult condition
- OEM (Original Equipment Manufacturers) are directly promoting their systems to the customer

Anti-rollover systems are likely to benefit as well from these actions. Some gyro manufacturers are event expecting a NHTSA regulation to even push ahead the pass to full safety equipments features for high centre of gravity cars.

The performance requirement of chassis control application increase complexity and competition among players. Few degrees per second bias stability is required, depending of the OEM electronics. This is a strong goal to achieve for manufacturers. But the 22\$ ASP (in 2005) makes it an attractive application. We estimate that nearly 90% of the components are supplied by only three main challengers in 2005: BEI Technologies, BOSCH and Panasonic. We expect an aggressive competition of new entrant in the 2006-2008 periods.

Gyroscope Manufacturer Market Share on ESC application in 2005

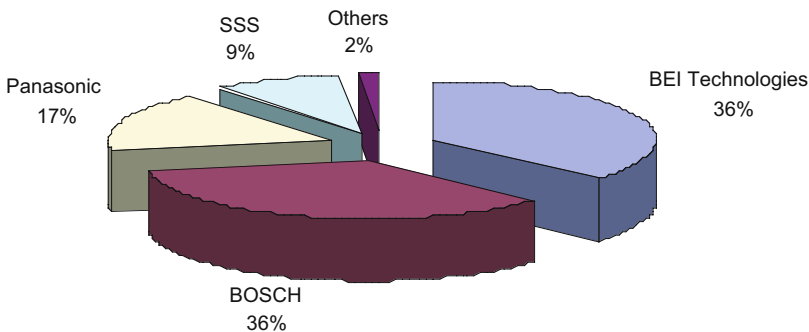


Fig. 1. Gyroscope Manufacturers' 2005 market share on ESC application

The year 2008 will be of high interest for the industry. More than 10 players would likely offer gyroscopes for stability control and the specific agreement between Continental and BEI will end. Only few gyro suppliers will last on this application, time will see...

2 Accelerometers for Automotive Applications: a 320M\$ Industry in 2010

Acceleration sensors in the automotive industry have been widely used since more than 30 years : motion sensing was key in order to be able to assure safety functions. But the real development of the market has started in 1988 when an un-known Norwegian company named Sensoror has realised on the market the first silicon accelerometer able to detect accurately chocks for airbag applications.

This first application has been really booming during 15 years, with now a clear saturation of the market and with key changes we will highlight in this article. But during that time, several other applications have emerged. The following list provides today applications of MEMS accelerometers in the car industry.

- ▶ Airbag sensors : detection of front, back and side shock
- ▶ Active suspension : adaptation of the suspension to road condition and speed
- ▶ Electronic stability program : system able to control the relative position of the car compared to the road and adjust it in order to be stay in safety conditions
- ▶ Safety testing: off road applications, use of accelerometers during crash test in order to monitor the acceleration in different points of the car and at passengers.

Tab.2 presents the status of the different applications:

	<i>Mature applications</i>	<i>Growing applications</i>	<i>Emerging applications</i>
<i>Accelerometers</i>	Airbag, safety testing	Active suspension, Electronic stability program (ESP)	No new applications are seen at the moment. GPS is using some times accelerometers instead of gyroscopes.

Tab. 2. Status of the different automotive applications

The total accelerometer market value (see Tab. 3) has been estimated to be \$355 million in 2005 and \$614 million in 2010 for a production of 150M and 260M units respectively. We estimate that the automotive field accounts for 89% of the total volumes which generate 81% of the global market value. 140 million of accelerometers will be necessary in 2006 for the automotive field only.

The major trends that is likely to change the accelerometer business today is a technology shift in airbag sensors applications. Siemens VDO soon released its Crash Impact Sound Sensing (CISS) sensor in which a MEMS microphone will act as a replacement sensor for several accelerometers.

The sound caused by the car's body panels/structure as they deform under impact is used to recognize the severity of the accident. The fact that minor collisions and serious collisions have the same rate of deceleration makes it dif-

difficult to adapt an airbag system to different crash scenarios. The CISS sensor offers strong benefits:

- ▶ Airbag deployment can take place up to 15 milliseconds earlier than with conventional systems
- ▶ Directly integrated into the ECU, it might be able sense omni-directional impacts, thus eliminating the needs for satellite airbag accelerometers. g crash sensors integrated into the ECU would still be required for cross-checking features.

	2005			2010		
	Million units	ASP (\$)	Market (M\$)	Million units	ASP (\$)	Market (M\$)
<i>Airbag sensor (per axis)</i>	120	1,6	192	143	1,3	182
<i>Active suspension (per axis)</i>	1,0	9,0	9,0	1,80	7,4	13,3
<i>ESP acceleration sensor (per axis)</i>	12,0	7,0	84	24,9	5,0	125
<i>Safety related testing (per axis)</i>	0,012	100,0	1,2	0,018	85,4	1,5
<i>Other consumer and medical applications</i>	17,20		68	90,435		292
<i>Total accelerometer market</i>	150		355	260		614

Tab. 3. Markets for MEMS based accelerometers 2005-2010. "Others" applications include oil exploration, pedometers, HDD free fall detection, auto key-stoning for projections, mobile phone, toys and human-computer interface.

We believe that if this technology is adopted, it would strongly impact accelerometers shipments for airbag applications. Its first implementation on the Audi A8 2007 model will say if MEMS microphone technology can enter the automotive field.

3 A Path through the Automotive Inertial Measurement Unit?

Several trends are today very important in the automotive business and are impacting very heavily the MEMS business. We will review it in the next paragraphs.

One sensor for several systems or one system with its own sensor ?

More and more car manufacturers are pushing the system manufacturers to share sensor data between systems in order to save money and complexity in the cabling and system architecture.

One of the key trends is to have a central inertial measurement unit (IMU) able to deliver acceleration sensing (3 axis) and gyro movement (3 axis) to all the car systems. Several companies like Systron Donner (USA), Bosch (D), Honeywell (D), Invensense (USA) ... have or will have devices available very soon of automotive IMU.

The road is long to replace all accelerometers and gyroscopes in a car by a central IMU but the trend is there. Only few companies have the access to the right devices, electronics and software to be able to deliver a good and cost effective IMU (this is mainly the companies mentioned, Systron Donner, Bosch, Honeywell and Invensense).

Sensor redundancy?

For several key safety applications like airbag and ESP, the car manufacturers are willing to have redundancy for sensors which are key for the safety system, for example for the yaw rate for ESP and the side crash sensor for airbag. This trend is becoming very important and also could impact the market on the right way : more sensors will be needed, generating more business for all the sensor manufacturers.

Sensor flexibility?

ECUs have often different location and positions into each car model. This a great challenge for OEMs who need to customise systems. As an example, an ECU dedicated to stability control and anti-rollover systems needs 250°/s roll rate sensitivity whereas stability control yaw sensitivity is 75°/s.

We identified two ways components manufacturers will solve this issues: to develop a specific packaging so that one sensor can be soldered on different positions, or ultimately having an 6DOF ECU in which components sensitivity and characteristics could be adapted upon the ECU position.

These three trends are key opposite in their impact on the acceleration sensor market for automotive applications: we have tried to take into account these

different trends in our market forecasts but the next months and years will be very important for the development of acceleration sensing in the automotive industry. These applications are key for all the players.

4 Conclusions

The MEMS inertial sensor markets are widely dominated by automotive applications for the years to come and the new applications (both low-end and high-end) are driven by the availability of adapted-cost devices with right specifications. 2008 year will be a key date for the MEMS inertial industry where both gyroscope and accelerometer based applications will be challenged.

J.C. Eloy, M. Potin, Dr. E. Mounier, Dr. P. Roussel

Yole Développement
45, rue Sainte Geneviève
69006 Lyon
France
potin@yole.fr

Keywords: inertial sensor, accelerometer, gyroscope, market forecast, IMU, microphone

Three-Dimensional CMOS Image Sensor for Pedestrian Protection and Collision Mitigation

P. Mengel, L. Listl, B. König, C. Toepfer, M. Pellkofer, Siemens AG
W. Brockherde, B. Hosticka, O. Elkhaili, O. Schrey, W. Ulfig, Fraunhofer IMS

Abstract

Future car safety systems increasingly depend on the availability of robust sensors with vital improved technical perception output. For this objective, we develop a pulsed laser based time of flight range sensor in fully solid-state microsystems technology for more reliable detection and classification of road users, vehicles and traffic obstacles. The development aims on pedestrian protection and mitigation of collisions comprising the short distance around vehicle perception up to 25 m. The 3D sensor technology based on a chip design of 64x8 pixels and image repetition rates of up to 100 Hz will be presented and the performance of a first 3D line sensor prototype will be demonstrated for typical road test scenarios. Furthermore, an outlook on the final 3D array camera development for road safety applications will be given.

1 Introduction

Advanced car safety systems and sensor employment aim to reduce the numbers of road fatalities drastically by providing total awareness to the drivers in and around the car and to warn or even actively assist or intervene in situations of imminent danger. However, currently available sensors employed for the dynamic surveillance of the vehicle environment provide neither the degree of reliability and robustness, nor the overall availability of the perceptual output that would be required for safety critical applications. Radar and lidar sensors, for instance, yield excellent distance and velocity measurement precision, but virtually no lateral resolution. Video cameras feature excellent lateral resolution, but the state-of-the-art computer vision processes required for scene interpretation are often insufficient to identify all the relevant objects depending on contrast variations and environmental illumination conditions. Laser scanners exhibit much better lateral resolution as compared to radar sensors, but they come with comparatively slow scanning repetition rates, considerable physical size and comparatively high production costs.

In contrast to these drawbacks of the state of the art sensors, the novel pulse-operated time of flight (TOF) range sensor approach features detailed distance information with lateral resolution at an image repetition rate of up to 100 Hz.

The benefits for industrial employment comprise:

- ▶ Laser Pulse Based Parallel Time of Flight Method
- ▶ Combination of Precise Range Data with Lateral Resolution (φ, θ)
- ▶ Full Solid State Approach (Standard CMOS), No Mechanical Parts
- ▶ Low Cost, No Maintenance
- ▶ Robust with respect to
 - ▷ Object Surface Reflectivity
 - ▷ Background Illumination (i.e. Sun Light)

In this paper the principles of the sensor technology and the achieved technical data will be demonstrated. Further, the results of comprehensive evaluation in typical traffic test scenarios will be illustrated and discussed with relevance to the advantages of machine based 3D perception for semi-autonomous braking situations.

Essential features concern:

- ▶ Faster detection of collision partners
- ▶ Pre-conditioning of the brake in danger situations
- ▶ Application of full braking pressure in emergency situations
- ▶ Short delay, high confidence and high repetition rate of perception

2 3D Sensor Technology

The three-dimensional CMOS image sensor is based on a laser pulse-operated time of flight method providing parallel distance information to every single sensor pixel. In comparison with time-of-flight (TOF) cameras based on the principle of CW modulated light emission the pulse-operated method represents a unique performance characteristic by featuring vast independence of background illumination since laser pulses can be made quite short but nevertheless keeping the amount of energy per pulse at a constant level. Consequently, the background irradiation level is irrelevant as compared to the much greater emitted light intensity. With continuously emitted light, this is not feasible and the range cameras based on the CW modulated principle suffer from notoriously poor signal-to-noise ratios as well as of insufficient suppression of background illumination.

2.1 TOF Measuring Principle

The sensor concept calculates the time of flight (TOF) indirect from the intensity measurement of single laser pulses in high-speed shutter windows. Several laser pulses are averaged on chip to reduce the required laser power and to increase the measurement accuracy [1, 2]. The approach is called MDSI (Multiple Double Short Time Integration) and will be illustrated by the figure below:

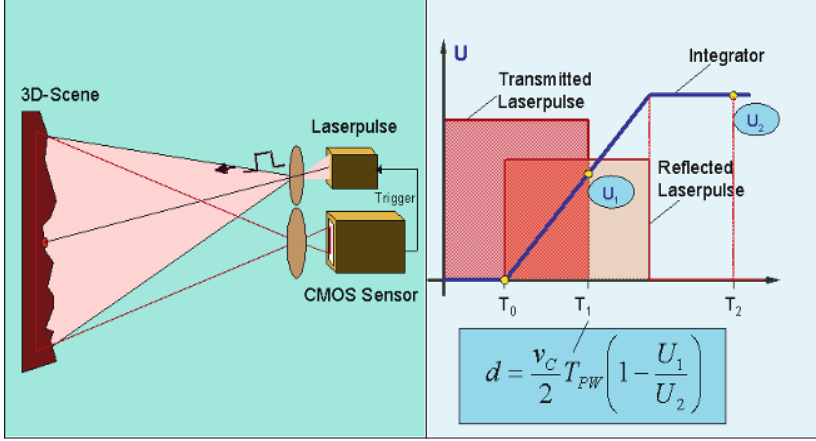


Fig. 1. MDSI (Multiple Double Short Time Integration) measurement principle

The transmitted light pulse synchronized with the start of the integration window always illuminates the complete 3D scene. The received pulses give rise to a linear sensor signal U after the light propagation time T_0 , which is measured at two integration times T_1 (short time shutter) and T_2 (long time shutter). While in the short time shutter only a certain fraction of the light pulse is detected depending on the distance of the object point, the long time shutter always receives the full reflected light intensity. By computing the quotient of the two integrated shutter intensities U_1 / U_2 an exact calculation of the propagation time T_0 and hence the distance d of each individual object point can be derived according to a simple mathematical relationship (see Fig. 1).

A unique feature of the MDSI method is the analogue real-time on-chip accumulation process and correlated double sampling procedure (CDS) at each individual sensor element using multiple pulses for each shutter window. The amount of received light reflected from an object not only depends on the emitted laser irradiance, the reflectance of the object and its distance, but also on the amount of background light due to effects of other present light sources,

i.e., sunlight. The influence of background light can be widely eliminated by measuring solely the background irradiance without laser pulse. Thus each measurement must be performed with laser pulse on and off and only the difference being stored on the corresponding capacitance in the analogue sensor memory. By this means the signal-to-noise ratio increases and leads to an improved distance accuracy. Repetitive integration of laser pulses will be performed adaptive up to the saturation level at each pixel element. Intelligent procedures can be employed to cover a large dynamic range of different surface reflectivity of targets with this adaptive flash illumination method.

2.2 Chip Design and Functionality

The 3D CMOS sensor chip contains a photodiode array and readout and control electronics. It employs the multiple double short-time integration (MDSI) principle mentioned above. This time-of-flight (TOF) approach ensures the best background light suppression, non-ambiguity, and, using the adaptive integration mode, a very high dynamic range. Adaptive integration means multiple non-destructive readout of the accumulated signal during integration of the reflected laser pulse train. The sensor allows on-chip analogue integration of more than 128 pulses.

<i>Parameter</i>	<i>Specification</i>
<i>Pixel count / size</i>	64x8=512 / 130μm x 300μm
<i>Pixel principle</i>	Photodiode with single buffer and CDS
<i>Noise equivalent power (30ns)</i>	1 W/m ² (Design goal)
<i>Minimum shutter width</i>	30 ns
<i>Dynamic input range</i>	54 dB + 21 dB (variable # of pulses)
<i>Image acquisition</i>	50...200 fps (1...128 pulses/frame)
<i>Readout scheme</i>	Non-destructive readout
<i>Background light suppression</i>	> 40 dB
<i>Operating wavelength</i>	850 nm...910 nm

Tab. 1. Sensor chip parameters

The most challenging sensor specifications are the optical dynamic input range (DR) and the noise performance (NEP). The DR is determined by the distance range and the reflectivity range (min/max). With a given optics, the received optical signal decreases with the square of the object distance. Thus, the required distance range of 2 m - 25 m and reflectivity range of 5% - 100% call for a minimum DR of 70 dB.

The number of photons reflected by the objects in the scene back into the sensor lens is quite low. Therefore, minimizing sensor noise is of prominent importance. Careful photodiode and readout electronics design and detailed noise analysis and optimization yielded a significant reduction in noise equivalent power, NEP. The key sensor specification data is summarized in the Tab. 1.

The sensor chip has been designed in the standard 0.5 μm CMOS process (1P3M) of Fraunhofer IMS with no process modifications. The mask layout of the CMOS sensor is shown in Fig. 2. The chip dimensions are 11 mm x 9 mm, and the photosensitive area in the centre measures 8.4 mm x 2.4 mm. The chip is mounted in a standard ceramic CQFJ84 package.

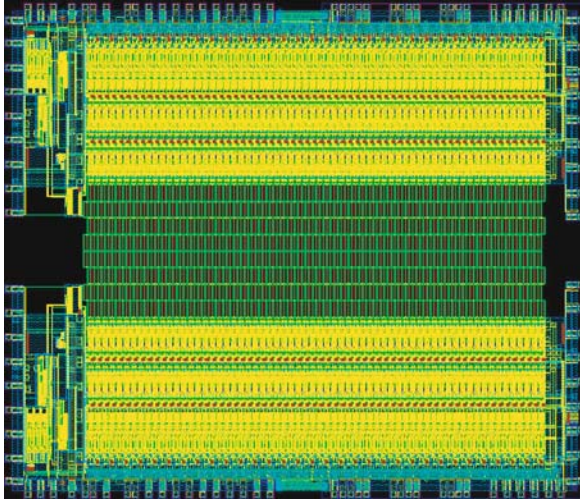


Fig. 2. Mask layout of 64x8 pixel CMOS TOF sensor chip

2.3 3D Test System

A first prototype system has been established for validation of the sensor concept in typical road safety related test scenarios. The prototype consists of an intermediate CMOS line sensor with 64 x 1 photosensitive elements, appropri-

ate designed electronics, optics and the laser pulse illumination. An image of the test system is shown in Fig. 3.

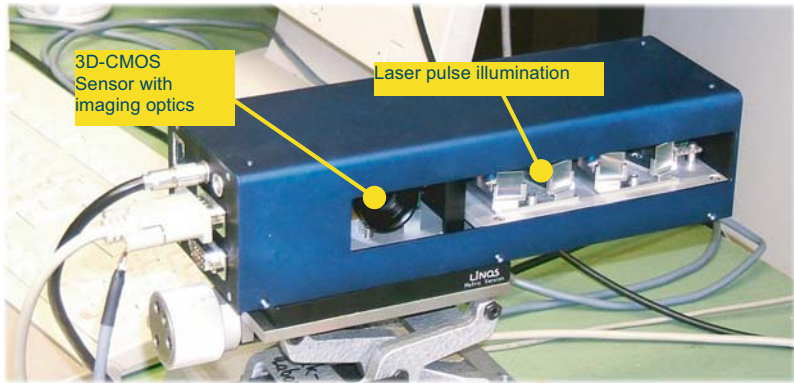


Fig. 3. Prototype test system

The design of the sensor electronics is based on a multi-board architecture to provide high flexibility for operation in different applications, Fig. 4. The main board contains the 3D-CMOS sensor, ADC-analogue-to-digital conversion and an integrated FPGA platform for sensor control, data acquisition and image processing, respectively. For noise optimization, special emphasis has been put to the placement of analogue and digital components and to the selection and design of voltage regulators. The interface board includes a 12 V power supply and various application interfaces as RS 232, TBase100 Ethernet and User I/O. The synchronisation to the laser source is realised by a trigger timing signal from the FPGA to the electronic driver circuit of the laser module.

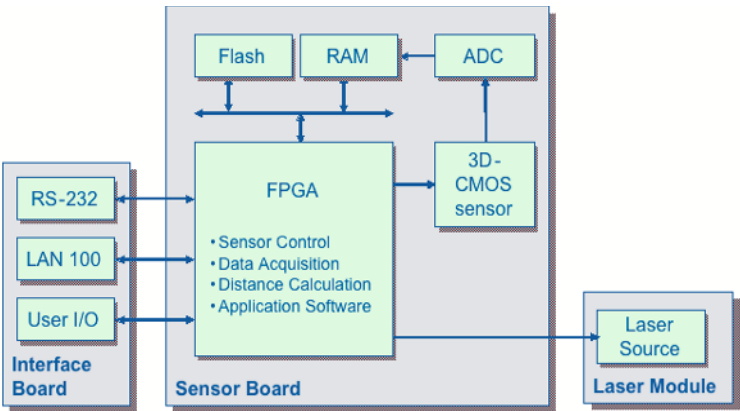


Fig. 4. Sensor system design

The laser modules with integrated driver electronics fulfil the high requirements on output power and variable pulse width with fast rise time. Thus, adjustable pulse widths between 100 ns and 300 ns with rise times of a few tens of ns can be reached with energy of 75 μ Ws at 10 kHz pulse repetition rate. Special beam forming optics has been constructed with custom designed cylindrical lens arrangements. According to the application requirements the illuminating laser light source can be formed with a homogeneous or anisotropic beam profile corresponding to the scene and the cameras field of view.

3 Road Safety Applications

The intended road safety applications and recognition tasks suitable for the 3D CMOS image sensor comprise:

- ▶ Near to intermediate front and side distance range of cars (20 m - 25 m)
- ▶ Lateral proximity of trucks (blind spot surveillance)
- ▶ 3D-algorithms for object (obstacles, pedestrian) detection and classification independently of surface reflectivity and ambient illumination conditions
- ▶ Performance investigations with car/truck demonstrators on typical traffic scenarios and obstacle occurrence

The application specific requirements for the 3D camera system have been analysed considering various traffic scenarios and relevant accident statistics [3]. From these investigations the essential consideration of pedestrian protection and collision mitigation will be demonstrated in the following chapters.

3.1 Accident Analysis between Passenger Cars and Pedestrians

Most front-end collisions with pedestrians occur in urban traffic situations. Therefore, the speed of the involved vehicles is typically 50 km/h or less. Walking pedestrians reach a characteristic speed of up to 6 km/h. It is assumed that approximately 0.5 seconds will be needed to detect a pedestrian in front of the vehicle and an additional 0.5 seconds for preconditioning of the brakes to achieve full braking performance. The required observation range of the 3D camera is shown in Fig. 5.

Pedestrians outside the blue lines are not at risk of a collision with the vehicle. A vehicle travelling with 50 km/h has a stopping distance of about 23.5 meters and therefore requires a longitudinal measurement range of 25.5 meters. A

pedestrian can walk about 3.6 meters within the stopping time of the vehicle and therefore requires a lateral measurement range of 4.5 meters. For lower vehicle speeds the stopping time and distance becomes smaller and also the walking distance of the pedestrian becomes smaller. Therefore, the required measurement range of the camera is much smaller for lower speeds but the required aperture angle becomes larger because of the smaller relative speed between vehicle and crossing pedestrian.

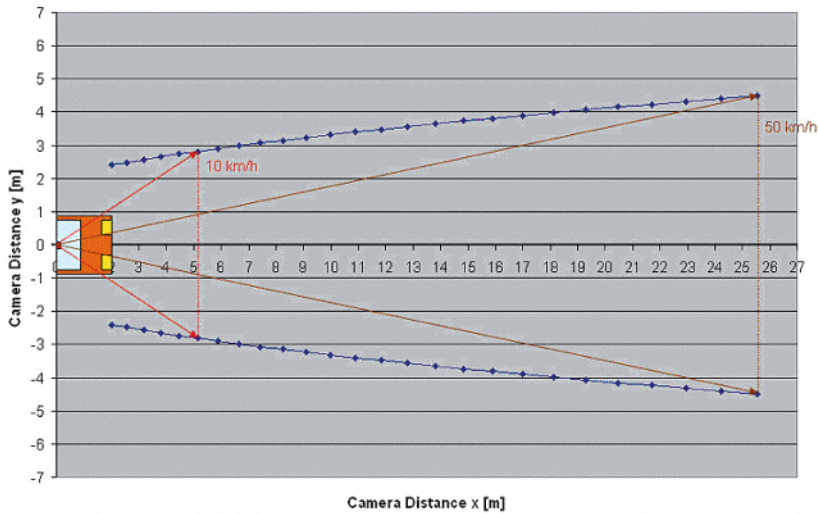


Fig. 5. Required observation range of the 3D camera

The relationship between the required measurement range and the measurement direction is shown in Fig. 6. For a vehicle speed of 50 km/h, the required measurement distance range is up to 26 meters at an aperture angle of up to 10°. For lower speeds the required measurement range becomes smaller but the aperture angle increases. For a vehicle speed of 10 km/h the required measurement distance range is up to 6 meters at an aperture angle of up to ±30°.

From the considerations regarding the front-end collisions with crossing pedestrians we can derive the following requirements for the 3D camera measurement range:

- Minimum distance: 2 m (vehicle front end)
- Maximum distance: 26 m for $\alpha = \pm 10^\circ$ ($v = 50$ km/h)
- 6 m for $\alpha = \pm 30^\circ$ ($v = 10$ km/h)

This allows the design of an optimised beam shape for the active laser illumination of the 3D camera.

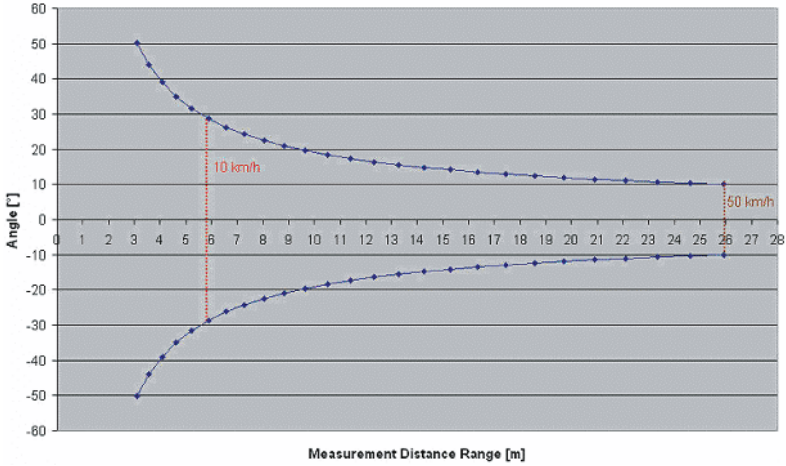


Fig. 6. Required measurement distance range characteristics

3.2 Front- to rear-end Collision caused by Passenger Vehicles

Like with accidents between cars and pedestrians, the geometry of the perception field required for the mitigation of front- to rear-end collisions between vehicles is characterised by a comparatively narrow strip parallel to the axis of the trailing vehicle. As with car-pedestrian encounters, a comparatively short distance range of a few meters is sufficient at an aperture angle of 30 degrees, while the maximum distance range is required at the central lines of sight close to the vehicle axis. This anisotropy can be used again to redistribute the emitted laser power accordingly, thereby gaining distance precision and/or distance range in the central field of view. Concerning the kinematics of the rear-end crash scenarios, one has to consider the distance, the relative velocity and the relative acceleration of the potential collision partners. Collision avoidance thus requires appropriate time to collision estimates, which in turn are based on appropriate measurements of the relative speed and deceleration. With a relative precision of distance measurements of 20 cm or less and a measurement repetition rate of 50 to 100 Hz, the 3D camera is in a good position to satisfy these essential features under the assumption of constant deceleration conditions. If this is not the case, the forecast of the time-to-collision and/or of the crash velocities becomes difficult to predict at any rate.

It can be shown that a machine-based accident avoidance / accident mitigation system can clearly outperform the average human driver. This is so, despite of the fact that the system is based on a perception device of some limited distance range of only about 20 m to 30 m. The outstanding performance of the mitigation system as compared to human drivers is rather based on the advantages of:

- ▶ Some best possible system response / delay times of only 0.5 s or less,
- ▶ The employment of maximum deceleration value of up to 10m/s^2 and
- ▶ A perception device that produces virtually no false alarms.

The 3D range camera appears to be a superior candidate for the type of accident mitigation perception device proposed in this section.

4 Car Evaluation Results

The 3D test sensor system has been integrated in an experimental car for evaluation on road safety related test scenarios.

4.1 Technical Data

The performance data are summarized in Tab. 2.

<i>Parameter</i>	<i>Value</i>
<i>Pixels:</i>	64 x 1
<i>Pixel size:</i>	$(130 \times 600) \mu\text{m}^2$
<i>Laser pulse energy:</i>	75 μWs / 150 μWs
<i>Pulse width:</i>	300 ns
<i>Pulse frequency:</i>	5 kHz
<i>Opening angle:</i>	36° / 60°
<i>Frame rate:</i>	theoretically, 25 fps @ 100 integrations (not reached due to data transfer and computing time of Matlab application)

Tab. 2. Performance data of the test sensor system

A typical distance calibration curve is represented in Fig. 7 for a target with 5% reflectivity (black velvet). Averaging over 10 single measurements is applied to lower the noise of the measured distance. The system was equipped

with an anisotropic illumination unit with pulse energy of 150 μ Ws per pulse and optics with 36° mm opening angle.

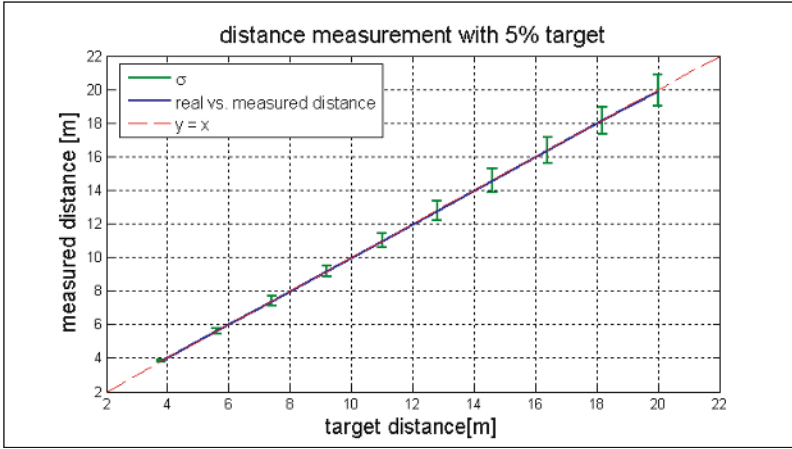


Fig. 7. Measuring accuracy

As can be seen from the measurements the sensor system provides high linearity between measured and real distance over the entire measurement range. The measuring accuracy, i.e. the standard deviation of the measurement results for one point on the curve, result in 5% of distance reading.

4.2 Road Safety related Test Scenarios

Different test scenarios were evaluated in order to investigate the ability of the test sensor to fulfil the requirements of the above mentioned road safety application. See Tab. 3 for an overview over the test scenarios and the particular conditions. For all following measurements, imaging optics with 8 mm focal length, resulting in an opening angle of about 60°, was used.

Test Scenario Situations						
	Scenario	Target	Laser	Theoretical image repetition rate	Target Distance	Example Picture
A	Frontal view from car	Vehicles	$E=75\mu\text{Ws}$ isotropic illumination	4 fps	5 m / 11 m	
B	Frontal view from car	Pedestrian	$E=150\mu\text{Ws}$ anisotropic illumination	6 fps	16 m	
					12 m	
					8m	
C	Blind spot surveillance for a truck	Pedestrian	$E=150\mu\text{Ws}$ anisotropic illumination	16 fps	< 2m	

Tab. 3. Test scenario descriptions

4.2.1 Scenario A: Vehicle Detection

In the test scenario, both cars (Renault and Mercedes) are visible to the test camera. The left figure shows the traffic scene taken with a photograph, the right figure shows the sensor response (shutter 1 in red, shutter 2 in yellow) and the estimated range data (in blue). The estimated range of 11 m and 5 m complies well with the actual situation. In the gap between both cars the reflected signal drops below the noise threshold, and thus yields no usable range data. This is probably due to the inclined lateral surface of the Mercedes. The metallic varnish has non-lambertian reflection properties. The depth pro-

file of the cars themselves is given by pixels 38 to 42 for the Mercedes and pixels 48 to 56 for the Renault. However, the depth variations in these regions are strongly influenced by (partly systematic) depth noise of about 0.3 m. But even though the individual obstacles have this noisy depth profile, the overall situation is well observable in the range data.

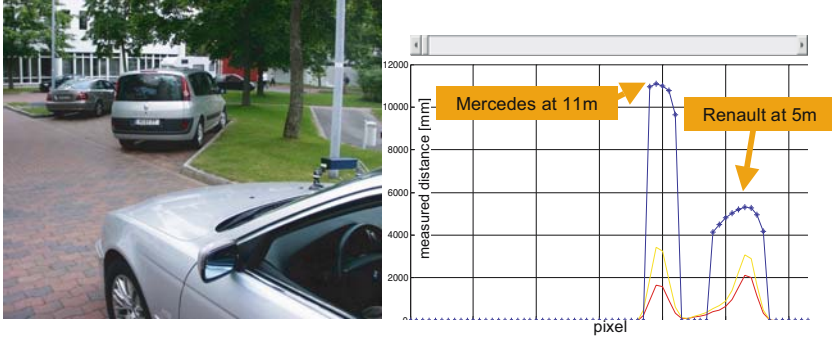


Fig. 8. Two cars in front

4.2.2 Scenario B: Pedestrian Detection

This scenario (Fig. 9) shows a pedestrian walking towards the car. For a distance of 18 m the sensor response (red and yellow line) is quite low, but though an accurate distance measurement is performed. The width of the pedestrian in the range image is only three pixels. At 12 m the distance measurement is still very accurate, the width of the person increased to 5 pixels. At a distance of 8 m one observes a margin effect: the pixel at the right boundary of the pedestrian only gets a partial reflection, thus the estimated depth is too high. Nevertheless, for the other pixel also here the measured distance fits well with the real distance. Thus it can be seen that the sensor provides good measuring linearity over the whole distance range.

4.2.3 Scenario C: Blind Spot Surveillance

This scenario (Fig. 10) shows a pedestrian walking towards the car. For a distance of 18 m the sensor response (red and yellow line) is quite low, but though an accurate distance measurement is performed. The width of the pedestrian in the range image is only three pixels. At 12 m the distance measurement is still very accurate, the width of the person increased to 5 pixels. At a distance of 8 m one observes a margin effect: the pixel at the right boundary of the

pedestrian only gets a partial reflection, thus the estimated depth is too high. Nevertheless, for the other pixel also here the measured distance fits well with the real distance. Thus it can be seen that the sensor provides good measuring linearity over the whole distance range.



Fig. 9. Sequence of pedestrian approaching the test car

Many severe road accidents at crossings, junctions or roundabouts are caused by truck drivers who are unaware that other road users are very close to, or beside their vehicles. This is illustrated in the above scenario where a child is crossing the street directly in front of the truck. As seen from the overlaid 3D-profile the safety of vulnerable road users can be improved considerably in such situations with direct 3D distance measurements.

Depending on the mounting position, of the sensor blind spot detection requires an opening angle of the sensor from 60° to 90°.

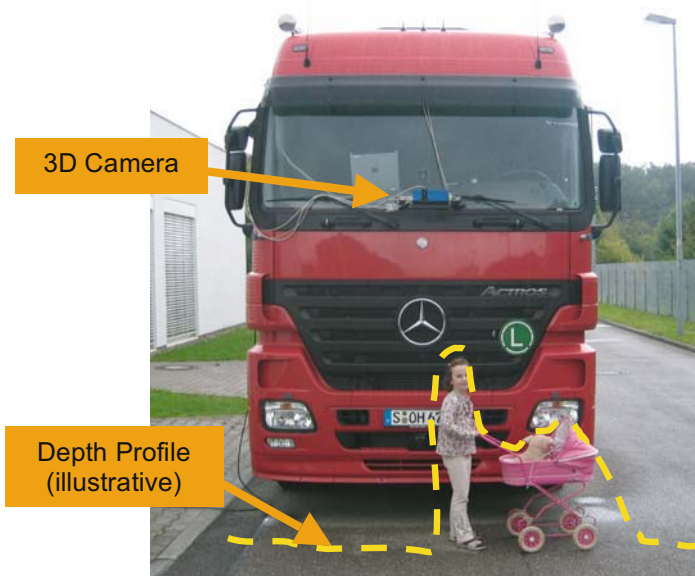


Fig 10. Blind spot surveillance

4.3 Conclusion

The current development platform shows the ability of the test camera to resolve the car proximity at distances of up to about 20 m. The sensor performance was successfully investigated in different test scenarios, including moving objects.

However, several areas have been identified that call for enhancement:

- ▶ **Vertical Range:** Currently, only a single line of the camera is functional. This limits the vertical field of view to about 2° . Thus, if the car approaches an object of small vertical size, it can disappear in the range data. The 64×8 – sensor (cf. 2.2) is necessary to overcome this problem.
- ▶ **Frame rate:** The current restrictions in illumination, sensitivity, serial communication and visualisation limit the frame rate to about 5 fps. Enhancements in all of these areas must strive for a frame rate of at least 50 fps to allow a reliable tracking of traffic objects.
- ▶ **IR transparent windows:** The car tests showed that the thermal insulation of the windscreen blocks the IR laser illumination. Thus the test car needs either a windscreen that is not insulated, or a cut-out area without IR block coating.

- Opening angle: At distances over 20 m a pedestrian would be represented by only one or two pixels. Thus, an object classification will not be possible at these distances due to the low resolution. Reducing the field of view for front view applications from 60° to 30° would double the number of pixels per object and still provide the necessary field of view for the intended tasks.

5 Outlook

The evaluation results showed that the camera offers outstanding potential not only in view of the required perception performance, but also with respect to sensor size, power consumption, package requirements and future production costs. In addition we expect the following performance enhancement for the final 3D range camera in the future project developments:

- Establishment of a CMOS array with 64x8 pixels providing lateral resolution in two directions instead of a line sensor
- Improvement of the sensor sensitivity of a factor of 2 (noise equivalent power $NEP = 1 \text{ W/m}^2$)
- Implementation of laser modules with higher output energy and higher repetition frequency (30 kHz). The laser illumination will still fulfil laser class 1 requirements
- Employment of a customised optics with lower f-number ($f\# < 1$) and a field of view of 30° to increase irradiance at sensor level, as well as scene resolution at larger distances for object classification

The planned modifications will result in improvements concerning distance range, accuracy of distance measurements and frequency of image acquisition.

6 Acknowledgements

The project work is funded by the European Commission as part of the Integrated European Project PREVENT/ Subproject UseRCam (<http://www.prevent-ip.org>).

The involved consortium partners of the UseRCams subproject are:

Siemens AG (Corporate Technology + Siemens VDO Automotive), BMW Forschung und Technik GmbH, Centro Ricerche Fiat, Technocentre Renault, Volvo Technology AB, Fraunhofer IMS, and Lewicki Microelectronic GmbH

References

- [1] P. Mengel, G. Doemens, and L. Listl, "Fast range imaging by CMOS sensor array through multiple double short time integration (MDSI)", Proc. IEEE International Conference in Image Processing (ICIP 2001), Thessaloniki (Greece), Oct. 7-10, 2001, pp.169-172.
- [2] O. M. Schrey, O. Elkhaili, P. Mengel, M. Petermann, W. Brockherde, and B.J. Hosticka, "A 4x64 Pixel CMOS Image Sensor for 3D Measurement Applications", Proc. European Solid-State Circuits Conference (ESSCIRC 2003), Estoril (Portugal), Sept 16-18, 2003, pp.333-336.
- [3] EC IP PRéVENT, UseRcams deliverable 52.300.1, http://prevent-ip.org/en/public_documents/deliverables/d523001_usercams_general_specifications.htm

P. Mengel, Siemens CT PS 9

81739 Munich, Otto Hahn Ring 6

Peter.Mengel@siemens.com

Keywords: 3D sensor, CMOS-technology, time-of-flight measurement, MDSI range detection principle, distance measurement, 3D range camera, pedestrian protection, collision mitigation, blind spot surveillance

EVENT-ONLINE – A Service Concept for large scale Events based on FCD Technology

R. Willenbrock, F. Steinert, gedas deutschland GmbH

W. Schönewolf, Fraunhofer IPK

K. Graze, Signalbau Huber GmbH

Abstract

Floating Car Data is a well known technology used in traffic science to detect travel time, average speed and disturbances with the help of probe cars moving as mobile sensors in a road network of interest. As GPS and GSM is available all over Europe, it is nowadays possible to generate FCD data with a simple software implementation on mobile devices such as PDA's, MDA's or navigation systems connected to a GSM module. After the generation of FCD based traffic data it can be sent to a service centre and help to improve fleet and traffic management. Results from field trials in Berlin, Hanover and Athens will be presented.

There are three different approaches to set up an FCD fleet for traffic management:

1. Commercial fleets with an on board GPS and communication system, e.g. cars or trucks.
2. Private or commercial fleets with an on board unit including GPS and GSM, e.g. navigation systems with an integrated mobile phone.
3. Public transport or shuttle fleets using a number of different technologies for the location of the fleet and for the communication to the centre where delay time and schedule have to be supervised.

Since 1990 all of these FCD approaches have been analysed within a number of research projects but costs and benefits were not balanced enough to run a commercial service centre based on FCD technology alone. In order to find a cost efficient FCD service concept gedas, Signalbau Huber and FHG-IPK developed a system which allows the control of costs and benefits, including implementation and operation of the service centre.

The idea is to equip public transport and shuttle fleets (see Fig. 1) in order to receive scheduled data in the service centre. After the service centre knows that parts of the road network are congested the fleet will be informed automatically and a deviation recommendation will be announced. This scheduled FCD approach allows an optimisation of fleet and traffic management during

large scale events and gives a reliable source of “mobile” traffic data to the organising entities responsible for schedule and security. The technology was developed within the “Eye in the Sky” project and tested in Berlin, Hanover and Athens. The vehicle and VIP sponsor of large scale events, e.g. Olympic Games, usually equips his fleet with mobile phones and navigation systems, thus the technology can be implemented with a simple software update.

As the Volkswagen Group was chosen by the National Olympic Committee of China to be the official auto sponsor for the Olympic Games in Beijing 2008, gedas will continue the first experiences of the “Eye in the Sky” tests in Germany and Athens to validate a possible transfer towards the Olympic Games 2008 in China. First step will be an FCD implementation within the traffic management centre of Hanover to support the park guidance system during the FIFA World Cup in Germany next year. The project started 2004 and is co-financed by the ministry of transport of the government of Niedersachsen.

The first live test of the “Eye in the Sky” high-tech system was presented the 1st of July in Berlin where a German consortium including the DLR (Deutsches Zentrum für Luft- und Raumfahrt, German Aerospace Center), Fraunhofer IPK (Institut für Produktionsanlagen und Konstruktionstechnik, Institute for Production Systems and Design Technology), the Bosch subsidiary Blaupunkt, ND SatCom, and gedas demonstrated the integrated “Eye in the Sky” system of airborne and terrestrial traffic detection. The “Eye in the Sky” project, a four million euros project funded by the EU, combines two different traffic monitoring strategies: capturing traffic data with the gedas CityFCD (Floating Car Data) and the local monitoring from a helicopter using special DLR cameras.

The resulting solution was breaking new ground. It offers a unique approach to improving security at major large scale events such as the Olympics or world championships. Real-time data capture is the key to enabling the smooth deployment of the police, emergency service vehicles and to supporting sponsors and organizers in their operations. The “Eye in the Sky” will allow traffic control centres to plan with more precision and to provide more accurate recommendations if the traffic threatens to become jammed or an emergency occurs. In addition, an ND SatCom antenna in the helicopter provides an independent radio channel for the police and emergency services. Such a safeguard is an invaluable aid in earthquake-prone areas or for preventing terrorist strikes. Vehicles equipped with CityFCD and gedas software implemented on Blaupunkt hardware were the core component of the live test in Berlin. They acted as mobile sensors on the streets. The data gathered from the “flowing fleet” were transmitted via SMS text message to the prototypical traffic

control centre at Fraunhofer IPK, where they were immediately evaluated on digital road maps. If the data suggested an upcoming traffic jam, the "Eye in the Sky" came into action – and the helicopter flew over the potential bottleneck. Scanning the streets from above, the special high-resolution DLR cameras within the helicopter fed the traffic control centre with image data via the ND SatCom radio connection. The data were immediately evaluated and made available to the traffic control centre. In effect, the system not only visualised but even measured the traffic volume at key traffic nodes. The advantage of this holistic solution is that it yields a high-quality, real-time data pool, which helps traffic controllers make the right decisions.



Fig. 1. System overview

References

- [1] Wayflow / City-FCD - Final Project Report for BMBF, March 2003
- [2] Eye in the Sky - Final Project Report for the European Commission, December 2004

Ralf Willenbrock

gedas deutschland GmbH
 Pascalstr. 11
 D-10587 Berlin
 Germany
ralf.willenbrock@gedas.de

Klaus Graze

Signalbau Huber GmbH
Niederlassung Berlin
Sickingenstraße 26-28
D - 10553 Berlin
Germany
klaus.graze@signalbau-huber.de

Werner Schönewolf

Fraunhofer Institut Produktionsanlagen und Konstruktionstechnik
Pascalstr. 8-9
D-10587 Berlin
Germany

Keywords: floating car data, FCD, event-online, traffic management, optimisation of fleet

Advanced Pressure Sensors with high Flexibility for Side Crash Detection

M. Brauer, Dr. K. Krupka, Infineon Technologies AG

Abstract

The implementation of advanced regulations for side impact crash tests require an improved and faster detection method for side impact crashes. Therefore the sensing principle must recognize the severeness of an accident with highest possible confidence and within shortest time. The use of pressure sensors inside a door cavity enables the system supplier to develop solutions to fulfill these requirements. Infineons 3rd generation of pressure sensors for side crash detection offers a high flexibility to implement customer specific communication protocols. Furthermore, proven diagnosis functionality as well as additionally new features are integrated to guarantee a high reliability of the sensors for this special safety application. All active components for the entire pressure satellite could be integrated within the sensor.

1 Introduction

Due to increased traffic accidents by side impact crashes and from it devoted rising number of hurt passengers of a car was intensified the guidelines for execution by side impact tests. Here increased requirements result to detecting such side impact crashes. The sensor system which can be used must recognize the heavy of the accident surely and within shortest time. The acceleration sensors used for this task show here however serious disadvantages: They can take up an impact by their preferential installation way in the b-pillar of a vehicle on the vehicle door only delayed. The use of a pressure sensor makes possible completely different beginning for detecting a side crash. Since by a side impact on a vehicle door this is distorted, an increase of pressure results within the door cavity. This pressure impulse can be measured by pressure sensors, which are in the door cavity. This pressure sensor was particularly developed for this dedicated application and is characterized by a high device complexity and many years proven high reliability.

2 Side Impact Tests

Conventionally, the tests for side impact crash were performed with a barrier, which meets the vehicle doors and the B-pillar from the side both parallel to the vehicle side (ECE-R95, 96/27/EG, euro NCAP, IIHS and FMVSS 214, Fig. 1).

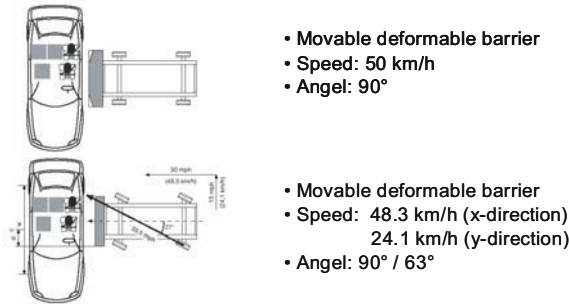


Fig. 1. Conventional side impact tests

Thereby the impact impulse was passed on directly to the B-pillar of the vehicle. An acceleration sensor located in the B-pillar can detect this impact sufficiently fast, in order to give the information for the release of the safety systems. By the rising license number of SUV (sport utility vehicle) and the higher type of construction of these vehicles it comes in the case of a side impact crash by such a vehicle however to an accident picture, which is not sufficiently covered by the conventional side impact tests. Accidents with such vehicles only met the vehicle door and not the entire vehicle side and thus the B-pillar. The consequence from these accident pictures is an advanced guideline for side impact tests (FMVSS 214 NPRM, Fig. 2).

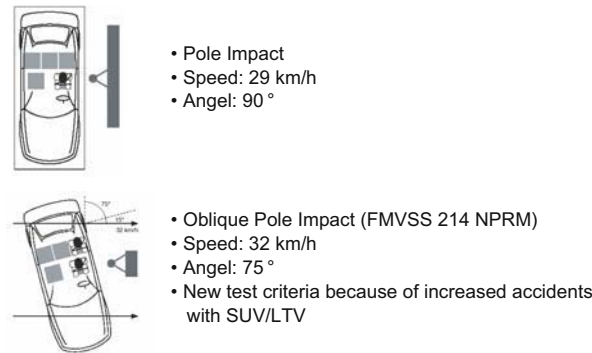


Fig. 2. Advanced side impact tests

3 Operational Principle

The guidelines for the advanced side impact tests, changed on basis of characteristic accident pictures, show an impact by means of a pole within the vehicle door. In that case the B-pillar is not directly affected by the impact, whereby acceleration sensors that are located at the B-pillar, can detect the collision due to inertia only delayed.

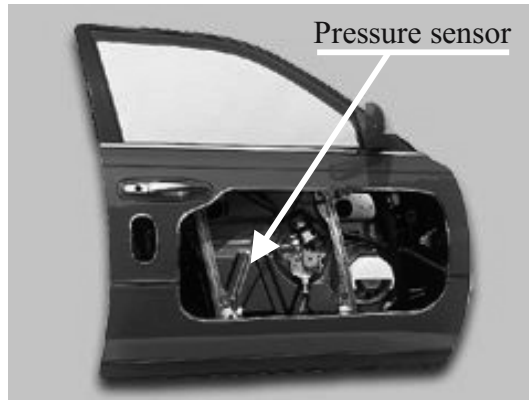


Fig. 3. Placement of the pressure sensor within a vehicle door

Measuring the impact at the place of the happening offers different detection possibilities. In the case of a sufficiently strong impact on a vehicle door it comes to the deformation. This causes a pressure impulse within the door cavity, since primarily the exterior of the door is pressed in the inside, the door inside paneling however a spontaneous pressure balance retarded. The pressure sensors developed particularly by Infineon for this application are located within the door cavity (Fig. 3). They are possible to detect the pressure impulse during an impact.

Fig. 4 shows the output signals represented by pressure sensors and acceleration sensors during a side crash impact. In each case two events are regarded: An impact is present after FMVSS 214, whereby the safety systems must be activated and an innocent impact of a ball is present, whereby safety systems may not be activated.

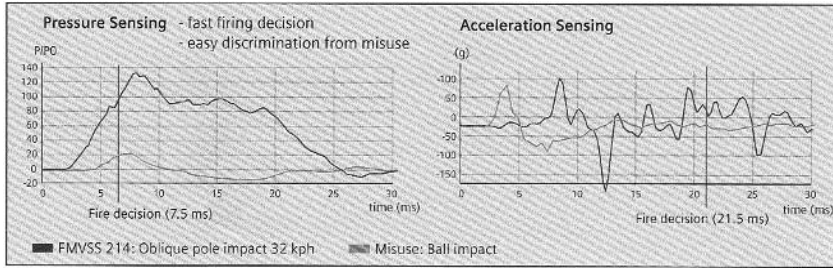


Fig. 4. Pressure sensor signals compared with acceleration sensors

Fig. 4 shows the advantages of the pressure sensors here clearly: On the one hand the reliable decision to activate the safety systems is known importantly faster. On the other hand pressure sensors show an output signal where it is substantially easier to differ between material accident and insignificant impulses.

A further advantage when using pressure sensors for side impact detection is that by the constant pressure distribution in the door interior the entire door serves as sensitive element. Thus the output signal is independent of in which place of the door the impact takes place, but only of the strength of the impact. From this a renewed advantage results concerning the placement within the door and the mounting technique: The output signal of the pressure sensor is of it independent. Further the pressure sensor will only then supply relevant initial values if it comes to an active destruction of the door; a wrong decision can be minimized in such a way. An interesting point is besides the direct linkage between impact strength and output signal of the pressure sensor. Here safety systems are conceivable, which can be activated gradually depending upon accident strength.

4 Special Pressure Sensors for Side Crash Detection

Already since 1998 with Infineon special pressure sensors are successfully produced for side crash detection, which today already find in many current passenger car platforms use. The improved guidelines for side impact tests show an intensified interest in this application. Based on no standard in the data communication but the necessity of each module manufacturer to have an adapted sensor for his system, larger product flexibility is in demand. Due to this request, Infineon develops the third generation of special pressure sensors for side crash detection. The higher flexibility for the customized transmission protocols could be achieved by the integration of an intelligent state

machine (iSM). Contrary to a fixed state machine, whose program sequence is firmly defined, the iSM gets its instructions from a firmware. This firmware is deposited within an integrated ROM. Changes mean only a change of the ROM. The used iSM already worked with several sensors from Infineon. Apart from the new flexibility it applies to receive however the proven reliability of these sensors. For this within the sensor several diagnosis modes are integrated.

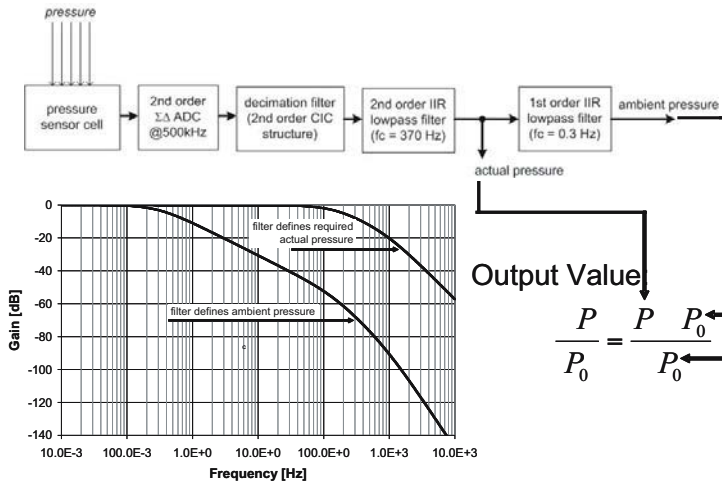


Fig. 5. Signal path

The sensor transfers not the absolute pressure, but the application adapted relative pressure ($\Delta P/P_0$). This is calculated by the difference of the absolute pressure with the ambient pressure, standardized on the ambient pressure (Fig. 5). The ambient pressure is produced thereby by means of a low-pass filter from the current pressure. In order to receive reliability over the correct function of the sigma delta converter and the following filters, during the starting phase the converter is supplied with a constant voltage and the system response of the filter is compared with the expectancy value. In the case of a deviation an error code is sent. The detection of the pressure is not made by a single large pressure cell, but within the sensor several pressure cells are integrated. 42 of such cells forms a pressure field, whereby altogether 2 sensitive pressure fields and 2 reference pressure fields are present (Fig. 6). During the normal operation these pressure fields are connected within a Wheatstone bridge. During the start-up phase the pressure fields are connected in such a way that a direct comparison of the sensitive pressure fields becomes possible. Thereby damages of the pressure cells can be recognized. In that case an error code is sent to the airbag control unit (ECU), which is able to shut down only the defect sensor. Pressure cells with only one single pres-

sure cell can provide this test only with the help of a reference sensor (right door - left door). In the case of an error both satellites would have to be driven down with such systems.

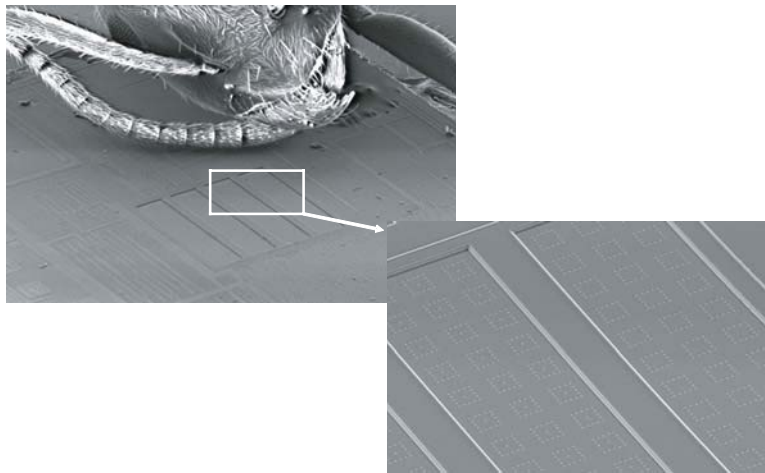


Fig. 6. SEM picture of the pressure cells in comparison to the head of an ant

Additional diagnosis modes like a self check iSM and the permanent monitoring of the ambient pressure are further characteristics of Infineons third generation pressure sensors for side crash detection.

Furthermore, these sensors feature a high integration of the components, which are needed for pressure based side crash detection satellites. Only few additional passive elements are needed (Fig. 7). Thereby costs can be saved regarding the application.

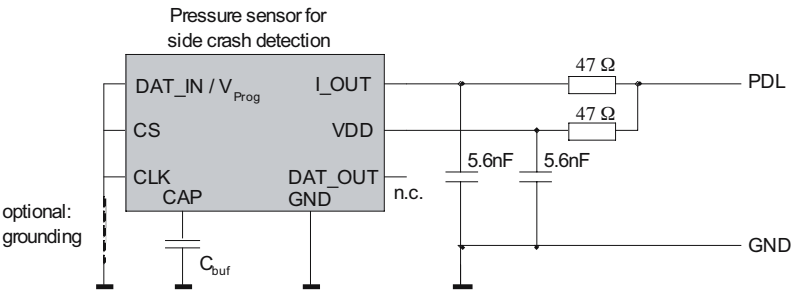


Fig. 7. Application circuit

Summary

The third generation pressure sensors for side crash detection is characterized by a large flexibility regarding the customer requirements for specific protocols. Furthermore, proven diagnosis modes as well as additionally new modes are integrated. Thereby a further high reliability of the sensors for this special safety application can be guaranteed. Additionally, all active components for the entire application could be integrated within the sensor. This high device complexity makes a cost reduction possible on module level.

References

- [1] "Advanced solution for pressure based side airbag systems" M. Wycisk. AMAA2003, 7th International Forum on Advanced Microsystems for Automotive Applications, Berlin May 2003
- [2] „Combining Acceleration and Dynamic-Pressure Sensing For Side-Impact Restraint Activation" G. Winkler, Th. Stierle, Th. Malbouef. Airbag 2002, 6th International Symposium, Karlsruhe Dec. 2002
- [3] Advanced Components for Pressure Based Side Airbag Systems" M. Wycisk. Airbag 2002, 6th International Symposium, Karlsruhe Dec. 2002

Michael Brauer, Dr. Kay Krupka

Infineon Technologies AG
 81726 München
 Germany
michael.brauer@infineon.com

Keywords: side crash detection, pressure sensor, side impact, door cavity

Detection of Road Users in Fused Sensor Data Streams for Collision Mitigation

L. Walchshäusl, R. Lindl, K. Vogel, BMW Group Research and Technology
T. Tatschke, FORWISS Institute for Software Systems, University of Passau

Abstract

This paper deals with a novel sensor fusion approach to detect and track cars and pedestrians to facilitate a collision mitigation application for vehicles. Robust collision mitigation requires a perception performance of an unprecedented degree of reliability, since an erroneous application of emergency braking caused by false alarms would greatly impede road safety improvement not lastly due to the major setback such an incident would represent for driver acceptance. However, current off-the-shelf single sensor approaches can hardly fulfil the challenging demands. Accordingly, we develop a multi-sensor recognition system. It is composed of a far infrared imaging device, a laser scanner and several radar sensors, which operate integrated into a BMW sedan.

1 Introduction

Statistic evidence of the European Union shows that accidents resulting in fatalities or serious injuries are caused to the highest percentage by collisions of cars with vulnerable road users. This fact points to the urgent need for active and passive automotive safety systems as a significant contribution to overall road safety.

Focusing on a novel approach for environmental perception based on a multi sensor-system this paper offers a collision mitigation application for cars by means of autonomous braking. To meet the application's requirements regarding accuracy and reliability of the perception result, we propose a fusion processing scheme, which operates only on slightly pre-processed sensor data. This "early fusion" approach uses the synergetic effect of a common and consistent data processing as well as an interpretation of sensor low-level data to tap almost the full sensor potential. To this end it relies on a combined modeling of the environment, which contains object assumptions as well as a-priori knowledge.

1.1 Related Work

Many research groups have contributed significantly in the field of sensor fusion. With regard to an automotive environment Kämpchen et al. [6] propose an adaptive cruise control system (ACC) based on a combination of an early and a track-based fusion approach. A laser scanning sensor and an imaging camera are used to detect vehicles. Schweiger et al. [8] utilize a radar and a monocular imaging sensor to build an ACC system. A collision warning and vision enhancement system is proposed by Polychronopoulos et al. [7]. Vulnerable road users and vehicles are identified by a far infrared camera and a radar sensor.

In this paper the multi-sensor perception system is composed of four radar sensors, a laser scanning device and a far infrared camera to detect both vulnerable road users and other vehicles utilizing a novel early fusion approach.

1.2 Overview

This publication focuses on a novel fusion approach based on only slightly pre-processed sensor data. The given sensor platform and its configuration is discussed in chapter 2. The envisaged safety application on top of the perception system is presented in chapter 3. Chapter 4 is dedicated to the perception system. After a short motivation with respect to the early fusion concept (4.1), section 4.2 is giving an overview on the fusion cycle and the system's main components. In the following sections (4.2.1 to 4.2.3) the data acquisition as well as the time prediction of our system is introduced, and the generation of predicted measurements is explained in detail. Sections 4.2.4 and 4.2.5 illustrate the data association process and the generation of new object hypotheses within the proposed fusion framework before the filtering of the object information is addressed (section 4.2.6). Finally, the last section gives an overview on the system architecture and implementation details of the fusion system.

2 Sensor Configuration

BMW has set up an experimental car with the following sensor configuration depicted in Fig. 1. Concentrating on the surveillance of the area in front of the vehicle, these cooperative sensors, which operate on the basis of distinct physical principles, complement each other both in effective range and spatial accuracy.

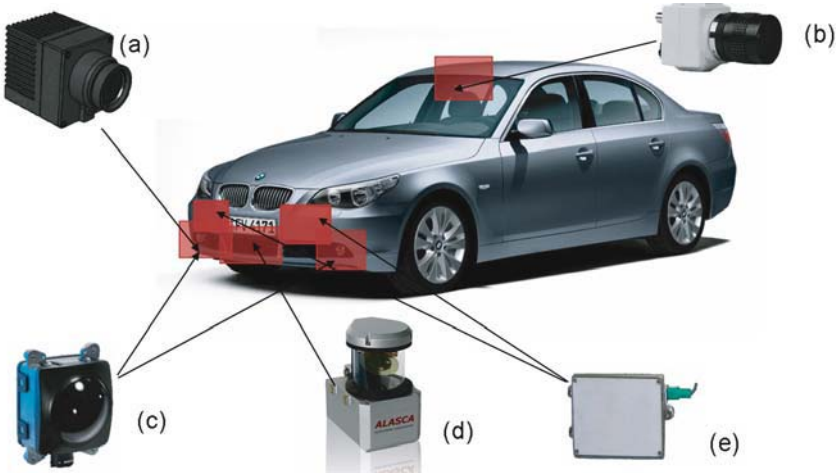


Fig. 1. BMW experimental car equipped with the following sensor configuration: (a) SAGEM far infrared camera, (b) Grey-scale camera, (c) Bosch SGU long range radar, (d) IBEO laser scanner and (e) MA/COM short range radar.

The usage of a far infrared (FIR) sensor guarantees both perception at bad lighting conditions and straightforward vehicle and pedestrian detection (see Fig. 2). As most pedestrian-scenarios covered by the experimental vehicle, are situated in the area to the right of the road, this sensor is mounted at the right of the front bumper. Long and short range radar sensors are surveying the environment ahead providing a seamless transition in distance and field of view resolution. Moreover, a laser scanning (lidar) device is mounted beneath the number plate to enhance the detection and tracking quality for both pedestrians and vehicles. The visual grey-scale cameras are used for supervising and controlling purposes only.



Fig. 2. (a) Pedestrian (FIR camera). (b) Pedestrian (grey-scale camera). (c) Vehicle (FIR camera). (d) Vehicle (grey-scale camera).

3 Collision Mitigation Application

The target application of the demonstration system is collision mitigation by means of autonomous braking. Accident statistics tell us that most of the accidents with severely injured persons happen through collisions of cars with vulnerable road users – often in urban areas on straight roads. These accidents can be attenuated or even prevented by our collision mitigation system. The second crash scenario addressed in our system deals with rear-end collisions.

The basis for any intra-system decision is a situation assessment. Taking into account the geometric and kinematic data of object-models provided by the perception system as well as probabilistic attributes and physical limits the collision risk is estimated. Only in case of an inevitable collision, the system engages the brakes autonomously. It uses the fact that technical systems are capable of reacting much faster than human beings.

Emergency braking caused by false alarms would greatly impede road safety improvement not lastly due to the major setback such an incident would represent for driver acceptance. Thus such an active autonomous intervention in the process of driving requires an outstanding degree of perception performance, particularly with regard to accuracy, availability and robustness. Therefore the attention is especially concentrated on the construction and design of the environment perception system.

4 Perception System

The central challenge for advanced driver assistance systems is an adequate perception of the vehicle's environment and the generation of an environment description out of these data.

A multi-sensor system containing a set of sensors based on distinct physical principles establishes a basis for an accurate and robust environment perception – notably if they complement each other in their sensing capabilities. Key ingredient of the perception system is the way how the diverse and sometimes conflicting measurement data from different sensors is combined in order to increase information content on the one hand and to reduce the amount of data on the other hand.

In track-based fusion approaches several sensor data streams are processed independently from each other until the level of object data is reached. Fusion on the object level runs the risk that useful data is discarded during early pro-

cessing steps (e.g. data reduction or feature extraction) because it doesn't seem to be significant enough from one sensor's point of view. That way contradictions could arise on object level, that are difficult to be resolved due to the lack of lower level information.

Therefore it is this paper's standpoint that the "early fusion concept" is the more promising approach to exploit the synergies of the different sensor data.

4.1 Early Fusion Concept

The term "early" means to combine data provided by multiple and even diverse sensors at an early stage of the data processing chain. These input data can be slightly pre-processed – limited to untracked and raw sensor data.

During the subsequent fusion algorithm, data from one sensor is assessed with regard to the relevance of its information, always in the light of data provided by other sensors.

The early fusion approach ensures consistency of models in the whole processing chain. In particular, one common environment model is used for describing the same aspect of reality seen from different sensors. Thus the whole sensor data contributes to one global environmental description, i.e. one outgoing result. With this early fusion approach it is expected to achieve a robust and reliable output of the environment perception system.

4.2 Fusion Cycle

Generally speaking an abstract inference problem is composed of three circular steps namely time prediction, data association (data matching) and measurement update (correction) [4]. On top of this basic pattern we added further steps to come up with multi-sensor and multi-object demands. The following subsections describe the fundamental structure of the implemented fusion cycle also condensed in Fig. 3.

4.2.1 Data Acquisition

As most of the used sensors are working on different clock rates and time is crucial in collision mitigation, we preserve a high time resolution by a semi-asynchronous data acquisition. The fastest sensor (master sensor) with respect to the refresh rate is used to trigger this step. The actual data acquisition is

done by polling every sensor for new data. This raw data is stored in a sensor specific coordinate system, which is relative to the sensor's mounting position. Measurements of sensors, which work asynchronously to the master sensor, obtain a time delay as these measurements occur between the last and the current cycle. Assuming a maximum object velocity of 15m/s in urban environments, this error is negligible compared to sensor specific errors. In addition, a slight pre-processing of the raw data, i.e. noise reduction or edge extraction, is performed. As the sensors have probably moved along with the own-car, a coordinate transformation from sensor specific to world coordinates can not be applied in this step. Nevertheless, this conversion is handled in the subsequent "time prediction" step.

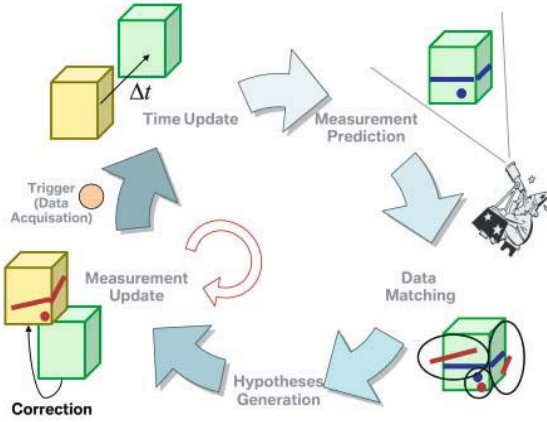


Fig. 3. Overview of Fusion Cycle. The cycle start is at the red circle. Yellow boxes symbolize tracked object-models. Green boxes and blue lines/circles represent predicted object-models respectively predicted measurements. Red lines/circles show real measurements.

4.2.2 Time Prediction

According to every objects' state (position, orientation, velocity ...) at the last cycle, these states have to be predicted to the current time. With the nomenclature from [3] the object-states \hat{x}_k and their prediction error covariances P_k are projected one time step ahead via x_k

$$\hat{x}_{k+1} = f(\hat{x}_k, u_k) \quad (1)$$

$$P_{k+1} = A_{k+1} P_k A_{k+1}^T + Q_k \quad (2)$$

on the basis of the objects' underlying dynamic models $f(\bullet)$ and their derivative A_k

A single track dynamic model [5] utilizing own car sensor data like current velocity, steering angle and lateral acceleration is used to predict the own-car's position. As all other sensors are mounted to the own-vehicle, their position is directly deducible and a world coordinate transformation is performed. In combination with a global coordinate system, this simplifies and standardizes the subsequent time prediction step of tracked vehicles and pedestrians. Currently for these object-models a linear dynamic model is applied.

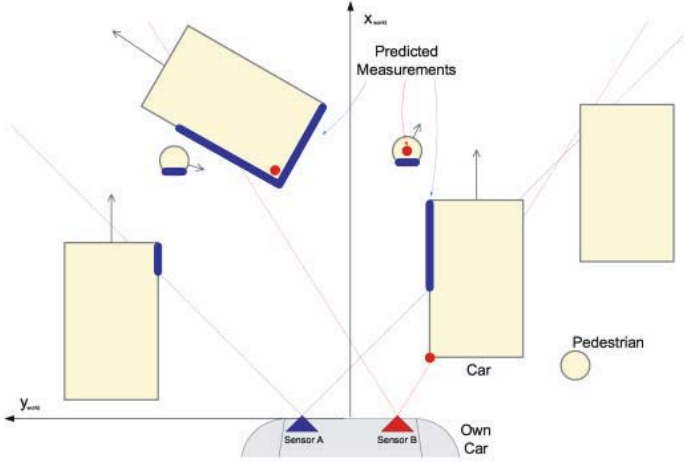


Fig. 4. Showcase for the predicted measurement generation. Using two different physical sensor principles predicted measurement generation is illustrated for both vehicles and pedestrian object-models, considering the sensors' view-port as well as partial occlusions. (Exemplified scene is in birds-eye-view and not in scale)

4.2.3 Predicted Measurement Generation

In the previous step for every object an updated representation (state) with regard to the current time is generated. These predicted states are the basis

for the following step, which estimates what each sensor would measure under the assumption that every objects' state was correctly predicted. With the notation of [3], this process reflects the non-linear function $h(\hat{x}_k)$, where \hat{x}_k represents the result of the "time prediction" step. In the following, a representation of the general task of the "predicted measurement generation" is given. The basic principle of this task is also shown in Fig. 4. Currently all object models are composed of simple polygons.

For all valid sensors within the current cycle the following steps are performed:

- ▶ **Sensor Transformation:** Transform all known object-models into the sensor coordinate system.
- ▶ **Back-face Culling:** Temporarily remove the objects' parts which are not "visible" to the sensor, because they are occluded by other parts of the object.
- ▶ **Clipping:** All objects residing outside the view-port of the sensor are ignored.
- ▶ **Occlusion Test:** Discard all objects which are "invisible" because they are occluded by other objects.

Measurement Generation: For the remaining objects respectively object parts the object specific predicted measurements are computed. This requires, that all object models have their own sensor specific representation.

Most of the necessary steps, like sensor coordinate transformation, clipping or occlusion testing, are strongly related to common computer graphics tasks. Therefore, we use a scene-graph representation for all object-models, which allow for an easy adaptation of these algorithms to the specific sensor characteristics.

4.2.4 Data Matching

The next step within the aforementioned fusion cycle is the data association that extracts and assigns corresponding pairs of real and predicted measurements. Due to the large data amount compared to most track-based fusion systems and the resulting complexity to determine the matching pairs, gating mechanisms are essential to support the fast finding of data correspondences. Thus, sensor data specific rectangular gates (derived from the object's shape model; see Fig. 5)

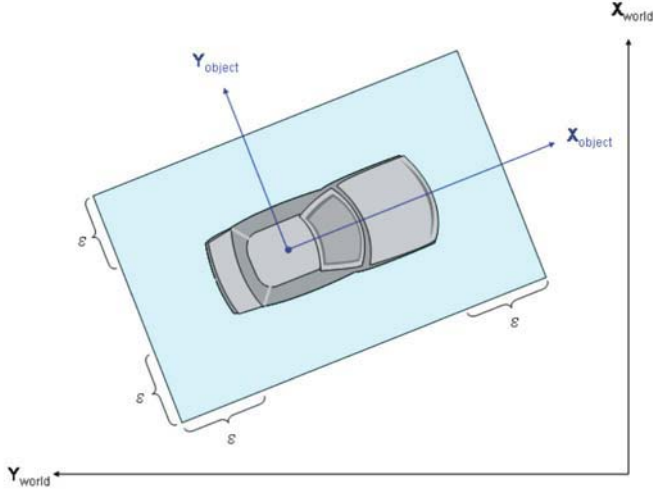


Fig. 5. Gate calculation of an object

are computed from the object's predicted estimation error covariance P_k^- , the Jacobian H_k of partial derivatives of the state-to-measurement function with respect to states and the sensor's measurement noise covariance R_k . Therefore

$$\varepsilon = \gamma \sqrt{s_i} \quad (3)$$

is added to the object's length and width respectively on each side, where $\gamma \in (0; \infty)$ and s_i denotes the respective element in the innovation covariance matrix

$$S_k = H_k P_k^- H_k^T + R_k \quad (4)$$

Now the real measurement data is tested for being inside one or more gates. Next, the data within the gating area of an object-model is assigned sensor-specifically to the object's predicted measurements (as calculated in 4.2.3) on the basis of a Global Nearest Neighbour approach.

4.2.5 Hypothesis Generation

A priority goal of the hypotheses generation is a direct and complete detection of all so far untracked and possibly relevant objects in the sensors' ranges. Thereto a high error of second kind is consciously taken into account. Usually a succeeding classification procedure as well as an observation of the objects over time can select and eliminate irrelevant assumptions. To limit the cost of computation, the hypothesis generation focuses to salient and unmatched sensor data in the detection range.

Currently the unmatched salient points, where new assumptions are placed, are radar responses, lidar segments within certain dimensions and vertical image edges from the far infrared imaging device. To limit the amount of assumptions a first coarse pre-classification step rejects impractical assumptions and a second aggregation step tries to combine overlapping hypotheses.

4.2.6 Extended Kalman Filter

A conventional Extended Kalman Filter (EKF) (see [1] for instance) has been chosen. It handles the nonlinearities of this application quite well. For every assigned pair of real and predicted measurement, which has been calculated before, a measurement update on the underlying object is performed. This procedure propagates the measurement information into the states of the respective objects. In doing so, the information of several measurements enhance the states by updating the objects' state values and furthermore, lowering the estimation error covariances. Thereby, for each assigned sensor data a measurement update step is conducted before the next cycle starts with the object's state prediction in time. With the notation of [3] the equations at time step k of the EKF's measurement update can be written as

$$K_k = P_k H_k^T (H_k P_k H_k^T + R_k)^{-1} \quad (5)$$

$$\hat{x}_k = \hat{x}_{\bar{k}} + K_k (y_k - h(\hat{x}_{\bar{k}})) \quad (6)$$

$$P_k = (I - K_k H_k) P_{\bar{k}} \quad (7)$$

Thereby the specific term $h(\hat{x}_{\bar{k}})$ has already been evaluated during the calculation process of predicted measurements and thus equation (6) can be written as

$$\hat{x}_k = \hat{x}_{\bar{k}} + K_k (y_k - y_{\bar{k}}) \quad (8)$$

for every pair of $(y_k, y_{\bar{k}})$ measurement and predicted measurement, matched by the data association process. As all sensor data is projected into the 3D global world coordinate system, the entries of the Jacobian H_k can be easily deduced from the underlying object-model without any further complex and time consuming calculations.

4.3 Implementation Details

A cyclic top-down architecture has been implemented to facilitate the detection, classification and tracking of relevant road users over time. The real world vehicle surroundings and the sensor configuration are reflected by a virtual environment, which is modelled as a hierarchical scene-graph structure [3], ensuring centralized data access and efficient spatial dependency processing (see section 4.2.3). To allow an efficient graph traversal as well as a decoupling of algorithm and data portions, the so called Visitor Design Pattern [2] has been used extensively.

5 Conclusion

This paper proposes a novel sensor fusion approach to detect and track cars and pedestrians in real-time to facilitate a collision mitigation application for vehicles. The perception system is composed of a far infrared imaging device, a laser scanner and several radar sensors which operate integrated into a BMW sedan. The proposed fusion framework in combination with the consistent use of global world coordinates for measurements, matching and the predicted measurement generation provides a high level of abstraction. Thus, more sensors at different view-ports up to a 360° sensor configuration could easily be implemented.

6 Further Work

There are still ample possibilities for improving the system. The most important ones to be tackled in future are to extend the system by a classification unit, to develop an auto-calibration of sensors and to apply alternative filtering approaches. In addition to these improvements, an extensive evaluation of the system performance is planned.

7 Acknowledgement

The fusion system presented in this publication is part of the main results achieved in the COMPOSE-project which is an application-driven subproject of the PREVENT Integrated Project, an automotive initiative co-funded by the European Commission's Sixth Framework Programme for active road safety. COMPOSE aims at collision mitigation and protection of vulnerable road users by (semi-) automated braking and to this end develops robust and reliable environment perception systems, one of which bases on a novel multi sensor fusion approach.

References

- [1] B.D.O. Anderson and J.B. Moore. Optimal Filtering. Prentice Hall, Eaglewood Cliffs, NJ, 1979.
- [2] Frank Buschmann, Regine Meunier, Hans Rohnert, and Peter Sommerlad. Pattern-Oriented Software Architecture: A System of Patterns, volume 1. John Wiley and Sons Ltd, 1996.
- [3] B.D. Allen Gary Bishop and Greg Welch. Tracking: Beyond 15 minutes of thought: Siggraph 2001 course 11. Technical report, University of North Carolina at Chapel Hill, 1995.
- [4] David A. Forsyth and Jean Ponce. Computer Vision: A Modern Approach. Prentice Hall, 2002. FOR d 02:1 1.Ex.
- [5] Marcus Hiemer. Model Based Detection and Reconstruction of Road Traffic Accidents. PhD thesis, Universitätsverlag Karlsruhe, 2004.
- [6] Nico Kämpchen, Kay Ch. Fürstenberg, and Klaus C.J. Dietmayer. Ein Sensorfusionssystem für automotive Sicherheits- und Komfortapplikationen. Aktive Sicherheit durch Fahrerassistenz, 2004.
- [7] Aris Polychronopoulos, Ullrich Scheunert, and Fabio Tango. Centralized data fusion for obstacle and road borders tracking in a collision warning system. Seventh International Conference on Information Fusion, 2004.

- [8] Roland Schweiger, Heiko Neumann, and Werner Ritter. Multiple-cue data fusion with particle filters for vehicle detection in night view automotive applications. IEEE Intelligent Vehicle Symposium, 2005.

L. Walchshäusl, R. Lindl, K. Vogel

BMW Group Research and Technology
Hanauerstr. 46, 80992 Munich
Germany
Leonhard.Walchshaeusel@bmw.de
Rudi.Lindl@bmw.de
Katrin.Vogel@bmw.de

T. Tatschke

FORWISS, University of Passau
Institute for Software Systems in Technical Applications Computer Science
Innstr. 43, 94032 Passau
Germany
tatschke@forwiss.uni-passau.de

Keywords: collision mitigation, early sensor fusion, pedestrian detection, vehicle detection, multi sensor system

Dynamic Pass Prediction – A New Driver Assistance System for Superior and Safe Overtaking

J. Loewenau, K. Gresser, D. Wisselmann, BMW Group Research and Technology
W. Richter, BMW Group Development
D. Rabel, S. Durekovic, NAVTEQ

Abstract

The paper introduces a new driver assistance system within the BMW ConnectedDrive concept. Based on the driving dynamics and navigation data, the Dynamic Pass Prediction (DPP) indicates road sections that are not safe for overtaking. By reducing the enormous driver workload before overtaking situations a safer and more comfortable driving is achieved without losing driving pleasure. This example shows how driver assistance systems can take advantage of navigation data especially if it contains curve and sign information. With the quality of navigation data available today the DPP function is feasible. Taking driving parameters into account, a situation adaptive recommendation provides even more benefit for the customer.

1 Introduction

Imagine you are driving on a curvy road, intentionally having disregarded the motorway access. You enjoy the acceleration, the force in curves, proud of the outstanding handling of your driving machine, fading out all the strains of the office. Crud! A truck! Too fast to pass on the fly and too slow to follow. You pull left in order to get a view over the upcoming road. No, too short to the next curve. Again – negative again! This time you fall back and accelerate before you pull out, thus shortening the necessary way to pass, but the run of the right curve is not visible at all. Brake! You start to get ambitious - two more unsuccessful attempts. After the next curve you will do it ...

Sounds familiar? Imagine that: You have a quick look at your navigation monitor and see that passing is not a good idea for the next two kilometres; an extra passing lane commences after that distance. You relax and change audio track: "*Country roads ...*"

About 43% of severe traffic accidents today occur on rural roads. Typically, severe accidents can be assigned to following accident sites: 33% on curved roads, 18% on sloped roads, 20% at or close to intersections, 29% on other places, see Ref. [1]. On rural roads, overtaking counts for about 10% of all severe accidents. Even though road traffic in Europe is steadily increasing, the number of fatal accidents was reduced by 40% within the last decade. This positive effect can be mostly attributed to automotive active and passive safety systems such as improved braking systems, DSC, air-bags, improved car structures, navigation systems as well as traffic regulation, infrastructure design, etc. However, the number of 40,000 casualties per year in Europe is still too high.

The BMW ConnectedDrive concept focuses on the intelligent integration of driver, car and environment concerning driver assistance and communication [2]. For BMW ConnectedDrive, driver assistance systems enhance safety and support drivers actively without interfering: they only make recommendations. Examples of available BMW systems are Active Cruise Control (ACC) using navigation data, Adaptive Light Control (ALC) and BMW Night Vision (NiVi), see Ref. [3-5].

Vehicle navigation based on map data will play a major role in future BMW driver assistance systems. The integration of precise navigation in vehicle control systems enables automatic adaptation of the system (its states as well as its parameters) depending upon the upcoming geometry of the roadway and memorized attributes/events using a GPS positioning system in combination with a digital road database. For the past years, the importance of accurate and up-to-date digital map information has increased dramatically. The digital maps are seen as a new type of sensors for the vehicles and could contribute to detect objects or dangerous curves beyond the horizon of the driver (and sensors). Driver assistance applications relying on map data need to be guaranteed of a certain level of reliability and accuracy in order to provide safe and efficient services.

In order to drive a vehicle well, the driver needs accurate information about the driving environment in addition to well-founded training, experience and the ability to perform routine functions. Ideally, the driver is able to estimate a situation fully and completely and then make the correct decisions. The driving environment is based on one hand on the position, movement and type of the other vehicles on the road, and on the other hand on the route and the nature of the road, on traffic regulations, weather, visibility etc.

However, because of the limitations of sensors, driver assistance functions at best possess only part of the information needed to describe the whole situa-

tion. Consequently, the driver will always experience a deficit in the expectations if the subjectively perceived information does not correspond to the full picture of the driving environment. The map preview as an electronic horizon can act as an additional sensor that will enhance the assessment of the situation of the vehicle.

In this context navigation systems and their associated databases are used as additional forward-looking environment sensors, which make part of the missing information available. The geometry of the road surface and other information about the road, such as its type, curves and the number of lanes or restrictions, results in an estimation of the driving environment. This gives rise to opportunities for optimizing the driver assistance functions.



Fig. 1. DPP system: red sections indicate 'not safe for overtaking'.

The outlined assistance system Dynamic Pass Prediction (DPP, Fig.1) offers a new function for recommending overtaking related handling strategies. The fundamental algorithms of the overtaking decision taking process, the HMI development as well as results from real drive tests are described.

2 Map Database

Prototype version of DPP is based on commercial NAVTEQ Digital Maps that can be found in most of today's in-car navigation systems.

To find out if a street segment is suitable for overtaking, the DPP system will examine a number of standard street attributes such as number of lanes, form-of-way (motorway, single-carriage road, roundabout ...), speed restrictions, etc.

Another important element in realization of DPP functionality is availability of street curvatures. While this data is not yet available in commercial Digital Maps, NAVTEQ pre-calculated the curvatures at shape points using existing street geometry. In general, such calculation can take place on-board. However, to achieve better results, sophisticated spline-interpolation algorithm is used. This method is calculation intensive and it is not practical to perform it in real-time on the navigation computer.

In the digital map database, calculated curvatures for street shape points are stored. In addition, on each crossing, one curvature value for every pair of streets is pre-calculated and stored in the database. Reverse-linear interpolation is used to emulate continuous curvature function over entire street length. During the road tests, it was found out that the curvature data is of good quality.

The legal overtaking restrictions are not part of standard NAVTEQ digital map attribute set. NAVTEQ collected and integrated to the database a number of street attributes that may affect the overtaking decision process. For instance, positions of pedestrian crossings, traffic lights as well as street markers are inserted in the database.

3 Electronic Horizon and Most-Probable-Path

Extract of the digital map containing streets that may be reached by the car in the near future is called Electronic Horizon (ADAS Horizon, Extended Driver Horizon). Path on Electronic Horizon that will be followed with highest probability is called Most Probable Path. Construction of the Electronic Horizon and Most-Probable-Path is outside of scope of this article, but it can be said that EH is generated using probabilistic algorithms that takes into account a number of street attributes as well as the calculated route (if available).

DPP algorithm examines only street segments along the Most-Probable-Path. While it is possible that the Electronic Horizon Most-Probable-Path does not correspond with the driver's intentions, this situation is very rare in DPP. Typically, DPP will be used on cross-country roads where frequency of crossings is not very high. In addition, on each such crossing EH algorithm will usually prefer most important road to follow; driver will turn to side roads either

when he know in advance which path he will follow (i.e. he is already aware of the crossing), or if calculated route follows that way. In the later case, since calculated route is used as parameter in EH algorithm, side road will be on Most-Probable-Path and the turn will be taken in account by the DPP algorithm.

4 DPP Driving Dynamics

Based on road geometry and other attributes in digital navigation maps as well as actual driving dynamic parameters DPP informs the driver about road sections that are not safe for overtaking. In the sense of the BMW ConnectedDrive concept the driver gets knowledge about roads ahead even when he is driving in unfamiliar areas. This avoids the continuously increasing willingness of the driver to take an overtaking risk. By using DPP in overtaking situations a safe, relaxed and comfortable driving is achieved.

Since the proposed system does not monitor oncoming traffic, it will *not indicate that overtaking is safe*. So the complete manoeuvre remains the driver's responsibility. As a matter of course the driver is obliged to obey effective traffic rules.

In order to adapt to the actual situation DPP also makes use of dynamic vehicle information like

- ▶ initial velocity
- ▶ rate of acceleration
- ▶ rate of deceleration

The given geometrical distance values during the overtaking manoeuvres are shown in Fig. 2, where vehicle 1 denotes the vehicle that is overtaken and vehicle 2 the overtaking vehicle.

The parameters for the overtaking distance are given by S_H describing the whole overtaking distance, S_1 and S_2 the safety distance to the vehicle in front of the overtaking vehicle and after the overtaking manoeuvres, respectively. l_1 and l_2 are length of the vehicles. S_L finally describes the distance that the overtaken vehicle has passed during the overtaking manoeuvres. The sum of the whole overtaking distance is than given by $S_U = S_H + S_L$, where S_H is given by $S_H = S_1 + S_2 + l_1 + l_2$.

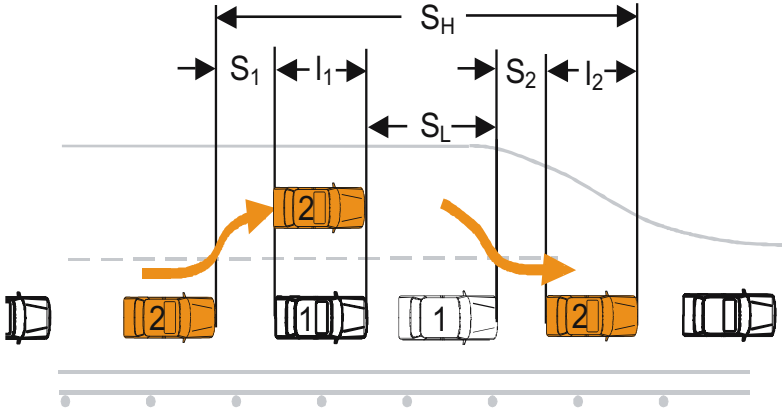


Fig. 2. Geometry parameters for the overtaking manoeuvre

S_U depends further on

- v_0 : the initial speed of the overtaking vehicle, which is assumed to be equal to the speed of the overtaken vehicle
- v_1 : the assumed velocity of the overtaking vehicle after the overtaking manoeuvre
- v_{\max} : speed limit
- a_a : acceleration of the overtaking vehicle and
- a_d : deceleration of the overtaking vehicle
- as well as the range of vision and the oncoming traffic.

Fig. 3-5 show speed plots for different situations. In Fig. 3 the overtaking vehicle accelerates to a turning speed v_m and subsequently decelerates to the desired speed v_1 . Applying standard motion equations

$$v = v_0 + a * t$$

and

$$S = v_0 * t + \frac{1}{2} * a * t^2$$

and eliminating variables v_m , t_a and t_d results in the required passing way (see Fig. 3-5).

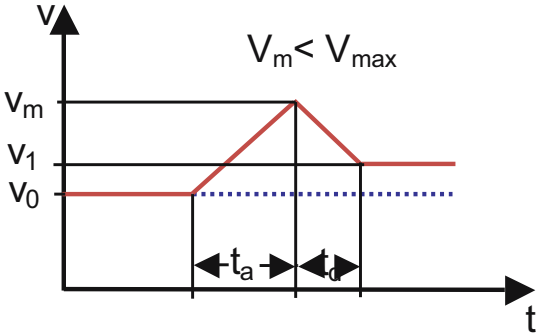


Fig. 3. Speed plot during the overtaking manoeuvres ($v_m < v_{max}$)

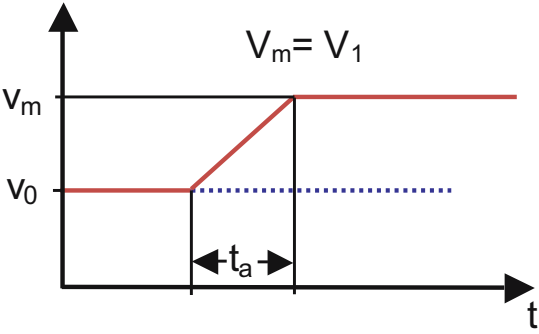


Fig. 4. Speed plot during the overtaking manoeuvres ($v_m = v_1$)

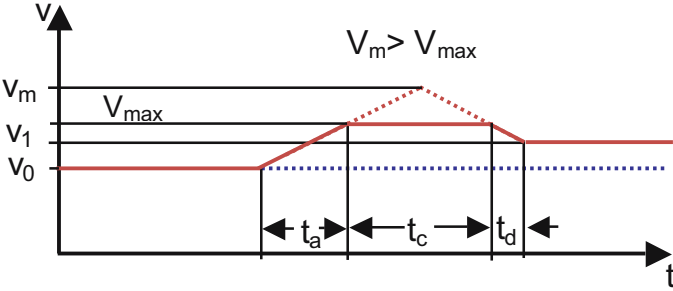


Fig. 5. Speed plot during the overtaking manoeuvres ($v_m > v_{max}$)

Fig. 4 shows the special case of acceleration to the desired speed without a deceleration phase. In Fig. 5 the maximum speed is limited by v_{\max} . Calculation of the passing way S_U is done analogously. The time values t_a , t_c and t_d will be calculated dynamically.

All road sections are marked as "overtaking not recommended" except those with curvature attributes below a limit continuously for at least the passing way S_U . The influence of velocity is shown in Fig. 6–8. Illustrated are map data on a rural road between Königsdorf and Bad-Tölz (South of Bavaria). The orange road sections show sections where overtaking is not recommended for various velocity parameters.

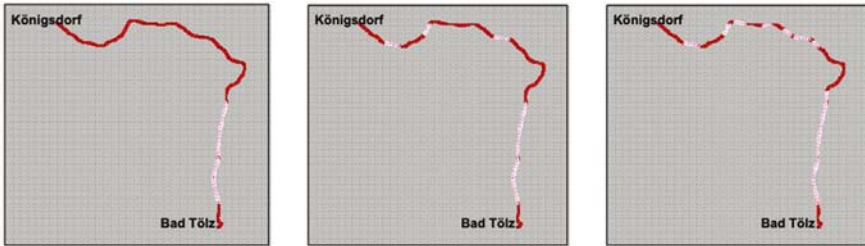


Fig. 6. – Fig. 8.

Orange road sections indicate "overtaking not recommend" for various velocity parameters

5 HMI, Visualization and Results from real Test Drives

Dynamic Pass Prediction is implemented in a 5er series sedan with navigation system and Head up Display (HuD). Results from real test drives tests have shown that the system enhances safety and supports drivers actively without interfering. The calculated distance is matched with map and navigation data where overtaking is not recommended.

The resulting information is shown on the head up display and on the navigation display (shown in Fig. 9 and Fig. 10). In Fig. 9 the orange colored bars indicate road sections that are not safe for overtaking and show the matched vehicle position and the electronic horizon in the navigation display. Fig. 10 shows the illustration on the head up display.

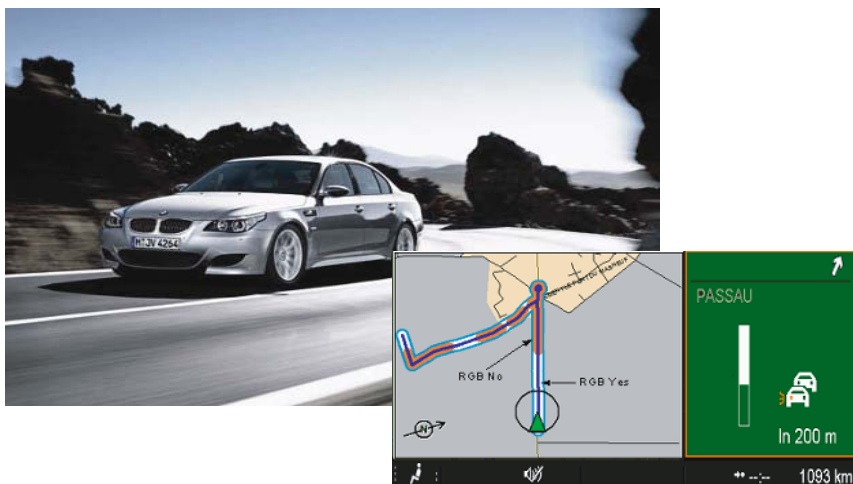


Fig. 9. Electronic Horizon indicating orange road sections in the navigation display where overtaking is not recommended



Fig. 10. Dynamic Pass Prediction integrated in the head up display

If a road segment is straight and free of crossings but too short for overtaking, it will be marked with light orange colour. Since the overtaking distance is a function of speed, it is possible that road segments that are too short become white if the vehicle changes speed.

Segments, which the DPP algorithm finds unsuitable for overtaking, are marked in orange colour (see Fig. 11). Most Probable Path (MPP) event signs symbolize the reason for the classification in the DPP engine. The Most

Probable Path (MPP) is part of the electronic horizon. If multiple reasons recommend not passing, an MPP event sign representing the first reason will be shown. All the colours in visualization are freely configurable. It is possible, for instance, to set the colour of 'too short' segments same as colour 'do not pass' segments.

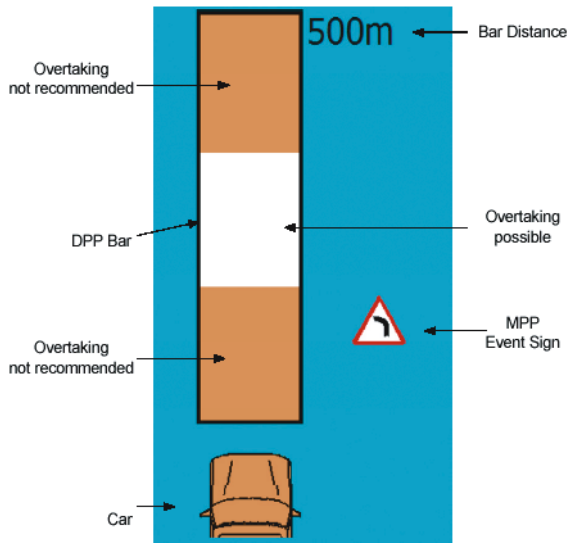


Fig. 11. Dynamic Pass Prediction design

As illustrated in Fig. 11, the vehicle on the display is orange if the start of an overtaking manoeuvre is not recommended at the moment and white otherwise.

6 Conclusion

Driver assistance systems heavily rely on remote sensing for road traffic situation perception. The concept of advanced vehicle navigation extends the driver's visual horizon to an electronic horizon with a much larger range. The ability to combine dynamic data (such as vehicle data) and map data (such as the roadway geometry from a vehicle navigation system), provides the means for a driver assistance system to generate a "clear" picture of the current traffic scene.

BMW has proven by series applications, that the integration of advanced vehicle navigation in driver assistance systems can bring substantial benefits in terms of reliability, robustness, increased functionality, fuel efficiency, active safety and performance. Driver assistance products using map databases as an additional source of information will most likely be introduced in phases. The Dynamic Pass Prediction is based on available GPS technologies and common map databases designed for driver assistance systems. Even with the quality of navigation data available today, BMW's DPP system can be enhanced by dynamics, which adapt to the situation, providing even more benefit for the customer. By using DPP in overtaking situations a safer, more comfortable and superior driving is achieved.

References

- [1] Quelle: Statistisches Bundesamt Wiesbaden, September 2005.
- [2] www.ConnectedDrive.com
- [3] Loewenau, J.P. et al (2005), MAPS&ADAS: Real Time Optimization of Active Cruise Control with Map Data using a Standardized Interface, 12th World Congress on ITS, San Francisco, USA 2005
- [4] Brandstaeter, M. et al (2004), "Functional Optimization of Active Cruise Control using Navigation Data", SAE 04AE-155, Detroit, USA 2004.
- [5] Loewenau, J.P. et al (1999), "Advanced Vehicle Navigation applied in the BMW", The Royal Institute of Navigation, Nottingham, England 1999, and Venhovens, P.J., et al (1999), "The Application of Advanced Vehicle Navigation in BMW Driver Assistance Systems", SAE1999-01-0490, Detroit, USA 1999.

Dr. Jan Loewenau

BMW Group Research and Technology
 Hanauerstrasse 46
 D-80992 Munich
jan.loewenau@bmw.de

Keywords: ADAS, driver assistance systems, ConnectedDrive, overtaking, digital map, vehicle navigation

Requirement Engineering for Active Safety Pedestrian Protection Systems based on Accident Research

R. Fröming, V. Schindler, TU Berlin
M. Kühn, VTIV

Abstract

The possibility to assess active safety measures for pedestrian protection is a prerequisite for the definition of reasonable driver assistance systems and their sensor need. The Verps+-index combines In-Depth accident data, driver models and vehicle tests in a new way. As an example, different brake assist strategies are analysed regarding their safety benefit for pedestrian protection. Additionally, requirements for the sensor system will be defined. Different sensing principles can be rated regarding their compliance to these requirements. It can be shown that by use of environmental sensors a brake assist strategy which keeps the driver in the loop already obtains remarkable safety benefits for pedestrians, while more advanced autonomous emergency braking strategies retrieve only limited additional performance. This means that mayor benefits in pedestrian protection can already be obtained by using "simpler" environmental sensors with reduced pedestrian recognition capabilities.

1 Introduction

A few years ago vehicle safety was all about occupant safety. The impact of the vehicle on its environment and to vulnerable road users (VRU) had less priority. Huge efforts have been made in the last decades to increase road safety. Therefore, modern cars are unprecedentedly safe in terms of occupant safety. Nevertheless, there is still a great potential to save the lives of VRU's and to minimise their injuries. During the last decade pedestrian and bicyclist safety discussion peaked at national and international levels. Calls have been made to implement measures to increase pedestrian safety. This has lead to European legislation concerning pedestrian safety and other VRU's. The recently released legislation is based on a component test procedure which assesses the vehicle front [1].

Nevertheless, active safety in general (infrastructural, educational and technical measures) has increased, helping to keep the number of accidents nearly constant while traffic density is increased. Against the background of the development of intelligent driver assistant systems (ADAS), the European pedestrian safety approach has to be adapted. These active safety systems might be able to sense a crash before it happens and reduce its severity or even avoid a crash by using advanced pre-crash sensors. The following chart (see Fig. 1) shows an expected penetration of the car market by active safety systems within the next ten years in Germany.

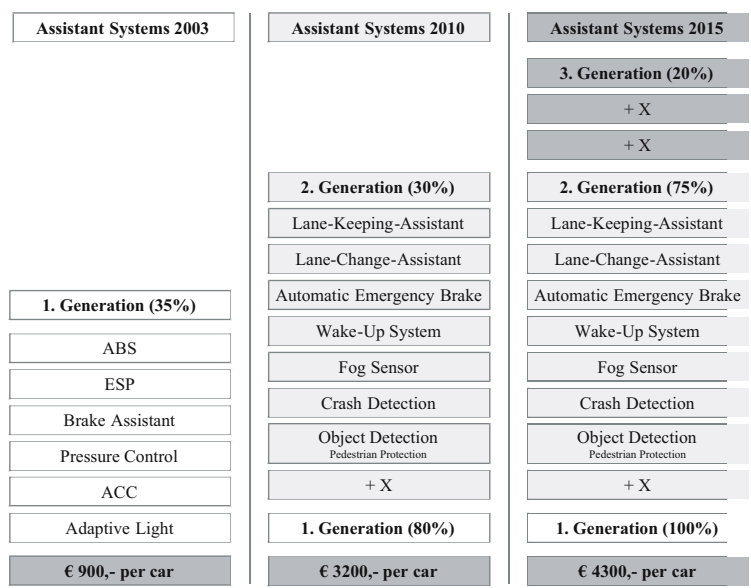


Fig. 1. Market share for driver assistant systems in Germany (based on [2])

1 Accident Research

Analysis of accidents involving vulnerable road users (VRU's) helps to deduce suitable measures of protection. Additionally, the effect in real world accident situations of certain measures can be proven by use of accident benefit research. In this chapter data related to pedestrian accident situation is summarized. The accident figures in Tab. 1 give an impression concerning the relevance of pedestrian and bicyclist accidents worldwide.

<i>Region</i>	<i>Pedestrians killed</i>	<i>Bicyclists killed</i>	<i>Pedestrian injured</i>	<i>Bicyclist injured</i>
<i>EU-25</i>	8.798 (2003)	-	184.300 (2003)	-
<i>Germany</i>	838 (2004)	475 (2004)	33.160 (2004)	73.000 (2004)
<i>USA</i>	4.641 (2004)	725 (2004)	78.000 (2001)	41.000 (2003)
<i>Japan</i>	2.332 (2003)	991 (2002)	85.592 (2003)	-
<i>Australia</i>	232 (2003)	26 (2003)	-	-

Tab. 1. International comparison of accident figures concerning killed and injured pedestrians and bicyclists (based on current governmental statistics).

Federal accident statistics are of limited use for detailed questions concerning the accident event or the cause of injuries. For more detailed questions, in-depth accident analysis can give the answers. In Germany, the "Bundesanstalt für Straßenwesen (BAST)" and the "Forschungsvereinigung Automobiltechnik e.V. (FAT)" cooperate in conducting such studies (GIDAS) [3]. Based on in-depth data of 663 pedestrian-car-accidents, occurred since 1994, detailed analysis of this accident type can be done. The results are limited to the suburbs of Hanover, slight changes are expected for accidents throughout Germany.

1.1 Accident Event and Location

Analysis of statistical data shows that 94% of all pedestrian accidents happen in the urban environment. Only 6% of accidents happen in rural areas, but accidents in rural areas cause more severe and fatal injuries. 71.4% of the killed pedestrians were involved in accidents in rural areas.

80.2% of all pedestrian accidents happen on roads classified as "city streets". 9.7% occur on country roads, 4.9% on federal roads and 3.2% on parking sites. On other road classes, only 2% of all pedestrian accidents take place. This is to differentiate between gateways (0.8%), autobahn (0.6%), cycle-, footways and trails (0.4%) and play streets for children (0.2%). Injury severity level depending on road class shows that the injury severity level increases with increasing speed limit. Straight road is the most common accident scene in case of pedestrian accidents. 60.3% of all pedestrian accidents happen in this scene. Other common accident scenes are crossroads with 19% of the accidents and gateways with 11% of the accidents.

82% of pedestrian accidents happen with an impact velocity up to 40 km/h. 87.8% of accidents causing slight injuries at this velocity level. The risk of

more severe injuries increases with increasing impact velocity. Severe injuries are sustained in 61.4% of accidents at an impact velocity level up to 40 km/h. No deadly injuries are found in the database up to 50 km/h.

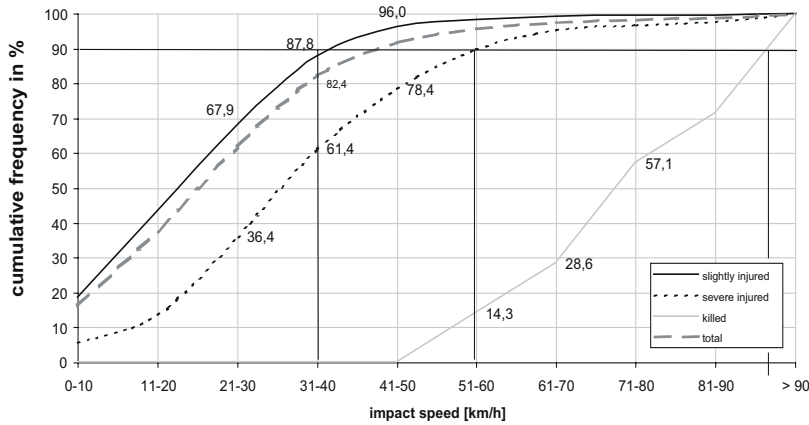


Fig. 2. Cumulative frequency of the injury severity (MAIS) depending on impact speed

In car-pedestrian-accidents, the vehicle front is the most commonly impacted part of the car. It is hit in 70.6% of all cases. The sides of a car are often hit as well. Impacts to the right side (15.9%) are twice as common as impacts to the left side (7.3%). The rear is involved in 5% of the accidents. This shows the necessity to establish a test procedure that makes it possible to evaluate the pedestrian compatibility of a vehicle front.

1.2 Pedestrian Data

39% of pedestrians involved in accidents are between 18 and 64 years old. 24% of all involved pedestrians are children between 6 and 12 years of age. 19% of all involved pedestrian are people older than 65 years. Small children up to 5 years (10%) and teenagers between the age of 13 and 17 (8%) are rarely found in the database. A more detailed analysis of age or gender could show further results (see Fig. 3). Children, between ages 6 and 12, are very often involved in pedestrian accidents. Six year old boys have the highest risk to be involved in a car-pedestrian-accident (23 cases).

In 92.2% of the cases, the pedestrian was crossing the carriageway of the vehicle before the accident happened. That is the reason why the pedestrian is hit

from left or right side by the vehicle. Along the vehicle front no special locations for the impact can be found, thus an equal distribution of pedestrian impact points can be assumed.

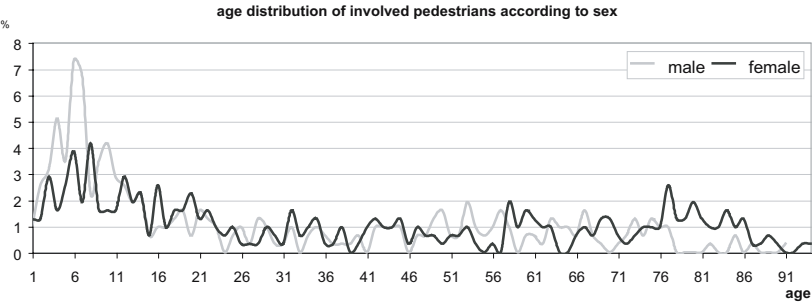


Fig. 3. Illustration of age distribution of involved pedestrians according to gender.

Walking velocity is known either from people involved in the accident or from witnesses. Therefore, it is important to analyse relative movements, sight conditions, angles between witnesses and people involved. Interpretation by the witness is important too: Short, fast steps resemble faster movement than wide, slow steps.

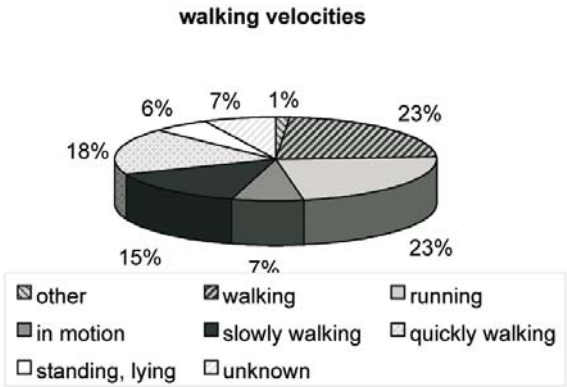


Fig. 4. Illustration of walking velocities of pedestrians.

Analysis of 609 pedestrian accidents shows that 94% of all pedestrian were moving directly before the impact. 152 of them were running (25%), 59.7% (364) were walking. Further division of this category shows that 33% (119) were walking quickly and 26% (96) were walking slowly. Some pedestrians were moving but it was impossible to characterise the movement. These cases

are summarized in the category called “in motion”. Only 6% of the pedestrians were not moving just before the impact.

1.3 Injury Frequency of Body Regions

Injury frequency of the various body regions is shown in figure 5. The most injured body regions are the lower extremities (35%) and the head (33%). Severity of injury can vary for each body region. Head injuries can be divided into slight (AIS 1 + 2, 89%), severe (AIS 3-5 10%) and fatal (AIS6, 1%).

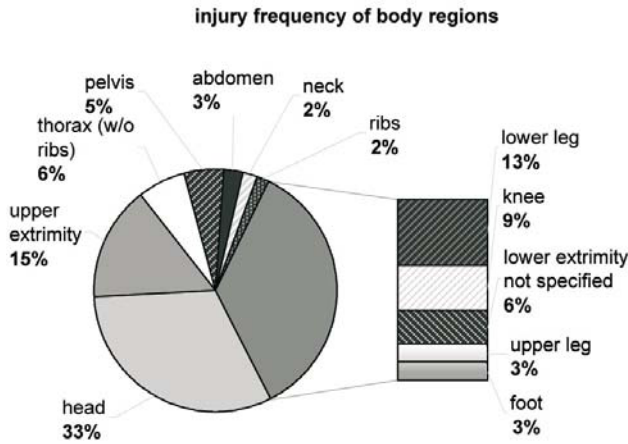


Fig. 5. Allocation of injuries according to body regions.

Analysis of all vehicle parts which caused head injuries shows that impact on the windshield is causing 44,3% of head injuries. Impact on the windshield causes twice as often head injuries and severe head injuries occur three times often as at the bonnet. Other vehicle parts mostly cause only slight injuries. An exception is the A-pillar. Head impact on the A-pillar causes severe injuries in 82% of the cases.

1.4 Causes of Injuries at Secondary Impact

A look at secondary impact shows that about 90% of the injuries received were caused by contact with road surface. A dependency of collision velocity or height of the pedestrian could not be proven. Injury frequency to head (37%), upper extremities (23%) and knee (11%) due to secondary impact is beyond

the average injury frequency to all body regions. Most injuries are slight non deadly injuries caused by secondary impact can be found in this database.

Otte and Pohleman have analysed in-depth data material in detail [4]. They revealed that with increasing impact velocity more injuries to the adult pedestrian are caused by primary impact than by secondary impact. At lower impact velocities more injuries are caused by the secondary impact (see also [5]). In general, primary impact causes twice as many injuries than secondary impact. At high impact velocities, three times as many injuries are caused by primary impact. Very often head and lower leg injuries are caused by impact with the road surface. Frequency of hand and knee injuries rises with increasing impact velocity. Head injuries caused by primary impact have the same level of severity as head injuries caused by secondary impact. In other body regions the level of severity due to primary impact is higher than the level of severity due to secondary impact. Injuries caused by secondary impact are not influenced by bonnet length and windscreen angle if the vehicle is ponton-shaped. Bonnet leading edge height, throw distance and collision velocity have major influences on injury severity due to the secondary impact.

1.5 Conclusions of Statistical Analysis

As shown in the paragraphs above, there are a lot of influences in a pedestrian car accident. A summary of the most relevant parameters of the pedestrian car accidents lead to the following conclusions:

- ▶ 94% of pedestrian accidents happen in urban environment.
- ▶ 70.6% of the main impact points on the vehicle are found at vehicle front. The sides were hit in 23.2% of the cases and 5% were hit at the rear of the vehicle.
- ▶ In 80% of the cases the pedestrian was crossing the carriageway of the vehicle.
- ▶ 82% of the accidents happen at an impact velocity of up to 40 km/h.
- ▶ Frequency of damages to the windscreen, a-pillar and roof increase with increasing impact velocity.
- ▶ In most cases the reason for the accident is exceeding the speed limit or unsuitable velocity.
- ▶ 84% of pedestrians suffered slight injuries, 15% received severe injuries and 1% were killed.
- ▶ In 58% of the cases, the pedestrian suffered head injuries. 10% of these were severe and 1% deadly.
- ▶ 34% of the injured pedestrians were under 13 years of age.

2 Assessment of Pedestrian Compatibility with VERPS+

Head impact by far results in the most severe and almost all fatal injuries in a pedestrian-car-collision. Therefore, our approach is focused on. Numerical simulations can provide knowledge about the kinematics of the event for each particular car and for diverse impact conditions. The results of the simulation are used to control a free flying head-form test device. The measured values provide the basis for the assessment of each analysed car.

Our assessment procedure therefore combines the following four modules:

- ▶ accident analysis
- ▶ numerical simulation
- ▶ component test
- ▶ quantification of pedestrian safety

The interfaces between the modules are well defined in a way that our “pluggable” method can take in new or other data in order to adapt the VERPS-Index on latest research results or new injury assessment approaches. In order to quantify pedestrian safety and to make sure that the results are comparable for all forms of vehicles on a linear scale, a Vehicle Related Pedestrian Safety Index is proposed (VERPS-index). In addition, it provides the opportunity to assess technical measures applied to the car’s front to increase pedestrian safety and allows to compare them with active safety measures applied to the vehicle (e.g. brake assist system).

Furthermore, the presented method makes it possible to influence the pedestrian compatibility of a product in a very early stage of the vehicle development process by making geometry changes with minor stylistic or functional effects or by triggering the development of additional pedestrian protection systems.

The results of the component tests can be represented by HIC values (Head Injury Criterion), calculated from the measured head form accelerations. They show a typical pattern of potentially dangerous regions at the vehicle front:

- ▶ parts of the bonnet with little deformation space beneath
- ▶ lateral bonnet edge and transition area between bonnet and wing
- ▶ bonnet area directly above the firewall
- ▶ lower windscreen frame
- ▶ A-pillars
- ▶ upper windscreen frame and roof frontal edge

All of these areas are characterized by stiff and hence less deformable vehicle structures. The degree of exposure of a pedestrian to these regions can differ

from car to car because of differences in dimensions and styling. A test procedure which stringently demands meeting specific test limits will unavoidably produce meaningless ratings in these areas. Because of differing vehicle geometries the potentially dangerous areas for the head impact are affected more or less frequently during a pedestrian impact. Some of these areas might be totally irrelevant for the head impact of a pedestrian (e.g. upper wind-screen frame at SUV's). That's why a weighting of the test results concerning their relevance in pedestrian accidents is necessary.

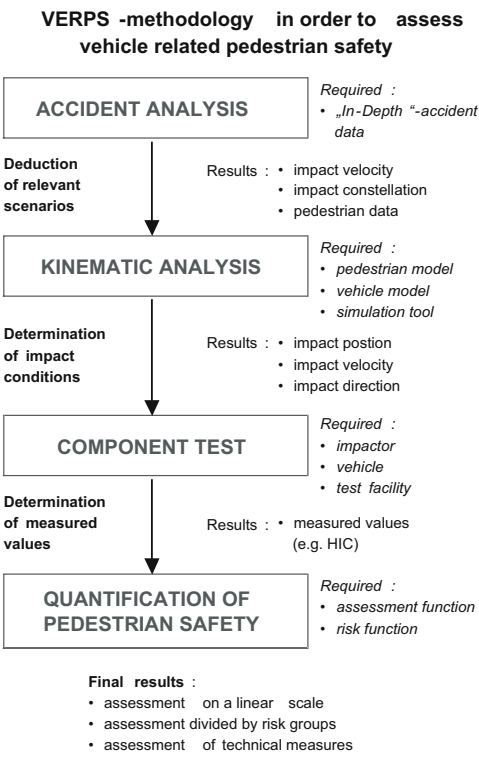


Fig. 6. Illustration of the methodology to assess vehicle related pedestrian safety.

In the following a Vehicle Related Pedestrian Safety Index (VERPS-index) is developed. This index assesses the level of protection which a specific vehicle can provide for the head of a pedestrian who is impacted by the front of the car. It allows to assess differences between particular vehicle designs and to compare technical measures applied to the vehicle front. The VERPS-index is the result of the quantification module in the proposed methodology (Fig. 6).

2.1 Mathematical Derivation of the VERPS-Index

The VERPS-index for the frontal impact is deduced in three steps from the values M_{ij} measured in the component test:

Mapping of M_{ij} to the degree of performance E_{ij} by an evaluation function $B(M_{ij})$.

$$E_{ij} = B(M_{ij}) \quad (1)$$

Weighting of the degrees of performances E_{ij} with relevance factors $R_{i,WAD}$ and $R_{j,Front}$ deduced from accident analysis.

$$R_{i,WAD} \cdot R_{j,front} \cdot E_{ij} \quad (2)$$

Summation of the degrees of performance for all subareas of the vehicle front to the VERPS-index.

$$VERPS = \sum_{i=1}^m \sum_{j=1}^n R_{i,WAD} \cdot R_{j,front} \cdot E_{ij} \quad (3)$$

To assess the vehicle front it is necessary to divide it in subareas. For each of them M_{ij} is measured. Subindex i describes the longitudinal direction of the vehicle front and subindex j the transverse one.

The definition of limit values is often used to assess measured values. But it allows only a binary assessment. It only distinguishes between good (limit met) and bad (limit exceeded). In order to derive a more refined evaluation an assessment function B can be used to get a functional link between measured values M and the degree of performance E . For the VERPS-index a functional relationship between HIC data and the occurrence of severe head injuries (AIS 3+) is used. In future, better injury risk assessment functions can easily be implemented.

The reduction of a HIC-value by 50%, e.g. from $HIC = 4.000$ to $HIC = 2.000$, improves the degree of performance E only from $E(HIC=4000) \approx 1$ to $E(HIC=2000) = 0,94$ (Fig. 8). In contrast to that an improvement from $HIC = 2.000$ to $HIC = 1.000$ leads to a significant improvement to $E(HIC=1000) =$

0,24; this means a probability for the occurrence of severe head injuries of 24%.

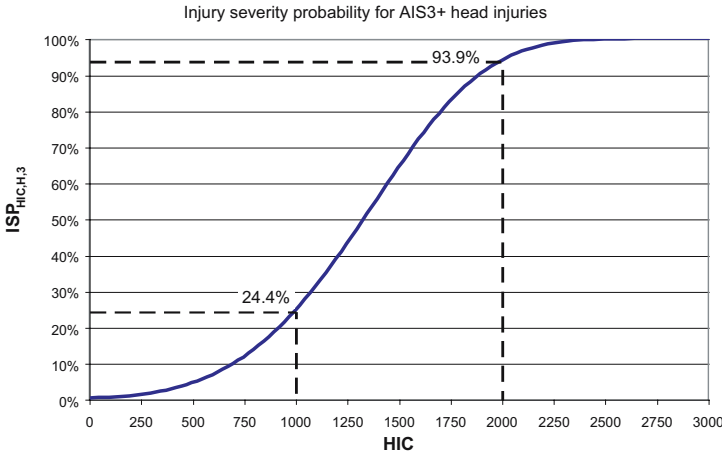


Fig. 7. Correlation between measured HIC data and probability of AIS 3+ injuries (ISP – Injury Severity Probability, based on [6]).

In the second step of the calculation of the VERPS-index the degrees of performance E_{ij} are weighed with their relevance in accident events. The importance of a test point obviously depends on the probability of hitting it in real life. In order to deduce the relevance factors, “in-depth” accident data of the Medical University of Hanover are used. The relevance factor in the longitudinal direction of the vehicle ($R_{i,WAD}$) describes the correlation between the vehicle specific kinematics factor f_K and the size of the pedestrian. In the transverse direction of the vehicle front an equal distribution for impact locations is assumed. This is supported by accident data.

We calculate the VERPS-index separately for children younger than 12 years and for adults and children older than 12 years. However, other separations are possible. Our choice considers the different requirements of pedestrian safety measures applied to cars for children and adults which result from different body heights. By use of the assessment function $B(M_{ij})$ the VERPS-index can be expressed as follows:

$$VERPS = \frac{1}{9} \sum_{i=1}^m R_{i,WAD} \cdot \sum_{j=1}^9 \left\{ 1 - e^{-\left(\frac{HIC_{ij} + 500}{1990} \right)^{4,5}} \right\} \quad (4)$$

Fig. 8 shows the division of the vehicle front in subareas and their relevance factors $R_{i,WAD}$ for a sample car.

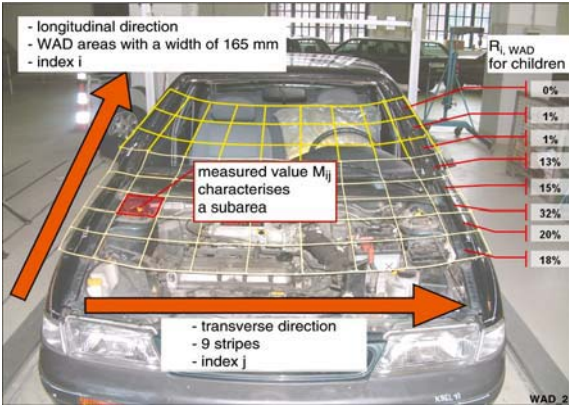


Fig. 8. Relevance factors in longitudinal direction ($R_{i,WAD}$) for car *F*.

The VERPS-index can run between (nearly) zero (no risk for AIS 3+ head injuries) and 1 (maximum risk for AIS 3+ head injuries). A car, which has a HIC-value of 1.000 in all subareas of its front, would have a VERPS-index of $VERPS = 0.24$. It can be shown that the proposed procedure allows to assess vehicle fronts on a linear scale within the limits of accuracy of the assumptions.

2.2 Application of the VERPS-Index on two Vehicles Passive Safety Measures

The VERPS-index is calculated for two sample cars. It can clearly be seen, that pedestrian safety has to be assessed separately for children and adults. Pedestrians hit different areas at the vehicle front because of their different body heights. This is the reason why a particular technical measure can positively affect all groups of pedestrians only in exceptional cases.

Two mass-production vehicles are compared with two modification levels of a possible pedestrian protection system. The first level represents a mechanical system which uplifts the bonnet in the rear area by around 0.1 m in case of a pedestrian impact. In the second level an airbag system is assumed which combines level one measures with an energy absorbing device covering critical areas of the A-pillars and the lower windscreen frame (see Fig. 9). Results can be seen in Tab. 2.



Fig. 9. Implementation of a system to uplift the bonnet by use of an airbag which also covers the A-pillars and the lower windscreen frame. [7]

		<i>vehicle F (mid-size)</i>	<i>vehicle G (compact)</i>
<i>production condition</i>	children	0.54	0.63
	adults	0.63	0.24
<i>uplifting bonnet</i>	children	0.22	0.43
	adults	0.60	0.24
<i>uplifting bonnet combined with an airbag</i>	children	0.08	0.11
	adults	0.25	0.17

Tab. 2. Assessment of two different cars and pedestrian protection systems by use of the VERPS-index.

For vehicle **F** the VERPS-index for adults could be reduced from 0.63 to 0.25, for children even from 0.54 to 0.08. The marked reduction of VERPS for children shows the great potential of active structural measures, if they are applied properly with respect to pedestrian body height and the vehicle dimensions. Head impact areas, which are mainly hit by adults, can only be protected with the uplifting bonnet and the additional airbag to cover A-pillars and lower windscreen frame taking into account.

The VERPS-index of 0.24 for adults of vehicle **G** in production condition is good compared to vehicle **F**. This can be traced back to the fact, that all relevant head impact areas for adults are in the windscreen area, which is considered uncritically concerning the HIC results unless the windscreen frame area or the A-pillars are included.

Because of the vehicle front geometry of car **G** an uplifting bonnet alone can protect only a small group of pedestrians. An additional airbag applied to the lower windscreen frame is able to improve the protection of smaller adults, but the relevant impact areas for larger ones are still not covered. Accordingly the VERPS-index is only reduced from 0.24 to 0.17. For children vehicle **G** in production condition performs poorer than for adults with an VERPS-index of 0.63, because children mainly hit the firewall and the lower windscreen frame with the head. By use of active structural measures the VERPS-performance can be clearly improved. The VERPS-index decreases from 0.63 in production condition to 0.43 for the uplifting bonnet alone and to 0.11 for the uplifting bonnet with the additional airbag.

It could be shown that an index can be formulated that allows to assess different vehicles with respect to their pedestrian safety on a linear scale. The VERPS-index allows to compare different vehicles and applied technical measures like the uplifting hood concerning their pedestrian protection potential. The injury risk induced by the secondary impact on the road is currently not assessed within VERPS.

The assessment of active safety measures (e.g. pre crash sensing devices, brake assist systems) on the VERPS-scale is also possible. The reduction of the collision speed of a vehicle, which can be attained with a certain probability depending on the system layout, can be included in the VERPS-calculation. The reduced collision speeds are used as an input parameter for the numerical simulation module. This finally results in specific VERPS-index for the analysed car.

2.3 The VERPS+- Index to assess Safety Benefits of Collision Speed Reduction

The reduction of collision speed results in a shift of the relevant head impact regions on the vehicle front and, leads to a reduction of the induced head accelerations, depending on the underlying vehicle structures. Four mayor effects can be noticed:

- On very stiff structures (e.g. A-pillars), the accelerations are reduced, but remain critical.

- ▶ "Critical" structures like the fenders induce lower accelerations, but still need structural improvements.
- ▶ Contact with stiff areas beneath the front hood can be avoided at a certain impact speed. This lowers the accelerations to a remarkable extent.
- ▶ "Uncritical" areas induce even lower accelerations.

Analysis of in-Depth accident data shows, that the head impact probability decreases with decreasing collision speed. This effect is taken into account in the VERPS+-Index by multiplication with the head-impact-probability factor $P_{\text{impact}}(v_k)$ (Fig. 10 and equation 5).

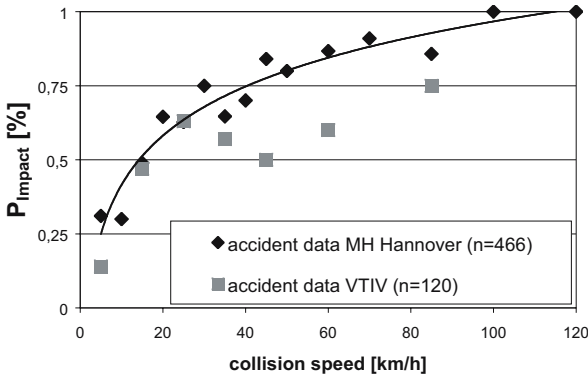


Fig. 10. Head impact probability derived from analysis of In-Depth accident data

The positive effect of collision speed reduction on pedestrian safety has been proven in a general approach in a couple of investigations related with the introduction of phase II of the pedestrian legislation starting from 2010. A retrospective estimation of the safety benefit does not take improvements of the vehicle structure into account, and is therefore always based on vehicle fleets, which are not optimised regarding passive pedestrian protection measures. Along with the new type approval requirements, some benefit in pedestrian protection can already be obtained, that could lower the additional benefit of brake assist systems (Fig. 11).

By replacing the component test within VERPS by a numerical one (Fig. 6), the injury risk estimation of multiple collision speeds becomes possible. On an exemplary vehicle, nine impact points have been virtually analysed for collision speeds from 20 km/h up to 50 km/h. The virtual test conditions for the analysed collisions speeds are calculated within the kinematic analysis of the

VERPS-procedure. As a result, a VERPS+-index for each analysed collision speed can be given (see equation 5). They can be interpolated to obtain a collision speed dependent head injury risk for the analysed vehicle.

$$VERPS+_k = P_{Impact}(v) \cdot \sum_{i=1}^m R_{iWAD}(v) \cdot \left(\sum_{j=1}^9 1 - e^{-\left(\frac{HIC_{ij}(500)}{1990} \right)^{4.5}} \right) / 9 \quad (5)$$

The VERPS+- Index can assess the mayor injury risk at different collision speeds vehicle-specifically. When applicated on the exemplary vehicle, a reduction of the head injury risk can be derived from the virtual component tests (Fig. 11).

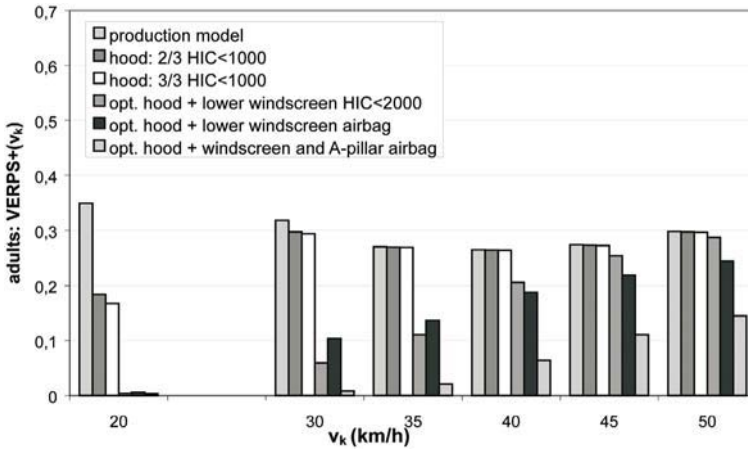


Fig. 11a. Vehicle specific impact of collision speed on the VERPS+-index for the analysed vehicle **H** (adults).

For children, a remarkable reduction of injury risk can be obtained. Starting from $VERPS+(50 \text{ km/h})=0.53$, a linear decrease of injury risk with lower collision speed is noticeable. This is mostly due to the head impact areas on the vehicles front hood. In this area, the head accelerations can be lowered to acceptable values by reduction of collisions speeds. In contrast to the injury risk for children, the injury risk for adults does not show a reduction over all collision speeds. At lower speeds, many adults have a head impact on the lower windscreen frame, which is a very stiff area. Therefore, reduction of collision speed alone is not sufficient to protect adult pedestrian in real life. But a reduction of collision speed in combination with basic structural measures shows a very good performance.

Additionally, one has to keep in mind, that the derived reductions of head injury risk is strongly vehicle specific. Other vehicle front geometries with different stiffness patterns will lead to different impact kinematics and head injury risks.

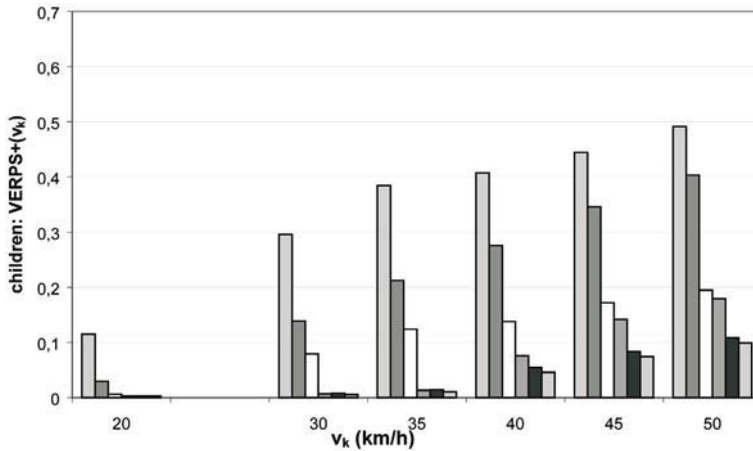


Fig. 11b. Vehicle specific impact of collision speed on the VERPS+-index for the analysed vehicle **H** (children).

3 Collision Speed Reduction of Different Brake Assist Strategies

The introduction of driver assistance systems has changed the understanding of an accident. In parallel to the upcoming of integrated safety approaches, the view of an accident has been widened onto the phase directly before an imminent crash. Up to now, only passive safety systems are assessed in type approval test and consumer tests. Nevertheless, active safety features like ESP offer a proven benefit for road safety [8]. For brake assist functions, a similar benefit is expected. A specific safety benefit of driver assistance systems could only be proven in retrospect accident analysis [9]. With VERPS+, the safety benefit of a reduced collision speed can be quantified prospectively and specifically for every analysed vehicle. Additionally, a comparison with passive safety measures regarding their safety benefit in real life accidents is possible.

Based on the drivers options to avoid a pedestrian accident, the precrash-phase can be divided into three phases ($v \sim 40$ km/h):

0. a collision warning is possible and reasonable (> 16 m, depending on the drivers reaction time $t_{\text{reaction}} > 1$ s)
1. collision can be avoided by braking only (~ 7 m)

- 2. collision can be avoided by steering only (~ 6 m)
- 3. collision can be avoided by combined steering and braking only (~ 5 m)

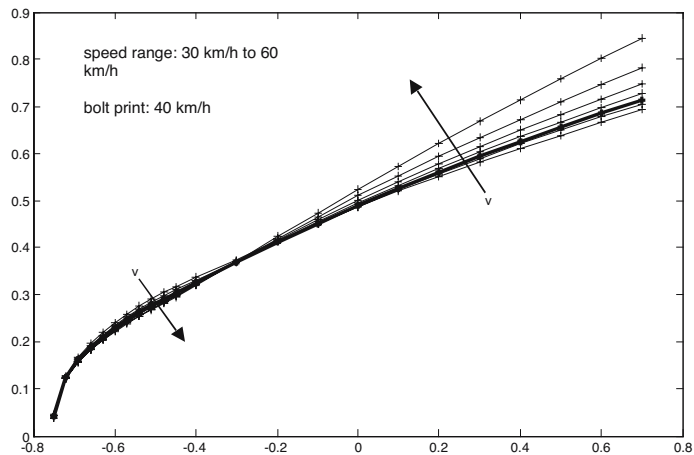


Fig. 12. Latest possible obstacle avoidance times (TTC), when only steering to the left is allowed (middle-class sedan).

The given distances have been derived from vehicle handling test with a middle-class sedan ($m = 1800$ kg) and an obstacle in the middle of the road strip. In a speed range from 30-50 km/h (mostly all pedestrian accidents happen up to this speed), an upcoming collision can be avoided by the driver up to a very short time period before the accident. Thus, autonomous braking systems, which are activated only during the last unavoidable time period, are limited regarding their safety benefit [10].

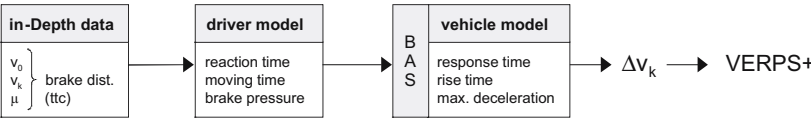


Fig. 13. Scheme of automated case-by-case-analysis of pedestrian accidents in order to assess potential reduction of collision speed using vehicle specific injury risks (Fig. 11).

In 64% of all analysed pedestrian accidents (data source MH Hannover), the driver performed a braking before the accident. The lifting of the throttle pedal during the drivers reaction can be used by future brake assistant sys-

tems (BAS) to initiate an optimised braking. Analysis of conventional BAS in driving simulations showed, that in pedestrian accidents only 50% of braking drivers could activate the brake assist system [11].

Based on the fact, that future driver assistance systems should only support the driver in performing the driving task and therefore, the driver has always to be in control of the vehicle, different brake assist strategies are defined, that fulfil these requirements. They are assessed by their potential reduction of collision speed. This is done by an automated case-by-case-analysis of each accident.

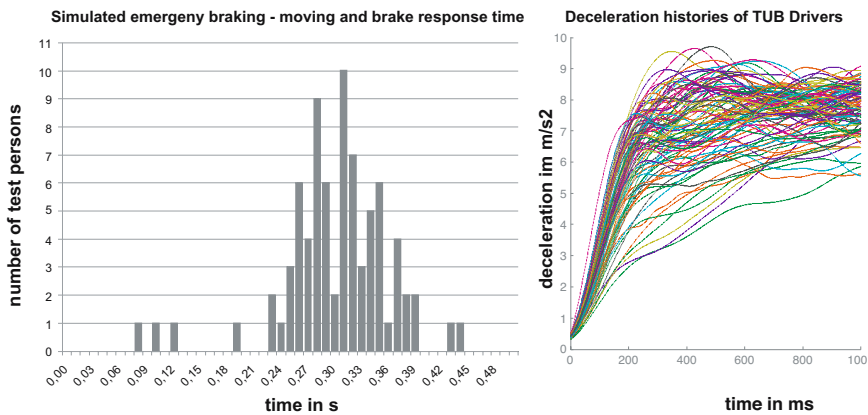


Fig. 14. Characterisation of TUB Drivers by moving time from throttle to brake pedal and brake pressure histories

The recorded In-Depth accident data (initial speed, collision speed, road friction) are used as input for a driver model, which currently consists of a set of 54 drivers performing an emergency brake (reaction times, moving times, brake pressure histories). The set of drivers used in this article is called TUB Drivers. Other sets of drivers can be implemented too, thus leading to differently reduced collision speeds. To determine moving times and brake pressure history from a realistic test, the subjects were instructed to drive on a free straight road with approx. 50 km/h. To the flash of a small lamp they should react with a full brake manoeuvre. The measured data was used to determine reaction times, moving times, brake pressure build-up time und histories of brake pressure and deceleration (Fig. 14). Wide dispersions of the histories are noticeable, which may be due to differences in the brake force. By using a brake assist system this time window can be minimised. The moving times show in contrast a low dispersion (Fig. 14). With the set of drivers that results

from the test it is possible to virtually reconstruct accidents which happened in reality and to predict the benefit, which can be obtained from different brake assist strategies.

The driver input controls a nonlinear single track vehicle model (open loop). For each calculated collision speed, a VERPS +-value is calculated, representing the induced head injury risk. By averaging all calculated VERSP+-Values, a safety benefit of the analysed brake assist system in real-life accident situations can be derived. Both the driver model and the vehicle model are derived and validated from dedicated tests with 98 subjects driving a fully instrumented mid-size sedan [12,13].

In this article, three different brake assist strategies are analysed:

- ▶ standard BAS: full brake, when certain levels of pedal velocities are exceeded
- ▶ advanced BAS I: full brake, when throttle pedal is lifted and an obstacle in front of the car is detected within a critical range
- ▶ advanced BAS II: partial brake with 0.3 g, when driving situation is critical ($t_{tc} < 1$ s to an detected obstacle) and full brake, when throttle is pedal is lifted and an obstacle is detected within a critical range

	<i>Brake Assist strategy: Full braking manoeuvre when:</i>	<i>Real-life activation probability</i>	<i>Operating state probabilities</i>			
			<i>Driver is braking</i>		<i>Driver is not braking</i>	
			<i>BAS active</i>	<i>BAS inactive</i>	<i>BAS active</i>	<i>BAS inactive</i>
<i>Standard-BAS</i>	certain levels of pedal speeds and pressure rise time are exceeded	50 % [11]	0,32	0,32	0	0,36
<i>aBAS I with environmental sensors</i>	Throttle is lifted and an obstacle is detected	85 % (est.)	0,54	0,1	0	0,36
<i>aBAS II with environmental sensors</i>	Throttle is lifted and relevant obstacle is detected Partial brake in critical driving situations ($t_{tc} < 1$ s)	95 % (est.)	0,61	0,03	Autonomous action! 0,34	0,02

Tab. 3. Analysed brake assist strategies and depending operation state probabilities.

All relevant operating state probabilities have to be defined and their depending lowered collision speeds have to be calculated. There are four possible com-

binations of driver is braking or not, brake assist activation or not, leading to four operating state probabilities. These reduced collision speeds are used to assess the safety benefit of the analysed brake assist system.

According to the previously defined brake assist strategies, a conventional BAS only affects 32% of all pedestrian accidents and aBAS I can affect 54% of all pedestrian accidents. The only way to cover the large number of unbraked accidents is to start an autonomous action. This is done by aBAS II in 32% of all pedestrian accidents. The advanced brake assist system I, which performs a full brake, when a critical obstacle is detected and the driver lifts the throttle, can start an optimised braking (at around 1 g) 0.3 s earlier (average over all analysed drivers), thus saving 11 km/h collision speed (median value of all braked accidents) and avoiding more than 22% of all pedestrian accidents. Nevertheless, the positive effect of aBAS I depends on the initiation of the drivers brake reaction. On the other hand, aBAS I does not need any pedestrian classification capability, but has to recognize pedestrians as obstacles up to a range of around 20 m (Tab. 5).

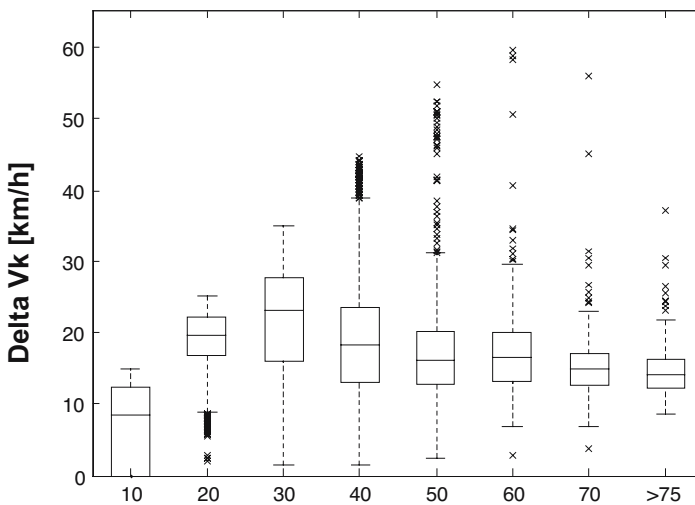


Fig. 15. exemplary boxplot of calculated reductions of collision speed for aBAS II [13], when TUB Drivers are applied on MHH data .

Additionally to aBAS I, the aBAS II systems performs a partial brake in critical situations and can reduce collision speed of unbraked accidents of 11 km/h. When the driver is braking, the collision speed can be reduced of 15.9 km/h

(median value of all braked accidents). More than 32.2% of all accidents (mostly those with lower collision speeds) can be avoided by the use of aBAS II. It has to be indicated, that only a light partial braking is performed autonomously. It depends on the specific layout of such a driver assistance system to minimise misuse cases and ensure driving pleasure.

	<i>Percentage of avoided accidents (TUB drivers)</i>	<i>median Δv_k when driver is braking (TUB drivers)</i>	<i>median Δv_k when driver is not braking (TUB drivers)</i>
<i>conventional BAS</i>	6.0 %	2,6 km/h	0 km/h
<i>aBAS I with environmental sensors</i>	22.3 %	11,5 km/h	0 km/h
<i>aBAS II with environmental sensors</i>	32.2 %	15,9km/h	Autonomous braking! 11,6km/h

Tab. 4. Analysed brake assist strategies and possible reduction of collision speed, when TUB Drivers are applied on MHH data.

By using the VERPS+-index to assess the safety benefit of the analysed driver assistance systems, a comparison of active and passive safety measures becomes possible. All calculated VERPS+- values are summarized and weighted taking the previously defined operating state probabilities in real life accidents into account.

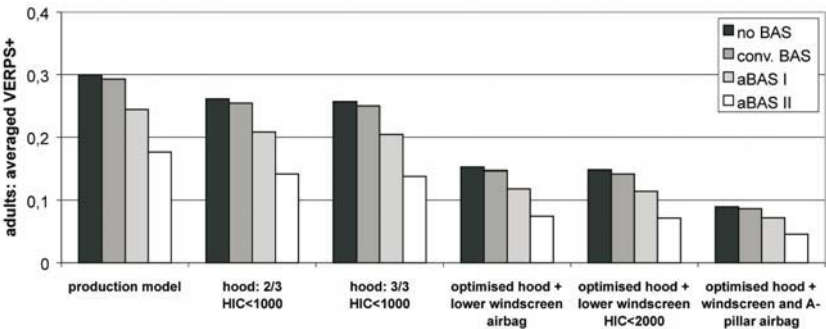


Fig. 16. Average risk for severe head injuries for adults depending on implemented structural and active safety measures applied on exemplary vehicle *H* (TUB Drivers and MHH data).

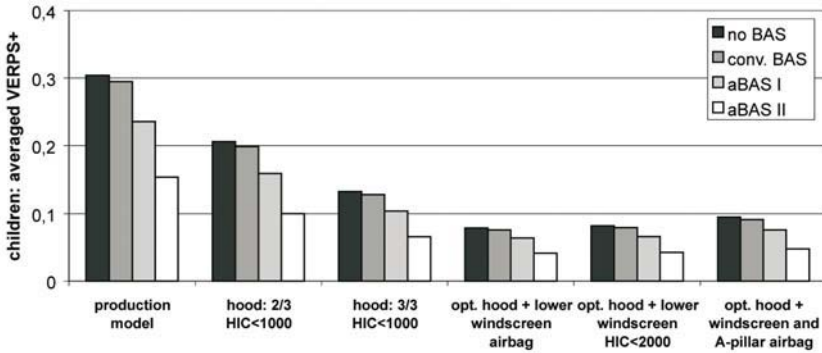


Fig. 17. Average risk for severe head injuries for children depending on implemented structural and active safety measures applied on exemplary vehicle *H* (TUB Drivers and MHH data).

4 Deriving Sensor Specification from Accident Data

Non-contact sensors detect a pedestrian prior to the first contact with the vehicle. The use of such sensors is therefore helpful to activate pedestrian protection measures in advance. Detection of a pedestrian prior to an accident can be based on different sensor principles. Of course all these sensor principles have advantages and disadvantages, but at least a pedestrian detection up to a certain range has to be possible. The sensor systems are assessed for their ability to trigger the analysed advanced brake assist systems. Therefore, a unique pedestrian classification performance is not necessary. All future environmental sensor systems must work under all possible weather conditions, offering a detection performance which is at least equal to the human eye. Optic sensors like lidar or computer vision system have disadvantages in this areas, but during the last years, these disadvantages have been minimized to a negligible amount.

4.1 Pedestrian Detection Performance

Depending on the type of brake assist system, a certain level of obstacle detection performance must be reached. It is assumed, that the first generation of environmental sensors cannot detect more pedestrians than 85% in front of the vehicle. A high false alarm rate cannot be obviated, thus making any

autonomous braking manoeuvre impossible. For autonomous partial brake manoeuvres in critical situations, the pedestrian detection performance should be as high as 95%, thus a false alarm rate near zero becomes possible. The near-zero false alarm rate makes light autonomous braking manoeuvres possible and reasonable.

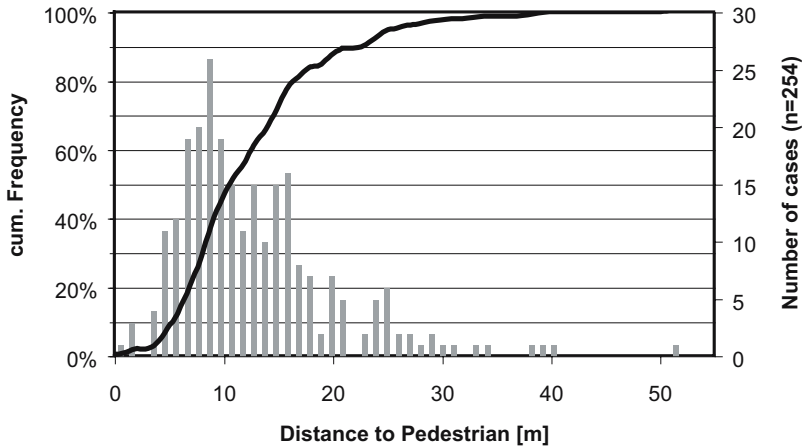


Fig. 18. Calculated distance to the pedestrian, when the drives starts to lift the throttle (virtually reconstructed from MHH data, $n=254$, using TUB Drivers, see Fig. 13)

4.2 Range and Field of View

Non-contact sensors are intended to detect a pedestrian over a certain distance. Due to the lower speed range of pedestrian accidents, range and field of view of pedestrian detection sensors are different from those used in ACC applications. Detailed analysis of pedestrian accident scenarios (MH Hanover data) shows, that the distance to the pedestrian is below 20 m in 90% of all cases, when the driver starts lifting the throttle. At this time, the driver assistance system has to “know” about the driving scenario, thus a range of 20 – 25 m would be adequate to implement pedestrian protection features. When talking about the sensors field of view, one has to keep in mind, that over 90% of all pedestrian accidents happen in urban environment, nearly 48% of urban pedestrian accidents happen at crossroads (VTIV data). Therefore, the environmental sensor system needs a much wider field of view than current ACC sensors. With the introduction of ACC Stop&Go functionality, a wider field of view is needed too.

4.3 Determination of Position, Sample Rate and Tracking Ability

The needed accuracy of position determination is crucial for system functionality. The driver assistance system has to decide whether a driving situation is critical or not. A clear view of the vehicles environment is needed. Detailed sensor specifications on position accuracy and sample rate must be estimated and verified in testing procedures. Scanning lidar systems fulfil all requirements regarding positioning accuracy very good, due to its high angular resolution. Radar signals are more cluttered and with inferior lateral and height resolution. The sample rate of Lidar and Radar systems is quite good already.

The positioning accuracy of computer vision systems is very much dependent on the resolution of the camera and the system setup. Monocular cameras need special environment models to gain depth information. Stereovision performs better in analysing 3D environmental information. A higher amount of data and therefore the more complexity of data analysis results in lower sample rates. Future pedestrian detection algorithms will run highly optimised on special ECU's.

The ability to track a pedestrian over a number of signal samples is helpful to understand the traffic situation, thus the false alarm rate is reduced and system activation probability in real-life accidents is increased. It is highly dependent on the quality of the received data and the analysing software algorithm. In some cases, neural networks are used for object tracking. As it can be seen in literature, the best performer in pedestrian tracking is the ALASCA laser scanner [10], followed by computer vision systems [14].

4.4 Pedestrian Classification

Many investigations and research work has been done in the last years in order to detect pedestrians in a traffic scenario and discriminate them from other relevant objects. Obviously, the desired driver assistance systems has huge influences on the demanded pedestrian classification performance. In this paper, two advanced brake assistance strategies have been presented, which do not need a pedestrian classification or discrimination from other objects at all. Keeping the driver in the loop means in that case, that the pedestrian classification task is not performed by the assistance system, instead it is delegated to the driver. By evaluating the drivers reaction on a detected obstacle, a check of the obstacles relevance on the current driving task becomes possible in a quite simple way. On the other hand, false activations of the driver assistance system are minimized.

Measurement category	Brake assist system	required values (Expert's opinion)	Computer vision		Radar	scanning Lidar
			Far Infrared	Visible and NIR		
Range	aBAS I and aBAS II	20 m (90 %)	+	+	++	++
Object tracking	aBAS I and aBAS II	helpful	+	+	0	++
Determination of position	aBAS I and aBAS II	± 0,1 m	++	++	+	++
Sample rate	aBAS I and aBAS II	min. 10 Hz	+	+	++	++
Object detection	aBAS I	85%	+	+	0	+
	aBAS II	95%	0	0	0	0

Tab. 5. Ranking of possible object detection technologies for active safety pedestrian protection systems

Due to the lack of a sensor that fulfils all requirements for pedestrian detection, the use of multiple sensors seems to be the way to go. A combination of a computer vision system (active NIR and visible light) and a laser scanner would be most promising. First results show that both techniques are able to detect pedestrians with appropriate performance (redundancy to decrease false recognition rate) but are complementary enough to each other to increase the overall pedestrian recognition performance due to sensor fusion effects (both sensors use data from the opposite sensor for pedestrian classification). Nevertheless, radar technologies may have advantages in vehicle package and life-time durability.

5 Summary

The VERPS-method to assess the pedestrian compatibility of a vehicle front has been presented. An evaluation of the influence of collision speed on the risk for severe head injuries has been done by expanding the VERPS-Index to VERPS+. The exact safety benefit of brake assist systems depends on vehicle specific properties, driving behaviour and accident scenarios. A group of drivers has been evaluated in order to verify the wide range of possible human interaction in emergency brake situations. It has been shown, that the additional introduction of brake assistance systems is equivalent to the protection potential of additional structural measures (active or passive). Nevertheless,

both types of pedestrian protection measures complement one another nearly ideally. It has been shown, that fully autonomous emergency braking manoeuvres are limited regarding their pedestrian protection potential. Keeping the driver in the loop and adapt driver assistance strategies in a way that the driver always keeps responsibility on the driving manoeuvres ensures customer acceptance and product liability.

References

- [1] EU-Directive 2003/102/EC on Protection of pedestrians and other vulnerable road users before and in the event of a collision with a motor vehicle
- [2] B&D (2004): Zukunftsmarkt „Aktive Sicherheitssysteme“. B&D-FORECAST-Studie, www.bd-forecast.de, access: 5.05.2004. B&D, 2004
- [3] Otte, D., Krettek, C., Brunner, H., Zwipp, H. (2003): Scientific Approach and Methodology of a new In-Depth-Investigation Study in German so called Gidas. 18th Esv-Conference, Proceedings, 2003.
- [4] Otte, D., Pohlemann, (2001): Analysis and Load Assessment of Secondary Impact to Adult Pedestrians After Car Collisions on Roads. Ircobi-Conference, Proceedings, 2001.
- [5] Ashton, S. J., Mackay, G. M.: Car Design for Pedestrian Injury Minimisation, 7th ESV Conference, 1979
- [6] ISO 13232: Test Analysis Procedures for Research Evaluation of Rider Crash Protective Devices Fitted to Motorcycles - Injury Indices and Risk/Benefit Analysis. Part 5 Rev. 1, ISO/TC22 Road vehicles, Subcommittee SC22, Motorcycles.
- [7] Kalliske, I., Kühn, M., Otte, D., Heinrich, T., Schindler, V. (2003): „Fahrzeugseitige Maßnahmen zum Schutz des Kopfes eines Fußgängers – eine ganzheitliche Betrachtung“; „Innovativer Insassen- und Partnerschutz - Fahrzeugsicherheit 2010“, Berlin, 20. – 21.11. 2003, ISBN 3-18-091794-6
- [8] Kreiss, J.-P., Schüler, L., Langwieder, K., The Effectiveness of Primary Safety Features in Passenger Cars in Germany, 19th ESV Conference, 2005
- [9] Busch, S., Entwicklung einer Bewertungsmethodik zur Prognose des Sicherheitsgewinns ausgewählter Fahrerassistenzsysteme, Fortschrittsberichte VDI Nr. 588, 2005, ISBN 3-18-358812-9
- [10] Fürstenberg, K., Pedestrian Safety Based on Laserscanner Data, Advanced Microsystems for Automotive Applications, 2005, ISBN 3-540-24410-7
- [11] Unselt, Th., Breuer, J., Eckstein, L., Fußgängerschutz durch Bremsassistentz, Conference Proceedings of „Aktive Sicherheit durch Fahrerassistenzsysteme“, München, 2004
- [12] Schulz, A., Fröming, R.: Experimentelle Untersuchungen zu Reaktionszeiten beim Führen eines Pkw unter Variation der Komplexität der Randbedingungen, TU Berlin, Institute of Automotive Engineering, internal Report, 2005

- [13] Weyer, F., Fröming, R.: Erstellung eines Einspurmodells zur Analyse der PreCrash-Phase von Fußgängerunfällen, TU Berlin, Institute of Automotive Engineering, internal Report, 2005
- [14] Gavrilă, D. M.(2004): Pre-Impact Pedestrian Sensing; Konferenz Fußgängerschutz 09.-11.03.2004 IIR Deutschland GmbH, CTI, 2004.

Dipl.Ing. Robert Fröming

ILS Kraftfahrzeuge, TU Berlin
Vehicle Dynamics / Pedestrian Safety
Gustav-Meyer-Allee 25, TIB 13
13355 Berlin
Germany
robert.froeming@tu-berlin.de

Dr.-Ing. Matthias Kühn

Verkehrstechnisches Institut der deutschen Versicherer
Friedrichstr. 191
10117 Berlin
Germany
m.kuehn@gdv.org

Prof. Dr. rer. nat. Volker Schindler

ILS FG Kraftfahrzeuge, TU Berlin
Gustav-Meyer-Allee 25
13355 Berlin
Germany
volker.schindler@tu-berlin.de

Keywords: pedestrian, brake assist, advanced driver assistance systems, sensor requirements, benefit analysis, VERPS, pedestrian compatibility, assessment, collision speed reduction

Biologically Inspired Multi-Sensor Fusion for Adaptive Camera Stabilization in Driver-Assistance Systems

W. Günthner, S. Glasauer, Ph. Wagner, H. Ulbrich, TU Munich

Abstract

The enhancement of comfort and safety is of major importance in today's research on automotive applications. Since visual information and image processing can significantly improve driver assistance systems, cameras are increasingly becoming an integral part of these systems. This paper presents an inertially stabilized camera platform for target tracking. The key point is the use of biomimetic algorithms for adaptive compensation of manufacturing tolerances. Therefore low-cost components can be used which make the system affordable in a wide range of vehicles. Initial road trials have shown the clear advantage of a stabilized camera over conventional car-fixed settings and demonstrated the usability of the proposed algorithms.

1 Introduction

Competitive driver-assistance systems are relying more and more on camera-vision systems. Wide angle cameras in the visible or infrared (IR) range are generally used to provide an overview of the environment and to detect road markers, cars and obstacles. However, a closer look at points of interest like number plates, traffic signs or children playing on the sidewalk requires cameras with a telephoto lens. These cameras have focal lengths of 16 to more than 25 mm and aperture angles of less than 10° ; they are thus extremely sensitive to motion, especially to rotation. Even a small bump can induce 100%/s rotation rates and cause the target on the camera chip to be lost. This makes active camera stabilization necessary. Since a camera operates at the usual frequency of about 25 Hz and a latency of 30 ms due to image processing, inertial camera/gaze stabilization with inertial measurement units (IMU) is the only way to ensure stable images during motion in the 2-15 Hz region. One of the goals of FORBIAS, a research cooperation of universities, car manufacturers and major automotive suppliers for biologically inspired driver assistance systems, is to achieve robust active camera stabilization with affordable and small hardware. The disadvantage in accuracy of relatively cheap MEMS sensors is compensated for by multi-sensor fusion of inertial and visual

information, and by using adaptive algorithms inspired by the latest developments in neuroscience.

2 Biological Analogy

Biological systems, from the earliest vertebrates to humans, have fulfilled the task of gaze stabilization by means of the vestibulo-ocular reflex (VOR), since a stabilization via visual signals would be too slow because of the long processing delays (~ 100 ms) of the visual system. The vestibular organ in the inner ear is the biological equivalent of a 6-DOF IMU and measures the motion of the head in space. The raw sensor signals are transmitted along a short-latency (7 ms) direct pathway through the brainstem to the extra-ocular eye muscles to stabilize gaze. A second adaptive path [1] utilizes the same vestibular information but distributes it onto the so-called parallel fibres, bundles of nerve fibres extending in the cerebellar cortex. Additionally, parallel fibres also carry visual information and internal feedback signals related to the current eye velocity. The parallel fibres form a multitude of adaptive synapses with the cerebellar Purkinje cells. These cells, gathering the synaptically weighted information transmitted by the parallel fibres, produce the output of the cerebellum, which is fused with the direct pathway in the brainstem. The adaptive process itself depends on the action of climbing fibres, another source of input to the cerebellum. Climbing fibres are driven by visual information about stabilization errors and act on a one-to-one basis on the Purkinje cells. By enhancing inertial with visual information, the biological system achieves excellent results in gaze stabilisation by adaptive calibration of the inertial sensors.

3 General System Description

This section gives a general overview of the whole system and detailed information about main subsystems. An IMU senses the vehicle motion in space and is the equivalent of the vestibular organ in the human inner ear. Its digitized output is sent via CAN bus to the main DSP (dSPACE DS1103 PowerPC) where all biomimetic algorithms for gaze stabilization are implemented. The DSP output, the required angles for each axis of the camera motion device, are transmitted to Maxon servo amplifiers (ADS). Motor positions measured by incremental encoders are fed back to the control algorithm. The camera motion device itself consists of two or three actuated axes in gimbal configuration.

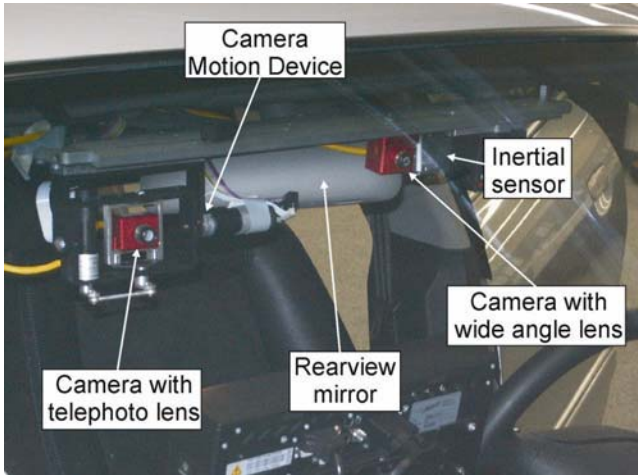


Fig 1. System setup for inertial camera stabilization

3.1 A highly miniaturized inertial Measurement Unit

The market for inertial measurement units is dominated by few global players, many of them being value-adding resellers of individual sensors from companies like Analog Devices Inc. Even the smallest IMUs currently available, like the Cloud Cap Technology's Christa IMU with dimensions of $50 \times 38 \times 25 \text{ mm}^3$ including analog-digital converter (ADC) and DSP, are far too big for the use with driver assistance systems where the IMU should more or less vanish behind or even in the rear-view mirror.

Therefore, a suitable inertial measurement unit was developed within the FORBIAS research project. In cooperation with the project's industrial automotive partners, main requirements for the new device were specified:

- ▶ Design envelope of less than 20 mm in each direction
- ▶ Mass less than 15 g
- ▶ Measurement range of up to $300^\circ/\text{s}$ and 2 g
- ▶ 12 bit resolution
- ▶ Bandwidth up to 100 Hz
- ▶ Frame rate up to 1 kHz
- ▶ CAN and RS232 Interfaces

Components

After intensive tests, the newly released LIS3LV02DQ sensor (STMicroelectronics) was chosen as a component for the IMU. This highly inte-

grated 3-axis accelerometer has a dynamically settable measurement range of 2g or 6g. The key advantage of this device is its small system size due to the integration of three axes on one chip and the direct digital output of the chip. Thus, it can be directly connected to a microcontroller using an SPI Interface. As angular rate sensor, the ADXRS300 (Analog Devices Inc.) has been chosen. Since it is pin-compatible to the ADXRS150, the same design can be used for applications which focus more on a better rate resolution with higher sensitivity and less on the measurement range. The sensor bandwidth can be set up to 100 Hz. The analog signals of the three gyroscopes are converted with a MAX1226 ADC (Maxim Integrated Products Inc.). Noise is significantly reduced by oversampling (up to $\times 32$) within the ADC. The whole inertial measurement unit is controlled by an AT90CAN128 microcontroller (Atmel Corp.). The on-board CAN controller and the small QFN64 package are ideal for miniaturization. With a 32 kB Flash version to come, the prize of the DSP will further decrease.

System Layout

Miniaturization was the highest priority for designing the new inertial measurement unit. In order to achieve an extremely small design envelope, we chose a six-sided completely closed cubical setup with an edge length of 15 mm. Except for the interface transceivers, all components of the IMU could be placed inside the cube (Fig. 2 left).

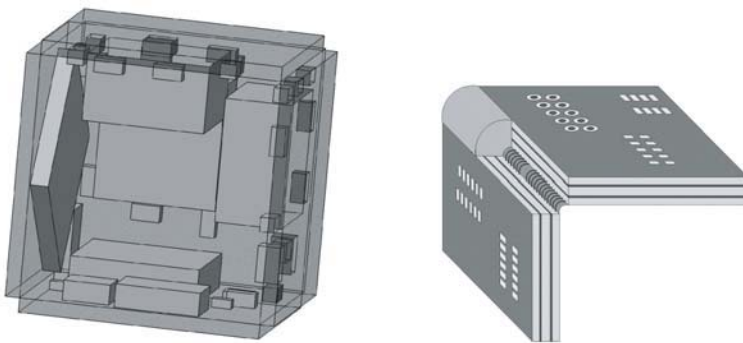


Fig. 2. Left: Model of cubical IMU (one side opened for clarity); right: Wirelaid PCB

One main challenge for inertial measurement units is the electrical connection of the necessarily more or less orthogonal circuit boards. On most commercially available IMUs, the boards are connected at their edges with soldering pads. However, these connections use several mm^2 on the circuit boards and

prohibit further miniaturization. Additionally, they lie open and are not very resistant to vibration. For our IMU we developed together with JUMA GmbH (Germany) stiff but foldable circuit boards using Wirelaid PCB technology. Connections of the rectangular boards are ensured by wires with a diameter of 150 μm which are welded onto the top or bottom layer inside the circuit board. In contrast to regular PCBs, these connections are maintained when folded. But since the board itself does not contain any completely flexible parts, the required stiffness for the IMU can be provided.

3.2 Systems for Gaze Control

For active gaze stabilization, a high precision camera motion device (Fig. 3) has been developed within the FORBIAS project. In a serial gimballed configuration the camera is actuated around two perpendicular axes. The inner frame containing the pan actuator and the pivoted camera is driven by the tilt actuator containing a 11 Watt Maxon motor (RE-max 24) combined with a backlash free HarmonicDrive HDUC-5-50 gearbox with a reduction ratio of 50:1. The pan actuator can be less powerful, so a 4.5 Watt motor (RE 16) is used. For the control of each axis differential encoders with 512 steps, i.e. 2048 quadcounts per revolution, provide sufficient resolution.

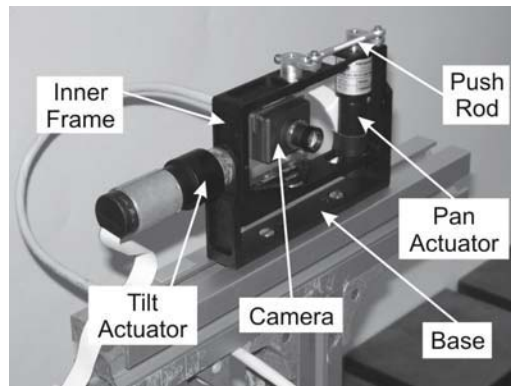


Fig. 3. Camera motion device, shown in a two-degree-of-freedom configuration

In this configuration, each axis can be controlled within tolerances of less than 0.05° . The camera module (Siemens VDO) features a CMOS sensor with an effective resolution of 750×400 pixels, 11 mm pixel size and a global shutter. The lens shown has a focal length of 16 mm.

For further miniaturization of the gaze control, a completely different hardware is in the process of development (Fig. 4). In the future, we will not actuate the camera itself but a small mirror in front of it. The actuator has a design envelope with edge lengths of less than 65 mm (not including the camera itself).

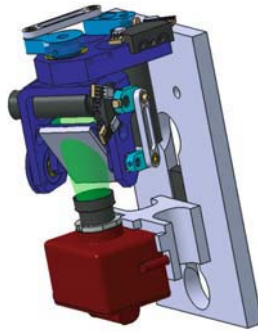


Fig. 4. New concept for miniaturized gaze control

3.3 Biomimetic Algorithms

The control algorithm for inertial camera stabilization is based on a computational model [2] of the angular vestibulo-ocular reflex (VOR, Fig. 5). The vestibular organ (IMU), in this case the semicircular canals, senses rotations of the head (car). In a direct pathway, an inverse stabilization command is sent to the eye's muscles (camera motion device). The direct pathway, even though it is very rapid due to only three neurons being involved, is not very accurate, because it cannot compensate for any changes in the system, e.g. due to development or aging. Therefore, a second parallel pathway through the cerebellum is continuously adapted to achieve perfect gaze stabilization. Vestibular signals, efference copies (feedback) of eye muscle commands and visual signals are sent to so-called parallel fibers in the cerebellum. A teaching signal containing visual and feedback information is formed in the inferior olive (lower brainstem) and passes through climbing fibers to the Purkinje cells. In each Purkinje cell, input from several thousand parallel fibers are combined for one output, using one climbing fiber teaching signal.

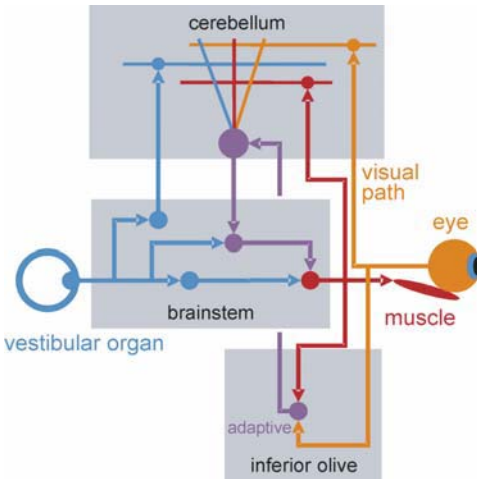


Fig. 5. Simplified outline of involved in adaptive vestibular gaze stabilization (VOR)

The task of the vestibulo-ocular reflex can be understood as active noise control [3], with the noise being the unwanted head movement which contaminates the visual signal. The noise is measured independently from the signal by the inertial sensors, and is then removed from the signal by actively moving the eyes in opposite direction. The adaptive component can, as first approximation, be seen as equivalent to what is known in engineering as filtered-x LMS algorithm [3]. Fig. 6 shows the block diagram of the gaze stabilization algorithm, assuming equal dynamic behaviour for each actuated axis.

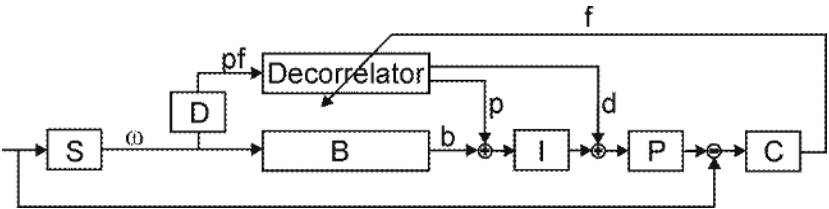


Fig. 6. Block diagram of biomimetic control for gaze stabilization. See text for explanation.

In the technical system, motion of the car is sensed by the gyroscopes of the inertial measurement unit S . The output of the “brainstem” B corresponds to the direct path and is calculated as

$$\mathbf{b} = \mathbf{JS}\omega \quad (1)$$

with the nominal diagonal sensitivity matrix \mathbf{S} and the Jacobian \mathbf{J} , projecting angular rates ω on the degrees of freedom of the camera motion device. Integrated in I, this part models the direct pathway in the neurological system.

In the adaptive path, angular rates ω are decomposed (D) into “parallel fibre” signals \mathbf{pf} . In our case, we chose to use measured angular rates and their derivatives, similar to a notch filter.

$$\mathbf{pf} = \left[\frac{\omega}{d\omega/dt} \right] \quad (2)$$

The basic idea of the adaptive algorithm is decorrelation of gyroscope signals and residual optic flow. Decorrelation control has already been proposed as the underlying mechanism in adaptation of the biological VOR [4]. Residual optic flow consists of three different parts: flow induced by vehicle rotation, translation of the camera (driving the vehicle) and changes in the outside world like self motion of other cars, pedestrians etc. For understanding the algorithm, it is important to know that only the first part, the vehicle’s own rotation and the corresponding optic flow (OF) is correlated to gyroscope signals. As soon as the algorithms manages to decorrelate OF from gyro signals, or better from their decompositions \mathbf{pf} , residual optic flow is no longer predictable from inertial angular rate measurement and therefore comes from either the vehicle’s translation or changes in the outside world.

As outlined below, flow caused by vehicle translation can be reduced by means of visual tracking (smooth pursuit) of space-fixed targets. Visual tracking also allows the camera to follow moving targets, e.g., other vehicle, thereby reducing local flow confined to the target.

In the decorrelator, all incoming decomposed signals are adaptively combined for each nominal axis. The underlying idea of adaptive linear combination is very close to the biological system with Purkinje cells extracting information from the parallel fibres. Due to the use of all gyroscope signals for adaptive adjustment of each axis, possible non-orthogonalities can be compensated for, thereby reducing the required tolerances and thus significantly reducing fabrication costs.

The proportional output of the decorrelator is added to the brainstem output \mathbf{b} and can be expressed as

$$\mathbf{p} = \mathbf{J} \begin{bmatrix} \mathbf{w}_p & \mathbf{w}_d \end{bmatrix} \begin{bmatrix} \mathbf{E}^{3 \times 3} & \mathbf{0}^{3 \times 3} \\ \mathbf{0}^{3 \times 3} & \mathbf{0}^{3 \times 3} \end{bmatrix} \mathbf{p}\mathbf{f}, \mathbf{w} = \begin{bmatrix} \mathbf{w}_p & \mathbf{w}_d \end{bmatrix} \in \mathbb{R}^{3 \times 6} \quad (3)$$

with ω_p and ω_d corresponding to weights of angular rates and their derivatives respectively. The output of the derivative path is fed into the system after the Integrator I with

$$\mathbf{d} = \mathbf{J} \begin{bmatrix} \mathbf{w}_p & \mathbf{w}_d \end{bmatrix} \begin{bmatrix} \mathbf{0}^{3 \times 3} & \mathbf{0}^{3 \times 3} \\ \mathbf{E}^{3 \times 3} & \mathbf{0}^{3 \times 3} \end{bmatrix} \mathbf{p}\mathbf{f}, \mathbf{w} = \begin{bmatrix} \mathbf{w}_p & \mathbf{w}_d \end{bmatrix} \in \mathbb{R}^{3 \times 6} \quad (4)$$

Note that $d\omega/dt$ is not used for either \mathbf{d} or \mathbf{p} directly, but is needed for weight updating, and has thus to enter the decorrelator. For weight update, an anti-hebbian learning rule is used

$$\dot{\mathbf{w}} = -\mathbf{f} \cdot \mathbf{p}\mathbf{f}^T \cdot \hat{\mathbf{a}} = - \begin{bmatrix} f_x \\ f_y \\ f_z \end{bmatrix} \begin{bmatrix} \omega_x & \omega_y & \omega_z & d\omega_x/dt & d\omega_y/dt & d\omega_z/dt \end{bmatrix} \begin{bmatrix} \beta_p \cdot \mathbf{E}^{3 \times 3} & \mathbf{0}^{3 \times 3} \\ \mathbf{0}^{3 \times 3} & \beta_d \cdot \mathbf{E}^{3 \times 3} \end{bmatrix} \quad (5)$$

where \mathbf{f} is the OF projected into the coordinate system of the IMU. β_p and β_d are learning rates of the proportional and derivative path. Following the idea of filtered-x LMS algorithms, $\mathbf{p}\mathbf{f}$ could be pre-filtered with an estimate of the plant's transfer function before the weight update. Laboratory experiments showed that this pre-filtering does not significantly improve the performance in the frequency range of gaze stabilization.

As mentioned above, inertial camera stabilization reduces overall optic flow caused by unwanted rotational motion and thus removes noise from the images. However, camera stabilization alone would not be suitable for collecting visual information, since perfect stabilization would not keep the line of sight on the road. We therefore implemented rapid changes of the camera's viewing direction, called saccades in biology [2]. These saccades may occur either when the line of sight is too far from the car's long axis (equivalent to vestibular nystagmus) or when a novel target should be looked at (equivalent to voluntary saccadic gaze shifts). As in the biological system, saccades and stabilization of the line of sight interact seamlessly and, most importantly, without affecting the efficiency of the adaptive adjustments.

Especially when using telephoto lenses, camera stabilization together with saccades are not sufficient for a driver assistance system, since closer inspection of road markers, other vehicles, etc., necessitates yet a third type of camera motion: visual tracking. Again, the basic principles can be adopted from biology: primates developed the smooth pursuit system for visual tracking. The smooth pursuit system is intimately linked to the VOR system, and exploits the same neuronal structure as used for VOR adaptation, the cerebellum, as final pathway to convey visual information to the eye muscles. Inspired by nature's solution, we implemented visual tracking in our system [5]. The problem of visual processing time in the order of 40-100 ms, which could cause instability of the tracking feedback loop, was solved by internally reconstructing target motion in space using a delayed combination of camera movement signal and IMU data. Fusion of tracking and stabilization commands was based on the simple consideration on how target velocity in space \mathbf{t}_s , camera velocity in the car \mathbf{c}_c , and car velocity in space ω (measured by the IMU) interact. Camera velocity in space can be expressed as $\mathbf{c}_s = \mathbf{c}_c + \omega$. Thus, the error between camera velocity and target velocity $\mathbf{e} = \mathbf{t}_s - \mathbf{c}_s = \mathbf{t}_s - \mathbf{c}_c - \omega$ can be used to drive camera motion. Note that, for simplicity, the equations are given for the one-dimensional case.

Visual tracking may, at least in the low frequency range, take over camera stabilization, thus compromising the success of the adaptive algorithm outlined above. Therefore, either adaptation or tracking was switched off in the evaluations shown below. However, a possible biomimetic solution has already been proposed [6] which is based on adaptation at multiple sites. Compared to other technical stabilization systems proposed on the basis of biological analogy [7], the present systems offers transparent algorithms together with flexibility and the same variety of camera movements as known from biology.

4 Experimental Evaluation under Laboratory Conditions

For experimental evaluation under reproducible conditions, a test setup with the Steward-Gough platform of the Institute of Applied Mechanics at the TU Munich has been chosen. The inertial measurement unit and the camera motion device are bolted to the upper platform (Fig. 7). The hexapod's tool centre point (TCP) is in the middle of the upper platform and was held constant during all experiments. The platform's orientation is defined with cardan angles α , β and γ . Due to the 2-dof-setup for camera motion, α was held at zero while β and γ were sine-waves with 12.5° amplitude and a frequency of 3 and 4.5 rad/s respectively. This motion led to sensed angular rates of approximately 100%/s.

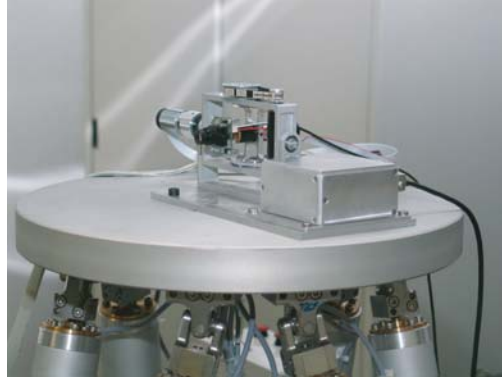


Fig. 7. Experimental setup on Steward-Gough platform

With the camera CCD being approximately 60 mm away from the stable TCP, translational displacements are limited to about 25 mm. The image from the analog camera with telephoto lens (focal length 16 mm) was digitized with a frame grabber (Bt787 chipset) and used for online optic flow calculation which was the teaching signal in these test.

We performed two different types of tests. In one series the algorithm started without any knowledge of the sensory system and the dynamic performance of the actuating unit. The gaze stabilization system learned to identify the three rotational sensors, their non-orthogonality and sensitivity. Additionally, the inverse of the system's transfer behaviour was approximated.

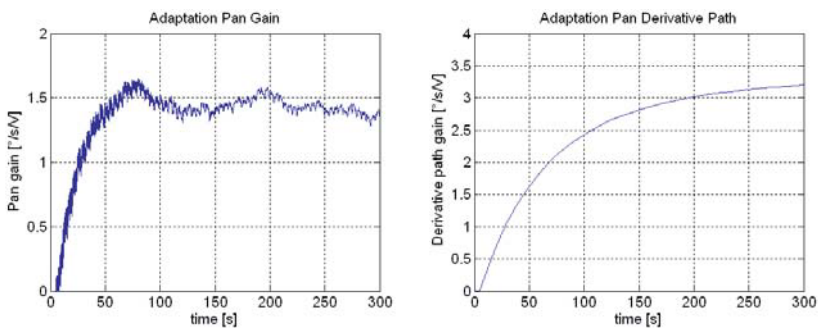


Fig. 8. Adaptation of sensitivity (left) and derivative path gain (right) for gyro corresponding to pan axis (in neutral position)

In a second series we started adaptation with nominal sensor characteristics, however non-orthogonality, errors in sensitivity from nominal values and

transfer behaviour still had to be compensated for. Fig. 8 (left) shows the adjustment of sensitivity. Although the difference to nominal sensitivity was only 0.75%, the corresponding difference in angular rate of about 1°/s was very disturbing and recognizable with a telephoto lens and an aperture angle of less than 15° in any direction. As explained above, the derivative path compensates for the transfer behaviour of the system approximated to have one pole.

At the beginning of adaptation, optic flow of the pan (horizontal) direction exceeded 6 pixel/frame (Fig. 9). The subjective impression of the camera video was quite bad, the video could hardly be used for any further purposes. After one minute of adaptation, residual optic flow reduced significantly to about 2 pixel/frame. After 2-3 more minutes, optic flow was down to the sub-pixel range. Image processing mostly detected 1 pixel/frame every few seconds. For the spectators, the video of the camera seemed completely stable.

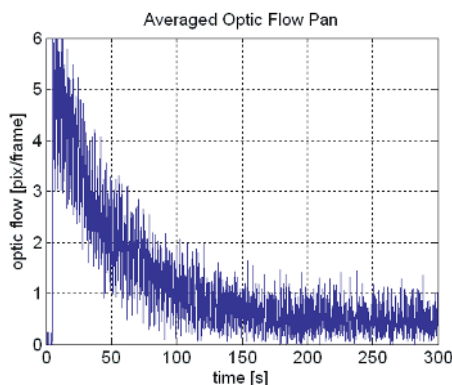


Fig. 9. Residual optic flow for pan axis

5 Verification in Road Trials

The adaptive system as introduced in chapter 3.3 and evaluated in chapter 4 was tested in road trials. With adaptation together with visual tracking being still in the phase of implementation, the parameters for the camera stabilization system were adapted under laboratory condition with a stable line of sight (LOS).

The inertial measurement unit and the camera motion device were mounted in the test vehicle as shown in Fig. 1. An additional camera with wide angle lens was used for the general overview of the environment and to detect a

point of interest for the camera with telephoto lens. The point of interest was coded in platform coordinates and defined the primary reference for the LOS. The camera was stabilized around this reference using the inertial measurement unit as described above. If the difference between the desired LOS and the camera axis was more than 1.5° , a saccade was initiated. For visual tracking, target velocity in space was fused with IMU data so that the point of interest remained stable on the telephoto camera. The required target position and velocity, which were determined by combining visual information with vehicle velocity and yaw rate, were sent via the framework's CAN interface to the gaze control system. Since translatory vehicle movement is known to the driver assistance systems, tracking of space fixed targets was considerably improved by fusing visual signals collected by the camera with information about vehicle motion.

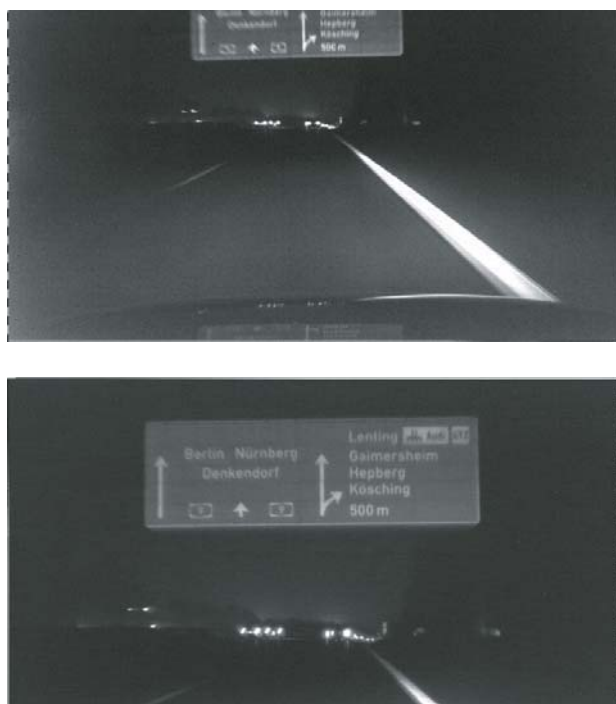


Fig. 10. Road trials with static wide angle camera (above) and inertially stabilized camera with telephoto lens

During the tests, three different modes were evaluated. In mode 1, a lane marker about 60 m ahead was chosen and then followed with the stabilized camera until it reached a distance of 20 m. Then the next marker was selected. In a second series, lane separation in a constant distance of about 40 m was

focused. In a third mode, no target was defined but the camera was stabilized around a constant line of sight.

In all modes, bumps in the road, as well as low frequency pitch could be well compensated for. Especially when driving in the dark, the inertially stabilized camera significantly improves the readability of road signs. While with longer exposure times indications are blurred in images of the wide angle camera, the camera with telephoto lens showed well readable writing on the signs (Fig. 10). This is especially remarkable since the effects of motion are more adverse when using lenses with longer focal lengths.

7 Conclusions

This paper introduced an inertially stabilized camera platform for driver assistance systems with the focus on biologically inspired multi-sensor fusion of data from an inertial measurement unit and image processing. Adaptive algorithms have been developed to compensate for non-orthogonality of sensitive sensor axes and deviations from nominal sensor characteristics due to loose manufacturing tolerances and variability of low-cost MEMS sensors. This helps reducing the cost of actively stabilized camera systems significantly since the use of expensive sensors and highly precise fabrication is not necessary. The system showed its capacities and improvements to current technology in first test drives. With a new miniaturized version of a gaze manipulation device being available soon, this can be the basis of driver assistance systems.

References

- [1] Lisberger SG. Physiologic basis for motor learning in the vestibulo-ocular reflex. *Otolaryngol Head Neck Surg* 119:43-48, 1998
- [2] Glasauer S. Cerebellar contribution to saccades and gaze holding: a modeling approach. *Ann N Y Acad Sci* 1004:206-219, 2003
- [3] Kuo SM, Morgan DR. Active noise control systems: algorithms and DSP implementations. John Wiley & Sons, NJ, 1996
- [4] Dean P, Porrill J, Stone JV. Decorrelation control by the cerebellum achieves oculomotor plant compensation in simulated vestibulo-ocular reflex. *Proc Biol Sci* 269:1895-1904, 2002
- [5] Glasauer, S., Günthner, W., Wagner, P., Bardins, S., Ulbrich, H., Adaptation in the vestibulo-ocular motor system: Technical realisation, ESF-EMBO Conference on

Three-Dimensional Sensory and Motor Space, San Feliu de Guixols, Spain, October 8-13, 2005

- [6] Günthner, W., Glasauer, S., Wagner, P., Bardins, S., Ulbrich, H., Technical Realisation of Adaptive Sensor and Plant Compensation for Three-Dimensional Gaze Stabilisation, No. 391.8, Society for Neuroscience, Washington DC, USA, November 12-16, 2005
- [7] Panerai, F., Metta, G., Sandini, G., Learning visual stabilization reflexes in robots with moving eyes, *Neurocomputing* 48: 323-337, 2002

W. Günthner, S. Glasauer, Ph. Wagner, H. Ulbrich

Institute of Applied Mechanics, TU Munich, BCCN Munich, LMU Munich
 Boltzmannstr. 15, 85748 Garching
 Germany
 guenthner@amm.mw.tum.de

Keywords: camera stabilization, gaze stabilization, driver assistance systems, inertial measurement unit, biologically inspired, adaptive control, neuroscience.

Low Speed Collision Avoidance System

J. Kibbel, H. Salow, M. Dittmer, IBEO Automobile Sensor GmbH

Abstract

Most collisions occur with ahead driving vehicles or at speed below 30 km/h, respectively. Driving in columns is tiring and can lead to inattention and distraction and is therefore one of the main sources of accidents. A Low Speed Collision Avoidance System can help the driver avoiding these kinds of accidents.

1 Introduction

Driving in urban areas can be a challenge not only for inexperienced drivers. The driver is distracted by information from inside the car like for example messages from the entertainment system, the navigation system, the telephone, the radio or passengers. Additionally the driver has to deal with all the information from outside the car like traffic signs or the behaviour of other road users. Just a moment of distraction is enough to cause a collision on city streets. The Low Speed Collision Avoidance System can help the driver avoiding these accidents by analyzing the area in front of the car. If an upcoming crash is detected the system will brake the car automatically to avoid the collision.

2 The Measurement System

The ALASCA XT Laserscanner used for environment detection is the latest member of IBEO Automobile Sensor GmbH Automotive Laserscanner family.

This Laserscanner can be integrated in the vehicle behind a plastic by consideration of the design of the vehicle. The sensor offers a horizontal field of view of up to 240° with an angular resolution between 0.1° and 1.00°, depending on the scan frequency, which can be modified from 12.5 Hz to 25 Hz during operation. The radial range for object detection is from 0.30 m up to 200 m.

The four scan planes obtain a vertical opening angle of 3.2° in the vertical direction. This allows a compensation of the vehicle pitch angle, as shown in Fig. 2.



Fig. 1. ALASCA XT multilayer Laserscanner

For more information on Laserscanner and their operating principle see [1].

Based on the measured scan data a tracking algorithm detects objects and calculates their velocity, size and class [2]. With these detailed information about the surrounding of the car many application can do individual things like collision mitigation.



Fig. 2. ALASCA XT Laserscanner with four individual scanning planes

3 Low Speed Collision Avoidance Application

The Low Speed Collision Avoidance System assists the driver to avoid rear end collisions in urban areas. To detect an upcoming accident a monitored area is calculated. The length of this area is depending on the ego velocity and on the velocity of a potential collision object. It consists of three parts (Fig. 3), the safety distance, the system delay and the braking distance.

The first part is the minimum distance between the ego vehicle and an object after the braking, the safety distance. To optimize the distance several test drives were made with different drivers. These tests showed that if the safety distance is too small the driver have less confidence in the system. If the distance is too large the system may brake the car even if the driver feels that he could still master the traffic situation. It seems that a distance of about one meter is the distance that is accepted by most drivers.

The delay time of the braking system is responsible for the second part, the system delay s_d . Even if the delay time of modern brakes was reduced in the last years, it still takes some time for the brakes to achieve the full deceleration that was requested by the system. The system delay s_d depends on the velocity of the ego car v_{ego} and on its maximum deceleration a_{dec} :

$$s_d = \left(v_{ego} + \frac{a_{dec}}{6} t_{SystemOffset} \right) t_{SystemOffset} \quad (1)$$

The third part, the braking distance offset s_b , is depending on the ego velocity and the velocity of a potential collision object. If we assume that the car in front has the same maximum deceleration than the ego vehicle but a lower velocity v_{obj} , we have to compensate the shorter braking distance of the car in front. The braking distance offset is the difference between the braking distance of the ego vehicle and the braking distance of a potential collision object. Because the velocity of the ego vehicle is already reduced during the system delay time, the offset can calculated as follow:

$$s_b = \frac{\left(\left(v_{ego} + \frac{1}{2} a_{dec} t_{SystemOffset} \right) - v_{Obj} \right)}{2a_{dec}} \quad (2)$$

Furthermore, the direction of the monitored area is depending on the front wheel angle. If an object like a car, truck, pedestrian or bike is entering the monitored area, the car is decelerated as long as the object is located within the monitored area to avoid a rear-end collision accident. If the collision object is leaving the monitored area or if the driver sidesteps the object, the braking is discontinued. Test drives showed that triggering the brakes puts the attention of the driver to the critical area in front of the car so that the driver can remedy the critical situation without any further support.

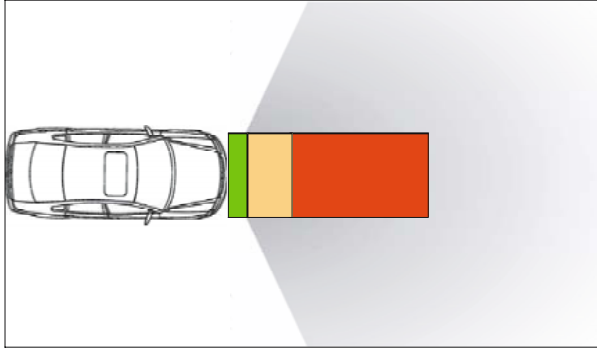


Fig. 3. Field of view of the Laserscanner (grey). Monitored area consisting of: Minimum distance to target after braking, the safety distance (green). System delay, depending on the vehicle velocity (orange). Braking distance offset depending on the ego velocity and the velocity of a potential collision object (red).

4 Typical Traffic Scenes

In the following three typical traffic scenes and the corresponding reaction of the Low Speed Collision Avoidance Application are analysed.

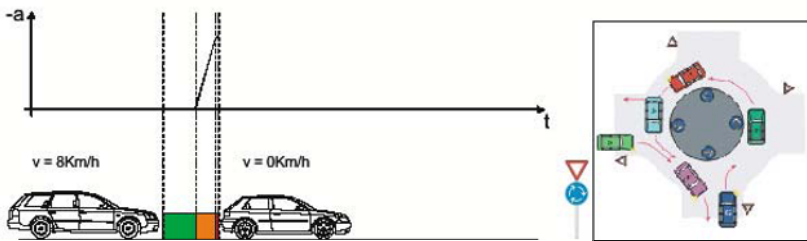


Fig. 4. Critical situation at roundabouts (right). Monitored area in front of the car (bottom left). The length of this area is dominated by the safety distance (green). The system delay distance (orange) is shorter than the safety distance. The braking distance offset (red) is much smaller than the safety distance. The time depending deceleration of the ego vehicle (top left).

One of the main sources of rear end collisions is entering a roundabout (Fig. 4). A car in front of the ego vehicle seems to enter the roundabout. The driver then puts the focus on trying to find a gap in the traffic inside the roundabout and starts entering the roundabout. If the car in front is still waiting to enter

the roundabout a rear end collision may happen. The Low Speed Collision Avoidance Application is monitoring the area in front of the ego vehicle and because of the low velocity of the car this area is dominated by the length of the safety distance. The driver can still get very close to vehicle in front, to observe the roundabout, without being disturbed by the system. Not until the driver is getting to close, the system will brake the vehicle to avoid an accident.

If the driver is distracted in urban areas he could easily oversight for example a traffic jam (Fig. 5). In this situation the Low Speed Collision Avoidance System could put his attention to the critical situation in front of the car. Then the driver has the possibility to control the situation on his own by braking the car or by giving way. Otherwise if the driver does not react appropriate the system will brake the car as long as there are objects inside the endangered area. Because of the relative low difference between the velocity of the ego vehicle and the potential collision vehicle the braking distance offset is small and the system delay distance is dominating the length of the monitored area in front of the car.

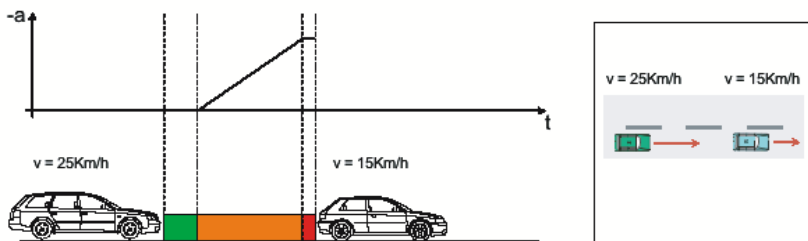


Fig. 5. Critical situation with a slow driving vehicle in front of the ego vehicle (right). Monitored area in front of the car (bottom left). The length of this area is dominated by the system delay distance (orange). The safety distance (green) and the braking distance offset (red) are shorter than the system delay distance. The time depending deceleration of the ego vehicle (top left).

A very dangerous situation can occur if the driver is approaching a stationary vehicle without noticing it (Fig. 6). Because of the huge different velocity of both cars the monitored area is much longer than in the previous example and is equivalent to the situation where no object is detected in front of the car. If a stationary object is detected in front of the car the Low Speed Collision Avoidance System has to trigger the brake much more in advance. If the system detects that the driver is aware of the critical situation the control of the brakes is put back to the driver. To detect the alertness of the driver, the move-

ment of the steering wheel as well as changes at the accelerator or the brake pedal are analysed.

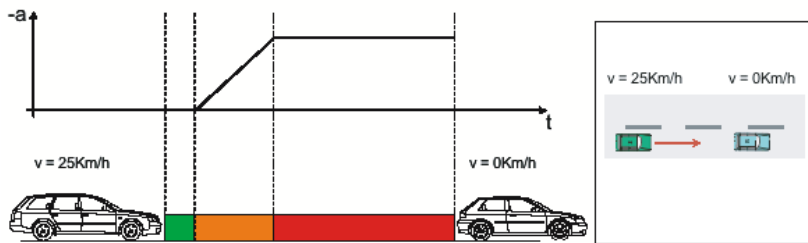


Fig. 6. Critical situation with stationary vehicle in front of the ego vehicle (right). Monitored area in front of the car (bottom left). The length of this area is dominated by the braking distance offset (red). The safety distance (green) and the system delay distance (orange) are shorter than the braking distance offset. The time depending deceleration of the ego vehicle (top left).

5 Conclusion and Outlook

The Low Speed Collision Avoidance System has the potential to decrease the number and the costs of rear end collision in urban area dramatically. To avoid a collision the system triggers the brakes if a dangerous situation is detected. By triggering the brakes the attention of the driver is put to critical area in front of the car. In most times the driver then takes control and can avoid a collision either by giving way, if possible, or by braking the car. If the driver is not reacting appropriate the system will bring the car to a halt or releases the brakes if the object in front left the endangered area.

References

- [1] www.ibeo-as.de

Jörg Kibbel

IBEO Automobile Sensor GmbH
Fahrenkrön 125
22179 Hamburg
joerg.kibbel@ibeo-as.com

Keywords: Alasca, laserscanner, collision avoidance

Laserscanner for Multiple Applications in Passenger Cars and Trucks

R. Schulz, K. Fürstenberg, IBEO Automobile Sensor GmbH

Abstract

Driver assistance systems for both passenger cars and commercial vehicles have made much progress throughout the past few years. Laserscanners have proven to meet the requirements for serving as their sensor backbone. This article focusses on the potential of automotive laserscanners supporting advanced driver assistance systems on passenger cars and trucks.

1 Introduction

The introduction of active and passive automotive safety systems has significantly contributed to the reduction of traffic accidents and injuries. Nevertheless european road traffic takes a toll of 40000 lifes every year. The next step to increase traffic safety will be taken by the introduction of advanced driver assistance systems as proposed by the European Comission. Its e-safety initiative [1] sets the goal of reducing the number of traffic accidents by the year 2010 by 50%. Applications like distance alert, lane guiding assist, collision mitigation, or drowsy driver warning assist will help to reduce the consequences of crashes for all collision partners. Before this background advanced driver assistance systems for passenger vehicles have been receiving much attention throughout the past few years. Less noticable, advanced driver assistance systems for trucks have also made much progress. For the general acceptance of advanced driver assistance systems reliable sensors with a high degree of availability -even under adverse environmental conditions- are indispensable. Infrared laserscanner technology stands in the first line amongst the sensor technologies of the choice.

This article focusses on the applications of laserscanners, developed by IBEO Automobile Sensor GmbH. Their capability of a high range finding distance of up to 200 m in combination with a fine horizontal resolution make it a favourable technology for applications in classic ACC systems in combination with applications like Stop & Go including automatic restart, Lane Departure Warning, Pedestrian Protection, Pre-Crash, and Automatic Emergency Brake. For commercial vehicles the applications Slow Moving Assist, Turning Assist,

and Cut-In Assist are of predominant relevance. All mentioned applications can be operated by one single laserscanner system.

2 ADAS Applications Overview

The ALASCA XT laserscanner series developed by Ibeo Automobile Sensor supports up to seven ADAS applications each, on passenger cars and commercial vehicles. While some of them like Automatic Emergency Brake and Lane Departure Warning are common for both vehicle types the Turning Assist and the Slow Moving Assist are specifically designed to serve the needs of commercial vehicles. An overview of the applications is presented in Fig. 1.

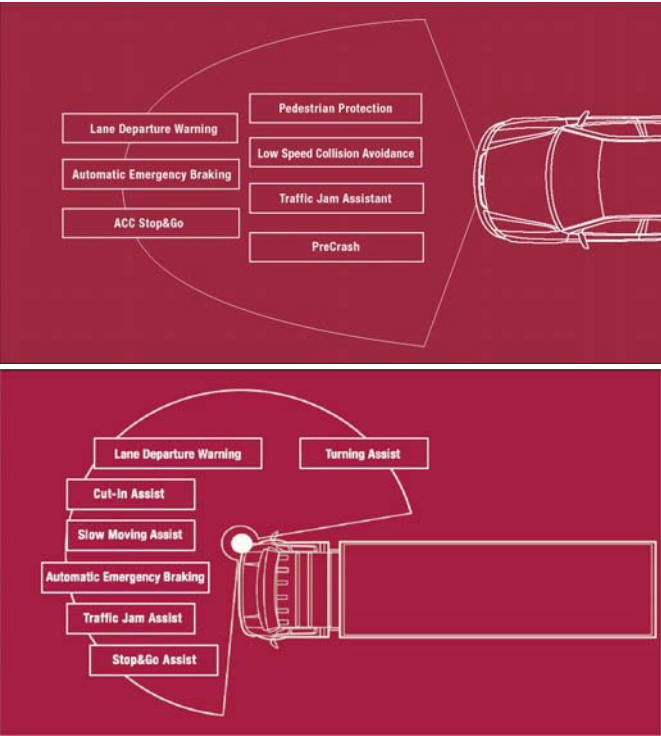


Fig. 1. ADAS applications for passenger cars (top) and trucks (below) supported by a single Laserscanner ALASCA XT system

In the following sections laserscanner performance under adverse weather situations will be addressed and specific attention will be paid to a selected set of ADAS applications on passenger cars and commercial vehicles.

3 Environmental Robustness of the Laserscanner System

The ALASCA laserscanner series developed by Ibeo Automobile Sensor was designed such that adverse weather conditions would not inhibit a reliable performance of the application. Specifically tests with dense traffic on expressways under heavy rain fall conditions proved full functionality (see Fig. 2). Problems of blooming, as known from video technology, are unknown to the laserscanner because it carries its own light source and sunlight is removed by an adequate filtering technique. Also there exists no danger of being blinded by other vehicles which themselves are carrying infrared sensors. The receiver characteristics of the laserscanner matches at the worst only for the fraction of a second the transmitter characteristics of the sensor on the other car which results in the drop-out of a small number of measurement points. These points can easily be removed by a software filtering process and do not affect the performance of applications.

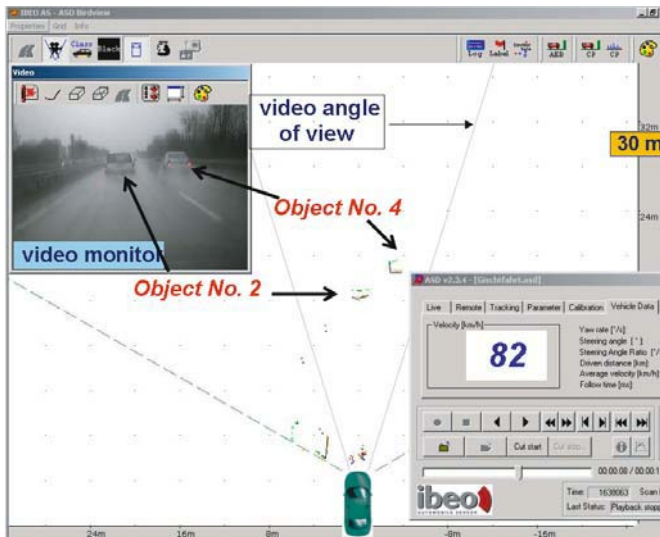


Fig. 2. Expressway driving scene under heavy rainfall conditions. Speed = 82 km/h. The main frame shows the laserscanner data and the tracked vehicles (objects). The top left insert shows the video monitor.

The performance of the ALASCA system was tested in Sweden during winter conditions. All automotive requirements were met. Fig. 3 shows a screen shot of a test driving situation where a passenger car is detected by the ALASCA XT system at a distance of 225 m.

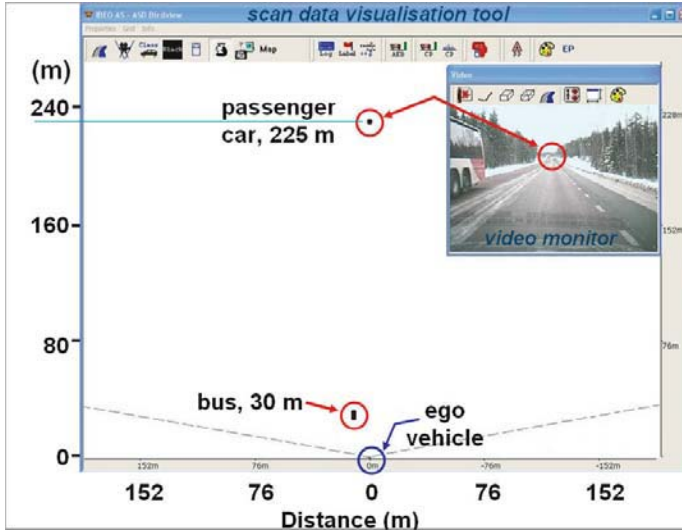


Fig. 3. Screen shot of a driving situation during winter test in Sweden where a passenger car at 225 m ahead is picked up by the laser-scanner system.

4 Vehicle Integration

The integration of a laserscanner into a vehicle includes two aspects of work. The mechanical part must ensure that the sensor can be accommodated within the contour of the vehicle body. The second part consists of its integration into the electronic network. Via the vehicle CPU the ALASCA applications transmit their commands, e.g. to the throttle or to the brakes of the vehicle. In the reverse direction the ALASCA CPU continually receives vehicle data, e.g. steering angle, yaw-rate, speed, and brake pressure.

For development purposes a recording system, consisting of a video camera and a computer, may be connected. The entire data stream of the ALASCA system together with the video image may be stored for later evaluation purposes. Meanwhile a number of vehicles from different manufacturers has been equipped with an ALASCA system by IBEO AS. Depending on the developmental requirements either a single central sensor with a horizontal opening angle of 150° or a sensor pair with 240° was built in. In the latter case the ALASCA data are fused in order to provide a unique stream of commands to the vehicle system.

5 Applications

5.1 ACC with Stop & Go

The first Adaptive Cruise Control systems (ACC) were introduced about 10 years ago as comfort systems in upper class passenger cars. However they only reached a relatively small market penetration. Starting at a minimum speed of about 30 km/h these radar-based systems control the speed depending upon distance and speed of the preceding vehicle. Below the minimum speed a control function is not available due to the fact that the low horizontal resolution of radar-based sensors does not permit a safe surveillance of the immediate proximity of the car.

With the new ALASCA XT it has become possible to simultaneously run long range and short range ADAS applications. Adaptive cruise control can now be operated within the full speed range from low speed city traffic (including full stop) to high speed expressway traffic. While for ACC a range of up to 200 m is of predominant importance, Stop & Go requires the wide horizontal scan angle paired with a fine angular resolution. This feature ensures an early detection of cut-in and cut-out procedures which results in a significant increase in comfort and safety for controlling the longitudinal speed. After an automatic stop the system has the capability of evoking a safe automatic restart because there exists sufficiently dense information about objects in the immediate proximity of the car.

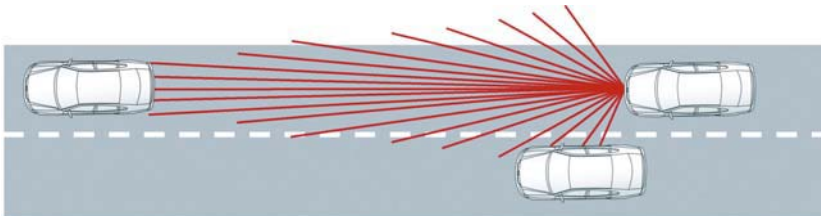


Fig. 4. Schematic of laserscanner supported full range ACC with Stop & Go. The integrated laserscanner ALASCA XT detects objects up to a distance of 200 m in a horizontal scan area of 150°.

A driving szenario with a laserscanner in a typical Stop & Go situation is shown in Fig. 5 as seen by the measurement system. The left part of Fig. 5 shows the screen shot of the laserscanner data from a bird-view perspective. The right part of Fig. 5 exhibits the corresponding video image which serves for reference purposes only.

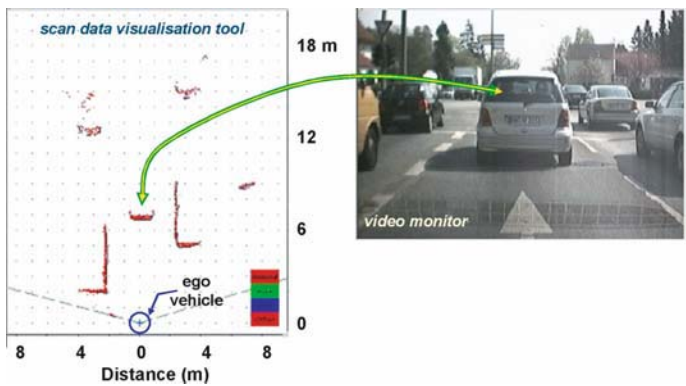


Fig. 5. Driving situation with ALASCA and Stop & Go operation. The left side shows the screenshot of measurement data in bird-view perspective. The right side shows the corresponding video image which has been taken for reasons of reference only. Note: The video image only partly shows the center part of the laserscanner screenshot data.

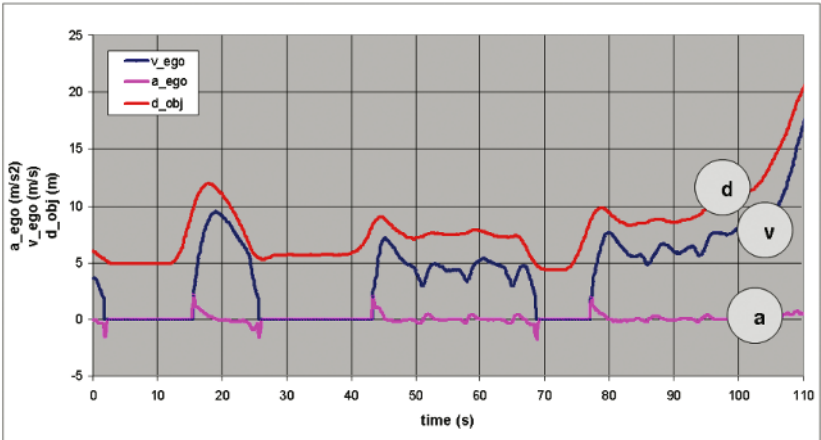


Fig. 6. Compilation of laserscanner data in a real traffic jam Stop & Go szenario on an expressway. The red trace (d) shows the distance to the leading object, the blue trace (v) the ego-velocity, and the pink trace (a) the ego-acceleration.

In order to demonstrate performance in a real Stop & Go situation the test vehicle was driven during a traffic jam on an expressway. Fig. 6 shows a compilation of the ALASCA XT data for a sampling time of 110 sec. The red trace shows the distance to the leading object, the blue trace is the test vehicle ego-velocity and the pink trace denotes the ego-acceleration. It can be seen that

the test vehicle controls its velocity according to the distance of the leading object. The parameters are set such that a minimum distance of about 5 m is kept when traffic comes to a stand still. Acceleration for the restart is evoked with a slight delay after the distance to the leading object has already increased again. Deceleration down to zero velocity is executed when the distance approaches the set limit of 5 m.

5.2 Pedestrian Protection

The e-Safety initiative of the European Commission proposes to cut the number of road accidents by 50% by the year 2010 [1]. Specifically Pedestrian Protection systems will become an essential safety function in future vehicles as legislation forces automotive manufacturers to improve pedestrian safety. For such systems the ability to detect, track, and classify pedestrians is mandatory.

The accident analysis describes the car-to-pedestrian accident mainly as a front crash with a moving pedestrian. The front crash of a car with a pedestrian is associated with about 70% of all car-to-pedestrian accidents. In addition 94% of the pedestrians involved are moving [2]. These accidents can be predicted by the ALASCA system which corresponds to 66% of all car-to-pedestrian accidents. As a safety measure in order to protect pedestrians in the moment in which an accident becomes inevitable, i.e. an active bonnet can be triggered such as presently realized by means of a bumper integrated impact sensor [3].

The strategy to classify pedestrians with a laserscanner is based on the following concept. An object with the shape of a pedestrian is classified as a pedestrian only if the object is moving or has moved during the period of tracking in the past [4]. This is a good assumption, as 94% of the pedestrians involved in car-to-pedestrian accidents are walking or running [3]. Otherwise the object will be detected as a non-moving obstacle. As long as a small obstacle is not moving towards the road, there is no risk of collision, neither for the vehicle nor for the object itself. In order to increase the robustness of the pedestrian classification, the typical oscillatory movement of the legs in the range image sequences and the history of the tracked object with respect to previous classification results are additionally taken into account [5].

If the pedestrian is detected in a well defined region in front of the car, the so-called region-of-no-escape (RONE), the car-to-pedestrian accident is defined inevitable (see Fig. 7). Every pedestrian colliding with the car's frontal region will enter the RONE in a certain time before the accident. This can be moni-

tored using Laserscanner data. The dimensions of the RONE are determined under consideration of the maximum deceleration and acceleration capabilities of the ego vehicle and the pedestrian, respectively. The potential initial acceleration of a pedestrian has been evaluated in detail. It was found that typical dimensions of the RONE are 1 m to 3 m in front of the vehicle, depending on the velocity of the vehicle and the pedestrian. The determination of the RONE parameters – in addition to pedestrian classification algorithms – provides a strategy to predict an impending car-to-pedestrian accident with a very high reliability.

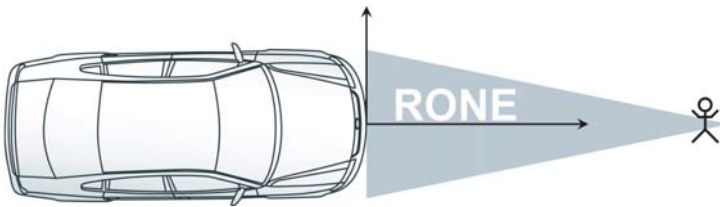


Fig. 7. Schematic of the region-of-no-escape (RONE) in front of a car

The verification results are generated with recorded real data of a laserscanner integrated in a passenger car, with a total driven distance of more than 10,000 km on different road types. The first results show a false alarm rate of 0.7 per 100 km for the Pedestrian Protection application, without use of the analysis of the oscillatory leg motion pattern. Adding the leg motion analysis first results indicate that a false alarm rate of 1 per 10^8 km should be possible.

The described system therefore shows the potential of an early detection of 66% of all car-to-pedestrian accident scenarios corresponding to 94% of pedestrian front accidents. In conjunction with active safety elements it offers the possibility to mitigate the consequences of car-to-pedestrian accidents.

5.3 Lane Departure Warning

Long rides under monotonous conditions may lead to a sudden loss of alertness, the so-called microsleep. This situation bears the risk of unintentional lane departure with the result of causing an accident. A Lane Departure Warning (LDW) system greatly reduces this risk. The task of LDW is to alert the driver before an unintended lane departure takes place. Video based systems [6] which monitor the lane markings ahead of the vehicle and infrared systems [7] measuring the markings straight down, are already commercially available.

An ALASCA system already built into the vehicle for supporting one or more of the applications mentioned above is capable of additionally supporting LDW. Additionally to monitoring the objects on the road in the proximity of the car ALASCA also measures the position of the lane markings. When the vehicle starts drifting off the lane an adequate warning signal is issued to the driver enabling him to prevent an accident by steering back into the lane.

Technically the LDW system is realized by utilizing an unused fraction of the 240° ALASCA scan angle. A mirror is positioned within the integration chamber such that an additional detection area on the road surface is created. This area is located at a distance of about 4 m ahead of the vehicle (Fig. 8). Different types of lane markings of varying quality can be recognized.

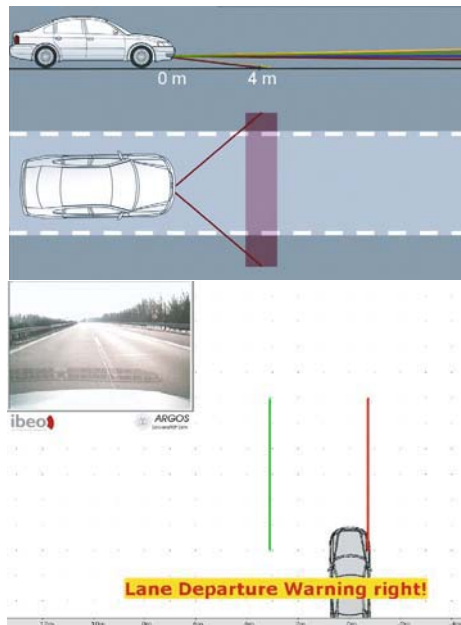


Fig. 8. Lane Departure Warning with a laserscanner system. The schematic (top) shows the beam directions for both, the standard set of beams and the additional LDW-beams. A corresponding driving situation is shown below.

5.4 Slow Moving Assist and Turning Assist for Trucks

Unlike cars, trucks have much larger front and side blind spots than passenger vehicles. Vulnerable road users located in these blind spots are exposed to a

high risk of accident. This situation is the reason for hundreds of fatal accidents per year only on German roads. These accidents occur in urban traffic situations such as pictured in Fig. 9. European legislation requires from January 2005 on an additional mirror as a first countermeasure. Eventhough mirrors are an easy-to-install low-cost solution they are often inadequate to provide a proper view when turning or when starting to move. The reason is that first some blind spot zones remain and second the number of mirrors (up to 6), the truck driver must supervise, may become too large for a fast and intuitive information processing. This is where the ALASCA laserscanner provides a suitable ADAS alternative. With its large scan angle and its fine horizontal angular resolution it is particularly suited for monitoring the entire blind spot area. A situation like the one shown in Fig. 9 either leads to a driver warning or, in case of an imminent collision, braking and disabling of the accelerator.

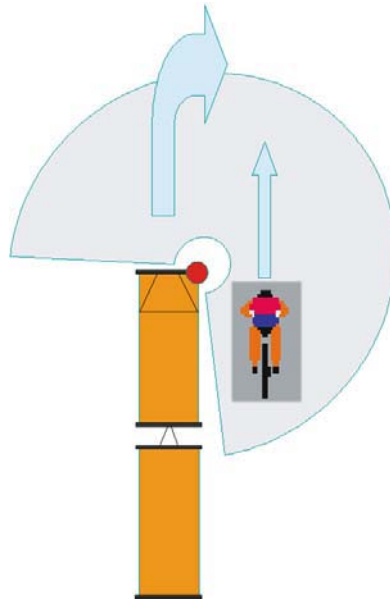


Fig. 9. Top view on a typical situation where high alert of the slow moving assist and turning assist is required. A truck is waiting at a traffic light with a bicycle located in its blind spot. The arrows indicate the intersecting paths of the two vehicles after the green light comes on. The ALASCA system prevents the accident at the red star-marked area.

The automotive laserscanner ALASCA was integrated into the right side of the front bumper of a commercial truck. The integration chamber harmonically fits in with the contour of the vehicle. The available scan angle is about 220°

such that monitoring of the immediate proximity of the areas in front of the truck and on the right side of the truck are warranted. Vulnerable road users like bicyclists or pedestrians entering the blind zones can now safely be detected. Warning signals can be issued and a collision will be inhibited.

A screen shot of a driving szenario is shown in Fig. 10. It can be seen that the wide scan area has been realized and that pedestrians are detected near the truck as well as at larger distances.

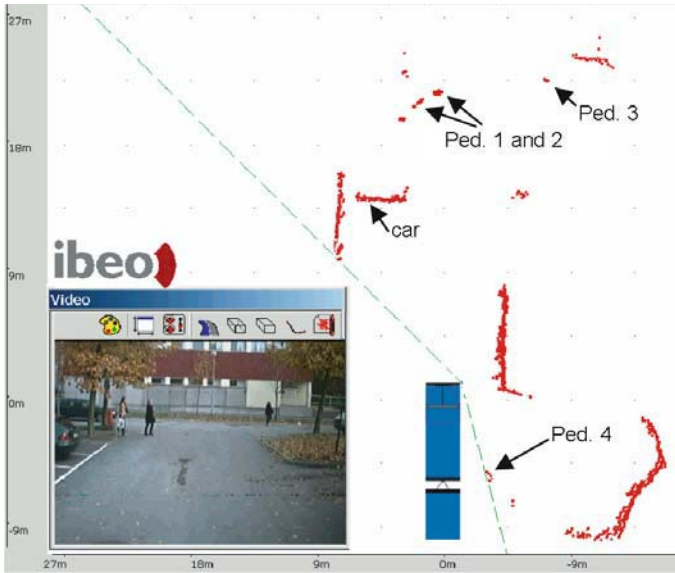


Fig. 10. Screen shot of a driving situation with commercial truck and integrated Laserscanner in a narrow road environment. Note the extreme wide scan area. The ALASCA system detects and classifies the pedestrians (denoted Ped. 1 to 4) within its monitoring zone and thus provides the required safety function.

Once the truck is equipped with the ALASCA there exists the option of also serving the other ADAS applications as mentioned above (Fig. 1). Their implementation is basically a matter of the dedicated software and the application specific HMI.

5.5 Cut-In Assist for Trucks

Another important safety application is the Cut-In Assist for trucks. This assist is designed to support drivers operating their vehicles on expressways. After

overtaking slower traffic the subsequent cut-in procedure frequently leads to dangerous situations and to accidents due to a misjudgement by the driver of the available gap on the slower lane. Here the laserscanner system supports the driver when moving back into the main lane (see Fig. 11). It outputs a Go-Signal when length and position of the gap in the right lane permits a safe lane change. Otherwise the driver is prompted with a No-Go-signal.

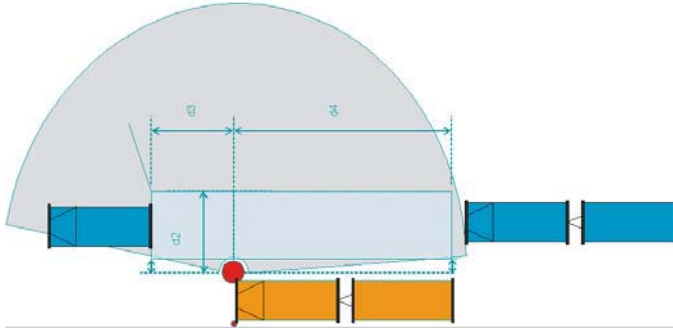


Fig. 11. Schematic of the application Cut-In Assist for commercial vehicles.

6. Conclusion

The ALASCA sensor integrated into the demonstrators showed the ability of operating a wide range of ADAS applications on passenger cars as well as on trucks. The combination of a long detection range of up to 200 m and a large horizontal scan angle of up to 220° provides the opportunity to simultaneously operate seven applications with one single sensor system.

References

- [1] www.eevc.org
- [2] Heinrich, T.: Bewertung von technischen Maßnahmen zum Fußgängerschutz am Kraftfahrzeug. Technische Universität Berlin, Studienarbeit, Berlin, 2003.
- [3] citroen.com/CWW/en-US/RANGE/PrivateCars/C6/default/C6_technologie.htm
- [4] Fuerstenberg, Kay Ch.; Dietmayer, Klaus C.J.; Willhoeft, Volker: Pedestrian Recognition in Urban Traffic using a vehicle based Multilayer Laserscanner. Proceedings of IV 2002, IEEE Intelligent Vehicles Symposium, June 2002, Versailles, France.

- [5] Fuerstenberg, Kay Ch.; Dietmayer, Klaus C.J.: Object Tracking and Classification for Multiple Active Safety and Comfort Applications using Multilayer Laserscanner. Proceedings of IV 2004, IEEE Intelligent Vehicles Symposium, June 2004, Parma, Italy.
- [6] Iteris's AutoVue in DaimlerChrysler Lastkraftwagen: www.iteris.com.
- [7] AFIL (PSA): www.citroen.com/CWW/fr-FR/TECHNOLOGIES/SECURITY/AFIL/

Roland Schulz, Kay Fürstenberg

Ibeo Automobile Sensor GmbH

Fahrenkroen 125

22179 Hamburg

Germany

rsc@ibeo.de

kf@ibeo-as.de

Keywords: ADAS, advanced driver sssistance systems, laserscanner

A new Approach for Obstacle Detection Based on Dynamic Vehicle Behaviour

M. Straßberger, BMW Group Forschung und Technik
R. Lasowski, Softlab GmbH

Abstract

Inter-vehicle communication has been one of the most emerging fields of interest in the automobile industry during the past few years. It is considered as one key enabler for active safety and foresighted driving assistance services. A very prominent example is a local danger warning service. Vehicles instantaneously inform others about critical situations like aquaplaning, accidents or obstacles on the road. The detection of such environmental conditions should be accomplished by means of already available and widely deployed on-board sensors. In this paper we present a new efficient and light-weight approach to estimate the existence of an obstacle, based only on the vehicles' driving dynamics. The approach is evaluated in terms of contribution to the application domain, operability and reliability. A prototype implementation is described and first results from real track driving tests are presented.

1 Introduction

Today, nearly all vehicles are already equipped with sophisticated on-board sensors to detect critical driving conditions and take appropriate actions. These systems are mostly reactive and only cover the vehicle's current position. They are not able to foresee critical situations, which the vehicle may potentially encounter in the future. During the last decade, car manufactures and suppliers put a lot of effort into developing foreseeing and proactive driver assistance systems like ACC. They are mainly based on near range sensing technologies such as radar, lidar, ultra-sonic or optical image processing. Some of these systems are already available in series products and perform very well. Unfortunately, these systems are usually very expensive and only available for upper class vehicles.

The paradigm central to this approach is different. Inter-vehicle communication based on vehicular ad-hoc networks will play an increasingly important role for future vehicle active safety systems. The main idea is to interlink the

on-board sensor systems of vehicles. Thus, vehicles have access to (abstracted and standardised) current sensor information from locations different from their own positions. This enables the enhancement of the drivers' horizon through safety related information that is gathered and provided directly by other vehicles. Therefore, inter-vehicle messaging is widely considered as a promising complementary technology to support foresighted driving and accident avoidance. One of the most promising active safety applications in vehicular ad-hoc networks is a local danger warning (LDW) service as described in [4]. Vehicles directly exchange information about the present road condition and dangerous situations. They are therefore able to warn their drivers of potential upcoming dangers in a timely manner. This will significantly reduce the likelihood that vehicles will get into a critical driving condition, because the drivers' attention will be systematically directed to the spot of the danger in the run-up of the situation. Obviously, this in turn will lead to a significant reduction of accidents.

This paper covers two key concepts towards a foresighted obstacle warning in the domain of local danger warning based on inter-vehicle communication. We present a lightweight approach to detect the occurrence of an evasion manoeuvre, which in turn can be used as an indication for a potential obstacle on the road that triggers additional subsequent evaluation algorithms.

The rest of the paper is organized as follows: First we point out the scope and objectives of the proposed solution. In chapter three we briefly describe the related work and our contribution. Section four describes the proposed approach in detail. Later, the prototype implementation and the system architecture are outlined. Finally, we will present an evaluation and conclusion of our work.

2 Scope and Objectives

The scope of this paper is limited to the domain of cooperative local danger warning based on inter-vehicle communication. The proposed approach will complement other existing and future foresighted driving assistance systems that help to avoid critical driving conditions. In contrast to these stand-alone in-vehicle systems, cooperative systems rely on information provided by other vehicles. Thus, the reliability of the overall system depends on both the reliability of the communication and the penetration rate of the system. Putting it differently, cooperative systems can only operate well if sufficient information from contributing vehicles is available. As a consequence, it is unlikely that those cooperative systems will (in the near future) take appropriate actions

autonomously. Instead, they will systematically direct the drivers' attention to dedicated information of particular interest in a certain situation. Nevertheless, once deployed in vehicles, they are cheap and easy to integrate and complementary to stand-alone sensor systems. In addition, the range is basically not limited to a few hundred meters in front of the vehicle, which is typically the case for on-board sensor systems. On top, the overall contribution and benefit to foresighted active safety will steadily increase over time [2].

In order to achieve a quick deployment and high market penetration, the system should be cheap and easy to integrate into the vehicles. In particular, no additional new sensor systems should be necessary. Instead, common and already widely deployed sensor systems should be used. Vehicles should not necessarily need to be equipped with any kind of navigation system or digital map. To enable quick market penetration, the system should also be available as an additional aftermarket solution.

For the following considerations, we assume that an ad-hoc communication system as well as a cooperative local danger warning service is available in some vehicles, and that these vehicles are equipped with a standardised positioning system with sufficient accuracy, like GPS or Galileo.

3 Related Work and Contribution

In recent years, a couple of national and international research programs and standardization committees have been dealing with inter-vehicle communication and the dissemination of warning messages [4 - 10]. Basically, they focused on communication issues and challenges, but did not address in detail the recognition of road obstacles.

We decided to deduce evidence for obstacles by means of vehicles' driving dynamics during an evasion manoeuvre similar to [FOR05]. This approach has two big advantages. First, it only depends on common on-board sensors, without the need of complex additional hardware like radar or cameras. Second, assuming a standardized interface to access basic sensor information, the system can be offered as an aftermarket add-on, almost independent of the brand and the model of a vehicle.

To understand the concept, we foremost have to get granular on the technique of obstacle detection by vehicle's driving dynamics. First of all we can mark out three distinct states a vehicle can reside in during an evasion manoeuvre, namely whether the vehicle is moving out of its lane, is driving past the obsta-

cle, or is moving back into its original lane. Each of those three states is defined by characteristic values of signals, like lateral acceleration, longitudinal acceleration, speed and yaw.

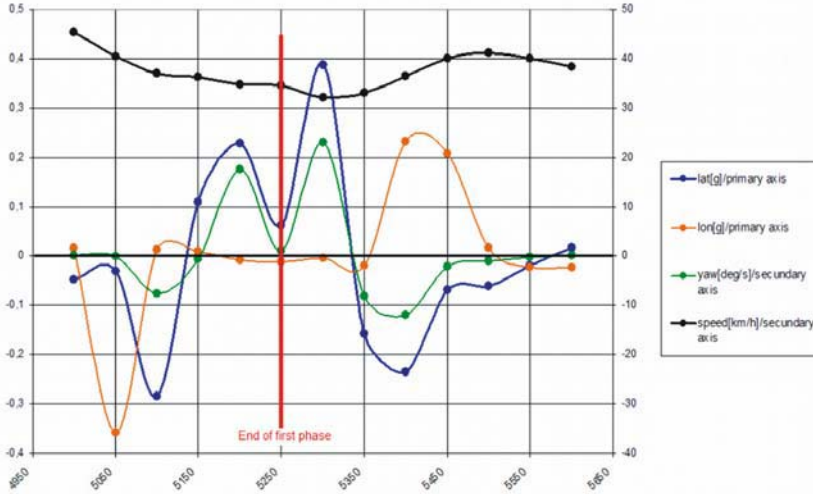


Fig. 1. Evasion manoeuvre [11]

As shown in [FOR05], there are some requirements which have to be fulfilled during signal analysis to reach a conclusion on the existence of an evasion manoeuvre. The most important aspect is the detection of a specific threshold of the lateral acceleration, both as negative and positive amplitude in a defined period of time, which means that the signal changes from one relative extremum to another. This aspect of curve progression is typical for all evasion manoeuvres (moving out of lane). However, concerning the varying occurrence of each following situation (which is significantly influenced by drivers' behaviour and the present road characteristics) it is hard to make a reliable statement about these situations by only analyzing this specific sensor information. Therefore, we have developed an enhanced but lightweight concept which is supposed to increase the reliability of the obstacle detection system.

4 Obstacle Detection

In this section we briefly describe the basic idea and workflow of our system in addition to some of the decision criteria to presume whether or not an obstacle has been detected.

The proposed obstacle detection consists of two distinct successive phases: An initial indication for an obstacle which is deduced from evidence for an evasion manoeuvre, and a subsequent verification process. For the first, we will adapt the suggestion presented in [11]. For the latter, we propose a systematic evaluation of the trajectory of the following vehicles. Fig. 2 shows the basic control flow.

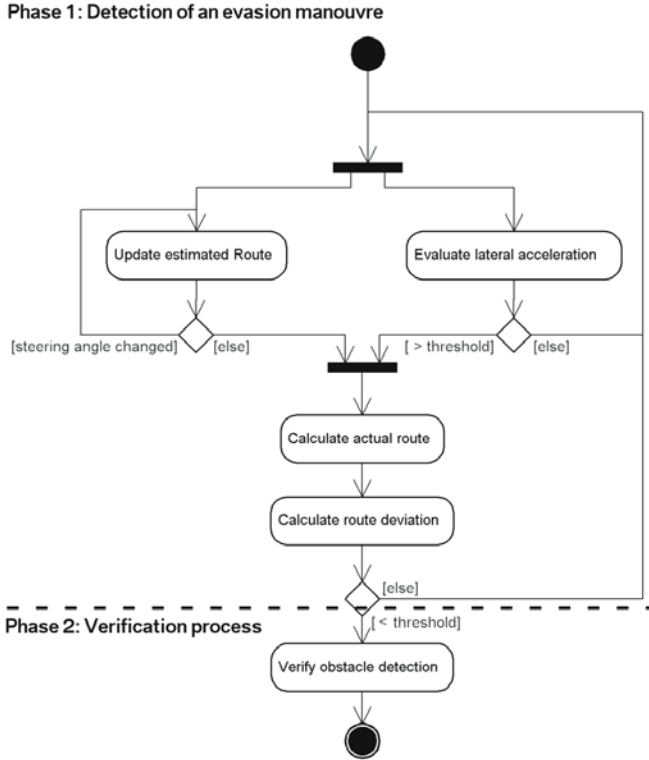


Fig. 2. Basic control flow

4.1 Phase 1: Detection of an Evasion Manoeuvre

The basic idea for the detection of an evasion manoeuvre is to simplify the evaluation of the vehicle's driving dynamics to the first state when it quickly moves out of its lane and countersteers again. The resulting characteristic curve is typical for all evasion manoeuvres and is basically independent from the present steering angle and the dimensions of the obstacle. However, a similar behaviour can be found in steep double curves. In order to distinguish evasion manoeuvres from similar accelerations caused by these particular road

geometries, it has to be verified whether or not the vehicle returns back on its designated route (Fig. 4). This consideration is based on the fact that usually road geometries do not consist of two successive double bends.

Thus, the proposed detection of an evasion manoeuvre consists of the following three parts:

- a) Forecast of the most probable route that will be driven by a vehicle in the imminent future.
- b) The detection of a sequence of unusual lateral accelerations, typical for evasion manoeuvres.
- c) An evaluation of the deviation of the actual trajectory from the forecasted route.

Since the system is required to be permanently active, there is one state which is characterized by regular drivers' behaviour, which means that no critical situation is on the road. In this section the car continuously calculates its hypothetical route whenever it changes its heading (a) according to [Derived from the steering angle. If the vehicle is equipped with a digital map or navigation system, such estimation is obviously not necessary. Instead, the known road geometry can be used.]:

$$r = \frac{d_w}{\tan(\gamma)} \quad (1)$$

where d_w is the particular wheelbase of the vehicle and γ refers to the present steering angle. Having the information of the estimated route, the car can build up its own local logical map with its own coordinate system where it is located in the origin (Fig. 3).

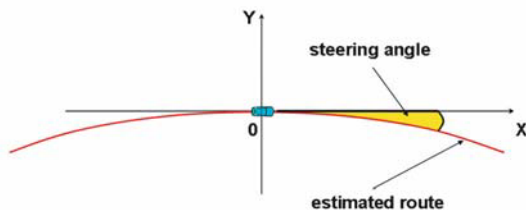


Fig. 3. Route estimation

Besides this route estimation the system concurrently analyzes the received sensor information with regard to a specified threshold of the lateral acceleration signal as described in the preceding section indicating a move out of lane

manoeuvre. In case of sufficient evidence for such manoeuvre (b), the route, which the car was supposed to reside on before the manoeuvre, will be considered as the reference route and a second evaluation will be initiated (c) where the real driven route will be compared to the reference one (Fig. 4).

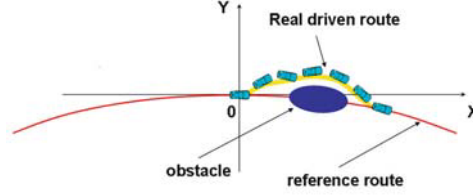


Fig. 4. Real driven route calculation

To perform this kind of evaluation, we have to take a closer look at the technique how the real driven route can be calculated without any global coordinate or positioning system. This is necessary because the current systems do not meet the requirements of availability and reliability for this kind of application.

The main idea is the abstraction of a car ride to single steps, where each is described by an appropriate orbit. This approach is similar to the calculation of the hypothetical route. However, it is more complex, because the car is moving in the deduced local map. Thus, it is not positioned in the origin anymore and therefore some different calculations have to be done. We will briefly describe these calculations in the following paragraphs.

After initiating the second calculation, the vehicle moves on the pursuant orbit, so that the current position has to be calculated. This position P (Fig. 6) can be described by the driven distance w , which can be assessed by the speed v measured during an appropriate time period.

$$w = \frac{v}{\Delta t} \quad (2)$$

On the basis of this data, the angle α and the current position P , where the vehicle is positioned on the circle, can be calculated as follows:

$$\vec{P} = \begin{pmatrix} \cos(\alpha \cdot \pi / 180) \cdot r \\ \sin(\alpha \cdot \pi / 180) \cdot r \end{pmatrix} + \vec{M} \quad (3)$$

where M refers to the centre of the corresponding circle. Considering, that our steering angle is changing continuously, the actual route can be calculated by getting the radius of the according circle. Therefore, the new centre of the new circle has to be calculated. This can be done by defining a direction vector from our current position to the old centre and calculate an appropriate unit vector. Multiplying the unit vector by the new radius and adding the result to the position of the vehicle finally leads to the new centre.

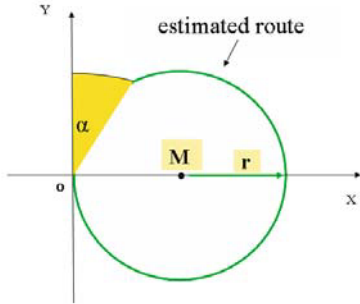


Fig. 5. Route estimation (mathematical view)

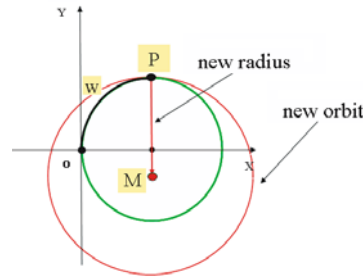


Fig. 6. Real route calculation (mathematical view)

After each position update, the system verifies, whether the vehicle returns back on the reference route or not. This verification is done by treating the resulting deviation between the predicted and the actual route. If this deviation still exceeds a certain threshold after a specific time t (which is derived from the speed that the vehicle had right before the evasion manoeuvre), the existence of an evasion manoeuvre is assumed to be true. To further improve the quality of service, both the deviation and the local extremum of the initial lateral accelerations can be used to deduce the likelihood for a particular evasion manoeuvre.

After running through that phase, the system resets and returns back to the first one.

4.2 Phase 2: Verification Process

However, an evasion manoeuvre obviously still does not give sufficient evidence for an obstacle that endangers other road users. Similar manoeuvres also occur when, for example, a driver rapidly changes his lane to overtake another vehicle. In addition, obstacles often move and disappear again very quickly (For example animals, a car door that has been opened carelessly etc.).

One very obvious consequence of the existence of a static obstacle that endangers others is the fact that vehicles will not pass over the respective location. This can be exploited for the subsequent verification process. The main idea is to systematically analyze the exact trajectory driven by the following vehicles. Note that because of performance issues, it is not (yet) possible to reduce the obstacle detection mechanism to only this phenomenon. This would require a permanent detailed evaluation of all trajectories of all vehicles at any time. In addition, all trajectories have to be permanently exchanged among the vehicles which would quickly lead to a congestion of the available communication channels. Again we assume that vehicles are equipped with a positioning system. The complexity of such trace analysis thereby depends on the accuracy and resolution of the deployed positioning systems. If the resolution and accuracy is significantly better than the typical width of a lane ($<0,5$ m), the exchanged trajectories can be used to detect any location that has not been passed over by any vehicle for a certain period of time. However, the resolution of currently deployed positioning systems is not yet sufficient enough. To overcome this problem, steering angles and speed reductions of the following vehicles can also be taken into account to further verify, if there is an unusual behavior of vehicles at (or close to) the reported location.

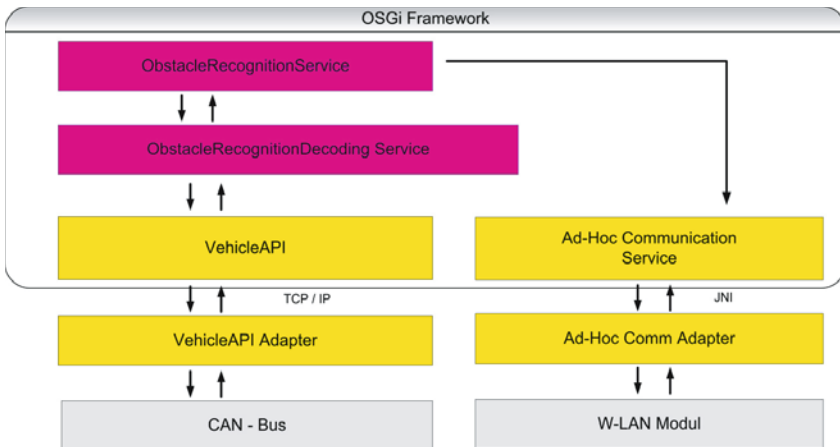


Fig. 7. System architecture

An additional verification may be based on vehicles that are equipped with sophisticated sensor systems like radar. Today, these systems typically still suppress static objects because of performance reasons. Again, having evidence for an evasion maneuver could initiate a systematic evaluation of static objects only at that particular location.

Given sufficient evidence for an obstacle as described, a warning message can be sent to other vehicles whose drivers can be warned in time and are therefore able to intervene adequately.

5 Prototype

For the purpose of verifying the operability of the proposed approach, we implemented the described algorithms into a BMW 5 series (E60) prototype vehicle. In addition, the system was linked to existing software modules that enable direct sensor access to the vehicle's CAN buses, and intervehicle communication based on IEEE 802.11a to populate warnings to other vehicles after an obstacle has been detected.

In order to enable data access, a dedicated interface (VehicleAPI) was designed providing any requested data with sufficient quality of service (QoS). This interface is not addicted to any specific brand or model.

The overall architecture is service oriented and based on the OSGi Framework (Fig. 7). Furthermore, a graphical interface was developed, where the car ride can be traced to check if data is interpreted correctly.

One of the core aspects of our concept is the fact that the system has access to common sensor data, usually provided by in-vehicle bus systems like CAN. This enables third party solutions that can be offered in the aftermarket and therefore ensure a quick deployment. If offered in the aftermarket, the only customization that has to be done is the adaptation to the particular CAN format of the respective vehicle.

6 Evaluation

In order to prove the developed concept, numerous test cases had to be established. To demonstrate the correctness of our approach, black box tests had been used, where primarily the overall functionality of the approach was tested.

There are basically three different situations that have to be distinguished: an evasion manoeuvre, regardless of the dimension of an obstacle, hectic driving style and regular driving conditions. Each case has been tested several times with different drivers. After configuring some settings like the lateral accel-

ation threshold and measurement time intervals, our planned results had been achieved strongly. Hence, our approach has been proved as a solid concept for obstacle detection without using additional complex hardware.

Even though we have reached a high success rate, it can not be assumed as a system which provides 100% reliability in the current state. One conceivable and powerful add-on could be the availability of a digital map, which is supposed to ensure a better forecast of the reference route. Instead of the present lightweight route estimation, the real road geometry at a certain location could be used.

7 Conclusion

We have presented a new, cooperative and lightweight approach to deduce evidence for the existence of a road obstacle. The main idea is to systematically analyze the dynamic behaviour of vehicles. Therefore, no additional sophisticated sensor systems are necessary. Instead, we assume that vehicles are equipped with an ad-hoc communication system. Thus, vehicles are able to share individual knowledge among each other.

In a first step, a potential evasion manoeuvre is deduced that indicates a potential obstacle at this position. In order to exclude false alerts, a subsequent verification process is started, exploiting the trajectories of the following vehicles.

We implemented the proposed approach into a prototype vehicle and showed that it performs well under real world conditions. The proposed system is cheap and easy to integrate, and intended to complement sophisticated but expensive stand-alone sensor systems that aim to reduce the number of accidents through foresighted driving assistance.

This work has been carried out in the context of the wireless local danger warning (WILLWARN) project within the PREVENT research programme, funded by the European Union.

References

- [1] F. Dötzer, M. Strassberger and T. Kosch. Classification for traffic related inter-vehicle messaging. 5th International Conference on ITS Telecommunications. Brest, France, 2005.

- [2] K. Matheus, R. Morich and A. Lübke. Economic Background of Car-to-Car Communication. 2. Braunschweiger Symposium Informationssysteme für mobile Anwendungen (IMA 2004), Braunschweig, Germany, 2004.
- [2] T. Kosch. Situationsadaptive Kommunikation in Automobilen Ad-hoc Netzen. Dissertation. Fakultät für Informatik, Technische Universität München. Munich, Germany, 2005
- [4] T. Kosch. Local Danger Warning based on Vehicle Ad-hoc Networks: Prototype and Simulation. 1st International Workshop in Intelligent Transportation (WIT 2004). Hamburg, Germany, 2004
- [5] L. Wischhof, A. Ebner, H. Rohling, M. Lott and R. Halfmann. SOTIS - A Self-Organizing Traffic Information System. Proceedings of the 57th IEEE Vehicular Technology Conference (VTC 03 Spring). Jeju, South Korea, 2003
- [6] Network-on-Wheels (NoW), <http://www.network-on-wheels.de>, last accessed: 05.01.2006
- [7] Vehicle Safety Communication (VSC), <http://www-nrd.nhtsa.dot.gov/pdf/nrd12/Camp3/pages/VSCC.htm>, last accessed: 05.01.2006
- [8] Car-to-Car Communication Consortium (C2C-CC), <http://www.car-2-car.org>, last accessed: 05.01.2006
- [9] Invent, <http://www.invent-online.de>, last accessed: 05.01.2006
- [10] PReVENT WillWarn (Wireless Local Danger Warning), www.prevent-ip.org/en/prevent_subprojects/safe_speed_and_safe_following/willwarn/, last accessed: 05.01.2006
- [11] Forgis – Institute for Vehicle Technology an Environmental Technology, Friction and Obstacle detection, Patent Nr: 10 2005 055 208.0, 2005

Markus Straßberger

BMW Group Forschung und Technik
 Hanauer Str. 46, 80992 München
 Germany
Markus.Strassberger@bmw.de

Robert Lasowski

Softlab GmbH
 Zamdorfer Straße 120, 81677 München
 Germany
Robert.Lasowski@softlab.de

Keywords: inter-vehicle communication, IVC, vehicular ad-hoc networks, VANETS, local danger warning, obstacle detection

Far Infrared Detection Algorithms for Vulnerable Road Users Protection

Y. Le Guilloux, R. Moreira, S. Khaskelman, J. Lonnoy, SAGEM

Abstract

Far Infrared (FIR) technology was originated a few decades ago in the military domain for its ability to detect any dissipation of heat, as this reveals not only the presence of moving threats or vehicles, but also of living creatures, including human beings, in a passive way, by daytime or night time, even in adverse conditions. More recently, FIR was found a valuable sensor to detect Vulnerable Road Users (VRU) in the automotive safety domain. After a first adaptation to VRU detection of typical FIR detection techniques used in the military domain, where most applications tend to rather concentrate on small objects at a great distance, we have also investigated more recent theoretical schemes, applying them to Far Infrared images. Candidate schemes include various learning methods, such as neural networks, support vector machine, boosting.

1 Introduction

Annual statistics recall the dramatic toll of road fatalities. As more advanced technology becomes available aboard vehicles with time, it seems only reasonable to use growing capabilities with utmost priority in order to help reducing the number of victims. A number of EC-sponsored projects are setting ambitious goals for on-going research in the domain of active safety. The study described here was developed within one of these, Integrated Project PReVENT (www.ip-prevent.org), and more specifically for the COMPOSE sub-project.

The “driver and vehicle” system is a complex one, which evolves within the road context and interacts with other road users, vehicles, pedestrians, etc. Accidentology shows that accidents can be explained by various sources of failures of this system, at the level of the perception of the environment, or at the decision level, or implementing the action decided. These different failure levels are addressed by various research initiatives, detecting potential threats or conflicts, or conveying important information to the driver, or taking the correct decision, or concretely triggering specific mechanical devices. Moreover,

some projects address more than one level of a given application, which can resort to intersection management, or longitudinal control etc.

PREVENT/COMPOSE subproject focuses on pre-crash and collision mitigation. Therefore, in relevant situations, collision can no longer be avoided, but active measures can still decrease the severity of damages. The overall idea behind dedicated devices is to decrease the amount of cinematic energy at the time of impact when it involves Vulnerable Road Users (VRUs), as active bumpers do for example. Along with reducing the amount of energy, the geometry of such devices aims at reducing the severity of consequences, trying not to impact fragile and vital parts of the VRU's body.

Deciding to trigger such a device is an important and often irreversible choice. Taking such an option must rely on a comprehensive perception of the overall environment and detection of VRUs. A main trend within the perception community in various applications includes considering an array of different sensors to properly assess the environment. Long range radars, visible, near-infrared or far-infrared (FIR) cameras, short range radars, laser-scanners are only examples of such sensors being scrutinized. Managing information coming from different sensors implies architecture, communication, registration issues and fusion algorithms which are not considered here.

We concentrate on FIR imagery, as this sensor proves to be very fit for VRU detection. After establishing the practical and geometrical context for taking images, we report different algorithmic approaches relevant for VRU detection.

2 Scope and Practical Context

2.1 Perception for VRU Protection in Pre-Crash and Collision Mitigation

The first point to set is the horizon monitored by the system. Pre-crash and collision mitigation are only concerned with objects within a short range, so close to the vehicle that collision can no longer be avoided. Practically, a range of 30 meters seems the maximum distance to consider.

Once range is set, the next key parameter is the field of view. We consider that selecting an horizontal field of view below 40° would result in too late a detection of a VRU crossing toward the space soon to be filled by the vehicle. A vertical field of view of the same order is always sufficient.

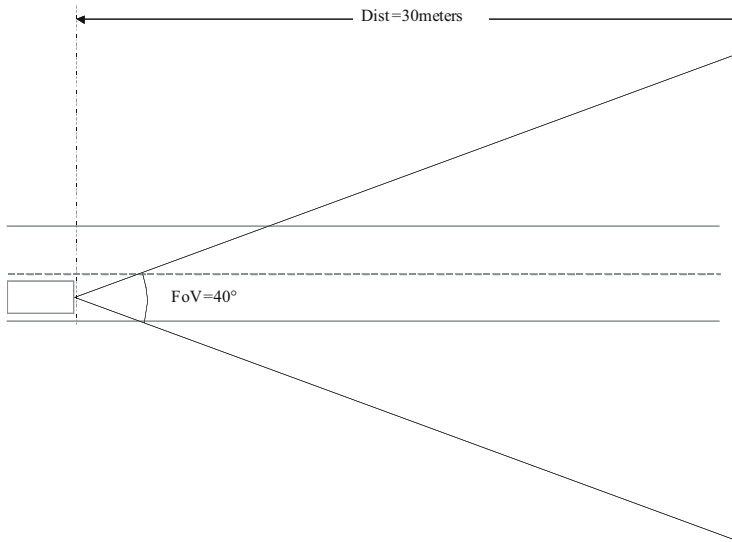


Fig. 1. Monitoring geometry

Once we know how far we should watch, the next question is which objects are relevant. Here, FIR technology was selected due to its capability to enhance VRU visibility. The order of magnitude of the height of a VRU will be roughly around 1.60 meter, not as an accurate dimension, but rather to properly dimension image capture.

2.2 Additional Constraints

Since the price of a FIR camera is a key factor of the cost of a VRU protection system, and knowing that its cost depends mainly on image resolution, we have to consider using sufficient, but not oversized images. A common alternative opposes 160x120 images to 320x240 images.

Finally, the vehicle is already packed with many devices, and integration of the sensor aboard the vehicle can be a touchy subject. The most common location acceptable for a camera lies inside the front bumper.

2.3 Image Capture Geometry

The previous sections has set figures for perception geometry.

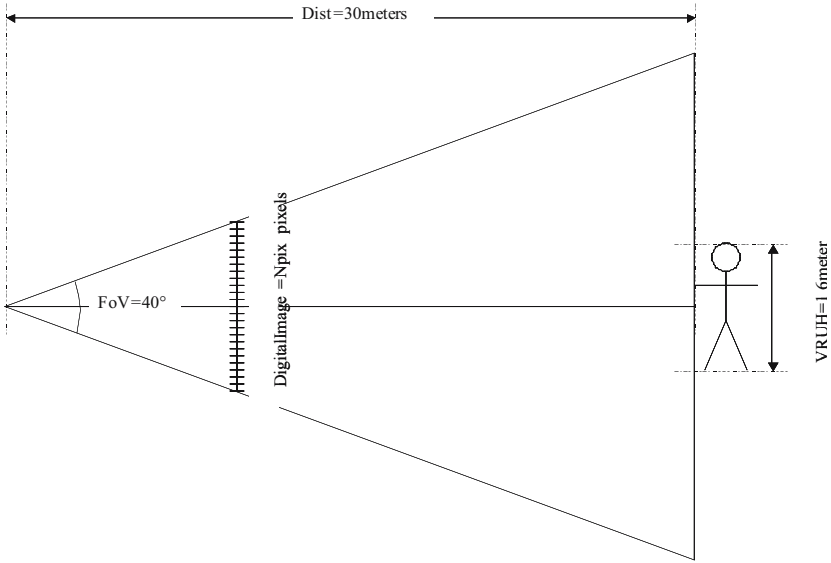


Fig. 2. Image capture geometry

Based on these assumptions, we can easily derive the number of pixels corresponding to the height of a VRU at the maximal relevant distance.

$$VRUh_{pix} = \frac{VRUH \times \frac{N_{pix}}{2}}{Dist \times \tan\left(\frac{FoV}{2}\right)} \quad (1)$$

which yields approximately 23 pixels for the height of a pedestrian, assuming a 320x240 image.

Fig. 3 is an example of a 32x16 pedestrian sub-image, extracted from a regular image. Intuitively, we can assume that recognizing VRU using images with less pixels can hardly be thought of. However, the order of magnitude of the image dimension selected seems to make the task feasible, provided that adequate algorithms are implemented.

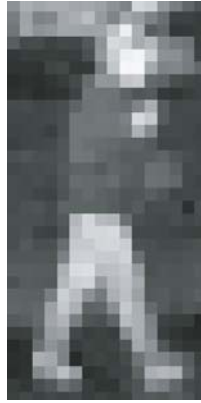


Fig. 3. Pedestrian image example

3 General Properties of Detection-by-Learning Schemes

3.1 Sub-Image-based Recognition

With increasing computing power, most advanced recognition techniques tend to turn from dedicated algorithms, which are fine-tuned to zoom on one given shape or very similar instances, to learning algorithms, which follow a general-purpose procedure to elaborate a basic recognition module based on a set of examples. The resulting module, given a candidate image, decides whether it represents an object of the category it was trained to detect. The object must basically fill the input image to make positive decision possible.

Therefore, the whole problem of detecting VRU, as an example, can now be split in two parts:

- Image scanning: selecting and/or building sub-images from the image delivered by the camera to present to the basic recognition module
- The basic recognition module itself

Both parts are of major importance, as they may influence performances, time response and required computing power with similar weights.

3.2 Image Scanning Mechanism

Scanning the image consists in extracting a number of sub-images from the camera image and feeding them to the basic recognition module. For pedes-

trians, for example, we might want to consider vertical rectangles (height = double of width). Assuming a given size for a pedestrian (like 32x16 pixels), we shall consider a whole grid of candidate positions for a pedestrian sub-image, as displayed below. Note that neighbour sub-images will generally largely overlap.

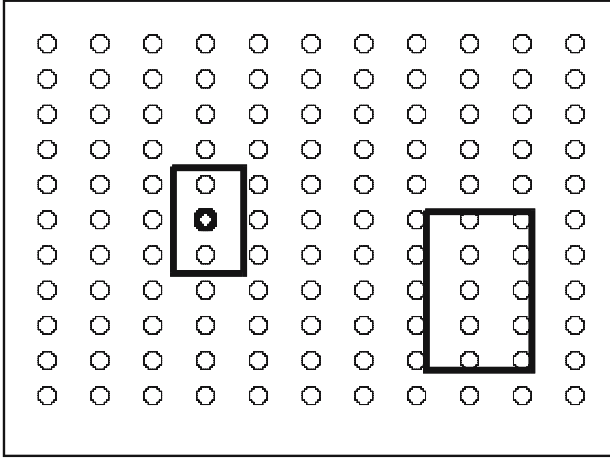


Fig. 4. Image scanning mechanism

Moreover, pedestrians may appear in the image with different sizes, depending on their real size and the distance to the camera, so we shall consider different scales, i.e. different sub-image sizes, and in turn different grids for different scales. Grids naturally become sparser as the sub-image grows. However, the total number of positions to consider for recognition includes all locations from all scales. This number can be a few 10^5 for a brute force scanning of a single image. This will result in a high number of candidates presented to the basic recognition module, so in turn not only in heavy computation, but also possibly many false positives, regardless of the performance rate of the basic recognition module.

3.3 Sub-Image Positive Databases

To elaborate an efficient learning-based recognition, the first step consists in gathering a great number of sub-images representing full frame candidate objects, VRUs in our case here. Here, we benefit from the relative invariance of infrared images, which remains largely unaffected by light changes, weather conditions, a.s.o.

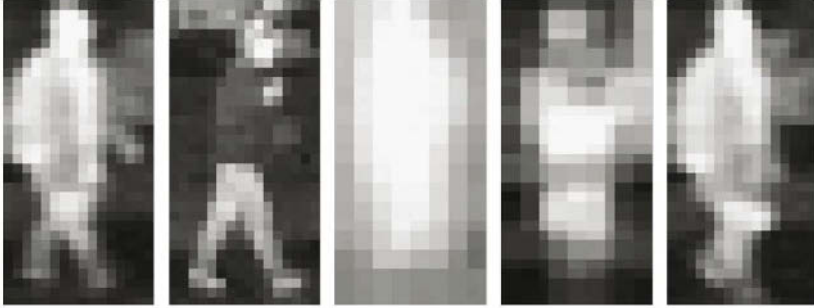


Fig. 5. VRU sub-image examples

This can be a tedious and lengthy phase, for which no fully automated tool exists. Therefore, we shall rely on observations made and recorded by an operator pointing at pedestrians in existing images. Sub-images are systematically scaled to an appropriate standard size.

3.4 Sub-Image Negative Databases

Although this point might not be so intuitive, a learning algorithm also needs an important set of counter-examples on which it knows it should give a negative answer. The size and pertinence of the negative database should not be underestimated.

Practically, building a consistent negative database can be made much easier than it is to build its positive counterpart. Various procedures can deliver appropriate sub-images a priori not centred on VRUs, and it is enough to invalidate any sub-image appearing to display a full frame VRU.

4 Boosting Techniques

4.1 Introduction to Learning Techniques

Having earlier experience with using neural networks for classification, we have carried no further experiment on this approach.

A survey of literature reveals many articles about pedestrian detection using image processing techniques. A short list of relevant references which were analysed and discussed is given in the "References" section, [1-14]. More ref-

erences are also given, pertaining to learning techniques in general, or applied to different applications.

In any case, we shall always assume a training set, including positive and negative examples – with/without the objects of interest – and a training phase using this set to tune the algorithm. Then the algorithm is tested and evaluated on a test set, which does not overlap the training set.

4.2 Boosting

Boosting is a general technique applied in learning. It consists, during the learning phase of the algorithm, in reinforcing misclassified examples weights, so as to pay more attention to them during the following learning step. Fig. 6 illustrates how boosting can converge toward a better solution.

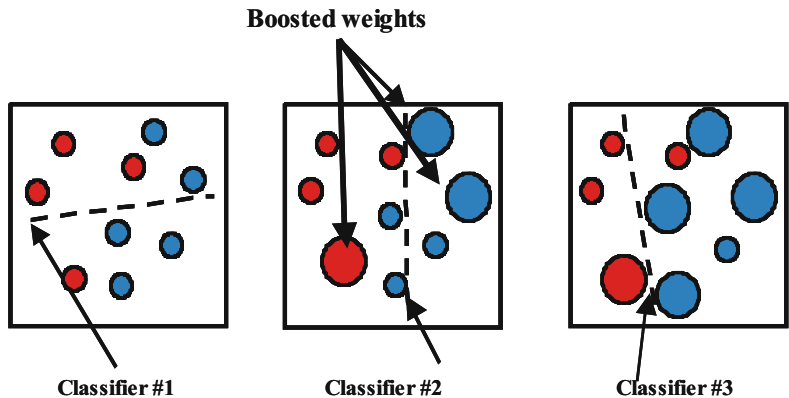


Fig. 6. Boosting

Classifier #1 has achieved a reasonable classification of positive and negative example, displayed by a line. Therefore, the three misclassified examples will be given increased importance during the next step. Not surprisingly, classifier #2, selected based on updated weights, will classify these examples correctly, leaving other examples out, which will in turned be given increased importance when selecting classifier #3, which, combined with predecessors, will improve overall performance.

Freund [17] proposes to build up a series of strong classifiers, each of them combining many weak classifiers. Strong classifiers are lined up in a serial way, so that the second strong classifier only knows candidates accepted by the first classifier, and so on.

Practically, a weak classifier can be based on thresholding some simple feature which can be computed from the candidate sub-image in a very short time. Learning means selecting a good list of classifiers from the acceptable dictionary of features, with correct threshold. Tuning the threshold is illustrated in Fig. 7.

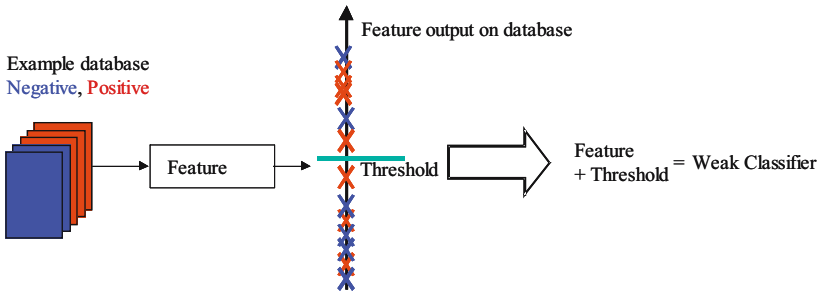


Fig. 7. Weak classifier tuning

Tuning the threshold of a classifier consists in selecting the value which best separates negative and positive feature values.

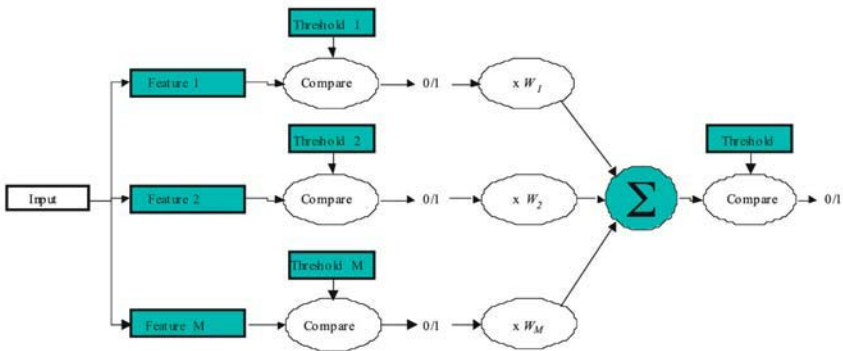


Fig. 8. Strong classifier structure

A strong classifier combines linearly binary output of weak classifier through weights, and compares the sum with a threshold. This structure allows boosting during the training phase.

Strong classifiers are built up one by one, starting from the first step. In order to achieve a given false positive rate for the whole classifier, we may relax the specification for each single step. Once the first step meets this specification

on the whole initial database, the second step is trained to achieve the same performance, but only on the examples which were classified positively by the first classifier. Following steps are built in the same manner.

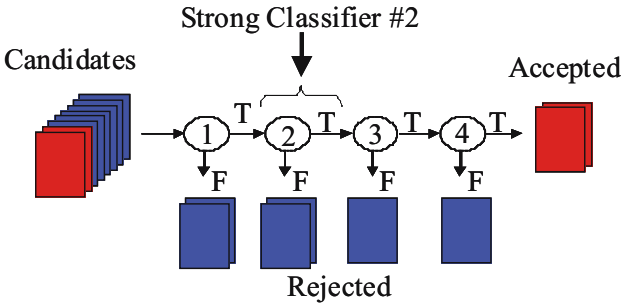


Fig. 9. Full classifier structure

4.3 Application to Pedestrian Detection

A comprehensive description of a training/recognition scheme has been given above. However, we still have to define the family of features to consider to build weak classifiers. Viola and Jones [26] suggest a family of simple integrating kernels, adding the pixel values where the shape is marked white, subtracting where it is marked black, ignoring other pixels.



Fig. 10. Simple sub-image features

Roughly, the features illustrated above aim at capturing successively edge information (first two templates: vertical edges, horizontal edges), line information (templates #3 and 4: vertical lines, horizontal lines) and local minima and maxima (last template). These templates are considered for all sizes, which amount to a fair number of candidate features.

Such features can be easily and quickly computed over a whole sub-image, and used during training phase to derive a cascade of strong classifiers as described in previous sections.

4.4 Experiments and Results

The technique described here is only a basic recognition module, which should be at least combined with a scanning mechanism. We give performance estimates of the basic recognition module, and translate it in a straightforward manner into a overall performance.

The overall performance of such a basic recognition module, although reaching a detection rate around 85% on the training set, falls down to 50% on a different database. The false positive rate is very low, but we should keep in mind that a great deal of candidates will be presented. These figures only represent the performance of the internal recognition module, not the performance of the FIR VRU detection.

Building a very straightforward VRU detection system using only such a detection technique would roughly achieve a 50% detection performance – equal to the basic recognition module performance – and give an average of 1 false positive for each image processed. This may seem a poor performance, and clearly does not meet practical requirements. However, taken into account that such the basic recognition module processes a huge number of sub-images, its performance can be thought as perfectly fair.

Many experiments were conducted, restricting or enlarging the family of features, or changing the algorithm at many levels, resulting in only slight gains.

A major point of this recognition technique is the level of performance achieved with respect to the amount of computing required at detection time, which is very low. From this point of view, this technique seems to have little, if any, competitors.

Finally, the positive conclusion of this study, is that the recognition module exhibits extremely interesting and relevant capabilities, but that building a complete VRU detection system requires integrating the combination with complementary modules as found in most – if not all – detection system: pre-processing , tracking, confirmation, etc.

5 Support Vector Machines

5.1 SVM Principle

Vapnik [25] introduced SVM classification, a technique supported by a solid theoretical background. Basically, the descriptors are points of a high dimension space. A nice property of such a space is that separation of positive and negative examples by a hyper-plane may be a likely hypothesis, which is highly unlikely in 2D/3D spaces with which we are naturally more familiar.

Then the problem becomes: "How can we find a right hyper-plane to separate both sets?".

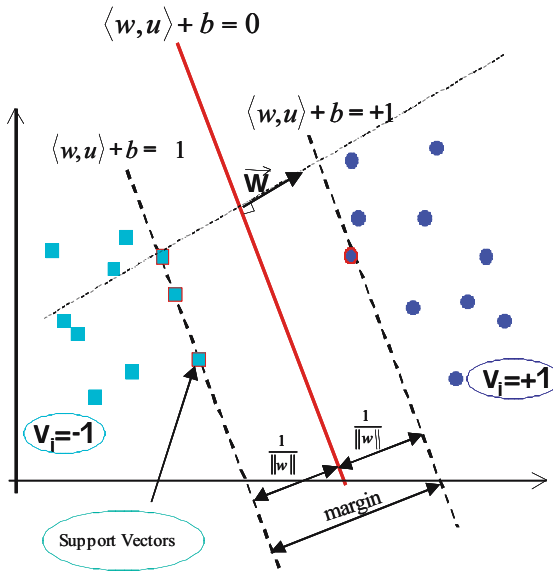


Fig. 11. Support Vector Principle

SVM defines the margin as a quality measurement of the hyper-plane. It can be understood that without a sufficient margin, the classifier might be extremely touchy, and it would become unlikely that any classification quality evaluated on the training set might still hold on a different testing set.

An extensive literature on SVM (see [15], [16], [21], [22], [23], [24]) provides hints on how to represent examples, and how to compute a hyper-plane with good separation properties. In some cases [22], the whole processing algorithm boils down to solving a least squares linear problem.

5.2 Implementing SVM for Pedestrian Detection

A straightforward implementation of SVM uses sub-images as input vectors and computes a separating hyper-plane, similarly to how boosting algorithms were implemented, using the benefit of infrared image invariance. As for any classification problem, the performances are evaluated in terms of detection rate and false positives.

We tuned the parameters of the algorithms in an attempt to reach a decent – not too high – false positive rate. As a consequence, this translates into a lower detection rate.

5.3 Results

Learning performances obtained with SVM on our training sets appear somewhat similar to what boosting algorithms achieved. However, the generalization capabilities, evaluated on different testing sets, seems lower. The general tendency in the results we obtained is a high false positive rate (>20 per image) when trying to achieve a decent detection rate (> 70%!) and a low detection rate when trying to contain the false positives.

We have also shown that the full dimension of sub-images was not necessary to achieve the performances, which might open ways to further reduce computation effort.

As a conclusion, our problem turns out to be too difficult to be solved single-handedly by such a SVM technique.

6 Conclusion

We have investigated different learning-based VRU detection algorithms on infrared images. The diversity of technical conclusions cannot be fully accounted here, but in a synthetic way, we found that boosting-based recognition techniques, although not delivering the final performance that we need for a standalone system, exhibit excellent capabilities when compared to the amount of computation required.

SVM techniques seems to give rather permissive performances, that is, giving a important number of false positives. Therefore, like boosting, SVM does not seem a sufficient tool to detect VRUs reliably.

However, both techniques have individual qualities that ought to be considered, not using either as a full classifier – as was naively thought in the first place – but as modules of a complete classifying system, together with more classical blocks such as tracking a.s.o.

This direction is currently under investigation.

References

- [1] C. Papageorgiou, T. Poggio. CBCL and AI Lab. Cambridge. Article 1 : Pedestrian detection using wavelet templates. CVPR – June 1997
- [2] C. Wöhler, J.K. Anlauf, T. Pörtner, U. Franke, A time delay neural network algorithm for real-time pedestrian recognition, 1997
- [3] K. Tabb, S. George, R. Adams, N. Davey, Human shape recognition from snakes using neural networks, Hertfordshire – UK – 1998
- [4] L. Zhao, C. Thorpe, The Robotics Institute, CMU – USA, Stereo and neural network - based pedestrian detection, ITSC -Tokyo - Japan - October 1999
- [5] Y. Song, X. Feng, P. Perona, California Institute of Technology - Pasadena – USA & Università di Padova – Italy, Towards detection of human motion
- [6] H. Nanda, L. Davis, Probabilistic template based pedestrian detection : infrared videos Maryland – USA – 2002
- [7] F. Xu, K. Fujimura, Ohio State University , Honda R&D America, Pedestrian detection and tracking with night vision, USA – 2002
- [8] D. M. Gavrila, J Giebel, Daimler Chrysler Research, Chamfer System Shape-based Pedestrian Detection and tracking, Germany – 2002
- [9] P. Viola, M. Jones, D. Snow, Mitsubishi Electric Research Laboratories - July 2003, Detecting pedestrians using patterns of motion and appearance
- [10] A. Shashua, Y. Gdalyahu, G. Hayun, University of Jerusalem, MobilEye Ltd., Pedestrian detection for driving assistance systems : single frame classification and system level performance, Jérusalem – Israël – 2004
- [11] H. Sidenbladh, Swedish Defense Research Agency, Detection human motion with support vector machines, Stockholm – Sweden – 2004
- [12] J. Denzler, H. Niemann, Universität Erlangen – Nürnberg, Real-time pedestrian tracking in natural scenes, Germany – September 1997
- [13] A. Broggi, M. Bertozzi, A. Fascioli, M. Sechi, Dip. Informatica e Sistemistica – Univ. Pavia, Dip. Ing. Dell'Informazione – Univ. Parma, Shape-based Pedestrian Detection, Italy – 2000
- [14] A. Broggi, M. Bertozzi, A. Fascioli, P. Lombardi, Vision-based pedestrian detection: Will Ants help ? Parme – Italy – May 2002
- [15] C. Burges, A tutorial on Support Vector Machines for Pattern Recognition. Knowledge Discovery and Data Mining, 1998

- [16] J. Callut, Implémentation efficace des Support Vector Machines pour la classification, Mémoire pour le grade de Maître en Informatique, Bruxelles, Belgique 2003
- [17] Y. Freund, R.E.Schapire, A decision-theoretic generalization of on-line learning and an application to boosting. *Computational Learning Theory*, 1995.
- [18] J.Friedman, T.Hastie, R.Tibshirani, Additive logistic regression: a statistical view of boosting, 1998.
- [19] R. Lienhart, A.Kuranov, V.Pisarevsky, Empirical analysis of detection cascades of boosted classifiers for rapid object detection, Microprocessor Research Lab, Intel Labs, 2003.
- [20] S. Romdhani, P. Torr, B. Schölkopf, A. Blake, Computationally Efficient Face Detection, *ICCV* 2001.
- [21] John Shawe-Taylor, Nello Cristianini, An Introduction to Support Vector Machines, The Press Syndicate of the University of Cambridge, 2002.
- [22] J.A.K. Suykens, T. Van Gestel, J. De Brabanter, B. De Moor, J. Vandewalle ; Least Squares Support Vector Machines, World Scientific, Singapore, 2002 (ISBN 981-238-151-1).
- [23] J.A.K. Suykens, Introduction to SVM and kernel-based learning, *ESANN*, 2003.
- [24] J. Valyon, A sparse least squares support Vector Machine Classifier, *Periodica Polytechnica Hungary*, 2003.
- [25] V. Vapnik, The Nature of Statistical Learning Theory, Springer-Verlag, 1995.
- [26] P. Viola, M.Jones, Rapid object detection using a boosted cascade of simple features. *Conference on Computer Vision and Pattern Recognition*, 2001.

Y. Le Guilloux, R. Moreira, S. Khaskelman, J. Lonnoy

SAGEM Défense et Sécurité
BP 72 - 95101 Argenteuil CEDEX
France
yann.leguilloux@sagem.com

Keywords: far infrared, vulnerable road user protection, precrash, collision mitigation, learning-based techniques, boosting, support vector machines

iBolt Technology – A Weight Sensing System for Advanced Passenger Safety

K. Kasten, A. Stratmann, M. Munz, K. Dirscherl, S. Lamers,
Robert Bosch GmbH

Abstract

In 2004 the NHTSA FMVSS-208 ruling became effective, to avoid injuries of children by unwanted deployment of the passenger airbag. To fulfil the requirements of this law, several technical principles are under development or had a first product launch recently. The key technologies are weight sensing by measuring strain or displacement or mat solutions either fluid filled or as pattern recognition. This paper presents the Bosch iBolt technology, a direct weight measuring system, which is an integrated and therefore functional part of a seat. The advantages and properties of this technology will be described depending on the main questions, like insensitivity against lateral forces and moments, temperature behaviour and packaging issues both on component and seat level. The weight sensing iBolts are installed directly into the seat frame, replacing existing bolts, so no H-point shift is caused by integrating the iBolts sensors.

1 Introduction

Since 2004 the NHTSA FMVSS-208 ruling (National Highway Traffic Safety Administration; Federal Motor Vehicle Safety Standards and Regulations 208) is effective. It was introduced for reduction or prevention of (fatal) injuries of children by unwanted deployment of the passenger airbag. In order to fulfil this regulation several technical solutions are being currently developed or have been launched recently. The working principles are based mainly on weight sensing utilizing strain or displacement measurement. Other systems are utilising a gel-filled or keypad-like mat-solution for pattern recognition. Every sensor system has to fulfil all the NHTSA FMVSS-208 rules. Under all circumstances the occupancy status of the passenger seat has to be determined accurately. On top of the 208 requirement, customers demand field robustness over lifetime to prevent any misclassification. This indicates the exceedingly high requirement on the functionality of a standardized sensor system. At the same time the various environmental influences, such as floor

panel, seat type, seat cushion, seat cover, seat installation tolerances, etc. have to be considered.

This paper addresses the BOSCH iBolt™ technology, a direct measuring system, directly integrated – and therefore a functional part – into the seat structure. Properties, performance and advantages of the BOSCH iBolt™ technology are described. Various key areas, e.g. sensitivity against lateral forces and moments, temperature performance, hysteresis, packaging issues, are discussed on both component and system level.

The working principle of the BOSCH iBolt™ is based on measuring the deflection of a bending beam. The deflection is monitored by measuring the change of static magnetic field utilising a specific Hall-sensor-to-magnet field arrangement. The BOSCH iBolt™ is designed in such way that the change of magnetic field is proportional to the load present on the seat. The unique design of the BOSCH iBolt™ enables an exceptional insensitivity against lateral forces and moments. Consequently the BOSCH iBolt™ is capable of measuring the correct load under a wide range of environmental strain conditions. This in return permits simple and inexpensive seat structure integration. Utilising a high strength steel in combination with a limit stop design ensures the outstanding accuracy and temperature behaviour of the BOSCH iBolt™. The limit stop design prevents yielding of the bending beam at low speed crashes.

The particular design of the BOSCH iBolt™ allows for an assembly within a common seat structure simply replacing an existing bolt. Hence no H-point shift is caused by integrating the BOSCH iBolt™, which is a major advantage compared to systems mounted underneath the seat track. Additionally, since the BOSCH iBolt™ is integrated into the seat structure there are no effects of seat type or seat cushion on the iBolt™ performance. In case of implementing the iBolt™ above the seat belt attachment point a customized algorithm in the ECU usually handles correct occupancy detection without an additional belt tension sensor. Incorporating the BOSCH iBolt™ below the seat belt attachment point eliminates the necessity of an additional belt tension sensor.

2 System Design

The BOSCH iBolt™ system consists, depending on the application, out of up to four iBolt™ sensors integrated into the seat structure and an Electronic Control Unit (ECU). A customized algorithm stored in the ECU classifies the passenger according to the weight signals of the sensors. This classification is

used by the Airbag-ECU to enable or disable the firing of the passenger airbag. Fig. 1 shows a schematic system layout.

The communication of the weight signals to the ECU is based on an analogue point-to-point connection to the ECU. Furthermore it enables a localization of each sensor in the seat. This is necessary for diagnosis and service purposes in case of exchanging a sensor. For diagnostic purposes the ECU enters a digital communication mode with the sensor. This enables the ECU to read out several parameters stored in the sensor.

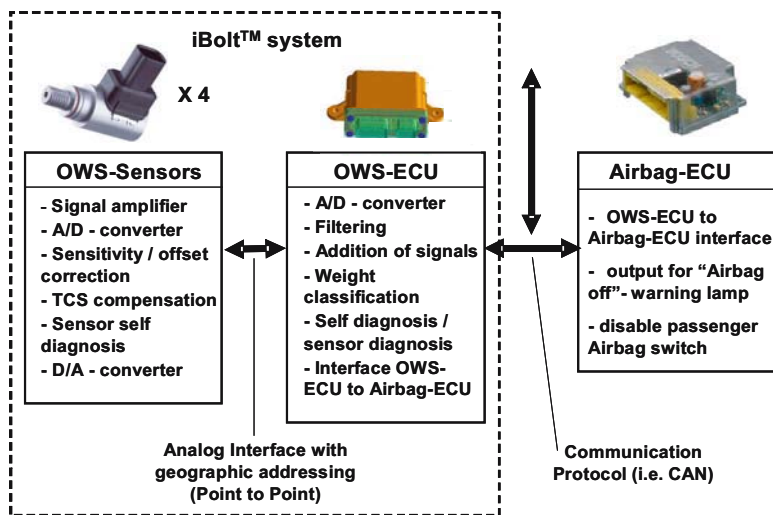


Fig. 1. System layout of the BOSCH iBolt™.

The sensor design allows for calibration of sensitivity and offset on sensor level as well as a temperature calibration. Hence the weight signal generated by each iBolt™ is fully temperature compensated.

The analogue output signals of the iBolt™ are converted into digital values. Next the ECU low pass filters the sensor signals and summarizes them to a weight signal. The weight of the seat itself, stored in a non-volatile memory, is continuously subtracted from the actually measured weight signal. Primary part of the algorithm incorporated in the ECU is the classification of the passenger. The main focus is on the differentiation between a child and a small adult. The trigger area is only 6 kg whether a passenger seat is occupied by a small child in its child seat (6 year old ATD in the heaviest NHTSA Booster) or by a so called 5 %-female (NHTSA specified 5%-female). Software filter stages are used to ensure a stabilized classification particularly under transient or

dynamic events. Additionally diagnostic functionality is implemented to guarantee correct classification of the system.

The result of the classification is transferred to the ECU using either CAN or other OEM specific protocols. Depending on the detected class the airbag ECU enables or disables the airbag. Alternatively an adjusted level of airbag firing is possible.

3 Working Principle

3.1 The Sensing Principle

One function of the iBolt™ is to transform the effective force caused by the weight of a passenger into an electrical signal. The automotive coordinate system defines the driving direction as X, the vertical and horizontal orientation as Z and Y, respectively. The iBolt™ combines a bending beam with the Hall measuring principle. It is designed in a way that preferably the Z-component of the weight of a passenger causes the displacement of the bending beam. The Hall-to-magnet arrangement within the iBolt™ is such that a linear change in the electrical signal is achieved. Thereby a static magnetic field, running through a Hall-sensor, causes an output signal linear to the deflection of the bending beam. The unique design of the iBolt™ inhibits a horizontal displacement of the magnet relative to the Hall. Additionally the iBolt™ features a mechanical limitation of the maximum strain on the bending beam.

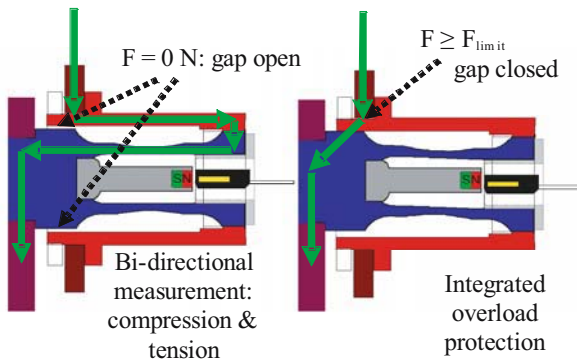


Fig. 2. Schematic of the measurement principle of the BOSCH iBolt™ technology.

Gaining a linear signal has been obtained due to a constructive detail. The load caused by a passenger is led from the upper seat structure into the sleeve and further into the bending beam (Fig. 2). From the bending beam the force is led into the seat track of the car. The bending beam is constructed as a double bending beam. Typically a double beam shows an S-type deflection line. Thereby both vertical joints of the double bending beam remain in a vertical position for any deflection. This feature ensures a parallel movement of the magnet to the Hall. Hence a linear output signal is achieved (Fig. 3).

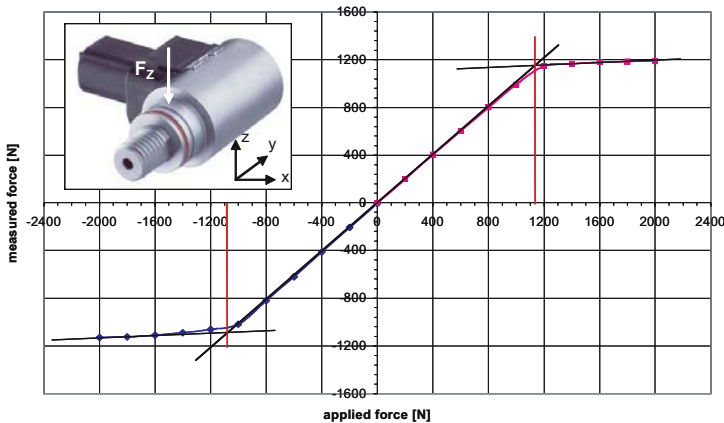


Fig. 3. Typical output signal of a BOSCH iBolt™ sensor as a function of the applied force.

Tests in passenger seats have shown that sensors are exposed to positive and negative forces. The origin of these forces is twofold. First, seat-inherent preloads are effected due to manufacturing and assembly tolerances as well as from fitting into the car. Secondly different load situations are caused by the seating position of the passenger and tilt of the backrest (Chapter 4 and 5). Therefore the iBolt™ is designed to measure loads in positive and negative Z-direction. This allows for an unambiguous interpretation of the weight of the passenger. Due to the symmetric design of the iBolt™, it measures pulling and pushing forces at equal magnitudes and tolerances. This unique feature allows for using the same iBolt™ weight sensor at the four linkages of upper seat structure and seat tracks in both vertical assembly directions.

3.2 The Seat Linkage

As mentioned earlier, the BOSCH iBolt™ has a second feeding. Like described above the accurate measurement of the weight of the passenger is only one

requirement of the system. Secondly the iBolt™ is designed as the linkage between upper seat structure and the seat tracks. It replaces an existing structural part of the seat adopting an essential safety feature. In case of a crash the iBolt™ in conjunction with the seatbelt have to divert the occurring forces to the floor panel anchorage points.

In practice two crash situations are looked at, first a low speed crash up to 12 mph must not cause any change in performance of the iBolt™. Secondly at a high speed crash the iBolt™ must ensure the integrity of the seat structure. Therefore, to limit the maximum stress the bending beam experiences, a mechanical limit-stop design is implemented into the iBolt™ assembly. While exceeding the maximum load F_{limit} the front joint of the bending beam mechanically engages with the limit-stop sleeve. This causes a direct transmission of the load from the upper seat structure into the seat track by-passing the bending beam (Fig. 2, right hand side). As a result the force-sensitive bending beam is protected against plastic deformation. The FMVSS-208 regulations do not require a determination of loads above a certain value. Furthermore the loads in the relevant area can be determined more accurately.

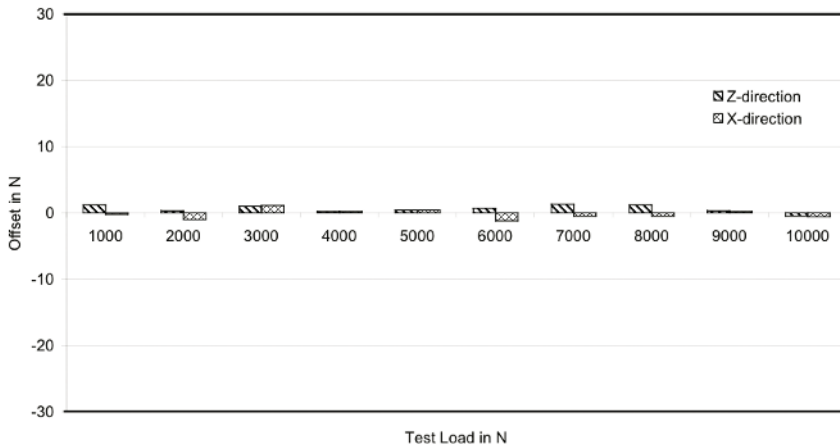


Fig. 4. Component performance after low speed crash separated in X- and Z-component.

3.3 Component Performance

Measurement results on component level have shown that there is a sound linear relation between the forces applied and measured with the iBolt™. The output signal is linear within the guaranteed measurement range of $\pm F_{limit}$.

Above the mechanically limited measurement range the output signal describes a significantly reduced gradient. This occurs once the bending beam joint starts to engage with the limit-stop sleeve at higher loads. None the less it does not affect the accuracy of the iBolt™ at all.

As described above requirements on the functionality of the iBolt™ are twofold. One is that the iBolt™ is not affected by a significant offset after a 12 mph crash. Since the force of a frontal crash can be disaggregated in a force in X- and Z-direction the errors caused in X- and Z-direction are evaluated separately. Forces occurring during a low speed crash are in the range of 6,800 N and 4,200 N in X-direction and in Z-direction, respectively. Fig. 4 shows the offset of the iBolt™ for a simulated low speed crash which does not exceed ± 1.3 N. The results are calculated from the original offset of the sensor compared to the offset after a test load is applied in the range of 1,000 to 10,000 N. The results shown in Fig. 4 demonstrate the outstanding performance of the BOSCH iBolt™ technology.

4 Influences of Lateral Forces and Moments

Measuring weight correctly at a seat environmental conditions set high demands for a sensor concerning insensitivity to lateral forces and moments. The seat tolerances are usually in the range of several millimetres. Therefore seats with such tolerances lead inevitably to high preloads (up to ± 300 N) in all possible directions.

There are basically two options to handle such preloads in a weight sensing application:

1. Gimbal integration of the sensor in the seat.
2. Designing the weight sensor towards insensitivity against any lateral forces or moments.

Obviously the first option will introduce a high amount of additional costs and effort to integrate and decouple the sensor in the seat. However the BOSCH iBolt™ is particularly designed for insensitivity against any lateral forces or moments. Aiming for this option additionally eases the entire seat integration process. The existing joints usually only need moderate modification. Low sensitivity against lateral forces and moments is achieved by a special design of the bending beam together with an improved magnet-to-Hall-sensor arrangement.

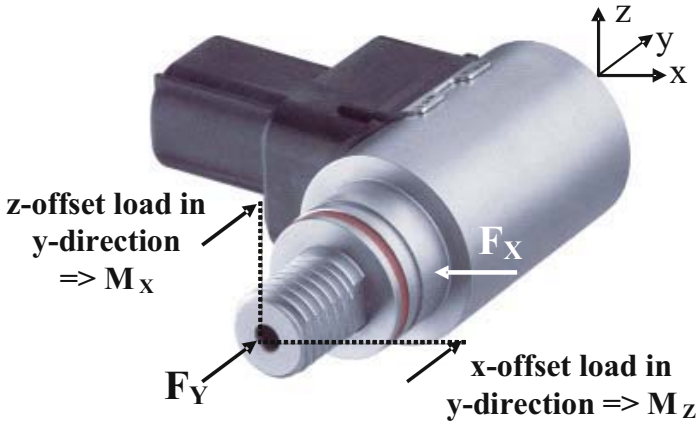


Fig. 5. Definition of cross-axis loads. Moments are applied by offset loads in y-direction.

In general preloads can be divided in forces and moments. Fig. 5 shows the definition of these loads for the iBolt™. F_z is the only designated sensing direction. Hence the iBolt™ is distinctively designed to minimize the influence of loads and moments adding unwanted signals to the output of the sensor. The actual sensitivities in F_x - and F_y -direction are established by applying a force (~ 600 N) to the sensor in the corresponding direction. The sensor output is referred to the applied load and calculated as percentage (Tab. 1).

The moments M_x or M_z are engendered at the iBolt, by applying a force F_y (~ 600 N) with a geometrical offset of 1 inch (0.0254 m) to the Y-axis of the sensor in Z- and X-direction, respectively. This method implies a combined load case of F_y and the corresponding moment to the sensor. Hence, the sensor output is corrected by the sensitivity in Y-direction times the applied load in Y-direction. This corrected sensor output is referred to the applied moment ($M_{\text{appl}} = F_y * 0.0254 \text{ m}$) to calculate the moment sensitivity of the iBolt™ in N/Nm.

Tab. 1 shows the measured cross-sensitivities (F_x , F_y , M_x , M_z). The results were measured at numerous samples. All measured cross-sensitivities are close to zero. This excellent behaviour of the iBolt™ under the influence of lateral forces and moments is reflected in the seat level measurements shown in chapter 5.2.

<i>Cross Sensitivity</i>	<i>Mean</i>	<i>Sigma</i>
<i>F_x Sensitivity</i>	0.13 %	0.08 %
<i>F_y Sensitivity</i>	0.14 %	0.08 %
<i>M_x Sensitivity</i>	0.41 N/Nm	0.11 N/Nm
<i>M_y Sensitivity</i>	0.06 N/Nm	0.04 N/Nm

Tab. 1. Overview of Cross-Sensitivities for iBolt™.

5 Seat Integration and Performance

5.1 Requirements for Seat Integration

As discussed earlier the major tasks for the sensor design is to ensure the seat integrity, even at a high speed crash, as well as accurately determine the actual load on the seat. Furthermore all the FMVSS-208 requirements have to be fulfilled. This in return affects the seat integration. The unique design of the BOSCH iBolt™ is an unified sensor system resulting in no H-point shift. Therefore no major design changes at vehicle level are necessary compared to systems integrated underneath the seat tracks. As mentioned previously the iBolt™ design shows a distinct insensitivity against lateral forces and moments. This results in an ample degree of freedom for designing the seat structure.



Fig. 6. Example of the BOSCH iBolt™ integrated in a seat between seat track and upper seat structure.

The iBolt™ design features integrated overload protection as well as allowing for a flexible connector design. Fig. 6 shows an example of an integration of the BOSCH iBolt™ between the seat tracks and the upper seat structure. A CAD schematic is given in Fig. 7 showing the lever arm of the height adjuster from the upper seat structure which is secured with a clip ring. The second attachment point of the iBolt™ is the seat track featuring a poka-yoke design to ensure correct orientation of the sensor in the seat structure. The iBolt™ is fixed with a nut (M10) to the seat track.

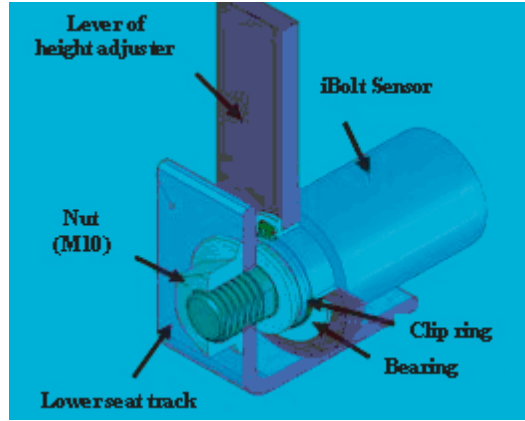


Fig. 7. CAD schematic of the BOSCH iBolt™ integration in a seat structure.

Essential for the performance of the iBolt™ arrangement is to avoid any load shunts by-passing the measuring system. Therefore the selected position in the seat structure, the seat structure design and the connector design has to ensure free movement between upper seat structure and the seat tracks for all seat positions. Integration of the iBolt™ into the seat structure below the seat belt attachment point eliminates the necessity of an additional belt tension sensor. However a customized algorithm in the ECU usually allows for an implementation of the iBolt™ above the seat belt attachment point still safeguarding correct occupancy detection without an additional belt tension sensor. Beneficial is a seat structure design preventing shunting of any parts between sensor and floor panel.

5.2 Seat-Level Performance of the BOSCH iBolt™ Technology

In addition to component testing seat performance at system level is evaluated. Measurements are carried out to reflect various mechanical tolerance influ-

ences, e.g. floor panel and seat track tolerances. Therefore a series like seat is fitted with four BOSCH iBolt™ sensors and an ECU. All shown measurements are carried out at room temperature ($\sim 25^{\circ}\text{C}$) with an unloaded (0 N) and a loaded (~ 400 N) seat. The measurements cover the entire range of seat positions as shown in Fig. 10 and Fig. 11. Starting and end point is the so called design position where the seat is in a mid-mid position. This is not necessarily the geometrical middle position of seat height and seat track. Further seat positions are front (-f), middle (-m) and rear (-r) of the seat tracks. The seat height is varied between down (-d), middle (-m) and up (-up). The system is only once zeroed before a measurement cycle including all seat positions for the unloaded and loaded seat. For the system accuracy and hysteresis test the weights are placed on the seat as shown in Fig. 8. The seat is in design position and the weight is increased in steps of 200 N up to a maximum of 800 N. For all other measurements the weight is placed in the middle of the seat right in front of the back rest (dotted line).

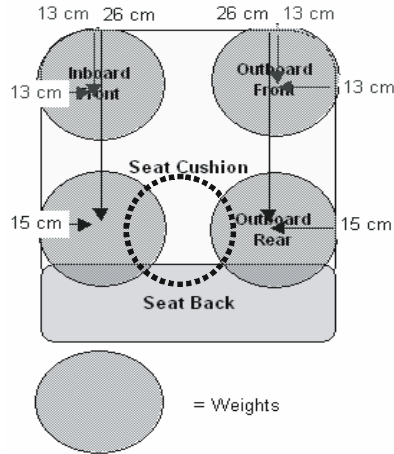


Fig. 8. Schematic of the weight positions on the seat.

Fig. 9 shows the applied load compared to the measured output signal of the system. The maximum deviation observed is 11 N is at a load of ~ 601 N. The maximum hysteresis (8 N) occurs at an applied load of 201 N. These output weights are computed by the ECU out of the signals of the four iBolt™ sensors. Note the seat used is a slightly modified series seat to accommodate the iBolt™ sensors. No additional adaptations are made to reduce seat-embedded preloads and moments.

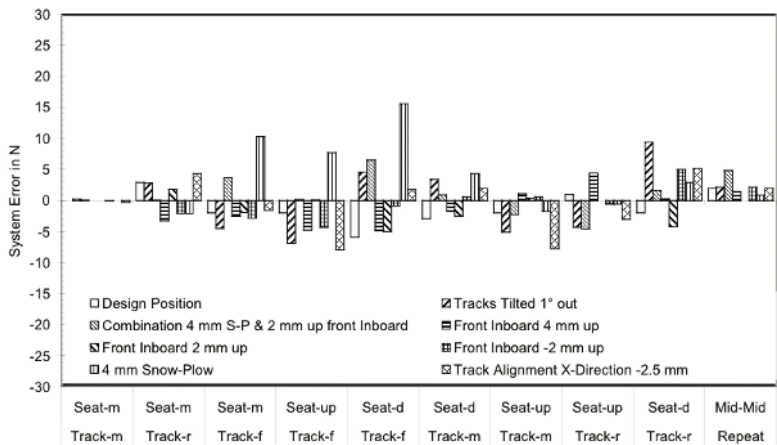
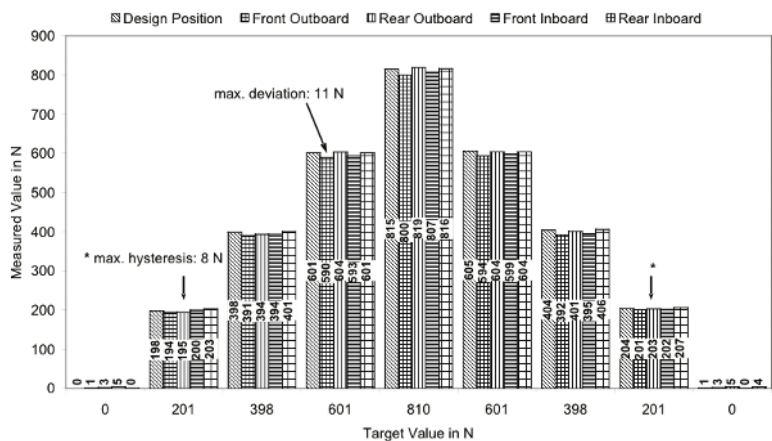


Fig. 10. System performance over entire seat positions at a variation of mechanical tolerance of e.g. floor panel at no additional load on the seat.

Looking at the system performance for a variation of possible misalignments of the seat tracks on the floor panel the BOSCH iBolt™ technology shows outstanding performance. In Figs. 10 and 11 the deviation of the output signal of the iBolt™ is shown as function of different misalignments without and with an additional load of 398 N respectively. Within the figures the maximum error bands (± 30 N) are given. In total six different misalignment situations

are investigated. Additionally a combination of two misalignments is tested. As a reference the design position is shown without any misalignments. The maximum deviation over all misalignments is 15 N and 22 N for the unloaded and loaded seat, respectively. This maximum occurs at a so called 4 mm snow-plow situation where both front attachment points are moved inward by 1 mm and both rear attachment points outward by 1 mm. Interestingly the combination of snow-plow and one raised attachment point shows no further increase of deviation. Hence for a certain seat structure a maximum deviation is expected caused by the system-implicit preloads.

Seat tests performed focus on the variation of the relative position of the four anchorage points of a passenger seat to each other. Therefore in one test one by one the four anchorage points are raised by 2 and 4 mm as well as lowered by 2 mm (-2 mm up). A further experiment varied the distance between the anchorage points 1 mm inside or outside. A variation of that test is the so called snow-plow situation where the front and the rear anchorage points are moved inside and outside, respectively. In the track alignment test inboard and outboard seat track are moved in X-direction by 2.5 mm to each other. The seat tracks also can be tilted inside or outside. Hence one or both seat tracks is tilted either inside or outside by 1°.

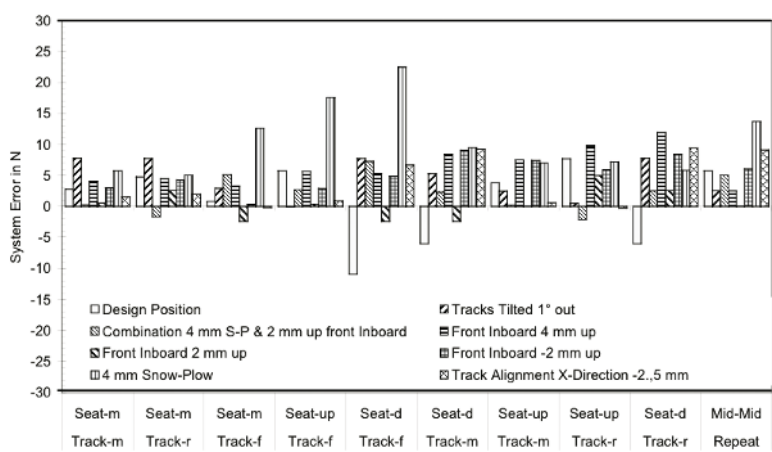


Fig. 11. System performance over entire seat positions at a variation of mechanical tolerance of e.g. floor panel at 398 N additional load on the seat.

All these misalignment positions are thought of reflecting the tolerances of floor panel and assembling of the seat structure. Hence combinations of these misalignments can occur. This is accounted for in the combination of the snow-

plow and one raised attachment point. Results shown in Figs. 10 and 11 give the worst case scenario of the different misalignment tests.

Further investigations included temperature cycling measurements on seat level with and without load. Fig. 12 shows the deviation of the sensor output related to the temperature. The temperature scale is on the right hand side the deviation is shown on the left hand scale. Interestingly, the maximum observed temperature related deviation is 16 N and 13 N for the unloaded and loaded seat, respectively. This effect is addressed to the additional load of ~ 400 N which is orientated opposite to some of the movement in the seat due to the temperature influence.

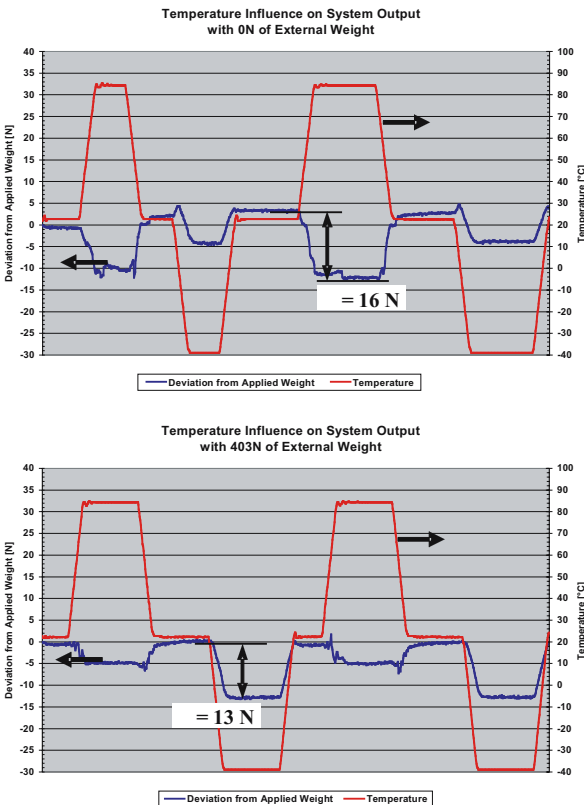


Fig. 12. Temperature behaviour of a unloaded (above) and ~ 400 N loaded seat (below).

FMVSS 208 requirements include 35 mph, 50% and 95% male ATD sled test on a rigid barrier according to US-NCAP and static anchor pull test (FMVSS 207/210) with a maximum load of $F_{\max} = 19 \text{ kN}$. The BOSCH iBolt™ sensors passed all tests and maintained their structural integrity.

Additionally 12 mph low speed non-fire frontal crash and 10 mph rear impact, 50% male ATD, sled test with vehicle buck as well as 10 mph side impact (SID) according to FMVSS214 are passed without performance degradation.

6 Summary and Outlook

In order to fulfil the requirements of the FMVSS 208 Robert Bosch GmbH has developed a seat integrated weight sensor (iBolt™). A complete sensing system for weight classification consists of 4 iBolts™ and an ECU (Electronic Control Unit). The ECU filters the input signals of the iBolts™, computes the sum and delivers the occupancy status of the passenger seat. The occupancy classification is communicated to the airbag ECU.

The measurement principle of the iBolt is based on a deflecting bending beam utilizing a particular magnet-to-Hall-IC configuration.

The main advantages of the presented iBolt™ concept are:

- a. Low and high speed crash robustness: The iBolt™ is designed such that yielding or fracturing of the sensor is prevented by an integrated limit stop feature.
- b. Ease of application: The iBolt is easily integrated into a seat structure not causing any H-point shift, because it replaces an existing bolt of the seat structure.
- c. Low cross coupling: The iBolt™ design is optimized for insensitivity to lateral forces and moments.

Overall this allows for an inexpensive and simple integration into the seat structure. Furthermore no additional measures are required at seat level to limit or reduce lateral forces and moments affecting the iBolt™. This insensitivity leads to an excellent seat level performance, even in heavily distorted seat structures.

Additionally, the iBolt™ is optimized for temperature performance leading to minimal temperature dependency within the operating range of -40°C to $+85^{\circ}\text{C}$.

The next iBolt™ generation will feature a digital bus solution replacing the analogue point-to-point connection. Furthermore the integration of the iBolt™-ECU into the airbag ECU is in development, to reduce the overall system costs.

Dr.-Ing. Klaus Kasten

PO-Box: 1342

72703 Reutlingen

Germany

Klaus.Kasten2@de.bosch.com

Keywords: weight sensing, occupant classification, FMVSS 208, Hall-sensor, force sensor, passenger airbag, iBolt

Object Classification exploiting High Level Maps of Intersections

S. Wender, T. Weiss, K. C. J. Dietmayer, University of Ulm
K. Ch. Fürstenberg, IBEO Automobile Sensor GmbH

Abstract

An object classification system is introduced. The system observes the vehicle's environment with a laser scanner. Preprocessing and object tracking algorithms are applied. The object classification combines a pattern classifier with rule based a priori knowledge and high level map information. The pattern classifier uses significant features to calculate membership values for each class. These membership values are verified and corrected by a priori knowledge. Furthermore, a precise position of the test vehicle is estimated. The positions of observed objects in the high level map can be determined exploiting this information. As the object position is restricted for some object classes, this knowledge can be used in the classification, which significantly improves its performance. Finally, the system is evaluated with labeled test data of several sequences at different intersections.

1 Introduction

Nowadays, automotive research focuses on active safety systems. Since many applications need similar sensor data processing, a common algorithmic base for all applications can reduce the overall processing time. The output of these common algorithms can comprise a detailed vehicle environment description. This description should consist of position, size, orientation and velocity of observed objects. In addition, the type of the objects can be important. This information might be useful for several applications. Vulnerable road user protection, for example, is based on the identification of pedestrians. Sometimes, also the identification of bikes is required to protect their drivers. Another example may be precrash applications. The airbag deployment can be controlled depending on the estimated weight of the type of the crash opponent. For this application, a separation of cars, trucks, small road users, and stationary objects will be interesting.

Especially the vehicle environment perception at intersections is an important and challenging task. It is important as a large amount of accidents occur at intersections and challenging as the road users move in multiple directions. It is not possible to restrict the orientation and the direction of motion as it is possible on highways or motorways. Additionally, a high traffic density may increase the complexity of intersection scenarios (Fig. 1). Therefore, present research concentrates on special algorithms for intersections [1].

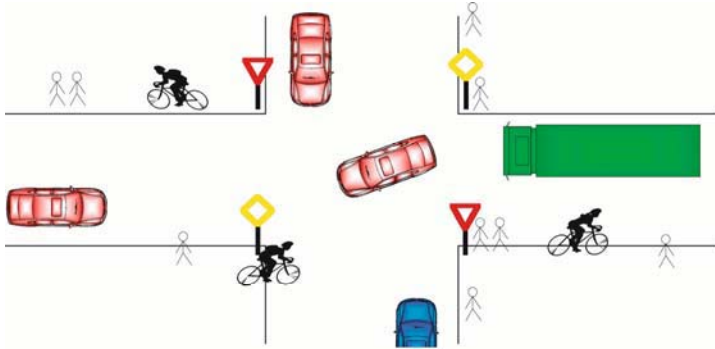


Fig. 1. Complex situations at intersection scenarios: Environment modeling algorithms need to handle high traffic density, multiple directions of motion and partial occlusions

Our approach distinguishes five types of objects. There are four moving object types: "pedestrian", "car", "truck" and "bike". Motorcycles and bicycles belong to the class "bike". The remaining class of stationary objects is called "unknown". The focus of this work is on the improvement of the object classification at intersections.

2 Sensor Configuration

The algorithms use sensor data of a scanning laser range finder (laser scanner). This laser scanner is manufactured by IBEO AS, Germany. It is integrated in the front bumper of the test vehicle (Fig. 2). Technical details of this sensor can be found in [2].



Fig. 2. Integrated laser scanner: The integration allows for an adaptation to the vehicles design. The sensor technology enables the usage under adverse weather conditions.

3 Preprocessing and Tracking

A segmentation algorithm clusters close distance measurements, which possibly belong to the same object [3]. The measurements are assigned to observed objects of former time steps. This object tracking is based on Kalman Filter estimation. Detailed tracking algorithms are described in [4].

In this work, all object models are free mass models. The reference point is the centre of gravity. An improved feature association is used. This feature association provides the possibility to assign more than one segment to an object. This was necessary, because objects can disintegrate in several segments in some cases. This disintegration is due to the distance based segmentation. If different parts of large objects are measured, the distance between these parts can be too large to assign all measurements to the same object (Fig. 3).

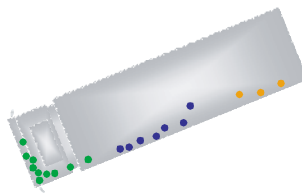


Fig. 3. Object disintegration: Objects can sometimes disintegrate into several segments. If different parts of large objects are measured, the distance between these parts can be too large to assign all measurements to the same segment.

The association of all segments to the same object can improve the classification task, because the object size is a significant criterion for the object classification. Especially cars and trucks can often only be distinguished by their size. The multiple segment assignment concentrates only on the classes "pedestrian", "bike", "car", and "truck". The identification of multiple segments for background objects is quite difficult, because there are no assumptions or restrictions for the shape of background objects.

Two methods are applied to assign multiple segments to an object, which was already observed in former time steps. The first method uses the fact that disintegration causes the appearance of new segments. Usually, all objects in the environment of these segments are already assigned to other segments. A segment will now be assigned as additional segment, if several conditions are fulfilled. The additional segment must not be located at the boundary of the field of view. In this case, the observation of a new object is more probable. The resulting object must not be transparent. That means the laser scanner may not provide measurements behind the object (Fig. 4, left). The resulting object must be convex (Fig. 4, middle). This restriction is used, because pedestrians, bikes, cars, and trucks are usually convex. Finally, a smooth contour is expected for these objects. Therefore, the corresponding endpoints of two assigned segments must be closer than all other pairs of points. (Fig. 4, right)

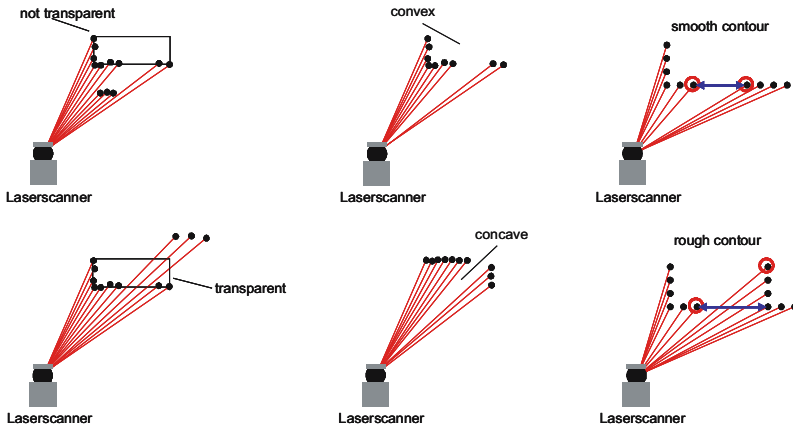


Fig. 4. Criteria for the first method to assign additional segments: New segments will be assigned to objects with segments, if they cannot be assigned to an object without segments. The combined object measurements must not be transparent (left). They must be convex (center) and have a smooth contour (right).

The second method to associate additional segments is the usage of object speed. Moving vehicles must keep a safety distance to the next vehicle. This distance depends on the vehicle's speed. Drivers in Germany are already high fined, if they do not keep a safety distance of a quarter of the speed indicator's value in m. That means the safety distance d in meter can be calculated based on the object speed v in meter per second:

$$d > v * 3.6s / 4$$

Studies have shown that drivers do not keep even this minimal safety distance. Therefore, the algorithm uses a minimal distance of an eighth of the speed indicator's value in m:

$$d_{\min} > v * 3.6s / 8$$

If the tracking algorithm can reliably estimate an object speed with former observations, the minimal safety distance will be used. All segments in front of or behind the object will be assigned to the object, if they are closer than d_{\min} . All assigned segments are now used to calculate a new value for the measured object size (Fig. 5). Afterwards, the method is applied again to assign additional segments. This loop is stopped as soon as the algorithm can not find any more new segments.

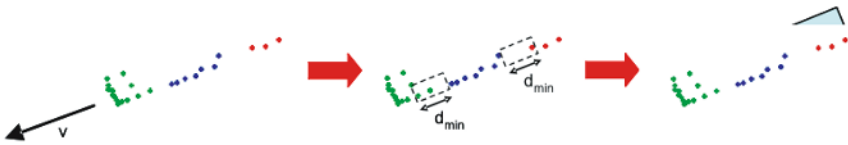


Fig. 5. Second method to assign additional segments: If the tracking algorithm can reliably estimate an object speed, all segments will be assigned, which are closer than a safety distance in front of or behind the object. New measurements of the object's size will be calculated.

Both methods add only segments of the actual time step. The calculated size is used as measured feature for the Kalman Filter, which also filters the object size. The association of multiple segments must be repeated in the next time step.

Based on the tracking and preprocessing algorithms, significant features are extracted. These features are used by the classifier to estimate the object class. There are three types of object features. The first feature group is the contour

information. This group consists of features like width or length. The second group consists of dynamic features like speed, which are extracted from the object tracking. Furthermore, observed reflectors are used as features. The calculated features are described in detail in [5].

3 Classification

3.1 Classification Overview

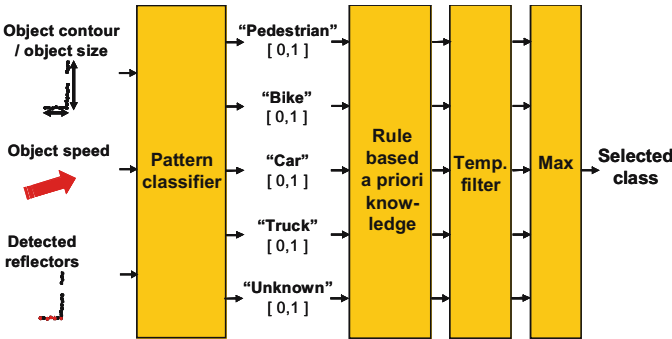


Fig. 6. Classification system: A pattern classifier estimates a membership value for each class based on the features of the object. Rule based a priori knowledge is used to verify and correct the output of the pattern classifier. A temporal filter combines classification results of several time steps. The output class is selected by the maximum membership value.

The object classification consists of four parts. The first part is the pattern classification. The pattern classifier calculates a membership vector for each object based on the object features. This vector contains a membership value for each object class. The membership value 0 means, the object is improbable. The membership value 1 means, the object is very probable.

The pattern classifier is based on neural networks, which provide low processing time and good classification results. The detailed pattern classifier architecture is described in [6]. The classifier estimates its internal parameters by a sample data based training procedure. The pattern classification is the application of the trained classifier to new sample data.

The second part comprises the verification and the correction of the class vector. A priori knowledge is used to correct implausible membership values. Restrictions with respect to the objects size and speed are applied. The membership values of implausible classes are set to zero. In addition, information about the location of observed objects in a high level map will be used to restrict the object class. The usage of maps is described in Section 5.

The third part applies a temporal mean to the membership vector. This filter includes classification results of former time steps in the actual classification.

Finally, the object's most likely class is chosen for the output by the maximum membership value.

3.3 Sample Data

The pattern classifier is trained with a set of training samples. This set consists of 38 sequences. These sequences provide laser scanner distance measurements of 10.000 time steps (10.000 scans). The system was evaluated with 12 additional sequences, which consist of approximately 5.000 scans. These sequences are not part of the training data.

4 Precise Ego-Localization using Precise Digital Maps

Today's common digital navigation maps contain information about the traffic infrastructure, such as the number of lanes and their positions as well as special locations, such as hospitals, fuelling stations or restaurants. The position accuracy is in the meter level, which is sufficient for navigation purposes. This work uses more precise environmental description, which can be measured with sensors like laser scanners. In this section an approach for the precise localization of the test vehicle using landmarks is proposed. This information will be used in connection with precise digital high level maps to improve the object classification algorithms significantly.

4.1 Determination of the Precise Position of Landmarks

4.1.1 Grid Maps

The position of landmarks used for the determination of the precise position and orientation of a vehicle in a specific street section is determined using grid

maps. Therefore, a mapping vehicle equipped with a laser scanner passes a street section. The distance profiles provided by the laser scanner are accumulated. The position of the vehicle during the mapping process must be known precisely to generate a consistent and accurate grid map. Therefore, a RTK-GPS (Real Time Kinematic) receiver in conjunction with an IMU (Inertial Measurement Unit) can be used. The accuracy of the position measurements of those systems is in the centimeter level. For limited regions up to about 80 m the integrated wheel speed encoders and yaw rate sensor can be used to determine the position and orientation of the vehicle during the mapping process. In Fig. 7 a grid map of an intersection is shown.

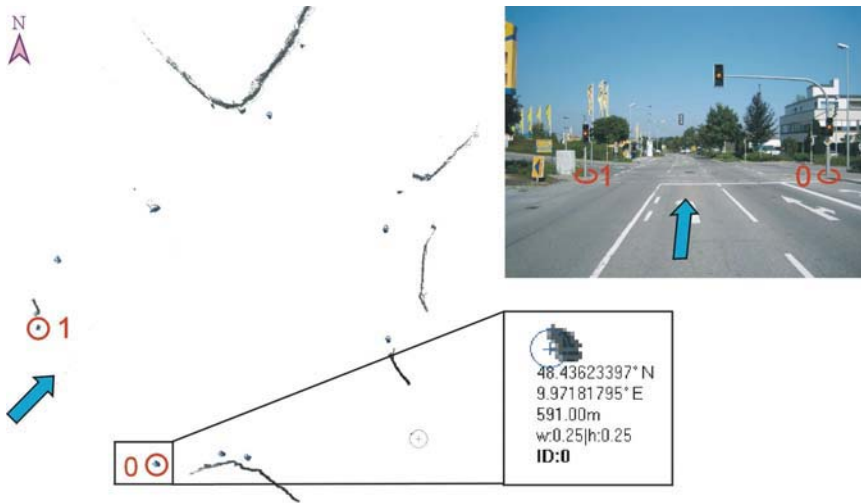


Fig. 7. Grid map of an intersection: The posts of the traffic lights are used as landmarks (features) for the ego localization approach. The WGS-84 coordinates of the features are shown.

4.1.2 Landmarks

Vertical elongated stationary objects, such as posts of traffic lights and traffic signs, which can be detected by a laser scanner, are used as landmarks (features) to determine the precise position and orientation of the vehicle.

As mentioned above, the positions of these stationary objects are determined using grid maps. Therefore, a reference coordinate system for the features and the grid map is required. Most GPS receivers provide their position measurements in the geographic WGS-84 (World Geodetic System) coordinate system.

Many common navigation databases based on GDF (Geographic Data File) also use the WGS-84 coordinate system.

For this reason, the positions of the features are determined in the WGS-84 coordinate system as the features can be related to GPS measurements and the features can be added to common map databases. For this purpose, a reference point of the grid map and its orientation to geographic north must be known. This reference point coincides with the starting point of the mapping process. The WGS-84 coordinates of this point can be determined using a precise RTK-GPS system providing position measurements in the cm-level.

If RTK-GPS is not available, surveillance points, which can be found in urban areas in low distances, can be used to determine a reference point of a grid map. The determination of the WGS-84 coordinates of features is described in detail in [7]. In Fig. 7 extracted features and their WGS-84 coordinates are shown. These landmarks are added to a high level map.

4.1.3 Ego-Localization

As mentioned above, the position and orientation of the vehicle is determined using features. In the first step the features are transformed into the laser scanner coordinate system with respect to the position measurements of a standard GPS receiver. These standard receivers are already integrated in modern cars for navigation purposes. As the accuracy of the GPS position measurements are in the meter level, the transformed landmarks are translated and rotated in the scan of the laser scanner as shown in Fig. 8. The main challenge is to associate the features to the distance measurements of the laser scanner as the environment is rapidly changing and features are often occluded in urban areas.

In order to solve the association problem a translation and rotation invariant representation of geometric arrangements was defined. In the first step the scan is clustered as described in section 3. Several segments are combined to a mesh. The mesh is then represented by a set of parameters which define the geometric constellation of the segments. However, the representation is position and rotation invariant. This set of parameters is then compared to a mesh constructed from features of the high level map. A new algorithm TrAss (Triangle Association) finds the optimal association between a segment-mesh and a feature-mesh. This algorithm allows the detection of visible features in the scan in one time step. After an established association, the feature shapes are matched with the shape of the segments in order to determine the exact

position of the features in the laser scan. Fig. 8 shows an example with real data. The localization algorithm is described in detail in [8].

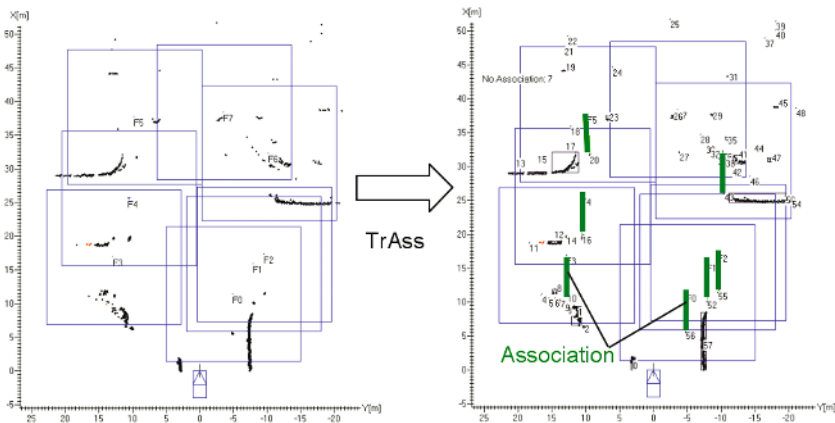


Fig. 8. Left: The features were transformed into the laser scanner coordinate system with respect to the position measurements of a standard DGPS receiver providing position measurements with an accuracy of several meters. Right: The segments of the clustered scan are associated to the transformed features using the TrAss (Triangle Association) algorithm. This association is visualized by the green lines. The successful association allows a correction of the test vehicle's position and orientation.

4.2 High Level Maps

The infrastructure is represented by precise high level maps. These maps contain information about the topology of traffic lanes and other static objects like traffic lights or traffic signs. In addition, they can store attributes, like the driving direction of a traffic lane.

The high level maps can be stored in the GDF format, which is used by current navigation systems. Compared to existing navigation maps, the position of the traffic lanes is measured more precisely. It is possible to convert the lane information to polygons, which describe the traffic lanes. The combined polygons form the road area of the intersection (Fig. 9).

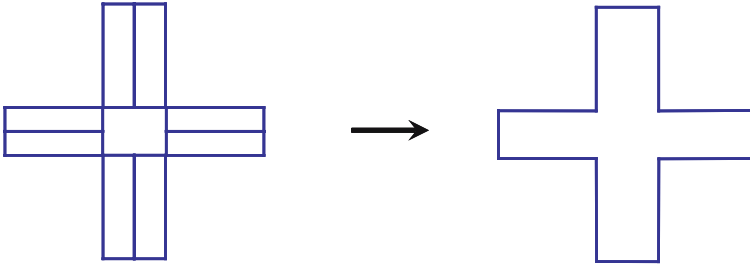


Fig. 9. All traffic lanes of the high level map are combined to a road mask.

The information about the road is used in the rule based part of the classification. The precise position of the test vehicle can be used to determine a precise position of observed objects in the high level map. It is assumed, that cars or trucks can not appear beside the road. Thus, the membership value of the classes "car" and "truck" will be set to zero, if an object is located beside the road. Background objects are not assumed to appear on the road. Therefore, the membership value of the class "unknown" is set to zero for all objects, which are located on the road. These rules allow a classification of objects by their position even if the objects' contour is identical (Fig. 10).

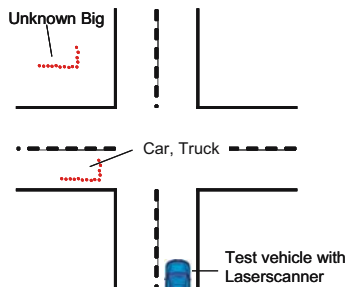


Fig. 10. The position of measured objects can be used for classification. Objects, which are observed in areas, which certainly belong to the road, cannot be stationary objects. Cars and trucks cannot appear in areas, which certainly do not belong to the road.

Furthermore, high level maps can contain areas, which are not of interest for the tracking and classification algorithms. These areas can be houses or gardens, for example. The areas should be ignored by all algorithms (Fig. 11). This is realized by removing all distance measurements of the laser scanner, which are located in such areas. The remaining area is the region of interest (ROI).

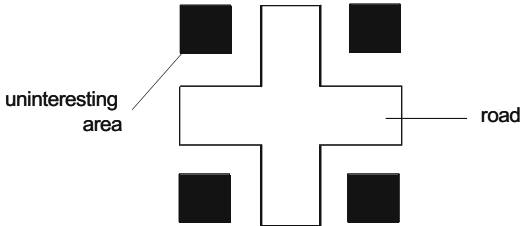


Fig. 11. Some areas at intersection such as houses or gardens may be not of interest for tracking and classification algorithms. These areas can be stored in the high level map and all distance measurements inside these areas will be ignored.

4.3 Application of Uncertainties

The test vehicle’s position is calculated with a position uncertainty and an orientation uncertainty. Applying these uncertainties to the high level map establishes several areas of confidence. The first area is the area, which certainly belongs to the road. The second one is the area, which might belong to the road. The remaining area certainly does not belong to the road. The uncertainties are also applied to the areas, which should be ignored. The areas, which certainly should be ignored by tracking and classification, are calculated.

The test vehicle’s position uncertainty reduces the area, which certainly belongs to the road. At the same time, the area, which might belong to the road, is increased with respect to the road mask. The remaining area does certainly not belong to the road (Fig. 12).

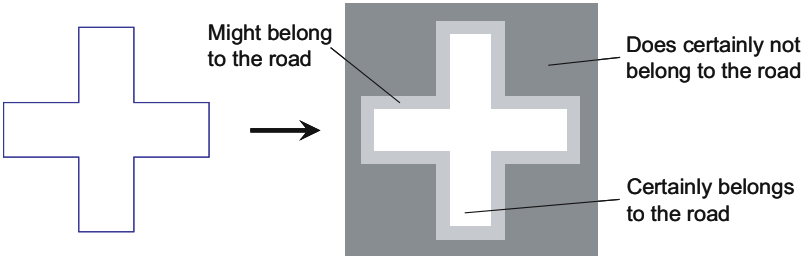


Fig. 12. The uncertainty of the test vehicles position reduces the area, which certainly belongs to the road, while increasing the area, which might belong to the road.

The uncertainty of the ego vehicle's orientation also reduces the area, which certainly belongs to the road. The area, which might belong to the road, is increased. When rotating the mask by this uncertainty to the left and the right, the whole covered area might belong to the road. The area, which certainly belongs to the road, must be covered by the rotated mask at all possible rotation positions (Fig. 13). When the mask is rotated, the points of the polygon move on a circular arc. This arc is approximated as a straight line (highlighted in red), because the rotation is performed with a small angle.

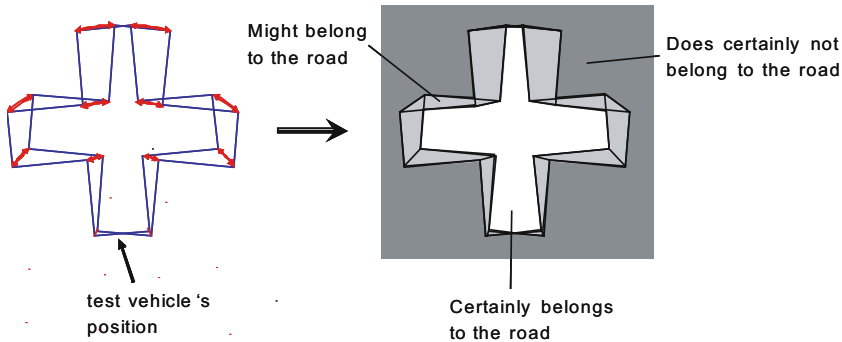


Fig. 13. The uncertainty of the ego vehicle's orientation can be taken into consideration by rotating the road mask. Every point, which is covered at least once, might belong to the road. The area, which is covered by all rotated masks, certainly belongs to the road. The remaining area certainly does not belong to the road.

The translative and rotational uncertainties are combined to calculate the areas of confidence. First, the road mask is enlarged by the position uncertainty. Then it is rotated by the orientation uncertainty to the left and to the right. The two increased road masks with maximum rotation are used to determine the areas. The corresponding polygon points are connected with lines. The whole area, which is covered by this rotation, might belong to the road. The area is calculated by starting at the point with the minimal x value. The algorithm successively chooses polygon lines of the outer contour of the structure (Fig. 14, left).

The area, which certainly belongs to the road, must be covered by both rotated decreased masks. A point of this area must be inside the first mask and stay inside the other mask during the whole rotation. This fact is used to find a starting point for the area estimation. A polygon point of one mask is chosen. The connection to the corresponding point of the other mask must completely be inside this other mask. Again, the algorithm successively chooses lines of the inner contour (Fig. 14, right).

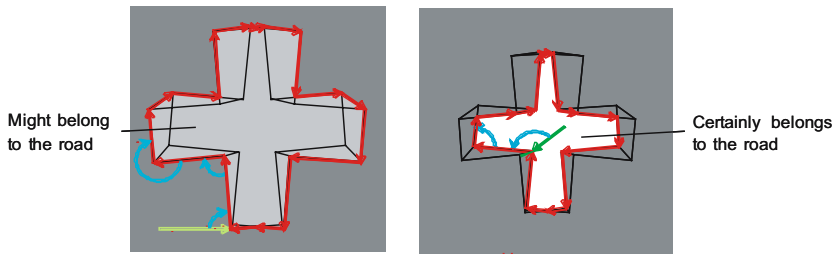


Fig. 14. The area, which might belong to the road, is calculated based on two increased road masks, which are rotated by the maximum angle to the left and the right. The corresponding points are connected with lines. The outer contour is extracted. The area, which certainly belongs to the road, is calculated with two decreased masks with maximum rotation. An inner contour is extracted.

The uncertainties are also applied to all stored uninteresting areas. The areas, which should certainly be ignored, are estimated. This is similar to the calculation of the area, which certainly belongs to the road. All calculated areas are shown in Fig. 15.

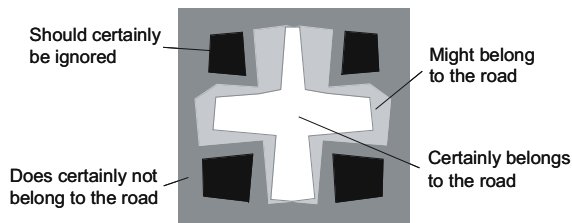


Fig. 15. High level map with applied uncertainties: Several areas of confidence are calculated by applying the test vehicle's position and orientation uncertainties to the high level map.

5 System Evaluation

The system was evaluated with test data of several sequences at different intersections. Of course, the test data was not used to train the classifier. Two measures were calculated to analyze the system performance. The detection rate describes the percentage of objects, which are correctly detected and classified:

$$\text{detection rate} = \frac{\text{true positives}}{\text{true positives} + \text{false negatives}}$$

True positives are objects of the classes "pedestrian", "bike", "car", and "truck", which are classified correctly. This number is divided by the number of all objects of these classes.

The false detection rate is the ratio of false detections to all detected objects of the classes "pedestrian", "bike", "car" and "truck".

$$\text{false detection rate} = \frac{\text{false positives}}{\text{false positives} + \text{true positives}}$$

In this case a false positive can be a misclassification of a background object, but also misclassifications of other objects as "pedestrian", "bike", "car" or "truck" will be false positives. That means that even a car, which is classified as "truck", is a false positive.

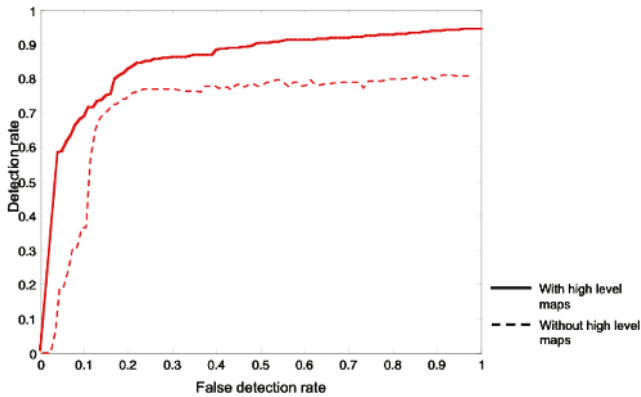


Fig. 16. System evaluation: The system performance is evaluated based on complex intersection scenarios. The operating point curves show the possible combinations of detection rate and false detection rate. The dashed line shows the performance without high level maps. The improved results of the classification with high level maps are shown by the solid line.

Different possible combinations of the described measures are shown by an operating point curve in Fig. 16. The solid line shows the performance with

high level maps at complex intersection scenarios. The dashed line shows the performance without high level maps for the same scenarios.

The algorithms are implemented on an Intel Pentium M with 1.7 GHz. The processing time for one time step is 17 ms. As the used sensor sample rates are 10 Hz and 20 Hz, the system is applicable in real time.

6 Conclusions

An object classification system was described, which combines pattern classification and a priori knowledge. Significant improvements in the classification performance were achieved by the usage of high level maps of intersections. Localizing the road users with respect to a high level map enables the application of object class depending constraints. Additionally the preprocessing could be improved by the assignment of multiple segments to one object in case of object disintegration. The complete system is designed to be applicable in real time.

Current work aims at an extension of the scenarios. The presented results show the system performance for complex intersection scenarios. However, it is to be expected that other a priori knowledge of scenario environments, such as "driving on a highway", can enhance the performance of the object classification. Further improvements may be achieved by adapting the system to the requirements of a specific application.

References

- [1] K. Ch. Fuerstenberg, U. Lages, "New European Approach for Intersection Safety – The EC-Project INTERSAFE", Proceedings of 2005 IEEE Intelligent Vehicles Symposium, Las Vegas, 2005
- [2] Homepage of the IBEO Automobile Sensor GmbH, <http://www.ibeo-as.de>, January 2006
- [3] K. Ch. Fuerstenberg, K. Dietmayer, "Fahrzeugumfelderfassung mit mehrzeiligen Laserscannern", Journal Technisches Messen 71 (2004) 3, Oldenbourg Verlag, Munich, 2004
- [4] N. Kaempchen, M. Buehler, K. Dietmayer, "Feature-Level Fusion for Free-Form Object Tracking using Laserscanner and Video", Proceedings of 2005 IEEE Intelligent Vehicles Symposium, Las Vegas, 2005

- [5] S. Wender, M. Schoenherr, N. Kaempchen, K. Dietmayer, "Classification of Laserscanner Measurements at Intersection Scenarios with Automatic Parameter Optimization", Proceedings of 2005 IEEE Intelligent Vehicles Symposium, Las Vegas, 2005
- [6] S. Wender, K. C. J. Dietmayer, "Statistical Approaches for Vehicle Environment Classification at Intersections with a Laserscanner", Proceedings of ITS 2005, 12th World Congress on Intelligent Transportation Systems, San Francisco, 2005
- [7] Fuerstenberg, K.; Weiss, T. "Feature-Level Map Building and Object Recognition for Intersection Safety Applications" Proceedings of IEEE Intelligent Vehicles Symposium 2005, Las Vegas, USA, June 2005
- [8] Thorsten Weiss, Nico Kaempchen, Klaus Dietmayer, „Precise Ego-Localization in Urban Areas Using Laserscanner and High Accuracy Feature Maps", Proceedings of IEEE Intelligent Vehicles Symposium 2005, Las Vegas, USA, June 2005

Stefan Wender, Thorsten Weiss, Klaus C. J. Dietmayer

Department of Measurement, Control and Microtechnology
 University of Ulm
 Albert-Einstein-Allee 41
 89081 Ulm
 Germany
 stefan.wender@uni-ulm.de
 thorsten.weiss@uni-ulm.de
 klaus.dietmayer@uni-ulm.de

Kay Fürstenberg

IBEO Automobile Sensor GmbH
 Fahrenkrön 125
 22179 Hamburg, Germany
 kf@ibeo-as.de

Keywords: object classification, high level maps, ego localization, intersection, laser-scanner, multiple segment association

Performance of a Time-of-Flight Range Camera for Intelligent Vehicle Safety Applications

S. Hsu, S. Acharya, A. Rafii, R. New, Canesta Inc.

Abstract

A variety of safety-enhancing automobile features can be enabled by microsystems that can sense and analyze the dynamic 3D environment inside and outside the vehicle. It is desirable to directly sense the 3D shape of the scene, since the appearance of objects in a 2D image is confounded by illumination conditions, surface materials, and object orientation. To overcome the disadvantages of 3D sensing methods such as stereovision, radar, ultrasound, or scanning LADAR, we present Electronic Perception Technology, an advanced range camera module based on measuring the time delay of modulated infrared light from an active emitter, using a single detector chip fabricated on standard CMOS process. This paper overviews several safety applications and their sensor performance requirements, describes the principles of operation of the range camera, and characterizes its performance as configured for airbag deployment occupant sensing and backup obstacle warning applications.

1 Introduction

A variety of safety-enhancing automobile features can be enabled by microsystems that can sense and analyze the dynamic 3D environment inside and outside the vehicle. Safety features may include collision warning and avoidance, smart airbag deployment, obstacle detection such as backup warning, and parking assistance. Common to these applications is the need to detect, isolate, measure, locate, recognize, and track objects such as people, traffic, and road-side features.

It is often proposed to perform these tasks using conventional 2D imaging sensors and analysis software, but achieving cost-effective and reliable performance during all vehicular usage scenarios is a formidable challenge. The appearance of objects in a 2D image varies greatly, depending on illumination conditions, surface materials, and object orientation. These variations in the image complicate the task of software that must interpret the scene. On the other hand, the 3D shape of objects is invariant to those confounding effects.

Stereovision based 3D recovery is computationally complex and fails on un-patterned surfaces. RADAR, ultrasonic, scanning LADAR, and other ranging technologies are similarly proposed, but they have difficulty discriminating objects due to limited temporal or angular resolution; moreover, the need for specialized sensors for each safety function poses system integration challenges. A single high frame rate focal-plane-array 3D sensor is desirable because it can serve multiple safety and convenience functions simultaneously, allowing applications to jointly exploit shape and appearance information in a dynamic scene. The output of the sensor should be a sequence of 2D arrays of pixel values, where each pixel value describes the brightness and Cartesian X , Y , Z coordinates of a 3D point on the surface of the scene.

Canesta has developed Electronic Perception Technology (EPT), an advanced range camera module based on pixels that measure the time delay of modulated infrared light from an active emitter. Electronic Perception technology permits machines, consumer and electronic devices, or virtually any other class of modern product to perceive and react to objects and individuals in the nearby environment in real time, particularly through the medium of "sight," utilizing low-cost, high-performance, embedded sensors and software.

The camera module contains a light source constructed from a bank of infrared LEDs (or laser diodes), a lens system for the detector chip, a detector chip with 160×120 phase-sensitive pixels fabricated on standard CMOS process, and an embedded CPU for application processing.

This paper first surveys several automotive safety applications. Next, quantitative performance metrics are defined for range cameras, which are necessarily evaluated on a different basis from 2D cameras. It explains geometric uncertainty, accuracy, and dynamic range as important factors in the performance of range sensors. Then it describes how the automotive applications requirements map to the sensor performance metrics. Next, the paper describes the principles of operation of the EPT range camera, highlighting design features that overcome challenges to this sensing method, including resilience to full-sunlight illumination. Finally, the paper presents two application-specific configurations of the range camera and characterizes its performance for those applications.

2 Safety Applications and Sensor Requirements

Growing government legislation, increasing liability concerns, and the inevitable consumer desire for improved safety make the introduction of new

safety features a high priority for automakers. Today, various sensing technologies play a key role in delivering these features, detecting conditions both inside and outside of the vehicle - in applications like parking assistance, adaptive cruise control, and pre-crash collision mitigation. Each of these applications is characterized by a unique customized technology (e.g. ultrasonic, RADAR, LADAR, digital image sensing, etc.), which generally provides either a ranging function or an object recognition function.

The need for investment in multiple disparate technologies makes it challenging to deploy individual safety features as quickly or as broadly as desired.

Future applications pose even more difficulties, as multiple features must be provided in a single vehicle. Plus, virtually all of the new sensing applications on automakers' roadmaps (e.g. pedestrian detection being planned in Europe and Japan) require both ranging and object recognition functions. Combining two incongruent technologies to accomplish this task (such as RADAR and digital image sensing) is expensive, difficult to implement, and poses the additional problem of inefficient development.

The use of vision gives added levels of discernment to the air bag systems by providing static or dynamic occupant classification and position sensing. Further, the addition of a vision system inside the cabin enables other value-added applications such as abandoned baby/pet detection, personalization, and security. Applications for vision-based sensing outside the car are blind spot detection, vehicle lane departure, safety in rear vision, proximity of other vehicles around the vehicle, and off road and heavy equipment proximity sensing. The benefits of vision sensors are two fold. They provide enhanced visual feedback to assist the driver in operating the vehicle. But more importantly, when vision sensors also provide range data, they provide the necessary information for advanced algorithms to achieve higher level of discernment and more accurate analysis of object motion dynamic. With such sensors, for instance, the system can use the shape differences between a person and a large box sitting in the front seat to deploy the air bag or not.

We consider the requirements of some of these applications after defining the relevant range sensor performance metrics.

2.1 Range Sensor Performance Metrics

An imaging sensor's lateral resolution can be measured in pixels per degree (pixels/°), but field distortion in typical lenses tends to reduce the resolution in the periphery of the image.

The geometric measurement performance of a range camera can be characterized by several statistics. For any quantity repeatedly measured over time, we define accuracy as the RMS error between the time average of that measurement and ground truth, uncertainty as the RMS error between instantaneous measurements and the time average, and total uncertainty as the 3-sigma confidence bound between the instantaneous measurements and ground truth. The spatiotemporal extent of the averaging regions for these statistics should be chosen based on the application. For occupant sensing, head-sized regions spanning 20 cm x 20 cm over 40 frames are appropriate.

Specifically, the range camera produces a 3D measurement $\mathbf{P} = (\mathbf{X}, \mathbf{Y}, \mathbf{Z})$ for each image pixel i at each frame t . By convention, the coordinate system is defined with respect to the camera, with the \mathbf{Z} axis in the viewing direction, and \mathbf{X}, \mathbf{Y} being lateral directions. If \mathbf{Z}' denotes the time average of \mathbf{Z} measurements, and \mathbf{Z}^* denotes the ground truth, then we may compute the statistics as follows:

- ▶ Accuracy in \mathbf{Z} is the RMS error

$$\sqrt{\sum_i n_i (\mathbf{Z}'_i - \mathbf{Z}^*_i)^2} / N.$$
- ▶ Uncertainty in \mathbf{Z} is the RMS error

$$\sqrt{\sum_i \sum_t (\mathbf{Z}_{it} - \mathbf{Z}'_i)^2} / N.$$
- ▶ Total uncertainty is

$$|\mu| + 3\sigma,$$

where $\mu = \sum_i \sum_t (\mathbf{Z}_{it} - \mathbf{Z}^*_i) / N$ and $\sigma = \sqrt{\sum_i \sum_t (\mathbf{Z}_{it} - \mathbf{Z}^*_i - \mu)^2} / N.$

Performance statistics for \mathbf{X} and \mathbf{Y} are analogous.

For a conventional imaging camera, dynamic range is defined as the ratio of the largest non-saturating (i_{\max}) input signal to the smallest detectable input signal (i_{\min}), and is reported as $20 \log_{10} (i_{\max}/i_{\min})$ dB. The objective of a high dynamic range imaging camera is to reproduce brightest and darkest segments of the scene. The ambient light works in favor of a conventional camera as it illuminates the scene for better imaging. On the other hand, the goal of a range camera is different. A range camera is evaluated based on its ability to detect range regardless of the ambient light condition. Therefore, the dynamic range of a range camera is defined as the ratio of the largest non-saturating input signal for detecting a range to the smallest detectable range signal. The dynamic range of a range camera can be further refined as the value of the usable dynamic range that satisfies certain \mathbf{Z} uncertainty requirements.

Ambient illumination from the sun and artificial lights is pervasive in automotive applications. A critical requirement, therefore, is for the sensor to meet performance specifications even when viewing sunlit surfaces. Indeed, the sun at noon will project roughly 1 kW/m² on sunlit surfaces. The EPT camera mod-

ule's optics contains an IR filter to pass only light whose wavelength matches the active emitter (e.g. 870 nm), reducing the amount of surface sunlight that reaches the sensor to about 50 W/m². Still, compared to roughly 2 W/m² projected by the active light source of the camera, a significant amount of sunlight reaches the sensor. The range camera must provide the technology to cancel the effect of the remaining ambient light that reaches the sensor.

Another challenge in automotive environments is operational temperature range, at least -40°C to +85°C. The sensor performance must remain within the specification required by each application for the range of automotive temperatures. Finally, for exterior applications, the sensing modality must be robust to degraded viewing conditions of rain, mud and fog. The mud and rain effect can be mitigated by either placing the sensor inside the car (e.g. behind the window glass), or by carefully protecting the lens by designing appropriate enclosures, or providing a washing and cleaning system.

2.2 Occupant Sensing for Advanced Airbag Deployment

The functionality of high volume production air bag systems was once limited to detecting a collision and then deploying the air bag. Improper seating of children in the front passenger seat, small stature adults, and out-of-position occupants were therefore major considerations. Of concern is the firing of an air bag when a person's head is too close to any of the vehicle air bags or there is something blocking the effective deployment of the air bag. The critical out-of-position (COOP) zone near the dashboard is an area where a person is likely to be injured by airbag deployment.

Government and Consumers are pushing the Automotive Industry for improvements to the air bag systems in vehicles on the road today. The U.S Department of Transportation's (USDOT) National Highway Traffic Safety Administration (NHTSA) has a legislative mandate under Code of Federal Regulations (CFR) Title 49, Chapter 301, Motor Vehicle Safety, to issue Federal Motor Vehicle Safety Standards (FMVSS) and Regulations to which manufacturers of motor vehicle and equipment items must conform and certify compliance. Occupant crash protection (571.208) lists the requirements for the air bag systems [Dot04]. This document is the basis for the vehicle manufactures to improve the air bag systems.

Advanced air bag systems are requiring additional input information. A smart sensor system would be desired that can discern presence, size, location within the passenger space, and category of object. Through the real time monitoring of the space, the air bag system will have the ability of making more

informed decisions on when, if, and with how much force the air bag will deploy. An air bag system with smart sensors has also the potential of warning the passenger of unsafe seating posture during the normal operation of the vehicle.

Today's "advanced airbag systems" are primarily based on weight sensors located in the seat cushion or floor. However, weight sensors alone cannot provide all the necessary information for intelligent deployment and furthermore pose implementation challenges for the automaker. They are difficult to integrate with the vehicle, e.g. requiring designing the seat around the sensor, and are different for each vehicle model, contrary to a common components strategy across the product line.

In contrast, Electronic Perception Technology is ideally suited for passenger localization [Gok04a] and classification [Gok05]. The EPT range camera updates three dimensional data to the air bag system every 16 msec. This gives the air bag system time to calculate the passenger's velocity and distance to the COOP boundary. With this information the air bag system can determine the air bag deployment strategy that is required by the situation, based on FMVSS requirements.

For the front passenger occupant sensing application, the volume that should be monitored is the space from floor to roof, from seatback to dashboard. With the range camera mounted in the center of the headliner, the required field of view is typically 110° vertical \times 80° horizontal, and the farthest object may be up to 100 cm from the sensor. Within this volume, the geometric uncertainty should be 0.5 cm or better, and commensurately the image lateral resolution should be 4 pixels/ $^\circ$. The geometric accuracy should be 2 cm or better in the region likely to be occupied by the passenger's head. These specifications are needed by intelligent algorithms that predict the location of the head from the dashboard after a crash is detected. Furthermore, the distance of head from the side window pillars is useful for the decision on the deployment of the side air bags. The range camera should provide 3D measurements at least 60 times per second, with latency not exceeding 16 ms, to give the airbag system sufficient time to calculate the person's velocity and distance to critical zone boundaries. Lower latency values are possible by reducing the window of interest size of the camera frame and obtain a rapid burst of data for a subset of field of view.

2.3 Backup Obstacle Warning

The current trends in car styling and vehicle configuration, as in SUVs and Minivans, have reduced backup visibility of the driver. Video and ultra-sound backup warning systems are now fairly common in vehicles. A backup system provides visual and/or audio feedback to the driver when the object appears too close in the trajectory of the car. A backup system can warn the driver if an object is in the blind spot of the driver, or assist the driver during the parking. Backup systems are presently implemented by placing multiple ultra-sound sensors in the bumper of a car.

For the backup sensor to be useful for the driver, it has to correctly estimate the distance of the car to an object that is in the trajectory of the car, even if close to the ground. It should not be triggered by roadside objects or the road itself. Otherwise, the sensor can become a nuisance rather than being a useful tool for the driver. The 2D video sensors have the advantage of giving a good view of the back of the car. However, estimating the real-world distances from a video image is a difficult task for the driver. The 3D image sensors have the advantage of providing both the visual and positional information in this application.

It is estimated that 90% of backup collisions with pedestrians occurred at a vehicle velocity of 8 km/h or more. At that speed, it is necessary to monitor 4 m behind the car just to achieve 95% successful accident aversion [Gla05]. Accordingly, for the backup warning system, the volume that should be monitored is a 4 m wide lane from the back of car to 10 m behind the car, from ground to 1 m. The geometric accuracy should be 10% of the radial distance or better and the uncertainty should be 1.5% of the radial distance or better. This suffices to detect a 15 cm thick person or object lying on the ground at 4 m distance. The image lateral resolution should be 4 pixels/° in order to detect a standing person at 10 m range. Per ISO recommendation, the backup detection system including range camera should provide an audible alert to the driver within 350 ms of the manifestation of a hazard.

3 Principles of Operation

A time-of-flight sensor module measures distance by observing the time delay ΔT between emission and detection of light that travels from an active light source, bounces off a surface in the scene, and returns to the camera. For a light source modulated at frequency f and surface at radial distance r , the

delay can be expressed as a phase $\phi = 4\pi r f / c$; hence, distance can be recovered by measuring phase.

This section describes the principles of operation of the EPT range camera, highlighting design features to overcome challenges to this sensing modality, including resilience to full-sunlight illumination [Gok04b]. First we describe the operation of the detector pixels in the sensor chip, and then we detail the calculations performed by the CPU to recover phase and 3D coordinates.

3.1 Detector Pixels

The light source in a typical EPT range camera module is a bank of IR LEDs at 870 nm wavelengths, switched on and off with 50% duty cycle at a frequency on the order of 44 MHz. Each pixel in the detector array contains a pair of charge accumulating gates, called **A** and **B**, which are alternately enabled in-phase and out-of-phase with the light source. The gates are reset to 0 at the start of each frame and integrate over the frame exposure time **S**, typically 1 to 32 ms. As the surface distance and phase of received light varies, the amount of integrated charge in gates **A** and **B** will vary (Fig. 1).

Even in the absence of modulated light, the charge in **A** and **B** would be biased from 0 due to dark current and ambient scene illumination. The offset is independent of the received phase, and the two pixels are enabled for the same amount of time, so the biases could be canceled by measuring only the differential signal $D = A - B$. The latter signal is digitized by an ADC and stored in a frame memory accessible to the CPU.

While ambient illumination does not theoretically affect the **D** signal, it could potentially cause the gates **A** and **B** to saturate. To prevent this effect, the sensor implements a patented Common Mode Reset (CMR) process that removes the same amount of charge from **A** and **B** gates, leaving the differential signal unchanged. Typically, 20 resets are applied during each exposure. The camera detector has also the ability to prevent the saturation of the differential signal. These measures to avoid saturation of the detectors are among key innovations that enable the EPT range camera to operate in high ambient illumination conditions typical of automotive applications.

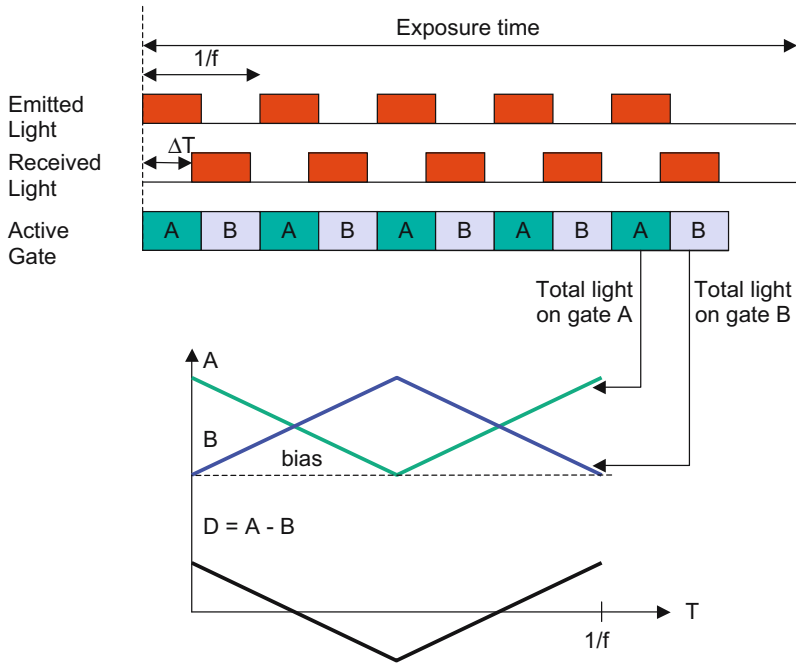


Fig. 1. Principle of Operation of the EPT Detector Pixel

3.2 Recovery of Phase and Scene Geometry

While D depends on ϕ , phase cannot be determined from a single observation of D . Accordingly, the same process is repeated, sequentially or in parallel, wherein the light source modulation is delayed by 0° , 90° , 180° , and 270° with respect to the A/B clock. Then phase can be estimated by

$$\phi = \tan^{-1} \frac{D_{90} - D_{270}}{D_0 - D_{180}} \quad (1)$$

Ideally, $\tan^{-1}(D_{90} / D_0)$ would suffice to recover phase, except that subtracting pairs of D observations with light phase 180° apart has the benefit of canceling residual biases found in the differential signals. In the sequential phase measurement, multiple exposures each of duration S results in lower uncertainty in depth data, whereas, in parallel operation, one exposure captures all four phases and the motion blur effects are minimized.

In sequential mode, since four exposures are required, it would seem that the EPT range camera can output a result only once every 4S seconds. However, since the light source modulation is cyclically varied in 90° steps, phase can actually be computed using the formula at the end of any one exposure because the last four exposures have four different modulation phases.

In an ideal system with co-located point light source and sensor, with non-distorting optics of known focal length, and perfect square wave signals, it would be possible to convert ϕ directly to radial distance r and then to X, Y, Z coordinates in space by simple geometry. In practice, $\phi = 4\pi r f / c$ however, does not hold exactly, due to pixel-to-pixel variations in gate timing, imperfect square wave signals, and use of a distributed light source. Moreover, a real lens distorts the field of view. Accordingly, a per-pixel calibration function may be used to map from measured ϕ value to Z . This function may be determined empirically for each pixel by measuring ϕ as a planar test target is moved to known Z positions. In addition, a calibration function can be used to map from each pixel (row, column) to a 3D direction ray ($X/Z, Y/Z, 1$). That function is obtained by imaging a grid pattern of known dimensions. Scaling that vector by Z yields the desired 3D coordinates. By these means, the EPT range camera is capable of reporting accurate position information in an absolute sense, not just relative, when required by an application.

Active brightness, a measure of the strength of the received modulated signal, can be defined as :

$$I_A = \sqrt{(D_0 - D_{180})^2 + (D_{90} - D_{270})^2} \quad (2)$$

If active brightness in some pixel falls below a threshold, ϕ is deemed unreliable and no coordinates are returned. This feature is important because it informs the application on the confidence level of the depth data that is returned in the pixel. The application can take corrective actions by reconstructing the depth from other good pixels, or take a default action related to the application.

4 Performance Characterization

In this paper we describe range cameras for two applications that mate the 160×120 pixel detector chip with appropriate optics and light source. The geometric measurement performance of a range camera for occupant sensing

has been measured. The uncertainty of the backup obstacle warning camera has been predicted using a system model.

Ongoing work includes characterizing the measurement performance of the EPT range camera over the full range of sunlight illumination and temperature conditions expected in an automotive environment, as well as verifying the frame rate and latency.

4.1 Occupant Sensing System

For the front passenger occupant sensing application, a lens was chosen to cover 104° vertical \times 81° horizontal. Due to field distortion, the relative resolution is raised in the image center to 1.6 pixels/ $^\circ$. A light source was constructed from forty IR LEDs, radiating 5 W peak optical power into a volume matching the lens field of view.

In order to measure the geometric performance of this EPT camera module, a planar test target with IR reflectivity of 0.5 was placed at six different distances from 15 cm to 105 cm. For each placement, sequences of 40 frames were acquired by the range camera for different values of exposure time S up to 32 ms.

For analytical purposes, forty-three $20\text{ cm} \times 20\text{ cm}$ regions were chosen within the occupant detection volume at the six distances. Within each region, the metrics defined in 2.1 are calculated for the best S for that region. (The best S is selected as the exposure time minimizing the Z uncertainty metric. Typically S is 32 ms, except for brightly lit regions that could saturate with such a long exposure.)

Fig. 2 shows histograms of the performance metrics. Z uncertainty varies from 0.3 cm to 1.5 cm for different analysis regions, due to non-uniformity of the light-gathering power of the lens, non-uniform radiation from the active light source, and $1/r^2$ fall-off of power with distance. The median of each metric in each dimension meets the goals stated in 2.2.

In the sensor chip, the maximum non-saturating signal with 50 common mode resets is 2×10^5 ADC units, while the noise level in the signal is around 5, yielding a raw dynamic range of 92 dB. On the other hand, for range cameras a more relevant metric is the range of signal levels that satisfies a measurement performance goal. A regression model can be fit to the relationship between active brightness and Z uncertainty, predicting that $I_A = 480$ suffices to achieve

uncertainty of 1 cm. On that basis, the dynamic range for satisfying the performance specification is 52 dB.

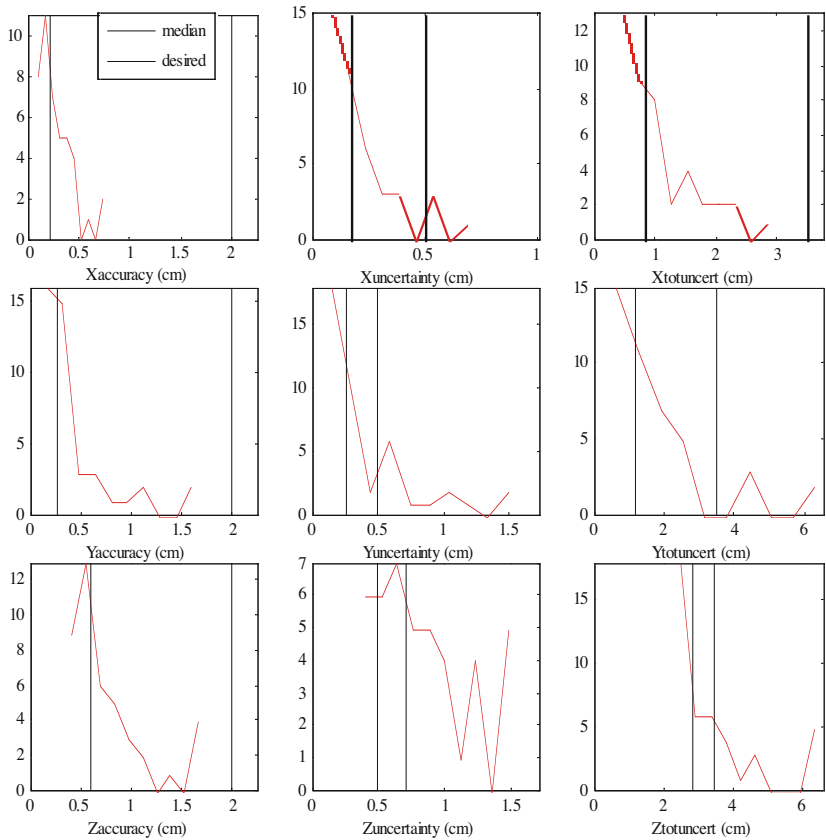


Fig. 2. Histograms of Geometric Performance Metrics for Occupant Sensing EPT Range Camera

4.2 Backup Obstacle Warning System

We have developed a system model to predict the depth precision for a given active light source, target object, and optics, or alternatively the locus of 3D points where a specified precision is achieved. The model could be inverted to design the light source to achieve a specified precision on a given locus. The parameters of the model include:

- Light source model: optical wavelength, total power, angular distribution (assumes point source co-located with sensor)

- Object model: reflectivity and radial distance (assumes surface is perpendicular to line of sight)
- Optics model: focal length, $F/\#$, transmission losses of lens and IR filter (assume no vignetting or field distortion)
- Pixel model: pixel area and quantum efficiency
- Analog to digital converter model: quantization step, voltage swing, exposure time
- Range estimator model: modulation frequency

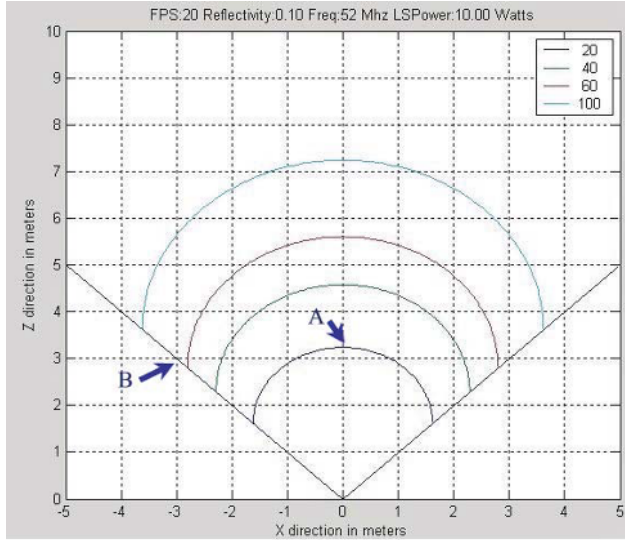


Fig. 3. Iso-Uncertainty Contours, showing loci of 20, 40, 60, 100 mm uncertainty.

The object model converts the emitted light to received light at the lens, which the optics model converts to light power falling on a pixel. Assuming received and emitted light are in phase, the pixel model converts light power to a voltage, which the ADC model converts to a digital differential signal D_{\max} . Depending on actual phase, D will vary from 0 to D_{\max} in steps of 1. The range estimator model converts this to the corresponding step in radial distance.

Fig. 3 illustrates the result of the model assuming 10 W of light source power, 52 MHz modulation frequency, 0.1 object reflectivity, 90° field of view and 20 frames per second. The figure shows iso-uncertainty contours for 20, 40, 60 and 100 mm values as a function of distance from the sensor and the light source. For instance, the lower curve shows the set of points with uncertainty of 20 mm. Clearly, the points that are closer to the sensor and aligned with the

axis of the camera reflect more light to the sensor and thus produce better uncertainty values. The shape of the curves is influenced by the profile of the light source and the well-known \cos^4 -effect. If necessary, the light source can be designed to compensate for the \cos^4 -effect by increasing the concentration of the light on the boundaries of the field-of-view.

For the backup obstacle warning system, this configuration of the camera shows that distances for objects as far as about 3 m (see arrow A in Fig. 3) in the direction of the center axis of the camera can be measured with 2cm uncertainty. At center axis of the camera, 1.5% uncertainty requirement is easily met (2.3). In the perimeter of the field-of-view, the model suggests that the present light source only gives about 6 cm uncertainty (see arrow B in Fig. 3) for objects in a plane that is 3 m from the back of the vehicle where the camera may be mounted. The model suggests that an alternative light source with higher concentration of the light in off-center regions would be better suited for this application. We observe the clear advantages of using a system model for sensor performance analysis. The model provides the information that is needed for the camera system designer to tailor the camera and its light source for a vehicle application to achieve cost/performance goals of the application.

5 Conclusions

This paper described the advantages of Electronic Perception Technology, a high frame rate focal plane array 3D sensor, for automotive safety systems. Performance metrics and application-driven requirements were presented for two specific systems, occupant sensing and backup obstacle warning. We detailed the principles of operation of the range camera. We demonstrated the use of actual measurement and the use of analytical modeling to show how the two configurations of the camera module satisfy the requirements.

References

- [1] [Dot04] National Highway Traffic Safety Administration, U.S. Department of Transportation, Federal Motor Vehicle Safety Standards, 49CFR571.208, pp. 497-580, 2004.
- [2] [Gla05] V. Glazduri, "An Investigation of the Potential Safety Benefits of Vehicle Backup Proximity Sensors", in Proc. Int'l. Tech. Conf. Enhanced Safety Vehicles, 2005.
- [3] [Gok04a] S.B. Gokturk, C. Tomasi, "3D Head Tracking Based on Recognition and Interpolation Using a Time-Of-Flight Depth Sensor", in Proc. Computer Vision Pattern Recog., Vol. II, pp. 211-217, 2004.
- [4] [Gok04b] S.B. Gokturk, H. Yalcin, C. Bamji, "A Time-of-Flight Depth Sensor—System Description, Issues, and Solutions", in Proc. IEEE Workshop Real-Time 3D Sensors, 2004.
- [5] [Gok05] S.B. Gokturk, A. Rafii, "An Occupant Classification System—Eigen Shapes or Knowledge-Based Features", in Proc. IEEE Workshop Machine Vision Intell. Vehicles, 2005.

Dr. Stephen Hsu, Sunil Acharya, Dr. Abbas Rafii, Richard New

Canesta, Inc.
 440 N. Wolfe Rd.
 Sunnyvale, CA 94085
 USA
 shsu@canesta.com
 acharya@canesta.com
 arafii@canesta.com
 rnew@canesta.com

Keywords: range camera, time-of-flight camera, range video, lidar, 3D camera, 3D sensor, CMOS-sensor, airbag occupant sensing, advanced airbag, dynamic suppression, backup obstacle detection, pedestrian detection, pre-crash sensing, electronic perception technology

Coordinated Cylinder Pressure Based Control for Reducing Diesel Emissions Dispersion

M. G. Beasley, R. C. E. Cornwell, M. A. Egginton, P. M. Fussey, R. King,
A. D. Noble, T. Salamon, A. J. Truscott, Ricardo UK Ltd.
G. Landsmann, General Motors Powertrain Europe

Abstract

Future demands for very low emissions from diesel engines, without compromising fuel economy or driveability, require Engine Management Systems (EMS) capable of compensating for emissions dispersion caused by production tolerances and component ageing. This paper describes a collaborative project between Ricardo and General Motors (GM), aimed at reducing engine-out emissions dispersion and enabling alternative combustion modes, such as Ricardo's Highly Premixed Cool Combustion (HPCC), in real-world scenarios. Cylinder pressure based control is a key technology enabler for achieving the necessary high-level coordination of fuel, air and EGR in order to meet the conflicting performance requirements of current and future diesel engines. The paper describes the background to the project, the development toolchain using production intent sensors, control strategies developed for both testbed and vehicle application and preliminary results obtained.

1 Introduction

Future demands of very low emissions on diesel engines are presenting a significant challenge to the automotive industry. The need to remain cost competitive has deferred the adoption of expensive Nitrous Oxides (NO_x) aftertreatment systems thereby placing pressure on achieving even lower engine-out emissions. This has led to greater influence of manufacturing tolerances and aging on emission spread. Fig. 1 illustrates the effect of production tolerances on the NO_x /Particulate matter (PM) emissions dispersion cloud. Although the levels of emissions required for EURO V compliance are achievable, when current production tolerances are considered the resulting dispersion clouds are significant.

The Advanced Diesel Engine Control (ADEC), a collaboration between Ricardo and GM, is aimed at investigating the feasibility of applying advanced control

strategies to reduce the emissions dispersion incurred by production tolerances and ageing whilst maintaining competitive fuel consumption. This began with a sensor feasibility study which included a number of new sensing technologies appropriate for future mass production. Two sensor types were selected to demonstrate varying degrees of benefits versus sensor technology cost. These were based on two sets of engineering targets for engine-out emissions of 0.15 g/km NO_x , 0.03 g/km PM and 0.08 g/km NO_x , 0.03 g/km PM over the NEDC cycle. The engine technology applied to achieve these levels, namely advanced EGR cooler with bypass, high specification turbocharging and model based air-path control, had already been demonstrated without the use of combustion feedback control in a prior Ricardo project [1].

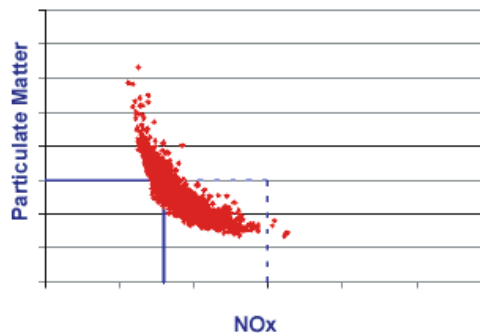


Fig. 1. Effect of production tolerances on the NO_x /PM emissions dispersion cloud relative to EURO V guideline emissions limits

The objectives of the ADEC Project are:

- ▶ to investigate sources of emissions dispersion and sensitivity of engine emissions to key input variables and internal states
- ▶ to investigate sensor technology to support advanced control strategies for combustion and charge feedback
- ▶ to compare available sensors and select options for demonstrating the above emissions targets
- ▶ to develop new control architectures and functions for the sensor options
- ▶ to validate the potential of the two selected systems for addressing emissions dispersion on a testbed and vehicle

2 Engine Application

The engine application is a 1.9 litre Family B engine. A schematic diagram of the base engine is given in Fig. 2.

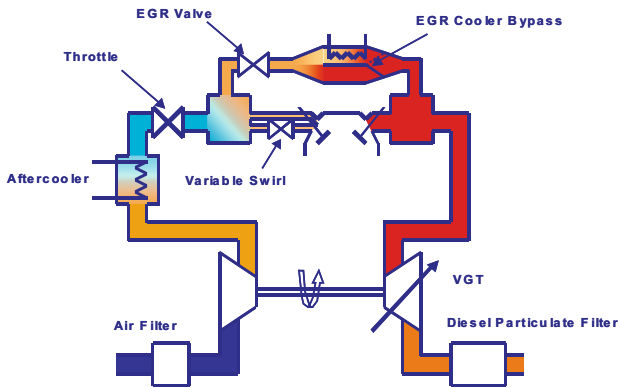


Fig. 2. Schematic diagram of 1.9 litre Family B engine, the base engine for the ADEC programme

3 Sensor Feasibility Study

A sensor feasibility study was carried out at part of the project. The objectives of this task were:

- ▶ to investigate sensor technologies required to support advanced control strategies for combustion feedback control
- ▶ to compare available sensors and select options for demonstrating feedback control in order to meet emissions targets

A total of nine different sensors covering each of the following technologies were tested to evaluate their potential for use in closed-loop control of Diesel combustion:

- ▶ Direct in-cylinder pressure sensing
 - Piezo-electric
 - Piezo-resistive
 - Optical measurement of deflected membrane
- ▶ In-direct cylinder pressure sensing
 - Deflection of cylinder head
 - Change in cylinder head sealing gap (Head Gasket)
- ▶ Non-cylinder pressure sensing technologies

- Ion current (combustion) sensing
- Block mounted accelerometer

Direct measurement of cylinder pressure would certainly provide the best means of estimating combustion states such as P_{max} , Indicated Mean Effective Pressure (IMEP), angle of 50% fuel mass fraction burn (B50). However, in view of the cramped conditions inside the 16-valve diesel engine, it was clear that any cylinder pressure sensor required for mass production would have to be integrated within an existing engine component. The direct sensors were therefore chosen to be glow-plug mounted types. Although it is true that the term “direct” becomes less meaningful if the sensor is mounted further away from the cylinder in such a way as to measure the deflection of the glow-plug probe (compared to the traditional flush-mounted Kistler sensor), for the purpose of this study, in order to differentiate them from sensors used to measure cylinder head deflection, they were considered as “direct sensors”.

The response characteristics of the cylinder pressure candidate sensors were compared with a Kistler 6053BB60 reference sensor. Figs. 3 and 4 show associated Lissajous for five such glow-plug pressure sensors, depicting the spread of candidate versus reference sensors at extreme operating conditions from low to high speed and load. These results provided useful information concerning signal repeatability, linearity, hysteresis, etc.

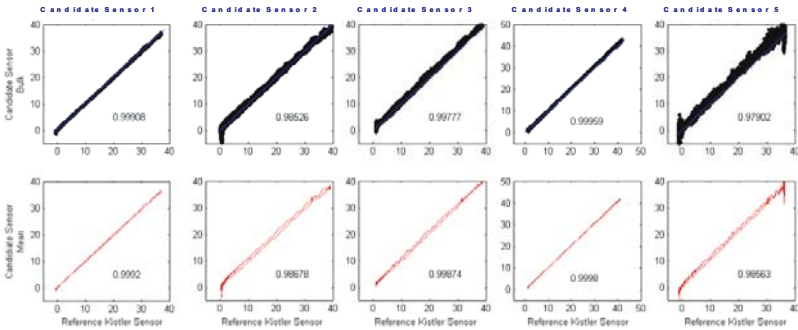


Fig. 3. Lissajous plots (candidate sensor output vs. reference sensor output) for five different candidate cylinder pressure sensors at 1500rpm, 2bar BMEP

Ricardo’s Cylinder Pressure Processing Tool (CPPT), which incorporates the Heat Release algorithm, HREL, was then applied to estimate the various combustion states. This was performed for each of the five candidate sensors using both filtered and un-filtered signals at six operating conditions across the

speed/load range. Results were compared to the reference sensors and a regression technique was applied to determine the correlation.

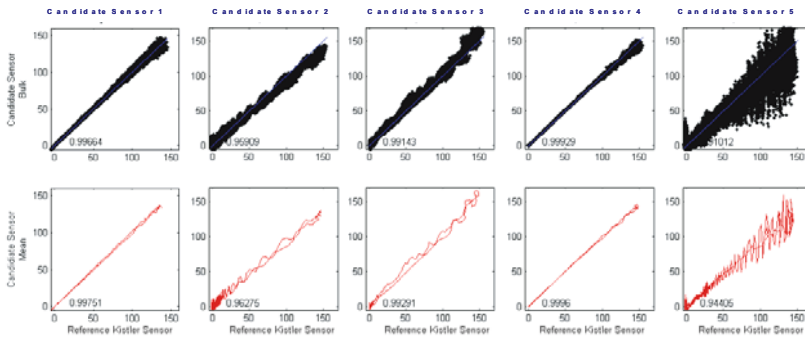


Fig. 4. Lissajous plots (candidate sensor output vs. reference sensor output) for five different candidate cylinder pressure sensors at 4000rpm, Full Load

The correlation data was combined with other factors including product development maturity, production cost and ease of integration into vehicle electronics/ECU and signal processing/filtering requirements to select the target sensor option for the further phases of the programme.

Cylinder pressure traces from in-direct cylinder pressure sensors suffered from noise and interference from combustion and valve events in neighbouring cylinders, making engine state estimation more problematic and reducing the correlation with the states estimated from the reference sensors. A pressure sensor integrated in a glow-plug (utilising direct measurement of the in-cylinder pressure) was therefore selected as the target sensor option. These sensors were carefully designed to overcome a number of technical issues including robustness to temperature variations related to glowing/non-glowing action as well as thermal shock, and minimal noise interference.

From non-cylinder pressure type sensors, it is only possible to estimate temporal (combustion phasing) engine states such as Start of Combustion (SOC). Taking this into account, and combined with their low production cost, block mounted accelerometers were selected as a low-cost alternative option for evaluation. Details of this study will be published at a later date.

4 Control Strategy Development

Cylinder pressure feedback control has attracted much attention in recent years, as there are many potential benefits [2, 3]. This section describes the development of such a system as the target sensor option to meet the programme objectives.

The control strategy was defined based on a number of system requirements. These include:

- ▶ High-level coordination of fuel and air in order to meet the conflicting demands of fuel economy, low emissions and good driveability
- ▶ Adaptability to production tolerances and aging
- ▶ Modularity to allow transferability to different sensor types

A top-level system diagram of the control strategy is given in Fig. 5.

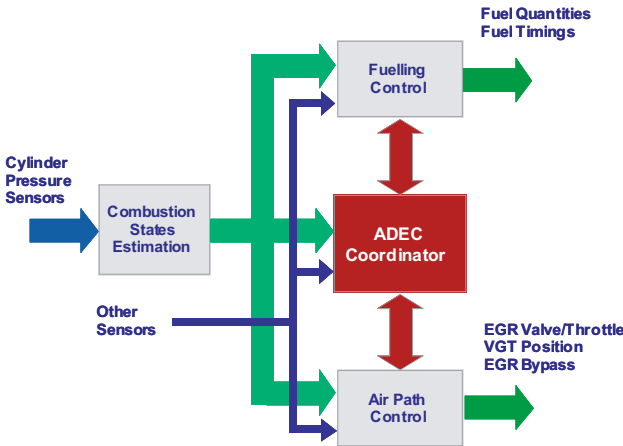


Fig. 5. Control Strategy Overview

4.1 Estimation of Combustion States

Certain key combustion states were estimated for feedback control. Unlike the offline estimation strategies applied in CPPT as indicated in section 3, this necessitated approximations appropriate for real-time computations. Furthermore, these were applied to each successive engine cycle thus requiring moving average filtering of the states. Any consistent errors based on the approximations applied could be calibrated out.

Combustion state estimation algorithms were also developed around the sensing technology applied. The objective was to avoid the imperfections in the sensor signal or to compensate for them. This allowed the use of less refined sensors more appropriate to near-future mass production.

The combustion states considered were:

- ▶ Crank angle at which 50% of the total fuel is burned (angle of B50)
- ▶ Peak cylinder pressure (P_{\max})
- ▶ Rate of Combustion (ROC)
- ▶ Combustion Instability (CIS)
- ▶ Indicated Mean Effective Pressure (IMEP)
- ▶ Top Dead Centre (TDC)

The angle of B50 is estimated based on the Rassweiler & Withrow approximation [4]. CIS is any appropriate measure of cycle-to-cycle variation of some combustion state related to the given cylinder. TDC is estimated during overrun to compensate for crank-sensor offset.

4.2 Fuelling Control

Fuel quantity and timing are controlled separately for each cylinder. Start of Injection (SOI) is controlled to match a target angle of B50 for good fuel efficiency and, together with mass airflow/EGR, low NOx. Fig. 6 describes the feedback controller that compensates for both injector and combustion uncertainties.

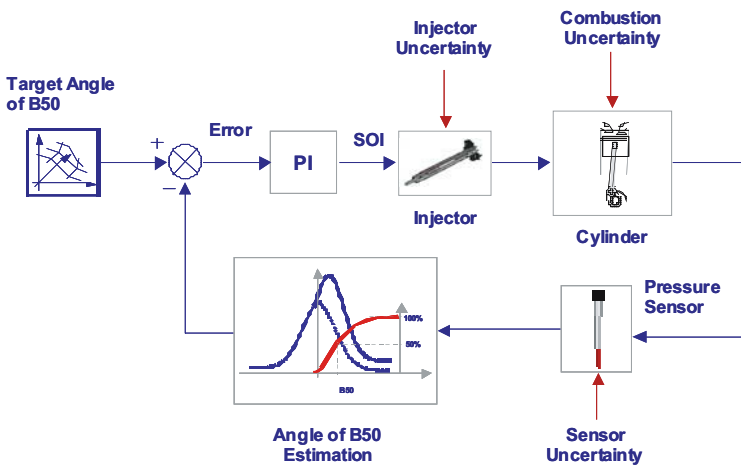


Fig. 6. Angle of B50 control for each cylinder

Although sensor uncertainty is also introduced, this is mitigated by the Rassweiler & Withrow approach applied which does not require sensor gain calibration.

During normal fuelling operation, P_{\max} and CIS are maintained within limits as described below.

4.3 Air Path Control

The air path controller controls EGR and boost pressure. EGR is controlled as standard by adjusting the EGR valve and throttle to match a target Mass Airflow (MAF). Corrections are also made to compensate for variations in intake manifold conditions and to maintain combustion stability (see below). The EGR cooler bypass valve is actuated using a model-based estimate of the intake manifold temperature in order to maintain the correct EGR temperature. The boost pressure is closed-loop controlled at high loads using the VGT.

4.4 ADEC Coordinator

At the heart of the control strategies is the ADEC Coordinator. This high-level coordinator adapts control setpoints harmoniously in order to meet the various conflicting performance requirements as well as responding rapidly to any sensor failure (Fig. 7).

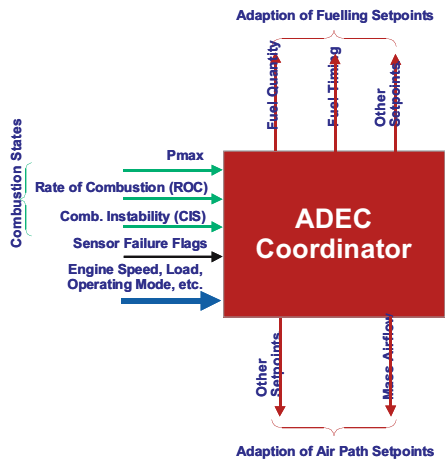


Fig. 7. ADEC Coordinator

To ensure stable operation at high levels of EGR, and when running in alternative combustion modes (e.g. HPCC) both fuelling and air path controllers are adapted. Once combustion instability increases above a given threshold, the target B50 angle is immediately advanced for rapid stability control followed by a slower increase in target MAF as illustrated in Fig. 8.

In order to protect the engine, the P_{\max} of each cylinder is controlled separately within a limit by altering the fuel commands. Firstly an offset is applied to the target angle of B50 to directly retard the combustion once the P_{\max} limit has been exceeded. If the retard authority limit (due to exhaust temperature limitation) is reached and further reduction is required, the fuel quantity is reduced accordingly as illustrated in Fig. 9. Control action is therefore applied in two stages: combustion retard, then fuelling reduction, in order to minimize the impact on torque felt by the driver.

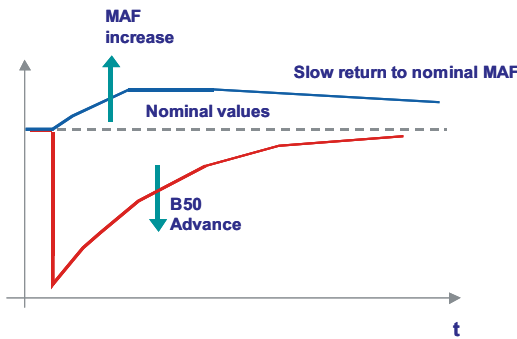


Fig. 8. Combustion Stability Control

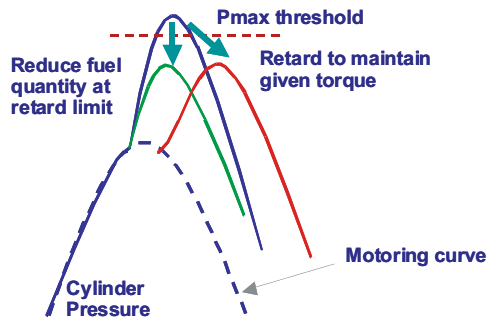


Fig. 9. P_{\max} Control

There is no conflict in timing between P_{max} and CIS control as the CIS is active only at part-load.

An ROC controller is also integrated within the ADEC Coordinator.

5 Control Strategy Implementation and Testing

5.1 Prototyping System

One of the key enabling factors for the combustion feedback strategies based EMS is a suitable hardware prototyping system. To obtain the appropriate resolution of the combustion state estimates a high quantity of data per engine cycle had to be processed in real time – much higher than today’s ECU technology.

To this requirement the prototyping EMS was based around Ricardo’s high-powered ECU platform, rCube [5]. This enables one-degree sample resolution over the combustion phase as high resolution was necessary for effective ROC estimation. All combustion states are estimated once per cycle for all four cylinders in the rCube as shown in Fig. 10. rCube utilises two processors to split between fast interaction with external world (MPC565) and computationally extensive tasks of combustion states estimation performed by MPC8260.

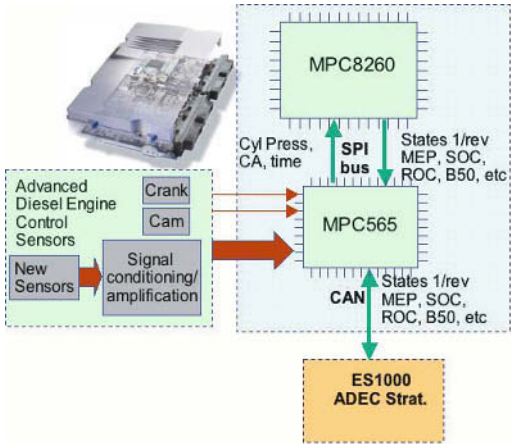


Fig. 10. rCube Dual Processor System Architecture

Calculated combustion states are fed over CAN to an ETAS ES1000 which provides the necessary closed-loop control, interfacing with the Bosch EDC16 over

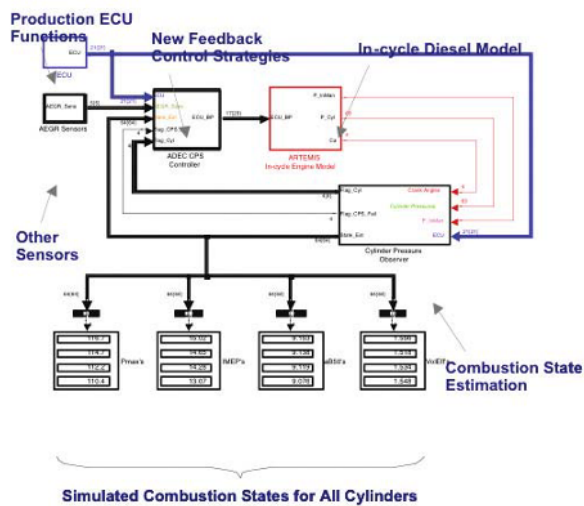


Fig. 12. Software-in-the-Loop Testing Environment

In the final stage, the control strategies were implemented in ASCET-SD® to run on the Prototyping System. This was first tested in a dSPACE Hardware-in-the-Loop environment before commissioning on the testbed.

6 Test Results

Preliminary results have been obtained to demonstrate the performance of the various control algorithms. Specifically, these were angle of B50 balancing, P_{max} and stability control. These were tested first using reference Kistler sensors (Kistler 6053BB60) followed by the glow-plug integrated pressure sensors selected in the Sensor Feasibility Study. For the purpose of this paper the glow-plug sensor results are presented for B50 balancing, P_{max} control as well as for the combustion stability control.

6.1 Angle of B50 Control Results

The angle of B50 controller performance is demonstrated in Figs. 13 and 14. The first of these indicates the effect of switching the controller on and off under steady-state conditions. It is clear how the spread in B50 is reduced accompanied by a corresponding spread in SOI as the fuel timings are individ-

ually adjusted in order to balance the combustion phasing. The second figure demonstrates how the controller is able to track changes in the B50 set-point.

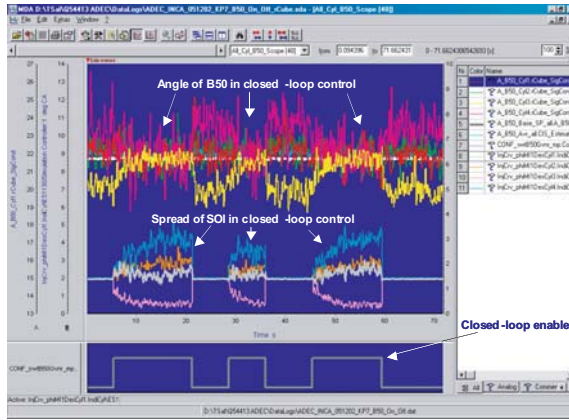


Fig. 13. Steady-state angle of B50 control

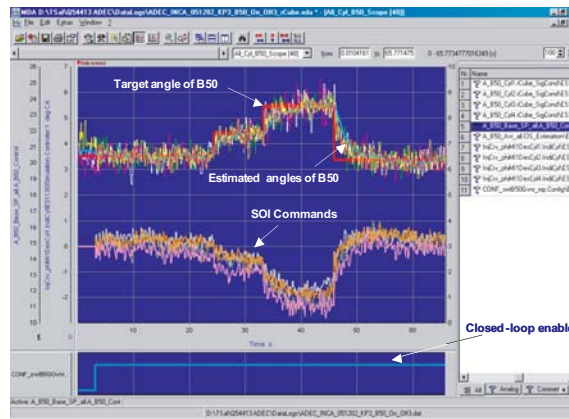


Fig. 14. Transient angle of B50 control at 2000 rpm, 76 Nm at 1500 rpm, 30 Nm

6.2 P_{\max} Control

The control of P_{\max} in response to an increase in driver demand is demonstrated in Fig. 15. Two tip-in/tip-out manoeuvres were applied, first without then with P_{\max} control. The results clearly demonstrate how P_{\max} is successfully limited by a combination of fuel retard and fuel quantity. Here calibration thresholds for P_{\max} and SOI retard limit were set purely for demonstration purposes.

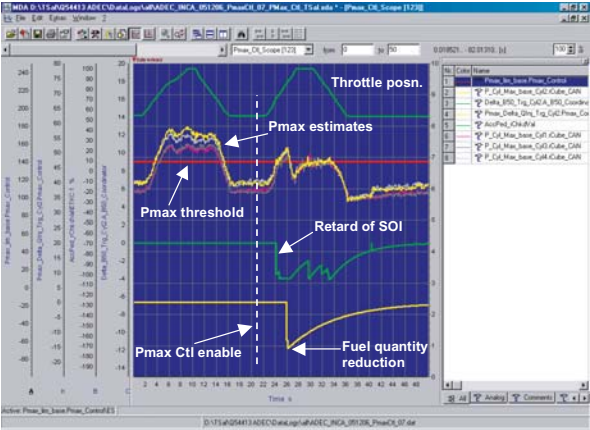


Fig. 15. P_{\max} control results at 2000 rpm, accelerator pedal 60-100%

6.3 Combustion Stability Control

Maintaining stable combustion in response to forced instabilities was demonstrated successfully. At high EGR levels, the timing was suddenly retarded on all cylinders resulting in an increase of CIS above a given threshold. As indicated in Fig. 16, the target B50 angle was immediately advanced to compensate followed by an increase in target MAF triggered by saturation of the B50 advance controller.

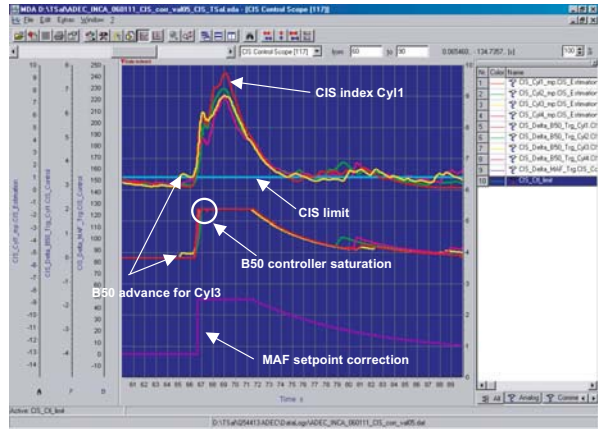


Fig. 16. Combustion stability control at 1500 rpm, 2bar BMEP

These are gradually wound down to their nominal set-points until the next threshold crossing occurs (compressed timescale for demonstration).

7 Conclusions

This paper describes the on-going developments in the ADEC Project, a collaboration between Ricardo and General Motors. The conclusions so far are as follows:

- ▶ a sensor feasibility study has identified a glow plug mounted pressure sensor type as the target sensor option
- ▶ a cylinder pressure feedback control system was developed and has demonstrated successful control of angle of B50 timing, P_{\max} limiting for engine protection and good control of combustion stability.

The next steps in the project are as follows:

- ▶ Validation of robustness of control system to dispersion tests carried out on the testbed
- ▶ Demonstration of control system on a demonstrator vehicle
- ▶ Application of accelerometers sensor strategies

Acknowledgments

The authors would like to thank the directors of Ricardo and GM for their funding of, and permission to publish this work.

Special thanks are due to the rest of the project team at Ricardo. These include Leo Xenakis, Matthew Bent, John Bailey and Dave Penwarden.

References

- [1] B. Cooper, I. Penny, M. Beasley, A. Greaney and J. Crump, Advanced Diesel Technology to Achieve Tier 2 Bin 5 Emissions Compliance in US Light-Duty Diesel Applications, SAE 2005
- [2] P. Moulin, A. Akoachere, A. Truscott, A. Noble, R. Müller, M. Hart, G. Krötz, C. Cavalloni M. Gnielka and J. von Berg., Benefits of a Cylinder Pressure Based Engine Management System on a Vehicle, Advanced Microsystems for Automotive Applications 2002, VDI/VDE Conference, May 2002
- [3] M. Sellnau, F. Matekunas, P. Battiston; C. Chang and D. Lancaster, Cylinder-Pressure-Based Engine Control Using Pressure-Ratio-Management and Low-Cost Non-Intrusive Cylinder Pressure Sensors, SAE 2000-01-0932
- [4] G. Rassweiler and L. Withrow, Motion Pictures of Engine Flames Correlated With Pressure Cards, SAE 800131

- [5] S. Channon and P. Miller, An Advanced Network Vehicle Controller (NVC) to Support Future Technology Applications, Advanced Microsystems for Automotive Applications 2003, VDI/VDE Conference, May 2003

M. G. Beasley, R. C. E. Cornwell, M. A. Egginton, P. M. Fussey, R. King, A. D. Noble, T. Salamon, A. J. Truscott

Ricardo UK Ltd.

Shoreham Technical Centre

Shoreham-by-Sea

West Sussex

BN43 5FG

United Kingdom

Matt.Beasley@ricardo.com

Richard.Cornwell@ricardo.com

Martin.Egginton@ricardo.com

Peter.Fussey@ricardo.com

Richard.King@ricardo.com

Andy.Noble@ricardo.com

Tomasz.Salamon@ricardo.com

Anthony.Truscott@ricardo.com

G. Landsmann

Technology Development, TL Engine Controls

GM Powertrain Europe

General Motors Powertrain - Germany GmbH

IPC T2-02, 65423 Rüsselsheim

Germany

Gerhard.Landsmann@de.gm.com

Keywords: diesel engine, engine management systems, cylinder pressure sensing, coordinated control, combustion feedback

A High Temperature Floating Gate MOSFET Driver for on the Engine Injector Control

P. Delatte, V. Dessard, G. Picún, O. Stevens, L. Demeûs, CISSOID S.A.

Abstract

This paper presents a High Temperature Floating Gate MOSFET Driver ASIC for on-the-engine Injector Control. The circuit was specifically designed for this harsh environment and has been realized using Silicon-on-Insulator (SOI) Technology. The first section describes the operation of the system sub-blocks: low- and high-side drivers, the current sense and the fault detector. In the second section, measurements show the proper operation of the circuit up to 225°C.

1 Introduction

Placing the injector control electronics on the engine allows removing cables thus reducing weight. Moreover, having the control electronics on the motor could enable the stand-alone testing of the engine. The challenge is to have electronics that can reliably sustain the engine harsh environment, especially the large temperature range (-40°C to +200°C). Silicon-on-Insulator (SOI), providing fully dielectric isolation and leakage reduction, has already demonstrated to be the best technology in designing high temperature analogue and digital circuits [1, 2]. This paper presents a prototype of low side and high side power MOS drivers integrated in a system-on-chip ASIC. It has been realized in a high temperature and high voltage SOI process with tungsten metallization for long-term reliable operation at high temperature. Besides drivers, current sense and fault detector circuits have also been implemented in order to have all analogue functionalities required for driving power MOS on inductive loads at high temperature.

2 System Overview

Fig. 1 depicts the ASIC prototype schematic and layout. Beside the digital control part that will not be considered hereafter, the ASIC includes three main analogue functionalities: the drivers, the current sense and the fault detector.

2.1 Drivers

Drivers are required in order to interface the digital control with external power MOSFET's. Two kinds of drivers can be distinguished in Fig. 1. The first and simplest one, called the low-side (LS) driver has its output voltage referred to ground. In the ASIC prototype, this LS driver is controlled by digital 5 V logic. Its output can swing between 0 and 10 V levels versus ground. The second driver, called the high-side (HS) driver is more complex. Its input is also controlled by digital 5 V logic and its output can also swing 10 V. The difference is that the output is completely floating versus the ground. This allows keeping the POWER MOSFET turned ON with its source connected to an inductive load. An external capacitor is required for the HS driver in order to be able to drive the gate of HS MOSFET with a voltage higher than the supply voltage. This way, the ON resistance of the HS power MOSFET is always kept very low. For applications where the HS MOSFET has to be turned ON for a long time (i.e. without switching it), an internal charge pump has been integrated in the driver in order to maintain the charge in the external capacitor. Measurement results are shown in section 2.

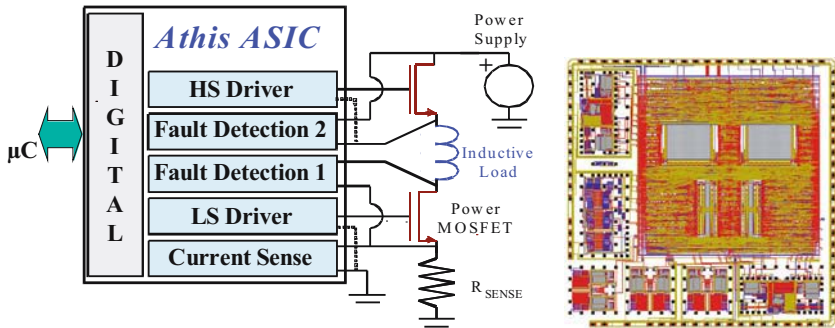


Fig. 1. ASIC prototype (digital control + drivers) schematic and layout

2.2 Current Sense

In order to control the LS and HS drivers, the digital controller needs to know the actual current flowing across the inductive load. The Current Sense (CS) circuit is responsible for comparing this current (measured across a grounded sense resistor in Fig. 1) with a digital threshold. The comparison result is a fed back to the digital controller. Therefore, the current sense block is implemented by a "mixed-mode" comparator, comparing an analogue voltage with a digital threshold D , which is a much simpler way than those used so far. In the implemented prototype, D is an 8-bit word. Fig. 2 depicts our CS measurement

at 25°C and 200°C for 8 bits digital threshold arbitrarily fixed at D_{128} and D_{255} respectively. The comparator needs no more than 1.4 μ s to switch at 200°C. The measured thresholds for D_{128} and D_{255} are also very close to the theoretical values. Note that the CS 5 V reference voltage is internally generated with a buffered 5 V voltage reference. The supply voltage must be at least 6 V in order to correctly generate the internal 5 V reference voltage.

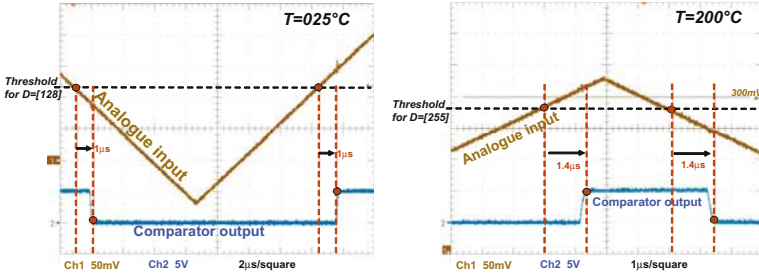


Fig. 2. Current sense measurements at 25°C and 200°C for digital threshold of respectively D_{128} and D_{255}

2.3 Fault Detector

In order to avoid inductive load or battery damaging, it is important to verify that the power MOSFET's operate as expected. A simple way to check this is to monitor each power MOSFET drain-to-source voltage (V_{ds}). When the digital controller requires turning ON a MOSFET, it is expected that V_{ds} of this device drops under a threshold voltage after a small delay. Similarly, when the MOSFET is turned OFF, the V_{ds} voltage should be higher than this threshold. Any mismatch between the expected MOSFET state (ON or OFF) with the actual measured V_{ds} is interpreted as a failure. In such case, the digital controller should turn OFF all the MOSFET's in order to avoid any damage caused by an over-current. The Fault Detector (FD) is also simply implemented by a "mixed-mode" comparator, comparing a floating differential voltage (V_{ds}) with a pre-defined digital threshold. In this prototype, the digital threshold can be set to 2 V or 2.4 V. Fig. 3 depicts quasi-static measurements at 25°C of the comparator output voltage versus the differential input voltage (V_{ds}). The common mode (CM) of this differential voltage is swept from -1 up to 50 V. The measured threshold is very close to the expected 2 V. We only observe a small influence of the CM voltage on this threshold. (50 V shift on CM corresponds to 100 mV shift on threshold, i.e. $\Delta_{threshold}/\Delta_{CM} \approx 2$ mV/V). The FD switching time is shorter than 1 μ s over temperature.

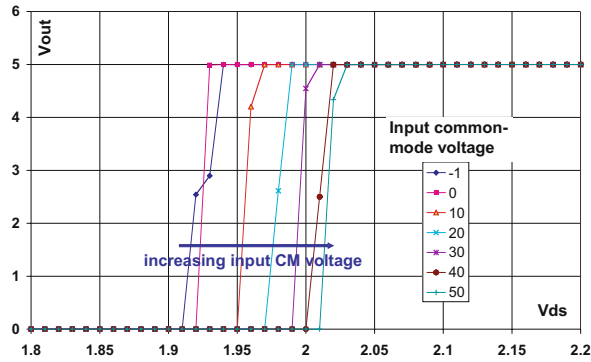


Fig. 3. Measured fault detector output voltage versus differential input voltage as function of the input common mode voltage at 25°C.

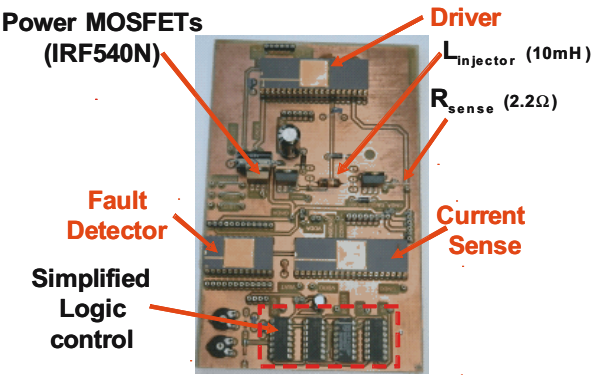


Fig. 4. Full system measurement setup (Driver, current sense, fault detector). Only the driver can be under thermal stream on this board.

3 System Measurement

The full system, including a HS driver, a LS driver, a current sense and a fault detector has been tested (ASIC of figure 1 has been sub-diced in order to test separately the analogue parts). In the setup, only the driver can be heated up to 225°C with a thermal stream. Other parts are at 25°C. However, they have been previously tested separately up to 225°C. External components of Fig. 1 setup are:

- Power MOSFETs: IRF540
- Inductive load: 10 mH
- Sense resistor: 2.2 Ω

Fig. 4 shows the test measurement board. Digital control is such that the current target is set to 100 mA during 300 μ s and to 60 mA during 600 μ s, before turning off. Note that the current levels in the inductive load and the sense resistor represent a scaling down with respect to the final application (few Amps). This scaling down is acceptable since the driver load is a MOSFET able to drive up to 33 A.

Fig. 5 is a screen shoot of the sense resistor voltage, the HS MOSFET gate-to-source voltage (V_{gs}) and the HS fault detector output. Measurement results are very similar at 25°C and 225°C. Fig. 5 is relative to a 12 V battery voltage. However, the driver can sustain battery voltages up to 55 V at 225°C.

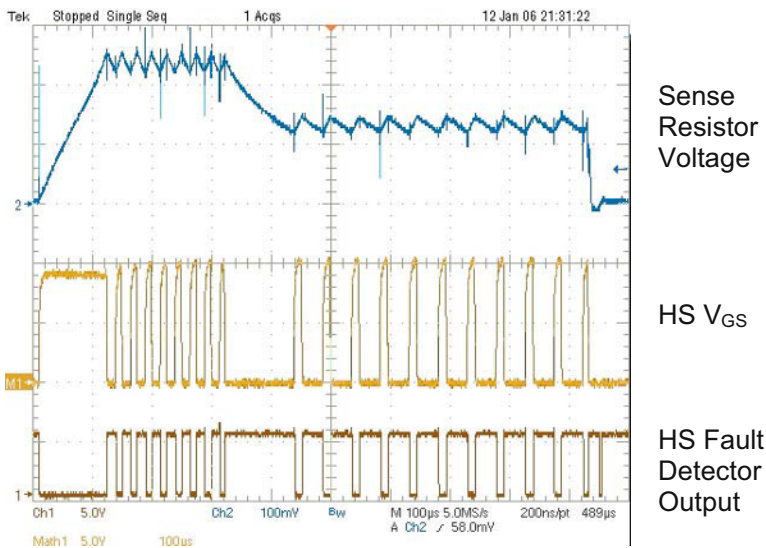


Fig. 5. Measured sense resistor voltage, HS V_{gs} and HS fault detector output (from top to bottom) at 225°C with a 12 V battery voltage (Results are very similar to those at 25°C).

From Fig. 5, we can see that the fault detector output (bottom wave) is in accordance with the MOSFET gate-to-source voltage (middle wave). The system is working correctly.

Concerning delays, Fig. 6 shows a zoom on one HS switching at 225°C. Waves are the sensed voltage, the voltage on HS MOSFET source and the HS V_{gs} from top to bottom respectively. Switching time is between 1 μ s and 2 μ s with the used MOSFET (IRF540). Results are similar for the LS driver.

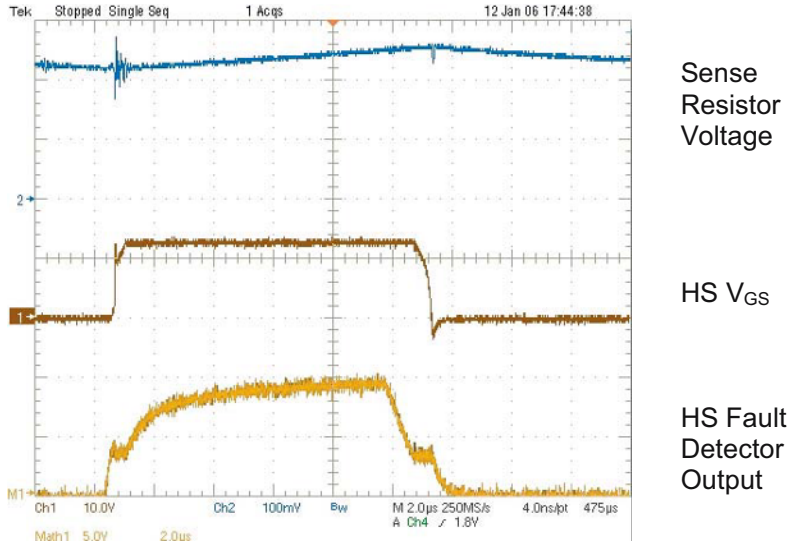


Fig. 6. Zoom on one HS switching period at 225°C with 12V battery voltage. Waves are the sense resistor voltage, the HS MOSFET source voltage and the HS V_{gs} (top to bottom wave respectively).

4 Conclusion

Taking advantage of the full dielectric isolation and the high temperature performance of SOI Technology, all the blocks of Floating Gate MOSFET Driver have been successfully designed, fabricated and tested up to 225°C. This ASIC shows the opportunity to place the Injector Control Electronics directly on the engine. This would enable the stand-alone testing of the engine while removing cables thus reducing weight.

Acknowledgements

This ASIC has been developed in the frame of EC FP5-Growth ATHIS (Advanced Techniques for High Temperature Systems-on-Chip) project with partners UCL, Xab, CRF, CNM, IMMS, UNEW.

References

- [1] "High Temperature SOI Voltage Reference, Voltage Regulator and ~~Val~~ Oscillator Driver", V.Dessard, G. Picún, P. Delatte, L. Demeus, HITEC Conference, Santa Fe, May 2004.
- [2] "A Low Power 80C51 Microcontroller in SOI High Temperature Technology", Ph. Mannet, R. Ambroise, D. Bol, L. Demeus, J.-D. Legat, HITEN Conference, Paris, Sept. 2005.

V. Dessard, P. Delatte, G. Picún, O. Stevens, L. Demeus

CISSOID S.A.

Chemin du Cyclotron 6

1348 Louvain-la-Neuve

Belgium

demeus@cissoïd.com

Keywords: driver, half-bridge, floating, high temperature, SOI, ASIC, engine control, automotive

Distributed Pressure Sensor Based on Electroactive Materials for Automotive Application

E. Ochoteco, J.A. Pomposo, H. Grande, Cidetec
F. Martinez, G. Obieta, Ikerlan
J. Lezama, P4Q Electronics
J. M. Iriondo, Maser Microelectronica

Abstract

The development of distributed pressure sensors based on conducting polymers for automotive application is described. These pressure sensors can be placed on large surfaces due to its flexibility and low cost. As a consequence, pressure data are obtained not only from some discrete points but also from continuous surface points. 256 of these sensors have been placed on an automotive seat, giving the so-called "smart automotive seat". These sensors are able to provide information about the person on the seat (adult, child, size, weight, etc.). This information can be used by the central electronic system in the vehicle for activation and modulation (or deactivate if necessary) of security systems (airbag, seat belt's prestress system, etc.). Response time is lower than 2 milliseconds, and it works in pressure ranges of 0.05-10 kg/cm², showing a lifetime of more than 10 millions of actuations.

1 Introduction

The field of automotive industry increasingly demands higher accuracy security requirements. As a result, the accuracy of safety measurements in a car are progressing enormously. One of the most demanded and needed security systems is based on the presence detection, providing information about the person on the seat. In this sense, the elucidation of whether the person on the seat is an adult, or a child, and the size and weight of this person should led the activation or deactivation of security systems (airbag, seat belt's prestress system), and in case of activation, the adecuation of its actuation to the specific person.

Until now, no pressure sensor with appropriate performance for its application in automotive field has been developed. Traditional presence detecting sensors based on metallic wires, permanent magnets or electromagnetic induced cur-

rents are adequate to obtain information from discrete surfaces or areas but not to inform about a whole surface [1]. Moreover, they are not quantitative sensors, but only qualitative (on-off) sensors informing about presence or not presence of an object. Recently, a new generation of pressure sensors begins to be developed and used for these kinds of applications. It consists on the use of piezoresistive polymer film elements, between plastic substrates, showing a decrease in electrical resistance when a normal force is applied [2]. These sensors constitute a new generation of pressure sensors enabling monitoring along a whole specific surface area, and not only discrete points pressure monitoring. However, their use for large surface applications seems unlikely due to the high cost of materials used. The electroactive materials incorporated in currently developed configurations use metallic microparticles (silver) embedded on a polymer film or metallic central films (silver) separated by a pressurable elastomeric polymer film. In this sense, some devices which are now in commercial state have been already developed, showing several variations in its configurations, being either capacitive [3-4] or resistive [5-6] pressure sensors. Among resistive ones, Tekscan [5] technology uses a silver ink layer on each of plastic electrodes, followed by a pressure sensitive material layer. The sensor is formed laminating together two layers of substrate. This configuration gives a resistivity decrease when different pressures are applied on it. On the other side, Peratech [6] technology is based on metal-filled polymers as electroactive materials. This composite material behaves like a perfect insulator in absence of force, and metal like when deformed by compression, twisting or stretching. As a consequence, an exponential resistance drop with the pressure is observed. In spite of these valuable advances, the use of such high cost materials as silver is without any shadow of doubt a very important inconvenient since large surface applications can not be afforded by these types of sensors.

In this work, the construction of an intelligent seat is described, using a patented new technology of distributed pressure sensors [7]. This new technology uses conducting polymers as electroactive materials for construction of pressure sensors. The use of two thin conducting polymer films onto plastic substrates and the presence of a roughness at microscopic level lead a resistivity decrease when different pressures are applied. This new technology shows great advantages for application on high-surfaces, as on automotive "intelligent seats": A) Plastic sheets being used final sensor devices are light. B) Sensors being low cost, it is thus a competitive technology to be incorporated in automotive industry. C) Flexibility in final sensor devices makes feasible its incorporation in a flexible surface as it is the case in automotion seats.

The new sensors are based on ICPs such as polypyrrole (PPy), polyaniline (PAni) or polyethylenedioxythiophene (PEDOT) are emerging electroactive

materials useful for several industrial applications [8]. ICPs are already being employed in electronic capacitors [9], electrochemical (bio)sensor arrays [10], polymer light emitting displays [11], through-hole metallization of multilayer printed circuit boards (PCBs) [12], long-term solderable lead-free tin surface finishes for PCBs [13], transparent antistatic coatings for insulating substrates [14], conducting fibres, textiles [15] and anticorrosion coatings [16]. New emerging applications being studied are electromagnetic shielding applications in electronic equipments [17], conducting hot melt adhesives [18], electromembranes [19], cathode materials for lithium-ion batteries [20], electrochromic devices [21], organic solar cells [22], electroactuators [23] and nano-electronic devices [24]. For some of these applications, and specifically for application as thin film for pressure sensors, a good processability in ICP is crucial, in order to get an easy applied polymer film on the substrate. Thus, being conducting polymers insoluble in common solvents, aqueous dispersions of these polymers are used in these cases.

Conducting polymer dispersions are usually prepared by chemical oxidative polymerization of monomer in water in the presence of a polymer steric stabilizer [25]. By using different water soluble polymers during the polymerization such as poly(vinyl alcohol), poly(ethylene oxide), poly(N-vinylpyrrolidone), cellulose derivatives and poly(styrene sulphonate) salts, macroscopic precipitation of the ICP is prevented and sub-micrometer dispersed particles are obtained [26]. Reaction conditions such as temperature, oxidant, monomer concentration, etc. as well as the chemical structure, molecular weight and concentration of the polymer steric stabilizer strongly affect the size and stability of the colloidal dispersions and the conductivity of the resulting PPy film upon water removal. The presence of the insulating polymer steric stabilizer in the dried PPy film leads to lower conductivity values ($< 10^{-1}$ s/cm) when compared to raw PPy. If such PPy aqueous dispersions are employed as additives in water borne paints, the conductivity of the resulting coating after drying is usually very low ($< 10^{-5}$ s/cm). In a previous paper [27] new conducting polymer dispersions with average particle size below 100 nm are obtained by using sonochemical techniques during the oxidative polymerization process. These dispersions can be directly applied on substrates obtaining a conducting continuous film.

The development of a new low cost and flexible pressure sensor technology based on the deposition of conducting inks onto plastic flexible sheets has previously been described [7]. In this work, this conducting polymers based thin film technology is used for the construction of a smart automotive seat. Placing them on the surface of the seat, pressure data are obtained not only from some discrete points but also from continuous surface points. This smart automotive seat, based on 256 of these sensors, is able to provide information about the

person on the seat (adult, child, size, weight, etc.). This information can be used by the central electronic system in the vehicle for activation and modulation (or deactivate if necessary) of security systems (airbag, seat belt's pre-stress system, etc.).

2 Sensor Construction: Experimental

Experimental procedures for distributed pressure sensor construction are described below:

2.1 Conducting Ink Preparation

A conducting polymer dispersion was used as conducting ink for its application on a flexible plastic sheet. Poly(3,4-ethylenedioxythiophene) (PEDOT) was chosen as conducting raw material, and aqueous dispersions of this polymer were prepared for the preparation of conducting inks. PEDOT aqueous dispersions were prepared by using an Ultrasonic Processor (model UP 400 S from Dr. Hielscher GmbH) during the synthesis. As an example, ethylenedioxythiophene (1 ml, 9.4 mmol) and 3.5 g of poly(styrene sulfonate, sodium salt) were dissolved in 100 ml of distilled water. To this mixture, an equimolar amount of ammonium peroxydisulphate (6.58 g, 28.8 mmol) dissolved in 50 ml of water was added dropwise over a period of 4 minutes. After 1 hour of reaction under ultrasonic irradiation a dark blue PEDOT aqueous dispersion was obtained. Dispersion particle sizes were measured using a Beckman Coulter N5 Submicron Particle Size Analyzer.

2.2 Conducting Flexible Sheet's Preparation

Conducting flexible sheets were prepared placing a PET (polyethyleneterephthalate, 5×5 cm² in surface, 125 µm in thickness) plastic sheet on a spin coater. 50 µl of conducting polymer ink were dispensed on it and it was rotated at 1500 rpm. After 1 minute, it was stopped and left drying at room temperature. A thin conducting film was created onto the plastic sheet, giving a conducting flexible plastic sheet.

2.3 Sensor Configuration

In the construction configuration adopted, an additional flexible plastic sheet is also used together with the conducting polymer sheet, with conducting and non-conducting paths printed on it. The conducting paths act as electrodes, enabling the electrical connection of the different sensor elements, and they are printed on the sheets by either serigraphy or photolithography. The configuration and distribution of the conducting paths determines the size of each sensor element and their spatial distribution. The insulating paths allow the working pressure range of the sensor to be controlled. The configuration used for incorporating the sensors to the seat was a 4 x 4 array of sensor elements with an element size of 1 cm².

2.4 Interface Software

Real-time graphic representation of the information was acquired creating an application in the Labview programming environment. The current values measured by each of the sensor elements were converted to pressure data, using the calibration values previously obtained by the sensor configuration to make this conversion. The value of each of the pressure elements is displayed in real time on a colour scale going from blue (minimum pressure) to red (maximum pressure). The program thus enables real-time display of the pressure being exerted at each of the different points of the sensor.

3 Results and Discussion

Aqueous conducting polymer dispersions synthesized with mechanical stirring led to a broad distribution of particle size from tens of nanometres to several microns. When applied by sping coating onto plastic sheets for fabrication of conducting films, surface inhomogeneity of the coatings is significantly enhanced as a consequence of the presence of large conducting polymer particle sizes. The objective for a pressure sensor construction being an homogeneous and continuous conducting plastic sheet, lower particle sizes have to be obtained in starting conducting polymer dispersion. For this purpose, sonochemical techniques such as ultrasonic irradiation have been employed during the synthesis of the conducting polymer dispersion (PEDOT dispersion) in the presence of ammonium peroxydisulphate, as oxidant, and poly(styrene sulfonate) as steric stabilizer and dopant, as already described in our previous work [28]. Fig. 1 illustrates the particle size distribution obtained using the sonochemical technique. In this case, the average size of the particles in the

ultrasonic irradiated PEDOT dispersion is about 70 nm as determined by Light Scattering (LE).

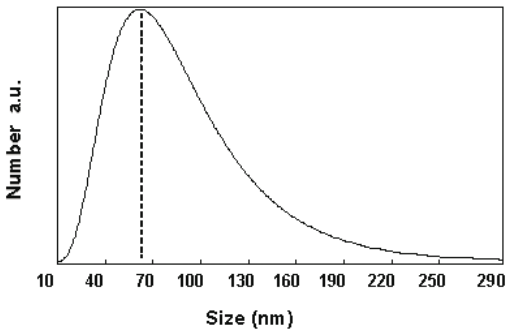


Fig. 1. Particle size distribution obtained in a sonochemical synthesis procedure

This PEDOT dispersion has been deposited by sping coating onto plastic flexible sheets obtaining a nanosized thin conducting film on it. Fig. 2 shows the surface picture obtained by atomic force microscope of these conducting films.



Fig. 2. Surface picture of conducting plastic film obtained by Atomic Force Microscope

A surface roughness can be observed at microscopic level, with an average grain size of about 50 nm, in good agreement with LS measurements. This roughness at microscopic level is thought to be the main point defining the working mechanism in the sensor. A sensor device is constructed by superposition of two conducting sheets by leaving conducting film inside. With no pressure on plastic sheets, there is no contact between conducting material or the contact is extremely light, due to existing microscopic irregularity on these

conducting surfaces. As the pressure on plastic sheets increases, the contact between the peaks in the conducting surfaces becomes higher and higher. Conducting rough surfaces progressively overlap until a full contact is obtained at a specific pressure value. In fact, a calibration plot is obtained by deposition of different masses on the sensor surface and recording the corresponding electrical intensity values. As it is shown in Fig. 3, a linear conductivity increase (or resistivity decrease) is observed until a constant value is reached. This is associated to the full contact point between conducting surfaces. Consequently, the conducting polymer film used as electroactive material in this technology acts as a bifunctional part: on the one hand, as the conducting material (as the silver in previous configurations); on the other hand, as the part allowing more or less contact between sheets with pressure changes (the pressurable elastomeric polymer film in previous configurations).

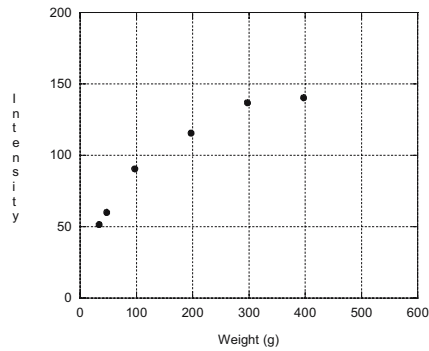


Fig. 3. Calibration plot for a flexible pressure sensor. Electrical intensity values for different masses on the sensor surface

The conducting plastic sheet and the lithographed plastic sheet having conducting and non-conducting paths printed on it are superposed. Thus, a 4 x 4 array of sensor elements with an element size of 1 cm² is obtained in an unitary device (Fig. 4).



Fig. 4. Sensor layer structure

Then, 16 of these unitary device elements were used to obtain a total of 256 measurement points distributed over the surface of the seat (Fig. 5). For their integration into the flexible structure of the seat, the sensors were simply glued onto it. Their location was chosen taking into account the optimum seat parts for providing information about the person on the seat (adult, child, size, weight, etc.). Most of the sensors (160 elements) were therefore located on the seat base, with the rest distributed over the back. More specifically, 16 of the sensor elements were located on the seat headrest, to provide precise data on its position. This information could be of great use for automatic headrest position adjustment or optimum opening of the airbag.



Fig. 5. Sensor location in the automotive seat

Each of the sensor elements acts electronically as a variable resistor in accordance with the applied pressure. The range of this electrical resistance varies among several $k\Omega$ at low pressures and a few ohms when maximum pressure is applied (before plastic deformation occurs). Multiplexing electronics was used to create a sample of the 256 sensors. To maintain the low cost of the sensors, simple electronics were used based on a voltage divider configuration or current-to-voltage converter. A control circuit sequentially connects each sensor element to a measurement unit, which makes an analogue/digital conversion of the pressure value obtained. In this way, a sample of the individual pressure exerted on each of the 256 sensors in a time of less than 2 ms is obtained.

Using this configuration, we have deduced the calibration parameters relating the voltage obtained at the output of the D/A converter (measurement unit) to the pressure exerted on the sensor. The data obtained show that sensor

response is exponential. The sensor resistance decreases abruptly when a determined initial pressure is applied and tends towards a constant final value on applying the maximum pressure. Thus, the sensor is designed to work in the intermediate part of its operating range where its behaviour is more linear and stable. This range is normally between 2 k Ω and 100 Ω .

A real-time representation is obtained converting current values measured by each of the sensor elements to pressure data. Calibration values previously obtained by the sensor configuration were used to make this conversion. The value of each of the pressure elements is displayed in real time on a colour scale going from blue (minimum pressure) to red (maximum pressure). The graphic representations of each of the sensor elements are shown spatially on a picture representing the sensorized vehicle seat. The program thus enables real-time display of the pressure being exerted at each of the different points of the seat. Fig. 6 shows the graphic representation as seen on the computer screen.



Fig. 6. Graphic representation of pressure values in the smart automotive seat

The way these sensors have been constructed allows the spatial configuration of the different sensor elements to be easily modified and tailor-made designs to be created. For example, sensor elements can be made with different spatial resolutions and/or non-uniform distribution to adapt to the application's requirements. The range of working pressures can be adjusted by altering the space between the conducting paths acting as electrodes, and/or the thickness or spacing between the non-conducting paths that act as spacers between the conducting layer and the electrodes.

An aspect to be simplified in future developments is the connectivity of the different sensor elements. There are no particular problems with the present configuration, as long as a large number of sensors are not used. However, in applications that require sensorization of a large surface area with a high spatial resolution at the same time, it would be convenient to adopt new ways of making the connections between the various sensor elements and the measurement unit.

4 Conclusion

A distributed pressure sensor is developed by using conducting polymer thin films on flexible plastic surfaces. Conducting formulations can be produced and deposited by dip-coating and printing high scale deposition technologies. The low cost and flexibility of final sensor units make them suitable for placing and adapting them on large surfaces, obtaining pressure data not only from discrete points but also from continuous surface points. Pressure ranges of 0.05-10 kg/cm² and lifetimes exceeding 10 millions of actuations are obtained with this technology based sensors, that shows a response time lower than 2 milliseconds and are passive elements versus electromagnetic interferences (EMI).

By placing 256 of these sensors on an automotive seat, a "smart automotive seat" has been developed. The smart automotive seat is able to provide information about the person on the seat (adult, child, size, weight, etc.). This information can be used by the central electronic system in the vehicle for activation and modulation (or deactivate if necessary) of security systems (airbag, seat belt's prestress system, etc.).

5 Acknowledgements

Authors wish to thank Basque Country Government (Proyecto Etortek "ACTI-MAT" and INTEK Cooperación), Ministerio de Educación y Ciencia (PROFIT-TIC), and Diputación Foral de Gipuzkoa for their financial support.

References

- [1] W.J. Karl, A.L. Powell, R. Watts, M.R.J. Gibbs, C.R. Whitehouse, *Sensors and Actuators*, 81(1) (2000) 137.
- [2] S.K. Yeung, E.M. Petriu, W.S. McMath, D.C. Petriu, *IEEE Transactions on Instrumentation and Measurement*, 43(2) (1994) 277.
- [3] www.micronavlink.com/technology.html
- [4] www.dactyl.com/scratchpad/pps/conformableSensor.html
- [5] www.tekscan.es
- [6] www.peratech.co.uk/science.htm
- [7] J.A. Pomposo, E. Ochoteco, H. Grande, F. Martinez, G. Obieta, CIDETEC & IKER-LAN, P200501698.
- [8] S.Kirchmeyer, K. Reuter, *J. Mater. Chem.*, 15 (2005) 2077.
- [9] T. Kazuhiro, Y. Mutsumi, K. Mamoru, Sanyo Electric Co., US 6894890 (2004).
- [10] A. Guiseppie-Elie, Allage Associates Inc., WO9306237 (1993).
- [11] K. Bremen, M. Buechel, S. Winter, S. Vulto, Koninkl Philips Electronics N.V., WO2005015654 (2005).
- [12] H. Juergen, K. Walter, Blasberg Oberflaechentech GmbH, US,5,373,629 (1994).
- [13] B. Wessling, Zipperling Kessler & Co., EP0807190 8 (1997).
- [14] J. Friedrich, Bayer A.G., DE4229192 (1994).
- [15] H. Kuhn, Milliken Res. Co., US5108829 (1992).
- [16] K. Guido, H. Ulrich, H. Martin, Bosch GmbH, DE10234363 (2004).
- [17] S. Fauveaux, J.L. Wojkiewicz, J.L. Miane, *Electromagnetics*, 23 (2003) 617.
- [18] J.A. Pomposo, J. Rodriguez, H. Grande, *Synthetic Metals*, 104 (1999) 107.
- [19] J. Ding, W.E. Price, S.F. Ralph, G.G. Wallace, *Polym. Int.*, 53 (2004) 681.
- [20] R.P. Ramasamy, B. Veeraraghavan, B. Haran, B.N. Popov, *J. Power Sources*, 124 (2003) 197.
- [21] D. Mecerreyes, R. Marcilla, E. Ochoteco, H. Grande, J.A. Pomposo, R. Vergaz, J.M.S. Pena, *Electrochim. Acta*, 49 (2004) 3555.
- [22] C.J. Brave, *Sol. Energ. Mat. Sol. C.*, 83 (2004) 273.
- [23] D.Z. Zhou, G.M. Spinks, G.G. Wallace, C. Tiyaipiboonchaiya, D.R. MacFarlane, M. Forsyth, J.Z. Sun, *Electrochim. Acta*, 48 (2003) 2355.
- [24] J. Ackermann, D. Crawley, M. Forshaw, K. Nikolic, C. Videlot, *Surf. Sci.*, 532 (2003) 1182.
- [25] S.P. Armes, B. Vincent, *Chem. Commun.*, 4 (1987) 228.
- [26] J. Stejskal, *J. Polym. Mat.*, 18 (2001) 225.
- [27] M. Magini, T. Radnai, *J. Chem. Phys.*, 71 (1979) 4255.
- [28] J.A. Pomposo, E. Ochoteco, C. Pozo-Gonzalo, P.M. Carrasco, H. Grande, J. Rodriguez, *Polymer for Advanced Technologies*, 17 (2006) 1.

E. Ochoteco, J.A. Pomposo, H. Grande

CIDETEC, Center for electrochemical technologies
Parque Tecnológico de Miramón
P^a Miramón 196, 20009 San Sebastián
Spain
eochoteco@cidetec.es

F. Martinez, G. Obieta

IKERLAN, Technological Research Center
P^o J.M. Arizmendiarieta, 2
20500 Arrasate-Mondragon
Spain

J. Lezama

P4Q ELECTRONICS
Alonsotegi Elkartea, 27-29
48810 Alonsotegi
Spain

J.M. Iriondo

MASER MICROELECTRÓNICA
P^o Industrial Mendarozabal
Edif. OFICINAS, 20850 MENDARO
Spain

Keywords: distributed pressure sensor, flexible plastic sensor, conducting polymer ink, presence detection, large surface monitorization, smart automotive seat

Intelligent Infrared Comfort Sensors for the Automotive Environment

L. Buydens, V. Kassovsky, R. Diels, Melexis NV

Abstract

We will discuss the advantages of contact-less infrared thermometers as main sensor in automotive climate control systems and address the practical considerations one should take into account when developing such a system. In order to offer a price competitive solution with the more commonly known aspirated thermistor sensor, Melexis developed an integrated infrared thermometer targeted at size reduction, improved ease of installation, multi zone temperature control and cost improvement. The features of this new product are highlighted. Furthermore we discuss the functional and reliability requirements that have to be met by automotive infrared sensors and how these requirements are met in a modern sensor design. Finally, we show the results of the development of low cost infrared array sensors for next generation air-conditioning systems in combination with safety applications.

1 Introduction

As many people spend several hours a day in their car or truck, it is important to provide a good thermal environment, which gives comfort and optimises performance for both the driver and passengers. In recent years, infrared contact-less sensors have become widely accepted and implemented as the comfort sensor for mobile air-conditioning (MAC) applications [1]. In such a system, passive long-wavelength (5 to 15 micrometer) infrared sensors based on thermopile technology are being used. This paper discusses the different applications of these infrared sensors in the automotive environment.

The application of infrared sensors can be split in two broad categories: comfort and safety applications.

In the comfort application, the infrared sensor is used to track the comfort feeling of driver and passengers. The signal output of the sensor is used as the input to control the settings of the automatic air-conditioning system. We describe the specific demands that MAC applications ask from the infrared

thermometer and highlight the technical solutions for these requirements. There is a growing penetration of the infrared thermometer in the automotive air conditioning market. Melexis started volume production of infra red thermometers 3 years ago. Current volume is more than half a million pieces per year for 5 different car models of Japanese and US car manufactures. Production volume grows in the next two years above one million pieces per year for European, US and Japanese car manufactures.

Safety applications of infrared sensors are not yet widely commercialized. This paper discusses the possible applications in an automotive environment, derives the requirements for the infrared sensor, and again discusses the technical solutions that have been developed.

2 Automotive Comfort Sensing Application with Infrared Thermometers

An automatic air-conditioning system needs to measure the comfort of the passengers in order to take the appropriate air-conditioning action.

The thermal comfort feeling of the driver or a passenger in a car is a function of six parameters:

- ▶ Cabin air temperature
- ▶ Air blowing speed on exposed skin
- ▶ Radiation: sunlight radiation and thermal radiation level inside car
- ▶ Humidity of the air
- ▶ Activity of the person
- ▶ Clothing worn by the person

When a person is highly active, he needs a lower air temperature in order to feel comfortable. For a car climate control system, the activity level of the occupants is known and relatively constant. A person driving a car dissipates about 160 W which needs to be carried off to make him feel comfortable.

The amount of clothing a person wears is of course a personal choice and depends on the season. A person wearing thicker clothes requires a lower operational temperature in order to feel comfortable. Each person will set the desired temperature according to his own preferences. This is recognized in both references [2] and [3]. Reference [2] gives comfort temperature zones for typical summer and winter clothes worn in an office environment. Reference [3] lists different types of clothes and their impact, in °C, on the comfort temperature.

The other 4 parameters mentioned above are taken into account by one single infrared sensor. The infrared sensor measures the average temperature of the surface within its field of view. Depending on the position of the sensor, the surface inside the field of view is made up of parts of the car interior, clothes of the persons inside the car, and skin of the persons inside the car.

All of these surfaces change temperature under influence of air temperature, air blowing speed and sunlight radiation. These three parameters are thus directly measured by the infrared sensor, using the relation between surface temperature and infrared radiation emitted by the surface.

As mentioned in reference [2], humidity is a special case. When the humidity is high, the evaporation of sweat becomes more difficult. As a result, the persons in the car will get a wet skin and wet clothes, and will feel sticky and uncomfortable. As skin and clothes are not cooled by evaporation, their temperature will rise. This rise in temperature of skin and clothes will be sensed by an infrared sensor, which will indicate to the air conditioning controller that more cooling is needed. Reference [2] mentions that the air temperature comfort zone is moved about 1°C lower when the relative humidity increases from 30% to 60%.

To take into account humidity in the infrared measurement, it is necessary to view the persons inside the car, as their surface temperature will be affected by relative humidity of the air in the car through the mechanism of evaporation of sweat. However, it has also been demonstrated that an extremely effective and energy-efficient automatic climate control system can be realized by measuring only the average surface temperature of the front windshield and the dashboard: see references [4] and [5]. By combining infrared sensing with an optimized A/C loop, the authors of [5] were able to save 40% to 70% of the energy needed for climate control, while maintaining optimum comfort for the car passengers.

As an infrared sensor can take into account the 4 main parameters influencing comfort feeling, i.e. air temperature, air-speed, sunlight radiation and humidity, it is appropriate to consider an infrared sensor is rather as a comfort sensor than as simply a contact-less thermometer. Compared to the more commonly used aspirated thermistor, the infrared sensor offers the opportunity to achieve an improved, stable thermal comfort for the car occupants. Even though the sensor does not measure directly the direction of the sunlight, it is possible to take the effect of the sunlight into account as sunlight will immediately increase the surface temperature.

Compared to the often used aspirated thermistor, the infrared comfort sensor offers the following advantages to the MAC system designer:

- ▶ The sensor takes into account more parameters which influence the comfort feeling of the passengers;
- ▶ The controller receives a measurement of the temperature in the car interior, not just of the temperature in front of the dashboard;
- ▶ By nature, the infrared sensor has a small thermal mass, giving a fast response to changing temperatures and external factors (thermal time constant in the order of 30 ms, digitisation and linearization time around 300 ms). This enables the designer to use simple control algorithms while still achieving a tighter control and stability of the passengers' comfort;
- ▶ By taking into account more parameters which influence directly the comfort of the passenger, a MAC system with infrared sensors can be more easily adapted to car model changes as it is easier to adjust the MAC control algorithm to changes in cabin design such as window size changes;
- ▶ Reduced size and easier integration in the air conditioning control unit;
- ▶ Direct multi zone control using a single sensor with multiple thermopiles for a marginal additional cost.

3 Automotive Comfort Sensing Requirements on Infrared Sensors

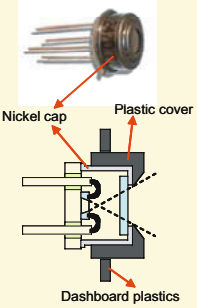
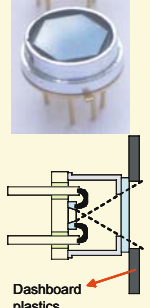
In order to allow application in automotive comfort sensing, an infrared sensor needs to meet the requirements in Tab. 1.

4 Automotive Comfort Sensing Solutions

4.1 Present Day: Infrared Sensor with Signal Processing ASIC on PCB

In its development of infrared sensor modules for automotive climate control, Melexis was able to meet all of the requirements of the preceding paragraph, by making design trade-offs and using advanced mixed analog-digital signal conditioning techniques.

To meet the requirements of reliability, stability over time and wide temperature operating range, we decided to use only CMOS materials and processes in the manufacture of its thermopile sensors. The design trade-off made concerns the sensitivity of the thermopiles over e.g. Bi/Sb solutions. However, it also makes that the thermopiles benefit from the reliability, stability over time and temperature operating range offered by CMOS technology.

Parameter	Requirement
Number of pixels	1 or 2
Operating temperature range	$[-40^{\circ}\text{C}, +85^{\circ}\text{C}]$
Typical range of object temperatures T_o where measurements can be made ¹	$[0^{\circ}\text{C}, +50^{\circ}\text{C}]$
Typical range of ambient temperatures T_a where measurements can be made ¹	$[-20^{\circ}\text{C}, +85^{\circ}\text{C}]$
Object temperature measurement accuracy in and directly around the comfort range; valid for objects with emissivity of 99.2% ² .	Error $< 1^{\circ}\text{C}$ for T_a within $[0^{\circ}\text{C}, +50^{\circ}\text{C}]$ and T_o within $[15^{\circ}\text{C}, +40^{\circ}\text{C}]$
Maximum drift on object temperature measurement over 10 years of operation	Lower than 1°C
Aesthetical integration in car interior	<div><p>The thermopile sensor is packaged in a metal TO can. The metal cap is not suited to appear in the car interior. The only part of the sensor that should be visible is the IR window of the TO cap. There are two proven solution: a: TO can with window inside and plastic cover hiding the cap, or TO can with window outside. Both provide a satisfactory appearance, and have their own application in function of installation method and thermal environment.</p><div></div><p>Figure 1: Photograph of thermopile sensor with window inside.</p><div></div><p>Figure 2: Photograph of thermopile sensor with window outside.</p></div>
Automotive qualification	Passing automotive testing; high-temperature operation; temperature/humidity cycling, thermal shock; mechanical shock, vibration; chemical resistance (cleaning fluids, soft-drinks,...); EMC: electromagnetic compatibility, ESD tests;
Failure rates over 10 years of operation	Sub-ppm

Tab. 1. Requirements. ¹ Outside these ranges, a temperature overflow or underflow signal is generated.² See the remark on emissivity in chapter 6.2

For the signal processing of the thermopile signal, an advanced mixed analog-digital signal conditioning MLX90313 ASIC is combined with the thermopile infrared sensor in the TO-can. The ASIC is manufactured in standard CMOS technology. The amplifier used for the thermopile signal has an offset limited to 4 μV , and input referred noise of only 25 $\text{nV}/\text{Hz}^{1/2}$.

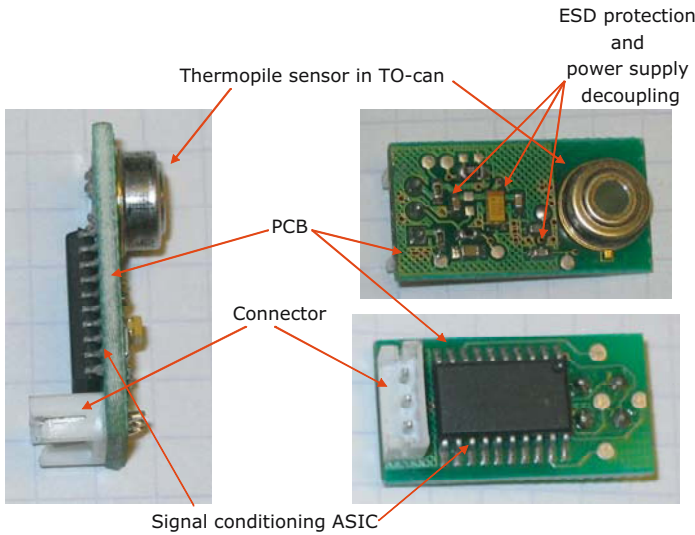


Fig. 3. MLX90601: automotive module assembly with thermopile sensor and signal conditioning ASIC

The high accuracy on the object temperature measurement within a wide range of ambient and object temperatures is obtained by making the ambient compensation and linearization in the digital domain. Both thermopile and thermistor output are amplified and converted to digital. The ambient temperature is calculated on basis of the amplified thermistor voltage and the thermistor calibration constants stored in EEPROM. The object temperature is calculated by solving the 4th order equation

$$V_{TP} = \alpha (T_o^4 - T_a^4) \quad (1)$$

In this equation, T_o is the object temperature we want to measure, T_a is the ambient temperature of the sensor itself; V_{TP} is the amplified thermopile voltage and α is the calibration constant determined during object calibration of the module in front of a precision black body.

The 4th order equation (1) is solved exactly in the digital domain. As the equation is not approximated by a first or second order Taylor approximation around a working point, good accuracy is obtained over a wide range of temperatures, and not only directly around the working point.

The absolute object temperature accuracy is mainly determined by the tolerance on the temperature of the laboratory bath used during ambient calibration, and the tolerance on the temperature of the black body used during object calibration. These tolerances lead to small errors on the measured ambient temperature T_a , and on the calibration constant α . Equation (1) shows that the measured object temperature T_o is not impacted by the error on α if $T_o = T_a$ (and $V_{TP} = 0$). As the difference between T_o and T_a increases, the error on the measured value of T_o will also increase.

The calibration constants are stored in the EEPROM of the signal conditioning ASIC. Although the EEPROM has passed testing for 10 years data retention at 85°C and 1 year at 125°C, extra safety for data retention is built in by applying a 5 bit Error Checking and Correction (ECC) code. The ECC is based on Hamming coding. Error checking and correction is run after each power up; it allows automatic correction of single bit errors. Multiple bit errors lead to an error message.

4.2 Integrated Sensor/ASIC Solution

The newest development in the area of automotive passive infrared sensors is the integration of the temperature sensing element and the signal conditioning ASIC into a standard 4-pin TO-39 can.

This infrared thermometer combines the functionality, accuracy, reliability and know-how of the current MLX90601 module in a very small package, made possible by the design of a reduced size thermopile chip and a small signal conditioning chip in standard 0.35 μm CMOS technology. The assembly supports both a single and a dual sensor version suitable for dual zone air-conditioning and blind spot detection applications. The factory calibrated, measured temperature is available at the TO-can pins as a standard PWM signal or the information can be read using the 2 wire SMBus protocol. The thermometer supports both 3 V and 5 V supply voltage operation as a standard and 12 V supply voltage operation for remote installation.

To the MAC system manufacturer the advantages are multiple:

- ▶ Standardized factory calibration leads to shorter development time and lower product cost.
- ▶ Reduced part count improves reliability further and lowers cost.
- ▶ Integration on customer PCB without extra sensor PCB is possible.
- ▶ Reduced size, space saving in a more and more cramped area as more and more applications need to find a place behind the dashboard;
- ▶ Complete single/dual zone thermometer in one package;



Fig. 4. MLX90614: digital, fully calibrated, infrared thermometer in a TO can

The Mlx90614 is built from 2 chips developed and manufactured specifically for this purpose: a reduced size infrared sensor and a signal conditioning ASIC, specially designed to process the output of IR sensor. Thanks to a low noise amplifier, a high resolution ADC and powerful DSP unit the thermometer can achieve a high resolution and accuracy over wide temperature ranges. The infrared thermometer is factory calibrated in wide temperature ranges: -40 to 125°C for ambient temperature and -70 to 380°C for object temperature. For object temperatures in range 0°C to 50°C the measurement error is below 0.5°C. Outside that range the error is below 1%.

The 10-bit PWM is configured to transmit continuously the measured object temperature for range of -20 to 120°C, which corresponds to an output resolution of 0.14°C. The PWM can easily be customized digitally for any temperature range desired by customer without affecting the internal calibration of the device. Using the SMBus, the measured temperature is directly accessible with a resolution of 0.01°C.

Compared to the MLX90601, the new MLX90614 thermometer in a can has some improvements:

- ▶ The user has the opportunity to adopt the sensor for any emissivity coefficient below one (see chapter 6.2) without affecting the factory calibration of the sensor.
- ▶ The measurement bandwidth and associated noise level can be chosen independently from the output refresh rate. By a software implementation of an Infinite Impulse Response filter, we can keep the refresh rate constant while at the same time achieving a low noise level for the measured signal.
- ▶ Using the SMBus protocol, the user can build a sensor network of up to 10 infrared sensors connected with only 2 wires, each device having its unique 8-bit ID.

The thermometer is available in 2 versions: 5 V compatible and 3 V (battery) compatible. Additionally, the 5 V can be easily adopted to operate from higher supply voltage (6-16 V) by adding only one external bipolar transistor, one resistor and a capacitor.

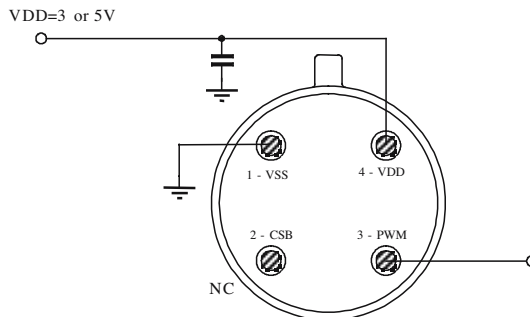


Fig. 5. 3 or 5 V supply voltage version of the MLX90614

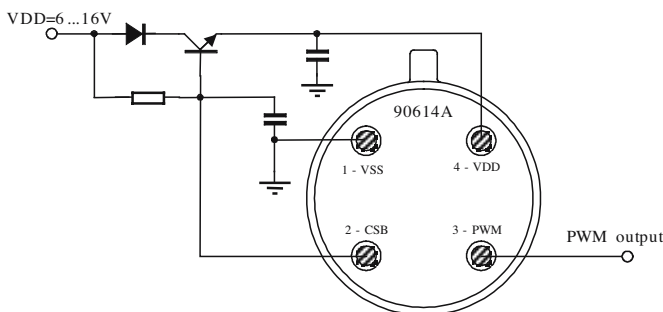


Fig. 6. 12 V supply voltage version of the MLX90614 for remote applications

5 Possibilities of Infrared Arrays in Automotive Comfort Sensing

Dual pixel and multi-pixel (array) sensors have the following benefits in comfort applications:

- ▶ Independent sensing of comfort in two or more zones: thereby providing a real dual or multi-zone automatic climate control using a single sensor with multiple thermopiles integrated. This approach can drastically reduce wiring cost, since the mounting location of the sensor is decoupled from the area that is being measured. Also it is no longer necessary to use a sunlight sensor as the effect of sunlight radiation is directly captured by the array thermometer;
- ▶ Distinction between skin and clothes: The extra information may allow making the control system more intelligent;
- ▶ Filtering of anomalies such as the hot tip of a cigarette: Such anomalies can be detected very clearly when using an array, as an array is equipped with a lens and individual fields of view per pixel can be made quite small without compromising the signal to noise ratio. Melexis made 4x4 array prototypes with individual field of view of 10°, and 10x10 array prototypes with individual field of view in the order of 5°;

The main advantages of an array can be realized by using the same sensor for two applications: comfort and safety. This will be discussed in chapter 7.

6 Practical Aspects of Automotive Comfort Sensing

6.1 Sunlight Immunity

Direct sunlight incidence in the thermopile sensor should not impact the accuracy of the object temperature reading. To this end, the sensor window filters out the short wavelengths below 5.5 μm . Long wavelength infrared radiation emitted by the objects in the car will pass the filter window. Long wavelength infrared radiation emitted by the sun is blocked by the windows of the car (glass is not transparent for long wavelength infrared radiation!). The combined filtering of the Si-window of the sensor and the glass of the windows of the car reduces the impact of direct sunlight at orthogonal incidence to an error of +0.5°C to +1°C on measured object temperature. The error can be further reduced by mounting the sensor in such a way that direct orthogonal illumination by the sun is impossible or rare.

If windows are open, long wavelengths emitted by the sun are NOT blocked by glass, and direct sunlight incident on the sensor can lead to important

changes in object temperature readout. This should however not be for the climate control application, as it is normally not designed for functioning with windows open.

6.2 Emissivity

Emissivity is the ratio of power radiated by a surface to the power radiated by a blackbody at the same temperature. Melexis infrared sensor modules are calibrated in front of a black body with emissivity 99.2%. That means that the calibration constant α is determined in such a way that the correct object temperature is obtained when measuring objects having an emissivity of 99.2%. Typical surfaces in a car have somewhat lower emissivities [8]: skin (0.97 to 0.98), glass (0.92), black plastic (0.95), textile fabrics (Hessian fabric, green coloured, reported 0.9).

For simplicity, we further assume that the calibration black body has emissivity = 1. In that case, we can take into account the emissivity of the object by changing equation [1] into:

$$V_{TP}' = \alpha(\varepsilon T_o^4 - T_a^4) \quad (2)$$

Where ε is the emissivity of the object.

However, equation (2) is not completely correct for following reason. An object with infrared emissivity ε reflects $1-\varepsilon$: the lower the emissivity, the higher the reflection of infrared radiation. So, the sensor will also see radiation from the surroundings/environment reflected by the directly observed objects. In a first approximation, we assume the surroundings in the comfort application to be at a uniform ambient temperature T_a . In that case, a more correct formula taking into account the infrared radiation reflected by the object is:

$$V_{TP}'' = \alpha(\varepsilon T_o^4 + (1 - \varepsilon) T_a^4 - T_a^4) = \alpha\varepsilon (T_o^4 - T_a^4) \quad (3)$$

The simplified model of formula (3) shows that the measured thermopile voltage is a factor ε smaller than what it should be for a correct measurement, which results in a too small difference between the measured object temperature and the ambient temperature. If the object has emissivity lower than 99.2% the following will happen: an object at higher temperature than ambi-

ent T_a will be measured too low; an object at lower temperature than T_a will be measured too high. The importance of the error grows with the difference between T_o and T_a , and with the value of the emissivity: the lower the value of the emissivity, the larger the error. The phenomena predicted by the simplified model (3) have been experimentally confirmed by Melexis. The order of magnitude of the error can be easily derived from (1) and (3). For $T_a = 45^\circ\text{C}$ and $T_o = 20^\circ\text{C}$, and $\varepsilon = 0.95$ (instead of 0.992), the measured T_o using formula (1) will be about 21.2°C , or a positive error of 1.2°C . This error should not prohibit the use of the sensors in automotive climate control: the effect can be taken into account in the design of the climate control system, by checking out typical operating conditions. If needed, the sensor ASIC can easily take into account the effect of a different emissivity without affecting the calibration. The processor of the climate control system can make a compensation on basis of both T_o and T_a . The main sensor characteristic of importance for the climate control application is the stability and repeatability of the temperature reading.

6.3 Field of View

The temperature an infrared sensor measure is an average of the temperature of all surfaces the sensor sees in its field of view. The field of view required for a comfort application is determined by the vehicle dimensions and the design-principles of the manufacturer of the air conditioning control panel. As a thermopile die is sensitive to radiation coming from all angles (180° front view; even sensitivity to radiation coming from the back of the die), it is not difficult to make thermopile sensors with wide field of view. Reducing the field of view is possible by reducing the diameter of the opening of the TO-can. However, this technique has its limits. At a certain moment, the amount of energy received from the object becomes too low, and instabilities occur. Typically, it is advised to work with a viewing angle of at least 60° . Smaller field of views can be realized through lenses, but these make the application considerably more expensive.

A special case is the dual thermopile sensor. In the sensor are two thermopile chips which are placed off centre. Fig. 7 shows a typical field of view for such a sensor. Each of the thermopiles sees a different area of the car such that one looks at the driver and his/her surroundings and the other looks at the front passenger and his/her surroundings. Both the temperature of the driver side and the passenger side can be measured separately and transmitted to the air conditioning controller. This makes this sensor especially suited for multi zone car air conditioning.

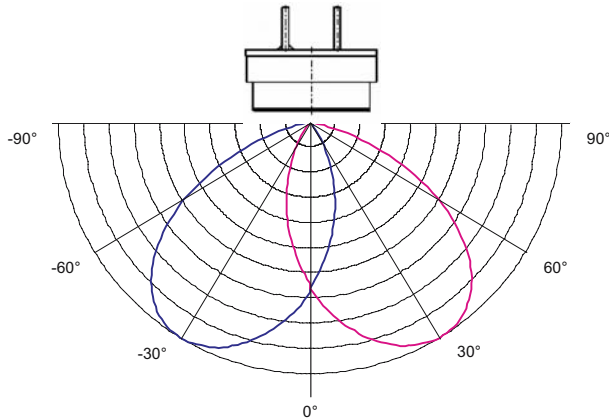


Fig. 7. typical horizontal field of view of a dual thermopile infrared sensor

6.4 Thermal Gradients

An infrared thermometer module is calibrated in front of a reference black body (perfect thermal emitter with $\varepsilon=1$). During the calibration, the module itself is operated at room temperature, and the module is isothermal: the differences in temperature over the surface of the module are very small. When used for measurements under isothermal conditions, the measurement results will be correct. However, when used under non-isothermal conditions, errors may occur. A typical automotive example is the example according to which the module is mounted in the dashboard. The back of the module is behind the dashboard and the thermopile sensor looks into the cabin through an opening in the dashboard. High-power electronics mounted close to the module heat the back of the module; the front part of the sensor is cooled by the air-conditioning. In such situation, the top of the sensor package has a slightly different temperature than the thermopile chip, and emits radiation according to its temperature. This infrared radiation is an error signal added up to the infrared radiation emitted by the object. The error can become important when the field of view is small, and radiation received from the object is low.

This problem was solved by providing thermopile sensors in metal cans of highly thermally conductive material; so the thermal gradient over the sensor is kept small. For demanding applications where the sensor has to be used under high thermal gradient, the thermopile sensor of Fig. 2 has best performance, among others thanks to its thick aluminium cap. For stable operation, it is always advisable to limit the thermal gradients over the thermopile sensor by avoiding placing of the sensor close to strong heat sources.

6.5 Cigarette Smoking

A property of IR radiation is that it is almost not influenced by smoke in the air. Smoke from cigarettes will therefore in all practical circumstances not influence the temperature reading of the IR sensor. The temperature of the tip of a lit cigarette can reach up to 800K. The size of the tip is very small however and when the cigarette is not too close to the sensor (> 50 cm) the temperature readout influence will stay below 0.5°C (measurement with a wide-angle sensor with an opening angle of about 90°). When the cigarette is drawn the temperature of the tip can reach 1000K and the readout may react up to 1°C . Normally this is only a very short effect which can be averaged out easily by the MAC controller or by setting the sensor to a lower bandwidth.

7 Safety Applications

7.1 Windshield Defogging based on Dew-Point Detection

Windshield fogging presents a double safety issue, as it deteriorates the view on the road, and it distracts the driver who is looking for manual activation of the defogging. Reference [6] describes how the fogging of the front windshield can be measured and predicted by using an infrared sensor for measurement of the temperature of the windshield. According to [6], the infrared sensor can simultaneously be used to make a highly efficient climate control system. This can lead to considerable cost savings as expensive and difficult to install contact sensors can be avoided.

Infrared comfort sensors used in air conditioning control systems can be directly used in windshield defogging applications. The operating temperature ranges are equal; there are no special accuracy requirements. The requirements related to automotive reliability are equal to the ones used in automotive comfort sensors.

7.2 Blind Spot Detection

System designers are examining different types of sensors to help drivers be aware of vehicles in their side blind spots when changing lanes and making turns. Dual infrared sensors integrated in mirrors, taillights or side fascia can measure adjacent lane temperature over time to detect vehicles entering the side blind spot. Such systems ignore stationary objects, minimizing false

alarms and are immune to noise. Dual infrared comfort sensors used in MAC systems can also be used for blind spot detection.

7.3 CO₂ Concentration Measurement

Future climate control systems in Europe will most likely use CO₂ as a cooling agent. In these systems, CO₂ will be used under high pressure. Several studies on the safety and health risks of CO₂ in automotive cooling/heating systems are being made. According to the study [7] made by the EPA (Environmental Protection Agency, USA), it is strongly recommended to use CO₂ detection inside automotive climate control systems in order to activate system fault indicators, and to automatically activate fast release of the CO₂ cooling agent and air exchange in the passenger cabin. The open air CO₂ concentration is 365 volume-ppm. Sustained exposure to 40.000 volume ppm (1 hour) is considered as harmful, as well as short exposure to 60.000 volume ppm (minutes): see [7]. The infrared absorption line of CO₂ around 4.26 μm can be used to make accurate and reliable CO₂ concentration measurements.

CO₂ concentration measurements require the use of thermopile sensors with a filter window centered on the CO₂ absorption wavelength of 4.26 micrometer. The concentration measurement is based on the use of an infrared radiation source having strong emittance around 4.26 μm . Reliable sources operating at a temperature around 402°C (= black body temperature with peak radiation 4.26 μm) are commercially available. The radiation of a black body at 402°C is strong enough to emit a power level in the narrow absorption line around 4.26 μm that is of the same order of magnitude as the power emitted by a black body at room temperature over the whole width of the spectrum, thus bringing the module in its normal operating range.

7.4 Presence Sensing, Seat Occupancy and Pedestrian Detection

The passenger airbag should not be activated if a passenger seat is not occupied. An infrared array can be used to detect the presence of a person in a seat by detecting differences in measured temperature among pixels.

Intelligent airbags need to do more than just detect whether a seat is occupied. The activation of an intelligent airbag depends upon the type of person (baby in seat, child or adult) and the position of the person (sitting straight, bent over, feet on dashboard). As such, an intelligent airbag needs one or more sensors to distinguish among the different situations. Thermopile-based infrared sensor arrays can make rough thermal images, which allow to learn about the

type of person and to detect the position of a person using minimal image processing.

Infrared sensor arrays can also be used to detect obstacles outside the vehicle. The advantage of using infrared above visible detection is in the extra dimension provided by the temperature information. Thanks to this extra information, image processing power and complexity can be greatly reduced, and the number of erroneous detections can be strongly reduced. A visible camera with image processing system might have difficulty in distinguishing a real person from its shadow; for an infrared camera, such problem does not exist.

Presence sensing, seat occupancy and detection of pedestrians all require arrays. They are based on the detection of differences in temperature between the surface of a person and its environment. Three parameters of the arrays are of importance for the applications:

- ▶ Spatial resolution, determined by the number of pixels;
- ▶ Temperature resolution: the smallest temperature difference distinguishable between two pixels;
- ▶ Detection speed;

Sensing the presence of a person in a car seat is the simplest application of the three; a limited number of pixels will be enough to determine whether a person is present in the seat or not. Typically, a 4x4 thermopile array should be sufficient.

In order to sense the type of person (child, adult) and the position of the person, more information is needed. A minimum of 10x10 pixels is advised.

In order to detect a person at sufficient distance to stop (25 m braking distance at 60 km/h on a wet road), we assume that the width of the person (0.5 m) should fill a single pixel, and that we scan the road over a width of 10 m and a height of 3 m. These assumptions lead us to the need for a minimal horizontal resolution of 22 pixels and a minimal vertical resolution of 7 pixels, leading to a 154 pixel array.

During a nice summer day, the surface temperature of the seats can get quite hot. In such situations, the temperature difference between the skin of the person and the surface of the seat can become small. Most probably, it will not be possible to make a failure-free detection system. In some cases, the presence of a person will not be detected, as the difference in temperature between the person and its environment is not clear enough. An infrared array can only be an aid in detecting, but cannot faultlessly cover 100% of the practical situations. In order to reduce the number of detection failures, it is important to

have a good temperature resolution and stable readout, typically better than 1°C or even 0.5°C .

Presence sensing and seat occupancy can deal with quite low frame refresh rates: changes in presence and changes in position of a person do not happen within fractions of seconds.

Pedestrian detection however, needs quite fast frame rates. At 60 km/h, a car moves 17 m every second. If the frame refresh rate is above 1 s, a pedestrian detection at 25 m is of no use. To make detection at 25 meter distance useful, the frame should be refreshed within about 1 meter travelling distance, or within 60 ms, for a vehicle travelling 60 km/h.

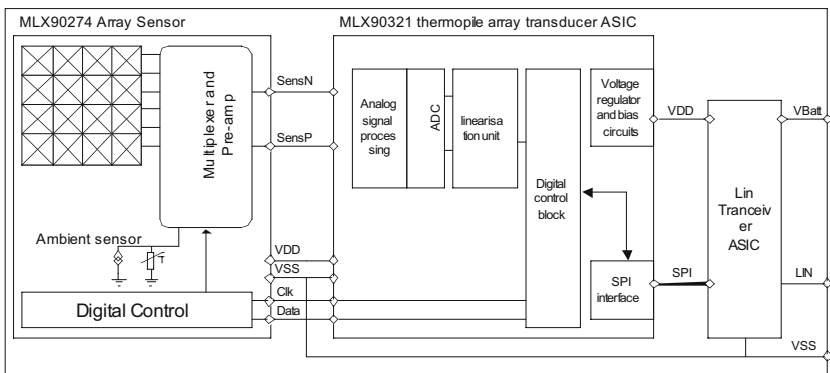


Fig. 8. 90611 Block diagram

In order to yield good temperature resolution, infrared sensors need some integration time. A larger integration time results in lower noise and better temperature resolution. So, speed is a requirement that is in conflict with temperature resolution.

We have made a 4x4 prototype infrared array module MLX90611 which can be used in presence detection and seat occupancy by developing a thermopile sensor die with integrated multiplexer electronics, as well as the infrared signal conditioning ASIC MLX90321, that is capable of handling up to 32 pixels (Fig. 8).

The MLX90321 reads out 4 pixels simultaneously, thereby increasing the frame refresh time considerably. A key feature of the MLX90321 is its ability to communicate through virtually any protocol (up to 4-wires) with external sensors, actuators or other devices, as all SPI pins can be reconfigured as gen-

eral purpose input-outputs. The data from these devices can be processed by the MLX90321, combined with infrared temperature measurements and sent back to the same or other devices. This option provides flexible control of the module as well as economical (in terms of wiring) and safe transfer of data.

The MLX90611 IR array module has a 4x4 array sensor with wide viewing angle. The total field of view of the complete array is 70 by 70 degrees, each pixel having a field of view of 10 degrees. Each individual pixel has its own constants stored in the ASIC EEPROM and is fully calibrated by Melexis. The temperature information of each individual pixel can be communicated to the ECU through an SPI or LIN interface.

The 4x4 array prototype can be used as a combined sensor for comfort sensing and presence detection. The photograph in Fig. 9 shows a picture of the 4x4 array module, while Fig. 10 gives a schematical drawing of the field of view of the module.

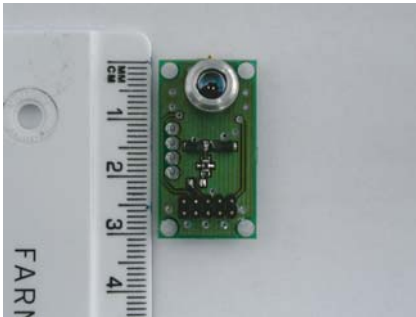


Fig. 9. 4x4 array prototype module; thermopile array in TO-39 package with electronics on PCB.

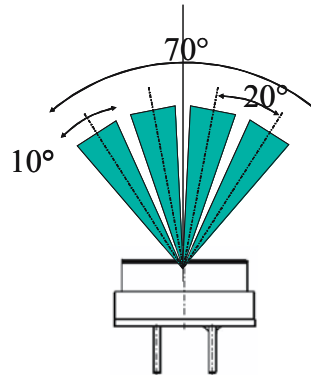


Fig. 10. Field of view of 4x4 array prototype.

In addition, Melexis developed a 10x10 thermopile array module. This prototype is based on the MLX90313 signal conditioning ASIC, which reads out all pixels sequentially. An example of possible application of the 10x10 array is shown in Fig. 11. The figure shows an overlay of a low-resolution infrared picture taken with the 10x10 array, and a photograph taken in the visual domain. The right photograph shows a situation with the driver sitting upright; in that case, the airbag can blow off at full energy. The left photograph shows a situation where the driver grabs a map lying under the windshield. The chest of the driver is against the steering wheel. In that position, the airbag should not

blow off. The two photographs show that the position of the driver can be easily detected by identification of the hottest spots in the 10x10 matrix. As there are only 100 pixels, image processing requirements are very limited, while the probability of correct detection is rather high. It should be clear that the 10x10 array can at the same time be used for comfort sensing.

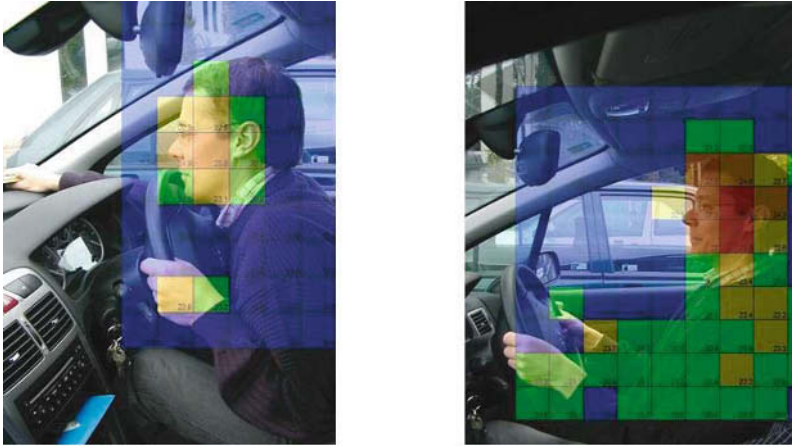


Fig. 11. Application of 10x10 infrared arrays for seat occupancy / position detection

At this moment, no prototypes suitable for pedestrian detection are available. Although the application can probably be realized using thermopile array technology, the high frame renewal rate combined with the good temperature resolution will require massively parallel processing of pixels, which might become only commercially viable using future microelectronics technology generations.

8 Conclusion

In this paper, an overview has been given of thermopile based infrared sensor applications in automotive comfort and safety. For each of the different applications, the sensor requirements put have been discussed and a number of practical considerations related to the practical use of infrared sensors in an automotive environment have been discussed.

The application of infrared thermopile sensors as the comfort sensor for air conditioning systems in several car models has shown that this is a mature, reliable technology. Further advances in integration will result in an even more versatile technology with widespread applications. The cost reduction

coming from the higher integration level will make the infrared thermometer cost competitive with other automotive cabin temperature sensors.

References

- [1] "Reliable, High Quality Infrared Sensors Have Found Their Way Into Automotive Climate Control", Roger Diels and Domenic Pompei,, Advanced Microsystems Automotive Applications 2003, pp. 359-376;
- [2] "Building air quality: a guide for building owners and facility managers", published by the US Environmental Protection Agency, September 1991.
- [3] "New Developments in International Standards for the Indoor Thermal Environment", B.W. Olesen, D.F. Liedelt, Proceedings of the International Conference HB2000, Helsinki, 5-10 of August 2000, Finland.
- [4] "Equivalent Temperature Estimator using Mean Radiant Temperature Sensor", S. Mola, M. Magini, C. Malvicino, Sensors and their Applications XI/ISMCR 2001, London, September 2001.
- [5] "HEAC (High Efficiency Air Conditioning) Prototype: Comfort Improvement with Reduction of Impact on Fuel Consumption", Stefania Martini, Massimo Magini, Stefano Mola, Giulio Lo Presti, Carloandrea Malvicino, Guglielmo Caviasso, Antonio Tarzia, Denis Clodic: paper presented at 2004 MAC Summit, Washington DC, USA.
- [6] "Estimating Incipient Fogging Windshield Conditions by Means of Mean Radiant Temperature Sensor", Stefano Mola, Giulio Lo Presto, Massimo Magini, Nicola Presutti, Carloandrea Malvicino, Gennaro Bisceglia, Massimiliano Mandrile, Antonio Tarzia, Guglielmo Caviasso, presented at FISITA 2004 World Congress, Barcelona.
- [7] "Implications of HFC 152° and Carbon Dioxide Risks to the Future of Vehicle A/C", Erin Birgfeld, presentation made at the VDA Alternate Refrigerant Winter Meeting, February 2004
- [8] List of material emissivities in <http://www.infrared-thermography.com/material-1.htm>

Luc Buydens, Victor Kassovsky, Roger Diels

Melexis NV
Transportstraat 1
3980 Tessenderlo
Belgium
lbu@melexis.com

Keywords: air conditioning, climate control, thermometer, infrared temperature sensor, comfort

Gesture Recognition Using Novel Efficient and Robust 3D Image Processing

B. Liu, T. Sünkel, O. Jesorsky, R. Kompe, 3SOFT GmbH
J. Hornegger, Friedrich-Alexander University, Erlangen-Nuremberg

Abstract

Hand gestures as a natural form for communication have attracted many research efforts. In this paper we present a hand-gesture control system for drivers or passengers based on a new generation of a 3D imaging sensor, which generates both a grey image and a range image of the scene. In this gesture recognition system, we take the hand as one entity, and only the 3D position or the trajectory of the hand centroid is interesting for the system. The advantages of the proposed system over other gesture recognition techniques are its robust and real-time recognition, effective suppression of background illumination, and no need of additional devices or markers to be attached. As a driver assistance system, the proposed gesture-recognition system is natural, robust, efficient and practical.

1 Introduction

With the rising number of intelligent driver-assistance functions emerging in modern car architectures, it becomes more and more important to look for more natural, comfortable and efficient Human Vehicle Interfaces. Gesture recognition provides a new channel of input and enhances usability.

Hand gestures as a natural form for communication have attracted many research efforts [3, 10]. Many researchers focus their work on the analysis and recognition of the articulated hand motion. Some use reflective markers or gloved-based devices with e.g. electromagnetic sensors [5]. These systems are cumbersome, intrusive or expensive. Efforts were also made to track motion of bare hand [11], however, which are either limited by user-specific hand models or by well-designed background to make hand segmentation easy. Others work on the combination of two or more modalities, e.g. speech and gesture [8], in order to maximize the usability.

In this paper we present a hand-gesture control system for drivers or passengers based on a new generation of 3D imaging sensor. The sensor developed

by PMD technology GmbH is based on the principle of Photonic Mixer Device (PMD) [12]. It generates a dense range image of the scene at video rates by analyzing the phase shift between a modulated infrared signal emitted by a LED array and the reflected signal captured by the sensor. The phase shift is caused by the time of flight of the light signal from the light source to an object point and backwards to the sensor as shown in Fig. 1.

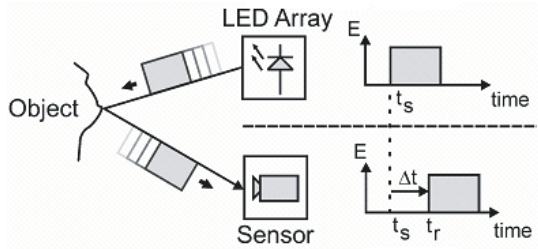


Fig. 1. The PMD Principle: A PMD system consists of a combined illumination unit and a sensor unit. A modulated infrared signal emitted by an LED array travels from the light source to an object, where it is reflected, and then travels back to the sensor. Due to the time of flight, a phase shift occurs between the emitted and the sensed signal. Based on this phase shift, the distance between the PMD system and the object is calculated.

The production process of the PMD sensor is similar to that of a standard low-cost CMOS imaging sensor. Therefore, the complete system can be produced at a very low price on embedded platforms.

In our gesture control system, we take the hand as one entity, and only the 3D position or the trajectory of the hand centroid is interesting for the system. The advantages of the proposed system over other gesture recognition techniques are its robust and real-time recognition, effective suppression of background illumination, and no need of additional devices or markers to be attached.

In the proposed system, the 3D sensor is used to capture the motion of the driver's or the passenger's hand in real time. Through processing the range image obtained from the 3D sensor, the hand position is estimated within the camera's field of view. An object tracking method, based on the Kalman filter, is used to stabilize the hand-tracking performance, even under rough conditions. We included two modes of control in the system. In the first mode, the estimated 3D hand position functions similar to a 3D computer mouse. In the

second mode of control, movement patterns of the hand are classified with a set of pre-defined/trained Hidden Markov Models in order to recognize complex gestures. Both modes can serve to press buttons, select menu items, scroll windows or lists, or move or zoom maps in a navigation view.

The presented system architecture consists of a PMD camera and a separate processing unit for analyzing the 3D data. The imaging and the image-processing technologies presented in this paper can be extended and perfectly used for applications like out-of-position sensing and occupant classification.

In the following section we present our hand-gesture control system in detail. We report our experiment results in section 3 and at last conclude the paper in section 4.

2 The Proposed Gesture Recognition System

In this section we present a hand-gesture control system based on a 3D imaging sensor. The hand motion of the driver or a passenger is captured by the sensor in real time. Through analyzing the image data provided by the PMD camera, we can estimate the 3D position of the hand within the camera's field of view. A Kalman-filter tracking method is employed to stabilize the hand-tracking performance.

In the following we first describe the algorithm of hand position detection, and then propose a Kalman-filter model for hand tracking. Afterwards two control modes are presented for monitoring the system.

2.1 Hand Detection

To determine the hand position we need to segment the 3D hand points from the background. From the range image and the extrinsic and intrinsic parameters of the PMD camera we can compute directly the corresponding 3D points for every pixel on the image. But not all the 3D points in the field of the camera's view are of interest for us to estimate the hand position, since the hand of the driver or the passenger is supposed to be placed only within a certain 3D volume, when it "monitors" the system. Therefore, we define a 3D-volume of interest where the hand is expected to move, and the process of hand segmentation works only on the 3D points within this volume. We name this 3D volume action volume. Fig. 2 shows a possible setup of the camera's view and the action volume. Note that the system is easy to handle and no calibration is

needed. The camera can be positioned more or less anywhere. The action volume can be arbitrarily adjusted within the field of the camera's view.

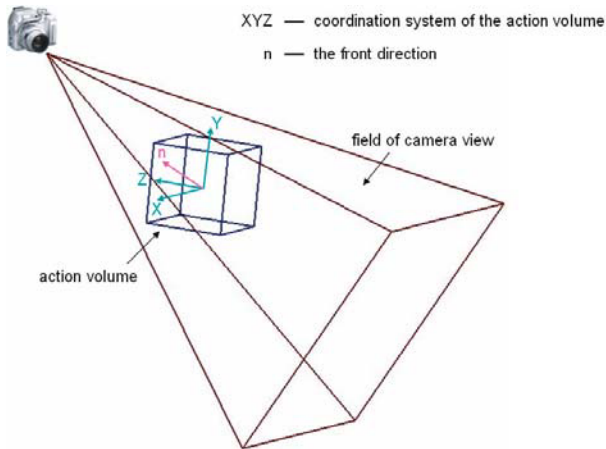


Fig. 2. An example setup of the camera's view and the action volume

The following five steps are implemented to detect the hand points and estimate the hand position. Fig. 3 gives an overview of the complete hand-tracking process.

Smooth the raw data

In order to enhance the quality of range data, we apply a standard mean filter on the sensor's raw data. According to our practice, smoothing upon the raw data obtains better result than smoothing upon the range image.

Remove out-of-range 3D points

As mentioned above, only the 3D points within the pre-defined action volume are of interest for hand detection. Moreover, in the next section we will describe a Kalman-filter model used for hand tracking. The Kalman filter can give a prediction of the hand position in the next frame. Hence, we define a certain neighborhood around the predicted position, and search for the hand points within the intersected volume of this neighborhood and the action volume.

Remove noisy points

The quality of the range measurement directly depends on the fraction of the emitted light being reflected by an object. The lower the fraction is, the lower the reliability of the depth measurement is. Therefore, we remove points with low fraction values based on a variable threshold.

Remove edge-points

Additionally, to segment the hand from the scene we are interested actually only in points on planes instead of edges. With respect to 8-neighbour relationship, we define the 3D points with less than two near neighbours as edge-points. Near neighbour here means the Euclidean distance between two neighbour points is less than a certain threshold.

Segment the hand points and compute the centroid

We define a 3D front direction for the action volume and sort the 3D points descendingly along this direction. We take a certain number of the front points as the hand points, and compute their centroid as the estimate of the hand position. In this operation we assume, the hand points are always in the front of the action volume.

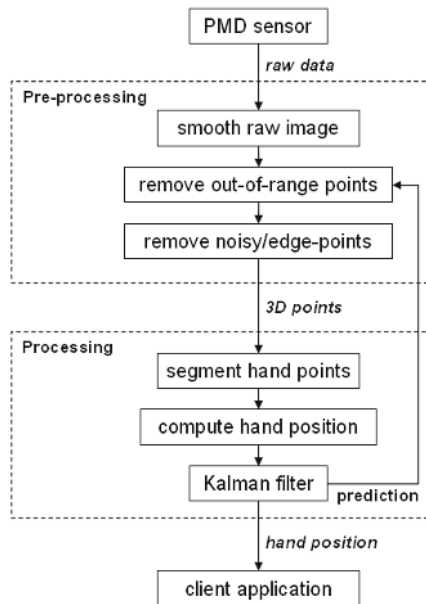


Fig. 3. Diagram of the hand-tracking process

2.2 Hand Tracking Using the Kalman Filter

In the previous section, we presented an algorithm for detecting the hand position from a single PMD frame through analyzing its image data. The main idea is to assume the hand points to be the front points within the action volume. However, due to noise and disturbance, this assumption may not always

be true. In this section we propose a Kalman filter model, which not only smoothes the motion of the hand but also deliver a prediction of the hand position in the succeeding frame.

The Kalman Filter tries to deduce an optimal estimate of the past, present, and future state of a linear system using a time sequence of measurements, given a statistical model of the system and an initial estimate of the state [9].

In our hand-tracking problem the state \mathbf{x}_k is the true 3D hand position at the time k . The measurement \mathbf{z}_k is the estimated hand position as presented in the last section. Our Kalman filter model for hand tracking is based on the assumption of the relatively consistent acceleration of the hand motion, which yields the equations

$$(\mathbf{x}_k - \mathbf{x}_{k-1}) - (\mathbf{x}_{k-1} - \mathbf{x}_{k-2}) = (\mathbf{x}_{k-1} - \mathbf{x}_{k-2}) - (\mathbf{x}_{k-2} - \mathbf{x}_{k-3}) + \mathbf{w}_{k-1},$$

i.e. $\mathbf{x}_k = 3\mathbf{x}_{k-1} - 3\mathbf{x}_{k-2} + \mathbf{x}_{k-3} + \mathbf{w}_{k-1}$

and $\mathbf{z}_k = \mathbf{x}_k + \mathbf{v}_{k-1}$

where \mathbf{w}_k is the process noise and \mathbf{v}_k is the measurement noise. We assume both of them follow the isotropic Gaussian distribution. The complete process of the Kalman filtering is composed of the iterations of two main operations: prediction and correction. For detailed derivation of the Kalman filter please refer to the Kalman filter tutorial [9].

In this system we use the hand-detection method as stated in the previous section, to estimate the hand position at the time $t=0$ and $t=1$. Then apply the above Kalman-filter method to the succeeding time. The initial estimate of the state \mathbf{x}_2 at time $t=2$ is the result of the hand-detection method. The Kalman filter is applied to “correct” the estimate and deliver a prediction for the next moment. As mentioned in Section 2.1, the prediction from the Kalman filter is used to guide the detection of the hand points in the next frame. Please see Fig. 3 for the complete process of hand tracking.

2.3 Hand-Control Modes

Two hand control modes are implemented in our system. In the first mode, the estimated 3D hand position functions similar to a 3D computer mouse. In the second mode, movement patterns of the hand motion are classified with a statistical model in order to recognize complex gestures. Both are used to press

virtual buttons, scroll within selection lists or to move or zoom maps in a navigation menu.

2.3.1 3D Hand-Mouse Control

In the 3D hand-mouse control mode, the auto driver or passenger can use his/her hand to control the mouse-icon on the screen. It behaves like a 3D computer mouse. The plane of **X**- and **Y**-axes in the 3D action volume resembles the 2D surface of the screen; and the **Z** coordinate of the hand position decides whether or not to press a button, select a menu item, or hold the cursor to shift a map or to scroll a window.

However, not like the “real” mouse that we hold on a flat table, the hand mouse vibrates in the 3D volume, due to noises and the natural vibration of the human hand motion. Accordingly, the mouse-icon will be flickering significant on the screen, if the **X**- and **Y**-coordinate of the 3D hand position reflects directly the mouse position. Therefore, we also implemented an anti-flickering process to stabilize the displayed mouse icon. The basic idea is to update the mouse position only when the next mouse position is outside a certain size of the local neighborhood around the current mouse position.

There are several ways to realize the pressing of a button. One possibility is to interpret any significant forward movement of the hand as a button press. Another possibility is to take the absolute distance to a fixed display as the criterion. Currently we are working on the interpretation of the hand posture (e.g. “opened” and “closed”) in order to solve this task.

2.3.2 Gesture-Pattern Control

The second mode is intended to control functionality of the client application only by moving the hand according to previously defined or trained movement patterns. Each item of this gesture vocabulary corresponds to a gesture command which can be performed if a movement pattern is recognized by the system. Typical gestures that can be modelled are commands like “select”, “back”, “play”, “pause” or “zoom in” and “zoom out”. A typical movement pattern for the zoom commands can for example be a circular motion of the hand performed clockwise or counter clockwise in order to distinguish between “zoom in” and “zoom out”.

The big advantage of this approach compared with the 3D hand-mouse mode is that the passenger has seldom to have a look at the screen (for example only

to receive the results of the navigation system), because for most commands no steering of a cursor is needed. Hence the driver is much less distracted in this mode.

We use Hidden Markov Models trained on a previously recorded training set of gestures to classify observed movement patterns. Hidden Markov Models (HMMs) are stochastic models used in many pattern recognition systems. They are commonly applied in speech recognition systems. There they are usually used to model time consecutive feature vectors extracted from speech signals [7]. Hence it makes sense to use them in our gesture recognition system where the movement patterns of the hand have to be classified which are also time consecutive.

Hidden Markov Models have already been used in other gesture recognition systems [6]. Our approach differs from the existing methods in that point that we calculate our features based on real 3D hand positions which are the results of the segmentation step described earlier in this paper.

The simplest way of coding a feature sequence belonging to a gesture is to use the sequence of the raw 3D positions $\mathbf{o} = \mathbf{o}_1, \dots, \mathbf{o}_k$ as a feature sequence $\mathbf{f} = \mathbf{f}_1, \dots, \mathbf{f}_n$ as shown in Fig. 4. Advanced representations of \mathbf{f} also used by other researchers, such as the cartesian velocity ($d\mathbf{x}, d\mathbf{y}, d\mathbf{z}$), the polar velocity with angular velocity term ($d\mathbf{r}, d\phi, d\mathbf{z}$), the polar velocity with tangential velocity term ($d\mathbf{r}, rd\phi, d\mathbf{z}$) or other comparable features [2].

In our system, we train individual models HMM_i , with $i = 1, 2, \dots, N$, for each gesture command out of a set of N gestures (e.g. the commands mentioned in the beginning of this section) with a large number of training samples. The parameters of each model HMM_i are estimated using the *Baum-Welch Re-estimation* procedure [1].

After finishing the training procedure, we can use the HMM models to classify previously un-trained movement patterns represented by their corresponding feature sequences \mathbf{f} . According to the Bayes' Theorem, the optimum classifier decides for the class with the maximum a posteriori probability

$$\operatorname{argmax}_i \{P(\mathbf{C}_i | \mathbf{f})\} \quad \text{with } i = 1, 2, \dots, N$$

for a set of classes \mathbf{C}_i . The rule of Bayes yields

$$P(\mathbf{C}_i | \mathbf{f}) = P(\mathbf{f} | \mathbf{C}_i) * P(\mathbf{C}_i) / P(\mathbf{f}).$$

Looking for the maximum value, the probability of occurrence $P(\mathbf{f})$ can be skipped because it is constant for all classes, and hence only the product of the a priori probability $P(\mathbf{C}_i)$ and the class conditional probability $P(\mathbf{f} | \mathbf{C}_i)$ is left.

Using our HMM approach, the conditional probabilities for a set of N gestures are given by the probabilities $P_1(\mathbf{f} | \text{HMM}_1), \dots, P_N(\mathbf{f} | \text{HMM}_N)$. The values of the probabilities can easily be calculated with the Viterbi Algorithm [4]. The values of the conditional probabilities give an indication of the similarity between the observed movement pattern represented by the feature sequence \mathbf{f} and the training sequences of each model.

In a gesture recognition system the a priori probability $P(\mathbf{f})$ strongly depends on the current state of the system. For example in "CD player mode", the a priori probability for the class "play" should be higher than for the class "zoom in". In our current work, we assume the same a priori probability for all gestures. In this case $\text{argmax}_i \{P(\mathbf{C}_i | \mathbf{f})\}$ is reduced to $\text{argmax}_i \{P(\mathbf{f} | \text{HMM}_i)\}$.

Implicitly we decide for the model – in other words for the gesture – with the biggest similarity to the tested sequence \mathbf{f} . Fig. 4 shows the entire recognition process for a set of N trained models.

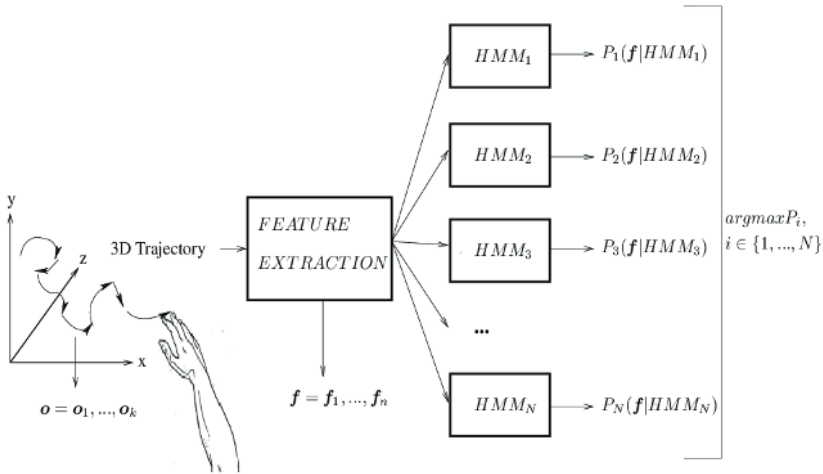


Fig. 4. Gesture recognition with HMMs

3 Experiments

The presented system architecture consists of a PMD camera and a separate processing unit to perform the computation of hand tracking and gesture recognition. We used two types of PMD sensors: PhotonICs® PMD 1k-S and PhotonICs® PMD 19k, with the resolution of 64x16 and 160x120 pixels, respectively. We chose a frame rate of around 20 fps.

Fig. 5 shows a screenshot of a sample user interface being controlled by our gesture recognition system. In this case we modelled a “touchless touch-screen” device. The yellow “hand” in the image is the icon for the hand-mouse. In the 3D-hand-mouse control mode, a user can use his/her hand to control the hand icon on the screen. When the user’s hand moves forward within the action volume, the hand icon will get “held”, which means the according target on the sreen is chosen. For example the “hand” could hold the city map in the navigation window, and then move it in arbitrary directions.

As stated in Section 2, we set several thresholds for detecting the hand points and tracking the hand position, e.g. the number of hand points, or the size of the neighbourhood around the predicted hand position by Kalman tracking. These thresholds are pre-defined for the system according to our practices.

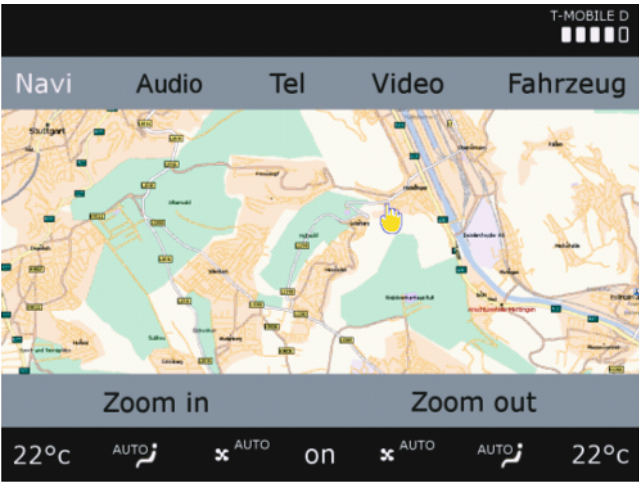


Fig. 5. A sample user interface controlled by our gesture recognition system

Tab. 1 gives the statistical evaluation of the performance of the PMD sensors and the processing time for tracking the hand in one frame. As we have men-

tioned above, the processing unit for computation is separate from the PMD camera. That means the computation process and the image-capture process can be run simultaneously. Therefore, in this case, the whole processing time of one frame just equals the time for capturing the images in the 3D hand-mouse control mode.

<i>PMD sensors</i>	<i>Image Capture (ms)</i>	<i>Hand Tracking (ms)</i>
<i>PMD[Vision]® 1k-S (64x16 pixels)</i>	21	17
<i>PMD[Vision]® 19k (160x120 pixels)</i>	47	46

Tab. 1. Performance of PMD sensors and the computation to process one frame

4 Conclusions

In this paper we present a hand-gesture control system for drivers or passengers based on a new generation of 3D imaging sensor, which can generate a range image of the scene at video rates. In the system, the 3D sensor is used to capture the motion of the driver's or the passenger's hand in real time. A Kalman filter model is created to stabilize the hand tracking. Additionally, two control modes are introduced in the paper. Both modes can be used to press buttons, select menu items, scroll windows or lists, or move maps in the navigation view. In the first mode the estimated 3D hand position is used to model a 3D mouse as input device. In the second mode complex movement patterns are classified with Hidden Markov Models. The advantages of the proposed system over other gesture recognition techniques are its robust and real-time recognition, effective suppression of background illumination, and no need of additional devices or markers to be attached.

The presented system architecture consists of a PMD sensor and a separate processing unit for the evaluation of the 3D data. The complete system can be produced at a very low price. For the first time a robust application of 3D machine vision can be realized on embedded platforms. The technology presented in this paper can be extended and perfectly used for applications like out-of-position sensing and occupant classification.

References

- [1] L.E. Baum and J.A. Eagon, An Inequality with Applications to Statistical Estimation for Functions of Markov Processes and to a Model of Ecology, *Bulletin of American Mathematical Society*, volume 73, pp. 360-363, 1967.
- [2] L.W. Campbell, D.A. Becker, A. Azarbayejani, A.F. Bobick and A. Pentland, Invariant features for 3-D gesture recognition, *Second International Workshop of Face and Gesture Recognition*, pp. 157-162, Killington VT, October 1996.
- [3] C. Cohen. A Brief Overview of Gesture Recognition, *Cybernet Systems Corporation*, 1999.
http://homepages.inf.ed.ac.uk/rbf/CVonline/LOCAL_COPIES/COHEN/gesture_overview.html.
- [4] G. Forney, The Viterbi Algorithm, *Proceedings of the IEEE*, volume 61, no. 3, pp. 268-277, March 1973.
- [5] S. Malassiotis, N. Aifanti and M. G. Strintzis. A Gesture Recognition System Using 3D Data, *First International Symposium on 3D Data Processing Visualization and Transmission (3DPVT'02)*, p. 190, Padova, Italy, June 2002.
- [6] P. Morguet and M. Lang, Spotting Dynamic Hand Gestures in Video Image Sequences using Hidden Markov Models, *International Conference on Image Processing*, pp. 193-197, Chicago, Illinois, October 1998.
- [7] E.G. Schukat-Talamazzini, *Automatische Spracherkennung*, Vieweg Publisher, ISBN 3-528-05492-1, Braunschweig/ Wiesbaden, 1995
- [8] R.P. Shi, J. Adelhardt, V. Zeissler, A. Batliner, C. Frank, E. Noeth and H. Niemann, Using Speech and Gesture to Explore User States in Multimodal Dialogue Systems, *International Conference on Audio-Visual Speech Processing*, pp. 151-156, St. Jorjios, France, September 2003,.
- [9] G. Welch and G. Bishop, An Introduction to the Kalman Filter, *Technique Report 95-041*, University of North Carolina at Chapel Hill, 1995.
- [10] Y. Wu and T.S. Huang, Hand Modelling, Analysis and Recognition for Vision-Based Human Computer Interaction, *Proc. IEEE Signal Processing Magazine*, vol. 18, pp. 51-60, May 2001.
- [11] Y. Wu, J. Lin and T.S. Huang, Analyzing and Capturing Articulated Hand Motion in Image Sequences, *IEEE Transactions on Pattern Analysis and Machine Intelligence*, vol. 27, No. 12, pp. 1910-1922, 2005.
- [12] Z. Xu, R. Schwarte, H. Heinol, B. Buxbaum, T. Ringbeck and Smart Pixel – Photonic Mixer Device (PMD): New System Concept of a 3D-imaging Camera-on-a-Chip, *International Conference on Mechatronics and Machine Vision in Practice*, pp. 259-264, Nanjing, China, 1998.

B. Liu, T. Sünkel, O. Jesorsky, R. Kompe

Vision Solutions Group, 3SOFT GmbH

Frauenweiherstr. 14, 90765 Erlangen

Germany

bing.liu@3soft.de

thomas.suenkel@3soft.de

oliver.jesorsky@3soft.de

ralf.kompe@3soft.de

J. Hornegger

Head of the Chair of Pattern Recognition

Friedrich-Alexander University, Erlangen-Nuremberg

Martensstr. 3, 91058 Erlangen

Germany

Joachim.Hornegger@informatik.uni-erlangen.de

Keywords: gesture recognition, hand detection, driver assistance systems, 3D image processing, human machine interface, 3D vision, out-of-position detection

Network of Excellence HUMANIST - Human Centred Design for Information Society Technologies INRETS & ERT

A. Pauzié, French National Institute for Research in Transport and Safety

Abstract

HUMANIST is a Network of Excellence gathering the main research institutions from 15 European countries. The partners involved in this network are working in the area of new technologies in Transport, with a specific concern on human centred design, to ensure matching between provided systems and services, and users needs and requirements, in addition to concern with road safety improvement.

1 Introduction

In the coming years, the development of the new technologies of information and communication is going to transform deeply the uses and the practices in transport. In the field of road telematics and driver assistance systems, the current developments can constitute a real opportunity of help for the mobility and a real improvement of the road safety. Nevertheless, implementation of ITS raises numerous questions about acceptability by drivers and about possible modifications of behaviour or attitudes.

The human factors competencies exist in Europe but are scattered. To obtain effective results, it is necessary to integrate the research capacities in Europe.

For this purpose, a panel of research institutes, members of the European Conference of surface Transport Research Institutes (ECTRI) and the Forum of European Road Safety research Institutes (FERSI) joined to build up a network of excellence HUMANIST aiming at federating the researches in the domain of user/system interactions and their applications on in-vehicle information systems and advanced driver assistance systems. The aims of this network of excellence is to federate the researches in the domain of user/system interactions and design, and their applications on road telematics and driver assistance systems.

2 Context

If the driving task has little evolved since the creation of the motor vehicle, this situation is changing today under the combined effect of the widespread of driver information and communication systems implemented in-vehicle and the emergence of advanced driver assistance systems.

These various systems propose or will propose a certain number of functions to the driver, with the objective to facilitate driving task and to improve safety of travelling. For example, the access to navigation information allows a lowering of the attentional level involved in orientation process of the driving situation. The diffusion of traffic information in real time can be at the origin of critical situations avoidance. The messages of alert, concerning road or meteorological events arisen downstream, and diffused as quickly as possible to the driver, allow the activation of anticipation process. The adaptive cruise control, while maintaining a safe headway with the ahead car, decreases the drivers' stress and mental load. Finally, in direct connection with objectives of road safety, the active assistance systems conceived specifically to take effect in accidental situations, can balance some reaction latencies and decision uncertainties, inherent to the human functioning in driving situation.

But the effective realisation of the expected benefits will depend on conditions of systems design and implementation: in particular, in which measure the system responds to drivers needs, is compatible with their functional capacities whatever their age and satisfies the criteria of relevance, usability and acceptability.

Finally, the emergence of automation technologies, that is assistance systems being able to take care of some control tasks traditionally assigned to the driver, brings the problem of the tasks dispatching between human and machine, as well as the choice of the logic used for the management of this control sharing, substitute or co-operative. Particularly in the case of co-operative assistance, further researches are needed regarding the emergent human driving tasks of system supervision, system status awareness, and system response representation.

All this argues for a more active participation of the Human Sciences in the various stages of systems conception and for a concept of technological development determinedly centred on Human, in which the assistance is designed according to the needs and the capabilities of the human being and not driven by the technological offer. When, in the end, the systems will be able to modulate its assistance according to the analysis of the driving situation requirements, one can then speak about cognitive engineering, where a cor-

rect matching between the system design and the specificity of human being is ensured, for positive consequences in terms of road safety.

The area of road telematics and driving assistance systems is characterised by a fast technological development and a strong competition in the industrial world between Europe, Japan and USA. The success of the deployment of these new products needs, beyond technological research efforts, strong and continuous actions in the domains of human factors to guarantee the usability and the acceptability of these systems and consequently a real improvement of the safety and the mobility.

In addition to federate the research activities in this area, HUMANIST, like the others NoEs, has the objective to progress towards the creation of a Research European Virtual Centre. The network has built a joint program of research, integrating, spreading and management activities with the purpose of sustainability.

3 Joint Research Activities

In the area of human factors and ergonomics for ITS, the objective of the joint research activities is to converge, in the coming decade, towards a coherent research programme with complementary approaches.

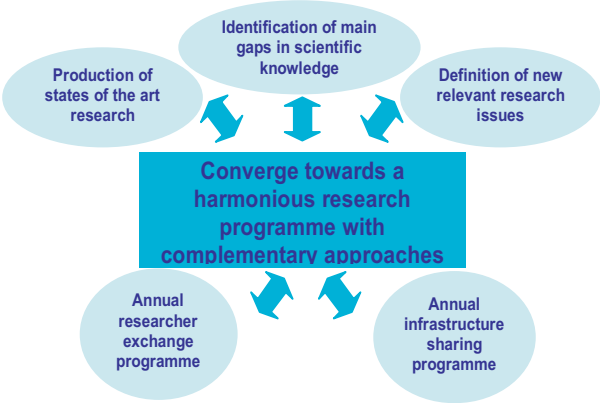


Fig. 1. HUMANIST task forces

It is not intended in this paper to make an exhaustive presentation of the 7 research Task Forces, but rather to give examples about the topics that have been more specifically developed during the past year.

3.1 Task Force A: Identification of the Driver Needs in Relation to ITS

Identification of drivers needs according to new technological development requires several types of investigations and a lot of effort, as there is a wide heterogeneity of the population in terms of functional abilities and requirements.

The methodology to investigate driver needs covers a wide area. Driver needs, especially for driving task support, are investigated often by analysing driver errors and accidents. Driver and traveller information needs are often studied by interviews and questionnaires.

Age and driving experience seem to be the most important factors when defining driver needs for support. Especially, the elderly would need support in many situations, e.g. merging and turning in intersections. There are, however, not many systems available for supporting them, yet. Another group with high relative risk in traffic is young drivers, especially male.

One specific group to take into account is professional drivers. They need communication systems while driving, more often than private drivers. Communication while driving is often highly important for their work, and therefore, this fact must be taken into account while planning different restrictions for the use of communication aids. Use of alcohol and/or drugs is an important factor in traffic safety work.

3.2 Task Force C: Joint Cognitive Models of the Driver-Vehicle-Environment for User centred Design

In order to produce really suitable and customised design solutions for the automotive domain, in-vehicle systems should be designed following the approach known as User-Centred Design. A crucial element in the UCD process is the overall model of the "joint" cognitive system represented by the Driver, Vehicle and Environment (DVE Model). In the framework of HUMAN-IST activities, a book about Modelling Driver Behaviour in Automotive Environments has been published; it gathers the state of the art in modelling and simulation of DVE systems and in particular of driver behaviour that can be applied and used in nowadays and tomorrow automobiles.

3.3 Task Force D: Impact Analysis of ITS on Driving Behaviour

With the increasing development and implementation of ITS on the market, the issue of assessing and evaluating their effects on various road traffic related criteria becomes more and more up to date. Thus, one main objectives of this Task Force is to describe and continuously update the state-of-the-art on the impact of in-vehicle information and communication systems (IVIS) on relevant criteria of driver workload and behaviour.

3.4 Task Force E: Development of innovative Methodologies to evaluate IT Safety and Usability

Knowledge and experience of partners, about methodologies for the evaluation of IVIS both in terms of safety and usability, have been shared in order to build up a Matrix of Methodologies. Objective of this matrix was to identify and to categorise existing and proposed methods for evaluation of ITS. When assessing usability and safety, different metrics are used. These metrics are collected using specific techniques and often require specific tools. The metrics are collected in one or more physical environments. The combination of metric/technique/ tool/ environment is what is referred to as a method. Additional information in the matrix includes the type of data obtained; the effectiveness of the method, practical issues of application, scientific references and a list of HUMANIST partners with experience or knowledge of the methods. Partners were asked to indicate their favourite methods. From this, a selection of 22 broad ranging methods were indicated as 'favourites', demonstrating the variety of methods available and that methods used depend heavily on the objectives of a study. The matrix can be updated as new information becomes available and can serve as a source of reference. It will form the basis for consideration of more integrated methodologies within the project.

3.5 Task Force G: Use of ITS to train and to educate Drivers

Driving simulators and e-learning communication technologies hold considerable promise for enhancing driver training, testing, and licensing and improving road safety. One of this Task Force objectives is to assess the present state of the art in the application of simulators to driver training, and to identify what additional R&D effort is needed to achieve the potential effectiveness in using simulators to improve the driver training process at a European level with harmonized procedures. At this stage, some main statements can be made:

- Driving simulators or e-learning are already being used in driver training, both of novice drivers and of professional drivers. On the contrary, there are few alternatives to cover the needs of disabled or elderly drivers.
- The validation of simulators is also an area where there is still a need for further advances. A methodological approach to driver simulator validation for training is required.
- In parallel, teaching skills have to improve, by including these new methodologies in a global training curriculum, by applying them to the different driving task levels of matrix and by developing performance measurement tools to monitor in real-time driver's progress and to improve the trainee's feedback.



Fig. 2. Four generations of driver training simulators; TNO Human Factors, The Netherlands



Fig. 3. Simulated urban traffic environment for a bus drivers training simulator developed at Madrid Polytecnic University

4 Integration

The set of integrating activities has been created in order to manage and to consolidate the NoE research structure.

In order to promote the **mobility** of researchers inside Europe, a number of **PhD** thesis have been funded by HUMANIST in the following topics:

- Development of assessment methodologies
 - Definition of reference interfaces and reference models of driver interaction for comparing the distraction potentials of in-vehicle devices
 - Feasibility study using Event-Related Potentials to analyse the effects of secondary driver assistance information on primary driving task information extraction and processing

- ▶ Study of the impact of ITS enforcement systems on driver behaviour
Influence of speed adaptation system on the communications between road users in urban areas. Investigation of the psychological, legal and technical issues of video enforcement systems to reduce driving offences and to quiet drivers' behaviour
- ▶ Study of the influence of ITS on driver behaviour
Investigation of which components of the situation awareness could be affected by driving with ITS Study of the impact of multiple visual and auditory inputs on driver behaviour, by identifying the age-related difference in the driving task performance. Subjective evaluation by professional drivers of the impact of on-board devices, on driver's stress and mental workload
- ▶ Driver modelling and cognitive simulation
Driver behaviour modelling and cognitive engineering tools development in order to assess driver's situation awareness
Analysis and modelling of driving activity and driver's behaviour for the design of on-board systems

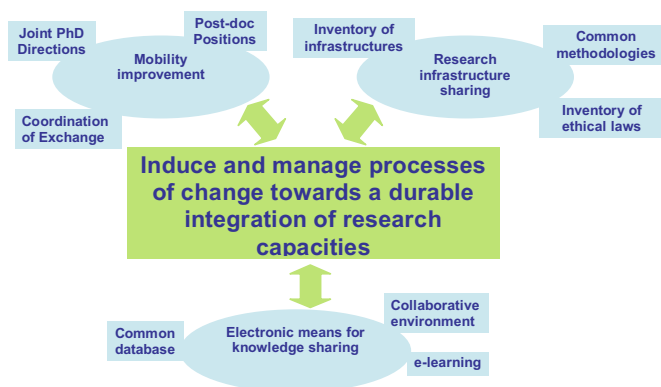


Fig. 4. HUMANIST activities

The following Post-Doc topics will be also supported by the HUMANIST NoE

- ▶ Information technology and older female drivers
- ▶ Incorporation of parameters related to its Into traffic simulation models
- ▶ The effects of in-car speed information systems on Driving behaviour
- ▶ Situation awareness when using in-vehicle Systems
- ▶ Its and unprotected road users - challenges and potential
- ▶ Nomadic devices – use and impact on driving behaviour

5 Dissemination

There is a set of activities devoted to organise and to strength exchanges between research activities developed inside the network, and relevant stakeholders belonging to various areas of interest: automotive industries, transport services, European Integrated Project in this area, EC representatives from the eSafety initiative, Standardisation bodies, European Universities, Final users, Insurance companies,

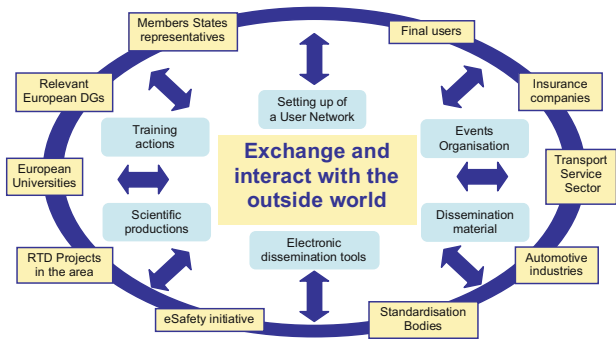


Fig. 1. HUMANIST dissemination

This activity is developed through the organisation of Stakeholders Forum, with interactive debates between participants from various backgrounds and the HUMANIST partners. An electronic forum available for open discussion will be set up on the Electronic Collaborative Work Environment with a dedicated access to identified users. This access will allow external stakeholders to be able to raise specific issues, and to communicate with HUMANIST partners in an interactive way in order to get feedback regarding some of their concerns.

A training program has been set up toward European students, young researchers and professionals of the field willing to be informed about new development of the research in the area of ITS design. The training program for professionals is open to any interested stakeholders and is composed by lecturers and by practical exercises.

- [1] HUMANIST is a Network of Excellence funded in the framework of the FP6 "Information Society Technologies IST eSafety for Road and Air Transport"
- [2] HUMANIST Co-ordinator: Europe Research Transport SAS, Jean-Pierre Medevielle, Chief Executive Officer, Loïc Courtot.
- [3] HUMANIST Management Team: INRETS, Corinne Brusque, Annie Pauzié; ERT, Jean-Pierre Medevielle, Loïc Courtot ; CDV, Karel Schmeidler; HIT, Angelos Bekiaris; EC-JRC, Carlo Cacciabue; UPM, Jose Menendez.
- [4] HUMANIST partners: ERT SAS, INRETS, BAST, Christhard Gelau; FACTUM, Ralf Risser; CDV, Karel Schmeidler; CUT, Josef Krems; DTF, Lotte Larsen; EURISCO, Guy Boy; CERTH/HIT, Angelos Bekiaris; BIVV, Mark Tant; ICCS, Angelos Amditis; EC-JRC, Carlo Cacciabue; IFADO, Sascha Sommer; NTUA, Ionnis Golias; SWOV, Divera Twisk; TNO, Wiel Janssen; TOI, Truls Vaa; TRL, Alan Stevens; UNIMORE, Roberto Montanari; UPM, Jose Menendez; UTL/FHM, Anabela Simoes; VTI, Lena Nielson; VTT, Juha Luoma.

Pauzié Annie

INRETS/Laboratory Ergonomics Cognitive Sciences in Transport
 25 avenue François Mitterrand
 Case 24 - 69675 -Bron Cedex
 France
 pauzie@inrets.fr

Keywords: intelligent transport systems, design, human machine interaction, human factors

High Speed 1Gbit/s Video Transmission with Fiber Optic Technology

T. Wipiejewski, F. Ho, W. Hung, S. Cheng, E. Wong, St. Ng, W. Ma, Th. Choi, G. Egnisaban, K. Yau, T. Mangente, ASTRI

Abstract

We demonstrate a 1 Gbit/s video transmission over up to 15 m of polymer cladded silica (PCS) optical fiber using high speed fiber optic transceiver (FOT) technology. The video link consists of a camera with an electrical S800 LVDS interface and a high resolution monitor. A pair of fiber optic cable connects the two ports replacing and extending the regular electrical cable. In contrast to the electrical cable the optical fiber is thin, light weight, and highly flexible. The high power budget margin of the link allows 3 in-line connectors for the 10-15 m link length. For other applications a longer link length is feasible using higher bandwidth optical fiber.

The FOTs are high speed versions based on the technology we have developed for the 50 Mbit/s infotainment network. The transmitter contains a vertical-cavity laser (VCSEL) light source operating in the infrared wavelength regime at 850 nm, an electronics driver chip, and some passive components. The package is a low cost leadframe style for through-hole or surface mounting. The output power of the transceiver is limited to 0.7 mW to meet eye-safety class I requirements. An internal control circuit stabilizes the optical output power over the entire operating temperature range from -40°C to +105°C to within 1 dB. Due to an integrated lens we achieve a wide coupling tolerance of the VCSEL into the PCS fiber of ± 80 μ m over a long longitudinal tolerance range of 0.5 mm. The large alignment tolerance ensures a stable coupling over temperature and time and enables the usage of very low cost plastic molded connector ferrules.

The FOT receiver module contains a high speed MSM photodetector. The special design of the MSM photodetector enables high speed operation up to 3.2 Gbit/s in combination with a large active area for easy alignment.

1 Introduction

Photonics technology has been applied in many ways for automobiles. As shown in Fig.1 photonics applications in automobiles can be categorized into three main areas which are connectivity, lighting, and sensing. Light emitting diodes (LED) have been used for dash board illuminations for many years, because of its color purity small size, and high efficiency. White light LEDs are now making it into interior lighting. LEDs are used for brake lights and sometimes for turn signals, due to their long life time and high efficiency. A new stage of development is the replacement of light bulbs for front lights such as fog lamps. Optical sensors have also been used in a variety of applications for measuring different physical or chemical parameters. New developments include examples such as optical fiber sensors for seat occupancy detection, light curtains for window blocking detection, infra-red sensors for night vision, and others [1-4]. Fiber optic connectivity has been implemented for the infotainment system of many automobiles. MOST and IDB1394 are standards for the it [5-6]. The typical data rate is 50 Mbit/s for MOST and 250 Mbit/s for IDB 1394 S200. These numbers are the physical data rates including some overhead load due to the implemented coding schemes.

Many European car manufacturers have already adopted the MOST system in their car models. The fiber optic transceiver production volume for automotive applications is already more than ten million units per annum. Besides the infotainment system fiber optics has been introduced to the safety system. The Byteflight system of BMW [7] is pioneering fiber optic links in their airbag control system. Today, camera and video links are under development for driver assistance to provide visual information in the applications such as lane detection, traffic sign recognition, or object identification. These applications require even higher data rates of 500 Mbit/s up to 1 Gbit/s (IDB1394 S800) to transmit uncompressed visual data for real time reactions.

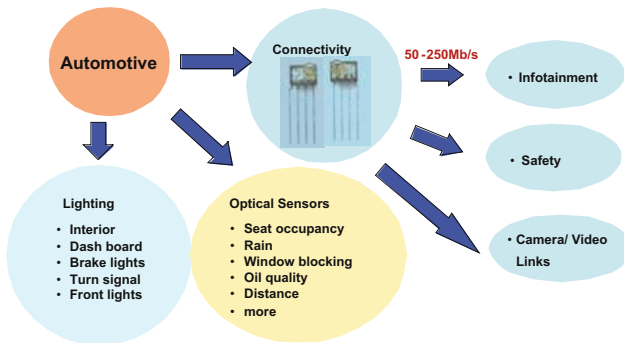


Fig. 1. Photonics applications in automobiles

At high data rates electrical cables require relatively good shielding to minimize electromagnetic interference (EMI). Both coaxial type cables and shielded-twisted-pair (STP) become quite bulky. It is also more difficult to include in-line connectors, because of the shielding and required mechanical precision. To overcome these drawbacks, we have developed a 1 Gbit/s video transmission over up to 15 m of polymer cladded silica (PCS) optical fiber using high speed fiber optic transceiver (FOT) technology. The video link consists of a camera with an electrical S800 LVDS interface and a high resolution monitor. A pair of fiber optic cables connects the two ports replacing and extending the regular electrical cable. In contrast to the electrical cable the optical fiber is thin, light weight, and highly flexible. The high power budget margin of the link allows 3 in-line connectors for the 10-15 m link length. For other applications a longer link length is feasible using higher bandwidth optical fiber.

The infotainment system in automotive usually includes a variety of devices like digital radio, DVD/CD player, video displays or GPS navigation system to provide on-road entertainment and information to the drivers and passengers. In many European cars which adopting MOST standard, these devices are connected with optical links as shown in Fig. 2. A basic optical link consists of a pair of optical cables and two pairs of fiber optic transceivers which are installed in the device. The fiber optic transmitter converts the electrical signal form electronics board into optical signals and transmits them through the optical cable. The fiber optic receiver detects the optical signals from the optical cable and coverts them back into electrical signals for the electronics board circuitry. The transmission distance of the optical link is usually from 10 cm to 30 m. The key benefit of fiber optic link is the absence of electromagnetic interference (EMI) noise creation and susceptibility. In addition, fiber optic cables are thin, light weight, and highly flexible. The fiber optic connectors are robust and can carry high speed signals up to Gbit/s easily.

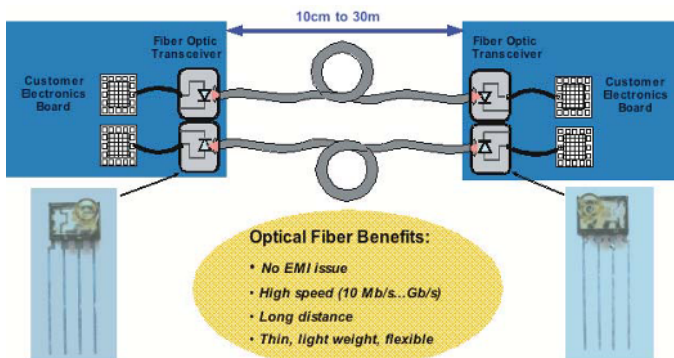


Fig. 2. A basic optical link in automotive infotainment system

Currently plastic optical fiber (POF) and 650 nm LEDs are used in the MOST fiber optics system [1]. This system run with a power budget of around 14 dB over an operating temperature range from -40°C to +85°C or +95°C. Therefore the current fiber systems are limited to the passenger compartment. For roof top implementations a maximum temperature of 105°C would be required and for the engine compartment even up to 125°C. PCS fiber is under consideration to overcome the current operating temperature limitations. This fiber can be operated even at 125°C. Tab. 1 summarizes the technical requirements of different standards and corresponding fiber optics technologies. The IDB1394 standard has four standard data rates ranging from 100 Mbps to 800 Mbps classified as S100, S200, S400 and S800. POF and 650 nm LED are proposed for the S100, if the operating temperature up to 85°C is sufficient. For S200, some people use 650 nm resonant cavity (RC) LED as light source to work with PMMA POF [8-9], however, the operating temperature is still limited up to 85°C or 95°C. For higher temperature (105oC) and higher data rates (S400 and S800) PCS fiber and 850 nm VCSEL provide the desired performance and relatively low cost solution.

Standards	Technical requirements			Fiber optic technologies	
	Data rate	Physical bit rate	Operating temperature	Light source	Optical fiber
<i>MOST</i>	25Mbps	50Mbps	-40°C to 85°C	650nm LED	PMMA SI POF
<i>MOST, advanced (preliminary)</i>	25Mbps	50Mbps	-40°C to 105°C	850nm VCSEL	SI PCS fiber
<i>IDB 1394 S100</i>	100Mbps	125Mbps	-40°C to 85°C	650nm LED	PMMA SI POF
			-40°C to 105°C	850nm VCSEL	SI PCS fiber
<i>IDB 1394 S200</i>	200Mbps	250Mbps	-40°C to 85°C	650nm RC LED	PMMA SI POF
			-40°C to 105°C	850nm VCSEL	SI PCS fiber
<i>IDB 1394 S400</i>	400Mbps	500Mbps	-40°C to 105°C	850nm VCSEL	SI PCS fiber
<i>IDB 1394 S800</i>	800Mbps	1000Mbps	-40°C to 105°C	850nm VCSEL	SI PCS fiber

Tab. 1. Summary of the technical requirements of different communication standards and corresponding fiber optics technologies

2 Fiber Optic Transceivers

2.1 Through-Hole Package Design

Based on conventional semiconductor packaging technologies, we have developed VCSEL based ultra small form factor fiber optic transceiver (FOT) modules for large core fiber systems. A photo of the FOT modules is shown in Fig. 3. The outer dimensions of 9.7 mm x 6.2 mm x 3.6 mm are very small compared to standard SFF (small form factor) modules used in data communication for computer networks. The opto-electronic components and ICs are directly assembled on a lead frame platform and encapsulated with polymers with suitable mechanical and optical properties. The maximum operating tempera-

ture is up to $+105^{\circ}\text{C}$, much higher compared to typical datacom ($+85^{\circ}\text{C}$) devices.

The transmitter and receiver modules are mirror images of each other. They both contain four electrical leads for through-hole mounting. Two are for power supply, one for data channel, and one for control purposes. There is a wake-up and sleep mode function implemented in the design for power saving applications.

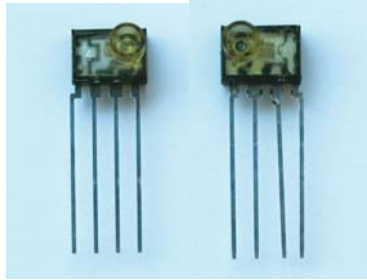


Fig. 3. High speed fiber optic transmitter for a wide operating temperature from -40°C to $+105^{\circ}\text{C}$.

2.2 Output Power Stability of Transmitter Module

One critical design concern of the VCSEL transmitter module is to stabilize the optical power coupled from VCSEL to the optical cable over wide temperature range. Our approach is to use a monitoring photo detector (MPD) to receive part of the optical output and feedback the photocurrent into the laser diode driver. The laser diode driver controls the bias current to the VCSEL automatically to stabilize the optical output power. Besides, a barrel feature is integrated with a lens in the module housing to facilitate an easy and robust coupling to the external optical cable. Fig. 4 shows the schematic diagram of the transmitter module with the optical feedback loop and coupling optics.

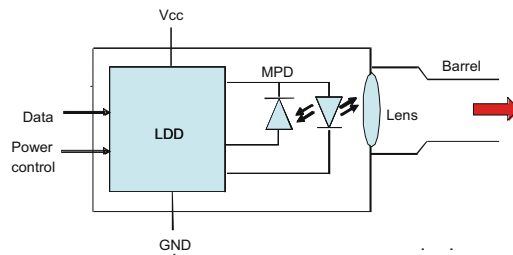


Fig. 4. Schematic diagram of the VCSEL transmitter module.

From the simulation results as shown in Fig.5, the optical coupling design of transmitter provides loose alignment tolerances of ± 80 mm in lateral axis for a working distance of 500 mm to a 200 mm core diameter PCS optical fiber. The coupling optics for the receiver is optimized for focusing the light from the fiber facet to the large area photodetector. The alignment tolerances are similar to the transmitter. We have confirmed our simulation results with experimental data as well. The wide alignment tolerance enables our customers to use very low cost plastic molded connectors with relaxed tolerance for their mechanical dimensions.

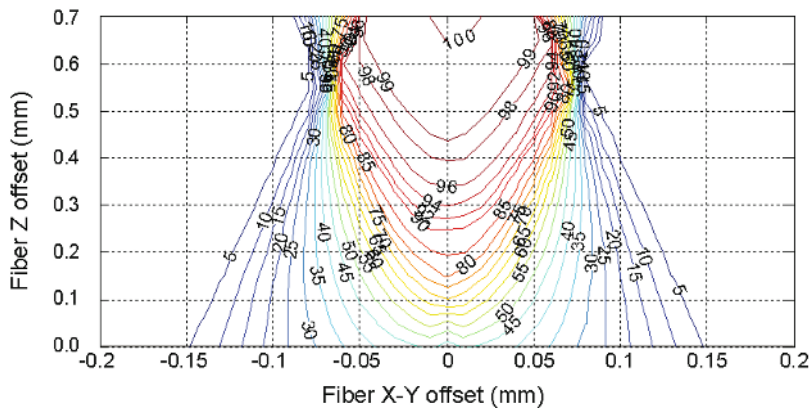


Fig. 5. Simulated coupling tolerances of VCSEL FOT to a 200 mm core diameter PCS fiber.

Fig. 6 shows the coupled power of the VCSEL transmitter into a 200 mm core diameter PCS fiber cable over a wide temperature range from -40°C to $+105^{\circ}\text{C}$. A variation of less than 1 dBm is measured. This excellent value enables a tight output power specification of the transmitter. The tight power specification results in a better link margin for the transmission system.

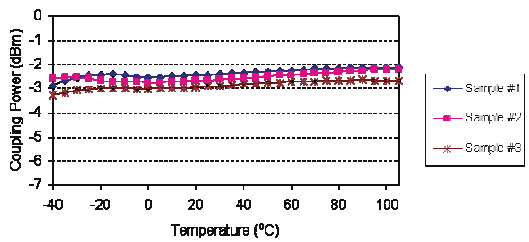


Fig. 6. Coupling power of the VCSEL FOT to a 200 mm core diameter PCS fiber over temperature from -40°C to $+105^{\circ}\text{C}$.

2.3 Surface Mount Package Design

Surface-mount-technology (SMT) has been widely used in electronics board assembling. Compared to the through-hole mounted device surface mount devices (SMD) have a number of advantages such as smaller size, higher degree of assembling automation, and higher circuit density. Components can be mounted on both sides of the board. They are more robust under mechanical stress and have a lower lead resistance and inductance leading to better performance for high frequencies. Adopting SMT in opto-electronic packaging is very attractive not only due to the advantages of this technology but also because the infrastructure of electronics manufacturing can be leveraged. However, it has been very difficult to make optical transceiver modules that are compatible with the reflow soldering process of SMT devices, because of the material used for the optical components such as lenses and optical coupling window.

We develop surface mount type packages for our fiber optic transceivers. This is to complement and extend our through-hole package product line. Fig. 7 shows a photograph of an SMT FOT prototype. It has a similar form factor as the through-hole type fiber optic transceivers. One challenge is to select the right molding material which has the suitable optical properties for efficient optical coupling and thermal properties compatible to reflow soldering.



Fig. 7. Photograph of an SMT fiber optic transmitter module prototype.

We have verified the reflow soldering compatibility of the SMT fiber optic transmitter module by measuring the optical alignment performance before and after undergoing a reflow soldering process. The reflow soldering temperature profile is set to 240°C for 46 seconds and to peak at 250°C. This profile complies with Pb-free soldering requirements. Fig. 8 depicts the optical power coupled from 5 samples of SMT fiber optic transmitter modules before and after undergoing the reflow soldering process, plus one control sample which has not undergone reflow soldering. No significant change in the coupled power is observed indicating the good stability of the packages.

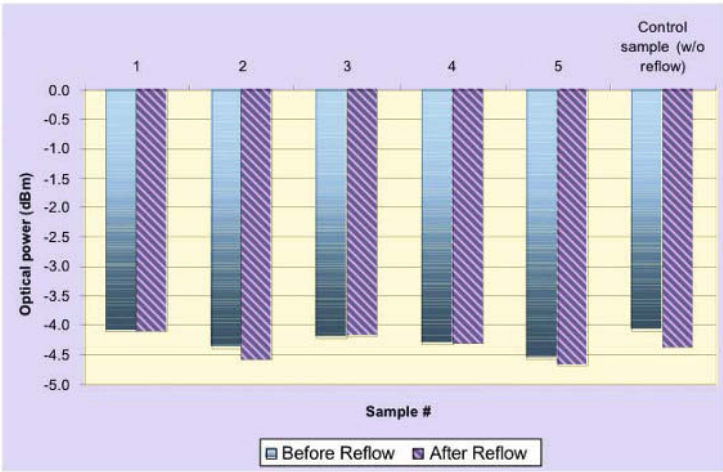


Fig. 8. Optical power coupled from five samples of SMT fiber optic transmitter modules before and after undergoing the reflow soldering process with 240°C for 46 seconds and a peak temperature of 250°C for lead-free soldering.

3 Transmission Performance

3.1 Transmission Performance over Wide Temperature Range

The current MOST infotainment system runs at a data rate of 50 Mbit/s. The VCSEL based FOT can easily meet the timing specifications of the link. The fast turn-on and turn-off signal transitions provide a low jitter value for the entire optical system. Fig. 9 depicts the eye diagrams of the transmitter module at 50 Mbit/s data rate for different temperatures of -40°C, +25°C, and +105°C. The eyes diagrams are wide open indicating a good and error free transmission performance. The extinction ratio is greater than 10 dB for all temperatures. The uncorrelated jitter is less than 150 ps.

Fig. 10 shows the eye diagrams of the Si-pin PD receiver module at 50 Mbit/s data rate for different temperatures of -40°C, +25°C, and +105°C. The eyes diagrams are wide open showing an excellent, error free transmission performance. The optical modulation amplitude of the input signal is -24 dBm. The uncorrelated jitter is less than 800 ps.

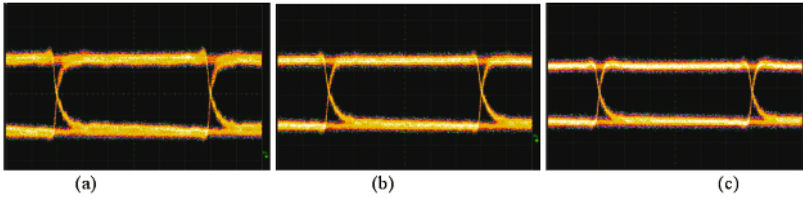


Fig. 9. Eye-diagrams of the transmitter module at 50 Mbit/s data rate at an ambient temperature of (a) -40°C , (b) $+25^{\circ}\text{C}$, and (c) $+105^{\circ}\text{C}$.

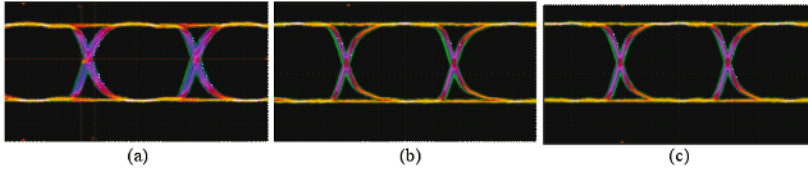


Fig. 10. Eye-diagrams of the receiver module at 50 Mbit/s data rate at an ambient temperature of (a) -40°C , (b) $+25^{\circ}\text{C}$, and (c) $+105^{\circ}\text{C}$.

3.2 High Speed Transmission Performance

For higher speed applications such as the IDB 1394b standard and video links, we have demonstrated the high speed performance of a pair of VCSEL transmitter and GaAs metal-semiconductor-metal (MSM) photodetector receiver over 10 m of PCS fiber as shown in Fig. 11.

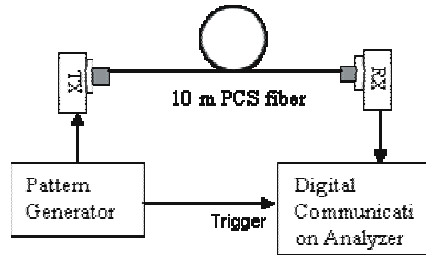


Fig. 11. Experimental setup of transmission over PCS fiber with VCSEL transmitter and MSM-PD receiver

The VCSEL transmitter is capable of much higher data rates from a few hundreds Mbit/s to Gbit/s range with a different electrical circuit design. The special design of the MSM photodetector enables receiver module to operate at 3.2 Gbit/s in combination with a large active area for easy alignment. Figure 12 depicts eye diagrams of the transmission at 300 Mbit/s, 600 Mbit/s, and

1.25 Gbit/s, respectively. The extinction ratio is greater than 9 dB in all cases. The total jitter is around 100 ps.

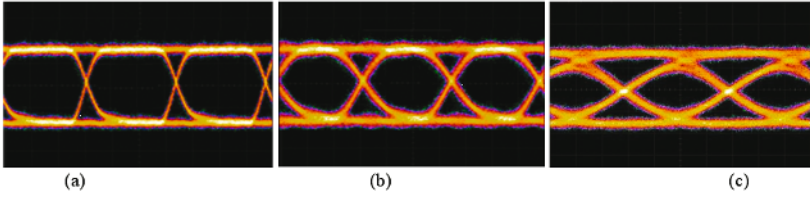


Fig. 12. Eye-diagrams after 10 m of PCS fiber transmission at (a) 300 Mbit/s, (b) 600 Mbit/s and (c) 1.25 Gbit/s.

4 Optical Video Link

We have set up an IEEE 1394b S800 video link with the fiber optic transceivers and PCS fiber. As shown in Fig. 13, the video link consists of a camera with an electrical S800 LVDS interface and a high resolution monitor. A pair of fiber optic cable connects the two ports replacing and extending the regular electrical cable. In contrast to the electrical cable the optical fiber is thin, light weight, and highly flexible.

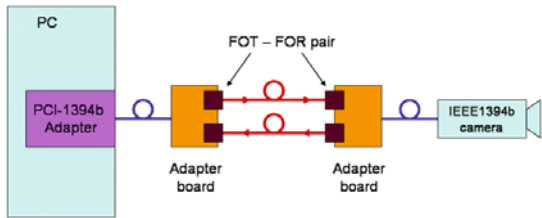


Fig. 13. System architecture of the IEEE 1394b S800 optical video link.

We have measured the bit error ratio (BER) of the optical links with fiber length of 1 m, 5 m, 10 m, and 15 m as shown in Fig. 14.

In this measurement, a $2^7 - 1$ pseudo-random bit sequence (PRBS) data stream at 1 GHz clock frequency is used. The launch power of fiber optic transmitter is -1.5 dBm. The power budget for the four different optical links are inferred from the BER measurement and listed in Tab. 2. We assume a 2 dB power budget margin and a transceiver coupling loss of 2 dB. The insertion loss for each connector is also 2 dB. We calculate the maximum numbers of in-line connectors for each optical link as listed in Tab. 2. The power budget margin of

the link allows 3 in-line connectors for the 10-15 m link length. For other applications a longer link length is feasible using higher bandwidth optical fiber.

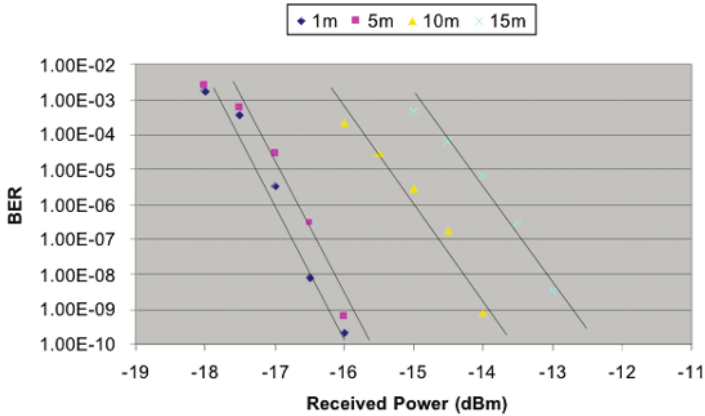


Fig. 14. Bit error ratios of the optical links with fiber length of 1 m, 5 m, 10 m and 15 m. A 27 -1PRBS data stream at 1 GHz clock frequency is used.

Transmission distance	1m	5m	10m	15m
Error-free operating power (dBm)	-15.5	-15	-13.0	-12.0
Maximum power budget (dB)	14	13.5	11.5	10.5
Approx. number of in-line connectors allowed	5	4	3	3

Tab. 2. Power budget and maximum number of in-line connectors for the optical video link of different length.

5 Conclusion

We have demonstrated a 1 Gbit/s video transmission over up to 15 m of PCS optical fiber using high speed FOT technology. The high power budget margin of the link allows 3 in-line connectors for the 10-15 m link length. For other applications a longer link length is feasible using higher bandwidth optical fiber. The FOTs are high speed versions based on the technology we have developed for the 50 Mbit/s infotainment network. The FOT package is based on low cost leadframe and plastic molding technologies. Packaging formats for through-hole or surface mounting are designed. The transmitter contains a VCSEL light source operating in the infrared wavelength regime at 850 nm, an electronics driver chip, and some passive components. The output power of

the transceiver is limited to 0.7 mW to meet eye-safety class I requirements. An internal control circuit stabilizes the optical output power over the entire operating temperature range from -40°C to +105°C to within 1 dB. Due to an integrated lens we achieve a wide coupling tolerance of the VCSEL into the PCS fiber of ± 80 mm over a long longitudinal tolerance range of 0.5 mm. The large alignment tolerance ensures a stable coupling over temperature and time and enables the usage of very low cost plastic molded connector ferrules. The FOT receiver module contains a high speed MSM photodetector. The special design of the MSM photodetector enables high speed operation up to 3.2 Gbit/s in combination with a large active area for easy alignment. The applications include video networks, information displays, and high speed cameras.

Acknowledgement

We gratefully acknowledge great support from our suppliers and partners. This work was financially supported by funds from the Hong Kong Innovation and Technology Commission ITC.

References

- [1] H. Poisel, M. Luber, O. Ziemann, "POF sensors for Automotive and Industrial Use Come of Age," Proc. 14th Intl. Conf. Polymer Optical Fiber, pp.285-289, Sep, 2005.
- [2] G. Kodl, G. Richinger, Ch. Weiss, " Dirtiness Sensor, based on the Changes in the Evanescent Field," Proc. 14th Intl. Conf. Polymer Optical Fiber, pp.225-228, Sep, 2005.
- [3] H. Y. Liu, H. B. Liu, G. D. Peng, P. L. Chu, " Strain Sensing using a Fiber Laser and a Polymer Optical Fiber Bragg Grating," Proc. 14th Intl. Conf. Polymer Optical Fiber, pp.229-232, Sep, 2005.
- [4] B. L. Henoret, M. Miedreich, "Fiberoptic sensor for pedestrian protection", Proc. 13th Intl. Conf. Polymer Optical Fiber, pp386-392, Sep, 2004.
- [5] Eberhard Zeeb, "MOST-Physical Layer Standardization Progress Report and Future Physical Layer Activities", Proc. The 3rd Automotive LAN Seminar, pp. (3-3) – (3-34), Oct, 2003.
- [6] W. Daum, W. Czepluch, "Reliability of Step-Index and Multi-Core POF for Automotive Applications," Proc. 12th Intl. Conf. Polymer Optical Fiber, pp.6-9, Sep, 2003.
- [7] R. Griessbach, J. Berwanger, M. Peller, "Byteflight – neues Hochleistungs-Datenbussystem für sicherheitsrelevante Anwendungen," ATZ/MTZ Automotive Electronics, Friedrich Vieweg & Sohn Verlagsgesellschaft mbH, January 2000.

- [8] J. D. Lambkin, T. McCormack, T. Calvert, T. Moriarty, B. McGarvey, d. O'Mahoney, "650nm RCLEDs and VCSELs for IEEE 1394b Applications" Proc. 12th Intl. Conf. Polymer Optical Fiber, post-dead line paper, Sep, 2003.
- [9] John D. Lambkin, "RCLEDs for MOST and IDB 1394 automotive Applications", Proc. 14th Intl. Conf. Polymer Optical Fiber, pp.51, Sep, 2005.

Torsten Wipiejewski

ASTRI, 5/F, Photonics Center

Hong Kong Science Park

Hong Kong

torsten@astri.org

Keywords: video transmission, fiber optic technology, fiber optic transceiver, VCSEL FOT, high speed photodetector, MSM photodetector, PCS optical fiber link, infotainment system

Integrated Giant Magneto Resistors – a new Sensor Technology for Automotive Applications

W. Rössler, J. Zimmer, Th. Bever, K. Prügl, Infineon Technologies AG
W. Granig, D. Hammerschmidt, E. Katzmaier, Infineon Technologies Austria AG

Abstract

The paper will give an introduction to the principle of the giant magneto resistive – GMR – effect and the silicon system integration of GMR sensors. The two main applications of a GMR are as a magnetic field strength sensor and as an angular field direction sensor. They will be discussed under consideration of automotive requirements.

The typical applications of a magnetic field strength GMR sensor in incremental position and speed sensing and those of GMR angular field sensors in position sensing will be summarized. Finally advantages of GMR in those applications will be discussed and conclusions on the use of GMR in automotive sensing will be drawn.

1 Introduction

The giant magneto resistive effect, which was discovered 1988, is the result of magnetic coupling in a stack of ferromagnetic layers. They are separated by non-ferromagnetic spacer layers. This effect can be used to construct different types of magneto resistive sensors. For our applications we focus on so called 'spin valve structures', which allow covering field strength sensitive or field direction sensitive constellations using the same basic technology.

For large scale introduction of GMR sensors in automotive applications a mass fabrication technology for the sensors is required. The most advanced high volume fabrication technology nowadays is CMOS (Complementary Metal Oxide Semiconductor) integrated circuit processing. CMOS in general is a good candidate for GMR integration. The techniques that are used in CMOS processes include methods for sputtering and structuring of thin layers of different materials. Alternatively bipolar technologies can be used for the basic signal processing chip.

Furthermore there is experience in handling magneto resistive structures available from the MRAM (Magneto Random Access Memory) technology, which is valuable for process optimization and fast ramp up of the new sensor technology.

The monolithic integration of the GMR will be focused on in the fourth section of this paper. The use of magnetic field sensors in modern cars is multifarious. The state-of-the-art technology uses the Hall effect. Besides simple magnetic switches there are two different basic modes of operation for automotive Hall sensors. These are incremental position and speed detection as the first and linear position and angle measurement as the second group of applications.

If a new technology is introduced there should be a significant advantage over the existing one. Thus, we will discuss the incremental, linear and angle applications more in detail in the fifth and sixth section of this paper and compare the existing Hall solutions with the potential that the GMR technology may offer [1].

2 The GMR Effect

The giant magneto resistive (GMR) effect can be explained as interface scattering when the mean free paths of minority spin and majority spin carriers of conducting electrons through successive magnetic layers alters. The magnetic layers are separated by a spacer layer, which is either a non-ferrous metal or a noble metal. Ferromagnetic transition metals like Ni, Co or Fe are commonly used as magnetic layers. The metal layers should be very thin such that the mean free path of the spin of the conducting electrons can be assumed to be much longer.

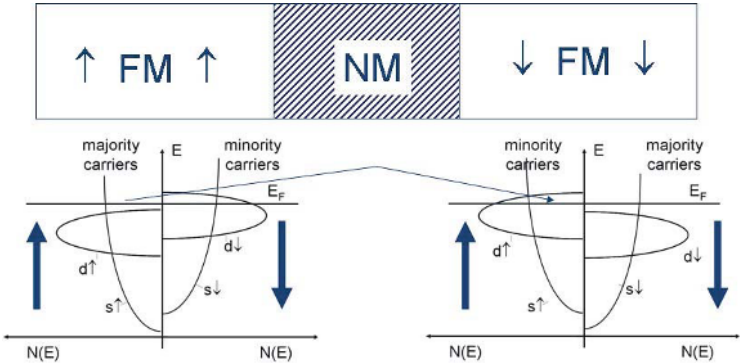


Fig. 1. Density of states model for a basic GMR system

The carriers can either exhibit spin-up or spin-down characteristics. Fig. 1 shows schematically the density of states of the s- and d-band electrons as a function of energy for anti-ferromagnetically coupled two layer system. The minority carriers exhibit a higher resistivity compared to the majority carriers due to a higher scattering probability of the d-band electrons (lower mobility). In the case when the magnetic layers have antiparallel aligned magnetization directions majority carriers traveling from one FM layer to the other FM layer become minority carriers combined with a higher resistivity there. Thus, anti-parallel alignment of neighboring FM layers results in an enhanced resistance.

In the case of parallel alignment majority carriers traveling from one to the other FM layer are still majority carriers there, resulting not in an enhanced resistance as is demonstrated in Fig. 2. This observation allows using the Mott two-current model. It assumes that the total resistance can be expressed as the sum of the separate contributions from spin-up and spin-down electrons, which can be seen as two separate channels added in parallel (Fig. 3)

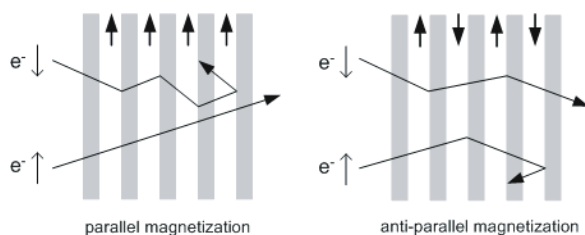


Fig. 2. Scattering of spin up and spin down carriers in a multilayer GMR structure

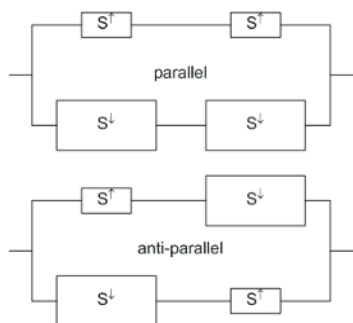


Fig. 3. Mott two current equivalent circuit

The GMR effect can be enhanced by increasing the delta resistance between spin-up and spin-down channels.

$$R_p = \frac{R^\uparrow \cdot R^\downarrow}{R^\uparrow + R^\downarrow} \quad (1)$$

$$R_{ap} = \frac{R^\uparrow + R^\downarrow}{2} \quad (2)$$

$$GMR_{rel} = \frac{R_{ap} - R_p}{R_p} \quad (3)$$

However, spin mixing can occur which lowers the GMR effect. For optimization of the GMR effect, micro structural features like grain size and texture and circuit configurations like Current-In-Plane (CIP) or Current-Perpendicular-to-Plane (CPP) have to be considered.

3 GMR Spin Valve System for Sensor Application

3.1. GMR Spin Valve

GMR multilayer configurations were the first structures suitable for device application. They consist of typically up to 20 non-ferromagnetic/ferromagnetic bi-layers resulting in high GMR values. They feature a bell-shaped resistance change with magnetic field and are suitable to detect in-plane magnetic field strengths independently of the field direction. However they can exhibit a pronounced hysteresis which complicates the application of this sensor type for highly accurate automotive magnetic field sensors. Furthermore, the bell-shaped signal characteristic of the multilayer structure can lead e.g. in the presence of an interfering magnetic field to a frequency doubling when measuring an oscillating magnetic field, since there is no clamping of the signal for extreme magnetic field values.

GMR spin valve structures possess improved properties combining high GMR values with low hysteresis, signal clamping and high stability. They were developed in the early 1990ies for read heads in magnetic storage devices. Compared to the GMR multi layer structure, the magnetic properties of a spin valve stack can be adapted to the specific application so that the measurement of the strength and/or the direction of a magnetic field are possible.

As described above, GMR spin valve systems basically consist of two ferromagnetic layers separated by a non-magnetic spacer layer as depicted in Fig.

5. One layer is the 'hard' or 'pinned' layer and the other the 'soft' or 'free' layer. In contrast to the multilayer system the pinned layer's magnetization direction is ideally fixed whereas the free layer magnetization can follow an external in-plane magnetic field with almost no hysteresis.

A defined alignment of the magnetization directions in the hard layer is achieved by "pinning" to a synthetic anti-ferromagnet (SAF) system. The SAF benefits the high stability of the system, because the pinned hard layer possesses a large magnitude of unidirectional anisotropy that is the tendency of a ferromagnet to have a preferential direction of magnetization. The hard layer is magnetically biased in direction of the 'easy axis' by the means of the exchange bias effect. The exchange bias describes the pinning of the magnetization of a ferromagnetic layer by an adjacent anti-ferromagnet.

The second magnetic layer, the so-called free layer is separated by a nonmagnetic spacer with an adjusted thickness resulting in an ideally zero coupling between the magnetic layers. Coupling between 'soft' and 'hard' layer is very weak, ideally zero. However, coupling can occur from residual exchange bias fields, interface roughness or magnetostatic coupling to neighbouring ferromagnetic layers.

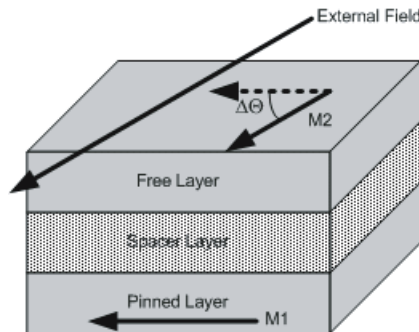


Fig. 4. Simplified spin-valve GMR stack

More sophisticated spin-valve systems have implemented a tri-layer artificial anti-ferromagnet instead of the pinned layer. This so-called reference system consists of a pinned layer which is exchange coupled to a natural anti-ferromagnet and an anti-ferromagnetically coupled reference layer. The (valuable) GMR effect takes place between the free and the reference layer. The advantage of such a reference system is the much lower net magnetic moment compared to the case with a pinned layer only which stabilizes the reference magnetization in an external magnetic field.

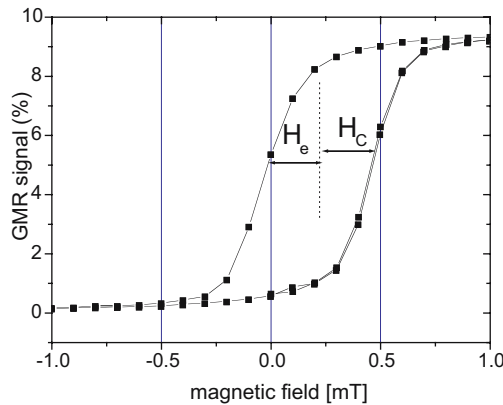


Fig. 5. Minor loop of a GMR magnetization curve

Fig. 5 shows a typical easy-axis (i.e. magnetic field parallel to the reference magnetization axis) minor loop characteristic of a GMR spin valve magnetization curve reflecting basically the free layer properties. H_e denotes the residual ferro-/antiferromagnetic coupling and H_c is the coercivity of the free layer. The dependence of the GMR value as a function of the magnetic field leads to the possible application as a magnetic switch where high sensitivities (small switching fields) and small coercivities are needed..

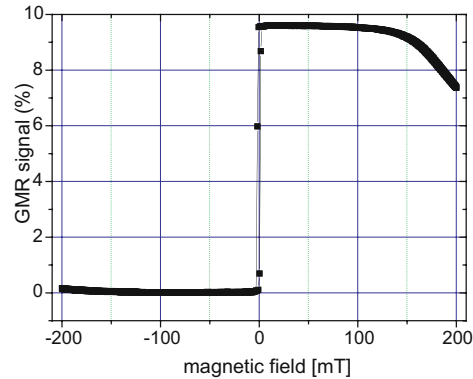


Fig. 6. Major loop (± 200 mT) of a GMR magnetization curve

In Fig. 6 presents the corresponding magnetic easy-axis behavior in the range ± 200 mT which characterizes mainly the properties of the spin-valve reference system. The stable plateaus in the low/high resistance regime beyond 120 mT demonstrates that the spin-valve structure can be designed to feature a stable reference system for magnetic field strengths which are relevant for

automotive applications. Furthermore, the exposure of even higher fields does not lead to irreversible changes of the sensor properties.

3.2 GMR Spin Valve System for Sensing the Angle of Magnetic Field

For magnetic fields in the range of some 10 mT, i.e. in the saturated range, the free layer is aligned to the direction of the external field. In this case the resistance of the GMR stack is a function of the cosinus of the angle between the magnetizations of free and pinned layer (Fig. 4). While the magnetization in the free layer follows the external magnetic field, the magnetization in the pinned layer is fixed by the exchange coupling in a reference direction. This reference direction is defined during the magnetization process using high temperatures and high magnetic fields.

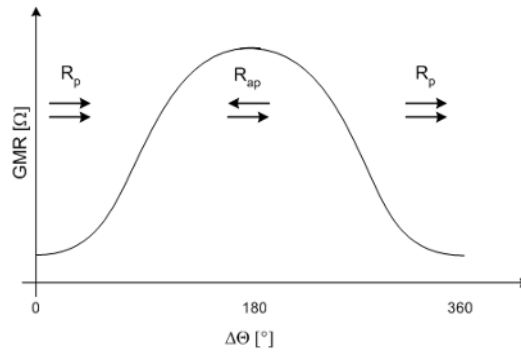


Fig. 7. Resistance of a GMR spin valve operated in saturation as a function of the field angle with respect to the magnetization direction of the pinned layer.

As shown in Fig. 7, the cosine dependence of the GMR effect upon rotating the free layer magnetization direction under a constant external field in the saturation region leads to the possible application as a rotary angle sensor. The following equation describes the relationship,

$$R_{\Delta\theta} = R_0 - \frac{1}{2} \cdot (R_{ap} - R_p) \cdot \cos(\Delta\theta) \quad (4)$$

whereas $\Delta\theta$ denotes the angle between the magnetization direction of the pinned and free layer and R_0 the resistance in the absence of any magnetoresistive effects. R_p is the resistance when magnetization directions between pinned and free layer are in parallel and R_{ap} is the resistance when the mag-

netization directions between pinned and free layer are anti-parallel. As a result, a single GMR resistor exhibits a 180° uniqueness. Compared to the AMR effect which has a angle uniqueness in 90° the GMR spin-valve structure features a significant benefit. As a result, a 360° angle sensor is enabled by using a bridge circuit having GMR resistances with reference directions oriented along two axis only.

3.3 GMR Spin Valve System for Sensing the Strength of Magnetic Field

For incremental speed sensors an approximately linear MR behavior around zero field is favorable in order to enable tooth decoding (correct identification of tooth characteristic) of a tooth wheel e.g. for a "true power on" function. If the magnetization direction of the reference layer is aligned perpendicular to the magnetization / anisotropy axis of the free layer, a linear MR behavior with respect to a magnetic field component parallel to the reference magnetization is obtained. The magnetic field which is necessary for a fully anti-parallel ($-H_k$) and parallel ($+H_k$) alignment of the free and reference layer describes the maximum linear range. Since the H_k is a property of magnetic anisotropy of the free layer only, sophisticated material and/or geometry engineering can be applied to adapt the magnetic performance. By choosing special growth conditions for the free layer it is possible to induce a certain anisotropy axis which can lead to an H_k greater than 8 mT. Furthermore, there are ferromagnetic materials where an anisotropic axis can be induced by an anneal in a magnetic field, thereby obtaining an H_k as high as 5 mT. Another possibility to tailor a certain strength as well as direction of the magnetic anisotropy axis is to make use of the shape anisotropy by adjusting the geometry of the GMR resistance. In order to minimize the free magnetostatic energy it is favorable for the magnetic layers to align the magnetization along the long axis e.g. of a resistance stripe. The higher the aspect ratio of the GMR structure is, the stronger is the magnetostatic energy.

Fig. 8 shows the simulated effect on the hard axis minor loop characteristic as a function of the width of a GMR structure with constant length. The strength of the magnetic anisotropy can be easily adapted to the sensor application: a strong anisotropy for applications where a wide linear range is advantageous, e.g. for rotary speed sensing or a vanishing anisotropy for applications which need the saturation magnetization to be obtained for low H-fields as it is necessary for angle sensors. Therefore, the GMR technology offers the possibility to cover the whole automotive magnetic sensor portfolio with just one GMR stack and slight variations of the sensor layer and/or GMR resistance layout.

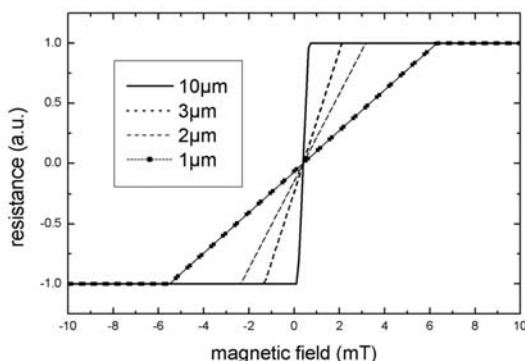


Fig. 9. Simulated hard axis minor loop as a function of GMR stripe width; stripe length of all structures is $250\mu\text{m}$.

4. Technology

4.1. Monolithic Integration

In contrast to AMR sensors where only one soft magnetic layer (e.g. permalloy) of several 10 nm thickness is processed, the deposition of a GMR layer system with single layers in the sub nanometer range has to be well controlled in terms of absolute film thickness and homogeneity over the wafer. In the beginning, GMR stacks were deposited by MBE (molecular beam epitaxy) which is highly sophisticated and time consuming. In recent years, sputter tools with a highly accurate and reproducible thin film deposition as well as a high wafer throughput were made available on the commercial market. Therefore, GMR sensor processing became suitable for mass production with benefits for price and quality of the sensor products.

Independently of the GMR stack composition, most of the processing of GMR sensors can be done using standard semiconductor equipment. The GMR multilayer stack is deposited in a low temperature sputter process on top of a fully processed IC separated by an insulating layer.

All GMR stacks start with a specific seed layer defining the growth mode of the subsequent films and end up with a capping layer which prevents the underlying material from being oxidized. In order to avoid a degradation of the GMR sensor performance, the temperature budget of the following process steps have to be kept below a certain degradation limit which is in the range between $250^\circ - 350^\circ\text{C}$ for minutes – hours depending on the stack type. The

structuring of the GMR resistor can be done either by a dry etch or lift-off process. In the latter case, before the GMR sputter process a photo resist mask has to be generated on the substrate.

Afterwards, a passivation with a GMR compatible temperature budget, e.g. by a sputter or specially developed low temperature CVD process, is deposited. After opening of the contact areas, a direct contact between GMR and the wiring metal is processed. Finally, depending on the sensor application, either a state-of-the-art magnetization process for the speed sensor or a special process for the local magnetization needed for angle sensing is applied.

So far GMR sensors are available as discrete devices, i.e. without any signal processing on the same chip. In order to gain an utilizable sensor signal the connected signal processing chip may have following tasks:

- ▶ Signal level amplification
- ▶ Offset compensation
- ▶ Gain compensation
- ▶ Trigger threshold generation for speed sensors
- ▶ A/D conversion for angular sensors
- ▶ Angular calculation

The signal processing chip has to be attached to the sensor chip e.g. by wire bonding or by a package-by-package solution. The results are higher inductive/capacitive parasitics, higher disturb signal sensitivity as well as increased leakage currents, thereby reducing the sensor performance. Furthermore, it could also be a major challenge to obtain a symmetric routing which is also important for excellent sensor properties. In addition, an input protection for the sensor chip is necessary.

These drawbacks can be avoided by an integration of the GMR sensor on the IC chip. Results of the Infineon MRAM development reveal a high compatibility of the integration of GMR materials in CMOS technology with respect to stack deposition, structuring, planarization processes and passivation.

Furthermore, CMOS technology offers a variety of ways to provide conditioned surfaces which are very important to adjust the GMR growth condition and therefore, magnetic properties. In principle, there are two basic concepts for GMR integration into CMOS:

- ▶ horizontal integration where the IC is beside the GMR sensor with no IC below and
- ▶ vertical integration, putting the GMR device on places with IC beneath

The second concept gives the possibility of maximum integration density, since no dedicated areas have to be provided. We have developed an integration concept for GMR elements which is fully compatible to the CMOS processing with only minor changes of the IC base process. This is very advantageous because almost any CMOS and bipolar technology can be chosen for the IC. As a consequence, a transfer into different technologies like bipolar processes for higher voltage and current applications is easily possible. This covers a plurality of applications like power applications or advanced digital logic for signal processing.

4.2 GMR Spin Valve thermal long Term Stability

For automotive application the long term stability of the GMR stack is a key characteristic. As a monitor for changes in the GMR stack and magnetic properties we will show exemplarily the influence of thermal stress on the signal height of a GMR angle sensor. Fig. 9 demonstrates the relative GMR signal normalized to the initial value after high temperature storage between 175°C and 275°C up to 2000h.

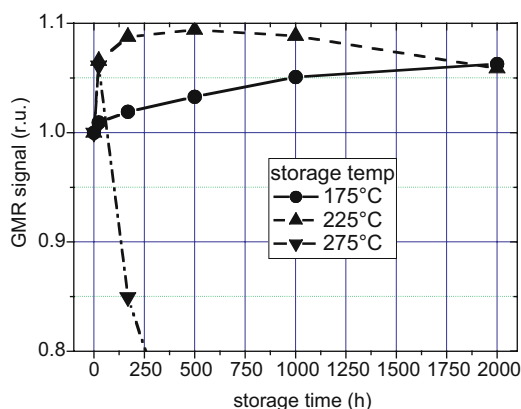


Fig. 9. GMR signal as a function of storage temperature and time

At the beginning, of the storage an increase of the GMR signal by up to 10% is observed as can be seen for $T=225^{\circ}\text{C}$. For longer storage times the signal drops down again which is strongest pronounced at $T=275^{\circ}\text{C}$. Origin is a strong decrease in the exchange bias strength between the natural anti-ferromagnet and the pinned layer. As a result, the reference system is turned significantly by the rotating external field, thereby preventing a full parallel and anti-parallel alignment of the free and reference layer. The signal increase and decrease processes seem to be thermally activated. Assuming an Arrhenius

behaviour, an activation energy for the first signal increase of ~ 1.5 eV can be estimated which corresponds to a quite highly activated process.

As a consequence, under typical automotive temperature condition of maximum 150°C a signal change of $\sim 1.5\%$ after 1000h is expected. Furthermore, a drop in the GMR signal is estimated to begin not before 240.000h at 150°C which is far beyond the required lifetime of automotive products.

These results reveal the compatibility of the GMR technology to automotive requirements also regarding long term thermal stability.

5 Incremental Position Sensors

5.1 General Speed Sensor Requirements

Usually toothed metal tone wheels are used as a target for speed sensors in powertrain applications. The general shape of the target wheels is not very predictable as it strongly depends on the application. Therefore very different magnetic signals may occur at a speed sensor. The wheel speed application uses widely pole wheels. The typical ambient operating temperature range for speed sensors is -40°C - $+150^{\circ}\text{C}$. Usually an air gap of up to 4.5 mm can be covered by Hall based speed sensors. GMR sensors allow now an increased air gap or better phase accuracy or repeatability. Table below shows general sensor demands for the specific application:

<i>Application</i>	<i>Air gap [mm]</i>	<i>Frequency [kHz]</i>	<i>Repeatability demands [%]</i>
<i>Wheel speed (ABS)</i>	0 ... 3.5	0 ... 4.5	Low
<i>Crankshaft</i>	0 ... 3.5	0 ... 10	High
<i>Transmission</i>	0 ... 5.5	0 ... 12	Medium

Tab. 1. Summarized requirements for incremental speed sensors in wheel speed, crankshaft and transmission application

5.2 Comparison of the Technologies

Variable reluctance (VR) sensors have been widely used in the past in all speed applications. Most important weak points on VR are the size and weight, which

limits the downsizing of modules. The output voltage of VR depends as well on the air gap and on the wheel speed which may cause additional efforts in the speed detection algorithm.

All these drawbacks disappear by using Hall or AMR principle. The digital output of the devices is very predictable and just need a cheap digital input and only low signal conditioning. Advanced sensors like TLE4941/42 for example use a current interface of 7/14 mA which allows wire break detection and saves wiring costs. Integrated digital algorithms and improved analogue circuitry enable new features like direction detection, vibration detection, air gap information and self calibration. Hall sensors allow a reasonable air gap and phase accuracy for most of the applications and can be fully integrated into the semiconductor standard production. In comparison the AMR devices are still very often not integrated and use a 2 or even 3 chips setup, which causes higher production cost.

<i>Condition</i>	<i>VR</i>	<i>Hall</i>	<i>AMR</i>	<i>I-GMR</i>
<i>Output signal</i>	analogue	digital	digital	digital
<i>ECU signal conditioning</i>	Schmitt-trigger/ ADC	digital input	digital input	digital input
<i>Module Size</i>	-	+	+	++
<i>Weight</i>	-	+	+	+
<i>Sensitivity</i>	+	0	++	++
<i>Temperature stability</i>	+	+	+	++
<i>Zero speed & true power on function</i>	No	Yes	Yes	Yes
<i>Direction detection and vibration detection</i>	No	Yes	Yes	Yes
<i>Voltage supply needed</i>	No	Yes	Yes	Yes
<i>Cost: IC + module + ECU conditioning</i>	0/-	+	0	+

Tab. 2. Comparison of different Sensor-Types (++ very good; + good; 0 average; - weak; — very weak; Yes/No means that this function or condition is/isn't possible for this sensor type)

Although discrete GMR have a better phase accuracy and allow a bigger air gap they struggle with the cost position. This can be improved by developing

an integrated GMR solution. The integrated GMR principle allows better phase accuracy and improved sensitivity, but should not increase the total module costs against Hall sensors. Therefore some percentage of the sensitivity improvement may be used to reduce the costs of the magnetic circuit. So the usage of cheaper magnet materials and reduced size of magnet is possible.

Furthermore the improved signal to noise ratio (SNR) reduces the demands on the internal signal conditioning circuitry. Signal amplification is getting less critical as well as the conversion from analog to digital world. All these points will cause further costs savings which should overcome the higher efforts to produce the GMR structures.

Tab. 2 below shows the performance of I-GMR in reference to the other possible sensor principles.

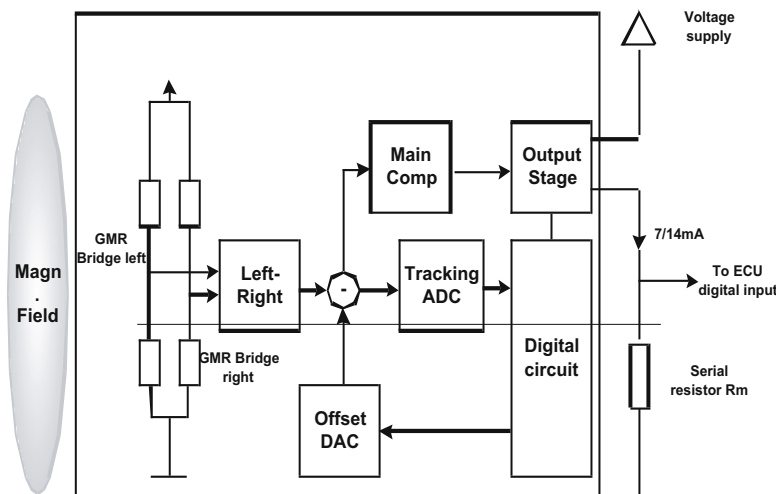


Fig. 10. Block diagram of Incremental Speed-Sensor.

5.3 Architecture of an Integrated Sensor

The general system realization of an integrated GMR sensor will be quite similar to the circuitry of an advanced differential Hall IC (Fig. 10). It contains a pair of GMR half bridges which are connected in a way to get a differential output signal. Then a summation point to compensate internal and external offsets will follow. Here the signal path can be split into an analogue path where a threshold comparator (main comp) will control the output stage. Depending

on the application, different threshold concepts already available on Hall products can be used. The other path is used to track the signal so that the calibration algorithm and the offset DAC can ensure that all internal and external offsets are compensated.

The output signal is current modulated. The current levels 7 and 14 mA correspond to logic 'low' and 'high' level. This allows a connection of the sensor with only 2 wires.

Of course, further GMR half bridges can be added to allow the direction detection and vibration suppression. Only the output stage has to be extended to support a PWM or digital coded protocols. In further development, a fully digital processing concept similar to the concept shown in the angle sensor section may be introduced.

6 Angular Sensors

6.1 Automotive Applications

Angular Sensors can be found in several automotive applications in both engine and passenger compartment. The required angular accuracy strongly depends on the application. The better the accuracy, the more applications can be served. A few examples for values of the angular measurement range are listed in the table below.

<i>Application</i>	<i>Measurement Range</i>
<i>throttle-valve angle</i>	110°
<i>steering-wheel angle</i>	±2 x 360°
<i>pedal position</i>	30°

Tab. 3. Ranges for different angular sensors applications

6.2 Measurement Principle

The GMR sensor circuit, like described in the previous technology section, changes its resistance according to the magnetic field components with

respect to the pinned layer of each GMR resistance. The change of the GMR resistance can be converted into a change of single-ended or differential voltages. These voltage-swings can be used to determine the correct angle of the magnetic field applied to the GMR sensor. The simplest way to detect the angle of the magnetic field is to calculate the angle out of the sine and cosine component of the magnetic field.

$$\alpha = \arctan\left(\frac{Y}{X}\right) \quad (5)$$

As only the relation of X and Y is crucial, all amplitude effects, which influence both measurement paths in the same way, are automatically compensated.

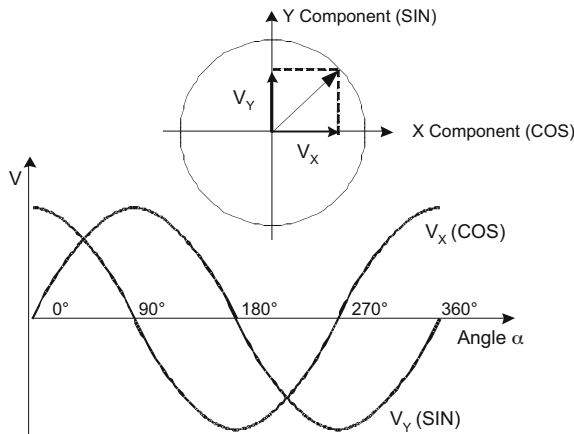


Fig. 11. Principle for 360° Measurement Range

6.3 Signal Processing Path

The two values X and Y are measured as voltages of two GMR bridges with perpendicular alignment of the pinned layers. X represents the cosine component and Y the sine component of the circular angle signal. Fig. 12 shows the orientation of the bridges on top of the signal processing chip.

A point to pay attention to is the inaccuracy of the converted angle components X and Y . The main errors amplitude and offset can be corrected by arithmetical operations. The offset can be subtracted from the X and Y components. Unsymmetrical amplitude variations of the two signal paths can be eliminated by a multiplication to achieve the desired gain for angle calcula-

tions. Today, these corrections can easily be done by digital logic or even a programmable microprocessor. This controller can be integrated in the signal processing chip. In this way the raw elliptic shaped GMR-outputs are corrected to a circle shaped figure to calculate the right angle by eliminating offset and amplitude variations. If a temperature measurement cell is integrated, additionally temperature dependent effects can be compensated. This increases the accuracy also in a wide temperature range.

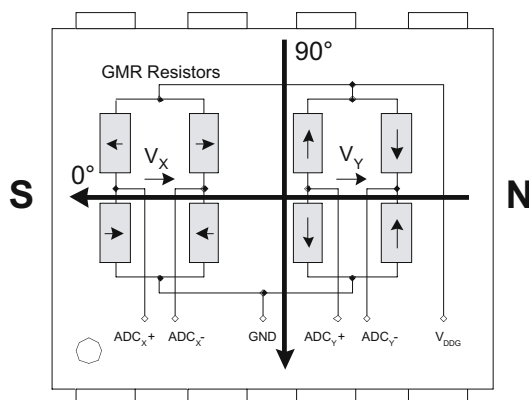


Fig. 12. Orientation of the bridges

The basic dataflow can be divided into two main parts, the analog signal area and the digital area. The analog area consists of the analog signal generation (GMR Signal Voltages), preparation for A/D-conversion and the A/D conversion itself. The digital part consists of component dependent digital signal processing, angle conversion and angle post-processing.

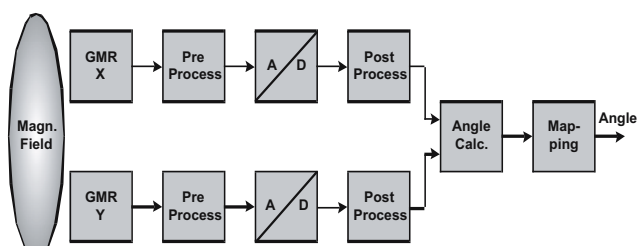


Fig. 13. Basic GMR based Angle Measurement

For the final 360° angle calculation 3 different methods can be used:

- Fully programmed software algorithm (so-called 'Cordic')
- Special hardware acceleration as additional logic module in a microcontroller

► Look-up table with interpolation

The analog parts include the blocks on the left side of the data path ending with the ADC, which converts the data to the digital domain. The angle calculation needs both components to calculate the angle, which is mapped afterwards to the right scale and angle offset.

Basically it is useful to convert values to the digital domain as fast as possible, because temperature and aging effects of analog circuits cannot occur in digital circuits. Only the calculation bit-width defines the calculation error in the digital domain. The signal speed is relatively low and the accuracy of each component is quite important. Therefore Sigma-Delta ADCs are most suitable in this application. With proper dimensioning of the ADCs, no preprocessing is required between the GMR sensor and the ADCs. This reduces the possible noise and error sources and the analog part becomes quite simple and short. Sigma-Delta ADCs generate a pulse-density 1 bit wide signal at a very high sampling frequency, which must be decimated and filtered to an appropriate useful signal-frequency.

<i>Benefit</i>	<i>Linear Hall</i>	<i>AMR</i>	<i>GMR</i>
<i>Sensor Size</i>	+	-	+
<i>Signal Level</i>	-	0	+
<i>Sensitivity</i>	-	+	+
<i>Temperature Stability</i>	-	0	+
<i>Weight</i>	-	+	+
<i>Module Size</i>	-	+	+
<i>Power consumption</i>	+	-	+
<i>System Costs</i>	+	-	+
<i>Angle Range</i>	120°	180°	360°

Tab. 4. Comparison between Hall, AMR and GMR

6.4 Comparison to other Technologies

To compare different types (Tab. 4) of angular measurement, different characteristics of sensors must be kept in mind. For angular measurements, linear Hall uses a different effect to sense one sensor component. Depending on the angle, the flux density is modulated. To achieve this, difficult and expensive

magnetic circuits are required. From the application point of view the signal may be the same. Therefore we compare these magnetic sensor types with each other. For AMR and GMR applications, only a simple turning magnet is used, as only the field direction is the key parameter. A grading is done in the following way: + good, 0 average, - weak performance. For example in the row sensor size a + for the Hall type shows that a good size is possible as it can be built very small.

7 Conclusion

The GMR functional principle is based on scattering of conducting electrons of opposite spin at the interface of adjacent magnetized ferromagnetic layers with different direction. To exploit the potential of GMR sensors for a wide range of automotive applications, a cost effective, reproducible and reliable fabrication technology is required. Therefore, The integrated circuit (CMOS and Bipolar) processing has been taken as the starting point for the development. It offers the advantage that it is widely established and qualified for all kinds of automotive applications. It uses well-known processing techniques like sputtering and structuring of thin metal layers. Furthermore, monolithic integration of electronic circuitry for readout and conditioning of the sensor signal makes the system insensitive to parasitic effects of interconnects and electromagnetic coupling.

In typical automotive applications the comparison with the established speed sensor types of variable reluctance, Hall and AMR showed significant advantages for the GMR technology. GMR sensors offer highest sensitivity and thus, allow performance gain by reduction of the jitter in the measured signals. On the other hand, an extension of the tolerable air gap between the sensor and the observed rotating targets is possible. The sensitivity gain may also be used to increase the allowable mechanical tolerances for the fixture of the sensor or to tolerate an operation using a less sophisticated back bias magnet. Both modifications open a cost saving potential compared to competitive sensor technologies. Furthermore, the GMR is the technology that exhibits the highest temperature stability. This allows increased performance by means of decreased tolerance over the automotive temperature range or reduced cost for time consuming temperature calibration measurements.

Angle sensing is supported by spin valve GMR sensors which can be operated in a saturated mode. In this operational mode, the sensitivity for changes of the field strength disappears. The sensor is only sensitive for changes of the field direction with respect to the pinned layer magnetization direction. Using two GMR bridges with orthogonally directed pinned layers a sine and a cosine

signal can be measured and used for direct 360° angle calculation. The range of possible applications is extremely wide and will benefit from temperature stability of the GMR technology and from the significantly reduced requirements for the magnetic circuit.

Summarizing all technology comparisons and the analysis of various automotive applications, the GMR technology has been identified to be the most promising magnetic field sensing technology for the next decade.

References

- [1] Hammerschmidt, Katzmaier, Tatschl, Granig, Zimmer, Vogelgesang, Rettig, Giant magneto resistors-sensor technology & automotive applications; SAE 2005 World Congress & Exhibition SAE2005-AE-247.

Jürgen Zimmer, Thomas Bever, Werner Rössler

Sense & Control
Infineon Technologies AG
Am Campeon 6
D-85579 Neubiberg
Germany
Juergen.Zimmer@infineon.com, Thomas.Bever@infineon.com
Werner.Roessler@infineon.com

Klemens Prügl

Infineon Technologies AG
Wernerwerkstr. 2
D-93049 Regensburg
Germany
Klemens.Pruegl@infineon.com

Wolfgang Granig, Dirk Hammerschmidt, E. Katzmaier

Sense & Control
Infineon Technologies Austria AG
Siemensstrasse 2
A-9500 Villach
Austria
Wolfgang.Granig@infineon.com, Dirk.Hammerschmidt@infineon.com
Ernst.Katzmaier@infineon.com

Keywords: giant magneto resistor, spin valve, angular sensor, speed sensor

Simulating Microsystems in the Context of an Automotive Drive Application

G. Pelz, Ch. Decker, D. Metzner, Infineon Technologies AG
L. Voßkaemper, D. Dammers, Dolphin Integration

Abstract

The opportunities to integrate more and more functionality into a (micro)system-in-a-package (SiP) heavily call for advanced methodologies in modeling and simulation for complete systems. For a microelectronics company like Infineon Technologies, the top-level simulation of our products, i.e. the above microsystems, is not a nice-to-have feature – it is a must! Iterating on the fabrication runs for design debugging simply is not feasible. Extending these simulations to application level can be accomplished and this paper shows how. An automotive drive application will serve as a demonstrator for that.

1 Introduction

Let's first take a look at the microsystem: it may comprise microcontrollers and power electronics. Behavioral modeling provides for sufficient simulation speed, while not sacrificing precision. For all analog and mixed-signal parts of the system, it is carried out in VHDL-AMS. This holds for electronics as well as for thermal processes, which always have to be taken into account when power electronics comes into play. The microcontroller is modeled in SystemC, which provides for an extremely fast, but still cycle-correct treatment. It takes real-life programs on assembly level and executes them as it is simulated.

The application side is the electric motor with gear, load and a hall sensor for position feedback. Again, VHDL-AMS is adopted for behavioral modeling. This allows for the simulation of the complete application, comprising the microsystem as well as the surrounding electric motor and position using a commercially available simulator. This complete system typically simulates at a performance of 20 CPU-minutes per second real-time on a recent Linux workstation, which allows for thorough system verification, software development and even concept assessment (in case the abstract behavioral models can be provided in time, which should be no problem for a design with substantial legacy content).

2 System Modeling

2.1 Introduction

When talking about system modeling and simulation, often block-oriented simulators are used like MATLAB/SIMULINK and similar tools. As the focus of a microelectronics company like Infineon is on electronic circuits, this kind of abstraction is too high, as even simple circuitry cannot reasonable be described in this way. Nonetheless, MATLAB/SIMULINK component models may be linked into the kind of simulations, which are proposed in this paper.

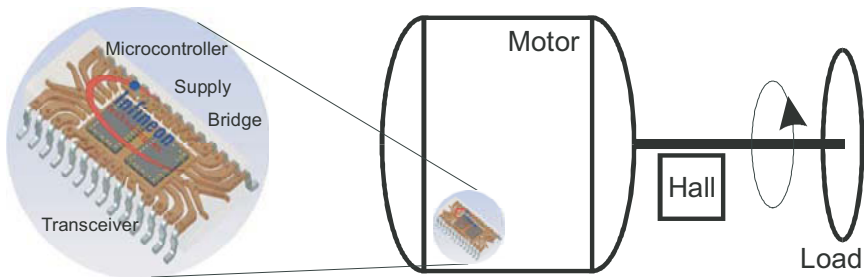


Fig. 1. Example drive system.

In general, this leaves us with two approaches for the modeling of systems spreading over more than one physical domain: simulator coupling and model transformation:

► **Simulator coupling**

In our case, the simulator coupling approach would have to bind together simulators for analog electronics, digital electronics, software, mechanics, thermal issues and magnetics. Even if it was possible to solve all the interface issues, we would end up with a big hunk of software, which would be extremely difficult to manage and configure. Moreover, the combination of several analog solvers would easily lead to very nasty convergence problems.

► **Model transformation**

The idea behind model transformation is to provide all models in one common form, so that they are simulatable by one solver.

We chose the second approach in which all domains are covered by one solver. Actually, we have got two solvers – one for analog and one for digital – which is due to the nature of the underlying descriptions. This co-simulation of the analog and digital domain has been a topic in microelectronics for twenty years now. The tools on the market are mature and reliable. The language to

formulate the analog models is VHDL-AMS. For the digital part we chose SystemC.

2.2 Power Electronics

The typical components of the power electronics are the following:

- ▶ Power switches, highside and/or lowside
- ▶ Motor bridges and bridge drivers
- ▶ Voltage and current regulators
- ▶ Transceivers

The basic behavior of these kind of components is determined by the behavior of the respective power MOSFETs and their gate drivers, several protection features (e.g. over-temperature, over-current, etc.), several diagnosis features and the environment, comprising of the loads (e.g. electric motors, bus lines etc.) and the attached microcontroller. With the reduction of the number of chips in an electronic control unit (ECU) and the resulting need for higher integration, many of the above features are integrated into one chip or at least into one package.

The modeling of power electronics – as any other kind of modeling – always requires a reasonable balance between precision and model complexity. Providing for more precision, i.e. adding more related physical effects into for instance the power MOSFET, directly leads to a longer simulation time. The art in it is to stay as precise as necessary and as abstract as possible. In our case, this means that the power MOSFET is to be modeled in higher precision and on an abstraction level, which is comparable with the device models for the circuit simulation. On the other hand, the protection features or the diagnosis features and even the gate drivers are modeled in a relative abstract fashion, as their impact on the outside world is limited or their contribution can be described in an event-oriented or even digital manner.

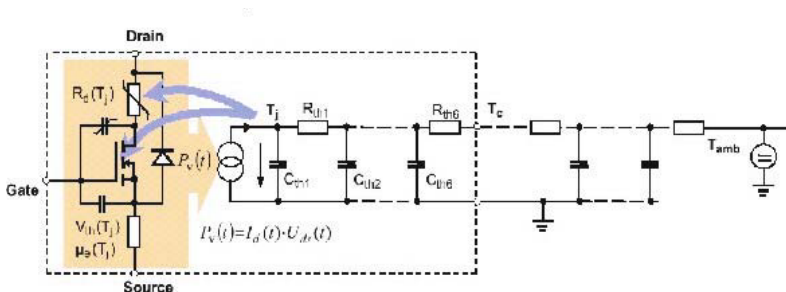


Fig. 2. Electro-thermal DMOS model.

When talking about power electronics, we also have to talk about self-heating and in general thermal issues. Even more, the circular dependency between the electrical and the thermal behavior of a power transistor has to be taken into account. This is due to the drain current which causes the self-heating and the resulting junction temperature which influences the drain current. Fig. 2 shows a DMOS model with attached network of thermal capacitances and thermal resistances.

2.3 Embedded Microcontroller and Software

The microcontroller's task is to run the embedded software and to provide for the interfacing to the outside world through its peripherals. Again, the issue of precision and abstraction comes up. The first question to answer for a microcontroller model is that of the underlying time base. In all practical cases up to now, it turned out, that microcontroller's clock cycle is precise enough for a reasonable system simulations. On the other hand, it allows for a simulation speed that is one or more orders of magnitude above the gate level simulations, which would form the next level of precision.

For the microcontroller in our case – a state-of-the-art 8-Bit controller – we provided for a SystemC model, which was attached to the VHDL-AMS models for the rest of the system. This was accomplished by using the standard SystemC interface as provided by the vendor of the commercial VHDL-AMS simulator. The modeling strategy again follows the rationale of as precise as necessary and as abstract as possible. As the underlying idea is not to enhance the respective microcontroller, it is sufficient to provide for a model that is only valid at its external interfaces. Basically this model is a command interpreter which reads the current assembler statement and runs the respective actions on its memory map. The models for the peripherals are attached to this command interpreter and bind it to the outer world. The embedded software itself is not modeled. At initialization time, it is loaded into the respective memory model. Then it is executed as the microcontroller model is simulated.

As the SystemC model just provides for digital behavior, an analog shell was attached to it, to accomplish for correct electrical behavior. This turned out to be extremely helpful, as mismatches can be detected easily in this manner.

2.4 Mechanics

2.4.1 Introduction

The demonstrator, which is driven by the microsystem, is an electric window winder like it is widely used in car doors, see Fig. 3. Such a macro-system consists of different components which comprise different domains, like electrical (DC-motor with Hall-sensor), mechanical (gear, cable, window, guide rails), electromechanical (DC-motor), electromagnetic (DC-motor, Hall sensor). As an example for the basic effect approach we have a closer look at the mechanical effects, which are:

- ▶ Inertia: gear wheels (rotational), window (translational)
- ▶ Static and dynamic Friction: gear, guide rails
- ▶ Transmission (rotation-rotation, rotation-translation) and clearance in a gear Note: the cable is implemented as gear with rotational input and translational output. This approach serves to convert the rotation into a translational movement.
- ▶ Mechanical stop: upper and lower limit, “children hand”

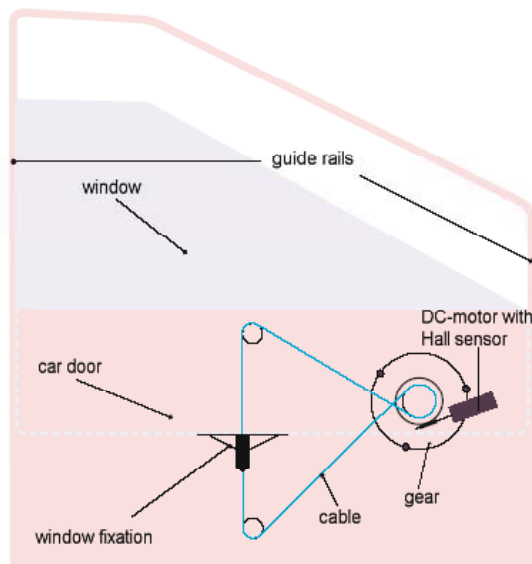


Fig. 3. Automotive window winder system

2.4.2 Modeling and Implementation of the Mechanical Parts

The electro-mechanical and electro-magnetic parts of the envisaged demonstrator is based on the modeling of basic physical effects which occur in or between single components of the mechatronic sub-system. The advantage of this kind of modeling is the high reusability of already modeled and validated effects. This approach benefits from the option that the designer is able to decide whether an effect will be considered or not and so influences the simulation precision and speed. Another advantage is that no knowledge of the model equation of the complete system is necessary – it is automatically build inside the simulator by combining the needed effect models.

In VHDL-AMS, we are not bound to given variables. This is an advantage, since we can implement variable types of non electric domains, which we want to simulate. VHDL-AMS offers outstanding possibilities for the definition of user-defined variable types. Tab. 1 shows the definitions of the flow and potential variables like they are recommended by the IEEE and for this system are excellent suitable.

<i>Definition of flow and potential variables</i>			
<i>Variable type</i>	Electrical network	Rotation	Translation
<i>Through flow-variable</i>	Current I	Torque T	Force F
<i>Across potential-variable</i>	Voltage V	Angle φ	Displacement x

Tab. 1. IEEE recommended definition of flow and potential variables

The restrictive port definition guarantees both the compatibility of the effect models among themselves, if one wants to interconnect them, and a simple expandability of the model library.

A simple example of physical effect implementation (the model of the gear transmission rotation/rotation without static friction or clearance) in VHDL-AMS is shown in Listing 1. The model contains two formulas:

- relation between the output torque and the input torque:

$$T_{out} = -T_{in} * g_r * \eta$$

- relation between the angle of the input gear wheel and the output gear wheel: $\theta_{out} = -\theta_{in} / g_r$

With T the torque, g the gear ratio, η the efficiency factor and θ the rotation angle.

```

01. LIBRARY IEEE;
02. USE IEEE.MATH_REAL.ALL;
03. USE IEEE.MECHANICAL_SYSTEMS.ALL;
04. ENTITY gear_rot_rot IS
05. GENERIC (g_r : REAL := 1.0; -- gear ratio
06.           eta : REAL := 1.0); -- degree of effectiveness (0 <= eta <= 1)
07.
08. PORT (TERMINAL rot_p_in, rot_n_in,
09.        rot_p_out, rot_n_out: ROTATIONAL);
10. END ENTITY gear_rot_rot;
11.
12. ARCHITECTURE simple OF gear_rot_rot IS
13. QUANTITY theta_in ACROSS T_in THROUGH rot_p_in TO rot_n_in;
14. QUANTITY theta_out ACROSS T_out THROUGH rot_p_out TO rot_n_out;
15.
16. BEGIN
17. T_out == - T_in * g_r * eta;
18. theta_out == - theta_in / g_r;
19. END ARCHITECTURE simple;
    
```

List. 1. VHDL-AMS implementation of the rotational/rotational gear transmission

2.4.3 Modeling and Simulation of the Mechanical Sub-system

For modeling the mechanical sub-system, the available models have to be interconnected. Due to the defined flow and potential variables the related models are port compatible. A symbol was created to each VHDL-AMS model, which can be interconnected then with another symbol in the schematic editor. The creation of the netlist of the system can be done automatically with the net list generator from the schematic editor. For exemplification the schematic of the sub-system is shown in Fig. 4.

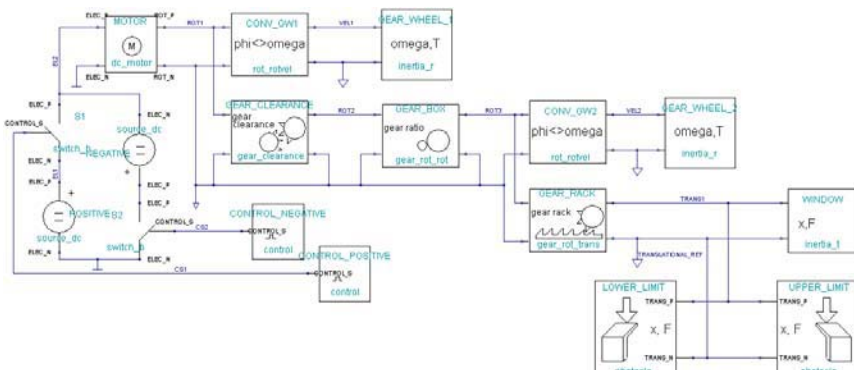


Fig. 4. Schematic of the automotive window winder sub-system with test-bench

After the fundamental physical effects were identified, implemented in VHDL-AMS and combined to the electro-magneto-mechanical macro system, the model of the mechatronic sub-system is ready to simulate.

3 Simulation Results and Conclusion

The model setup as described above has been simulated using 12 tests and related 12 embedded test programs. These were developed to verify the design of the (micro)system-in-a-package as described above. Virtually the complete functionality of the product can be assessed in its environment. These simulations turned out to be a cornerstone in the SiP-verification, as they helped to avoid a redesign. The simulation speed is in the range of 20 CPU-minutes per second real-time, which allows to accomplish extensive verification runs.

The limitation of this kind of simulations lies in the fact, that only those effects are taken into account, which have been introduced into the models. So if we know, that self-heating is an issue, we can take care of that. But if we do not take into account some certain effect, the system may later fail because of that, though the simulations were successful. In other words, this means that we get some information on whether the system can work under certain conditions rather than whether it will work under all conditions.

The shown drive system served as a demonstrator to assess the opportunities of complete system simulations. With that, the neuralgic scenarios can be assessed before tapeout of the chips. Even more, the complete controllability and observability of a simulation helps a lot in quickly tracking down the problems. All in all, the proposed approach will help to jointly get a much better understanding on the behavior of an even complex SiP in its environment.

References

- [1] G. Pelz, "Mechatronic Systems: Modelling and Simulation with HDLs", John Wiley & Sons, 2003.
- [2] L.M. Voßkämper, R. Schmid and G. Pelz, "Combining Models of Physical Effects for Describing Complex Electromechanical Devices", IEEE/VIUF Workshop on Behavioral Modeling and Simulation (BMAS), Orlando, Florida, 2000.

- [3] D. Dammers, P. Binet, L.M. Voßkämper and G. Pelz, "Motor Modeling Based on Physical Effect Models", IEEE International Workshop on Behavioral Modeling and Simulation (BMAS), Santa Rosa, California, USA 2001
- [4] D. Maurer and L.M. Voßkämper, "From Chip to System Design using a Co-verification environment", ECE Magazine September 2005, Page 34-36
- [5] G. Pelz, "The Virtual Disk Drive - Mixed-domain support for disk electronics over the complete life-cycle", IEEE International Workshop on Behavioral Modeling and Simulation (BMAS), Santa Rosa, California, USA 2001
- [6] M. Otter, "Objektorientierte Modellierung Physikalischer Systeme, Teil 1", at - Automatisierungstechnik 47 (1999) 1, R. Oldenbourg Verlag

Georg Pelz, Christian Decker, Dieter Metzner

Infineon Technologies AG
 Automotive Power
 Am Campeon 1-12
 85579 Neubiberg
 Germany
 Georg.Pelz@infineon.com

Dirk Dammers, Lars M. Voßkämper

Dolphin Integration GmbH
 Bismarckstr. 142a
 47057 Duisburg
 Germany
 mems@dolphin-integration.com

Keywords: microsystem, macrosystem, mechatronic, modeling, electro-magneto-mechanical effects, VHDL-AMS, multi domain, mixed-signal

Miniaturized Wireless Sensors for Automotive Applications

R. Thomasius, D. Polityko, H. Reich, TU Berlin

M. Niedermayer, S. Grundmann, S. Guttowski, Fraunhofer IZM

R. Achterholt, Global Dynamix AG

Abstract

Innovative packaging technologies and power aware design enable system shrinking considering automotive requirements. During the design process the coupling of very narrow positioned components and the interdependence of hardware, software, and packaging have to be considered. The relevant miniaturisation aspects are discussed on the exemplary application of a tire pressure monitoring system.

1 Introduction

Miniaturized wireless sensors become more and more important. They are increasingly applied to everyday objects, e.g. for tire pressure monitoring to enhance transport safety. Over 440 thousands people were injured or killed by traffic accidents on Germany's roads in 2004 [1]. Thereby maladjusted or improper filled tire equipments cause 30 percent of technical problems resulting in traffic accidents with personal injury [2]. Next to safety awareness satisfaction, correct pressure improves fuel economy and pollution control. Random inspection by NHTSA mentioned that pressure is erratically checked by drivers and over a quarter of tested vehicles have at least one improper filled tire [3]. As a result of this study the US American legislator passed a law [4], which claims to equip all new vehicles with tire pressure monitoring systems after September 1st, 2007. This measure affects about 8 million passenger cars per year [6] and implies a huge market for self-sufficient micro systems, while Germany exports about a half million cars per year into the United States [7].

Today's rapid development in packaging technologies enables direct tire pressure monitoring systems (TPMS) by additional downscaling of self-sufficient wireless sensors from some cubic centimetre to less than 1 cm. They allow efficient solutions for TPMS, which requires low weighted self-sufficient sensors to reduce out-of-balance forces. Furthermore the lowering of substrate area reduces mechanical stress applied to the electronic device. But not only tire pressure monitoring systems can benefit from miniaturized wireless sensors.

Tiny wireless ultrasonic sensors and cameras mounted on wing mirrors are imaginable to monitor blind angles and to be integrated into parking distance control systems. Ongoing system miniaturization at the Fraunhofer Institute for Reliability and Microintegration (IZM) targets self-sufficient wireless sensors with an edge length of 6 mm.

During the design process, the coupling of very narrow positioned components have to be considered in ultra dense 3D packaging more than in conventional 2D printed circuit board design. And also the low-power design benefits the overall system volume and dimensions due to usage of smaller batteries. So the development of tiny, low weighted and mechanical robust wireless sensor systems needs the reflection of multiple disciplines: hardware, software and packaging. Thereby exploitation of battery effects allows a reduction of battery volume. The relevant miniaturisation aspects are discussed on the exemplary application of a wireless tire pressure sensor unit.

In the next three sections, we will discuss the degrees of freedom in selecting components and packaging of miniaturized self-sufficient sensors like wireless tire pressure sensors. Beginning with the exemplary requirements on TPMS, we will introduce selection of components and interconnection technology as part of design flow to achieve miniaturized wireless sensors. Different design options are traded off to meet demands. Finally we present prototypes of network capable wireless sensors as well as sensor modules for a direct TPMS developed for Global Dynamix AG.

2 Requirements

Requirements on wireless sensors are defined by its application and lead the designer through the design space. Because we use it as an example, we want to introduce general requirements on tire pressure monitoring system:

Reliability: If a tire pressure system or another assistant system is at driver's disposal, it is trusted. Hence, reliability is intended by packaging. Wireless sensors mounted in rotating wheels are caught in crossfire of harsh environmental influences. Vibrations and acceleration forces necessitate mechanical robustness. A wide temperature range and thermal shock resistance are required by meteorological condition as well as heating by full braking. Sensor units must be shielded against electro magnetic irradiation and have to be resistant against chemical substances, i.e. salt-water, lubricating oil, sulphurous lotions, or cleaning supplies. In all cases, the integrity of sampled pressure values is a necessity and the driver has to be informed when a mal-

function is detected. Reliability also addresses fault-tolerant system behaviour (implemented in hard- or software), which is not considered in this paper due to limited space.

Low unit cost: Designed for mass marked, unit price has to be low. Reducing the number of electronic devices decreases component costs, and decreases the overall system weight and volume. Integrating analogue acquisition components, digital circuitry for computation and RF front-end for wireless communication into a single package allows a very compact single chip solution. Yield is primarily a function of die size. Therefore multi-chip solutions are sometimes preferred because of cost-effectiveness. However, the system requires the inexpensive integration of heterogeneous components, i.e. ICs, sensors, crystals, antenna, and passives.

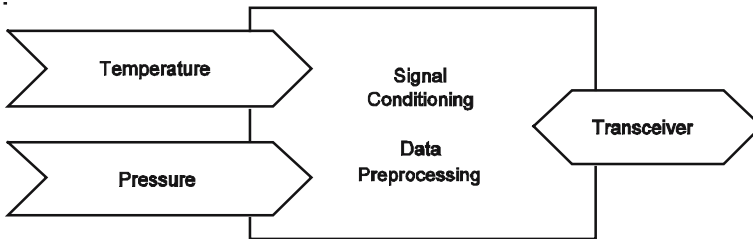


Fig. 1. Block diagram of an active bi-directional tire pressure monitoring unit.

Low installation and maintenance effort: Installation of tire pressure monitoring system should not influence established factoring processes. Amount of cabling should be as low as possible. Therefore systems with a single receiver are favoured over antennas in each wheel house. Reutilisation of keyless-entry board unit for tire pressure monitoring reduces installation effort and system costs. Exchanging batteries of tire pressure sensor units mounted in air chamber is time consuming and expensive. Therefore long operation time must be granted and a tire pressure sensor should work over a tire's life time by utilizing an ultra low power design.

In this paper we concentrate on techniques to achieve low system dimension and weight.

3 Selecting Components

Fig. 1 shows a block diagram of a wireless tire pressure sensor. It can be easily adapted to other wireless sensors applications: Temperature and pressure are acquired by sensors. After conditioning digitized signals are preprocessed and assembled into information packets, which are transmitted to the board unit using a radio link. The radio link can be used in opposite direction to receive calibration and configuration data. All components are powered by a power supply unit.

In the field of system miniaturization, the main question is which components mainly determine the final dimensions of the whole system. The optimization focus during the hardware development is to be put accordingly. Components like batteries, capacitances, high quality filters, crystals, and antennas normally dominate the volume of a wireless sensor node below a cubic centimetre. Several trade-offs often allow to adjust the requirements of a single component and to change volume share for a minimal size of the whole sensor node. For instance, a larger battery allows a smaller antenna with a reduced efficiency and vice versa. Our first design stage is to consider the manner, in which functionality will be realized. The subsections below discuss design options according to the requirements mentioned above, and keeping power consumption as well as system size in mind to achieve a long operation time and high mechanical robustness.

3.1 Sensors

Temperature, acceleration forces and supply voltage are reasonable measurements for TPMS next to obvious pressure. Temperature monitoring is necessary for temperature compensation and allows warning on overheated tire. Vibrations are indicators for a moving vehicle and can be used to wake up the TPMS from very deep sleep mode, while detection of low supply voltage is necessary to warn the driver about imminent sensor malfunction. The size and power consumption differs very much according to the type of sensor technology. With declining smaller sensor dimensions, the physical connection to the measuring medium also declines, so that miniaturization can considerably influence the precision. In this section we focus upon pressure and temperature measurement to avoid going beyond the scope of this paper. The selection of any transduction techniques affects the complexity and size of read-out circuitry.

	<i>Piezo-resistive</i>	<i>Capacitive</i>
<i>Nominal pressure [kPa]</i>	10 - 1000	10 - 1000
<i>Temperature range [°C]</i>	-40 - +125	-40 - +125
<i>Signal proportionality</i>	displacement	1 / displacement
<i>Electrical impedance</i>	low	high
<i>Signal drift</i>	high	low
<i>Signal noise</i>	low	moderate
<i>Offset signal</i>	moderate	small
<i>Relative signal change</i>	small (~2%)	large (~50%)
<i>Power consumption</i>	high	low
<i>Influence of parasitics</i>	low	high
<i>Read-out circuitry</i>	simple	complicated
<i>Overload-ability [nominal pressure]</i>	5x	100x
<i>Temperature sensitivity [%/K]</i>	-0,15	-0,01

Tab. 1. Comparison between piezo-resistive and capacitive pressure transducers [5]

Pressure: Miscellaneous pressure transducers are available on market: resistive wire strains, piezo-resistive and capacitive pressure transducers. Transducers used for TPMS operate in range between 100 and 500 kPa and must be insensible to acceleration forces. The first one is unsuitable, because resistive wire strains are less appropriate to pressures below 500 kPa appearing in tires and their miniaturization potential is limited [5]. Piezo-resistive pressure transducers change their resistance when deformed by applied pressure, while capacitive pressure transducers alter their capacity with distance of electrodes. Tab. 1 compares both pressure transducer types. Capacitive transducers are less sensitive to temperature but have high requirements on read-out circuitry. Influence of parasitic capacities is high due to measuring capacities in the range of 10 pF. Their low power consumption is less weighted, because sensors are low frequently used and activated for a very short duration. Specific package have to be attended to reduce disturbances by thermal mismatch between chip and package, whereas mechanical restraint due to fixed assembly of chip and package can be seen as reason.

Temperature: A sensor module for TPMS must operate in temperatures between -40°C and 125°C. Suitable transduction techniques are realizable in compact form. Metal resistors, negative and positive temperature coefficient

thermistors, silicon-spreading-resistance, and integrated sensors allow simple read-out circuits, while crystal sensors offer higher accuracy [5]. Tire pressure monitoring systems do not require high temperature accuracy.

3.2 Data Processing and Device Control

Signal conditioning and communication management is done by digital back-end. Pre-processing allows the reduction of transmitted data in order to save energy. The corresponding algorithms can partly be implemented energy efficiently as hardware or more flexible as software (Fig. 4). Hybrid approaches will often represent the most suitable solutions. Low level functions like the signal acquisition and base band processing are often realized via application specific, integrated circuits. This represents a benefit for computation-devices regarding computation speed and size. Depending on production volume and required flexibility, high level functions are implemented either in hardware or in software. In the case of our TPMS standard, microcontrollers with hardware support for data acquisition are used to achieve a short time to market. However, power consumption and battery size benefiting application specific integrated circuits are predicted due to high TPMS quantities.

Next to signal conditioning and communication management the digital back-end implements the power saving policy. An efficient power adaptation for single components allows a considerable reduction of size determined by energy supply. The standard measure is to switch off all components which are not in operation. In case of TPMS the impact of power down current increases due to very low duty cycles (below 0.1%). The microcontroller requires an operation mode with a very low leakage current and a possibility for periodic wake-up. U.S. Federal Motor Vehicle Safety Standards No. 138 [4] allows relaxed duty cycles for TPMS by an acceptance of reaction time up to 20 minutes.

3.3 Radio Interface

The design of radio interface and communication protocol is driven by following intentions: a) reliability of communication channel, b) size and weight of required components, c) power consumption. The selection of carrier frequency plays a key role. Higher carrier frequencies allow smaller antennas and higher data rates, whereas longer ranges and less reflection on surfaces are possible with lower transmission frequencies. Frequencies selection is limited by national frequency assignment plans. We choose 868/915 MHz for TPMS due to antenna size and transmit power consumption balance.

Antenna design is not only influenced by the limited space but also by shielding effects of the electrical circuitry and the power supply. Apart from the development of an efficient antenna, the optimum for the whole system can be a smaller antenna of reduced efficiency, where the saved volume allows a higher energy buffer capacity. In the case of the proposed TPMS lower battery weight has a higher priority than antenna size. The system has to work with a single antenna attached to the board unit. It is not satisfying to mount antenna in each wheel house due to wiring effort, which provides optimization criterion for antenna design in case of TPMS.

A further task of the radio interface is the reception of configuration data. Reconfigure ability of alert thresholds, duty-cycles and carrier frequency allows a very flexible system which can be used in different vehicles and countries. This makes integration of a receiver necessary, which also enables whole-system calibration after module assembly. The communication protocol has to reduce idle-listening, i.e. power-waste of an active receiver without incoming messages.

3.4 Clock Generating Components

Because clock generating components can take a high volume share, they are discussed separately. For the clock generating components a decision had to be made which frequency tolerances could be admitted. On-chip RC oscillators of a very low volume show a drift of 3 - 25% due to aging and temperature dependency. Frequency of larger crystals vary below of 0.1%. The clock source for radio frequency synthesis is most critical to keep radio frequency drift low. This clock source must be quite temperature and long term stable, because the tire pressure sensor is exposed to wide temperature range over several years. It is only possible to apply a frequency trimming factor in dependence of temperature if aging effects are negligible. In that case the avoidance of expensive temperature stable crystals with relative high volume share is possible.

3.5 Power Supply

An essential component of the self-sufficient wireless sensors is their own energy supply, which strongly determines size. The energy supply of tire pressure sensors is often based on electrochemical batteries due their relative high energy density and relative low costs. The selection of appropriate micro batteries can raise issues. Not only high energy densities for small volumes, but also the nominal voltage, the self discharge current, and the maximal load have to be considered for the choice of material. For instance, zinc air cells

with a very high energy density (Fig. 2) can be used only for a few weeks due to their high self-discharge current. On the other hand, lithium button cells can only drive relatively low currents, which can cause non-tolerable voltage drops in transmission phases. Here, electrode area is a major factor.

Furthermore, the estimation of the necessary battery volume for a given operation time is quite complex. The capacity of a small battery decreases rapidly at higher loads, whereas the capacity increases during intervals of reduced currents. This is known as the rated-capacity effect and the recovery effect. Additionally temperature dependency of chemical reactions, aging of battery caused by side reactions have to be considered – especially in case of long operating TPMS. Hence, determination of required battery size depends massively on the load profile and climatic environment.

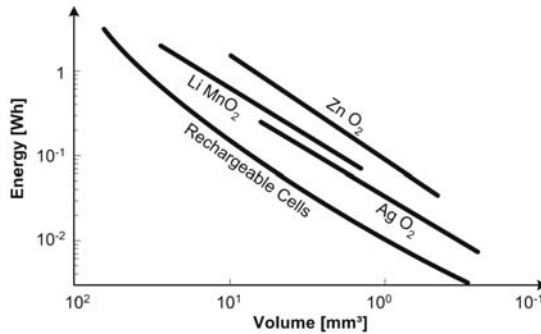


Fig. 2. Energy capacity of some batteries [9].

Indeed batteries have the lowest primer costs, but we have to think about the huge amount of batteries, which have to be disposed as hazardous waste after TPMS operation time ends. Some applications allow a replacement of large energy buffers by energy harvesting using movement, heat, radiation or bio-chemistry. The size of energy converters depends on energy demand and available intensity. Energy buffers will be necessary for most cases, because the harvested energy will rarely satisfy the total power consumption at any-time. Piezoelectric devices are imaginable in TPMS to benefit from vibration, but they require huge vibration pick-ups and oscillating weight, which increases wheel unbalance. An additional option is the usage of wireless charging techniques to enhance the system life time. Besides electrical charging via radio antenna or inductive coupling, the same principles of energy harvesting can be taken into account depending on coupling factor, shielding, and directivity. Charging by inductive coupling adds unwanted wiring effort in case of TPMS, because coils have to be mounted in each wheel house.

4 Integration Technology Selection

As have been shown above, a system like TPMS consist of several heterogeneous components. Design methodologies and reliable packaging technologies of heterogeneous components are research objects of Fraunhofer Institute Reliability and Microintegration and Technical University of Berlin.

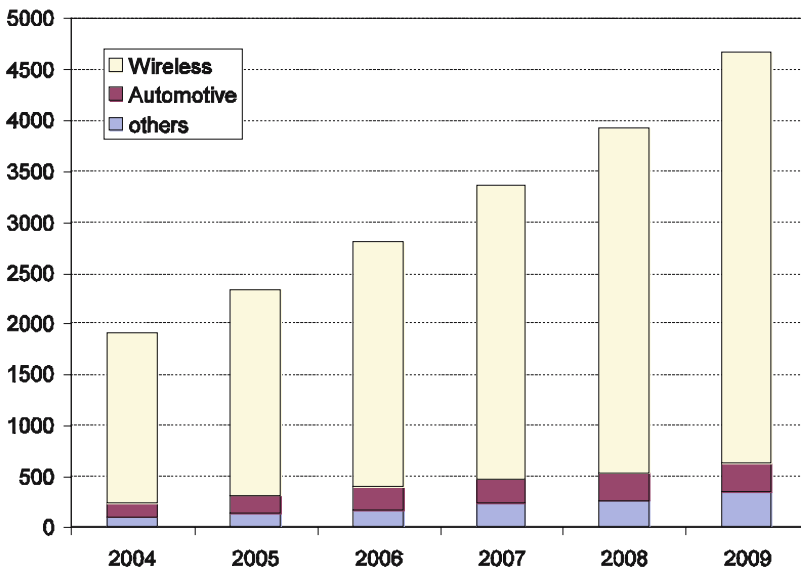


Fig. 3. SiP market projection, millions of units [10]

The common planar On-Board integration techniques like SMT (Surface Mounted Technology) allow low cost realization. But the increasing system complexity and high miniaturization demand for the automotive applications require another integration technologies, which have to be applied to achieve a size constraints. On-Chip integration of heterogeneous elements is challenging from design as well as from technological point of view. A promising solution for achieving highest integration density in smallest volume has been seen in vertical integration of heterogeneous components as a System-in-Package (SiP) (Fig. 5). This integration approach is well established in the area of wireless communication and it is also gaining for automotive market more and more in importance (Fig. 3, [10]).

The selection of the optimal integration technology as well as geometrical arrangement of components and preparing of the manufacturing data are obvious parts of the physical system design. It begins after the previously

described functional units are defined and their electrical schematic is finished. In the beginning of the physical design, the component set (ICs-bare dice, passives in their values etc.) for the realization of TPMS and their electrical interconnection (net list) are defined by the schematic. Within the 2.5D integration, where the functional layers are vertically integrated on each other, the physical design could be subdivided into two stages [8]:

- Global Layout, which can be abstracted away from any certain technology,
- Detailed Layout/implementation, which is obviously based on definite technology.

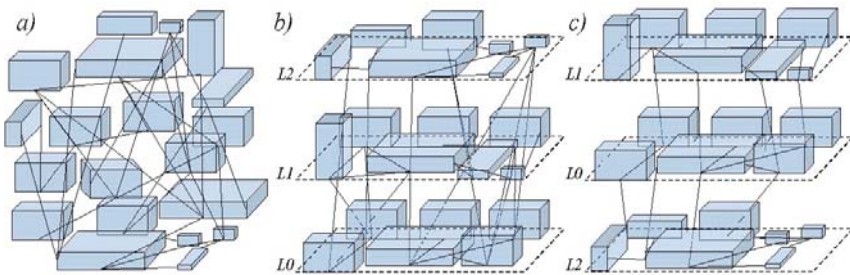


Fig. 4. Global layout for 2.5 D systems - Components and Nets: a) on the beginning, b) after partitioning, c) after placement and routing

In analogy to PCB/MCM- and IC-Design, both stages consist of three main steps: Partitioning, Placement and Routing. The aim of global partitioning is to group the components and to allocate them on certain vertical layers. Global placement means the arrangement of layers in stack, and global routing is in this case the optimization of the electrical wiring/nets between the layers (Fig. 4). All these steps can be formulated as a mathematical problem with a number of boundary conditions and objectives, such as floor plan and volume minimization for partitioning, minimization of wire length in the placement, the reduction of nodes quantity in the routing, testability of the layers and of the complete system as a general task etc.

Whilst a designer of “traditional” planar applications such as PCB or MCM has several clear technological criteria to make a decision regarding substrate and interconnection technology (e.g., wiring density, via types, the number of layers of laminated, thin film or ceramic substrates, interconnect pitch, cf. Tab. 2 and 4), there is no clearly defined criteria for choosing optimal SiP technology for vertical integration. The system designer is faced with many different

technological solutions presented by several industrial and research institutions. The currently available and practicable technological 2,5D SiP solutions for realization of highly miniaturized wireless sensor systems such as TPMS can be exemplary subdivided in four main groups [8] (Fig. 5):

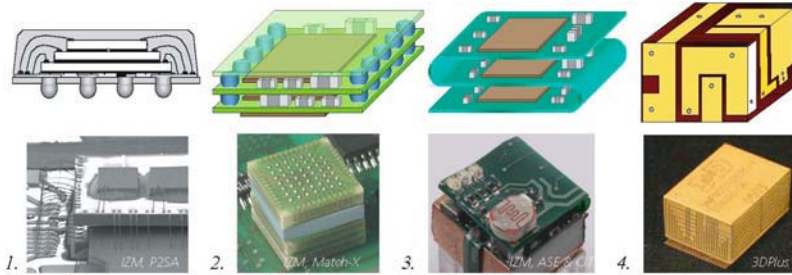


Fig. 5. Four main integration schemata and application examples of 2,5D SiP

1. Systems, where no signal redistribution in vertical wiring (In this case, it can be called vertical interconnect – VIC) and lower signal redistribution level in lateral wiring possible, so the routing can be down only in lateral level (mostly represented by wire bonded die stakes, e.g. Sharp),
2. Systems with no signal redistribution in VICs and high signal redistribution / routing capability in lateral levels (represented by solutions with functional layer on stacked modules e.g. North),
3. Systems, where signal redistribution level in vertical and lateral wiring is high and approximately equal (represented by solutions with components on the folded flexible substrate, e.g. Tessera),
4. Systems with medium and approximately equal redistribution level in vertical und lateral wiring, represented by stacked and molded devices with connecting metallization on the surface/sidewalls (3D Plus, Irvine).

For the compare and choice of optimal technology for the realization of TPMS at the beginning of the detailed layout/implementation stage, the designer needs objective criteria, as they are usual in the two dimensional design flow (Tab. 2 and 3). Tab. 4 demonstrates partly a parameter set for the four labeled technology groups. The parameter set is currently been explored at Fraunhofer IZM and practically verified by the prototypes, which are discussed in the section 4. The parameter provide not only key data for a qualified comparison and selection of integration technologies, they can also be used for the constrained placement of the components in 2,5D-Room in global layout stage. The available CAD tools for PCB-, MCM- and Packaging-Design include highly automated autoplacer and autorouter for the two-dimensional applications. But for vertical SiP- In-teg-ration of heterogeneous systems like TPMS, the designer still places components manually over the number of lay-

ers. The Fraunhofer IZM is working currently in cooperation with Fraunhofer ITWM on the novel 2,5D auto placement procedure, which is based on the volume optimization algorithms constrained by investigated technological parameter, targeting higher design effectiveness for TPMS- and further automotive applications. Furthermore, the automotive applications require very smart and robust concepts for the system encapsulation. In the traditional packaging design, the system molding issues are often been seen as an additional post design step. In the case of 2.5D integration for automotive area, the encapsulation concept influents the design flow in early stage for example during layer planning and components placement. Fraunhofer IZM investigates also molding technologies for the application environments with high temperature and mechanical stress, as they are usual in the automotive area.

	<i>MCM-L</i>		<i>MCM-C</i>	<i>MCM-D</i>
	<i>HDI</i>	<i>PCB Standard</i>	<i>Ceramics</i>	<i>Thin Film</i>
<i>Line width [μm]</i>	50...75	125	75..100	10
<i>Line space [μm]</i>	50...75	125	250	10
<i>Via land diameter [μm]</i>	100...225	650	200	30
<i>Number of layers</i>	8...10	8...30	15...30	2...5
<i>Dielectric constant [mm²]</i>	2,3...4.7	4,7	6...10	2,7...3,5
<i>Material</i>	FR4	FR4	Alumina	Si, Metal...
<i>Price approxim.</i>	Medium	Lowest (cents/cm ²)	Medium	High (\$/cm ²)

Tab. 2. Design relevant parameters for laminated (MCM-L), ceramic (MCM-C) and thin film (MCM-D) substrate technologies [8]

		<i>Wire Bond</i>	<i>Flip Chip</i>	<i>TAB</i>
<i>Min. Pad Pitch [μm]</i>	Die	50	100 ... 120	60
	Substrate	120	100 ... 120	200
<i>Mounting</i>		serial	parallel	serial/par.
<i>Electrical Performance</i>	L [nH]	1 ... 5	0.06 ... 0.2	1 ... 3
	C [pF]	0.2 ... 0.6	0.02 ... 0.03	0.2 ... 0.6
<i>Mechanical Protection</i>		glob top	underfill	none

Tab. 3. Design relevant parameters for different interconnect technologies [8]

		<i>Stacked Dice</i>	<i>Stacked Modules</i>	<i>Folded Flex</i>	<i>Moulded Devices</i>
<i>Redistribution capability</i>	Vertical	-	-	high	medium
	Lateral	low	high	high	medium
<i>Passive Integration Capability</i>	Discrete	low	high	high	high
	Embedded	low	high	medium	medium
<i>Wire Length</i>	WL	high	low	high	medium
<i>No. Functional Layer</i>	L	up to 5	7	10	32
<i>Layer Thickness</i> $L=G+C$	Layer Gap G [μm]	negligible	100 ... 1200	200 ... 1200	50 ... 600
	Carrier C [μm]	200 ... 600	50 ... 1200	20 ... 100	50 ... 200
<i>Vertical Interconnect Density</i>	[1/mm ² mm]	0.5; ~f(G)	0.5 ... 12; ~f(G)	5 ... 30	10 ... 50

Tab. 4. Parameter set for labelled SiP technology groups

5 Prototypes

For evaluation of high integration packaging techniques tiny wireless sensor are implemented on flexible substrates (Fig. 6a). These sensors measures brightness and temperature and interact in multi-hop sensor networks. All components are integrated in volume of 1 cm³. A self-sufficient tire pressure sensor unit developed for Global Dynamix AG is shown in figure 6b. They allow the reconfiguration of the tire pressure sensor module using radio communication like measure intervals, thresholds and radio frequency. The system uses 868/915 MHz-ISM-band and allows the usage of a single antenna integrated in the board unit.



Fig. 6. a) Components of wireless sensor mounted on folded flex
b) Electronic of a tire pressure monitoring sensor developed for Global Dynamix AG

6 Conclusion and Future Work

In this paper we discussed the degrees of freedom in designing miniaturized self-sufficient sensors considering a TPMS as an example. Especially tire pressure sensors electronics can be extended to equip a tire with intelligence and to allow vehicle adaptation to weather and road condition. The tire ID in future will prevent the usage of ineligible tires in dependence on vehicle type, road and weather conditions. This addresses a further main source of accidents with damage to persons. Thereby, miniaturization of application specific autarkic sensors requires system knowledge and multidisciplinary overview due to interdependences of different domains. Today's advances in packaging and manufacturing technology allow the enhancement of the miniaturization level, which enables the integration of reliable self-sufficient sensors into objects like valves. Further power efficiency is needed to achieve long operating light-weight systems.

7 Acknowledgements

A part of reported work, especially the introduced tire pressure monitoring system, was created in cooperation with Global Dynamix AG. Another part, especially in the section four was carried out in the frame of the project "AVM-Autarkic Distributed Microsystems", also known as eGrain-Project (refer to <http://www.egrain.org/>). This project has been supported by the BMBF (Bundesministerium für Bildung und Forschung) of the Federal Republic of Germany under the grant 16SV1658. The general Task of the AVM/eGrain Project is a preparation of future miniaturization technology on several levels (hardware, software, energy, communication etc.) The reported particular results are part of a task, which aims the development of design methodology for system miniaturization within advanced 3D packaging integration. The responsibility of this publication is held by the authors only.

References

- [1] Zeitreihen Verkehr 2004, Statistisches Bundesamt, Wiesbaden, Germany, 2005
- [2] Unfallursachen/Technische Mängel 2004, Statistisches Bundesamt, Wiesbaden, Germany, 2005.
- [3] Thiriez, K.; Bondy, N.: NHTSA's Tire Pressure Special Study, US DOT/National Highway Traffic Safety Administration, Paper Number 256, United States of America, February 2001
- [4] Federal Motor Vehicle Safety Standards; Tire Pressure Monitoring Systems; Controls and Displays, DEPARTMENT OF TRANSPORTATION, National Highway

- Traffic Safety Administration, 49 CFR Parts 571 and 585, Docket No. NHTSA 2005-20586, RIN 2127-AJ23
- [5] Tränkler, H.-R.; Obermeier, E. (Hrsg.): Sensortechnik - Handbuch für Praxis und Wissenschaft, Springer Verlag, Berlin, Heidelberg, New York, 1998
 - [6] Bureau of Transport Statistics, <http://www.bts.gov/>, Washington D.C., 2005
 - [7] Association of German Automobile Manufacturers, Export Statistics, <http://www.vda.de/de/aktuell/statistik/>, Frankfurt/M., 2005
 - [8] Polityko, D. D.; Guttowski, S.; John, W.; Reichl, H.: "Physical design and technology parameters for vertical system-in-package integration," Electronics Technology: Meeting the Challenges of Electronics Technology Progress, 2005. 28th International Spring Seminar on Electronics Technology, no.pp. 413- 419, May 19-20, 2005
 - [9] Niedermayer, M.; Polityko, D.; Guttowski, S.; John, W.; Reichl, H.: Entwurfsmethodische Grundlagen zur Miniaturisierung von Autarken Verteilten Systemen, 10. GMM-Workshop Methoden und Werkzeuge für den Entwurf von Mikrosystemen, Cottbus, 21.10.2004
 - [10] Vardaman, E.-J; Carpenter, C.; Matthew, L.: "System-in-Package, The New Wave in 3D Packaging", Market and Technology Research Report of TechSearch International, Austin, Texas, USA, September 2005

R. Thomasius, D. D. Polityko, H. Reichl

Technische Universität Berlin, Sekr. TIB 4/2-1
 Gustav-Meyer-Allee 25
 D-13355 Berlin
 Germany
 thomasius | polityko | reichl@izm.fraunhofer.de

M. Niedermayer, S. Grundmann, S. Guttowski

Fraunhofer IZM
 Gustav-Meyer-Allee 25
 D-13355 Berlin
 Germany
 niedermayer | grundmann | guttowski@izm.fraunhofer.de

R. Achterholt

Global Dynamix AG
 Mövenweg 17, CH 8597 Landschlacht
 Switzerland
 Global-Dynamix-R.Achterholt@bluewin.ch

Keywords: wireless sensors, tire pressure monitoring, 3D integration, 3D packaging

3D-MID – Multifunctional Packages for Sensors in Automotive Applications

D. Moser, J. Krause, HARTING Mitronics AG

Abstract

The MID (molded interconnect devices) technology provides selective metallization in three dimensions on injection molded thermo-plastic substrates and housings. Different technologies can be used to metallize plastic parts. Automotive applications for MID technology are pressure and flow sensors for engine management, air conditioning and crash detection. MR (magnetoresistive) sensors precisely positioned in MID packages are used for motion and position detection. MID provides 3D-positioning of laser diodes and LED's (light emitting diodes) for applications varying from lighting to "adaptive cruise control". Tip switches e.g. for steering wheel can be realized on 3D-MID structures. They require reduced space and allow therefore the integration of more electronic functions.

1 MID Technology Overview

The different MID technologies are primarily separated by the manner how to structure the metallization. The most popular MID methods are 2-shot-molding, LDS (laser direct structuring), LSS (laser subtractive structuring) or hot embossing. These technologies are well known and will not be further discussed here. Each of these technologies has its advantages and drawbacks for specific applications. Relevant criteria of selection are feasibility aspects due to the specific limits of each technology, the required design flexibility and the appropriate cost to investment relationship. Due to the high volumes and the full 3-D capability we usually recommend 2-shot molding as the primary MID technology in automotive applications, mainly driven by cost issues.

2 Advantages of MID Technology for Automotive Applications

Based on current customer projects and requests we identified the following major and unique benefits of MID in automotive applications:

Existing mechanical systems in a car can be “upgraded” with electronics (e.g. with sensors) by means of MID structures without having to redesign the complete system.

3D-MID structures (e.g. for tip switches) allow the integration of more electronics in the limited available space.

Especially for sensor packaging applications the MID technology has the additional advantage of multifunctionality:

- ▶ the package can also serve as substrate for sensor chip,
- ▶ a flow channel can be integrated,
- ▶ pressure port or a tube connection can be realized ,
- ▶ RF antenna can be part of a housing,
- ▶ shielding is a possible option,
- ▶ switches are easily implemented and
- ▶ mechanical and electrical interfaces are part of the housing.

2.1 Design Options

Some of the available MID technologies offer a high design flexibility because high efficient laser processes are used to write the interconnect lines. Therefore customer specific solutions are possible without additional tooling costs. Not only can the electrical connection lines within one package be changed easily, it is also possible to use the laser writing process for marking the devices piece or lot wise if this is required. An advantage of this procedure is that the traceability is realized at an early state of production.

For MID components in micro packaging applications high performance thermoplastic materials such as LCP (liquid crystal polymer) are available. They offer compatibility with lead-free soldering and the processes for chip mounting. The outstanding compatibility with harsh environments is another important aspect of the system integration advantage offered by MID devices, because peripheral devices must withstand hard conditions outside the central electronics boxes.

To complete the functionality of a peripheral electronic or sensor device it has to be connected to the wiring harness in most cases. For actual solutions press-in contacts, with additional soldering or conductive gluing are used to achieve a reliable connectivity interface to the harness. In the near future it is predicted that direct to MID pluggable contacts will be qualified.

2.2 The Options of Multifunctionality using MID in Detail

Mounting chips to a precisely preformed mold body allows to keep narrow tolerances in position and angle with reference to application specific demands. Since high accuracy and high precision (precise angles) are already given by the injection molded part no additional costs for accurate positioning or trimming occur (Fig. 1).



Fig. 1. 3D-MID Package with 2 MR Sensors in 90° tilted position. NCA flip-chip assembly. SMD Package, 1,7 mm overall height

Die bonding, wire bonding, flip-chip and soldering of SMT (surface mount technology) devices are possible on MID substrates (Fig. 2). Consequently MID packages offer the possibility to integrate the entire system functionality into one package. Integration is also the handle to reduce the amount of components. A PCB or Flex-Circuit Board is substituted by the package integrated interconnects.

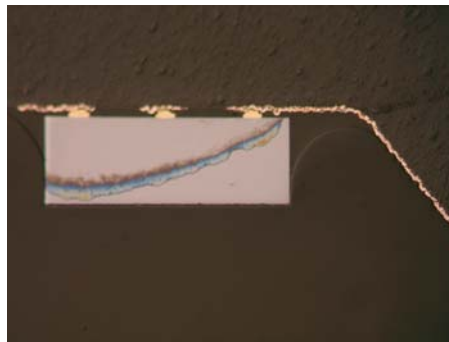


Fig. 2. NCA flip-chip assembly in detail. Cross-section through the contact pads

Keeping the production efforts nearly at device level, but reaching the functionality of a system device, offers potentials for miniaturization and ratio.

3 Examples of MID Sensor Packages in Automotive Applications

Based on running customer projects and requests we identified four main automotive sensor applications where MID based packages are very well suited:

3.1 Pressure and Flow Sensors for Engine Management, Air Conditioning and Crash Detection.

The 3-dimensional design space available using MID technology allows the placement of sensing element and signal conditioning ASIC in optimized positions (Fig. 5). Requirement like

- ▶ short lines between sensor and ASIC for signal quality,
- ▶ double pressure inlet for differential pressure sensing,
- ▶ additional SMD peripherals inside the housing and
- ▶ stress minimizing sensor mounts (Fig. 4)

are achievable.

For a concrete realization a concept with stacked arrangement of the chips and wire bond technology was chosen (Fig. 3).

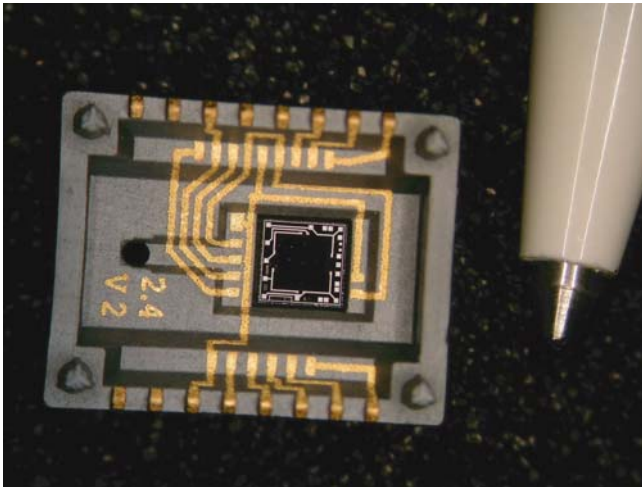


Fig. 3. Pressure sensor in MID package. View into the open package with sensor element mounted

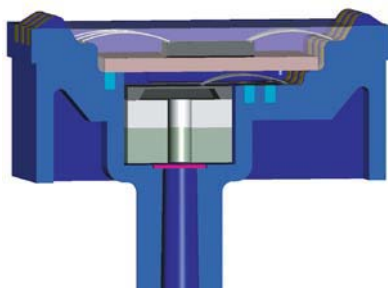


Fig. 4. CAD-cross-section through the completed sensor device. Interposer layers minimize stress on sensor chip.

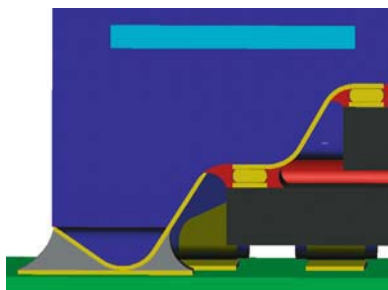


Fig. 5. CAD-cross-section through an alternative design using NCA-flip-chip assembly technology

3.2 MR (Magnetoresistive) Sensors for Motion and Position Detection

MID allows accurate 3D-positioning of MR chips. Special requirements like the nearly coaxial arrangement of two rectangular oriented sensor chips are realizable using MID technology (Fig. 6 & 7).

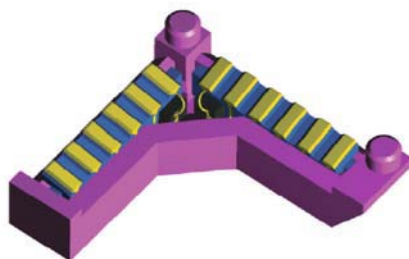


Fig. 6. Rectangular arrangement of 2 MR angular sensors promising precise coaxial alignment [1]

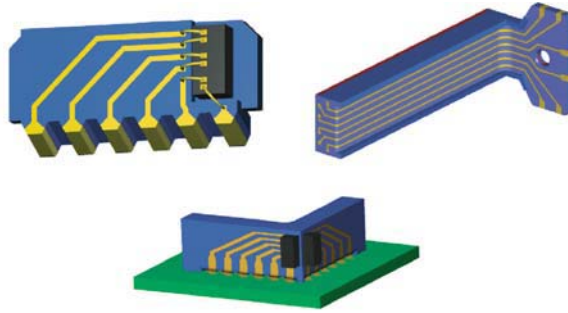


Fig. 7. MID substrates for MR positioning and angular sensors [1]

3.3 Switches on MID

Tip switches are more and more used to make parts of a car to become intelligent. The steering wheel is an example where a human to electronics interface is integrated into a mechanical part. 3D-MID structures require reduced space and allow a 3-dimensional, handling optimized arrangement of switches. A snap dome placed on a MID part makes a switch possible nearly everywhere it is needed. Consequently the integration of more electronic functions can be performed with high customer acceptance.

A switch application using snap domes has been pre-qualified. It was found that MID metallization layers fulfill the requirements for industrial application. After more than 4 Mio cycles the switch samples were still working. This indicates that the industrial requirement to achieve a guaranteed shelf life of 1 Mio. cycles can be fulfilled.

4 Qualification Status

HARTING currently qualifies MID technology including chip and SMD assembly on MID substrates for automotive applications.

The proof of reliability for a new technology is typically given after a decade in field application. HARTING used the established procedures to predict the reliability of MID devices.

Potential failure mechanisms were identified and appropriate accelerated aging test were applied to test samples. Today the reliability of the substrate materials, the metallization layers and the important interconnections are suc-

cessfully proofed. For Laser-Direct-Structuring (LDS) technology in the combination with SMD-and NCA-flip-chip-assembly the full range of standard aging procedures has been successfully passed. This includes 1000 cycles thermal shock -40°C - $+125^{\circ}\text{C}$ and storage in wet heat 85%rH/ 85°C and dry heat 125°C .

To achieve a high design quality for new products, design rules have been derived from the results of the qualification procedures.

Today it is possible to predict a sufficient reliability for selected materials and design conditions.

References

- [1] Franz Jost, Sensitec, Lahnau "Automotive Sensorlösungen in magnetoresistiver Technologie mit besonders kompakter Aufbautechnik" MID Academy, Zürich, November 2005

Dr. David Moser

HARTING AG
Leugenestrasse 10
CH-2500 Biel
Switzerland
david.moser@harting.com

Dr.-Ing. Jens Krause

HARTING Mitronics AG
Technical Marketing
Simeons carré 1
32427 Minden
Germany
jens.krause@HARTING.com

Keywords: MID, molded interconnect devices, substrates, housing, packaging, metallized plastic, 2-shot-molding, LDS, laser direct structuring, LSS, laser subtractive structuring, pressure sensor, positioning sensor, angular sensor, switch on MID, qualification

Towards the Automotive HMI of the Future: Mid-Term Results of the AIDE Project

J. Engström, J. Arfwidsson, Volvo Technology Corporation
 A. Amditis, ICCS I-Sense Group
 L. Andreone, Centro Ricerche Fiat
 K. Bengler, BMW Group Forschung und Technik GmbH
 P. C. Cacciabue, European Commission – Joint Research Centre
 W. Janssen, TNO Human Factors
 H. Kussman Robert Bosch GmbH
 F. Nathan, PSA Peugeot Citroën Automobiles

Abstract

AIDE is an integrated project funded by the EC in the 6th Framework Programme. The project, which involves 30 partners including all major European vehicle manufacturers, deals with behavioural and technical issues related to automotive human-machine interface (HMI) design, with a particular focus on HMI integration and adaptation. The project involves tightly integrated empirical research, driver behaviour modelling and methodological- as well technological development. This paper provides an overview of the mid-term results achieved about half-way through the four-year project.

1 Introduction

Every year, about 45 000 people die and 1.5 millions people are injured in traffic accidents in Europe. It is believed that the great majority of road accidents (about 90-95%) involve human error in the causal chain [1]. Recent empirical work, such as the US 100 car naturalistic field study, has providing an increased understanding of the nature of these errors, pointing to the key role of inattention. For example, 93% of the lead vehicle crashes recorded in the study involved inattention to the forward roadway as a contributing factor [2]. While conventional vehicle safety measures (e.g. seatbelts and airbags) have contributed significantly to the reduction of fatalities in the last decades, their safety contribution is reaching its limits and currently further improvement is difficult to achieve at a reasonable cost. Today, the development of new Advanced Driver Assistance Systems (ADAS, e.g. collision avoidance-, lane-keeping aid- and vision enhancement systems) offers great potential for further improving road safety, in particular by means of mitigating driver errors.

In addition, the number In-vehicle Information Systems (IVIS) increases rapidly in today's vehicles. This systems has the potential to greatly enhance mobility and comfort (e.g. navigation aids & traffic information systems, media players, web browsers, etc), but at the same time increase the risk for excessive and dangerous levels of inattention to the vehicle control task. Furthermore, many IVIS functions are today featured on portable computing systems, often referred to as *nomadic devices*, such as PDAs or advanced mobile phones, which are generally not designed for use while driving. In the near future, these many of these functions could be expected to be easily downloadable from a remote service centre, directly to the vehicle or the nomadic device.

This proliferation of systems and functions that interact with the driver in one way or another leads to a number of challenges, both technical and human factors related, for the designer of the future automotive HMIs. These challenges include the HMI design for the individual systems as well as the question how to integrate a range of different systems into a functioning whole with respect to their interaction with the driver. Another challenge concerns how to best exploit the technological possibilities of adaptive interfaces in the automotive domain. The general objective of the AIDE (Adaptive Integrated Driver-vehicle InterfaceE) project is to address these challenges by means of tightly integrated interdisciplinary work, involving leading human factors as well as technical expertise. Specific topics addressed by the project include:

- ▶ The development of a detailed understanding of the behavioural effects of interacting with different types of in-vehicle functions
- ▶ The design of human-machine interaction (HMI) strategies for ADAS that maximises the safety potential of the systems
- ▶ The design of HMI strategies for IVIS that minimise the added workload and distraction to the driving task
- ▶ The development of strategies for integrating multiple in-vehicle functions into a coherent interface towards the driver
- ▶ The development of technological solutions, e.g. multimodal input-output devices, driver-vehicle-environment monitoring techniques, and an underlying software architecture that supports this
- ▶ The development of solutions for the safe integration of nomadic devices into the driving environment
- ▶ The development of valid and cost-efficient methods for in-vehicle HMI evaluation with respect to safety and usability.

A general goal of the project is the realisation and demonstration of the *Adaptive Integrated Driver-vehicle Interface concept*. This entails a unified human-machine interface that resolves conflicts and exploits synergies between different in-vehicle functions. Some key features of the AIDE concept, further illustrated in Fig. 1, are:

- ▶ *Multimodal HMI I/O devices* shared by different ADAS and IVIS (e.g. head-up displays, speech input/output, seats vibrators, haptic input devices, directional sound output)
- ▶ *A centralised intelligence* for resolving conflicts between systems (e.g. by means of information prioritisation and scheduling).
- ▶ *Seamless integration of nomadic devices* into the on-board driver-vehicle interface.
- ▶ *Adaptivity of the integrated HMI* to the current driver state/driving context. The adaptive interface should also be re-configurable for the different drivers' characteristics, needs and preferences. This requires techniques for real-time monitoring of the state of the driver-vehicle-interface system.

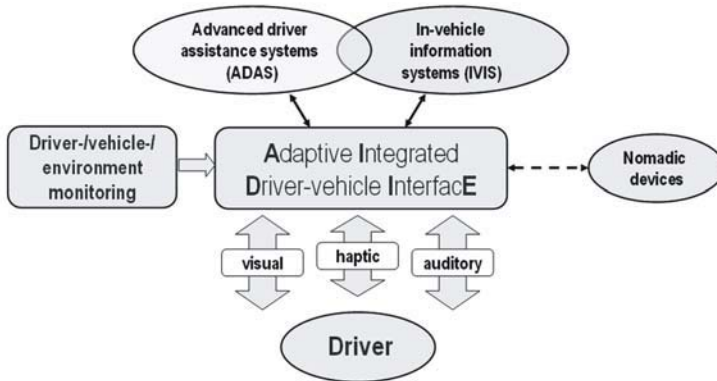


Fig. 1. Illustration of the AIDE Concept

AIDE is a so-called Integrated Project, funded by the European Commission in the Sixth Framework Programme (FP6). It involves 29 partners, including all major European vehicle manufacturers, the main suppliers and a range of leading research institutes and universities. It is part of the EUCAR Integrated Safety Program, which also includes the parallel projects PreVENT, EASIS, GST and APROSYS. The project started in March 2004 and will continue for four years. The objective of this paper is to provide an overview of the results achieved half-way through the project.

The following chapter briefly describes the general structure of the project. Chapter 3 then provides a review of the main results obtained in the four sub-projects so far, and some hints on the next steps to be taken in the second half of the project. Finally, Chapter 4 provides a general discussion on the results obtained so far in relation to the general project objectives.

2 Project Structure

As mentioned above, AIDE is a so-called Integrated Project. This a new instrument introduced by the EC in FP6, where a set of relatively large sub-projects (SPs) are integrated towards a common goal. AIDE consists of four such sub-projects:

- ▶ *Sub-project 1: Behavioural effects and driver-vehicle environment modelling:* The main goal of this sub-project is to develop a generic model and computer simulation of driver-vehicle-environment interaction, focusing on drivers' interaction with ADAS and IVIS. This will be based on empirical results from experiments on short- and long-term behavioural effects of different driver support functions.
- ▶ *Sub-project 2: Evaluation and assessment methodology:* The main goal of this sub-project is to develop a generic valid and cost-efficient methodology for safety- and usability evaluation of in-vehicle functions and to apply this method in the final evaluation of the AIDE prototype vehicles developed in SP3.
- ▶ *Sub-project 3: Design and Development of an Adaptive Integrated Interface:* The general objective of this sub-project is to design the AIDE system and develop the AIDE demonstrator vehicles. This includes the requirement specification, development of the system architecture, HMI design and the definition of HMI strategies, solutions for nomadic device integration, development of DVE monitoring modules and demonstrator vehicle implementation.
- ▶ *Sub-project 4: Horizontal issues:* While most of the research and technological development (RTD) is performed in SP1-3, SP4 contains a number of horizontal activities such as project administrative and technical management, dissemination and exploitation, development of HMI guidelines and standards and internal review and assessment.

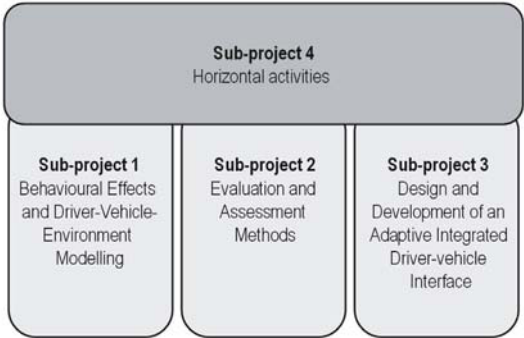


Fig. 2. General structure of the AIDE project

The main expected result from the project is the demonstration of the AIDE concept in three demonstrator vehicles, one city car, one luxury car and one heavy truck. The evaluation methodologies developed in SP2 will be used both during the iterative HMI design and development and in the final evaluation of the demonstrators. Both the SP3 HMI design- and the SP2 methodology development is supported by empirical and analytical results from SP1 on the short- and long-term behavioural effects of in-vehicle systems. Thus, in addition to supporting the overall goal of developing and demonstrating the AIDE concept, each sub-project will deliver important results on their own, in particular the SP1 DVE model/simulation and the SP2 validated evaluation methodology.

3 Review of Mid-Term Results

After about 2 years of work, the project is in the middle of its most intense development and experimental phase. The present chapter provides an overview of the results achieved to date. Naturally, due to the limited space, only general descriptions can be provided here. However, references are provided to sources where more detailed information can be obtained, in particular the AIDE deliverables most of which are available on www.aide-eu.org (where also summaries of the confidential deliverables can be found).

3.1 Sub Project 1: Behavioural Effects of Driving Support Systems and Driver-Vehicle-Environment Modelling

The main goal of SP1 is to develop a detailed understanding about the mechanisms that govern the interaction between the driver, the vehicle (in particular with IVIS and ADAS) and the environment, to be embodied in testable models as well as a computer simulations. The model development is supported by empirical studies on behavioural effects of different types of support systems. Below, the main results to achieved so far are reviewed.

3.1.1 Driver-Vehicle-Environment Modeling and Simulation

The main expected result from this activity is a testable model of the DVE, implemented in a computer simulation, which can be used to investigate potential behavioural effects early in the design process. The results of this work is also an important input to the DVE monitoring module development in SP3 (see section 3.3.6).

The development of the AIDE DVE model is an iterative, incremental procedure which is based on data collected in the AIDE empirical studies on behavioural effects of driver support systems (see next section) as well existing results in the literature. The basic requirements on the model and a preliminary model structure were outlined in Cacciabue et al., [3]. The modelling is based on the general SHELL architecture [4], which is a suitable framework for representing interactions between humans and other elements in the working environment such as support systems and other humans. A major focus so far has been on the identification of the key parameters of the model. At the current stage of development, the following parameters have been identified: (1) Attitudes/personality, (2) experience/competence, (3) task demand, (4) driver state, (5) situation awareness and (6) driver intention/goals. For each parameter, the correlation to measurable variables and other parameters are investigated. The results are documented in Cacciabue et al. [5]. (It could be noted that these parameters correspond roughly to the output vector of the DVE monitoring modules developed in SP3 – see below)

Moreover, a first high-level specification of the simulation software architecture has been developed. The DVE simulation architecture is intended as a generic tool where different types of driver, environment and vehicle models could be implemented and tested. For a further description of the initial DVE simulation specification, see Carusi [6].

3.1.2 Empirical Results from the Learning Phase Experiments

Behavioural effects of in-vehicle functions could be divided into *direct* and *indirect* effects. The former refer to behavioural changes that are intended by the designers of the functions, such as reduced speed resulting from the introduction of a speed alert function. By contrast, indirect effects are non-intended side-effects resulting from the use of a system. Moreover, when studying behavioural effects it is important to distinguish between *short-term effects* that occur during when the driver is learning to use the system, and *long-term effects*, which refers to behavioural changes over a longer period of using the system. For a literature review of known behavioural effects of in-vehicle functions, performed within AIDE, see Saad et al. [7].

In AIDE SP1, two sets of experiments were defined, one focusing on the learning phase, with a particular focus on integration and adaptivity, and the other focusing on long term effects. To date, the learning experiments have been completed. These studies included three coordinated simulator experiments investigating adaptivity of a forward collision warning (FCW) function to (1) driver distraction, (2) road friction and (3) individual driver characteristics.

Moreover, a field experiment addressed learning effects of a standard Adaptive Cruise Control (ACC) system and another field experiment looked at learning effects of speed limiter and cruise control functions with a common interface towards the driver. Finally, yet another field experiment looked at individual and combined effects of forward collision warning (FCW) and lane departure warning (LDW) systems.

An interesting finding from the LDW-FCW experiment, conducted by the Hellenic Institute of Transport, was that subjects tended to properly adapt their behaviour in the intended way when exposed to one of the two systems, while these positive effects did not occur to the same degree when the two systems were active simultaneously. This strongly indicates the behavioural effect of combining two warning systems is not simply additive (i.e. sum of the effects of the systems in isolation) and points to need for integrated warning strategies.

A common finding from the learning phase studies was that individual driver characteristics, such as personality traits, is a key factor influencing behavioural effects and acceptance of driver support functions. For example, in one of the studies on adaptive FCW, conducted by Leeds University, the warning criterion was adapted to the individual driver's reaction time, measured in the simulator prior to the main trials. Thus, in the adaptive system condition, drivers with fast reaction times received the warning later than drivers with slow reaction times. Moreover, personality traits such as sensation seeking were measured as well as the driver's preferred headway. In general, the results showed that both the non-adaptive and adaptive FCW reduced the reaction time to critical events indicating a clear safety benefit of the FCW function. Moreover, for non-aggressive drivers (long-followers and drivers with low-sensation seeking scores), there was no difference in acceptance ratings between the adaptive and non-adaptive systems. However, aggressive drivers (short followers with high sensation seeking scores), rated the adaptive system significantly more useful and satisfactory than the non-adaptive system. Since acceptance of a driver support system is the key to market- and safety impact, this result strongly indicates the value of adapting warning thresholds to individual driver characteristics. Besides feeding the DVE model development, these results thus provide important input to the development of adaptive warning strategies in AIDE SP3, especially with respect to the development of the Driver Characteristics module, with the purpose to record and monitor both static and dynamic driver characteristics (see section 3.3.6). The results from the learning phase experiments will be reported in Deliverable 1.2.3 (which will be finalised after the submission of this paper).

3.1.3 Next Steps, SP1

The main next step of the empirical work in SP1 is the long-term experiments, which will be finalised by August 2006. These experiments will include: (1) The continuation of the FCW-LDW study mentioned above, beyond the learning phase, (2) a larger-scale study of the speed-limiter/cruise control system mentioned above, (3) a long-term study of a product LDW system and (4) a study on long-term effects of Intelligent Speed Adaptation.

The DVE modelling work will continue with refinement of the model based on the empirical results reviewed above, the implementation into a running simulation and the final validation of the model/simulation.

3.2 Sub-Project 2: Evaluation and Assessment Methodology

The main objective of AIDE Sub-project 2 is the development of a generic methodology for evaluation of automotive HMI solutions with respect to safety and usability. In the final stage of the project, the developed methodology will be used in the final human factors evaluation of the AIDE prototypes. Initial work focused on extensive reviews of existing safety and usability methods and tools (see Cherri, Nodari and Toffetti, [8] and Johansson et al., [9]). Subsequent work has focused on parallel development of the individual building blocks of the evaluation methodology, in particular evaluation scenarios, workload/distraction assessment techniques, and methods for relating behaviour/performance measures into measures of risk. The results from the latter activities are reviewed below.

3.2.1 Evaluation Scenarios

The scenario specification is a central topic in the development of a generic HMI evaluation methodology. The scenario specifies the context in which the evaluation takes place, including the test vehicle, the road infrastructure, the traffic conditions and the environmental conditions. The work in AIDE SP2 on evaluation scenario definition has so far focused on collecting relevant information from within and outside the project, and identifying the key building blocks for AIDE evaluation scenario definition. An important first step was to review, and define a taxonomy for, IVIS/ADAS systems (Floudas et al., [10]). Moreover, categorisation schemes for driving simulators, subject groups etc. were defined, and the AIDE design scenarios, defined in SP3, were reviewed and related to the evaluation methodology development. Also, key results from the HASTE and COMUNICAR FP5 EU-funded projects were reviewed.

Based on this, the key building blocks for the AIDE evaluation scenario definition were identified. These building blocks were grouped into three main categories: (1) Road type and conditions (e.g. highway, rural road, visibility conditions), (2) Traffic type and actors (e.g. oncoming traffic, pedestrians etc.) and (3) Tasks and goals (e.g. car following, overtaking, distraction task etc.). The building blocks were then mapped onto the different IVIS/ADAS categories, defined in [10], by means of a matrix representing experts' judgements on the relevance of the different scenario building blocks for the evaluation of each type of system. A similar matrix was also constructed for the simulator/test-vehicle categories. These results are described in Rimini-Döring et al. [11].

3.2.2 Workload and Distraction Assessment Methods and Tools

Substantial work in SP2 has also been performed on methods and tools for offline driver workload and distraction assessment. Key results from this work include:

The Visual Demand Measurement Tool: A software tool for eye and head movement analysis, known as the VDM (Visual Demand Measurement) Tool, was developed. This tool can be used for automated analysis of eye- and head movement data from different eye-tracking systems and contains the basic signal processing algorithms for noise filtering and glance segmentation, a comprehensive set of functions for data management and visualisation as well as an easy-to-use graphical user interface.

Secondary task-based methods: This involved the development of improved methods for secondary task-based measurement of driver workload, resulting in new versions of the Peripheral Detection Task (PDT) method (see e.g. [12] for a description of the original PDT method. While the standard PDT is based on the ability to detect visual stimuli presented in the periphery, the present work investigated a range of different detection task methodologies, including versions where the stimuli were presented in tactile and auditory modalities. In a set of parallel experiments, it was found that the placement of the visual stimuli did not have a significant impact on the sensitivity to secondary task workload. Moreover, the sensitivity was relatively consistent even across modalities. Based on these results, specifications for new tactile and visual detection task methodologies were derived, where tactile was recommended as the default modality. The results from this work are further reported in Merat et al., [13].

Driving performance metrics: Part of this work addressed traditional vehicle control metrics such as speed, headway, lateral control performance and steer-

ing wheel movements, while another sub-task focused on a new influential methodology known as the Lane Change Test (LCT) [14]. The work on traditional metrics was largely based on results and data from the HASTE FP5 EU-funded project, and addressed a number of issues that were left open from this project. Based on some re-analysis of the HASTE data, a subset of vehicle control metrics, considered suitable for the AIDE Evaluation Methodology, were selected and specified in detail. One specific focus in this task was the development of improved steering wheel metrics for workload and distraction assessment. A modified steering reversal rate metric, with different parameter settings for visual and cognitive load, was defined. A set of experiments were also conducted on the Lane Change Test. For example, one of these studies compared LCT results from three different simulator setups: a PC-based low-fidelity set-up, a driving simulator with a plasma screen and a driving simulator with full projection. It was found that simulator set-up did have a significant effect on LCT results, where increasing simulator grade led to decreasing LCT scores (lane deviation values). However, no difference was found with respect to the IVIS tasks included, and thus it could not be determined whether the scores scale linearly between the different set-ups. The results from this work are documented in [15].

Subjective workload scales: This work focused on an experimental comparison of a number of existing subjective workload scales. The scales investigated were (1) PSA-TLX (PSA-Task Load index), (2) the DALI (Driving Activity Load Index) questionnaire and (3) the BMDMW (Behavioural Markers of Driver Mental Workload). The scales were evaluated in 3 parallel experiments: one in simulator and two in real-world conditions. It was concluded that all three methods were sensitive to workload but that they are applicable to different types of evaluation situations and purposes, and thus could be considered as roughly complementary. Recommendations for the application of each method were provided. See Chin et al. [16] for further details.

In the next step, the methods and tools resulting from all these sub-tasks will be empirically compared in a single study and the results fed into the general development of the AIDE evaluation methodology.

3.2.3 The Relation between Behaviour and Risk

One of the most important issues in the entire AIDE project, but at the same time one of the most difficult, is how to estimate the (positive or negative) safety effects of the changes in driver behaviour and state induced by IVIS, ADAS and different integrated/adaptive HMI solutions. This issue is specifically addressed as part of the SP2 work. While existing approaches, such as [2], has

focused on direct accident analysis, the work in SP2 has investigated a range of alternative approaches that should be considered as complementary to accident analysis studies. Specifically, the work has included the identification of basic driver behaviour-risk relations (e.g., between speed and accident risk), based on the literature as well as on new material generated by a re-analysis of data from the HASTE Project. Moreover, an empirical simulator study investigated the relations between situational demand, driving performance and accident risk. Finally, the potential of micro-simulation as a tool for getting to the desired functions was investigated. The results are documented in Jamson et al. [17]. Further work has looked into how the combined effects of behaviour parameters (e.g. speed) and driver state parameters (in particular workload) could be measured, resulting in a pragmatic and quantitative proposed method for mapping behaviour and driver state to risk. See Janssen, Brouwer and Huang [18] for details.

3.2.4 Next Steps, SP2

In the next phase of the project, the results from the parallel activities reviewed in sections 2.2.1, 2.2.2 and 2.2.3 above will be integrated into a generic evaluation methodology, which will be empirically validated in a number of empirical studies. Since the main part of the SP2 development work is focused on IVIS-related evaluation, further input on ADAS-related evaluation methods will also be incorporated from SP1 and the PReVENT sub-project Response 3. Based, on these inputs, the final AIDE evaluation methodology will be specified and applied in the final human factors evaluation of the AIDE prototype vehicles developed in SP3.

3.3 Sub-Project 3: Design and Development of an Adaptive Integrated Interface

SP3 is responsible for the actual design and development of the AIDE system. At the current stage, the specification phase has been concluded and the sub-project is now in the middle of its main design and development phase. The design of the adaptive integrated HMI is performed in an iterative, incremental, way, according to the standard User Centred Design (UCD) procedure. This implies that users are involved from the beginning of the design process, e.g. in evaluating early versions of the systems implemented in virtual prototypes. The final expected result from SP3 is the three prototype vehicles that will demonstrate the AIDE concept. The SP3 design process is supported by empirical results on behavioural effects of ADAS/IVIS from SP1 as well as evaluation methods and tools developed in SP2.

3.3.1 The AIDE use Cases, Design Scenarios and Requirements

The first step in the design and development of the AIDE system in SP3 was to define the scenarios and use cases that the AIDE system should address. This was partly based on a user needs analysis documented in Amditis et al [12]. As described in the introduction, the AIDE system is intended to work as an overall manager of the in-vehicle HMI. Thus the HMI management functions can be considered as meta functions, responsible for managing individual ADAS and IVIS with respect to their interaction with the driver. An example of such a meta function could be to block non-critical information (e.g. phone calls) in demanding driving situations. Since each such meta function generally covers a large number of specific cases (e.g. a phone call/traffic information/email is blocked in an intersection/during overtaking/in a sharp curve), a formal method for defining generalised use cases was needed. Since such a method did not exist, it had to be invented in the project. The result was the definition of a set of generalised problem scenarios, known as the AIDE design scenarios.

The AIDE design scenarios were specified in terms of a formalism using two main types of parameters: (1) application actions and (2) Driver-Vehicle-Environment (DVE) conditions. The actions represent an event initiated by the user or a system while the DVE conditions represent the momentary state of the Driver-Vehicle-Environment system. In order to obtain a generalised description, parameterisation schemes were developed for both the actions and DVE conditions. The actions were described in terms of eight parameters: Initiator {User, System}, Duration {Transient, Sustained}, Safety Criticality {None, Low, High}, Time Criticality {None, Low, High}, Real Time, Mandatory {Yes, No}, Driving Relevance {Yes, No} and Preference {Yes, No}. The DVE conditions were represented by five main parameters: Driving demand, Distraction, Driver Impairment, Driver Intent and Traffic and Environmental Risk. The actions were then classified into a set of priority classes, defined in terms of the action parameters. Based on this categorisation scheme, a set of general AIDE design scenarios were defined. The action and DVE condition parameterisation and classification schemes were also the starting points for the definition of the logic of the AIDE information management functions, implemented mainly by the Interaction and Communication Assistant (ICA, see section 3.3.3). In addition to the generalised AIDE design scenarios, a number of “normal” use cases were defined for nomad device integration and some adaptive HMI functions. The AIDE user needs, use cases and design scenarios are documented in Amditis et al. [12].

Based on the user needs analysis and the defined scenarios and use cases, a set of basic requirements for the AIDE system were derived. These included func-

tional as well as non-functional requirements, where the former refers to the required functionality of the system (e.g. the AIDE meta-functions, the supported I/O devices, supported nomadic device integration functionality etc.) and the latter refers to technological requirements such as scalability, modularity etc. In addition to these general requirements, a set of specific implementation requirements for the three demonstrator vehicles were defined. The AIDE requirements are documented in Kussman et al [20].

3.3.2 The AIDE Software Architecture

Based on the design scenarios and requirements, a general software architecture for the AIDE system was developed. This work focused on high-level, logical, architecture descriptions, which are largely independent of the underlying electronics HW and SW architecture (e.g. bus systems, gateways, middleware etc.). However, it is obviously important to identify the requirements that the AIDE logical architecture put on the general electronics architecture. This topic is currently addressed in cooperation with the parallel EASIS EU-funded project. The general role of the AIDE-specific architecture work was to define the main logical components, their roles and mutual relations.

The key components in the AIDE system are the Applications, the I/O devices, the Interaction and Communication Assistant (ICA) and the Driver vehicle environment (DVE) monitoring modules. The basic principles behind the architecture are illustrated in Fig. 3. Applications communicate with ICA by means of four types of messages. The *Application Request Vector (ARV)* is used to ask ICA for permission to execute an action (e.g. presenting output). The application request consists of a vector with action parameters, similar to the vector used in the AIDE design scenarios (described above). Based on the application request, the ICA assigns the action to a priority class. Based on this priority, the presence of other possible running actions and the current DVE state, the ICA decides which HMI strategy to apply. A *Reply Vector (RV)* is then sent back to the application which acts accordingly (e.g. by modifying postponing or terminating the action). If an application has finished an action it has to inform the ICA, using the *Channel Status Vector (CSV)*. Moreover, if a requested output becomes invalid during a postpone phase, the application informs ICA about the new status using the *Request No More Valid Vector (RNV)*.

An important property of this architecture solution is that, due to the fact that the ICA only operates on the action parameters (and not directly on the action content), applications can be added and removed without the need to change the ICA software. This greatly enhances flexibility and modularity. Moreover, since the priority assignment is done in the ICA, the vehicle manufacturer has

a certain control over the prioritisation strategy. However, it should be noted that this requires standardised protocols for the request and reply vectors. Another important issue concerns the role of the applications. While true HMI integration inevitably will influence the individual applications, it is desirable to keep this influence as small as possible. In the AIDE architecture, the main addition to the applications is the software needed to implement the communication with the ICA, a sub-component known as the *AIDE interface adapter*. By means of structuring the application according to the model-view-control pattern [21, illustrated in Fig. 3], a logical separation between the basic application SW and the AIDE-specific additional SW can be obtained, which greatly facilitates the SW development process.

The role of the Driver-Vehicle-Environment (DVE) monitoring component is to feed both the ICA and the applications with a momentary representation of the DVE state, which is represented by a DVE vector similar to the representation used in the AIDE design scenario descriptions. The DVE vector also includes a representation of static and dynamic driver characteristics, provided by the Driver Characteristics module. The DVE modules are further described below in section 3.3.6. See Kussman et al. [22] for a more detailed description of the AIDE architecture.

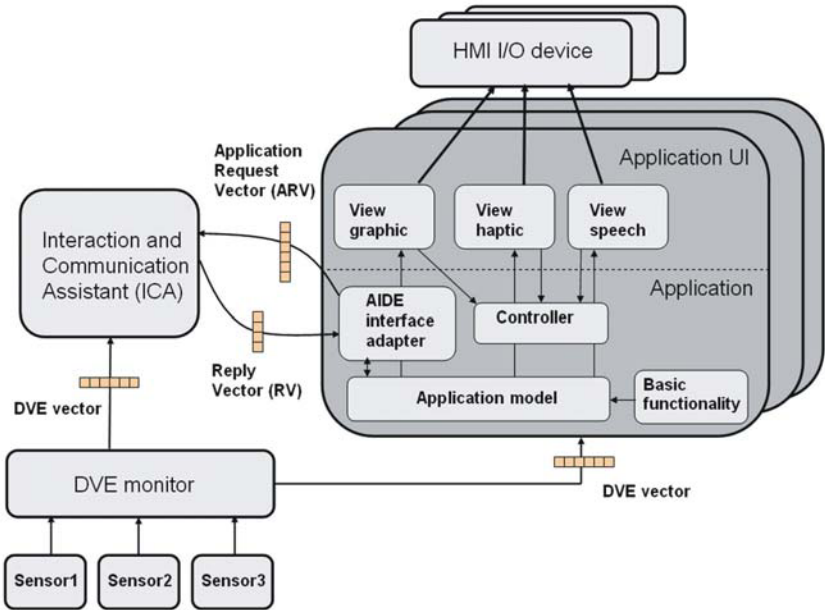


Fig. 3. Basic principles of the AIDE architecture

3.3.3 General HMI Strategies and the Interaction and Communication Assistant

The AIDE HMI strategies include the basic HMI design and configuration (i.e. the default mapping of actions, formats and input/output channels) as well as the dynamic information management taking into account the DVE state interdependencies (e.g. conflicts) between applications. The component with the main responsibility for realising the HMI strategies is the Interaction and Communication Assistant (ICA). The ICA can be viewed as the "brain" of the AIDE system and is responsible for the centralised management of the integrated HMI by implementing the AIDE meta functions mentioned above. This is based on real-time context awareness provided by the DVE monitoring modules. Specifically, the ICA implements the logic that determines if, when and how information should be presented to the driver. Thus, the ICA handles conflicts between applications (e.g. by means of prioritisation or change of output channel) as well as conflicts between individual applications and the driving task (e.g. by means of delaying non-critical information in demanding driving situations). As described above, a basic principle behind the AIDE solution for HMI integration is that each application always requests permission from the ICA before executing an action, using the application request vector (ARV) format described above. The application request is handled by the ICA logic series of steps, implemented in four distinct sub-modules:

- ▶ *The Priority Manager*: Receives the application requests and assigns a priority to the requested action based on the information in the ARV.
- ▶ *The Filter*: Decides whether the action can be presented given the current DVE conditions (as provided by the DVE monitoring modules).
- ▶ *Modality Selector*: Decides the whether modality (e.g. intensity, format etc.) of the message should be adapted according to the current DVE conditions. If not the request is put in a waiting queue until the DVE condition changes.
- ▶ *The Channel Selector*: Decides the output channel for the action. For each action, a primary (preferred) and optionally a secondary, output channel is specified in the ARV. The Channel module first checks whether the primary channel is free and, if not, the availability of the secondary channel is checked (given that the HMI strategies permit presentation in the secondary channel). If all channels are blocked, the request is put in a waiting queue.

When the HMI strategy has been decided, the ICA informs the application with a Reply Vector (RV) in a specified format. The internal ICA architecture and its relation to the other main AIDE components are further illustrated in Fig. 4.

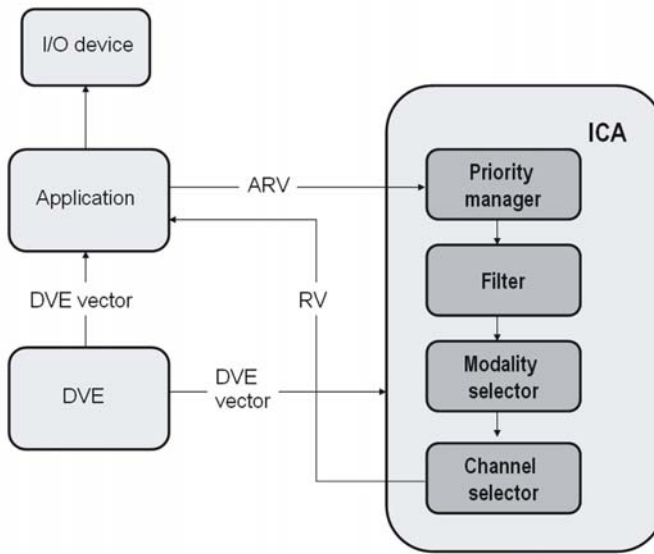


Fig. 4. Basic Principles of the ICA Logic

In order to perform early testing of the ICA logic, a special-purpose simulation tool has been developed. The main objective of this tool is to visualise and test the internal ICA logic and its interaction with other components. For more details on the ICA development, see Deregibus et al. [23].

In addition, specific work is devoted to the design of integrated and adaptive ADAS HMI strategies, in close collaboration with the INSAFES sub-project in the PReVENT IP (www.prevent-ip.org). It should be pointed out that, in the AIDE architecture, the ICA is not responsible for handling conflicts between strongly safety- and time critical warnings. The main reason for this is that this particular type of conflict resolution is difficult to separate from the application's own warning strategy. Thus, assigning this responsibility to the ICA would blur the responsibility between the ICA and the application which would create a dependency between the application and the ICA. Such a dependency would violate the basic requirements of modularity and scalability stated above. Thus, the adopted solution was to assign the responsibility for time-critical ADAS conflict resolution to a specific ADAS HMI manager (to be developed in INSAFES). However, the ADAS HMI manager always needs to an ARV request to the ICA, and await a reply, in order to avoid potential conflicts with other applications (e.g. the case when a sound warning is initiated while the radio plays loud music). Thus, the ADAS HMI manager has the same logical role in the AIDE architecture as a "normal" application.

3.3.4 HMI Input/Output Development and the AIDE Virtual Prototypes

While the AIDE solution should support the whole spectrum of input/output (I/O) HMI devices, the actual I/O device development in the project focuses on a smaller set of devices including speech input/output, multifunctional haptic input devices, head-up displays, configurable displays and tactile seats. While some software and hardware development of individual I/O devices is performed in the project, the main focus is on developing solutions for *integrating* multiple I/O devices into a functioning whole.

At the current stage of development, the first versions of the AIDE Virtual Prototypes (VPs) are being finalised. These represent first implementations of the AIDE system in driving simulator environments, which allow for early user testing of different HMI solutions. For the first user tests, two Virtual Prototypes have been developed, one car- and one truck version (the car VP will evaluate both the Seat and Fiat HMI solutions). The very first version of the Truck VP is illustrated in Fig. 5 below. The Virtual Prototypes will contain most of the envisioned AIDE HMI functionality, including simulated applications, dialogue structures, graphical layouts, I/O devices, and some of the AIDE meta functions. However, in these initial tests, some of the functionality will not be implemented in real-time but rather simulated by means of Wizard-of-Oz techniques.



Fig. 5. The first version of the AIDE truck virtual prototype: The graphics for the configurable instrument cluster (top left), the simulated infotainment application (top right) and the truck mock-up with some of the prototype HMI I/O devices (bottom)

3.3.5 Nomadic Device Integration

Another important topic addressed in the AIDE project is the integration of nomadic devices (ND), i.e. mobile devices such as Smartphones and PDAs. Work in AIDE on this topic involves both the technical development of possible solutions for ND integration as well as the establishment of the Nomadic Device Forum. Technical results to date include the identification of the key use cases and basic architectural requirements [19-21]. Moreover, a potential integration solution, based on a Bluetooth protocol developed by Motorola, has been identified. This solution will be implemented and demonstrated during the second half of the project.

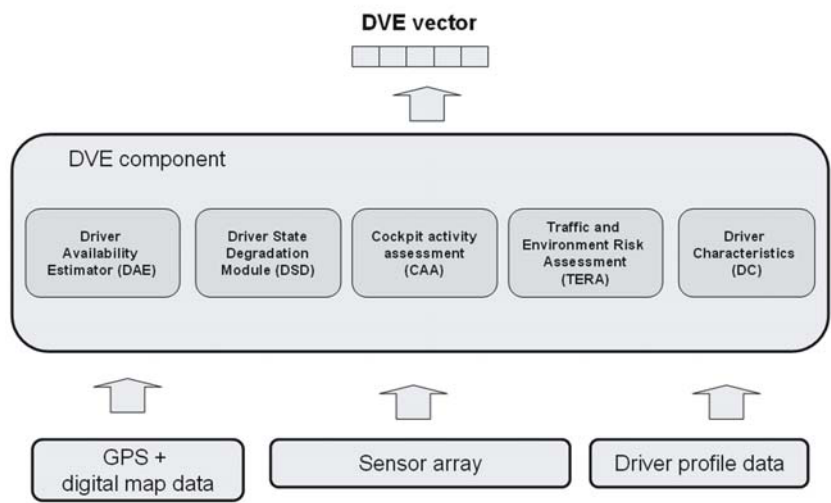


Fig. 6. The architecture of the Driver-Vehicle-Environment modules in AIDE

The Nomadic Device Forum is a consortium of vehicle manufactures, electronic device manufacturers and telecom industries, public authorities and other stakeholders with an interest in integration of ND into vehicles. The forum is being run by ERTICO and during its first year of operation, several workshops have been held. Topics addressed by the forum include both technical- (e.g. how can ND integration be achieved and which are the most feasible protocols) and strategical issues (e.g. which are the key business models for the different stakeholders). The forum can be accessed at: <http://ndf.itsnomadic.net/>

3.3.6 Real-Time DVE Monitoring

As described above, the purpose of the DVE monitoring is to provide a real-time assessment of the Driver-Vehicle-Environment state that can be used by the ICA, or directly by the applications, to enable the adaptive HMI functionality defined by the AIDE design scenarios and use cases. The general architecture of the DVE modules is illustrated in Fig. 6.

As illustrated in Fig. 5, all DVE modules have access to a shared sensor array. This includes driver sensors (e.g. eye-/head-/eyelid tracking), vehicle sensors (e.g. steering wheel angle sensor, pedal sensors, gyros etc.) and environment sensors (e.g. radar, laser, video). Moreover, a digital map database plus global position data is used. Other input data includes static driver profile data entered by e.g. a smart card.

Each of the DVE monitoring modules is responsible for a specific dimension of the DVE space. The main role of the respective modules are:

Driver Availability Estimation (DAE) module: Computes an estimation of the availability of the driver to receive information, as determined by the demand of the primary driving task. This is based on vehicle sensor- as well as digital map data.

Driver state degradation (DSD) module: Computes an estimation of the current drowsiness state, based on a combination of physiological and behavioural sensor data.

Cockpit activity assessment module (CAAM): Computes an online estimation of the driver's secondary task activity and (visual and cognitive) distraction level and. The main input is eye-/head tracking data, although other information sources such as lane tracking data and in-vehicle button presses are used as well.

Traffic and environment risk assessment (TERA) module: Computes estimates of traffic and environment risk mainly based on environment sensing, but also digital map data. This also includes estimation of drivers' intent to perform driving manoeuvres, partly based on input from the CAAM module.

Driver Characteristics (DC) module: Maintains a static record of driver characteristics and preference, based on driver identification (e.g. by means of smart card) but also computes a dynamic profile of driver characteristics (e.g. reaction time, preferred following distance etc.) computed from sensor data.

At the current state of development, first versions of the software for the modules have been released [26].

3.3.7 Next Steps, SP3

During the second half of the project, the development of the AIDE components will continue with iterative design and evaluation of virtual prototypes. In this process, AIDE simulations and prototypes will be developed and tested by a range of vehicle manufacturers, such as Seat, Fiat, Volvo, Ford, Renault and Peugeot-Citroën. In the final step, these components will then be integrated in the three main AIDE demonstrator vehicles, a city car developed by Seat, a luxury car from Fiat and a heavy truck from Volvo. When the demonstrator vehicles have been technically verified, they will be handed over to SP2 for human-factors evaluation. In parallel, the nomadic device forum will continue its activities.

3.4 Sub-Project 4: Horizontal Activities

While most of the work in SP4 is related to the day-to-day management of the project, some important technical work has been performed as well. In particular, this SP includes work on development of guidelines and proposals for new standards based on input from SP1-3. So far, this work has mainly included a review of existing guidelines and standards [27], while the actual development will take place in the second half of the project. This work has also supported the update of the European Statement of Principles on HMI, conducted during 2005.

Another result from SP4 is the development of a general conceptual framework, intended to be used as a common language to conceptualise key issues related to HMI and driver behaviour. The framework is based on the COCOM/ECOM model [28] and is further described in [29]. A short description of the framework and its intended application in the AIDE project can be found in [30] the AIDE Interaction Plan [29]. This deliverable also describes the plan for interaction between the AIDE SPs and with other related projects, such as PReVENT, EASIS, GST and HUMANIST. The

4 Discussion: Towards the Future Automotive HMI

This paper has provided an overview of the mid-term results from the AIDE project. This section provides a concluding discussion on these results in relation to the key objectives of the project, and points out some key issues that need to be further addressed in the second half of the project.

4.1 HMI Design for Maximising Safety Effects

The design of warning/intervention strategies is critical for the ability of an ADAS to increase safety by changing driver behaviour in the desired way. If the warning is not properly designed, the driver may ignore it or shut the system off altogether. An important point is that it is clearly not meaningful to separate the warning strategies from their application. Thus, the ongoing work on warning strategies in AIDE always needs to be tightly integrated with the application development in PReVENT.

A particular issue of great interest for AIDE is the possibility of *adaptive* warnings. Warning timing and/or intensity could be adapted to a number of situational factors, such as individual driving style, driver distraction, drowsiness and road condition. While this is clearly technologically feasible today (Toyota has announced that they will put a distraction-adaptive FCW system on the market early 2006), there are many tricky HMI-related issues still left open. For example, since the driver is also a (very advanced) adaptive system, it is likely that he/she will compensate for system adaptations that are not in line with his/her motives. Thus, the behavioural effects of adaptive warnings (e.g. in terms of brake reaction time) may not always be easy to predict. However, the SP1 results showed that adaptation of warning criteria to the individual driving style could enhance acceptance, especially for aggressive drivers. Another issue to consider is that system adaptivity also reduces predictability, which makes it more difficult for the driver to create a proper mental model of the system behaviour. Thus, while some types of adaptive functions may be useful, others may not. The potential of adaptive warnings will be further investigated in the virtual prototyping and testing in SP3, based on the empirical results from SP1. The prediction of the mutual adaptations between the driver and adaptive warning systems is also a key application for the DVE model/simulation.

4.2 HMI Design for Minimising Safety reducing Effects of in- Vehicle Systems

A further important aim of the AIDE project is to develop HMI solutions that minimise the negative effects of individual in-vehicle systems in terms of distraction and workload. A first step towards this goal is the development of valid and reliable methods for assessing distraction and workload and their effects on driving performance. The work in SP2 has focused on comparing and refining existing methods and resolving a number of open issues from previous projects such as HASTE, RoadSense and ADAM. However, a further key issue concerns how distraction, workload distraction and driving performance measures could be related to actual safety. Work in SP2 has investigated a range of approaches to address this difficult problem, as a complement to direct accident analysis [17-18]. In the next step, these approaches will, together with the work on evaluation scenarios [11], be integrated into the generic AIDE evaluation methodology. By applying this methodology, it should be possible to compare different HMI design alternatives with respect to their (positive and negative) effects on road safety.

Another approach for minimising excessive workload and distraction is by means of active workload management, e.g. re-scheduling of non-critical information in demanding driving situations. In AIDE, this functionality is implemented by the ICA, based on input from the DVE monitoring modules (in particular DAE and TERA). An important issue concerns the extent to which these types of functions are accepted by different user groups. An important issue for SP2 to consider concerns how to evaluate these types of meta-functions with respect to their expected safety enhancements.

4.3 HMI Integration

While the discussion so far has focused mainly on HMI issues related to individual systems, perhaps the most important issue addressed by the AIDE system is *HMI integration*. This is a problem that has to be solved if the full potential of driver support technologies, in terms of safety and mobility, should be realised. Perhaps the most straightforward reason for this is the packing problem - if every application had its own dedicated HMI, the HMI devices would simply not fit into the vehicle cockpit. However, there are also a number of human factors-related reasons for why HMI integration is needed. As the results from the SP1 learning studies show, the individual effects of two systems may not add up to their effects in combination. For example, if two warning systems are added on top of each without any further integration, the number of warnings presented to the driver will be doubled, with the possible

result that the driver's "acceptance threshold" is reached and the warnings ignored (this is one likely explanation for the results in the SP1 study).

HMI integration can be achieved in different ways. The most basic approach (which should always come first) is to take into account interdependencies between functions from the early stages of the design process. This also includes the design of the basic HMI configuration and the definition of a proper mapping between functions and I/O devices. A key human factors challenge here is to enable the user to establish a correct mental model of the relation between the shared I/O devices and the different functions that they control.

However, a further possibility is to use real-time centralised HMI management to resolve conflicts between applications, e.g. actions presented simultaneously. A key issue here which types of information that can be presented simultaneously and in which cases conflict resolution is needed, e.g. by means of prioritisation or a changing the output modality. These and other issues will be investigated in the forthcoming virtual prototyping tests in SP3, but also in the evaluation method development in SP2.

HMI Integration also leads to many technological challenges. In particular, how can a many-to-many mapping between applications and I/O devices be efficiently implemented, and how can we handle the strong requirements on re-configurability and scalability. The AIDE architecture [22] has been developed in order to satisfy these requirements. In the further work, it is important that the proposed architecture solution is continuously validated against these requirements, and discussed with external stakeholders, in particular architecture experts from related projects such as EASIS, PReVENT and GST.

4.4 Conclusion

The AIDE project integrates, for the first time in Europe, major efforts on driver behaviour research, evaluation method development and technological HMI development in a single multidisciplinary project. The mid-term results presented in this paper constitutes important steps towards a future integrated and adaptive automotive HMI, both from a technical and human factors point of view. However, much hard work remains in order to reach the final objective of the project, i.e. the on-road demonstration of the AIDE concept in three validated demonstrator vehicles.

References

- [1] Treat, J., R., Tumbas, N.S., McDonald, S.T., Shinar, D., Hume R.D., Mayer, R.E., Stansifer, R.L and Castellan, N.J. 1977. Tri-level Study of the Causes of Traffic Accidents: Final Report – Executive Summary. Technical Report DOT HS 805 099. US Washington DC: Department of Transportation, National Highway Safety Administration.
- [2] Neale, V. L., Dingus, T.A., Klauer, S.G., Sudweeks, J. and Goodman, M. 2005. An Overview of the 100-car Naturalistic Study Findings. Paper presented at the 19:th International Technical Conference on Enhanced Safety of Vehicles (ESV), Washington DC, June 6-9, 2005.
- [3] Cacciabue, P. C. Macchi L., Martinetto M., Saad, F., Tango, F., Cañas, J.J. and Alonso, M. 2004. Requirements for HMI Design and Driver Modelling. AIDE Deliverable 1.1.1b.
- [4] Hawkins, F.H. 1987. Human Factors in Flight. Gower: Aldershot, UK.
- [5] Cacciabue, P. C., Macchi, L., de Grandis, E., Alonso, M., Ramos, G., Plaza, J., Amditis, A., Carsten, O., Carusi, E., Engström, J., Hollnagel, E., Letziou, Z., Papakostopoulos, V., Saad, F. and Tango, F. 2005. Parameters and indicators of behavioural adaptation to ADAS/IVIS for inclusion in DVE model for preliminary design of AIDE system. AIDE Deliverable 1.1.3.
- [6] Carusi, E. 2005. DVE Simulation architecture and preliminary guidelines for model software implementation. AIDE Deliverable 1.3.1.
- [7] Saad, F., Hjälm Dahl, M., Canas, J., Alonso, M., Garayo, P., Macchi, F., Nathan, F., Ojeda, L., Papakostopoulos, M., Panou, M. and Bekiaris, E. (2004). Literature Review of Behavioural Effects. AIDE Deliverable 1.2.1.
- [8] Cherri, C., Nodari, E., Toffetti, A. 2004. Review of existing Tools and Methods. AIDE Deliverable 2.1.1.
- [9] Johansson, E., Engström, J., Cherri, C., Nodari, E., Toffetti, A., Schindhelm, R. and Gelau, C. 2004. Review of existing techniques and metrics for IVIS and ADAS assessment. AIDE Deliverable 2.2.1.
- [10] Floudas, N., Amditis, A., Keinath, A., Bengler, K. and Engeln, A. 2004. Review and Taxonomy of IVIS/ADAS applications. AIDE Deliverable 2.1.2.
- [11] Rimini-Döring, M., Keinath, A., Nodari, E., Palma, A., Toffetti, A., Floudas, N., Bekiaris, E., Pourtoui and Panou, M. 2005. Considerations on Test Scenarios. AIDE Deliverable 2.1.3.
- [12] Olsson, S., & Burns, P. (2000). Measuring distraction with a peripheral detection task. On-line paper. NHTSA Internet Distraction Forum. Available at www.nrd.nhtsa.dot.gov/departments/nrd-13/driver-distraction/welcome.htm
- [13] Merat, N., Johansson, E., Engström, J., Chin, E., Nathan, F. and Victor, T. 2005. Specification of a secondary task to be used in Safety Assessment of IVIS. AIDE Deliverable 2.2.4.

- [14] Mattes, S. (2003). The lane change task as a tool for driver distraction evaluation. In H. Strasser, K. Kluth, H. Rausch, and H. Bubbs (Eds.). *Quality of Work and Products in Enterprises of the Future*. (pp. 57-60). Stuttgart: Ergonomia Verlag.
- [15] Östlund, J., Peters, B., Thorslund, B., Engström, J., Markkula, G., Keinath, A., Horst, D., Mattes, S. and Foel., U. 2005. *Driving Performance Assessment, Methods and Metrics*. AIDE D2.2.5.
- [16] Chin, E., Nathan, F., Pauzié, A., Manzano, J., Nodari, E., Cherri, C., Rambaldini, A., Toffetti, A. and Marchitto, M. 2004. *Subjective Assessment Methods for Workload*. AIDE Deliverable 2.2.6.
- [17] Jamson, S., Batley, R., Portouli, V., Papakostopoulos, V., Tapani, A., Lundgren, J., Huang, Y-H. and Hollnagel, E. 2006. *Obtaining the functions describing the relations between behaviour and risk*. AIDE Deliverable 2.3.1.
- [18] Janssen, W. H., Brouwer, R.F.T and Huang, Y. 2005. *Risk trade-offs between driving behaviour and driver state*. AIDE Deliverable 2.3.2
- [19] Amditis, A., Bolovinou, A., Engström, J., Kussmann, H., Placke, L., Bekiaris, E., Panou, M., Gaitanidou, E., Andreone, L., Deregibus, E., Kompfner, P. and Robertson, P. 2005. *AIDE Scenarios and Use Cases Definition*. AIDE Deliverable 3.2.1.
- [20] Kussmann, H., Modler, H., Engström, J., Agnvall, A., Piamonte, P., Markkula, G., Amditis, A., Bolovinou, A., Andreone, L., Deregibus, E., Kompfner, P., Robertson, P., de Miguel Garcia, N., Feron, A., Berninger, H., Couvreur, C., Bellet, T., Scholliers, J. and Kutila, M. 2005. *Requirements for AIDE HMI and safety functions*.
- [21] Gamma E., Helm, R., Johnson, R and Vlissides, J. 1995. *Design Patterns. Elements of Reusable Object-Oriented Software*. Addison Wesley.
- [22] Kussmann, H., Modler, H., Bolovinou, A., Amditis, A., Robertson, P., Deregibus, E., Engström, J., Piamonte, P., Pringle, A., Scholliers, J., Feron, S., Kompfner, P., and Couvreur, C. 2005. *System architecture, data flow protocol definition*. AIDE Deliverable 3.2.2.
- [25] Deregibus, E., Bianco, E., Andreone, L., Bolovinou, A., Kussmann, H., La Tendresse, I., , van den Beukel, A., Pringle, A., Markkula, G., Marberger, C., Romera, M., Bellotti, F., and Couvreur, C. 2005. *Driver-vehicle interaction and communication management*. AIDE Deliverable 3.4.1.
- [26] Boverie, S., Bolovinou, A., Polychronopoulos, A., Amditis, A., Bellet, T., Tattègrain-Veste, H., Manzano, J., Bekiaris, E., Panou, M., Portouli, E., Kutila, M., Markkula, G. and Agnvall, A. 2005. *AIDE DVE Monitoring Modules – Design and Development*. AIDE Deliverable 3.1.1.
- [27] Schindhelm, R. and Gelau, C., Keinath, A., Bengler, K., (BMW); Kussmann, H., Kompfner, P., Cacciabue, P. C. and Martinetto, M. 2004. *Report on the review of the available guidelines and standards*. AIDE Deliverable 4.3.1
- [28] Hollnagel, E. & Woods, D. D. (2005). *Joint cognitive systems: Foundations of cognitive systems engineering*. Boca Raton, FL: Taylor & Francis/CRC Press.

- [29] Engström, J. and Hollnagel, E. 2005. Towards a conceptual framework for modelling drivers' interaction with in-vehicle systems. In *Proceedings of Modelling Driver Behaviour in Automotive Environments*, Ispra, Italy.
- [30] Engström, J. Interaction Plan, M13-30. AIDE Deliverable 4.0.1.

Johan Engström

Volvo Technology Corporation
 Götaverksgatan 10, 405 08 Göteborg
 Sweden
johan.a.engstrom@volvo.com

Jan Arfwidsson

Volvo Technology Corporation
 Götaverksgatan 10, 405 08 Göteborg
 Sweden
jan.arfwidsson@volvo.com

Angelos Amditis

ICCS-NTUA
 9 Iroon Politechniou str.
 15773 Zografou, Athens
 Greece
a.amditis@iccs.gr

Luisa Andreone

Centro Ricerche Fiat
 Strada Torino 50, 10043 Orbassano, Torino
 Italy
luisa.andreone@crf.it

Klaus Bengler

BMW Group Research and Technology
 Hanauerstr. 46 D-80788 München
 Germany
klaus-josef.Bengler@bmw.de

Pietro Carlo Cacciabue

EC, Joint Research Centre
 Institute for the Protection and Security of the Citizen
 21020 Ispra (VA)
 Italy
pietro.cacciabue@jrc.it

Wiel Janssen

TNO Human Factors
Kampweg 5, 3769 DE Soesterberg
Netherlands
janssen@tm.tno.nl

Holger Kußmann

Robert Bosch GmbH
Robert Bosch Straße 200, 31139 Hildesheim
Germany
holger.kussmann@de.bosch.com

Florence NATHAN

PSA-Peugeot-Citroen
VV014- route de Gisy, 78943 Vélizy-Villacoublay
France
florence.nathan@mpsa.com

Keywords: human machine interface, human machine interaction, integration, adaptivity, workload management, driver behaviour, modelling, HMI evaluation methods

Accidentology as a Basis for Requirements and System Architecture of Preventive Safety Applications

M. Schulze, DaimlerChrysler AG

J. Irion, Irion Management Consulting

T. Mäkinen, Technical Research Centre of Finland (VTT)

M. Flament, ERTICO - ITS Europe

Abstract

PREVENT takes a first comprehensive step towards realising the vision of a safety zone around vehicles by means of complementary safety functions. The most critical accident scenarios are covered by the applications developed. The integration aspects of the project demonstrate a number of different applications on one platform and making a seamless time to collision horizon from tens of seconds down to zero. Due to the multi-causal nature of accidents and a certain randomness, safety systems with continuous alert and early warning are needed. The foundation for requirements are laid in the analysis of driver behaviour and accidents, followed by a definition of functions needed from a vehicle to prevent the accident from happening or mitigating its consequences. The requirements database was created and requirements were classified into six main categories. A common PREVENT architecture is presented and highlighted with a detailed description of a sub-project focusing on lateral safety applications.

1 Introduction and Background

The Integrated Project PREVENT takes a first comprehensive step towards realising the vision of a safety zone around vehicles by means of complementary safety functions. Their subsequent integration into an overall safety system is expected strongly to reduce the number traffic accidents in the future. An additional step towards integration is taken by the INSAFES (INtegrated SAFETY Systems) subproject demonstrating a number of applications on one platform only.

Another integration aspect of the project is to create a seamless time to collision horizon from tens of seconds down to zero ranging from information from map navigation and wireless messages to potential danger warnings to colli-

sion mitigation (Fig. 1). This time continuum was deduced from the accident analysis and in-depth studies showing that both driver state and driver behaviour (accident causes) and accident situation (typology/scenarios) need to be known when optimal safety functionalities and applications are planned. Especially, knowledge of a multiple causation nature of accidents helps in creating applications concentrating on driver state and behaviour monitoring and communication systems beyond the on-board sensor capability.

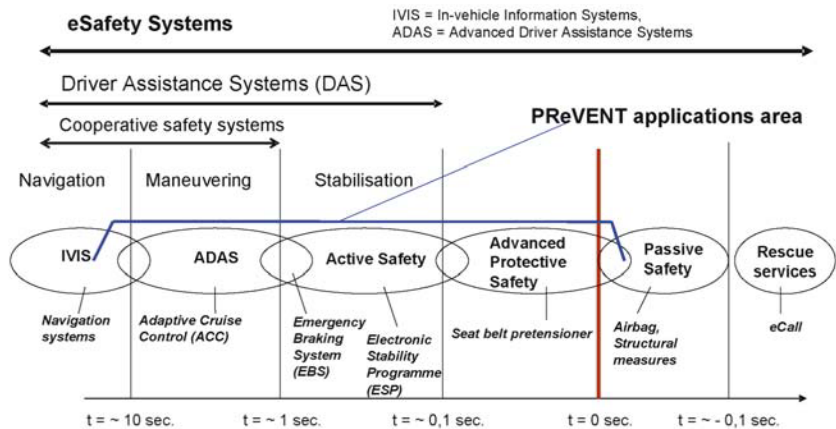


Fig. 1. Seamless time to collision horizon by means of different safety applications.

PreVENT focuses on the most critical accident scenarios such as the loss of longitudinal and lateral control leading to head-on and lateral collisions, run-off the road accidents and turning and crossing accidents. By analysing the driver behaviour and accidents, a set of requirements has been derived for each of the PreVENT applications. Eventually, the different requirements lead to a common PreVENT architecture.

Three basic layers are identified: perception, decision (application) and the action layer. The perception layer uses the sensors that range from onboard sensors such as short and long range radars, cameras and laser scanners to GPS signal in conjunction with digital maps and even to vehicle-to-vehicle and vehicle-to-infrastructure communication. In terms of enabling technologies, the project concentrates mainly on onboard sensors and digital map interface for ADAS applications. The perception layer performs low-level and high-level data fusion and sends a set of abstracted parameter representing the state of the vehicle to the application layer. The map interface supports the perception by providing a priori information on the known environment. The application layer assesses the situation such as the need for a collision warning, the need

for a lane keeping function or an emergency braking. It decides what to do and passes the decision to the action layer. The action layer issues warnings via an appropriate HMI or engages vehicle control actuators such as steering, brakes as demanded by the threat level of the potential accident situation.

The paper is organised as follows: First it is shown how the accident scenarios considered in PReVENT lead to the requirements of the active safety functions an how they are gathered to form a requirement data base that allows a systematic system specification and, later on, lead to their evaluation and assessment. The next section describes the overall PReVENT system architecture that is derived from the requirements and gives examples for their actual realisation. Subsequently it is elaborated how the singular safety functions will be integrated into a single platform in the later phases of PReVENT. Finally, a conclusion section discusses the significance and issues in realising the PReVENT vision.

2 From Accident Scenarios to Requirements

In addition to previous work in intelligent vehicle area, PReVENT safety requirements had its impetus from both EU- and national safety programmes. The foundation for requirements were laid in the analysis of driver behaviour leading to accidents, followed by actions needed from a vehicle to prevent the accident from happening or mitigating its consequences (Fig. 2).

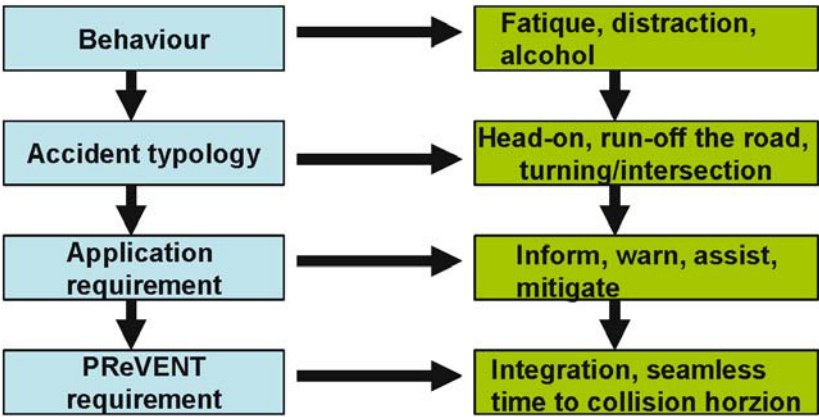


Fig. 2. Overall process of laying basis for the detailed definition of PReVENT requirements.

As indicated in Fig. 2, the most frequent accident scenarios are dealing with loss of longitudinal and lateral control leading to head-on and lateral collisions, run-off the road accidents and turning and crossing accidents. These scenarios are analysed, and a set of requirements has been derived for each of the PREVENT function fields and systems. After a grouping and classification process, a synthesis of the high level requirements covering the driving scenarios from information/warning tasks and manoeuvring tasks, to stabilisation and imminent pre-crash situations is formed and a need for a safety zone is expressed.

To manage numerous PREVENT requirements, a requirements database was created. Therein, a division of requirements into six different groups - where applicable - was followed (Fig. 3). The database presents, as a top-level element, a detailed accident scenario/unwanted behaviour to which the requirement was targeted. The first level describes the 'Functional requirements', i.e. it describes the function that the system needs to perform. The second level 'Technical requirements' lists the technical features of the system needed to perform the intended function. The third level, associated with the performance of the requirement, specifies in more detail what the system needs to perform to fulfil the intended function. The HMI requirements describe the actuator performance and details on how the information of the functionality is passed to the driver. User requirements describe the requirements in terms of usability and acceptance of the application to be developed. Finally, CoP (Code of Practise) details the requirements in terms of the system development, testing and evaluation and in terms of a requirement of reasonable safety when using the safety application.

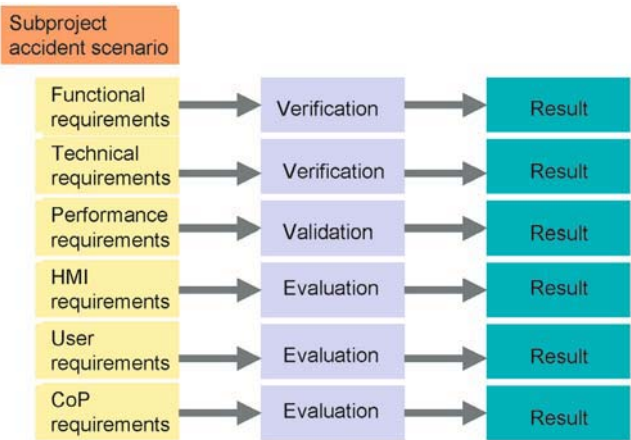


Fig. 3. Organisation of requirements levels for each PREVENT accident scenario.

Req_ID 32.2	Accident Scenario
Description	Tailgating scenario
Explanation	The traffic and environmental parameters priorities are: Gender: Male ñ Female (both priority 1) Age group: over 25 (priority 1) Day time: Daylight (priority 1), Dawn (priority 2) Weather conditions: No adverse
Verification / validation / evaluation	Pilots addressing LRM application will be performed upon these accident scenario and the combinations emerged from the defined traffic and environmental parameters.
Req_ID 32.2.1	Functional req's
Description	LRM (Lateral and Rear Area Monitoring): The application is intended to serve as a complement and extension to the rear view mirrors, and will enable the driver to detect and track vehicles in the rear and lateral area.
Explanation	The position, velocity vector and geometrical extents (length, width, height) of vehicles in the rear and lateral area will be displayed to the driver. The driver shall be able activate/deactivate the active parts of the output. I.e. sound/flashing and other attention attractions shall be controllable (on/off).
Verification / validation / evaluation:	Subsystem and component test in laboratory and simulator. Full function test with CRF test car on test track or real roads.
Req_ID 32.2.2	Technical req's
Description	The following tasks can be identified for the LRM-function: (T1) Measure ego-speed and yaw-rate. (T3) Measure object movement in sensor-range and characterise object dynamics in terms of object position & speed (lateral and longitudinal), and distance to the closest point. If possible other parameters like boundary points, etc. could also be estimated. (T5) Measure driver actions, e.g. direction indicator, steering wheel angle. (T9b) Identify objects of interest(e.g. moving / non moving). (T12b) Display objects of interest. See also requirements described in 32.1.2.3. ñ Long range radars: a detection range of at least 24m is desired but this is sufficient only for low relative speeds; Assume a relative speed of 100 km/h, assume a breaking force of 0.6g, the time necessary for speed adaptation is approximately 5s, with an extra second to accompany for reaction time it becomes necessary to have a window of 6s or more in order to give fast approaching cars a fair chance to avoid collision: 6s translates to 170m at a relative speed of 100 km/h.
Explanation	N/A
Verification / validation / evaluation:	The false and missing alarms/information will be recorded either in instrumented vehicle(s) raw data or in the simulator log files.
Req_ID 32.2.3	Performance req's
Description	A reliability factor of over 95% and an overall false display of less than 5% in total are basic requirements.
Explanation	N/A
Verification / validation / evaluation:	The overall system performance will be evaluated during the LS Pilots. LRM will be validated in a simulated environment and the CRF test car. Cross-check of the objects simulated and the objects in real environment will be the main validation criterion.
Req_ID 32.2.4	HMI req's
Description	LRM HMI has the purpose to inform the driver of the surrounding traffic situation in the lateral and rear-end area of the ego-vehicle. The LRM HMI should ñ be easy to understand. ñ have intuitive symbols. ñ be non disturbing but available when needed. ñ have different modes (colour, shape) for at least non-critical and cautionary situations.
Explanation	N/A
Verification / validation / evaluation:	HMI will be evaluated in terms of user acceptance in the final Pilots.
Req_ID 32.2.5	User req's
Description	Success will be assumed if the final limit of LS applications acceptance and usability remains above the average (acceptance limit) and the rate of answers is in accordance to the plan (i.e.15-20 questionnaires per Pilot site and application). (Success rates are defined upon the user acceptance indicators)
Explanation	In terms of the user acceptance assessment, usability, user acceptance and driversí workload while driving with the LRM applications will be evaluated.
Verification / validation / evaluation:	User acceptance will be assessed via a pre-pilots questionnaire and a post-pilots questionnaire on user acceptance, a short questionnaire on usability in both on-the-road and simulator Pilots and a driversí workload questionnaire.

Tab. 1. Extract of the PreVENT requirements and evaluation data base for the accident scenario 'tail-gating' within the subproject LATERAL SAFE

The Tab. 1 exemplifies how the requirements database is structured and how the contents are described in detail (Tab. 1). A full description and discussion can be found in the public deliverable oerequisites for preventive safety applications [1].

3 From Requirements to System Architectures for Preventive Safety Functions

3.1 Integrated Safety High-Level Architecture Principles

The creation of different architecture and specification levels requires first an agreement on an overall picture across the different activities in the EUCAR Integrated Safety Programme. In a draft version, a vehicle-centric layered logical architecture has been split into three environments between which information can flow: the “far environment”, specially from the point of organising information and services running on the infrastructure, linked to the “near environment” from the point of local communication (V2V and V2I) and environmental sensor arrangement leading to a large set of information made available to the “vehicle environment” for accurate and reliable perception (vehicle dynamics sensors), decision and actuation (HMI). In Fig. 4, the integrated safety architecture is depicted.

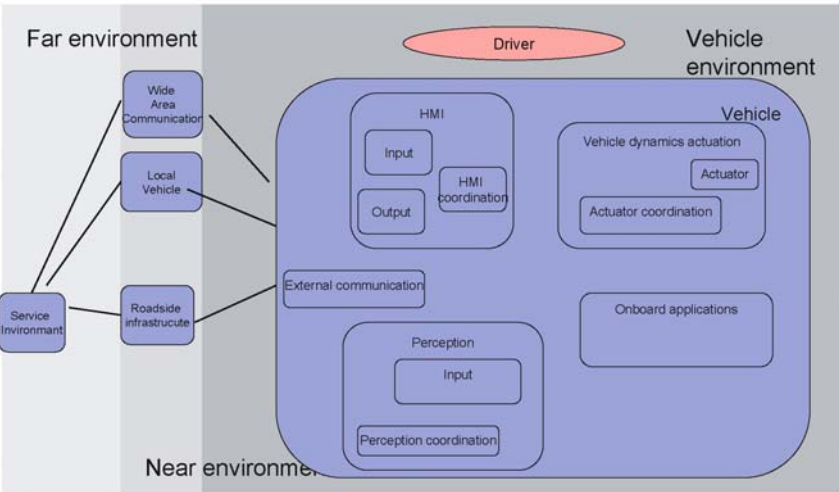


Fig. 4. Integrated Safety high level architecture: main blocks.

This basic decomposition of the architecture is quite general and applies to applications beyond PREVENT. It covers the scenarios found in the integrated projects GST, AIDE and EASIS. Together with PREVENT, this group of projects form the EUCAR integrated safety programme. Also applications that are purely based on telematic functions, such as e-Call, traffic jam information, floating car data, hot spot warning and speed limitations are encompassed.

3.2 The PREVENT Three-Layer Approach

Although the specific requirements necessarily differ for each individual safety application, they lead to a common overall PREVENT architecture. Reflecting from the EUCAR high-level architecture, three basic layers have been identified within PREVENT: the perception layer, the decision (application) layer and the action layer (Fig. 5). This basic layered architecture, depicted below was developed by the PROFUSION subproject and is described in more detail in the public deliverable 'Compendium on sensor data fusion' [2].

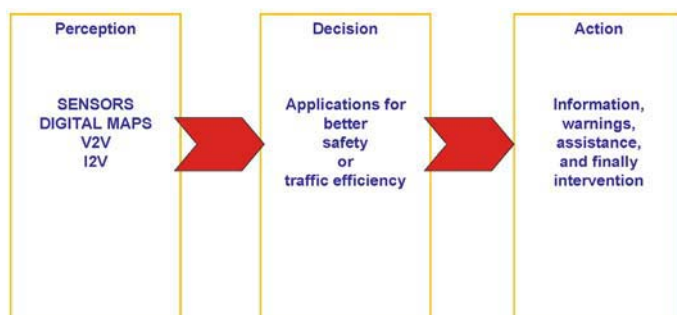


Fig. 5. PREVENT layers reflected from the high-level integrated safety architecture.

The perception layer uses the sensors that range from onboard sensors such as radars, cameras and laser scanners to GPS signal in conjunction with digital maps and even to vehicle-to-vehicle and vehicle-to-infrastructure communication. PREVENT applications rely mainly on the use of environmental sensors.

- ▶ The perception layer performs low-level and high-level data fusion and sends to the application layer a set of abstracted parameters representing the state of the driver, the vehicle, and the environment (DVE).
- ▶ The application layer detects and assesses dangerous situations such as the need for collision or lane deviation warning or even emergency braking. It decides what to do and passes the decision to the action layer.

- The action layer issues warnings via an appropriate HMI or engages vehicle dynamics actuators such as steering, brakes as demanded by the threat level of the potential accident situation.

Typical features of the PReVENT architecture can be characterised as having: modularity with add-on options, scalability with retaining the same architecture in different systems and common information bus such as CAN.

The various components that are used in the PReVENT applications, are shown in Fig. 6. They are highlighted. Each PReVENT subproject with its safety functions uses a subset of components in each layer needed to achieve its goal.

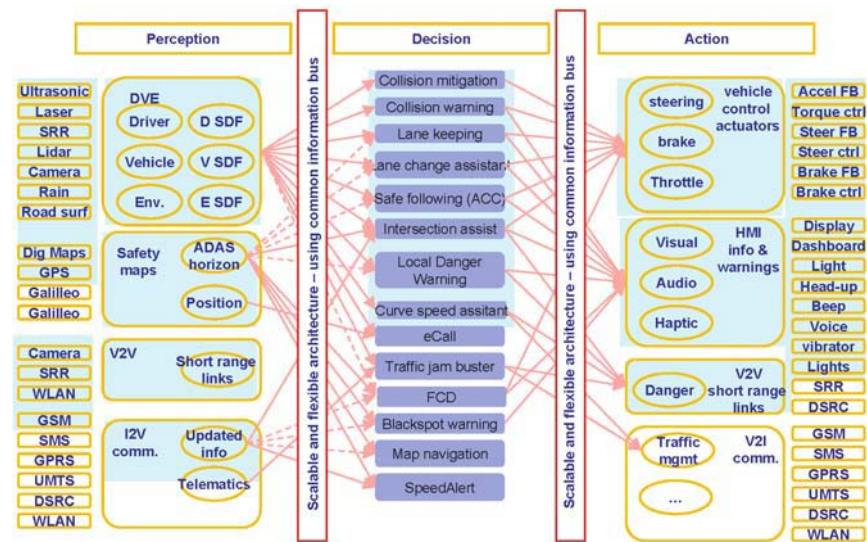


Fig. 6. PReVENT detailed view on perception, decision and action layers.

3.3 Purpose of the System Architecture: Lateral Control as an Example

In order to illustrate the purpose of the system architecture, we consider one of the PReVENT subproject in more detail: the LATERAL SAFE subproject.

This subproject introduces a cluster of safety applications of the future vehicles preventing lateral and rear related accidents and assisting the driver in adverse or low visibility conditions and blind spot areas. It covers all other directions around the vehicle without regarding the forward area. The appli-

cations make up a common multi-sensor platform and include: (i) Lateral collision warning system, (ii) Lane change assistant system (Lane Change Aid) and (iii) Lateral and rear monitoring system. The problems addressed in LATERAL SAFE are illustrated by the three-layered approach of the system including sensors, perception, applications and action (with Human-Machine Interface).

In the following sections, the individual layers are examined in more detail. The following architecture components are used within LATERAL SAFE. They are extracted from the public deliverable on specifications and architecture for PReVENT safety functions [3].

3.3.1 Perception Layer

The role of the perception layer is to provide a physical environment model to the application that decides and acts according to the defined functionality. The first step is to achieve a common temporal and spatial reference, transforming raw sensor data into a consistent set of units and coordinates; as a second step the perception layer interprets observations to detect objects and extract features in the current physical environment.

The Long Range Radar, the networks of Short Range Radars (one network on each side) and a set of cameras in Fig. 7 deliver signals and images to the perception layer, from which a description of the environment of the vehicle is derived and used by applications to decide appropriate actions towards the driver, implemented through adequate HMI.

The perception part also includes the processing blocks devoted to LRR, SRR and Vision signal and image processing, plus an additional Fusion block in charge of merging whatever information comes from the above processing blocks into a sound description of the environment. Vehicle sensor data are also available to all modules. This description of the environment is used in turn by three different applications Lane Change Assist (LCA), Lateral Collision Warning (LCW) or Lateral and Rear area Monitoring (LRM) which decide which controls should be sent to HMI in order to warn/inform/alert the driver of the current situation when found pertinent.

In conclusion the role of the perception layer in LATERAL SAFE is to:

- ▶ Carry out "perception enhancement" tasks independent of the application (generic)
- ▶ Describe in a formal way the environment and the traffic scenario (semantics) i.e. the current state of the objects, the driver, the vehicle and the road.

- Support LATERAL SAFE functions under request (specific)
- Act as a gateway between sensor systems and applications with defined interfaces and I/O protocols.

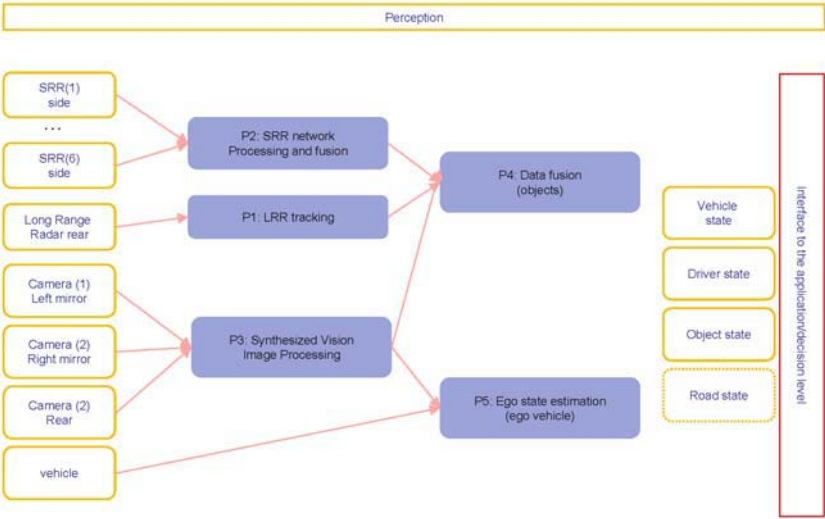


Fig. 7. Perception layer of LATERAL SAFE.

3.3.2 Decision/Application Layer

Based on the outputs of the perception layer, LATERAL SAFE develops three applications:

- Lane Change Assist (LCA) function: The application has two aspects. It informs the driver about presence of vehicles in the blind spot e.g. if the direction indicator is set, and it issues collision warnings in case of critical lane change manoeuvres of the ego-driver.
- Lateral Collision Warning (LCW) function: The LCW function will be able to warn the driver in cases of objects (e.g. cars, bikes, and infrastructure) getting very close to the side of the ego-vehicle
- Lateral and Rear Area Monitoring (LRM) function The application is intended to serve as a complement and extension to the rear view mirrors, and will help the driver to detect and track vehicles in the rear and lateral area.

The complexity of this first integration approach is illustrated in Fig. 8. The decision layer recommends the type of action needed in the event of a dangerous situation or inappropriate behaviour. This is determined by the type of

the perceived hazard and the previous interaction with the driver in form of information or warnings. Naturally, in individual applications, the decision concerns only the case whether to interfere by any means in driving or not. However, in the integrated approach, the decision means also a judgement upon the type of actions needed going from information to intervention.

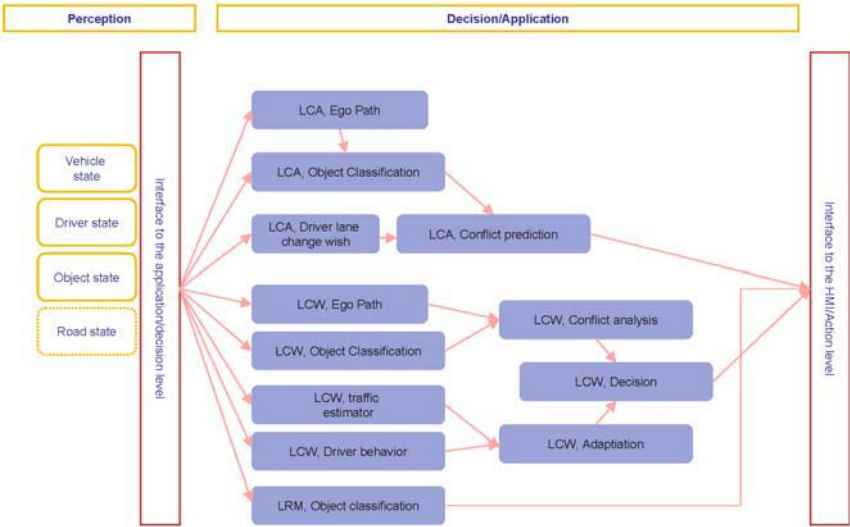


Fig. 8. Decision/Application layer of LATERAL SAFE.

3.3.3 Action Layer

The HMI Manager is responsible for decoding the outputs from the different applications. It also makes the decision on which and what information to convey to the driver and for how long a warning should be active. The HMI CAN controller, sound controller and graphics controller are modules that are responsible for the interface between the HMI software and the hardware.

The CAN controller is responsible for the CAN communication to and from the vehicle ECU. The Sound controller is responsible for activating the acoustic HMI. The Graphic controller is responsible for the graphic HMI.

Fig. 9 gives a schematic overview of the different modules involved in the action layer. The figure contains both software and hardware components and how they are connected.

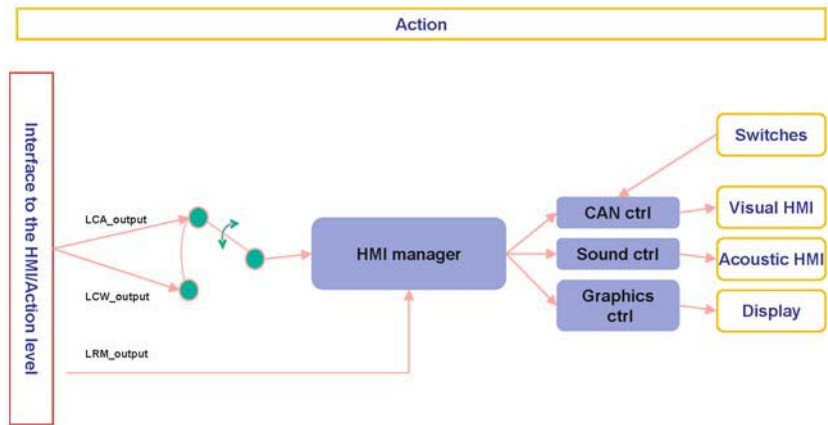


Fig. 9. Action layer of LATERAL SAFE.

3.3.4 HW & SW Platform

The following Fig. 10 illustrates how the different architectural building blocks discussed above are mapped onto the actual hardware architecture of LATERAL SAFE.

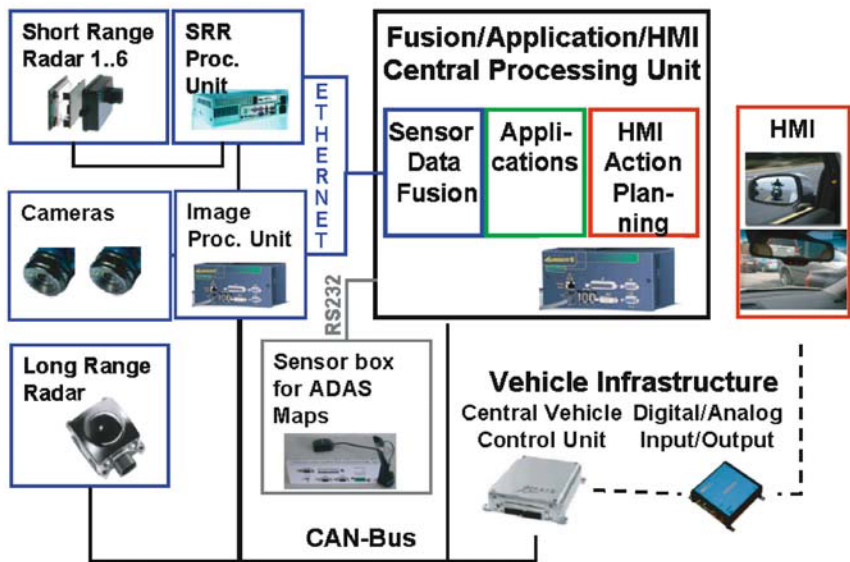


Fig. 10. Hardware architecture of LATERAL SAFE.

4 Towards an Integrated Preventive Safety

The PReVENT integration is further supported by horizontal projects aiming at both common use of sensors and vehicle positioning for different applications as well as common forum for validating the project work and results. As explained earlier, the first step towards a real integration is the new horizontal project INSAFES that will concentrate on showing the potential of integrating a number of safety applications on one platform. INSAFES will take a step beyond safety applications, targeting specific functions to an integrated system, covering a number of applications that are developed within PReVENT. In particular, INSAFES addresses the following different scenarios and use cases:

Enhanced longitudinal control functions

- ▶ Integration of Frontal collision warning and Collision Mitigation strategies - Semi-autonomous braking intervention: braking action confirmed by the driver on the brake pedal after a warning.
- ▶ Warning and intervention strategies optimised according to the data received from WILLWARN (e.g. about the friction parameters and the danger situations further ahead).

Enhanced lateral control functions

- ▶ Improvement of lane keeping support, optimised also w.r.t. the presence of lateral obstacles (e.g. close guard-rails or parallel vehicles)
- ▶ Side collision avoidance/mitigation for trucks within the ego-lane, typically in drifting situations.

Integration and synergies of Lateral and Longitudinal control applications

- ▶ All-around warning function, based on the reconstruction and the assessment of all-around traffic scenario.
- ▶ Improved Frontal collision warning/mitigation: Optimisation of the warning/intervention strategies, based on computation of a feasible evasive trajectory, taking the all around scenario into account.
- ▶ Collision Mitigation- Autonomous intervention: optimisation of the intervention strategies (for instance switch to semi-autonomous modality) depending on the surrounding detected traffic (e.g. evasive manoeuvre if feasible, close rear obstacles,...).

INSAFES goal is to find a methodological approach for functional integration, which should result in a higher level of functionality without introducing too many interconnections and dependencies between the different functions. The functions need to be integrated in order to gain performance and accept-

ance but they need to be modular to maintain a simple and flexible solution. The key is to find the balanced level of integration.

Starting from a number of stand-alone functions the three layered architecture is basically multiplied (Fig. 11). If no coordination at all is performed, it is likely that the different functions try to use the same output device (for example the brake system) at the same time. Due to the different perception modules it is also possible that the different functions don't have the same perception of a certain traffic situation.

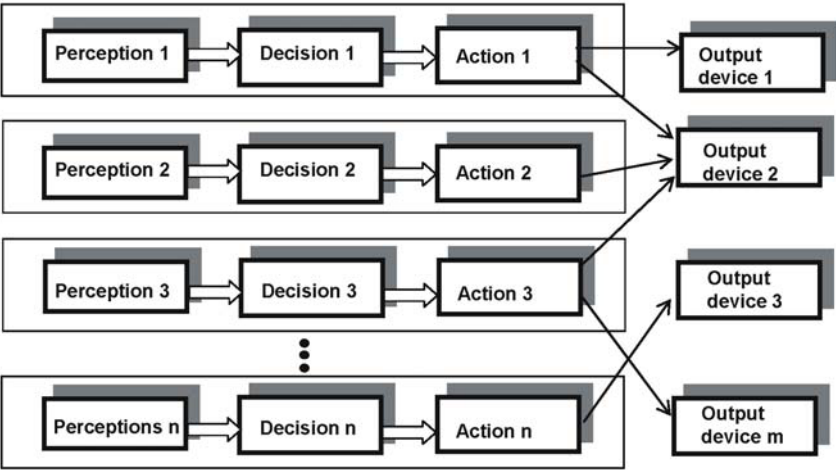


Fig. 11. Stand-alone functions with PReVENT functional architecture.

The easiest way to ensure that the different functions do not try to use the same HMI simultaneously, and that warnings and actions are transferred to the driver in a coordinated way is to introduce some kind of output coordination (Fig. 12). This is one of the topics examined by the integrated project AIDE, outside of PReVENT. This solution has the advantage that it can be used both for functions that are completely stand-alone or functions that use a common perception. Within ProFusion2 integration within the perception layer is handled. Through this common perception framework the different functions get a more unified view of the situation.

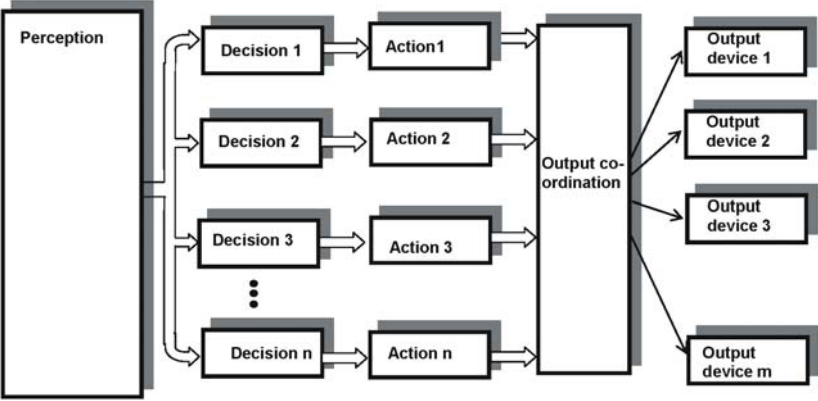


Fig. 12. Common perception and coordinated outputs.

A solution with a common perception and a coordinated uses a common view of the traffic situation and ensures that use of HMI units is coordinated. However, no major increase in functionality is obtained (other than what is expected from the forming of a unified perception).

The INSAFES approach to obtain a higher level of functionality is to use both a coordinated output and to integrate the functions themselves for a common decision. Through the common decision, a new functionality can be added.

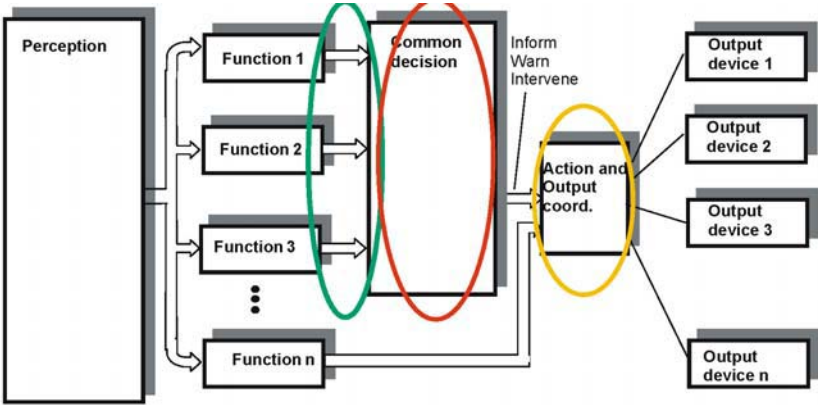


Fig. 13. Functions with a common decision.

The INSAFES project will thus develop a common decision layer and study the interfacing of different functions. One challenge will be to find a level of inte-

gration that results in an increased performance but still enables most of the different function components to be re-used. The INSAFES goal is to integrate already existing function components, and not to re-develop them or to create new ones.

Also, the action- and output coordination will be covered, in close cooperation with the AIDE project. Fig. 13 illustrates the idea of introducing a common decision layer and also shows how the action and output coordinator still is needed if there are functions that are not fully integrated in the common decision concept.

5 Conclusions and Discussion

As described, the vision of PReVENT is to create a safety zone around a vehicle by developing and realising a set of complementary safety functions. The justification for this vision comes from the previous work in active safety and ADAS area. It has been fragmented and lacking integration that would help the task of assisting drivers within one holistic system rather than by a number of isolated applications causing problems on HMI-level, at the latest.

PReVENT is actually a logical continuation and an outcome of previous work carried out in the former Framework Programmes and activities of automotive industry, suppliers and academia in the field. Moreover, there has been an increasing pressure from governments and EU to address the safety issue. Traffic safety work needs more vigour throughout Europe both in terms of implementing conventional and introducing new safety technologies.

Accident analysis, accidentology and review of driver behaviour theories has brought forth a number of useful facts when planning technical systems for driver assistance. The conclusion from these different analysis and findings is that, overall, drivers need a system with continuous alert. It is characteristic of any given driver to make occasionally mistakes that in certain conditions are fatal. Moreover, an accident to materialise, other contributing factors are often needed to trigger the harmful event. Furthermore, when being aware of drivers' typical time to react changes in his/her environment, it can be concluded that safety systems need to 'see' and above all, perceive more and further away than what the driver is able to.

The combination of drivers' reaction times and typical travel speeds in free flow conditions is such that that it is useful to have systems able to see even beyond a driver's field of vision. The most typical characterisation of an acci-

dent situation by survived parties is that it happened "all of a sudden" or very quickly. The answers reflect the fact that the driver had very little or no time to react, make a manoeuvre to escape the situation. For this reason, the basis of all safety systems that are in the first instance informative in a way preparing drivers for possible incidents along the way ahead. These systems should be able to collect information at the minimum, several seconds ahead of the driver to allow her/him to process the information and adjust behaviour accordingly. Eventually, any given safety system should, however, be more than serve as an information system only.

These systems need to be complemented by assistive functions aiming at correcting driver behaviour if - despite the pre-information, the driver does not change the behaviour. Most of safety applications under development have been targeted to adaptive functions. Knowing drivers' tendency to behave not by optimising safety but rather guided by other motives, there is still a great safety potential in this area. Recently published different accident studies on the safety impacts of vehicle stability systems support this assumption.

Finally, the third cluster of safety applications targeted to by PREVENT are systems to mitigate collision consequences. The sub-projects in concern have shown convincingly the assets of the collision mitigation systems such as reversible and irreversible safety systems to prepare the existing safety systems for a collision, active hood and bumper for the protection unprotected road users, brake pre-conditioning and finally, fully autonomous braking.

These applications of basically three different types are being developed in the four functional areas all having distinctive features: Safe speed and safe following, Lateral Support and Driver monitoring, Intersection safety and Vulnerable road users and collision mitigation.

Within PREVENT almost solely safety related applications are addressed. For this reason, there is a strong focus on safety validation throughout applications and functional areas. Especially, ADAS systems with new models of driver-vehicle interaction require a comprehensive validation of safety issues, not only the technical safety of systems but also the "safety of usage".

This question also includes the issue of how long the driver should be kept in the control loop. So far, the principle is that the driver will be controlling the vehicle as long as possible. Should the situation be allowed to develop so far that without vehicle's active safety system interfering in driving, the control of the driver will not be taken until at the last moment by the autonomous emergency breaking. Or should it be done earlier? Where is the point on time-axis, when the driver behaviour should be interfered? Today, there is no clear

answer to this. Different alternatives to keep the driver in the loop are being studied in Integrated Safety Programme. Above all, this issue is a user requirement. Currently, for example the increasing use of vehicle stability systems suggest that to some extent drivers allow control being taken momentarily off their hands. Whether this is a case with other active or proactive safety systems, is still unresolved. It is possible that if the system is felt assisting driving rather than restricting driving, the drivers accept the interference. This may be explained by the time the system is interfering in driving.

Even though, the above is a fundamental issue when decisions are made concerning the precise functions of various safety applications, eventually, it is a good starting point to let drivers themselves to decide on the application and function mode they want.

References

- [1] PReVENT Deliverable IP_D4: Requirements for Preventive Safety Applications PReVENT Consortium 2004. Available on <http://www.prevent-ip.org>.
- [2] PReVENT Deliverable Compendium on Sensor Data Fusion. PReVENT Consortium 2004. Available on <http://www.prevent-ip.org>.
- [3] PReVENT Deliverable IP_D5: Specifications and architecture for PReVENT safety functions. PReVENT Consortium 2005. To be published on <http://www.prevent-ip.org>.

Matthias Schulze

DaimlerChrysler AG
HPC 050 – G021
71059 Sindelfingen
Germany
matthias.m.schulze@daimlerchrysler.com

Joachim Irion

Irion Management Consulting
Taegermoosstr.10
D78462 Konstanz
Germany
joachim.irion@irion-management.com

Tapani Mäkinen

Technical Research Centre of Finland (VTT)
P.O. Box 1302, FIN-33101 Tampere
Finland
tapani.makinen@vtt.fi

Maxime Flament

ERTICO - ITS Europe
Avenue Louise 326
B-1050 Brussels
Belgium
m.flament@mail.ertico.com

Keywords: PReVENT, integrated safety, active safety, preventive safety, safety zone

ADAS Horizon – How Digital Maps can contribute to Road Safety

V. Blervaque, ERTICO

K. Mezger, Daimler Chrysler Research

L. Beuk, Siemens VDO, Eindhoven

J. Loewenau, BMW Group Research and Technology

Abstract

The paper introduces the ADAS Horizon concept and the first results from MAPS&ADAS project (PReVENT IP) of a standardized interface between ADAS applications and digital map data. As a predictive sensor called ADAS Horizon, in-vehicle digital maps are an important source of information providing look-ahead capability for ADAS applications and providing further information for on-board sensors to enhance environment perception. Therefore digital maps have large potential for road safety to enhance or enable preventive and active safety applications by extending driver horizon.

1 Introduction

The development of Advanced Driver Assistance Systems (ADAS) and, more generally, of in-vehicle ITS applications which support the driver in driving safely, comfortably and economically, are of major importance to the automotive industry. Typical examples of ADAS applications are Adaptive Cruise Control (ACC) or Adaptive Front Lighting System (AFS). ADAS currently perform their function on the basis of information generated by sensors observing the vehicle's environment. There is a significant potential for the use of a digital map and the vehicle's position to predict the road geometry and to track related attributes ahead of the vehicle. ADAS applications can benefit from this potential, and new functionality may likely be enabled. In particular, ADAS applications will use map data for recognising road infrastructure conditions at the vehicle's current position, and for a preview along the track ahead.

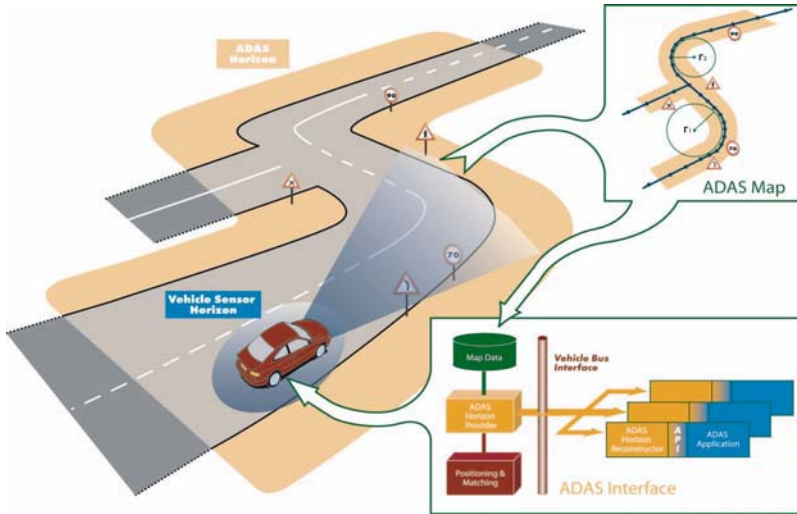


Fig. 1. ADAS Horizon concept

First approaches of map-supported ADAS entering the market will probably use the vehicle's navigation system as the map data source for this preview. The advantages of using the navigation system are that it already has a stored record of the map data, and it already performs the tasks of vehicle positioning and map matching. These functions can readily be used also for the ADAS preview. However, each navigation system stores map data in a system-specific format, and uses its own version of vehicle positioning and map matching. Moreover, when tailored to single ADAS applications, the variety of different map interfaces may expand even more – not only due to different data sources, but also due to application-specific differences. By standardising access to the map data, irrespective of the data provider and physical storage format, and by standardising the way that position and track ahead information is presented to the applications, ADAS software can focus on performing its main task without having to deal with the complexities of map representation.

The absence of a common standardised interface offering map access to ADAS applications has already been perceived in the industry community and has led to the foundation of an industry forum where ideas and requirements regarding such an interface have been deeply discussed. The extensive discussions and work already performed by the members of this group, known as ADASIS Forum [1], served as the basis for the MAPS&ADAS subproject part of the PREVENT Integrated Project [2]. Requirements and concept proposals discussed there among automotive OEMs, suppliers and map providers have already reached a certain maturity, stating the importance and close to mar-

ket position for the MAP&ADAS subproject goals: To develop, test and validate a standardised interface able to serve a spectrum of different ADAS-applications with map preview data.

2 Functional Architecture

Map data access for most ADAS-applications normally use only a small map extract around the current vehicle position. This ADAS-specific map extract is called the ADAS Horizon (AH) [3]. As shown in the Figure 2, the ADAS Horizon provider (AHP) is the entity responsible for the interactions with and transmissions to the ADAS-applications. The positioning module provides a map-matched position to both the navigation and the AHP. Using this position, the AHP extracts the necessary information from the navigation map and aggregates it into the ADAS Horizon (AH) which is sent to the application side

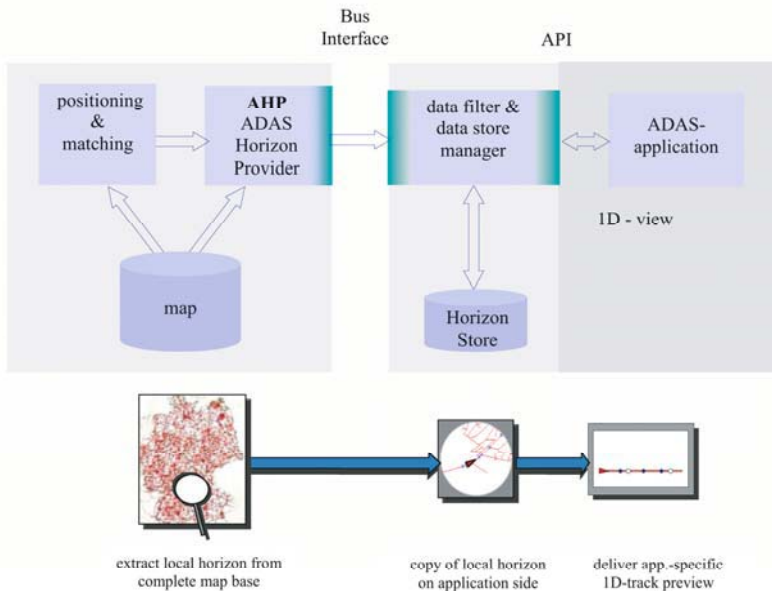


Fig. 2. Transformation and flow of map data from source via bus towards application

The map preview extracted by the ADAS Horizon Provider (AHP) is accessible by all map-supported ADAS applications through the vehicle bus interface. Incremental changes transmitted by the AHP are stored on application side by

the ADAS Horizon Reconstructor to build the 1D-track preview delivered to the ADAS application by means of an API.

3 Functional Structure on Application Side of ADAS-Interface

The ADAS-interface specification defines the content and organisation of a data stream which is sent by the AHP to all ADAS applications [3]. In a simple (near future) set-up with only one ADAS-application, this data stream may be dedicated; that means it only contains a configuration for data relevant to that application. In an advanced far future stage, several ADAS Applications may be listeners to the same data stream (e.g., transmitted via CAN bus). In this set-up, every ADAS application filters out the data it needs from this stream and stores it locally. If the AHP knows the individual needs of all listening ADAS applications, it can adapt the stream accordingly.

The data stream from AHP to ADAS applications consists of:

- Horizon map elements: parts of the road network with attributes together with additional content
- Vehicle position information together with driving dynamics
- Metadata

For the internal architecture of the receiving side, passing the data stream to the ADAS-application, see the Fig. 3.

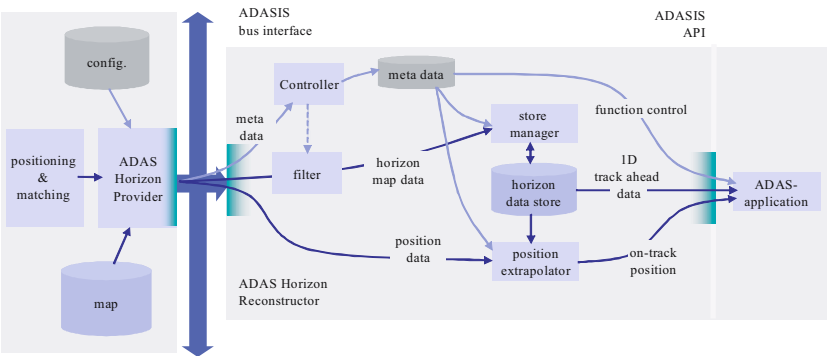


Fig. 3. Architecture layout on application side of ADAS-interface

The ADAS application will receive the data-stream and handle it in the following way:

- ▶ In the multi-application environment the horizon map elements are first filtered: only the road parts and attributes that are needed by the ADAS application are passed. For a single application scenario, this filtering is probably not necessary as according the configuration as only required data is transmitted. Then the horizon data store manager will store the filtered horizon map elements in the horizon map data store, assuming there is free storage space available. If there is no space, it will try to remove old elements that are no longer needed because the vehicle has advanced beyond them. For this, a mechanism to manage the available storage space is to be implemented.
- ▶ From this data store the relevant part for the application can be reconstructed - the left hand block of the application is called Horizon Reconstructor (AHR) for this reason. The AHR passes the relevant data to the application, generally in the convenient 1D-format for track preview functions, confined to its application-specific contents. The selection of the application contents should be performed to a maximum on the bus controller side (using e.g. message identifiers) and to a minimum by software mechanisms discarding non-relevant message parts in the application itself.
- ▶ Besides the basic geometry there is information that is continuous with respect to the along track distance (e.g. curvature) which can be modelled as profile along the track.
- ▶ The vehicle position, speed, heading, etc. is stored inside the AHR module of the application as the last known position, together with a time stamp. If the accuracy of the 'last known position' is sufficient for the ADAS application, it can use it directly for look-ahead calculations. If the application needs more accurate data, information about the delay of the transmission of the position information is provided by using time stamp or age information. Based on the last transmitted position and its time stamp, the position extrapolator may compute an extrapolated vehicle position with higher accuracy at any time, independent from the rate it is transmitted from the AHP. For the extrapolation it is also required that there is some basic prediction of the most probable path in order to provide preview across junctions.

Metadata is handled by the controller. Depending on the type of Metadata, it is passed actively to the respective module to influence functionality, or it is stored in a Metadata store for access by the modules.

3.1 ADAS Interface Implementation

Several components and systems have been developed and implemented within MAPS&ADAS to enable test and validation activities [4].

- ▶ An ADAS Horizon Provider (AHP) is a system that generates an ADAS Horizon and distributes it on a bus. Four AHP systems have been developed, 2 dedicated by Navteq and Navigon and 2 navigation based systems by Siemens VDO and Blaupunkt.
- ▶ An ADAS Client is receiving the ADAS Horizon from the bus. It includes an ADAS Horizon Reconstructor (AHR) that reconstructs the received ADAS Horizon, and makes its content available to the application via an API.
- ▶ The ADAS interface has been implemented in a sample ADAS application: Active Cruise Control. The implementation in the BMW ACC is based on an existing ACC, using the reference implementation of the AHR.
- ▶ A reference implementation of the AHR was developed for testing ADAS Horizon Providers systems and as the basis for the implementation of the ADAS horizon in an ADAS client.
- ▶ The Test Container is a separate system that can measure the impact of the protocol on the CAN bus for assessment.

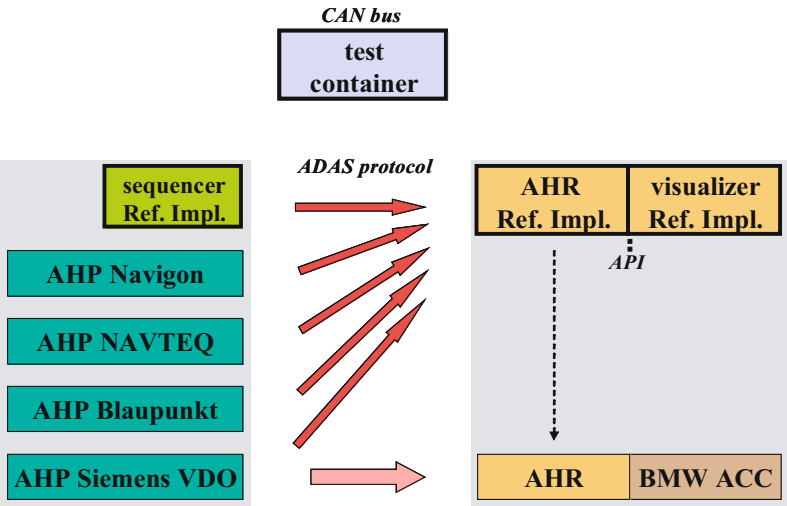


Fig. 4. Overview of implementations

3.2 ADAS Interface Testing

The test container provided by DC was intended for testing and evaluating the mutual influence of the original data traffic present on a vehicle CAN bus and the ADAS Horizon data stream injected onto this bus [5]. Mutual influence means how the characteristics of latency and transmission error statistics of one data stream are influenced by the presence of the other.

For these tests, the typical background CAN traffic of a vehicle that might use map supported ADAS function must be recorded and later replayed on a CAN bus injecting a corresponding data stream for transmission of horizon data using the ADAS interface. The reason why this must be done off-line in a 'sand-box' environment is, that it is not possible to introduce extra data on the CAN of a series vehicle under normal operating conditions (i.e. driving on public roads) without incurring danger of vehicle malfunction and safety risks.

Consequently, the tests involving real vehicle CAN data streams were performed by the four OEMs (BMW, DC, Ford, Volvo). On the other side, the four supplier companies (Blaupunkt, Navigon, Navteq, Siemens-VDO) helped by producing the ADAS interface data streams within the different vehicle CAN environments.

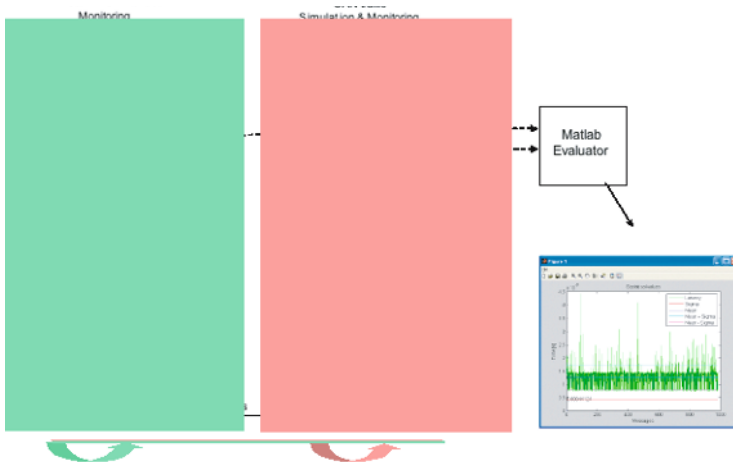


Fig. 5. Test architecture layout for online monitoring of MAPS&ADAS data stream and background data traffic on CAN bus

Of course it is interesting for each OEM how an implementation of the ADAS interface performs on his vehicles and how it does influence the existing CAN traffic. For this reason, the main test task for all the OEMs was to evaluate the

OEM specific properties of a possible interface usage on the own cars. Also, the OEMs were entitled to provide the background CAN traffic files for general testing, as they are able to produce relevant real life CAN traffic examples.

There are a number of factors that influence the behaviour of the MAPS&ADAS transmission within an existing background CAN traffic. These factors on one hand originate from the background traffic, into which the MAPS&ADAS transmission is to be injected. On the other hand, they are influenced by the properties of the injected transmission itself.

3.3 ADAS Interface Validation

As one of the major the objectives of MAPS&ADAS, the definition and the development of an interface between in-vehicle map data sources and assistance systems is of pure technical nature, the technical validation of the interface properties is the most important issue of the validation task [6].

However, there are properties, which obviously do not need to be examined, as they are known to be uncritical from state-of-the-art. On the other hand there are interface properties whose outcome is unsure at the moment of its definition, but which may be very important for success or failure of a market introduction of such an interface.

Consequently, the technical validation performed within MAPS&ADAS is focussed on these most critical or most important issues:

- ▶ Bandwidth usage: Does the interface as proposed by MAPS&ADAS efficiently use transmission bandwidth for standard application requirements? E. g. what bandwidth is spent for a typical ACC preview, consisting of geometry and road class information?
- ▶ Error properties and consistency of transmitted data: Is the interface transmission and interpretation error level sufficiently low? What level of Integrity (error recognition rate) can be reached?
- ▶ Timing Issues: How long does it take for the horizon and positioning data to be transmitted? How 'old' is the image presented to the application?
- ▶ Position and distance-to-object accuracy: How does the timing influence the knowledge and accuracy of the proper vehicle position and its relation to the event points of the preview?
- ▶ Interoperability: Is it assured that different horizon provider software solutions, based on different navigation systems and map databases deliver a horizon data stream fully compatible to the interface specification?

4 First Test Results

Test drives have been performed on different vehicles in different environments and the resulting data streams been mixed offline while varying several transmission parameters [5]. Of special interest were error and latency behaviour of the MAPS&ADAS data stream itself and also its influence on the background traffic which is already present on that bus for normal vehicle control purposes. The whole variety of performed tests, even the most challenging set ups have shown the following first results:

- ▶ Additional bandwidth requirement is normally around 0.1% of the busses capacity, reaching up to 1.5% for very demanding set ups.
- ▶ The maximum added latency charged to the background traffic (lower priority CAN frames) keeps below 0.37 ms for normal conditions and below 0.53 for more challenging setups.
- ▶ The total latencies experienced for the MAPS&ADAS data stream are around 0.25 ms (average) and 0.5 ms maximum for normal conditions, reaching up to 0.5 ms average and 1ms maximum for more demanding test conditions.
- ▶ The transmission properties of the more flexible, more general MAPS&ADAS protocol compared to the existing, dedicated BMW protocol are comparable. This is on one hand valid for the bandwidth usage figures and on the other hand regarding latency times and influence on background traffic.



Fig. 6. Examples of ADAS Horizon visualization from Daimler Chrysler, Navteq and Navigon

5 Conclusions

The encouraging first results achieved within MAPS&ADAS assess the technical feasibility of a standardised interface between ADAS applications and digital map data and therefore confirm the potential of digital map for road safe-

ty to enhance or enable preventive and active safety applications by extending driver horizon. As a predictive sensor called ADAS Horizon, in-vehicle digital maps are an important source of information providing look-ahead capability for ADAS applications and providing further information for on-board sensors to enhance environment perception.

These expected benefits of the ADAS Horizon concept are reflected by the increasing interest and support from the automotive industry. Since 2002 major industry stakeholders have joined the ADASIS Forum (26 Members from vehicle manufacturers, ADAS suppliers, navigation system suppliers and map providers) to promote and support implementation and near future market introduction by means of standardisation. The main direct impact of a standardised interface will be on the economic side. This impact may be roughly estimated in terms of economy on development efforts.

References

- [1] ADASIS Forum: <http://www.ertico.com/adasis>
- [2] PReVENT IP: <http://www.prevent-ip.org>
MAPS & ADAS: http://www.prevent-ip.org/maps_adas
- [3] K. Mezger (Editor) D12.32 Interface Requirements, Functional Architecture and Data Model, MAPS & ADAS project, Deliverable D12.32 revised version, Brussels, 2005
- [4] L. Beuk (Editor) D12.72.1 Implementation Report, MAPS & ADAS project, Deliverable D12.72.1, Brussels, 2005
- [5] J. Loewenau (Editor) D12.81 Interface Test Results, MAPS & ADAS project, Deliverable D12.81, Brussels, 2006
- [6] J. Loewenau (Editor) D12.92.1 Interface Validation Results, MAPS & ADAS project, Deliverable D12.92.1, Brussels, 2006

Vincent Blervaque

ERTICO
326 avenue Louise
1050 Brussels
Belgium
v.blervaque@mail.ertico.com

Keywords: ADAS horizon, advanced driver assistance systems, digital map, standardised interface, predictive sensor

Intersection Safety – the EC Project INTERSAFE

B. Rössler, Volkswagen AG

K. Ch. Fürstenberg, U. Lages, IBEO Automobile Sensor GmbH

Abstract

In the 6th Framework Program of the European Commission, the Integrated Project PREVENT includes Intersection Safety. The INTERSAFE project was created to generate a European Approach to increase the safety at intersections. The project started on the 1st of February 2004 and will end in January 2007.

The main objective of the INTERSAFE project is to

- improve safety and to reduce (in the long term avoid) fatal collisions at Intersections

In order to identify the most relevant scenarios for accident prevention, a detailed accident analysis was carried out. Based on the scenarios and the driver mistakes derived from the accident analysis a basic functionality is described. It considers for example the time budget, which is available in order to warn the driver.

The importance of these accidents leads to a deeper analysis of the scenarios. An in depth analysis of available data from reconstructed accidents in France and Germany show the central position of especially two accident types:

- Collisions with oncoming traffic while turning left and
- Collisions with crossing traffic while turning into or straight crossing an intersection.

Additionally the importance of the actual right of way regulation leads to the consideration of traffic light controlled intersections. The specification of the key technology components like sensors and communication technologies will be derived from the given requirements. Altogether, about 60% - 72% of all accidents in intersections are covered directly by the selection of these three scenarios. The possible coverage of other comparable accidents needs further investigations. This paper will describe the INTERSAFE approach of intersection safety and discuss the functionality to avoid fatal accidents at intersections for the chosen scenarios in detail.

1 Introduction

A general overview on the INTERSAFE subproject was given in [1]. The main focus of this paper is to give a better understanding of the functionality of the sensor based test vehicle used in this project.

The INTERSAFE test vehicle is equipped with two laserscanners, one video camera and additional communication systems. The video camera is used to process data about lane markings at the intersection while the laserscanner collects data of natural landmarks as well as data about other objects and road users. The fused data of the laserscanner and the video camera and a detailed map of the intersection (high-level map) are used for localisation of the vehicle within the intersection. Together with the object data collected by the laser-scanner a broad overall view of the scene is constructed.

The additional communication module allows wireless infrastructure to vehicle communication or, in extension, for communication via infra-structure with other road users that are equipped with such communication facilities. The test vehicle and the mounting positions of the sensors are shown in Fig. 1.



Fig. 1. Sensor integration in the INTERSAFE test vehicle

Due to the fact that this paper deals with the functionality of the application in the test vehicle only the laserscanner is considered, because this sensor detects and tracks the other objects which are essential for the application algorithms. Nevertheless, the video processing data and the fusion with the laserscanner data is crucial for the correct functioning of the host localization process [2].

In the first section of this paper the laserscanner based object detection, tracking and classification as well as the localization of the host vehicle is described. This serves as the input level for the scenario interpretation and risk assessment which is described in the second part.

2 Object Detection, Tracking and Classification

In order to meet the functional requirements of monitoring crossing traffic the laserscanner is integrated into both left and right front corners of the demonstrator passenger vehicle as shown in Fig. 2. With a scan area of 150° each and an overlap between both scanners of 80° a combined scan area of 220° was realised.

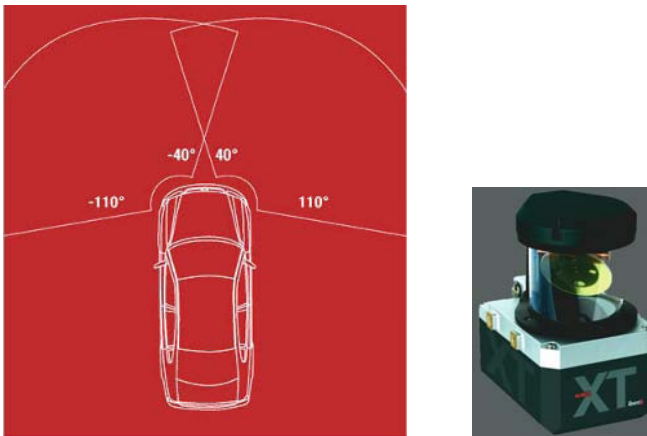


Fig. 2. Schematic of the ALASCA laserscanner scan area with the demonstrator passenger vehicle (left). laserscanner for detection, tracking and classification of road users (right).

The automotive laserscanner combines a 4-channel laser range finder with a scanning mechanism, and a robust design suitable for integration into the vehicle. The object data, as illustrated in Fig. 3, is suitable for various ADAS applications.

In the beginning the generated range profile is clustered into segments. Comparing the segment parameters of a scan with predicted parameters of known objects from the previous scan(s), established objects are recognised. Unrecognised segments are instantiated as new objects, initialised with default dynamic parameters.

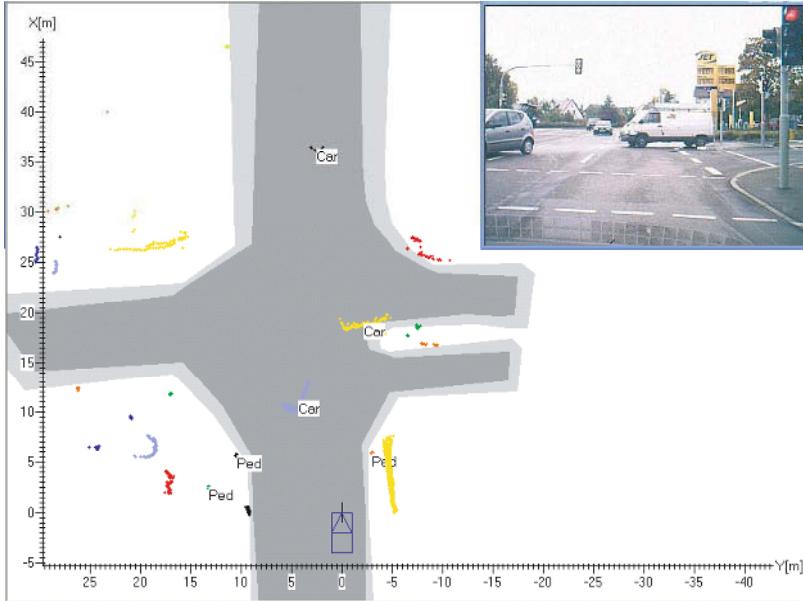


Fig. 3. Object recognition using laserscanners: Road users are tracked and classified crossing an intersection. The shape of the intersection, registered in the feature-level map, is painted grey. The coloured dots are measurements of the laserscanners at different objects. The host vehicle is drawn as a blue rectangle at (0;0) position.

In order to estimate the object state parameters a Kalman filter is well known in the literature and used in various applications, as an optimal linear estimator [3]. The Kalman filter was chosen, as it allows for more complex dynamic models, which are necessary for precise object tracking. We evaluated our data on different association methods, such as the nearest neighbour and the global nearest neighbour method [4].

Object classification is based on object-outlines (static data) of typical road users, such as cars, trucks/buses, poles/trees, motorcycles/bicycles and pedestrians. Additionally the history of the object classification and the dynamics of the tracked object are used in order to support the classification performance [5,6].

In a simple algorithm road users are classified by their typical angular-outline using only the geometric data [7]. Additionally the object's history and its dynamic data are necessary to enable a robust classification [8].

In case there is not enough information for an object classification a hypothesis is generated, based on the object's current appearance. The temporary assignment is valid, as long as there is no violation of limiting parameters. However, the classification is checked every scan to verify the assignment of the specified class [9].

An environmental model supports the selection of a suitable class. The understanding of the traffic situation may further improve the classification results. In recent projects the scan data fusion was very processing-intensive. The laserscanner gathers the range profile in a certain time while the mirror is rotating with the host vehicle usually moving. This leads to a shift in the distance, with respect to the vehicle coordinate system, of actually equidistant targets that are measured in different angles due to the time in scan. Every measurement is shifted to a common time base with respect to the host vehicle's movement.

Two laserscanners usually measure the same object at different times. If a fused scan just combined the two scans the same object would be at different places in the vehicle coordinate system. To minimise this effect, the scan data fusion is based on synchronised laserscanners to provide a consistent fused scan.

The ECU periodically sends signals (with the desired rotation frequency) to both laserscanners. The laserscanners adapt their rotation frequency to the synchronisation frequency and the angle of the rotating mirror to the sync-signal. The accuracy of synchronisation is about ± 2 ms.

3 Localisation of the Host Vehicle

GPS-based localisation is unable to provide sufficiently accurate or reliable localisation in areas where intersections are located. This is particularly true in urban areas where free view to sky is limited. The laserscanner system obtains a relative position within the intersection by detecting landmarks such as posts and other similar fixed objects at the intersection.

3.1 Map Building

In a first stage a grid map of an intersection is generated by moving the laser-scanner across the intersection under consideration of the host vehicle's movement. With known position and orientation of the vehicle at each time step the

distance measurement points of the laserscanner are transformed to a local map coordinate system. Therefore, the mapped region is discretised into small boxes (5 cm x 5 cm) and the number of measurement points in each box (hits) is accumulated.

The visualisation of the resulting grid map (GMAP) is done by standard bitmap images. Each pixel corresponds to a specific box of the discretised region. The more hits in a box the darker is the pixel in the bitmap image. Fig. 4 shows a GMAP of an intersection.

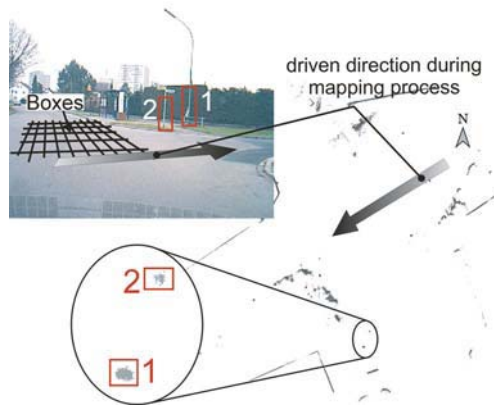


Fig. 4. laserscanner grid map and video reference image. The arrow shows the direction the vehicle drove along during mapping process.

The obtained GMAP is used to determine precisely the coordinates of static objects, like posts of traffic lights or traffic signs. These static objects (features) are later used as natural landmarks for an host-localisation algorithm.

3.2 Localisation

GPS provides approximate position measurements. Using this approximate position, the detected natural landmarks are transformed to the laserscanner coordinate system. The main challenge is to associate the transformed features to the data of the laserscanner. This is done by the algorithm proposed in [10]. After association the position and orientation of the vehicle's position is determined with respect to the known positions of the features, relative to the intersection coordinate system.

4 Functionality in the Test Vehicle

The following part describes the basic functionality of the application in the sensor test vehicle in order to assist the driver for the most relevant intersection accident scenarios. These scenarios were identified in a detailed accident analysis [11]:

1. Left Turn across Path
2. Turn Into/Straight Crossing Path
3. Red-Light-Crossing

Here the functionality for assisting the driver in the first two scenarios is described. This includes the scenario interpretation, risk assessment and the HMI level. The whole functionality considered within the INTERSAFE project including driving simulator and communication modules is described in [12].

5 Scenario Interpretation

As mentioned above, the sensors of the test vehicle permanently observe the environment and thus a consolidated view on the current, highly-dynamic scene is build. This includes the self-localisation of the host vehicle as well as the detection, tracking and classification of the other road users relative to the intersection. This allows the determination of all possible conflicts, hence, likely paths and finally the risk.

5.1 Conflicts

In a first step possible conflicts for the host vehicle at the intersection are identified. This is based on data from the high-level map. Since in the high-level map geometry of the different lanes as well as right-of-way regulations appear, it is possible to identify priorities for the traffic flow for each considered intersection. The computation of all theoretical conflicts within the intersection is a static process, which solely uses static data of the high-level map and needs to be computed only once each time when approaching an intersection. For this process it is urgently needed that the high-level map is up-to-date. Wrong information about the right-of-way regulations could lead in a total misinterpretation of the scene and therefore in a malfunction of the assistance system on the whole. An example of possible conflicts is shown in Fig. 5(a).

As soon as the localisation of the host vehicle and the other traffic participants is performed, the remaining conflicts are extracted as it can be seen in Fig. 5(b). These are the conflicts that could appear regarding mistakes of the host vehicle as well as the errors of the other vehicles.

Taking the right of way regulation into account the conflicts for ones own mistakes can be extracted in Fig. 5(c).

The extracted conflicts are only possible ones since they do not regard the time domain. This becomes important in the risk assessment evaluation later on.

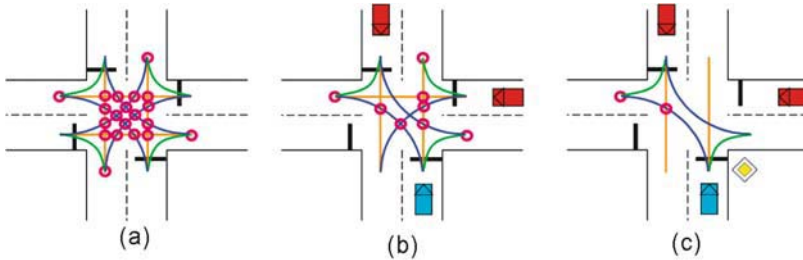


Fig. 5. Computation of conflicts

5.2 Plan Recognition

The conflicts, as computed above, are not necessarily dangerous if the plans of the vehicles will follow the conflict-free paths. Therefore, it is important to perform a plan-recognition in order to identify the possible manoeuvres for each traffic participant (including the host vehicle) and their degree of probability. The inputs for this process are precise lane information of the high-level map, the position and dynamics information of all vehicles and possibly the indicator information of the host vehicle and the other vehicles (transferred by car-to-infrastructure-to-car communication).

Bringing all this information together with the predefined typical occurrence and combination of these parameters for a special manoeuvre, a probabilistic model for the behaviour of the road users can be extracted (see Fig. 6).

These probabilistic plans are combined with the conflicts computed in the first step. The combination forms a consolidated scenario interpretation for the current scene that serves as basis for the risk assessment.

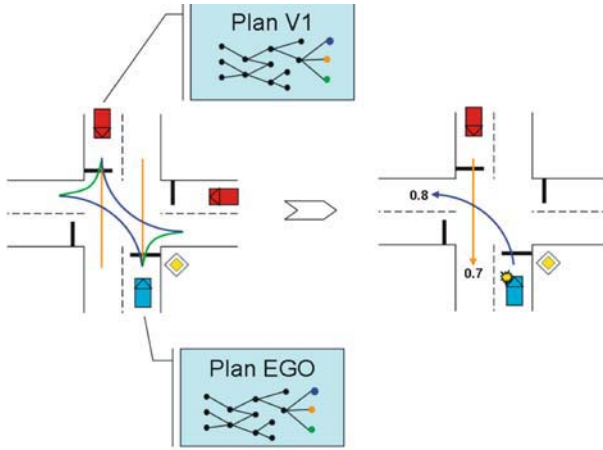


Fig. 6. Simplified diagram of plan recognition

6 Risk Assessment

The scenario interpretation provides all possible conflicts and the assigned probabilities of the driving behaviour of the vehicles, but, as mentioned before, omitting the time domain. The risk assessment takes these probabilities as weighting factors and computes a risk level for each possible conflict in time and space domain. Here, the time becomes important, because the risk of a conflict is highly dependent on the fact whether or not two vehicles are reaching the conflict point (i.e. a defined area around this conflict point) in the same time interval.

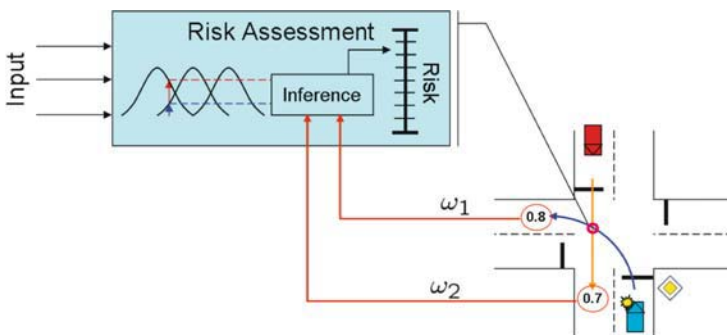


Fig. 7. Schematic diagram of risk assessment for one conflict

A fuzzy rule-base is built to reproduce “human thinking” for risk assessment so that an adequate strategy can be formulated in an easy way. Important input variables are speed, acceleration and distance to the conflict. But also inputs such as the type of the opponent could be of interest in order to translate it to a severity index for a possible crash. The results of the risk assessment module are different risk levels for all possible conflicts in the scene.

For a first approach the conflict with the highest assigned “risk level” will be considered to be the most important one. This conflict is passed to the warning strategy level.

7 Warning/HMI

A big challenge for humans while driving a car is to assess parameters like speed and distance of other approaching vehicles. These parameters are directly linked to the evaluation of the risk of a certain traffic situation. In order to assist the driver in such a situation an advanced driver assistance system has to estimate the risk level and present it to the driver in an adequate way.

Nowadays driver assistance systems mostly use warning strategies like appearing signals or sounds to alert the driver when a situation gets dangerous, i.e. when the computed risk rises over a defined level. The system approach used here is a warning interface that visualises the risk level in a continuous manner for the time of an identified situation that could become dangerous. The driver will have a direct visual link to those parameters that are difficult to estimate. For example, if the driver is approaching an intersection and intends to turn left, he has to watch out for oncoming traffic. The speed and distance of the oncoming cars is one measurement to determine if a turn-left manoeuvre is safe or not. Fig. 8 shows an example of our visualisation interface for an intended left-turn.

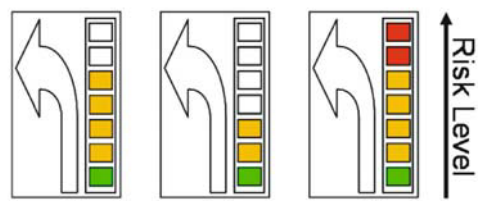


Fig. 8. Continuous HMI for visualisation of the risk level

During the whole approach the driver has the direct link to the risk level computed by the system (i.e. momentary value and derivative). The advantage is that there is no possibility to get surprised by a flashing light that tells him suddenly that a situation gets dangerous. Due to the continuous HMI interface he will be prepared for the situation and can estimate the risk for his intended manoeuvre more easily by taking his own driving skills into account. Beside the risk level visualisation there has to be additional information for which conflict the risk level is shown. The idea is to use simple pictures of well known traffic signs so that the driver ideally needs no long time to understand for what the warning is for. User acceptance tests at the end of the project will show the suitability of such an HMI visualisation.

8 Conclusions

A comprehensive approach was presented which enables new functions for increasing intersection safety by use of an autonomous on-board sensor system. Combining such a system with an additional communication module even more applications are possible. Two very precise laserscanner with a broad combined scan area of 220° around the front of the vehicle are used to localize the host vehicle within the intersection using natural landmarks as well as to detect, track and classify other road users. With this information and a detailed map of the intersection an overall view of the scene can be constructed. A scenario interpretation and risk assessment strategy that tries to emulate human way of thinking was introduced.

For the driver's recommendation it is fundamental not to have just binary information, but better a risk level assessment. With our HMI approach, the driver can easily assess, if a situation is risky for his driving skills, or not. Future work has to ensure that drivers don't use such a risk level based recommendation for risk compensation.

9 Acknowledgement

INTERSAFE is a subproject of the IP PReVENT. PReVENT is part of the 6th Framework Programme, funded by the European Commission. The partners of INTERSAFE thank the European Commission for supporting the work of this project.

The partners in the INTERSAFE project are:

- ▶ Vehicle manufacturer: BMW, VW, PSA, RENAULT
- ▶ Automotive supplier: TRW, IBEO
- ▶ Institute / SME: INRIA, ika/ FCS, Signalbau Huber

References

- [1] Fuerstenberg, K. Ch.: Intersection Safety – The EC-Project INTERSAFE. Proceedings of ITS 2005, 12th World Congress on Intelligent Transport Systems, ITS 2005 San Francisco, Paper 2686.
- [2] Heenan, A.; Shooter, C.; Tucker, M.; Fuerstenberg, K. Ch.; Kluge, T.: Feature-Level Map Building and Object Recognition for Intersection Safety Applications. Proceedings of AMAA 2005, 9th International Conference on Advanced Microsystems for Automotive Applications, March 2005, Berlin, Germany.
- [3] Welch, Greg; Bishop, Gary: An Introduction to the Kalman Filter. <http://www.cs.unc.edu>, 2001.
- [4] Blackman, Samuel: Design and Analysis of Modern Tracking Systems. Artech House, London 1999.
- [5] Willhoeft, V.; Fuerstenberg, K. Ch.; Dietmayer, K. C. J.: New Sensor for 360° Vehicle Surveillance. Proceedings of IV 2001, IEEE Intelligent Vehicles Symposium, IV 2001 Tokyo.
- [6] Fuerstenberg, K. Ch.; Willhoeft, V.: Pedestrian Recognition in urban traffic using laserscanners. Proceedings of ITS 2001, 8th World Congress on Intelligent Transport Systems, ITS 2001 Sidney, Paper 551.
- [7] Fuerstenberg, K. Ch.; Hipp, J.; Liebram, A. (2000) A laserscanner for detailed traffic data collection and traffic control. Proceedings of ITS 2000, 7th World Congress on Intelligent Transport Systems, ITS 2000 Turin, Paper 2335.
- [8] Fuerstenberg, K. Ch.; Dietmayer, K. C. J.; Willhoeft, V.: Pedestrian Recognition in Urban Traffic using a vehicle based Multilayer laserscanner. Proceedings of IV 2002, IEEE Intelligent Vehicles Symposium, IV 2002 Versailles, Paper IV-80.
- [9] Dietmayer, K. C. J.; Sparbert J.; Streller, D.: Model based Object Classification and Object Tracking in Traffic scenes from Range Images. Proceedings of IV 2001, IEEE Intelligent Vehicles Symposium, IV 2001 Tokyo, Paper 2-1.

- [10] T. Weiss, N. Kaempchen, K. Dietmayer, "Precise Ego-Localisation in Urban Areas Using laserscanner and High Accuracy Feature Maps", in IEEE Intelligent Vehicles Symposium Proceedings, Las Vegas, 2005
- [11] INTERSAFE Consortium: Requirements for intersection safety applications. Sub-project Deliverable D40.4 of the INTERSAFE project. To be found at: http://www.prevent-ip.org/en/public_documents/deliverables/.
- [12] INTERSAFE Consortium: Description of new active safety functionality. Sub-project Deliverable D40.41 of the INTERSAFE project. To appear at: http://www.prevent-ip.org/en/public_documents/deliverables/.

Dipl.-Inform. Bernd Rössler

Konzernforschung Elektronik, Fahrerassistenzelektronik
 Volkswagen AG Brieffach 11/17760
 38436 Wolfsburg
bernd.roessler@volkswagen.de

Kay Fuerstenberg

Director of Research, IBEO Automobile Sensor GmbH
 Fahrenkroen 125
 22179 Hamburg
 Germany
KF@ibeo-as.de

Keywords: intersection safety, laserscanner, map building, scenario interpretation, risk assessment

ProFusion2 – towards a Modular, Robust and Reliable Fusion Architecture for Automotive Environment Perception

T. Tatschke, FORWISS, University of Passau

S.-B. Park, Delphi Electronics Safety

A. Amditis, A. Polychronopoulos, ICCS, NTUA

U. Scheunert, Technical University of Chemnitz

O. Aycard, GRAVIR-IMAG INRIA

Abstract

This publication focuses on a modular architecture for sensor data fusion regarding to research work of common interest related to sensors and sensor data fusion. This architecture will be based on an extended environment model and representation, consisting of a set of common data structures for sensor, object and situation refinement data and algorithms as well as the corresponding models. The aim of such research is to contribute to a measurable enhancement of the output performance provided by multi-sensor systems in terms of actual availability, reliability, accuracy and precision of the perception results. In this connection, investigations towards fusion concepts and paradigms, such as 'redundant' and 'complementary', as well as 'early' and track-based sensor data fusion approaches, are conducted, in order to significantly enhance the overall performance of the perception system.

1 Introduction

In the European member states there are about 1.200.000 traffic accidents a year with over 40.000 fatalities. This fact points up the growing demand for automotive safety systems, which aim for a significant contribution to the overall road safety. For this reason a current technology field of the automotive industry focuses on the development of active safety applications and advanced driver assistant systems. These aspire a reduction or at least an alleviation of traffic accidents by means of collision mitigation procedures, lane departure warning, lateral control, safe speed and safe following measures.

The common nominator and key feature of all this novel safety systems is the accurate, robust and reliable perception of the vehicle's environment. However, current off-the-shelf single sensor approaches cannot always fulfil

these challenging demands. Therefore most of these applications base on perception systems, which process the data from multi sensorial platforms via data fusion methods.

The Preventive and Active Safety Applications project (PReVENT), which is part of the Sixth Framework Programme, contributes to the safety goals of the European Commission (EC). PReVENT addresses the function fields of Safe Speed and Safe Following, Lateral Support, Intersection Safety and Protection of Road Users and Collision Mitigation in order to cover the field of active safety. The majority of these functions are characterized by using perception strategies based on multi-sensor platforms and multi-sensor data fusion.

Hence, the strategy of PReVENT was to initiate a cross-functional subproject called ProFusion in order to streamline and to develop the subject of multi-sensor data fusion in a greater degree of depth and in a more systematic approach as compared to the primarily function-driven subprojects. The role of ProFusion, inside PReVENT, is to streamline the sensor data fusion by, e.g. gathering requirements, defining certain standards and developing fusion algorithms.

In this context we propose a multi sensor fusion architecture, which facilitates the robust and reliable processing of multi sensor data by providing different data fusion approaches, a common data structure and a common modelling within one framework. Due to the special design of the framework and the underlying algorithms it is not limited to a single use-case but can serve as a modular platform for environment perception and thus build the basis for different kinds of safety applications.

An additional rationale is motivated by the observation, that a variety of national and international research projects are devoted to the development and improvement of active and preventive safety systems, and that all of them are affected by the limited performance and even by deficiencies of the currently available sensor platforms. As PReVENT is considered as the core of the eSafety research and development initiative, it has been obvious to embrace a cross-functional subproject that adopts a variety of challenges and open issues in the field of multi-sensor perception.

2 The Fusion Architecture

As already outlined in the introduction the perception of the vehicle's environment is the crucial factor of a driver assistance and active safety system.

Therefore the major objective of the conducted research is to push the sensor data fusion techniques used for automotive environment perception beyond the current state-of-the-art ([6], [7]). This will be done by setting up a modular and interoperable fusion architecture for multi sensor systems, which integrates diverse approaches (e.g. low and high sensor data fusion, algorithms for situation refinement, etc.). In doing so the proposed framework is not limited to any special safety function but operational with all different kinds of applications like collision mitigation, lateral control, lane departure warning and others.

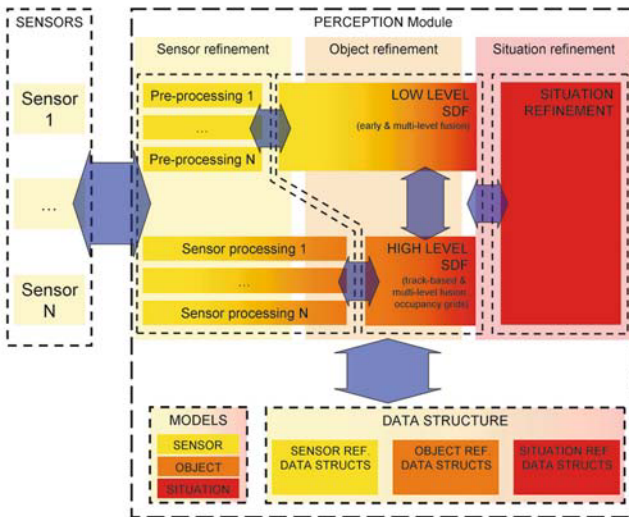


Fig. 1. The sensor data fusion architecture

Fig. 1 outlines roughly the concept and the components of the sensor data fusion framework:

The system will be based on an extended 4D scene / environment model [1]. Objectives are to deliver an extended view of the environment to applications (in terms of more detailed representations) and to define data structures for each processing step during the fusion process (e.g. for raw sensor data, signal features, objects detected in the environment).

For object refinement [2], one will develop existing and new algorithms for filtering, data association and object classification. Especially, chances for deducing confidence information from complementary and redundant sensor data for each processing result will be analysed. Additionally, the research work will be focused on new motion models.

Research topics on situation refinement will include trajectory classification and prediction for objects on the road, trajectory estimation of the ego-vehicle based on multi source information (e.g. detected lanes, ego-vehicle dynamics and map data), as well as on generic decision components for the prediction of the driver's intention.

The newly developed perception system [3,4], and especially the different fusion approaches, will be implemented, integrated and evaluated in open-loop real-time environments, and ultimately utilised in the closed-loop on-board systems of prototype vehicles (owned by BMW, CRF, DaimlerChrysler and Volvo Tec). These vehicles are equipped with distinct sensor platforms (including stereo vision cameras, FIR cameras, short and long range RADAR devices and LIDAR sensors) and serve diverse active safety application [5].

The succeeding paragraphs describe the main components of the fusion framework, especially the different fusion approaches, in detail.

2.1 The Early Fusion Approach

The term "early fusion" is derived from a fusion concept, which is based on only slightly pre-processed data. They are processed together from an early stage of the processing chain. Such an approach permits the fusion module itself to process all data from the different sensors "as a whole". Taking use of the redundant sensor information and matching these data to one common and consistent scene model of the environment it should be feasible to slash inconsistencies and to increase the robustness and reliability of the processing results.

Thereby an early fusion system is working as follows: Several sensors deliver raw sensor data, for example echoes from RADAR devices, images from vision devices or FIR cameras, etc. to the sensor pre-processing unit. During sensor pre-processing specifics of sensor signals are extracted (peaks, plateaus, regions with same properties, etc.) and grouped. The resulting features can be provided in different abstraction levels. Based on these features objects are detected, classified and tracked over time in further processing steps.

All processing steps make, more or less, use of presumptions related to the vehicle environment. These presumptions, stored in models, should be consistent in the whole processing sequence. Thus beside the one common environment model of the early fusion module there should not be used any other model in other processing steps. Therefore the input data to early fusion are required to be based on the same models or, if not possible because pre-pro-

cessing is contained and hidden in sensor components, to be based on minimal assumptions. As already indicated before, early fusion does not implicate to handle only some first processing steps, but takes data from early processing stages from all sensors, fuses and processes them together to one common result, the environment description of the vehicle.

Thereby the early fusion module is internally composed of several functional units, which are necessary to put the fusion process into practice. Fig. 2 illustrates the different components of the fusion module and shows their interaction. It mainly shows the circle of processing steps that have to be executed:

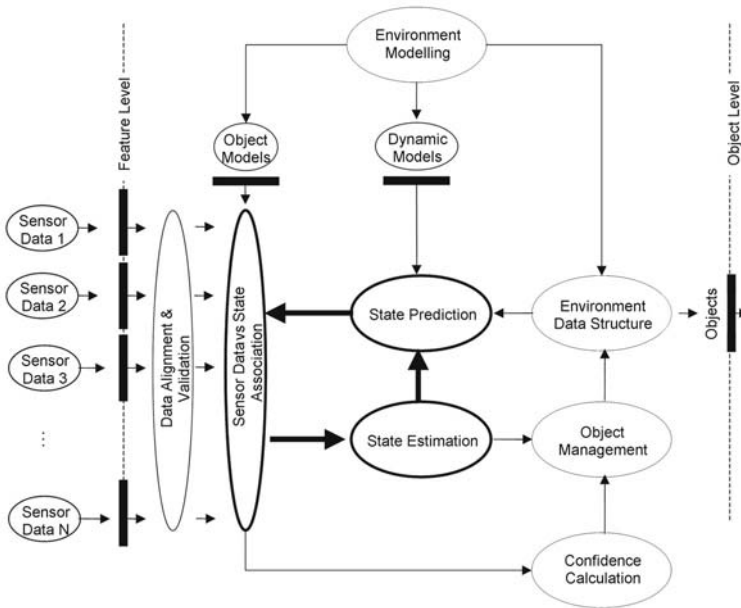


Fig. 2. Early fusion functional architecture

The following paragraphs develop the functionality of the fusion module's components in more detail:

The process of sensor data association or matching is a key challenge of the early fusion architecture. Like in other fusion systems feature vectors are extracted from the sensor output data. In the matching step these feature vectors have to be assigned to the respective corresponding objects in the modelled track history causing the measurement data of the feature vectors. In track fusion systems the data association is done based on the pure object data from the sensor processing units and the object data from track history. In the

early fusion module the data association poses the challenge, as this matching step has to be done for data on different level of abstraction, i.e. for edge to edge association up to edge to object / track assignment. Similarity measures are used to find the most probable and reasonable assignment of the acquired sensor data to the data of the object's history. Therefore they assess the association of the features based not only on their (Euclidian) distance, but in consideration of their covariance information and the origin of the sensor data.

As the early fusion approach is model driven, a further task of the matching module is the attribution and classification, respectively, of sensor data or features to different object models, which provide the basis for the characterisation of the environment. In the initialisation phase the matching module generates object assumptions for new features based on a set of given (shape and measurement) models (e.g. for the road, other cars and trucks, pedestrians, etc.) and allots the sensor data to the respective model that proves to be the most probable relative to the other ones. With the help of additional sensor data the respective object assumptions are either confirmed or discarded and newly reassigned over time. Whenever new features from the perception devices are available, the system checks if they can be associated to already existing objects in the environment description or if they are enough significant to create a new object assumption.

The handling and management of features, objects and tracks takes place in the environmental data structure. In this structure all information on the own car, the multi sensor system and the surrounding environment is stored just like the relations between these objects. Main task of the object management module is the addition, updating, fusing, splitting and deletion of features, objects and tracks to/from the environment data structure on the basis of new measurement data, data association operations and object hypotheses.

For the step of state estimation and prediction a realisation of the Extended Kalman filter is to be intended due to his simplicity, optimality and tractability in tracking and estimation of (non-linear) systems

The goal of the fusion module is to provide an as detailed as possible description of the own vehicle's periphery. This description, which contains all detected objects / tracks together with their attributes as well as their spatial interrelation in the surrounding area of the vehicle, can be easily generated at any time from the environment data structure. The format of the fusion module's output is generic and can be adapted to fit the respective application.

2.2 The Multi Level Fusion Approach

The holistic representation of the environment on the basis of the extended 4D environment model and the common data structures allows sensor data processing with the help of a multi-level fusion algorithm. Multi-level fusion means that not only one level of fusion exists but data components belonging to one physical object are scattered over different levels and evidently fused on several different levels too e.g. signal level, feature level and track level.

In general the chosen level of fusion is object and model dependent. Therefore for every object a certain hierarchical fusion strategy can be defined. This way the object tracking has inputs from tracked features, untracked features as well as from signal level.

A typical property of multi-level fusion is the use of back loops between the levels. Therefore feature models are used to describe which data from which level should be used to maintain an object track. This is organized by the multi-level fusion management. A special case of multi-level fusion is a processing on adaptive chosen levels. This allows the fusion strategy and selection of a certain fusion level to be dependent on the actual sensor data and the observation situation of an object. That's why a better processing strategy can be achieved in most cases.

The multi-level fusion approach means that several levels of fusion exist. Information and data which are generated by a specific object in the real world scene are fused on several different levels of abstraction. There are data components on the signal level, the feature level and the track level. At signal level all raw or pre-processed data coming from single sensors can be found. The data produced by different sensors are forwarded to the processing chain where they are processed and fused with data from the same, higher or lower level (Fig. 3).

Multi-level fusion can be performed in two oppositional ways – a bottom-up or a top-down strategy. Both strategies can be used at the same time parallel and sequential in the processing chain. By performing the bottom-up strategy, specific model knowledge about a real world scene and its objects is used to fuse more or less primitive objects to primitive objects at the same or at a higher level.

In the case of a top-down strategy the model of an object contains all relevant information about its physical properties called features (e.g. its shape or its composition by components / structural information). Of particular interest is the information about which component can be detected by which sensor.

Using this knowledge about a possible object the data of a lower level can be thoroughly analysed to increase or decrease the confidence in the assumption made before.

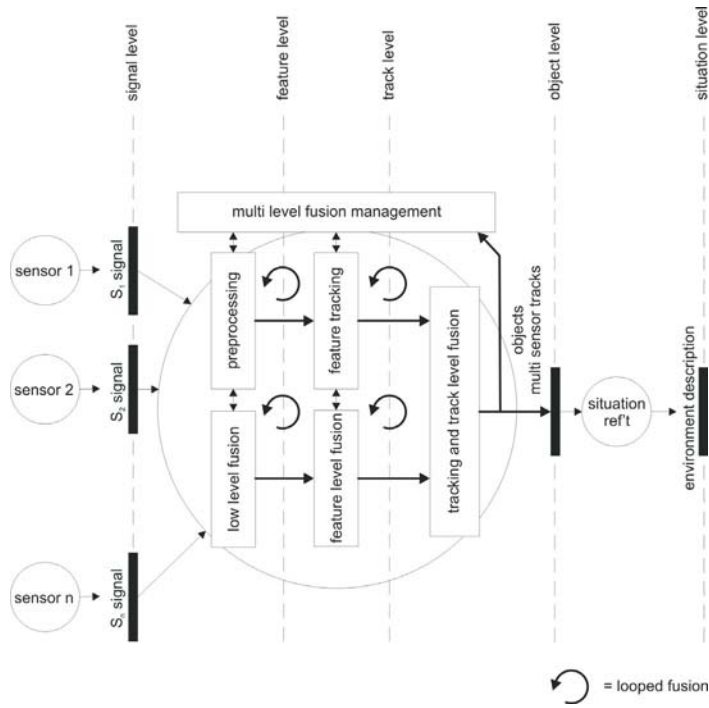


Fig. 3. Multi-level fusion functional architecture

There are three options to design the general fusion structure. This is sequential fusion, parallel fusion and a looped fusion structure. These are three basic structural mechanisms that are in real systems combined with each other: In a sequential processing approach the chain of data processing can be followed bottom up level by level performing fusion operations between data elements that come from the same sensor. Due to this strategy the degree of fusion as well as the degree of confidence is increased continuously. The second option – parallel processing chains – occurs, if several sensors are available and if parallel alternative processing is performed for the same sensor. Then the degree of composition increases, because components delivered from different sensors are combined and the sensor specific confidences are accumulated. Looped fusion can be implemented if detected features are assigned to a feature model and a back loop according to the degree of composition is initiated. Doing that it should be possible to assign additional features defined by the feature model to the object hypotheses. The use of feature models and the

mentioned methodology allows increasing certainty and confidence of object estimations by the perception process itself. If the quality of the interim results is not satisfactory the data can be passed through an adopted processing chain again to improve the results. The back loops are located between several levels. The repetition of certain processing steps can result in more accurate and stable results.

The state of the whole system represents a certain scenario in the real world how it is seen by multiple sensors. This overall information is the content of the environmental model. The environment description is a specific output of the environment model. This description can be used by an application to process certain information of the 4D environment model.

2.3 The Grid-based Fusion Approach

The main idea of grid-based fusion is to do sensor data fusion in an occupancy grid. This occupancy grid is a regular discretisation (sampling) of the environment in cells, where each cell contains the probability that the corresponding part of the environment is occupied. Sensor data fusion is done in a generic way in occupancy grid framework. This approach allows an important sensor flexibility and sensor independence. Sensor data fusion could be done at different levels: at a feature level, in this case, a precise model of each sensor is needed to build the grid, and at a track level, in this case, a geometric description of the processed data is needed.

The resulting occupancy grid is actually a snapshot of the current environment, i.e. an instantaneous view of the surrounding environment of the vehicle at a fixed frequency. In an occupancy grid, each cell contains the probability that there lies an obstacle. Advantages of the occupancy grid framework:

- ▶ the framework is sensor independent
- ▶ the framework could deal with raw data (low level fusion) and with pre-processed data (high level fusion)
- ▶ fusion of sensor data in each cell of the grid
- ▶ priors (i.e. the initial probability for each cell) according to the occupancy of the whole space could be integrated; For instance, if we are in a crowded environment, the prior of occupancy is very high and the rate of false alarm and missed detection is very high, and the fault tolerance of the system is increased

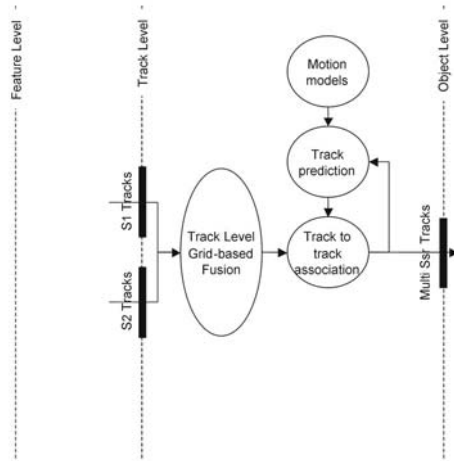


Fig. 4. Detail of the grid-based fusion architecture on the track/high level

In the case of high level fusion, the sensors return for instance velocity, of which a map of velocities is built as in an optical flow framework according to the discretisation of the occupancy grid. Thus in each cell, a probability distribution over a set of possible discretised velocities is built. If the sensors can return a classification of the obstacles, a map of category (such as car, truck, bicycle, pedestrian, none) is established and in each cell a probability distribution over all the possible categories is set up.

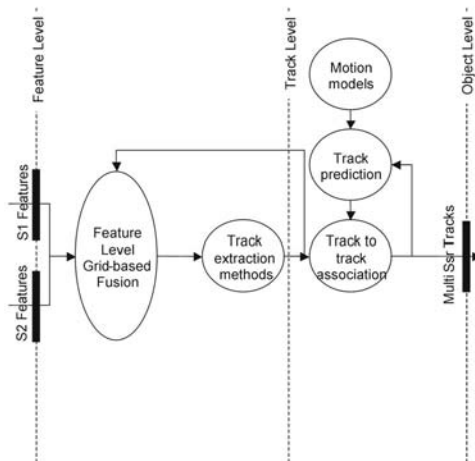


Fig. 5. Detail of the grid-based fusion architecture on the feature level

Based on the occupancy grid, we extract the objects in the grid: Moving obstacles are extracted by first identifying the moving area. We proceed by differencing two consecutive occupancy grids in time. Then extraction of features such as surface and velocity could be performed to classify the type of obstacle. In case of the possibility of using velocity or a category map the previous process is fused with these two maps to obtain the gravity centre of each object and a probability distribution over its possible category.

Data association algorithms are used to update the different tracks with extracted tracks. To deal with unobservable tracks, we use a particular process for handling occlusions. To deal with the particular topology of the environment: entry and exit areas, we use a particular process based upon the roadmap.

Thanks to the occupancy grid, we extract unobservable areas due to occlusions (Occlusion management). For each object, three cases arise:

- ▶ The object is seen by the sensors and then is associated with sensor measurement.
- ▶ The object is not seen due to occlusion, the sensors measurements define occluded areas and in each occluded area there is a uniform probability that the object lies.
- ▶ The object is not seen due to miss detection. When association is made, a probability over the velocity and the category is updated thanks to prediction models for each category of road users.

Thanks to the interpretation of the map, we are able to know areas where the objects could appear or disappear (entry and exit areas). This helps the robustness relative to false alarm and missed detection.

Object list are managed as a list of tracks. Each track is tagged with a specific ID and a set of characteristics. A track is created when consistent sensor information makes the existence of an object certain. One deletes a track only if this track disappears of the sensor view in a disappearance area. We also manage merge and split of objects and all other relevant problems that might appear. To perform the tracks update, tracking methods are used and a set of hypotheses of predicted position, velocity and category for each object is obtained.

In the situation refinement, we propose to perform trajectory prediction for the objects present in the environment. This trajectory prediction is performed using the classical “learn predict” paradigm. In a first step, the past trajectories of the objects are collected and are clustered to define some class-

es of typical trajectories. In a second step, these classes are used to predict the future trajectory of an object present in the environment.

2.4 The Track-Level Fusion Approach

The track-based fusion within the object refinement layer is a distributed approach. It assumes that tracking is carried out inside each individual sensor or system, and the tracks feed the track level fusion algorithms. It can be applied to automotive sensor networks with complementary or/and redundant field of view. The advantage of the approach is that it ensures system modularity and allows benchmarking, as it does not allow feedbacks and loops inside the processing.

Research and development for track level fusion is focused on developing innovative algorithms in the area of multidimensional (N-D) track-to-track association, track management and track fusion. Expected results from these efforts are more consistency and the avoidance of spurious or invalid perception information. The output of the track level fusion is aggregated tracks in the union of the sensor field of views.

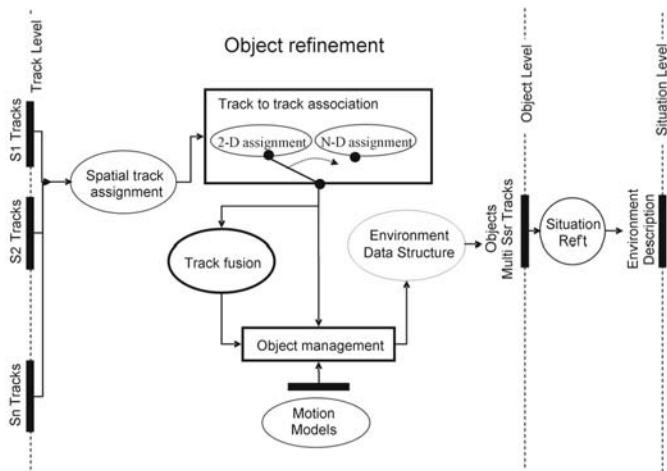


Fig. 6. Track-based fusion functional architecture

The research and development process for situation analysis consists of two main components: The first step is to develop the appropriate level of domain specific knowledge for the road elements (e.g. road borders, lanes, obstacles) and the second to develop a decision making process that is able to codify and manipulate the knowledge mentioned above. In situation refinement the sys-

tem is aware not only of the states of the road elements but has also knowledge of their relationships. The outcome of situation refinement enriches the environment model including additional attributes of the ego-vehicle and the obstacles (predicted paths, object to lane assignment, evidence for vehicle manoeuvres, etc.)

The track level fusion architectural modules are depicted in the Fig. 6. It is implied that a set of track arrays are entering the fusion system while the output of object refinement process is consisted of the fusion object list. The internal functionalities in this architecture are the association (spatial track assignment and 2-D and N-D association), the track to track update (fusion) and the fused object management. All these sub-modules are described in detail in this section.

The Fusion Area Track Assignment is the first function that is imposed to the tracks when they are entering the fusion system. The main objective of this is to decrease the computational load of the overall procedure and also to ensure the configurability and the interoperability of the procedure. A set of sensor configuration parameters are necessary for this module to work properly. At least it is required to have the sensors' maximum range, Field Of View (FOV), direction, location, accuracy resolution and a performance index - estimation error covariance matrix or overall confidence level. The main process of this module is to separate the sensor coverage area around ego vehicle and consequently to separate the available tracks. These areas could be blind areas not observed by any sensors, areas with one sensor and areas observed by two or more sensors. The main result of this process is to divide the fusion problem to a number of smaller fusion sub-problems.

The tracks that belong to areas without or single sensor surveillance are passing to the output without any additional processing. On the other hand, the tracks that are within the common sensors areas (2 sensors or more) an association measure will be defined. This metric is for generating the hypotheses for association between tracks, and then the relative association matrix or other metric passes to the next level where the track to track assignment takes place (Track to Track Association). In the case of 2 sensors tracks the 2-D association problem is solved. The input to this module is the output of track to track association and its output is the pairs of tracks that are suitable for fusion and the not assigned tracks that simply pass to the next module. In the case of tracks coming from more than 2 sensors then the solution to this problem the N-D with N to be 3 more takes place in this module. Usually this problem concerns the sequential generation of a 2-D problem out of the N-D and after that the solution is similar to this acquired in 2-D assignment.

The assignment tracks (2 or more) that come from the output of the assignment modules are fused by the track fusion module. They are updated and generate a fused object state and covariance that replaces the existing sensor level tracks.

Within the object management module the fused and the non-fused tracked objects are formatting the final object list output for the object refinement process. All the objects have an ID and in this module the initialisation, updates, deletion of objects based on ID information take place. Moreover, this module will handle, in a final step, object management issues such as duplications of objects, blind areas objects, transition of objects between different areas and all other relevant problems that might appear.

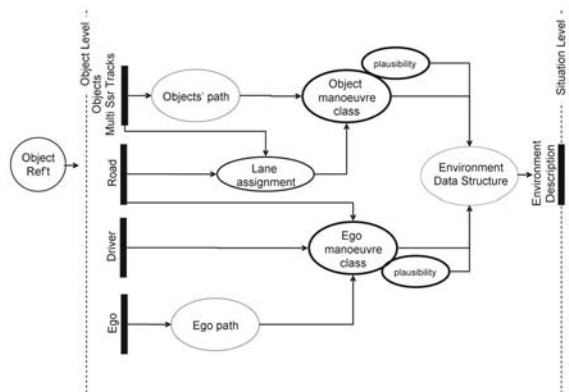


Fig. 7. The situation refinement internal functional module architecture

The model collection, containing also motion models, is a horizontal activity and not only internal in object refinement. It is a function that generates and uses the available dynamics models, static models, sensor models and the relative to the environment description models. This module is also necessary to the situation refinement process.

The internal situation refinement modules are depicted in the Fig. 7. The output of the object refinement process is the main input in this module. The internal functionalities that take place in this architecture are the assignment to objects in a specific lane and the prediction of the path of the ego and the other vehicles (moving objects). The final output is the ego-vehicle and moving objects manoeuvre classification together with a confidence index. The output of this module passes to the application.

The object path module and the ego path module concern the prediction of the expected future path of moving vehicles and the own car respectively for a short period of time (e.g. 4s).

The lane assignment module uses object position information and the available lane geometry and assigns a lane index to each of the vehicles accompanied with a confidence index. This information is very useful for the manoeuvre classification modules.

The objects and ego manoeuvre classification modules analyse the behaviour of objects and the ego vehicle and classifies them according to a predefined discrete set of classes (e.g. overtaking, exceeding speed, parallel to the lane, lane change, etc.). These modules assume the existence of an environment model – i.e. descriptions of the road attributes and the lane properties and the output of the objects' path and the lane assignment; they analyze relationships between "objects" and produce a new structure. Their output will be part of the environment model and will be defined in the relevant tasks. The decision is accompanied with a level of confidence.

2.5 The Fusion Feedback Approach

To overcome a limitation of track-based fusion, some approaches insist on injecting information coming from other sensors at an early stage of processing by a given sensor. This can be achieved by feeding unprocessed – or slightly processed data – from different sensors into a single module in charge of all processing across different sensors.

An original alternative way put forward here relies on fusion feedback. In track-based fusion architectures, taken as reference architectures, the output of fusion reflects information coming from different sensors. By feeding this processed multi-sensorial information into early processing of a given sensor (here sensor 1), we make it possible to sensor 1 processing to confirm some detection formerly only suspected by sensor 2.

As an example, a RADAR device and a FIR camera originally produce tracks. Track-based fusion will merge some of them, and logically leave some RADAR and FIR tracks unmatched, because of possible complex and/or misleading environment. With Fusion Feedback, the RADAR information available on output from Track-Level Fusion will allow FIR processing to further rescan the area corresponding to the RADAR-only tracks.

Fusion Feedback builds upon a track-based fusion architecture, providing a solution to overcome its limitations through little structural changes. To do so, we want the processing of some given sensor – sensor 1 – to be able to use some additional information including data from sensor 2. The output is an excellent candidate, as it already exists in a traditional track-based fusion architecture. It contains information provided by both sensors.

Therefore, we feed the output of track-based fusion into sensor 1 processing, as illustrated by the Fig. 8. Here, information coming from sensor 2 goes to track-based fusion, where some sensor 2 tracks might be left unmatched for various reasons. However, sensor 1 processing will use this information to better focus its search. This concept provides improved performance, without major reshuffling of the track-based fusion architecture, as it merely requires one additional link from fusion to the sensor processing, and customisation of the sensor processing.

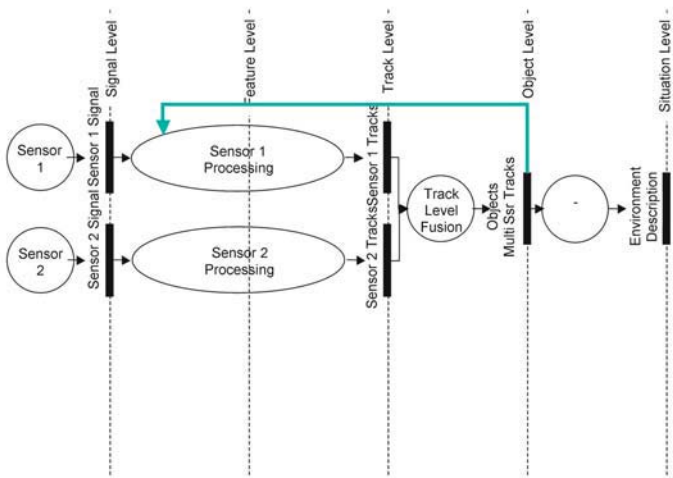


Fig. 8. Global Fusion Feedback architecture

According to the addition of the link illustrated in the Fig. 8, the sensor 1 processing must be able to take advantage of information coming from track-based fusion. Considering a FIR camera as sensor 1 the original sensor 1 processing can be described as acquisition, pre-processing, detection, tracking and output formatting. Now, to accommodate the use of extraneous information, we have to enhance this architecture with additional sub-modules, and some enhanced existing sub-modules (cf. Fig. 9).

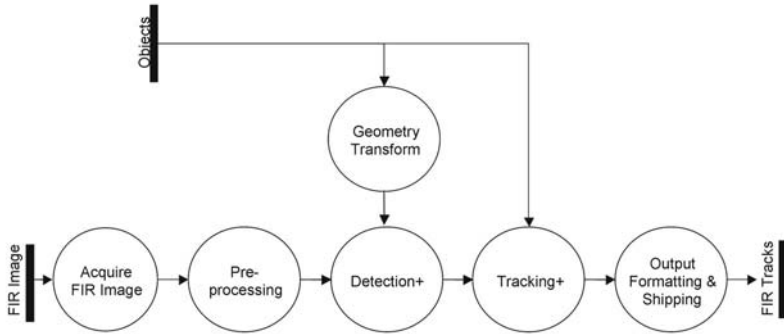


Fig. 9. Modified detection scheme

The information coming from the fusion module has to be converted into the natural representation for the sensor, here the FIR camera. Then detection must take into account the hint provided, possibly by releasing detection thresholds around given areas. Beside its usual functionality, tracking will now additionally have to check the compatibility between external track continuity and possible new FIR tracks detected using this hint.

3 Conclusion

In this paper we presented a modular framework for multi sensor data fusion, which addresses the crucial task of automotive environment perception. Thereby this interoperable architecture is not dependant on a special safety application but is designed on top of a multi sensor platform to serve diverse safety functions at once. Furthermore it will offer a robust and reliable perception performance due to the integration of diverse fusion approaches and algorithms for situation refinement beyond current state-of-the-art. Additionally this architecture with its extended environmental modelling provides an excellent basis for further enhancement in the field of automotive environment perception and thus contributes to the design and development of road safety systems.

4 Acknowledgement

The work described within this paper is part of the results obtained in the ProFusion2 project, which is a subproject of the PREVENT Integrated Project, an automotive initiative co-funded by the European Commission under the 6th

Framework Program. The long term goal of the subproject ProFusion2 is to streamline the sensor data fusion inside PReVENT by, e.g. gathering requirements, defining certain standards and developing fusion algorithms, which should be used by the application-oriented subprojects within PReVENT. Hence ProFusion2, whose consortium consists of CRF, DaimlerChrysler, Delphi, FORWISS, IBEO, ICCS, INRIA, SAGEM, the University of Chemnitz and Volvo Tec, addresses research work of common interest related to sensors and sensor data fusion including a modular architecture for sensor data fusion. This architecture will be based on an extended environment model and representation, consisting of a set of common data structures for sensor, object and situation refinement data and algorithms as well as the corresponding models.

References

- [1] U. Scheunert, Ph. Lindner, H. Cramer, T. Tatschke, A. Polychronopoulos, G. Wanielik, "The Extended 4D Environment Model for Interoperable Data Fusion", submitted to the IEEE Intelligent Vehicles Symposium 2006, Tokyo, Japan, June 2006
- [2] J. Llinas, C. Bowman, G. Rogova, A. Steinberg, E. Waltz, F. White. "Revisions and extensions to the JDL data fusion model II". In Proceedings of the 7th International Conference on Information Fusion, 2004
- [3] A. Polychronopoulos, et al, "PF2 Functional Model for automotive sensor data fusion", will be submitted to the International Conference on Information Fusion, Florence, July, 2006
- [4] Michael Darms and Hermann Winner, "A Modular System Architecture for Sensor Data Processing of ADAS Applications". In Proceedings of the IEEE Intelligent Vehicle Symposium 2005, Las Vegas, U.S.A., June 2006
- [5] F. Tango, A. Saroldi, et al, "Definition of System Requirements and Use-Cases", Public deliverable D15.31 of the PReVENT subproject ProFusion2, November 2005, available at www.prevent-ip.org
- [6] T. Strobel, C. Coue, et al, "State of the art of sensors and sensor data fusion for automotive preventive safety applications", Public deliverable D13.400 of the PReVENT subproject ProFusion, July 2004, available at www.prevent-ip.org
- [7] C. Coue, et al, "Recommendation for original research work", Public deliverable D13.400 of the PReVENT subproject ProFusion, July 2004, available at www.prevent-ip.org

Thomas Tatschke

FORWISS, University of Passau
 Innstrasse 43
 94036 Passau, Germany
 tatschke@forwiss.uni-passau.de

Su-Birm Park

Delphi Electronics Safety
 Vorm Eichholz 1
 42119 Wuppertal, Germany
 su.birm.park@delphi.com

Angelos Amditis

ICCS, NTUA
 Iroon Politechniou Str. 9
 15773 Zografou, Athens
 Greece
 a.amditis@iccs.gr

Aristomenis Polychronopoulos

ICCS, NTUA
 Iroon Politechniou Str. 9
 15773 Zografou, Athens
 Greece
 arisp@iccs.gr

Ullrich Scheunert

Technical University of Chemnitz
 Reichenhainer Str. 70
 09126 Chemnitz, Germany
 ullrich.scheunert@etit.tu-chemnitz.de

Olivier Aycard

GRAVIR-IMAG INRIA
 Rhône-Alpes 655 avenue de l'Europe
 Montbonnot 38334 Saint Ismier Cedex, France
 Franceolivier.aycard@imag.fr

Keywords: sensor data fusion, environment perception, fusion framework, environment modelling, early fusion, multi level fusion, grid-based fusion, track-based fusion, fusion feedback, ProFusion2

Integrating Lateral and Longitudinal Active and Preventive Safety Functions

A. Amditis, A. Polychronopoulos, Institute of Communications and Computer Systems

A. Sjögren, A. Beutner, Volvo Technology Corporation

M. Miglietta, A. Saroldi, Centro Ricerche Fiat

Abstract

Automotive safety functions are divided, on one hand, into passive and active safety according to a time factor before an accident or a critical situation could occur; on the other hand, they focus on single slices around the intelligent vehicle, even if more and more sensors are added to improve system accuracy. The paper proposes new integrated functions under INSAFES sub-project of PREVENT merging and harmonizing lateral and longitudinal support functions, collision mitigation protective functions and road users' protection systems. The advantage of INSAFES that is shown in the paper is that all functions share the same system resources – sensors and perception units – and trigger a given set of actuators and HMI controllers in order to communicate with the driver or intervene. The proposed system will be integrated and demonstrated in a passenger car and a truck.

1 Introduction

Existing sensing systems can identify the presence of obstacles and are able to support the driver, generally, in front of the vehicle or only on "single slices" of the scenarios around the vehicle. Consequently, different sensor technologies need to be integrated today in the vehicle in order to cover all the area around it and to provide a complete support in all traffic and environmental scenarios. The proposed work intends to allow the extension of the operative scenarios of the advanced driver assistance and protective systems beyond their current limits and allows enabling a considerable step forward of the actual development and implementation of data fusion techniques.

This problem is tackled in the INSAFES sub-project. The goal is to improve the functionality and reliability of applications developed within PREVENT Integrated Project (IP) and to advance from stand-alone safety applications,

targeting one specific function each, to an integrated system, covering a vast range of applications. This priority of INSAFES focuses on the full coverage of the surrounding of a vehicle, in order to warn the driver, intervene, or mitigate the effects of an accident. INSAFES addresses the proper use and interpretation of all the information available from sensors or functions that are being developed in PReVENT [1], and the subsequent situation and risk assessment. The paper studies INSAFES use cases such as:

- a) enhanced longitudinal control functions (e.g. integration of frontal collision warning and collision mitigation strategies, semi-autonomous braking intervention: braking action confirmed by the driver on the brake pedal after a warning; warning and intervention strategies optimised according to the data received from communication components).
- b) enhanced lateral control functions (e.g. improvement of lane keeping support, optimised also with respect to the presence of lateral obstacles e.g. close guard-rails or parallel vehicles; side collision avoidance/mitigation for trucks within the ego-lane, typically in drifting situations)
- c) integration and synergies of lateral and longitudinal control applications (e.g. all-around warning function, based on the reconstruction and the assessment of all-around traffic scenario; improved frontal collision warning/mitigation: optimisation of the warning/intervention strategies, based on computation of a feasible evasive trajectory; collision mitigation, autonomous intervention: optimisation of the intervention strategies – for instance switch to semi-autonomous modality – depending on the detected surrounding traffic).

The developed functions will be implemented, demonstrated and evaluated through validation and functional tests using a passenger vehicle from FIAT Research Centre and a truck from Volvo Technology. The equipped vehicles serve for test and validation purposes and will be used for testing the functionality and performance of the developed system and for evaluation of the driver acceptance of the human-machine-interface. INSAFES belongs to the cross-functional activities of PReVENT Integrated Project, which in turn is co-funded by the European Commission under the 6th Framework Program. The project is coordinated by Volvo Technology; it started in September 2005 and will finish in December 2007.

The paper starts with a layered conceptual framework borrowed from a PReVENT cross-functional activity, ProFusion2, which deals with sensor fusion, and implemented to cover INSAFES needs. A chapter that investigates how existing active and preventive safety functions can be improved in INSAFES follows. In Chapter 4, eight new functions are briefly presented which integrate different functional fields and are proposed for future implementation in the INSAFES passenger car and truck. The functions are classi-

fied with respect to the type of vehicle, but it can be considered without loss of generality, as integrated functions for future vehicles.

2 INSAFES System Design Layers

Due to the complexity of the information handled in INSAFES, the high quantity of information sources and the system requirements a sensor fusion approach is adopted. The same approach can be met in other sub-projects of PReVENT and is also recommended from the ProFusion PReVENT cross-functional activities [2]. ProFusion's major objective is to push the sensor data fusion techniques used for automotive environment perception beyond the current state-of-the-art. This is done by setting up a modular and interoperable fusion architecture for multi sensor systems, which integrates diverse approaches (e.g. low and high sensor data fusion, algorithms for situation refinement, etc.). In doing so, the ProFusion framework is not limited to any special safety function but operational with all different kinds of applications like collision mitigation, lateral control, lane departure warning and others, and thus is suitable for INSAFES.

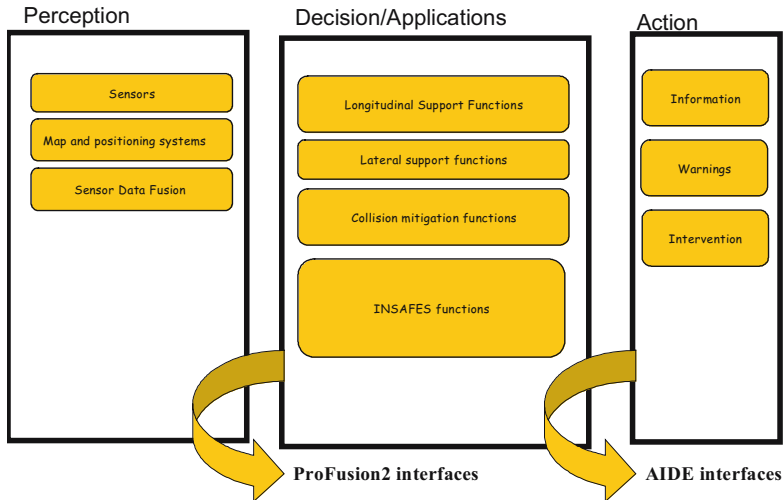


Fig. 1. Functional layers of a sensor fusion active/preventive safety system, the INSAFES paradigm

In general, sensor data fusion includes several processing steps which take the data of several single sensors and combine the information from them in order to achieve a certainly better result than the outcome of each single sensor's

processing could provide. This effect of getting better or more adequate results out of sensor data fusion compared to single sensor processing is called 'synergy' or 'synergetic effect'. A typical driver assistance system's architecture consists of at least three layers: the perception layer being responsible for the environment perception, the decision/application and the action layer, which are responsible for taking and executing actions respectively. Sensor data fusion, may take place on every individual layer depending on the approach or even in all layers. Usually, by sensor fusion, one can assume fusion in the perception layer (e.g. for obstacle detection), but this is not true, especially in the case of INSAFES project. However, in the system's perspective this is indifferent, if the layers support the same input output interfaces.

The INSAFES project develops the common decision layer and study the interfacing to it from the different functions. One challenge is to find a level of integration that result in an increased performance but still enables most of the different function components to be re-used. The INSAFES idea is to integrate already existing function components, not reinventing them from scratch again.

The action- and output-coordination will be covered, in close cooperation with the AIDE project [3]. The idea of introducing a common decision layer is depicted in the figure above; an action coordinator still is needed if there are functions that are not fully integrated in the common decision concept and it is described in AIDE related publications [4].

3 PReVENT Functions as a Starting Point of INSAFES

To clarify how INSAFES gives added value to the respective stand-alone functions – represented by PReVENT vertical sub-projects – the main goals of each of these projects are outlined here, together with a short description of the advantages of the INSAFES approach. This will supplement the description of the complementary character as well as the synergies between the projects highlighted throughout this paper.

The APALACI functions serve two principal goals: (1) the development of advanced obstacle detection functionalities, and (2) the development of longitudinal pre-crash and collision mitigation applications. Both functionalities are based on sensor fusion techniques in order to be able to detect and to classify objects including pedestrians.

Main INSAFES added value: Integration with the front collision warning functionality for the optimisation of the semi or autonomous braking intervention strategies with respect to the complete traffic scenario reconstruction; extension of irreversible pre-crash function to the lateral area (early detection of lateral obstacles for lateral air-bag pre-set).

The target functions for LATERAL SAFE are aiming to develop (1) a lateral and rear area monitoring application enhancing the driver's perception of risk of collision in the lateral and rear area of the vehicle. (2) a stand-alone lane change assistance system with integrated blind spot detection assisting the driver in lane change manoeuvres while driving on roads with more than one lane per direction and (3) a lateral collision warning function that detect and tracks obstacles in the lateral field and warn the driver about an imminent risk of accidents (collision, road departure or merging situations).

Main INSAFES added value: All-around collision warning function, integration of lateral support functions; reconstruction of the surrounding scenario for optimising the longitudinal functions and control strategies for warning or mitigation (e.g. strategies improved according to the computation of feasible evasive manoeuvre).

The SASPENCE concept aims at supporting the driver in avoiding accident situations related to inappropriate speed and/or insufficient distance (headway) to the obstacle ahead, by providing information through tactile primary commands. The system should support in maintaining an appropriate vehicle velocity (and distance) for any given driving situation in any conditions. Using such a system as starting point and collecting information from "all-around sensors", as well as complete data-fusion algorithms, more advanced information can be provided to the driver, concerning the suggestion of the optimal manoeuvre to perform, being a braking or obstacle avoidance.

Main INSAFES added value: Integration of longitudinal control functions; improved scenario reconstruction and warning strategies using WILLWARN information.

The SAFELANE application aims at enhancing traffic safety by supporting primarily the drivers of commercial vehicles in avoiding unintended lane or road departures on motorways and rural roads. The system operates safely and reliably in a wide range of even difficult road and driving situations. If an unintended lane departure is foreseen or detected, the driver is warned or an active steering system is activated to keep the vehicle within the lane or to bring it back into it.

Main INSAFES added value: Integration of lateral control functions

A basic WILLWARN system will focus on warning of reduced visibility or reduced friction or if the car has failed and has become an obstacle for other cars. Obstacle information will be derived from an ACC sensor and speed profiles or avoidance manoeuvres will be recommended. As INSAFES is using a multiple sensor approach for obstacle detection, the system will be capable of detecting and classifying obstacles in high quality. An INSAFES vehicle can warn other vehicles by car to car communication when an obstacle is detected using the techniques and protocols that are developed by WILLWARN.

Main INSAFES added value: integration of longitudinal control functions, radar systems integrated to WILLWARN functions.

The following highlights the complementary character of the project proposals by sensor technology and actuators.

PROJECT	FUNCTIONS	Maps and localisation	Long range front radar	Short range front radar	Front camera	Short range side radar	Long range back radar	Active steering	Active gas pedal	Reversible restraint system ive booster (brake system)	Non-reversible restraint system	
APALACI	Safety belt pre-trigger; air-bag deployment set; collision mitigation			X	X					X	X	X
SAFELANE	Lane keeping support	X	X		X			X				
LATERAL SAFE	Lane change assistance; lateral and rear area monitoring; lateral collision warning					X	X					
SASPENCE	Safe speed and safe distance	X	X	X	X				X	X		

Fig. 2. Sharing of resources for the realization of integrated functions

4 INSAFES Functions

4.1 Adaptive Lane keeping Support with Lateral Monitoring for Trucks

Lane keeping support function (represented in PReVENT as SAFELANE) assumes the centre position of the ego- lane as the optimal driving position. In

case of presence of a vehicle in the adjacent lane and especially if lanes are narrow and thus, lateral distance between vehicles is small, a lateral displacement of the own vehicle in the own lane is desirable to increase the lateral distance. In this function, the lane keeping algorithm is modified to consider a different desired lane position, when close vehicles in adjacent lanes are present, as shown in the following figure. The function may have different levels, starting from just modifying parameters in the lane keeping support algorithm up to actively correcting the vehicle's position in the lane by using a steering actuator. The existence of an adjacent vehicle will be presented to the driver from a different application.

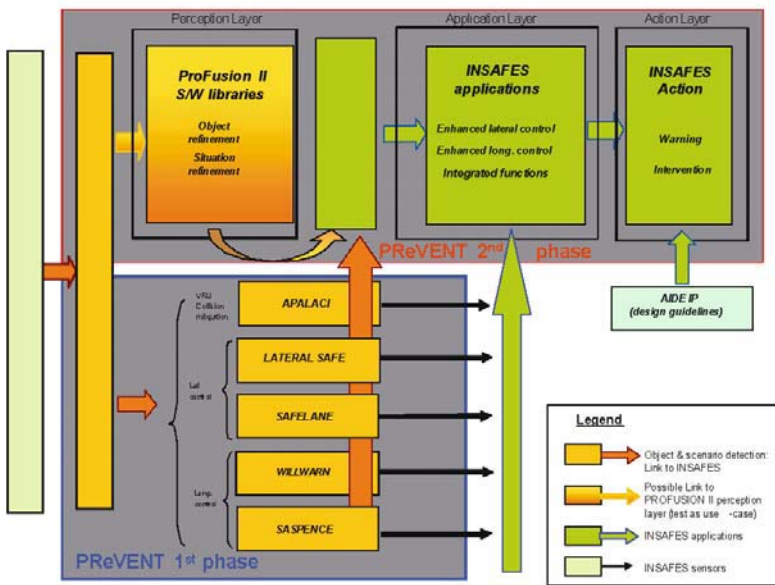


Fig. 3. INSAFES interactions with existing functions and cross-functional activities

The goal of the function is the enhancement of driving safety by adapting the desired lane offset for the Lane Keeping Support with respect to distance of other vehicles in adjacent lanes. The goal is to avoid safety critical driving situations by monitoring the lateral distance to vehicles driving in adjacent lanes and in case the distance is too small and thus implies an increased risk for accidents to adapt the desired lateral offset and position in the own lane of the lane keeping algorithm.

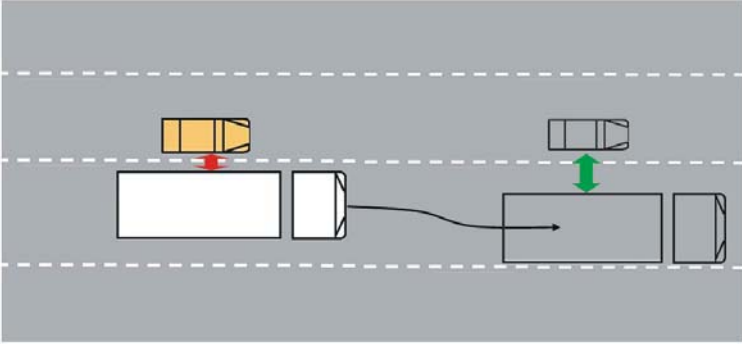


Fig. 4. Enhanced lane keeping with adaptive lane offset

4.2 Lane Change Warning with Haptic Steering Wheel Feedback and corrective Action for Trucks

The objective of this function is the enhancement of driving safety by combining an originally passive lane change warning function (cf. LATERAL SAFE) using only e.g. optical and/or audible warning with the possibilities provided by using SAFELANE’s active steering actuator for providing haptic feedback via the steering wheel. The goal is to avoid safety critical driving situations by monitoring the lateral area of the ego-vehicle and in case of an indicated lane change (e.g. usage of blinkers and actively steering) while another vehicle is present in the lateral area to issue a warning by haptic feedback (e.g. vibration and corrective action) by using the active steering actuator from SAFELANE.

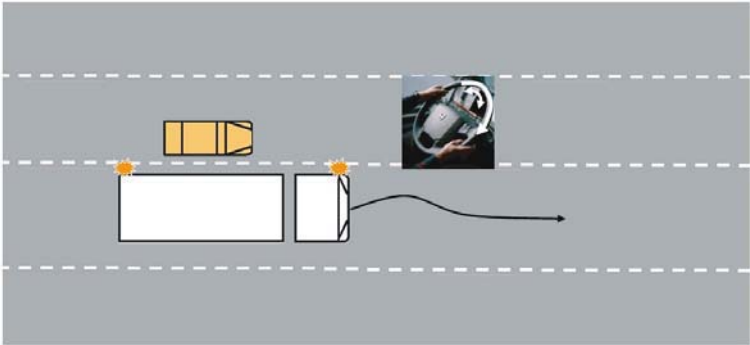


Fig. 5. Lane change warning with haptic feedback and correction

The lane change warning function uses visual and/or audible warnings. By alternatively or additionally using the SAFELANE active steering actuator a different HMI channel, a haptic warning, can be used. Furthermore, not only

a warning can be given, but by applying an overlay torque to the steering wheel a correction of the steering angle and “prevention” of lane change maneuver can be achieved as well, as illustrated in Fig. 5.

4.3 Enhancement of APALACI low Speed Obstacle Warning for Trucks

The objective is the enhancement of APALACI low speed obstacle warning and right-turn start inhibit with a blind spot sensor (right). This is a beneficial function as it covers a remaining blind spot between the APALACI front sensors and the lateral monitoring sensors used for the previously described functions.

The APALACI realization in the Volvo truck focuses mainly on the start-inhibit application, aiming at preventing run-over accidents in start-up situations, e.g. accidents when an object or a pedestrian in the proximity of the vehicle is hit by the truck taking off from standstill. Since the start-inhibit function requires the system to perceive the area close in front of the vehicle, it was also considered possible to extend the functionality to a general proximity-warning function: warning if there is an obstacle detected within the specified area, when the truck drives at low speed. The area of detection which has to be covered by the sensing system is shown in the figure below. The area for proximity warning is larger than the start inhibit area. In particular the right side of the vehicle needs also to be covered in order to include the main blind spots. This was not included in APALACI, but is considered here to enhance the APALACI function with the low speed obstacle warning, including especially the blind spot area as indicated with the red ellipse in Fig. 6.

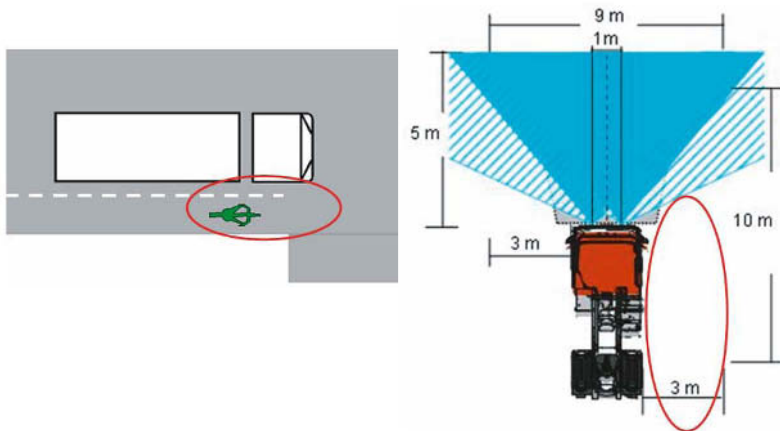


Fig. 6. Enhancement of APALACI low speed obstacle warning

4.4 Enhanced Curve Speed Warning Function for Trucks

The curve speed warning function is based on reliable perception of the road ahead. The road and lane curvature can be derived by a lane tracking system from SAFELANE – which is accurate for short distances – but still digital map data are needed for a longer electronic horizon and will be provided by MAPS&ADAS project. Considering the general condition of the truck, trailer, load weight and type (if known) or environmental conditions (if known) a suitable lateral acceleration and thus a suitable velocity for driving into and through the curve can be calculated and can e.g. be given as recommendation to the driver or in a second stage issue a warning. Finally even an active intervention by actively limiting or reducing the velocity is a possibility, but not considered within the scope of the project.

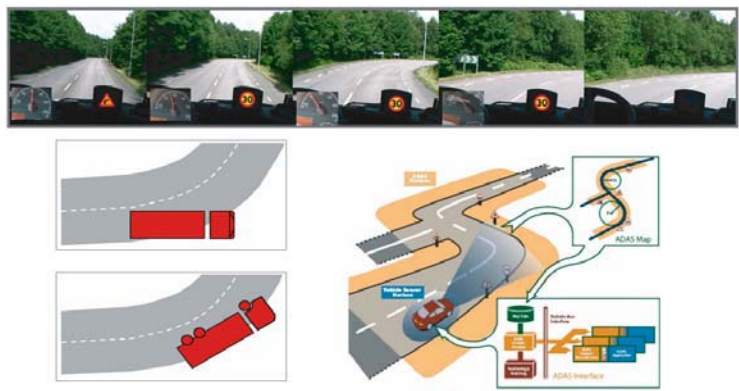


Fig. 7. Enhanced curve speed warning for trucks

4.5 Forward-Lateral-Rear-Monitoring Function for Trucks

The Forward-Lateral-Rear-Monitoring (FLRM) function is based on the Lateral-Rear-Monitoring (LRM) function developed for the simulator in LATERAL SAFE project. By using the lateral sensors, the additional blind spot sensor (right) and furthermore including the forward area obstacles information from the APALACI sensors the Monitoring functionality will be brought from simulation to a real application. As the right side blind spot is not visual in the original APALACI display, the FLRM display and visualization serves for the APALACI low speed obstacle warning functionality as well.

The overall objective of the FLRM function is to inform the driver of adjacent vehicles. This will assist the driver in the task of detecting and tracking sur-

rounding vehicles. FLRM thus extends and improves the visibility in direct (window openings) and indirect (mirrors) in the following ways:

Using multiple sensors will cover all of the vehicle surroundings, effectively eliminating the blind spots normally found in mirror systems.

The arbitrary placement of a sensor-display based system does not require an optical line-of-sight. This is especially valuable for trucks where ego vehicle/trailer typically blocks rear line of sight and where a significant blind spot area is to the right side of the cabin and even directly in front of the truck, as covered in APALACI.

The integration of sensors presented in a single consistent HMI will eliminate the fragmented viewing; all of the vehicle can be surveyed from a single point.

The nature of the FLRM function is thus passive, the function will present information; it is up to the driver to choose if and when to make use of the system and the information presented. The FLRM application presents the information in an abstract per-sector level and basically informs the driver of the presence of a vehicle in a designated sector around the vehicle as shown in Figure below.

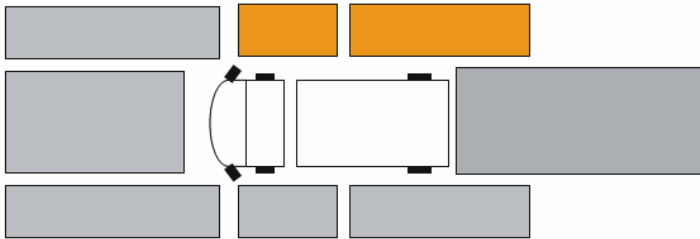


Fig. 8. Forward-Lateral-Rear-Monitoring Coverage

4.6 Integrated Longitudinal Support in Passenger Cars

This function results from a combination of functions developed inside WILL-WARN, SASPENCE, and APALACI subprojects as it merges preventive and active safety systems in the longitudinal driving axis. It provides support and protection in cases that an accident may occur in a few milliseconds or a critical situation or a hazard is foreseen for the future.

The driver is invited to follow a speed profile that avoids entering into dangerous situations with excessive speed (safe speed). This suggestion can be communicated to the driver through different perceptual channels, that is: visual display, sounds, haptic feedback on the accelerator pedal, and vibration on the seat-belts. When the driver pushes the brake pedal, but the force applied by the driver is not sufficient to avoid a collision, extra pressure is applied by the system on the brake (assisted braking). Finally, just before entering into a collision situation, safety belts are pretensioned to mitigate the effects of the accident.

4.7 All Around Collision Warning in Passenger Vehicles

The All-around Collision Warning function should warn the driver in case of a likely accident due to approaching objects from all sides. This includes traffic coming to close from behind, oncoming traffic from the side, and also oncoming traffic in the front useful e.g. in the case of driver distraction.

A network of sensors all-around the ego-vehicle is mandatory to sense the surrounding area. A threat assessment is calculated for all detected objects and a pruning algorithm selects the critical ones. Based on this, in case of a dangerously approaching object, a warning is given to the driver early enough to allow time for a situation analysis and a reaction.

To separate this application from other safety applications like pre-crash or collision mitigation, the focus has to be set to different main areas. Due to the fact that too many warning issues would annoy or overstrain the driver instead of leading to a real safety benefit, the target scenarios have to be limited by reducing the relative speed and operative speed intervals when the function is active. Most accidents occur in the urban scenarios which should therefore be the main scenario covered by the application. Another important argument for the limitation of the relative speed interval is the finite reaction time needed for the driver to recognize the situation and react in accordance to that. Due to the early warning function, it is intended that it is possible to reduce the number of accidents especially in the case of driver distraction or, at least, to reduce the crash severity by the reaction of the driver.

Warning information has to be given to the car driver by an unambiguous and appropriate readout. To allow the driver to understand the situation immediately this information has to include the direction/area of the critical situation in an intuitive way. Further investigations about an optimal solution for this task are clearly recommended.

4.8 Maneuver Suggestion Function

The objective of the function is to reduce the number of accidents due to a wrong maneuver undertaken by the driver, in particular when a decision has to be taken between staying in the lane or change lane (overtake). The driver receives a visual suggestion about the fact the he should stay in the lane or change lane, considering the position of the car on the road and the presence of obstacles. It is an extension of SASPENCE safe speed suggestion function.

5 Conclusions

The paper presented a new approach of merging different active and preventive safety functions and proposed integrated functions under the framework of PReVENT function taxonomy. The principles and basic requirements were set at the beginning of the paper; however, the actual design and implementation of the architecture is under development and results will be presented in the near future.

References

- [1] www.prevent-ip.org
- [2] T. Tatschke, S.-B. Park, A. Amditis, A. Polychronopoulos, U. Scheunert, "ProFusion2 – Towards a modular, robust and reliable fusion architecture for automotive environment perception", to appear in *Advanced Microsystems for Automotive Applications 2006*, Ed. Springer
- [3] www.aide-eu.org
- [4] A. Amditis, H. Kußmann, A. Polychronopoulos, J. Engström, L. Andreone, "System architecture for integrated adaptive HMI solutions", submitted to the *IEEE Intelligent Vehicles Symposium*, Tokyo, 2006.

A. Amditis, A. Polychronopoulos

Institute of Communications and Computer Systems
 Iroon Polytechniou Str. 9
 15773 Zografou, Athens
 Greece
a.amditis@iccs.gr
arisp@iccs.gr

A. Sjögren, A. Beutner

Volvo Technology Corporation
Götaverksgatan 10
SE-405 08 Göteborg
Sweden
Agneta.Sjogren@volvo.com
Achim.beutner@volvo.com

M. Miglietta, A. Saroldi

Centro Ricerche Fiat
Iroon Polytechniou Str. 9
15773 Zografou, Athens
Greece
Maurizio.miglietta@crf.it
Andrea.saroldi@crf.it

Keywords: integrated functions, active and preventive safety, sensor fusion, perception system, decision system, human machine interaction (HMI)

Lane Detection for a Situation Adaptive Lane keeping Support System, the SAFELANE System

N.Möhler, D.John, M.Voigtländer, Fraunhofer IVI

Abstract

The goal of the SAFELANE project is to develop a situation-adaptive system for enhanced lane keeping support. A prerequisite for lane keeping is reliable information of the vehicle environment. Especially the vehicle position within the lane and the course of the road ahead is important. This information is provided by the lane detection component. The lane tracker is mainly vision based but it is also supplemented by map, positioning and vehicle data. A high dynamic range camera provides the processing unit with image data. Measurement points of lane borders, calculated by a robust edge detection algorithm, are used to estimate a 3D clothoid model of the lane. A new approach for getting an initial lane model is introduced which can be dynamically adapted from map and positioning data. The detection is extended to the neighbour lanes and a lane markings type classifying component is added.

1 Introduction

The SAFELANE project is part of the Integrated European project framework PReVENT. The project's objective is to develop a lane keeping support system, which should go beyond the currently available systems and should function safely and reliably in a wide range of even difficult road and driving conditions. It should be usable in different type of vehicles from small passenger cars to commercial trucks and be operable on motorways and rural roads throughout Europe. Additionally to passive lane keeping support with haptic, acoustic and optic HMI elements it is intended that the system actively steers back into the lane in critical situations.

To reach that ambitious goal, reliable information of the vehicle environment is necessary. Especially the vehicle position in the driving lane and the course of the road ahead is important for lane keeping. Therefore, the lane detection system (lane tracker) is a key component of the overall system. Our lane detection is mainly vision based but is also supplemented by map and positioning

data, vehicle and radar data in cases of missing lane markings, so as the system to be always available.

This paper describes the specification and the current development status of our lane tracker. A special high dynamic range camera serves as input data source for the image processing lane tracking algorithm to cope with various lighting conditions. The image processing is done in real time on a common PC hardware platform. Measurement points of marked but also unmarked lane borders are calculated via a robust edge detection algorithm. The measured border points are projected onto the road plane and a lane model (clothoid) is estimated. To be as flexible as possible and to get accurate estimation results for the automated steering modus, a clear separation is made between camera calibration parameters and the estimated vehicle position parameters.

To enhance the system performance and robustness additional information about the upcoming road segment like lane width and curvature is taken from a digital map and several algorithm parameters are adapted accordingly. A lane marking type classification and a neighbour lane detection are introduced to get more information about the current traffic situation.

2 System Components

The central component of the vision system is the main lane recognition. If the main lane recognition was successful neighbour lanes are trying to be recognized near to the main lane. Measurement points which are generated during the lane recognition process serve as input data to the lane marking type classification. The obstacle area detection marks regions in the image where other objects are located like a vehicle driving ahead. The lane recognition uses this information to restrict the search of measurement points to free road areas. For the lane recognition as well as for the obstacle area detection the vehicle speed is needed. Map data are used to adapt certain lane recognition algorithm parameters like the current lane curvature and width.

3 System Requirements and Specification

The lane detection development and innovation were driven by the evaluation of existing state of the art lane tracker systems. Three different lane trackers were tested during the project concept and specification phase. Several critical scenarios were identified, where the trackers produced false results or

failed. The found scenarios were investigated to get new ideas and approaches for improving the performance of the current lane tracking technology. Some improvements and extensions came from lane keeping functional requirements (e.g. lane marking type recognition).

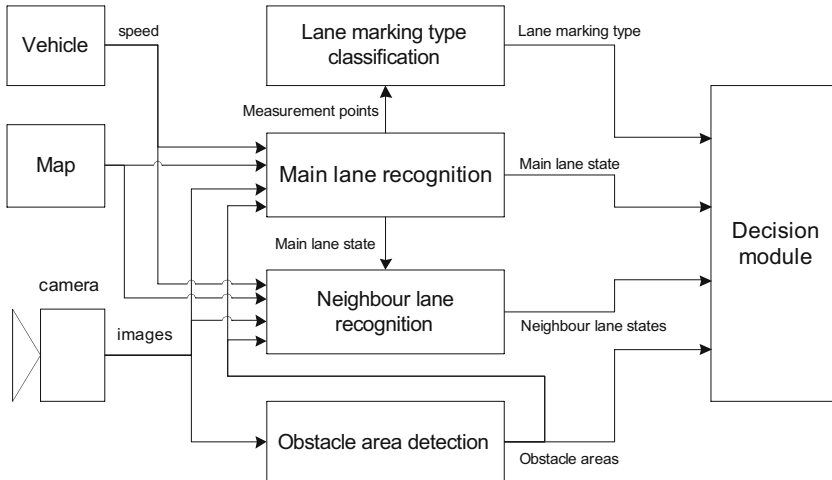


Fig. 1. System components overview

4 Main Lane Recognition

A model based approach with the lane as a clothoid was chosen for the lane recognition. Because highways, country roads and also rail tracks are built after a clothoid geometry, a clothoid suggest itself as lane recognition model. While some systems model the lane borders in the 2 dimensional image coordinates, Dickmanns et al. [1] was the first who showed the benefits of using a 3 dimensional spatial clothoid model for the lane recognition task. The road surface is assumed to be flat and therefore it can be modelled as a plane. The spatial vehicle state is described by its position and orientation relative to the lane. A model state vector comprises of the following parameters: lane width b , lane curvature c_0 , lane curvature change c_1 , lateral offset of vehicle relative to lane centreline y_0 , pitch angle relative to road plane φ_2 , yaw angle relative to lane tangent φ_3 .

In images taken from the camera search areas are set depending on the mode the system is currently in. Measurement points are searched on lines in the image plane. At program start or if the system "lost" the lane, no valid lane

state is at hand – the system is in initialisation mode. Because there are no spatial hints about the lane ahead available, the search area extends almost to the whole image on rigid wide lines (scan lines) in initialisation mode. If the lane recognition was successful in the previous image frame, a valid lane state exists and can be projected onto the image plane. Because the lane state frame to frame differences are usually small it is reasonable to set the scan lines along the lane projection. In both modes a list of scan lines serves as basis to search for lane contour edges in the measurement algorithm step. Now one edge per scan line has to be selected out of the calculated edges being most likely belonging to a lane border. Finally the selected edges are fed to the estimation stage where a new lane state is calculated.

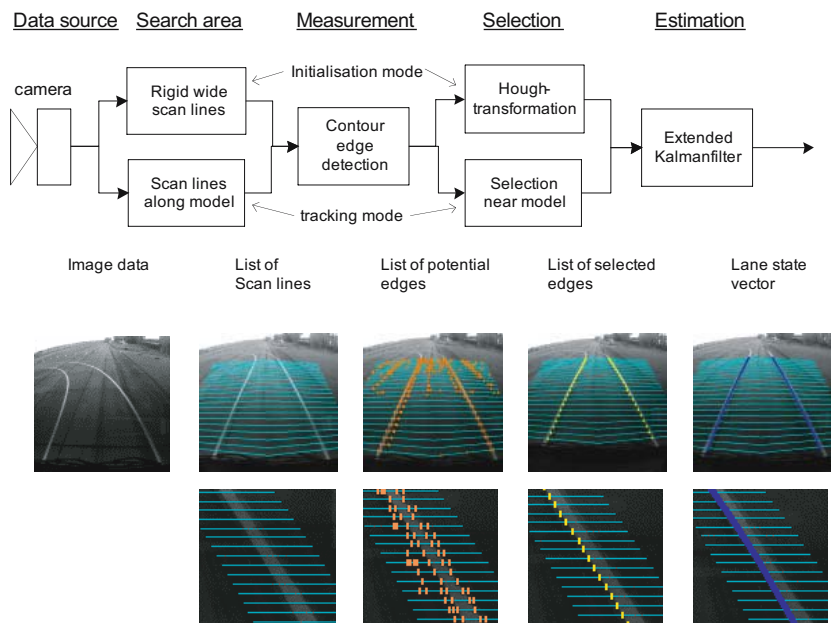


Fig. 2. Lane recognition processing steps, pictures above taken in initialisation mode and below in tracking mode

4.1 Camera Model

To be as flexible as possible concerning camera and lens hardware an extendable modular camera model is used. A camera model does the transformation from world coordinate points to image coordinate points (pixels). The reverse transformation from pixels to world points is a 2 to 3 dimensional transformation and needs an additional condition like world points belonging to a known

plane or having a certain distance from the camera in common. The model comprises 4 transformation stages: Sensor chip model, Distortion model, Projection model, Rotation and translation model. Sensor chip-, distortion- and projection parameter are usually called intrinsic camera parameters and rotation and translation parameters extrinsic camera parameters.

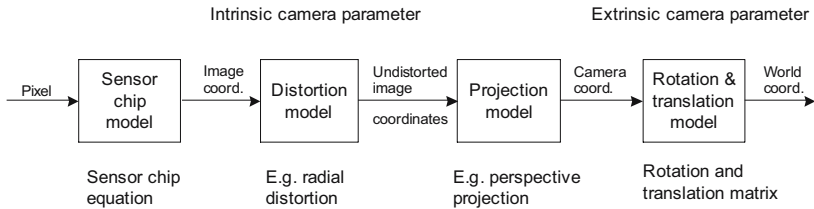


Fig. 3. Pixel to world coordinate transformation

The sensor chip model calculates an (may be distorted) image plane point (image plane: see below) out of a pixel position on the sensor chip. Given an image plane point the distortion model describes its distortion. There may be no distortion at all (pinhole camera) or e.g. radial, tangential, shearing distortion. Currently a radial distortion model is implemented. The projection model projects a camera coordinate point onto the undistorted image surface like a plane or a sphere. Models for central projection or central sphere projection are currently provided. The camera rotation and translation model describes the camera position and orientation in some world coordinate system. These systems are governed by a rotation matrix and a translation vector.

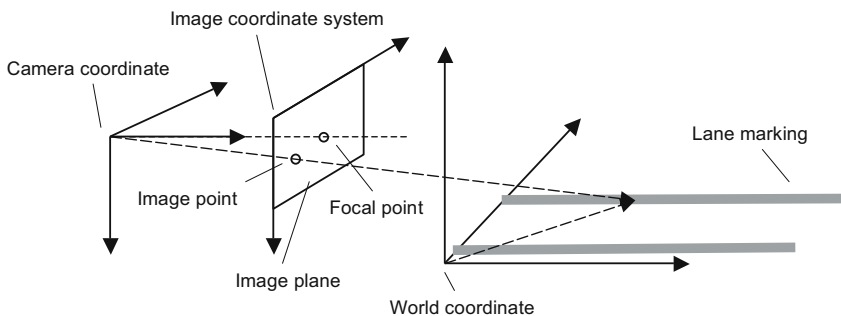


Fig. 4. Depiction of camera to world transformation

To obtain the calibration parameters (intrinsic and extrinsic) of a camera installation we use software for intrinsic and extrinsic calibration which generates calibration parameter files to be used directly in the vision system. It might be objected that this highly modularized approach creates "slow" code. But the

model is implemented with generic programming techniques (C++ templates) so that the compiler has the chance to do all the optimisation it would do as if a monolithic approach would followed. With the described flexible camera model much higher accuracy of lane recognition results are achievable which the automatic steering actuator module of the SAFELANE system benefits from. Above that it is possible to use wide aperture angle optics (radial distortion and sphere projection) to widen the field of view.

4.2 Lane Model

In lane tracking systems usually the position and orientation parameters (lateral offset, yaw and pitch angle) to be estimated are preset with calibration values and the rotational calculation is simplified ($\sin(x) \approx x$, $\cos(x) \approx 1$). It is assumed that the camera is mounted in the vehicle only with a small pitch, yaw, and roll angle.

One requirement of the SAFELANE system is that it should be able to operate on a variety of different vehicle platforms from small passenger cars to huge trucks. In a passenger car the simplification is justified. But in a truck with a high camera mounting position and relatively large calibration pitch angle, the assumption is violated. Therefore a clear separation is made between extrinsic camera parameters and vehicle position and orientation parameters to be estimated. This is done by dividing the world coordinate system into a vehicle- and a lane-coordinate system. Image points are first projected onto the ground plane of the vehicle coordinate system (XY -plane) with the camera model (intrinsic and extrinsic) and then transformed into the lane coordinate system in which the clothoid model is defined. The transformation comprises a rotational part (pitch angle φ_2 and yaw angle φ_3) and a translational part (lateral offset y_0):

$$p_l = \begin{pmatrix} 1 & -\varphi_3 & \varphi_2 \\ \varphi_3 & 1 & 0 \\ -\varphi_2 & 0 & 1 \end{pmatrix} p_v + \begin{pmatrix} 0 \\ y_0 \\ 0 \end{pmatrix} \quad (1)$$

where p_l is a point in the lane coordinate system and p_v a point in the vehicle coordinate system

A clothoid is mathematically unhandy, so it is approximated by a third order polynomial:

$$y(x) = \frac{1}{2}c_0x^2 + \frac{1}{6}c_1x^3 \quad (2)$$

where c_0 is the curvature and c_1 is the curvature change.

A lane border measurement point can be calculated with:

$$y_l(x) = \frac{1}{2}c_0x^2 + \frac{1}{6}c_1x^3 \pm \frac{b}{2} \quad (3)$$

where b is the lane width and $+$ ($-$) correspond to a left (right) lane border.

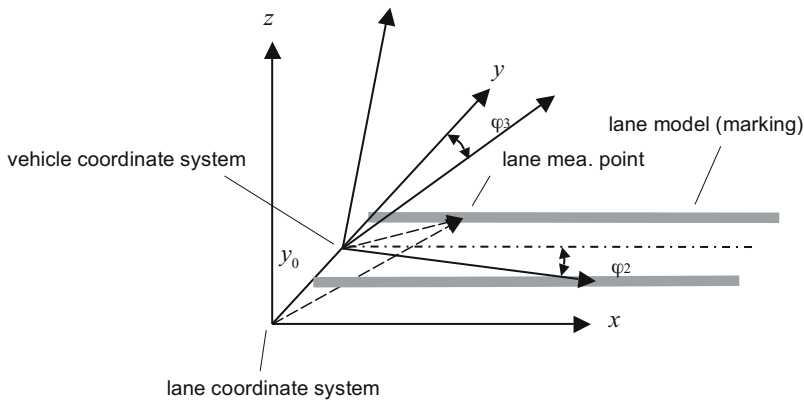


Fig. 5. Depiction of vehicle and lane coordinate system

4.3 Search Area

In initialisation mode the scan line generation is quite simple and follows a rigid setting scheme. In tracking mode scan lines are set along the projected predicted lane state. A scan line is set perpendicular to the local lane border tangent (not necessarily horizontal) in world coordinates. The line width and space to the next line are calculated depending on the look ahead distance. If the current lane border is classified as marked, the average lane marking width is calculated and will be added to the scan line width. Projected in the image plane the slope of the scan line is checked and the scan line is rejected if a certain threshold is exceeded.

4.4 Measurement Points

Fig. 6 depicts the process of generating measurement points. In a first stage it is sometimes helpful or even necessary to filter image data at pixel level. There are three mayor causes that can disturb the lane border measurement generating process: At dark lighting conditions cameras tend to get noisy, the road pavement structure can be coarse and heterogeneous and lane markings can be partially rubbed off. In these situations a filter is needed which on the one hand has smoothing characteristics but on the other hand retains strong edges. The median filter satisfies these needs. The median of a set of values is the middle value of the sorted set. In the image processing domain a median is calculated in a square area (called image filter mask) with a certain mask width. The median filter causes two problems: It is a computational expensive operator because of the involved sorting and structures disappear if smaller than the filter mask. We tackled the first problem by using an intermediate image, where already calculated median values are “cached”. This makes sense because in the following processing stages edge and structur tensor computation as well as segments calculation pixel are accessed several times. To prevent lane markings which appear small at further distances in the image from being smoothed away, the filter mask width is adapted according the look ahead distance.

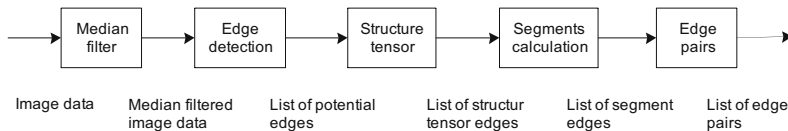


Fig. 6. Block diagram of measurement point generation

The well known Sobel operator [2] is used for gradient calculation as basis for the edge detection. Edges are detected where the gradient magnitude is maximal in gradient direction, a threshold is exceeded and the gradient points into the local direction of the lane. At the detected edge pixels the structure sensor [2] is computed. The quality of an edge pixel is computed by the ratio of its eigenvalues and the angle between the greater eigenvector and the tangent on the projected lane border.

If the quality of an edge is good enough a further validation is done by calculating little edge segments. The Search area of a segment is a small rectangle with the edge pixel at focus in the rectangle center, aligned along the lane border direction, bounded by the adjacent scan lines and with a width derived from the maximal allowed difference angle between the edge- and lane border-direction. Within the area neighbour edges in both lane border directions

are tried to be followed repetitively until the search area boundary is reached. If the segment is long enough with respect to the search rectangle length the segment is considered being part of a lane border.

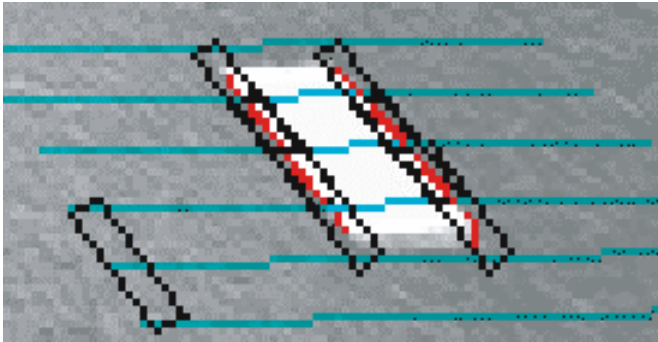


Fig. 7. Edge segments (red) at lane marking

4.5 Selection

In initialisation mode, where no lane state prediction of a previous time step is available an extended form of a Hough Transform [2] is employed. The Hough Transform is a technique which can be used to isolate features of a particular shape within an image. It requires that the desired features are specified in some parametric form.

The Hough technique is particularly useful for computing a global description of a feature, given (possibly noisy) local measurements. The motivating idea behind the Hough technique (e.g. for line detection) is that each input measurement (e.g. image point) indicates its contribution to a globally consistent solution (e.g. the physical line which gave rise to that image point).

As a simple example, consider the common problem of fitting a set of line segments to a set of discrete image points (e.g. pixel locations output from an edge detector). We can analytically describe a line segment with the linear equation $y = mx + b$. For any point (x, y) on this line, m and b are constant. In an image analysis context, the coordinates of the edge segment points (x_i, y_i) in the image are known and therefore serve as constants in the linear equation, while m and b are the unknown variables we seek. By plotting straight lines in an mb -coordinate system defined by each (x_i, y_i) , points in image coordinate space map to the so called Hough parameter space. If viewed in Hough parameter space, points which are collinear in the image space become readily apparent as they yield straight lines which intersect at a common (m, b) point.

The transform is implemented by quantizing the Hough parameter space into finite intervals (accumulator cells). As the algorithm runs, each (x_i, y_i) is transformed into a discretized (m, b) straight line and the accumulator cells which lie along this straight line in Hough space are incremented. Resulting peaks in the accumulator array represent strong evidence that a corresponding straight line exists in the image.

Applied to the problem of lane measurement selection the Hough transform equation is defined by the clothoid model, the vehicle position and direction parameters. To reduce the complexity and satisfy runtime constraints, not all parameters are taken into account and the look ahead distance where measurement points are searched is taken back comparing to the tracking mode. The clothoid model is further simplified by omitting the lane curvature change term and a pitch angle variation is not considered. Hence the resulting Hough parameter space is 4 dimensional and comprises the parameters b (lane width), c_0 (lane curvature), y_0 (lateral offset) and q_3 (yaw angle). The limits and the resolution of the Hough accumulator array are preset out of a configuration file. The parameter limits of c_0 and b are dynamically adapted through map data (if available). The algorithm takes each measurement point and stores a measurement reference in all accumulator cells satisfying the Hough transform equation. In a next step a number of accumulator cells are identified which accumulated most measurement points. To give more weight to measurement points of marked lane borders these points are counted double. To avoid initializing on guard rails or other lane marking like infrastructure the accumulator cell with smallest lane width parameter is chosen. All the accumulated measurement points in the chosen cell are used as input data for the following lane model estimation process.

The Hough parameter of the chosen accumulator cell is a good lane model hypothesis but far too inaccurate as a final model result. Still they can be used as initial lane state parameters for the lane model estimation.

Since the used estimator (Extended Kalman filter [3]) expects noisy measurements a variance value for each measurement has to be provided. The variances of all selected measurement points are set according the distance to the lane state, the pixel quantization error and the edge type (marked / unmarked).

During tracking mode the contour edge candidate next to the predicted lane state is used as a measurement point on a scan line. The variance of the selected measurement point is set the same way it is described for the initialisation mode.

4.6 Lane Model Estimation

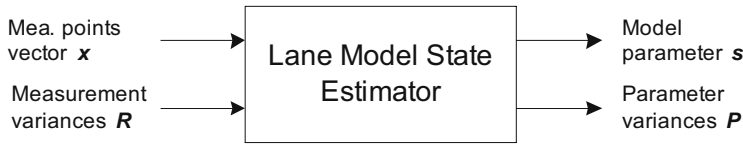


Fig. 8. Lane model state estimator

Assuming all measurement points are collected in a measurement vector \mathbf{x} , the optimal state \mathbf{s}_{opt} can be estimated by minimization of the square error:

$$\mathbf{s}_{\text{opt}} = \arg \min_{\mathbf{s}} (\mathbf{x} - \mathbf{f}(\mathbf{s}))^T \mathbf{R}^{-1} (\mathbf{x} - \mathbf{f}(\mathbf{s})) + (\mathbf{s} - \mathbf{s}_0)^T \mathbf{P}^{-1} (\mathbf{s} - \mathbf{s}_0) \quad (4)$$

The covariance matrices \mathbf{R} and \mathbf{P} of the measurement noise and the initial state \mathbf{s}_0 , respectively are assumed to be diagonal. I.e. no correlations among measurement points and among initial state parameters are assumed. The variances of measurement points and fixed variances of the initial state are used for the estimation.

Since the measurement function \mathbf{f} is quite complex and nonlinear the estimation is done by linearization and iteration within an Extended Kalman filter [3].

To check the plausibility of the new state, tolerance intervals for each state parameter are given, which describe the admissible range of the lane model parameter. If one of the parameters lies outside of its interval, the estimation is rejected and the system is put into initialisation mode.

5 Neighbour Lane Recognition

In the concept and specification phase of the SAFELANE project it was identified that the information of the presence of neighbour lanes can be helpful or even is necessary in critical traffic conditions for the lane keeping task. Thus the two directly neighboured lanes of the main lane where the vehicle is currently driving in are estimated as well. This is done with the same methods used for the main lane besides some deviations in the initialisation mode. If the main lane recognition was successful the neighbour lane recognition is triggered. The initial search areas of neighbour lanes can be set more precisely

comparing to the main lane because we know the location of one neighbour lane border and usually neighbouring lanes have about the same width. The pitch angle of the neighbour lanes is assumed to be identical with the main lane.

False detections can happen on structures that look like lane borders (e.g. crash barriers). Therefore two additional tests are applied. The first one compares the road texture of the main lane and the neighbour lane. If the texture difference exceeds a threshold the test fails. The second one checks if there are any obstacles inside the image area of the neighbour lane by means of the object mask image. If one of the tests is not successful the neighbour lane recognition will be rejected.

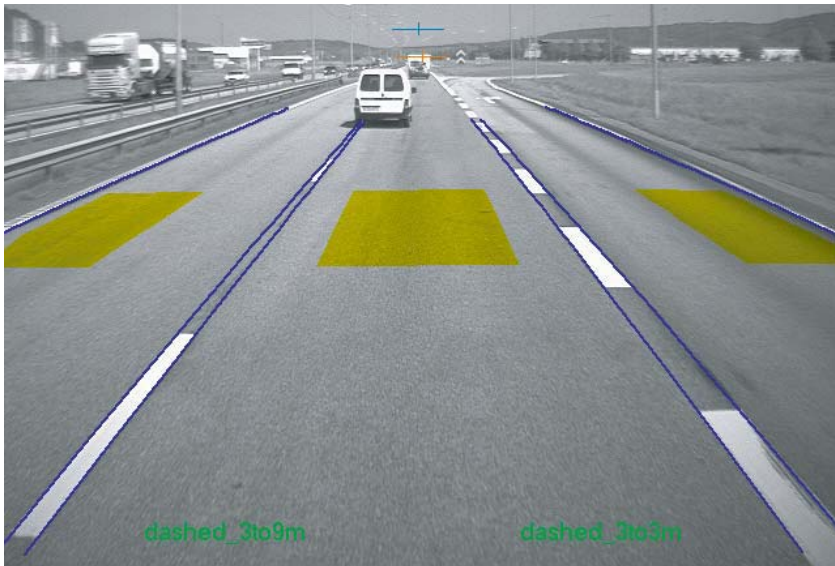


Fig. 9. Neighbour lane recognition, road texture check in yellow windows

6 Lane Marking Classification

The knowledge of the road marking types which delimits the own lane is of great importance for the lane keeping task. The system should e.g. react more sensitive regarding lane departure in case of solid lane markers comparing to dashed markers. One information source for road marking types is the digital map. But on a multi lane road the GPS and map data are not accurate enough to locate the vehicle in a dedicated lane.

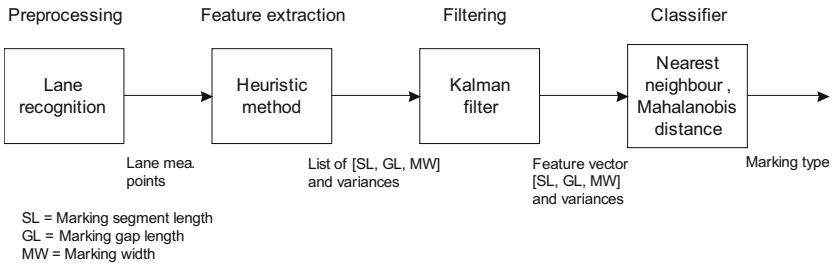


Fig. 10. Block diagram of lane marking classification

Lane markings are assumed to be solid or dashed marker lines. Dashed lane markings have certain constant marking line width, line segment length and line gap length. Therefore these three marking characterizing values are taken as features for the marking type classification. The needed information to determine the features are available in the lane border measurement points found in the course of lane recognition. The measurement points are first transformed to the lane (world) coordinate system before a heuristic method extracts all feature values of a lane border. That means we get for each marking measurement point a marking line width value and for each marking line segment and gap a length value. The extraction of segment and gap lengths benefits from the calculation of little edge segments within the lane border measurement process so that a one pixel accuracy can be achieved. The variances are calculated by transforming at each extraction position a one pixel difference from image coordinates to world coordinates.

For the classifier only one feature vector with the three characterizing width and length values are needed. Thus all the extracted values have to be merged in some way. We decided to use a Kalman filter for each feature (marking width, segment and gap length). Using a Kalman filter has also the advantage to time average the features so that occasionally false lane detection measurements or partially rubbed off markers are smoothed out.

Finally a nearest neighbour classifier determines the lane marking type. A nearest neighbour classifier calculates distances between the feature vector to be classified and sample feature vectors which represent different classes. Since we have variances of each feature a Mahalanobis distance function is employed. A Mahalanobis distance weight the distance according a covariance matrix (here the matrix is diagonal). That means high variances result in high distances.

For each marking type class a set of sample feature vectors must be specified in a configuration file. E.g. the file entry

```
dashed_3to9m = {{ 3, 9, 0.1}, { 3, 9, 0.2}, { 3, 9, 0.3}}
```

specifies a marking type class with line segment length of 3 m and line segment gap length of 9 m and marker width between 10 cm and 30 cm.

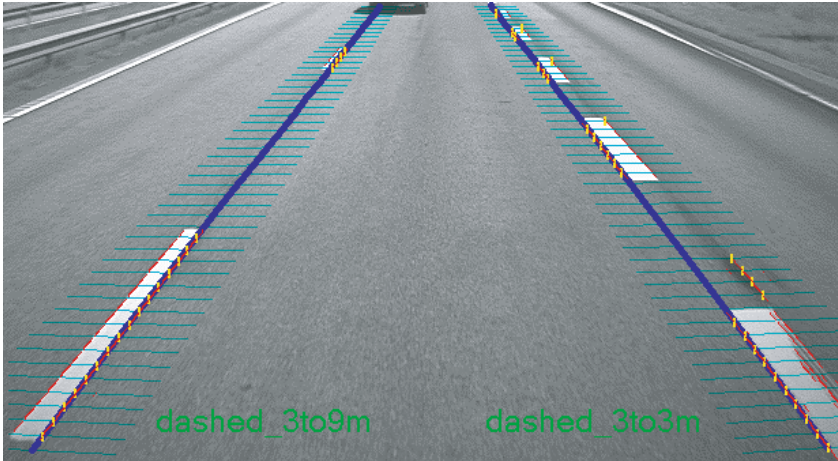


Fig. 11. Marking type “dashed_3to9m”: Marking segment length = 3 m and marking gap length = 9 m

7 Object Mask Generation

The function of this module is not to classify obstacles or other traffic participants. Areas on the road are detected and marked in an object mask image where objects are located. The main purpose is to support the lane recognition. The lane recognition cannot decide whether a measurement point is a point on the lane border or e.g. a vertical edge of a car driving in front of the own vehicle. A wrong measurement point can cause estimation errors. To avoid these errors lane detection search areas (scan lines) are trimmed where the object mask image is marked.

For the object mask generation an approach is chosen that analysis motion-compensated difference images assuming the vehicle moving on a planar road surface. The used motion compensation algorithm computes the required image warping parameters from an estimate of the relative motion between camera and ground plane. This is done for the last two consecutive images. The algorithm estimates the warping parameters from displacements at image corners and image edges.

8 Use of Digital Map Data

Besides the use of map data for the lane keeping decision module, the lane detection can also benefit of it. All lane tracking systems have certain fixed configuration parameters. The determination of a configuration parameter is often a trade off between different scenarios concerning environmental and lighting conditions. A parameter value may work well in one scenario while the same value doesn't work at all in another. So the general idea to enhance the performance of lane detection systems with map data is to adapt certain configuration parameters with respect to information about the vehicle environment coming from a digital map.

Several critical scenarios were identified in preliminary tests of state-of-art Lane Vision systems. Most of the problems were encountered in scenarios where external elements have visual features similar to lane markings or borders like guardrails and sidewalks. In these scenarios the resulting lane models deviate considerably from the real lane. If we would have some knowledge of the current lane in front of the vehicle, the estimated lane model could be validated. Here the digital map comes into play. Out of the GPS localisation and the digital map good estimates of the current lane width b and lane curvature c_0 can be provided.

If map data and a GPS signal are available the c_0 and b tolerance intervals of the lane state plausibility check (chapter 5.5) and the Hough accumulator parameter limits for c_0 and b are dynamically adapted. If the lane detection now starts tracking other elements and the estimated lane width and curvature get out of range, the state plausibility check triggers a re-initialisation of the system. Because the Hough accumulator space is limited in c_0 and b coordinates to the same values as the tolerance intervals, the chances are good that a proper lane detection restarts.

9 Conclusions

We proposed a lane detection system aimed at being used in lane keeping assistant systems. The development focus lay on a high system adaptability with respect to the vehicle platform and different environment and traffic situations. A clear separation of the camera calibration and vehicle position estimation is made to meet the vehicle platform flexibility requirement. The combination of a new initialisation algorithm and the use of positioning and map data lead to very robust detection results in varying traffic scenarios. The lane detection was furthermore extended to track the direct neighbour lanes as

well, an obstacle area detection algorithm was added and a lane marking type classification was introduced. One SAFELANE demonstrator vehicle (a truck at Volvo Technology in Sweden) is already equipped with our lane detection system and the so far conducted tests are very promising. In the next SAFELANE project phase extensive evaluation tests will be conducted on different vehicle platforms.

10 Acknowledgements

The work presented in this paper has been funded by the European Commission within the PReVENT subproject SAFELANE. This support is gratefully acknowledged. We also thank our SAFELANE project partners Volvo Technology, Delphi, Centro Ricerche Fiat, Ministerie van Verkeer en Waterstaat, Laboratoire Central des Ponts et Chaussées, Institute of Communication and Computer Systems and Ford Forschungszentrum Aachen.

References

- [1] E. D. Dickmanns, B. Mysliwetz. "Recursive 3D Road and Relative Ego-State Recognition. IEEE Transactions on Pattern Analysis and Machine Intelligence PAMI-14 (1992) 199-214.
- [2] Jähne, B., "Digital Image Processing", Springer Verlag, 1997
- [3] Brown, R.G. and Y.C. Hwang, "Introduction to Random Signals and Applied Kalman Filtering", Third edition, John Wiley & Sons 1997.
- [4] R. Risack, P. Klausmann, W. Krüger, and W. Enkelmann, "Robust Lane Recognition Embedded in a Real-Time Driver Assistance System", 1998, vol. 1, pp. 35-40.
- [5] <http://www.prevent-ip.org>
- [6] <http://www.prevent-safelane.org/>

Nikolaus Möhler, Dietrich John, Marina Voigtländer

Fraunhofer Institute for Transportation and Infrastructure System
 Zeunerstrasse.38
 01069 Dresden
 Germany
moehler@fhgde
john@fhgde
voigtlaenderi@fhgde

Keywords: lane keeping support, lane detection, clothoid, digital map, GPS, Hough transform, marking type classification, high dynamic range camera

Appendix A

List of Contributors

List of Contributors

Acharya	205
Achterholt	353
Amditis	379, 451, 471
Andreone	379
Arfwidsson	379
Aycard	451
Beasley	223
Bengler	379
Beuk	427
Beutner	471
Bever	323
Blervaque	427
Bouchaud	3
Brauer	45
Brockherde	23
Buydens	261
Cacciabue	379
Cheng	307
Choi	307
Cornwell	223
Dammers	343
Decker	343
Delatte	239
Demeüs	239
Dessard	239
Diels	261
Dietmayer	187
Dirscherl	171
Dittmer	123
Dixon	3
Durekovic	67
Egginton	223
Egnisaban	307
Elkhalili	23
Eloy	13
Engström	379
Flament	407

Fröming	79
Fürstenberg	129, 187, 437
Fussey	223
Glasauer	107
Grande	249
Granig	323
Graze	41
Gresser	67
Grundmann	353
Günthner	107
Guttowski	353
Hammerschmidt	323
Ho	307
Hornegger	281
Hosticka	23
Hsu	205
Hung	307
Irion	407
Iriondo	249
Janssen	379
Jesorsky	281
John	485
Kassovsky	261
Kasten	171
Katzmaier	323
Khaskelman	155
Kibbel	123
King	223
Kompe	281
König	23
Krause	369
Krupka	45
Kühn	79
Kussman	379
Lages	437
Lamers	171
Landsmann	223

Lasowski	143
Le Guilloux	155
Lezama	249
Lindl	53
Listl	23
Liu	281
Loewenau	67, 427
Lonnoy	155
Ma	307
Mäkinen	407
Mangente	307
Martinez	249
Mengel	23
Metzner	343
Mezger	427
Miglietta	471
Möhler	485
Moreira	155
Moser	369
Mounier	13
Munz	171
Nathan	379
Ng	307
Niedermayer	353
Noble	223
Obieta	249
Ochoteco	249
Park	451
Pauzié	295
Pellkofer	23
Pelz	343
Picún	239
Polityko	353
Polychronopoulos	471
Pomposo	249
Potin	13
Prügl	323
Rabel	67

Rafii	205
Reich	353
Richter	67
Rössler	323, 437
Roussel	13
Salamon	223
Salow	123
Saroldi	471
Scheunert	451
Schindler	79
Schönewolf	41
Schrey	23
Schulz	129
Schulze	407
Sjögren	471
Steinert	41
Stevens	239
Straßberger	143
Stratmann	171
Sünkel	281
Tatschke	53, 451
Thomasius	353
Toepfer	23
Truscott	223
Ulbrich	107
Ulfig	23
Vogel	53
Voigtländer	485
Voßkaemper	343
Wagner	107
Walchshäusl	53
Weiss	187
Wender	187
Willenbrock	41
Wipiejewski	307
Wisselmann	67
Wong	307
Yau	307

Zimmer

323

Appendix B

List of Keywords

List of Keywords

2-shot-molding	375
3D camera	219
3D image processing	293
3D integration	367
3D packaging	367
3D range camera	39
3D sensor	39, 219
3D vision	293
accelerometer	12, 19
active and preventive safety	484
active safety	425
adaptive control	121
adaptivity	405
ADAS	141
ADAS horizon	436
advanced airbag	219
advanced driver assistance systems	141, 436
air conditioning	280
airbag occupant sensing	219
Alasca	128
angular sensor	342, 375
ASIC	245
automotive	245
automotive markets	12
backup obstacle detection	219
biologically inspired	121
blind spot surveillance	39
boosting	169
camera stabilization	121
climate control	280
clothoid	500
CMOS-sensor	219
CMOS-technology	39
collision avoidance	128
collision mitigation	39, 169
combustion feedback	238
comfort	280
conducting polymer ink	260
coordinated control	238

cylinder pressure sensing	238
decision system	484
design	
diesel engine	238
digital map	436, 500
distance measurement	39
distributed pressure sensor	260
driver	245
driver assistance systems	121, 293
driver behaviour	405
dynamic suppression	219
early fusion	469
ego localization	203
electro-magneto-mechanical effects	351
electronic perception technology	219
engine control	245
engine management systems	238
environment modelling	469
environment perception	469
event-online	44
far infrared	169
FCD	44
fiber optic technology	319
fiber optic transceiver	319
flexible plastic sensor	260
floating	245
floating car data	44
flow sensor	12
force sensor	186
fusion feedback	469
fusion framework	469
gaze stabilization	121
gesture recognition	293
giant magneto resistor	342
GPS	500
grid-based fusion	469
gyroscope	12, 19
half-bridge	245

Hall-sensor	186
hand detection	293
high dynamic range camera	500
high level maps	203
high speed photodetector	319
high temperature	245
HMI	484
HMI evaluation methods	405
Hough transform	500
housing	375
human machine interaction	405, 484
human machine interface	293, 405
iBolt	186
IMU	19
inclinometer	12
inertial measurement unit	121
inertial sensor	12, 19
infotainment system	319
infrared temperature sensor	280
integrated functions	484
integrated safety	425
integration	405
inter-vehicle communication	154
intersection	203
intersection safety	449
IVC	154
lane detection	500
lane keeping support	500
large surface monitorization	260
laser direct structuring	375
laser subtractive structuring	375
laserscanner	128, 141, 203, 449
LDS	375
learning-based techniques	169
lidar	219
local danger warning	154
LSS	375
macrosystem	351
map building	449
market forecast	19

marking type classification	500
MDSI range detection	39
mechatronic	351
metallized plastic	375
microphone	19
microsystem	351
MID	375
mixed-signal	351
modeling	351, 405
molded interconnect devices	375
MSM photodetector	319
MST sensors	12
multi domain	351
multi level fusion	469
multiple segment association	203
neuroscience	121
object classification	203
obstacle detection	154
occupant classification	186
optimisation of fleet	44
out-of-position detection	293
packaging	375
passenger airbag	186
PCS optical fiber link	319
pedestrian detection	219
pedestrian protection	39
perception system	484
positioning sensor	375
pre-crash sensing	219
precrash	169
predictive sensor	436
presence detection	260
pressure sensor	12, 375
PreVENT	425
preventive safety	425
ProFusion2	469
qualification	375
range camera	219

range video	219
risk assessment	449
safety zone	425
scenario interpretation	449
sensor data fusion	469
sensor fusion	484
smart automotive seat	260
SOI	245
speed sensor	342
spin valve	342
standardised interface	436
substrates	375
support vector machines	169
switch on MID	375
thermometer	280
time-of-flight camera	219
time-of-flight measurement	39
tire pressure monitoring	367
track-based fusion	469
traffic management	44
VANETS	154
VCSEL FOT	319
vehicular ad-hoc networks	154
VHDL-AMS	351
video transmission	319
vulnerable road user protection	169
weight sensing	186
wireless sensors	367
workload management	405

